Heat Pumps in CHP Systems

High-efficiency Energy System Utilising Combined Heat and Power and Heat Pumps

Ommen, Torben Schmidt

Publication date:
2015

Document Version
Publisher's PDF, also known as Version of record

Heat Pumps in CHP Systems

High-efficiency Energy System Utilising Combined Heat and Power and Heat Pumps

PhD Thesis

$$(EIv'')'' = q - \rho A\ddot{v}$$

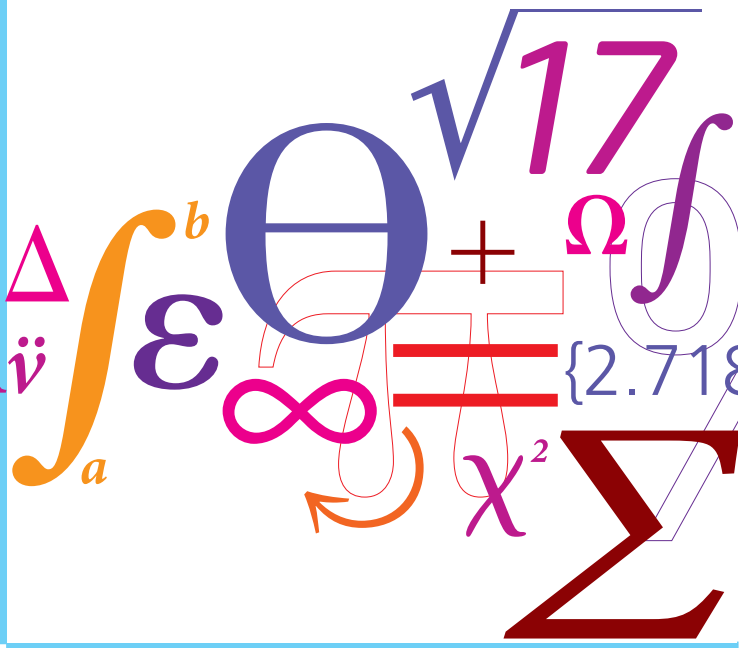

Torben Schmidt Ommen
DCAMM Special Report No. S187
April 2015

DTU Mechanical Engineering
Department of Mechanical Engineering

Heat Pumps in CHP Systems

High-efficiency Energy System Utilising
Combined Heat and Power and Heat Pumps

Torben Ommen

Ph.D. Thesis

Kongens Lyngby 2015

Technical University of Denmark

Heat Pumps in CHP Systems
High-efficiency Energy System Utilising Combined Heat and Power and Heat Pumps

Ph.D. Thesis

Supervisors:
Brian Elmegaard
Wiebke Brix Markussen

DTU Mechanical Engineering
Section of Thermal Energy
Technical University of Denmark
Nils Koppels Allé, Building 403
DK-2800 Kongens Lyngby
Denmark
Phone (+45) 45 25 25 25
Fax (+45) 45 25 19 61
www.mek.dtu.dk

Preface

This thesis was submitted as partial fulfillment of the requirements for the Ph.D. degree at the Technical University of Denmark (DTU).

The thesis was completed at the Section of Thermal Energy, Department of Mechanical Engineering at the Technical University of Denmark. The work was carried out in the three-year period which initiated 1^{st} of September 2011 and concluded 8^{th} of March 2015 under the supervision of Associate Professor Brian Elmegaard and the co-supervision of Assistant Professor Wiebke Brix Markussen.

An external research stay was undertaken from March 2013 to the end of May 2013. The external stay was at Politechnico di Torino, Turin, Italy. The purpose of the stay was collaboration with Associate Professor Vittorio Verda.

The thesis consists of a report and a collection of research papers written during the period 2012 to 2015, and published elsewhere.

This work was funded by several independent stakeholders. DONG Energy, Danish Technological Institute, the Technical University of Denmark and Copenhagen Cleantech Cluster as a GAP project administered by DTU.

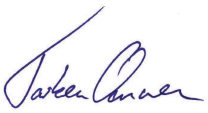

Torben Schmidt Ommen
Kgs. Lyngby, April 2015

Acknowledgements

I thankfully acknowledge the support of the Ph.D.-project by DONG Energy, Copenhagen Cleantech Cluster (CCC), Danish Technological Institute and Technical University of Denmark. In particular Katrine Bech Andersen, Mogens Bech Larsen and Lars Reinholdt from the collaborating companies should be acknowledged for their contribution to the project, by providing support, data and advice when needed.

My deepest gratitude should be expressed to the principal supervisor of the project, Brian Elmegaard. His support, advice, guidance and encouragement shaped this project from the initial grant applications to the finishing stage. I would also like to thank my co-supervisor Wiebke Brix Markussen for always being available for questions, discussions and linguistic assistance.

During my external stay in Turin, Vittorio Verda assisted with support and guidance, as well as recommendations for enjoying the city, for which I am grateful. I would also like to thank both H.P. Christensens and Myhrwolds foundation, who assisted with the economical support while abroad.

I also wish to thank my colleagues at the section of thermal energy for providing an inspiring scientific environment. You have each contributed to the project, either by active support, positive atmosphere or both. I am especially grateful for the wonderful collaboration and discussions with and support by Erasmus Damgaard Rothuizen, Jonas Kjær Jensen and Jorrit Wronski during the project.

Last, but not least, I am enormously grateful to my family and friends, who have been patient with me, also during the last part of the project. Especially to Nada for her love and understanding, and to Liva for being a necessary and loved distraction from academia.

Abstract

In the current Danish energy system, the majority of electricity and heat is produced in combined heat and power (CHP) plants. With increasing shares of intermittent renewable power production, it becomes a challenging task to match power and heat production to its demand curves, as production capacity constraints limit the efficient operation of the CHP plants. Heat pumps (HPs) can be used to decouple such constraints, but current state of the art are not competitive all things considered. Methods to improve the high energy efficiency are required to match the politically agreed carbon emission goals. The presented study investigates the possible introduction of HPs from both a thermodynamic and a system/operation management perspective, in order to find optimal integration schemes in both current and future energy scenarios.

Five generic configurations of HPs in district heating (DH) systems were identified and compared based on a thermodynamic analysis. The operational performance of the configurations were investigated at both local and system level considering different DH network temperatures, different fuels and different production technologies in the DH network. The analysis show that three configurations are particular advantageous, whereas the two remaining configurations result in system performance close to or below what may be expected from an electric heater. One of the three advantageous configurations is required to be positioned at the location of the heat demand, whereas the two remaining can be located at positions with availability of high temperature sources by utilising the DH network to distribute the heat.
A large amount of operational and economic constraints limit the applicability of HPs operated with natural working fluids, which may be the only feasible choice in Danish conditions. The limitations are highly dependent on the integration of heat source and sink streams. An evaluation of feasible operating conditions was carried out considering the constraints of available refrigeration equipment and a requirement of a positive net present value of the investment. Six vapour compression heat pump (VCHP) systems were considered along with the ammonia-water hybrid absorption compression heat pump (HACHP), corresponding to an upper limit of the sink temperature of up to 150 °C. The best available technology was determined for each set of heat sink and source temperatures. The results showed that five different HP systems propose the best available technology at different parts of the complete domain. Ammonia-water HACHP and ammonia VCHP systems utilising either low or

high pressure components are preferable very broad range of sink temperature and temperature lifts. With the considered economic constraints in place, the requirements in terms of sink temperatures and temperature lift are not met for many DH networks considering the configurations which heat to forward temperatures.
The specific performance for two DH HP configurations were studied in detail, using the finite temperature levels of a range of common DH networks. Eight systems were examined in terms of applicability, and the systems were optimised for each operating condition using exergoeconomic theory. The HPs were compared based on cost of heat. The results show that including the practical applicability of components causes a significantly increased cost at high temperature lifts, compared to the most competitive thermodynamic cycle. At high and medium temperature lifts cycle efficiencies of 45 - 50 % of the theoretical maximum (Lorenz cycle limit) can be achieved, whereas for low temperature lifts, efficiencies as low as 36 % may be expected.

Three frequently used operation optimisation methods were examined, in order to investigate their impact on operation management of energy system technologies. By focussing on the physical representation of a CHP-plant, it is clear that a simple representation allows infeasible production. Using MIP or NLP optimisation, the number of operation hours and the total production of heat from HPs are significantly increased, as the HPs may be used to shave the load patterns of CHP units in significantly constrained energy systems.
A MIP energy system model was developed with focus on the detail level of features for representation of CHP and HP units. Two energy scenarios were considered, one current, which is a validated model for 2011, and a future scenario, as proposed by energy planners for 2025, where reductions in carbon emissions for heat is of major interest.
The changed distribution of electricity generation technologies may suggest a reconsideration of optimum for DH network temperatures, in order to achieve low cost and minimum carbon emissions. The developed energy system model was used to investigate the changed operation. Production curves from typical CHP-plant technologies were used to represent the changed power and heat production for changed DH temperatures. The results show that both primary fuel consumption and cost can be reduced approximately 5-7 % at DH forward temperatures of 60 - 70 °C in 2025 scenario. Further reduction results in contrary tendencies as hot tap water requires increasing amounts of electricity to reach required temperatures. The results are network specific, as they represent the specific DH utility technologies and network constraints, but similar trends can be expected for other large DH networks.

Resume

I det nuværende danske energisystem bliver hoveddelen af den benyttede el og varme produceret på et kraftvarmeværk (KVV). Med stadig større produktion af el fra vedvarende energikilder bliver det en stadig større udfordring at tilpasse el og varmeproduktion til behovsprofilet, da produktions kapacitetens tekniske restriktioner begrænser den effektive produktion på KVV. Varmepumper (VP) kan benyttes til at afkoble sådanne begrænsninger, men den nuværende teknologi er ikke konkurrencedygtig. Metoder til at forbedre energi effektiviteten er nødvendige, for at kunne opnå de politisk fremlagte mål for CO_2-emmisioner. Det præsenterede studie undersøger den mulige introduktion af VP fra både et termodynamisk- og system/operationsanalyse perspektiv, for at finde optimale integrations løsninger for både nutidige og fremtidige energisystemer.

Fem generiske konfigurationer for VP i fjernvarme- (FV) systemer blev identificeret og sammenlignet ud fra en termodynamisk analyse. Den operative præstationsevne af konfigurationerne blev undersøgt både for den enkelte enhed og fra et system perspektiv for forskellige FV temperaturer, forskellige drivmidler og ved systemer med forskellige produktions teknologier i FV netværket. Analysen viste at tre konfigurationer er særligt fordelagtige, hvorimod de to tilbageværende konfigurationer, set fra et system perspektiv, præsterer tilsvarende eller endog dårligere end det der kan forventes af en elektrisk vandvarmer. Den ene af de tre fordelagtige konfigurationer skal lokaliseres hos forbrugeren, hvorimod de to resterende kan placeres på lokaliteter med særligt gunstige temperaturer, hvor FV netværket benyttes til at distribuere varmen. En stor mængde operative og økonomiske restriktioner begrænser anvendelsen af VP som benytter naturlige arbejdsmedier, hvilket kan være de eneste mulige valg for Danske forhold. Begrænsningerne er meget afhængige af integrationen af energistrømmene for varme kilde og dræn. En vurdering af fordelagtige operative anlæg blev udført ud fra restriktioner som tilgængeligt køleteknisk udstyr og behovet for en positiv nutidsværdi for investeringen. Seks kompressions varme pumper (KVP) blev analyseret sideløbende med ammoniak-vand hybrid absorption kompressions varme pumpe (HAKVP), hvilket korresponderer til en øvre begrænsning i dræn temperature op til 150 °C. Den bedste disponible teknologi blev bestemt for hver mulig kombination af kilde og dræn temperaturer. Resultaterne viste at fem forskellige VP systemer fremsætter den bedste tilgængelige teknologi ved forskellige dele af det samlede arbejd-

område. Ammoniak-vand HAKVP og ammoniak KVP systemer med enten lav eller højtrykskomponenter er fordelagtige for en meget stor del af de analyserede dræn temperaturer og temperaturløft. Krav til dræn temperaturer og temperaturløft kan ikke tilfredsstilles for mange FV systemer hvis VP varmer til fremløbstemperaturen, med de benyttede økonomiske begrænsninger inkluderet i analysen.
Den specifikke ydeevne for to FV VP konfigurationer blev undersøgt i yderligere detalje, hvortil der benyttes endelige temperatur niveauer som svarer til en række typiske FV netværk. Otte systemer blev analyseret for deres anvendelighed, og systemerne blev optimeret til hvert driftspunkt ved brug af exergoøkonomisk analyse. De enkelte VP blev sammenlignet baseret på prisen af den producerede varme. Resultaterne viser, at de tekniske begrænsninger medfører en betydeligt forøget pris på varme ved høje FV temperaturer, sammenlignet med den mest konkurrencedygtige termodynamiske kredsproces. Ved høje og mellemhøje temperaturløft er det muligt at opnå en kredsproces effektivitet på op til 45-50 % af det teoretisk mulige (i forhold til Lorenz processen), hvorimod så lave virkningsgrader som 36 % må forventes for lave temperaturløft.

Tre typisk anvendte operations analyse metoder blev analyseret for deres påvirkning på driftsstyring for energiteknologier. Ved at fokusere på den fysiske repræsentation af KVV, synes det klart at den simple repræsentation tillader ugennemførlig produktion. Når blandet heltals programmering (BHP) og ikke lineær programmering (ILP) benyttes, bliver antallet af driftstimer og produktionen af varme fra VP betydeligt forøget, da VP kan benyttes til at udligne driftsprofilet for KVV i energisystemer med betydelige tekniske begrænsninger. En BHP energi system model blev udviklet, med fokus på detaljeret repræsentation af KVV og VP. To energiscenarier blev benyttet til analysen, et nuværende, som er valideret for året 2011, og et fremtidigt scenarie, som modsvarer det energiplanlæggere foreslår for 2025, hvor reduktioner af CO_2-emissioner er en særlig indsats.
Den ændrede drift for elektricitets produktions enheder fører til genovervejelse af optimum for FV netværks temperaturer, for at opnå den laveste pris og de laveste CO_2-emissioner. Den udviklede energisystem model blev benyttet til at analysere den ændrede produktion. Produktions ændringer fra typiske KVV teknologier blev benyttet til at repræsentere den ændrede produktion af el og varme for ændrede FV temperaturer. Resultaterne viser at forbruget af primær energi og systemets omkostninger kan reduceres med ca. 5-7 % ved FV fremløbstemperaturer på 60 til 70 °C for 2025 scenariet. Yderligere reduktion i FV temperaturer resulterer i modsat rettede tendenser, da varmt brugsvand skal benytte stadig større mængder el for at opnå de nødvendige temperaturer. Resultaterne er netværks specifikke, da de repræsenterer specifikke FV forsyningsværker og netværk restriktioner, men tilsvarende tendenser kan forventes for andre store FV netværker.

List of publications

Journal Papers:

[P1] Ommen, T., Markussen, W.B., Elmegaard, B.. Comparison of linear, mixed integer and non-linear programming methods in energy system dispatch modelling. Energy 2014; 74:109–118. doi:10.1016/j.energy.2014.04.023.

[P2] Ommen, T., Markussen, W.B., Elmegaard, B.. Heat pumps in combined heat and power systems. Energy 2014; 76:989–1000. doi:10.1016/j.energy.2014.09.016.

[P3] Ommen, T., Jensen, J.K., Markussen, W.B., Reinholdt, L., Elmegaard, B.. Technical and economic working domains of industrial heat pumps: Part 1 - single stage vapour compression heat pumps. International Journal of Refrigeration 2015; xx: 1–15. doi:10.1016/j.ijrefrig.2015.02.012.

[P4] Jensen, J.K., Ommen, T., Markussen, W.B., Reinholdt, L., Elmegaard, B.. Technical and economic working domains of industrial heat pumps: Part 2 - ammonia-water hybrid absorption-compression heat pumps. International Journal of Refrigeration 2015; xx: xxx–xxx. doi:10.1016/j.ijrefrig.2015.02.011.

[P5] Ommen, T., Verda, V., Jensen, J.K., Markussen, W.B., Elmegaard, B.. Exergoeconomic comparison of heat pumps in district heating systems. 2015; [To be submitted].

[P6] Elmegaard, B., Ommen, T., Markussen, M., Iversen, J. Integration of space heating and hot water supply in low temperature district heating. Energy & Buildings 2015; doi:10.1016/j. enbuild.2015.09.003.

[P7] Ommen, T., Markussen, W.B., Elmegaard, B.. Lowering district heating temperatures - Impact to system performance in current and future Danish energy scenarios. Energy 2015. [Submitted].

Peer-reviewed conference papers:

[P8] Ommen, T., Elmegaard, B.. Exergetic evaluation of heat pump booster configurations in a low temperature district heating network. ECOS 2012. Firenze University Press.

[P9] Sigthorsson, O., Ommen, T., Elmegaard, B.. Thermoeconomic diagnosis of an energy system for ship propulsion. ECOS 2013. Chinese Society of Engineering Thermophysics.

[P10] Ommen, T., Markussen, W.B., Elmegaard, B.. Comparison of operation optimization methods in energy system modelling. ECOS 2013. Chinese Society of Engineering Thermophysics. Scientific contents corresponds to P1.

[P11] Ommen, T., Jensen, J.K., Markussen, W.B., Reinholdt, L., Elmegaard, B.. Technical and economic working domains of industrial heat pumps: Part 1 - vapour compression heat pumps. 11th IIR-Gustav Lorentzen Conference on Natural Refrigerants - GL2014. Chinese Association of Refrigeration. Scientific contents corresponds to P3.

[P12] Jensen, J.K., Ommen, T., Markussen, W.B., Reinholdt, L., Elmegaard, B.. Technical and economic working domains of industrial heat pumps: Part 2 - ammonia-water hybrid absorption-compression heat pumps. 11th IIR-Gustav Lorentzen Conference on Natural Refrigerants - GL2014. Chinese Association of Refrigeration. Scientific contents corresponds to P4.

[P13] Elmegaard, B., Ommen, T., Markussen, M., Iversen, J.. Integration of space heating and hot water supply in low temperature district heating. ECOS 2014. Åbo Akademi University. Scientific contents corresponds to P6.

[P14] Ommen, T., Jensen, J.K., Markussen, W.B., Elmegaard, B.. Enhanced technical and economic working domains of industrial heat pumps operated in series. International Conference of Refrigeraion ICR 2015; [Accepted for publication].

[P15] Jensen, J.K., Kærn, M.R., Ommen, T., Markussen, W.B., Reinholdt, L., Elmegaard, B.. Effect of liquid/vapour maldistribution on the performance of plate heat exchanger evaporators. International Conference of Refrigeraion ICR 2015; [Accepted for publication].

Other contributions:

[P16] Zvingilaite, E., Ommen, T., Elmegaard, B., Franck, M.. Low temperature district heating consumer unit with micro heat pump for domestic hot water preparation. 13th International Symposium on District Heating and Cooling 2012. District Energy Development Center.

[P17] Ommen, T., Markussen, W.B., Elmegaard, B.. Heat pumps in district heating networks. CoolEnergy 2013. Technical University of Denmark.

Contents

Preface i

Acknowledgements iii

Abstract v

Resume vii

List of publications ix

Contents xi

1 Introduction 1
- 1.1 Thesis statement . . . 3
- 1.2 Methodology . . . 3
- 1.3 Readers guide . . . 5

2 Heat pumps in combined heat and power systems 7
- 2.1 Heat pumps in finite reservoirs . . . 7
- 2.2 Potential heat sources . . . 9
- 2.3 Heat sink . . . 11
- 2.4 Heat pump configurations for district heating . . . 12
- 2.5 Summary . . . 16

3 Technical and economic working domains of industrial heat pumps 19
- 3.1 Heat pump working domains . . . 19
- 3.2 Vapour compression heat pumps . . . 22
- 3.3 Ammonia-water hybrid absorption-compression heat pump . . . 25
- 3.4 Vapour compression heat pumps operated in series . . . 28
- 3.5 Summary . . . 31

4 Centralised district heating heat pumps 33
- 4.1 Comparison of VCHP cycles for SF configuration at low forward temperatures . . . 33
- 4.2 Exergoeconomic optimal configurations . . . 34
- 4.3 SF configuration . . . 36
- 4.4 SR configuration . . . 37
- 4.5 Summary . . . 39

5 Energy system modelling **41**
5.1 Optimisation scheme 41
5.2 Mixed integer model 43
5.3 Current and future energy system scenarios 44
5.4 Examples of various heat pump integration schemes 45
5.5 Summary 48

6 Low temperature DH in current and future Danish energy scenarios **49**
6.1 Performance evaluation of LT DH distribution networks 50
6.2 Booster configurations 52
6.3 Impact to system performance from lowering district heating temperatures 52
6.4 Summary 55

7 Concluding remarks **57**
7.1 Summary of findings 57
7.2 Future work 60

Bibliography **63**

A Energy system model formulation **71**
A.1 Structure 73
A.2 Objective function 73
A.3 Economic constraints 74
A.4 Electricity and heat balances 78
A.5 Technology constraints 80
A.6 System reserves and operational constraints 84

B Energy system model validation **85**
B.1 Optimisation Criteria 85
B.2 Environmental reports 86
B.3 Environmental statements 87
B.4 Data from Energinet 87
B.5 Data from DONG 89
B.6 Summary 92

C Paper 1 - Energy **95**

D Paper 2 - Energy **107**

E Paper 3 - International Journal of Refrigeration **121**

F Paper 4 - International Journal of Refrigeration **139**

G Paper 5 - To be submitted **159**

H Paper 6 - Energy & Buildings **179**

I Paper 7 - Energy **203**

J Paper 8 - ECOS 2012 **237**

K Paper 14 - ICR 2015 **253**

L Paper 15 - ICR 2015 **263**

M Paper 16 - DHC13 2012 **273**

N Paper 17 - Coolenergy 2013 **283**

Chapter 1

Introduction

District Heating (DH) systems are implemented in many urban areas of northern Europe. The purpose is to increase overall energy efficiency, reduce consumption of fossil fuels and increase security of supply in areas with high population density (Gullev, 2006; Münster et al., 2012). In a Danish context waste incineration plants and steam networks were utilised from the beginning of 20th century, supplying both heat and electricity. During the years, the fuels for utility production have changed several times mainly according to fuel costs, and are now again changed towards renewable sources. Many different technology schemes exist, with various types of power plants, sizes, network types, substations, integration schemes in houses etc. In Lund et al. (2014) the systems are grouped by generations, with a particular focus on the influence of energy efficiency, supply technologies, fuels and operation strategy for each individual type.

The gain in terms of energy efficiency is typically obtained from utilisation of waste heat from power production in combined heat and power plants (CHP). The waste heat temperature is increased from ambient to a level which is applicable for utilisation. In terms of electricity production the corresponding performance reduction is low. Thus, the cost and carbon emissions from co-production of heat can be significantly lower than direct combustion of fuel for heating, even though distribution losses should be expected. Further steps towards reduction of fossil fuel exploitation and reduction of carbon emissions would typically require switching to renewable fuels in the CHP units.

As an alternative to thermal CHP units, integration of large amounts of heat pump (HP) capacity in the DH networks is proposed by several sources (e.g. (Lund et al., 2010; Rinne and Syri, 2013; Hedegaard et al., 2012)). If the heat source is high temperature, renewable and freely available, and the cycle efficiency of the heat pump is high, the technology may propose cost and carbon emissions, which are competitive to some CHP units. Besides this point, the technology may be used as a means to integrate yet higher amounts of intermittent electricity production capacity in a power grid (Lund and Clark, 2002; Meibom et al., 2007; Blarke, 2012).

Two motivations (not exclusive) are worth mentioning as drivers for changing utility strategy towards renewable energy sources and new technologies:

- political zero carbon emission ambitions (eg. Danish Government (2011))

- significant decrease in cost for renewable electricity production technologies, such as wind turbines or solar PV technologies (DONG Energy, 2015).

The latter may suggest that future power production is shifted towards intermittent sources. With less electricity from thermal power plants, the potential to exploit waste heat is highly reduced.
The city council of Copenhagen agreed in 2013 on a climate plan attempting to make Copenhagen the first CO_2 neutral capital in 2025 (City Council of Copenhagen, 2013). Naturally two of the main focus areas are to achieve CO_2 neutral heating and power production. CO_2 neutral DH is critical as the network supplies 98% of heat demand in Copenhagen municipality. A series of previously published reports named "Heat Plan Greater Copenhagen" (in Danish "Varmeplan Hovedstaden"), of which the newest at the time of writing is number 3, concludes that a limited share of central heat pumps, may provide small savings for heat consumers in 2035, but that the use of sustainable biomass is the major driver for cost and carbon reductions in the future system (CTR, HOFOR and VEKS, 2014b). With one dominant fuel type the system will experience a reduction in security of supply.
Based on the above studies, it is found that HP technology requires further development, or improved implementation in DH networks, to represent a feasible alternative to biomass. The key prevailing arguments for the study are listed below:

- Heat pump technology is ineffective at current stage, both as central installations and small de-central units, even at design specifications (heat to electricity ratio: 2-4:1). Relative to the theoretical limit of efficiency, state of art heat pumps perform poorly (30-50 % compared to the theoretical maximum), compared to other energy technologies.

- An increase in production of electricity from wind turbines and other intermittent sources will influence the production objective in the CHP plants, which today proposes the most efficient conversion of electricity to heat (ratio: 7-9:1), and propose the highest exergetic conversion efficiencies (60 % compared to the theoretical maximum).

- Current temperature levels for heat distribution are not optimal for integration of HPs. By obtaining a better match between sink and source heat reservoirs it would be possible to reduce primary energy requirement for the system.

- By shifting load to hours with low electricity cost, the largest benefit from installation of large quantities of HPs may be the increased value of intermittent power production (Meibom et al., 2007). Due to the higher investment cost and low HP performance in current DH networks,

taxation schemes for utilising the produced heat suggest to install electric heaters as an alternative.

1.1 Thesis statement

The present work aims at contributing to development of the heat pump technology by integrating two interdependent esoteric research areas: thermodynamics and energy system modelling. The focus of the research is mechanically driven vapour compression heat pumps in district heating networks.
An emerging synthesis of the energy system technologies in Denmark challenges cost, primary energy consumption and carbon emissions of current heat production schemes for DH. By investigating synergy relations between thermal CHP units and HP technology, the aim of the project is to propose efficient HP DH solutions in terms of economy and energy. A potential additional benefit is the possibility to integrate even higher amounts of intermittent power production.
More specifically, the research aims to answer the following questions:

- Which heat sources should be considered, how do they affect operation and where are they located in the network?
- From a thermodynamic perspective, how is the best performance obtained from heat pumps in cooperation with CHP technology, and how do different temperature sets of the network affect performance?
- Are there potential benefits from operating the HP by internal combustion engines (ICE) rather than electrical motors?
- How does the temperature of the DH network affect the performance of the heat pump technology? Which working fluids should be used for which configurations and temperatures?
- Is the benefit from lowering DH temperatures larger for HP technology, than for the residual technologies in the network?
- Which heat pump integration schemes result in largest benefit for the consumers and/or the system?
- For investment in a fixed capacity of heat pump integration, are there potential benefits from location of the heat pumps at the consumer, or is integration in the DH network the better solution?

1.2 Methodology

The project has focused on four different steps, of which number one to three has received the main attention.

1 The design and development of optimal HP configurations for cooperation with CHP-plants was investigated. This was done for current state of the art DH networks, where several technical parameters and interdependencies affect overall performance and cost of such solutions.

2 Investigation of heat pump economic optimal solutions for the technically preferable configurations of subject # 1. Two different analyses were performed, one was specific for DH vapour compression HP systems, and one with general interest for wide application of industrial scale heat pumps. The latter allowed detailed investigation of the performance of vapour compression heat pumps in comparison with the ammonia-water hybrid compression-absorption HP. The performance of the derived HP configurations may be seen as input to the subject # 3.

3 A numerical optimisation model of heat and electricity production has been developed, which was designed to match a specific energy system today and in future scenarios. Both CHP and HP technologies were represented with a high degree of detail in the model, and it was validated against several sources with good correlation on both yearly and hourly basis. By use of the advanced representation of CHP plants, it was possible to investigate the interdependencies of the two technologies. Recommendations for integration schemes for additional thermal capacity in the network were obtained for both current and future energy scenarios.

4 Current standard for effective heat pump technology for decentral units was examined, in order to derive recommendations and knowledge about the strength and weaknesses of the technology. Three experimental setups were build and analysed in the project.

a) The performance of the air-to-air HP system, which potentially may become a highly effective space heating technology, was initially considered a significant part of the research project. This part was assigned a lower priority after the initial phase, and was mainly carried out by various student projects either as master or bachelor thesis.

b) Investigation of the heat transfer properties and pressure drops for condensation of refrigerant in plate heat exchangers at elevated temperatures.

c) A decentral district heating heat pump configuration for boosting water temperature for hot tap water was developed in corporation with Danfoss and a large engineering consultant company. Elements of this research are presented in the thesis.

1.3 Readers guide

The thesis contains 7 chapters and two appendixes, along with 12 papers (out of 17 in total) which are published or submitted for publication.
Four of the listed conference contributions were invited for publication in scientific journals. In these cases only the latter of the two papers is included in the thesis. One conference contribution was not included due to discrepancy between the topic of the paper and the topic of the thesis.
The thesis, its chapters and the individual papers may be read independently. For reading the collected works, it is recommended to read the thesis prior to the collection of papers.

Chap. 1 Introduces the present project, its motivation and aim. The overall methodology of the project is presented, and the reader is introduced to the outline of the study.

Chap. 2 Two main topics are introduced and examined. Firstly, the availability of heat sources in the network, and their impact on the performance. Secondly, the cooperation of HPs and combined heat and power plants of various types.

Chap. 3 Technical and economic comparison of several vapour compression HPs and the compression-absorption hybrid HP. The comparison results in detailed working domains which highlights the areas were individual technologies are particularly competitive. The result may be seen as a strong tool for pinch analysis and for general integration of heat pumps in DH systems.

Chap. 4 A detailed analysis of working domains for two DH HP configurations. Exergoeconomic optimal vapour compression HP configurations are compared in terms of energetic efficiency, investment and the resulting cost of heat.

Chap. 5 A detailed energy system model is developed and presented. The purpose of the model is to investigate interactions between CHP and HP technology, in order to understand the influence of various HP integration schemes in terms of energy efficiency, carbon emission etc. Examples of HP integration is presented based on the calculated performance of Chap. 4.

Chap. 6 The possible benefits from lowering the temperature of DH networks are analysed for various cases. The performance implications of changing production temperature is analysed for two Danish energy scenarios.

Chap. 7 The chapter concludes the thesis, by summarising the main findings and key areas for future work.

Besides the main thesis, two previously unpublished appendixes are attached to present method and validation for the developed energy system model

App. A Energy system model structure, formulation of objective function and explanations of key technical and economical constraints.

App. B Validation of the energy system model considering data from several public and nonpublic sources.

Nomenclature used in the chapters of the thesis, can be found in the referenced paper(s) of the individual chapter. For Appendix A a seperate nomenclature is presented which correponds to the one presented in [p7].

Chapter 2

Heat pumps in combined heat and power systems

The purpose of this chapter is to establish a basis for analysing concepts for integration of heat pumps in combined heat and power systems.

Two main topics are introduced and examined. At first the availability of heat sources for the cycle, which may be considered a significant limitation for integration of the technology. Plausible options are introduced and discussed based on their locations in the network.

Secondly, several methods for utilisation of the heat source are considered, in a system with a high fraction of heat produced in extraction or backpressure CHP plants corresponding to Danish conditions. The results of the latter topic are part of the results presented in [P2].

2.1 Heat pumps in finite reservoirs

Heat pump operation in district heating systems is typically constrained by finite heat capacity in both sink and source streams. In this way the operation in district heating networks may be considered similar to that of most industrial heat pump integrations (Townsend and Linnhoff, 1983; Linnhoff and Hindmarsh, 1983). The result is different performance characteristics depending on the temperature and heat capacity of both sink and source streams. For this purpose the calculation method for a single stage heat pump is briefly introduced.
A principle sketch of a vapour compression HP and a temperature - heat load diagram for a pure working fluid are presented in Fig. 2.1. In Fig 2.1b the temperature variation of both sink and source is 10 K, which leads to pinch point temperature differences at the marked locations. In case of different temperature variations for either sink or source, the pinch point may be located elsewhere in the heat transfer process.
The operating conditions and performance of a heat pump were evaluated based on four variables, if the heat exchange parameters are fixed for the condenser

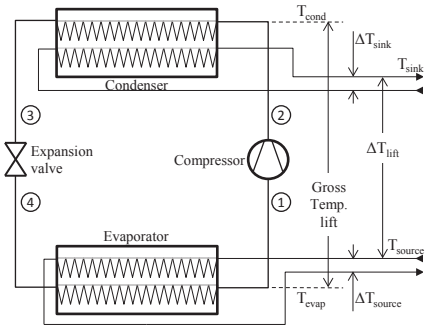

(a) Principle sketch of the vapour compression HP

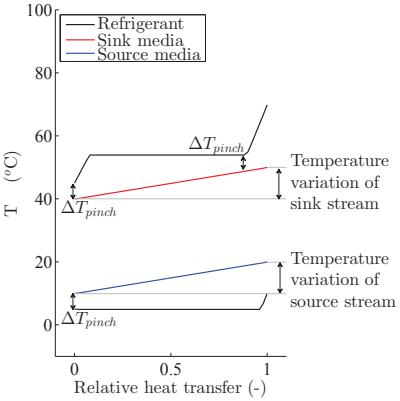

(b) Temperature - heat load diagram for condenser and evaporator. Temperature variation of both sink and source is 10 K

Figure 2.1: Principle sketch and temperature - heat load diagram of the vapour compression HP

and evaporator components. The required variables were the temperature of the sink process stream leaving the condenser (T_{sink}), the temperature lift (ΔT_{lift}) and the process stream temperature glides from inlet to outlet in both heat exchangers (ΔT_{sink} and ΔT_{source}).
The performance of the considered heat pump was calculated using constant efficiencies for compressor and electrical motor, as well as fixed temperature differences in the heat exchangers. The used values are presented in Table 2.1.

Table 2.1: Operational parameters for heat pump and drive shaft performance

Type of data	Value	Unit	Designation
Efficiency	0.8	/	Compressor isentropic efficiency
	0.8	/	Compressor volumetric efficiency
	0.95	/	Electric motor efficiency
	0.35	/	Gas engine shaft efficiency
	0.9	/	Gas engine total efficiency
Temperature	5	K	Evaporator superheat
	5	K	Minimum pinch point in heat exchangers

2.2 Potential heat sources

Heat sources can be distinguished by a set of key operational and economic parameters. Such parameters include the available temperature, heat capacity, concurrency with demand and required investment cost for utilisation. Considering the extent of many district heating networks, several heat sources are located within the area or close to the perimeter of the network. Co-location with available district heating transmission- or distribution facilities, may prove a significant asset, in order to reduce installation cost.

Heat sources are often classified by their origin as similar decision parameters may be assumed fixed for a given type. Smaller systems operate according to the available media and temperature at the location of the heat demand (Berntsson, 2002). By using a DH network, larger installations can be located near heat sources of elevated temperatures (compared to ambient conditions), such as sewage water (Berntsson, 2002), industrial waste heat (Lund et al., 2014), power plants (Blarke, 2012) etc. Such sources tend to have a low yearly temperature variation and a finite heat capacity rate of the stream. In some cases the heat source can also be ocean, lakes, air or ground (Mancarella, 2009) where yearly variation in temperature would be expected. A graphical overview of several possible configurations is presented in Fig. 2.2. Depending on the locations it may be possible to consider different types of fuels. Co-location with heat storages may further influence the operation.

A commonly used classification for heat sources is whether the point of departure may be considered renewable, and if not, the timeframe of the continued duration of the source. In current Nordic energy systems, the utilisation of non-renewable waste heat sources may propose higher temperatures than what is available from renewable origin. Assuming that utilisation of waste streams does not alter or encourage additional operation of its origin (etc. industry), the use of such sources may increase energy efficiency similarly to a renewable source.

Many of the proposed heat sources may be subject to intermittent availability or fluctuating capacity and temperature. These include the power plant flue gasses, industrial waste heat, waste (sewage) water and solar thermal heat. Sea or lake water may experience periods with icing issues, which would typically obstruct the flow of the heat source.

For utilisation of industrial waste heat sources, it is important to evaluate if the heat can be used elsewhere in the process before integration with the district heating network. In Hendriksen (2014) two sites (both in Copenhagen) are analysed in detail to estimate the potential for utilisation. Significant shares of unutilised waste heat are found. The recommendation for most of the investigated streams is to utilise the waste heat in the process at the site, which may be done with low pay back periods. A mapping of economic recommendations (Direct heat exchange, direct with heat pump, utilise for district heating,

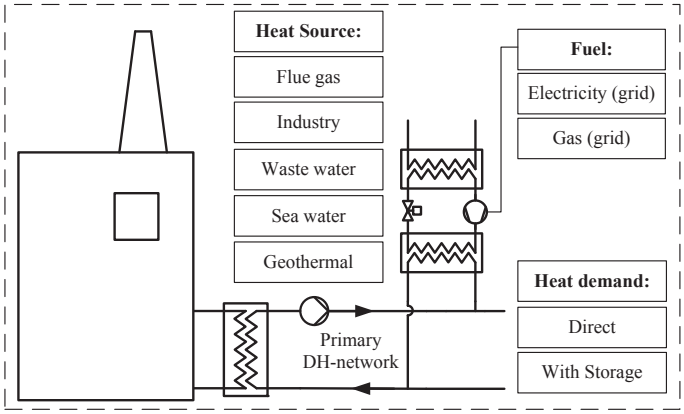

(a) Central locations in transmission networks, e.g. power plant sites.

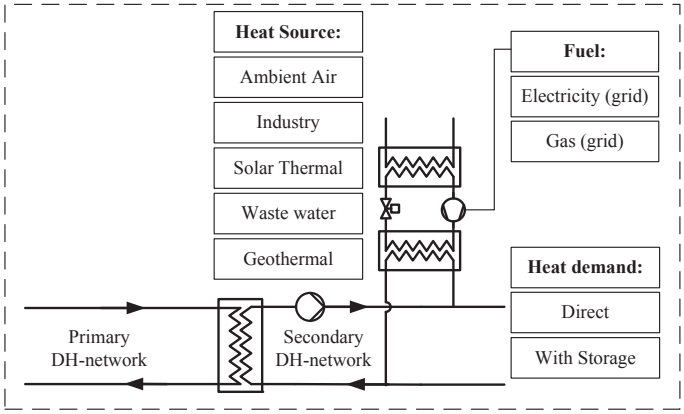

(b) Central locations in distribution networks.

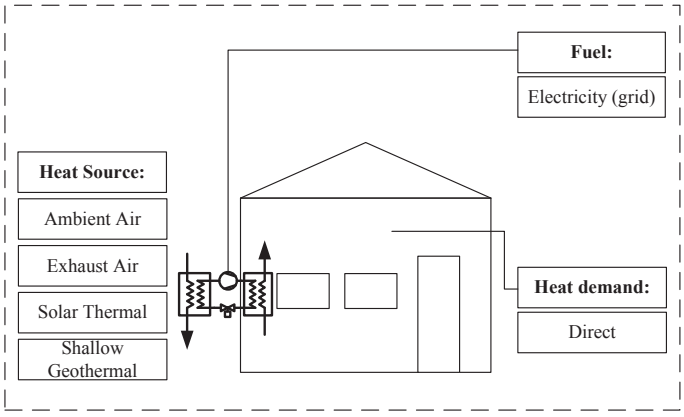

(c) Directly at location of the heat demand.

Figure 2.2: Potential heat sources at three different locations in a district heating network.

utilise for power production) for available waste heat streams is performed by Sørensen (2014). For many pinch temperature conditions (between 5 - 40 %) available heat should be utilised for district heating, depending on the economic scheme. For the case of a socioeconomic scheme 25 % of considered cases should be utilised. Configurations where heat pumps are used to upgrade waste heat to district heating networks are not considered in the study.

In Bach (2014) the most promising renewable sources for the Copenhagen system are found to origin from sewage-, drinking-, and sea water. It is found that total of around 87 MWth could be connected to sewage water facilities, and around 13 MWth could be connected to drinking water facilities. A total of 260 MWth heat pump capacity is distributed onto the Copenhagen district heating system, which is found to be barely sufficient to match future demand. Due to the hydrography of Øresund, this heat source may be expensive to exploit. Hubeck-Graudal (2015) implemented heat transfer correlations in a hydraulic model (EPANET) of the Copenhagen water supply in order to provide a detailed estimation of using the drinking water network as the heat source for district heating heat pumps. The potential heat source in Copenhagen is found to be 32 MWth, but by including the share of water, which requires reheating this figure is reduced by approximately 33 %. This implies additional electricity consumption for the produced heat, and while the heat pump unit may operate with a COP of around 3 for the given temperature levels, the resulting system COP is reduced to 2-2.1.

2.3 Heat sink

Generally, the temperatures for a district heating network are kept as low as possible in order to reduce heat losses and increase efficiency of electricity coproduction. The lower limit for forward temperatures is the case where the required temperature of certain constituents of the demand (often approximately 55 °C due to hot tap water) is no longer met.

In a Danish context the forward temperature ($T_{\mathrm{DH,Forward}}$) varies from 70 °C to 115 °C (Centralkomunernes Transmissionsselskab I/S, 2013; Dansk Fjernvarme, 2013) mainly depending on size of the network and its commissioning year. The corresponding network return temperature ($T_{\mathrm{DH,Return}}$) ranges from 35°C to 55°C. In some networks the forward temperature increases in cold seasons due to capacity constraints at high load and/or optimisation of pump work vs. reduction in co-produced electricity.

A qualified estimate of the relation between return and forward stream temperatures were found by interpolating temperatures for the range of $T_{\mathrm{DH,forward}} = 110 - 70$°C and $T_{\mathrm{DH,return}} = 55 - 35$ °C as presented in Fig 2.3. The lower limit for DH temperatures, with water as the working fluid, may be considered the 4GDH concept (Lund et al., 2014).

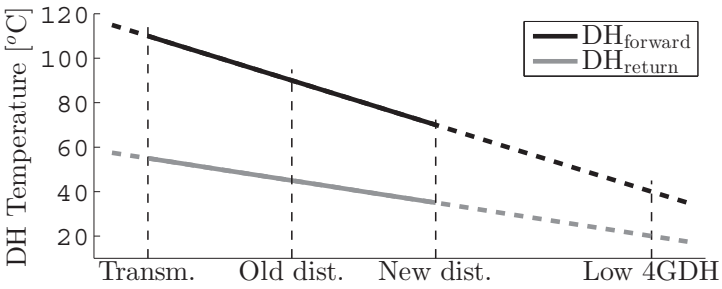

Figure 2.3: Estimate of relation between temperature of forward and return streams in district heating networks

2.4 Heat pump configurations for district heating

Not many relevant papers discuss the optimal cooperation of thermal combined heat and power production and heat pumps: Mancarella (2009) presents an approach for characterizing and assessing the performance of small decentralised cogeneration systems coupled with electric heat pumps. Blarke and Lund (2007) discuss the impact of two different heat sources for a parallelly coupled HP at a small decentral CHP plant considering optimal operation of the units. In Malinowska and Malinowski (2003) a study of exergetic efficiency is performed on a serially coupled HP and small-scale CHP plant. Lowe (2011) assesses the heat production capabilities of a CHP by considering the combination of a conventional steam turbine cycle and a HP at varying condensing temperatures of the CHP plant. He finds that heat production of CHP plant is highly effective with a performance advantage in the order of a factor of 3 when compared to the coefficient of performance of heat pumps.

Based on the identified temperature levels, as well as various sources in literature (Blarke and Lund, 2007; Berntsson, 2002; Granryd, 2005b; Ommen and Elmegaard, 2012), five possible heat pump configurations were identified. The configurations are presented in Fig. 2.4. White arrows indicate the temperature lift of T_{Source} to T_{Sink} for the various heat pumps, and the temperature variation of sink (ΔT_{Sink} and source ΔT_{Source}) are indicated by the dashed and full thin arrows, respectively. The temperature of the demand is represented by the hatched area.

The configurations are termed with the initial letter of both heat pump source and sink temperature levels (e.g., the combination "SF" for temperature of highest available heat source in the considered area and the temperature of the forward stream, respectively). The reader is referred to [P2], where the

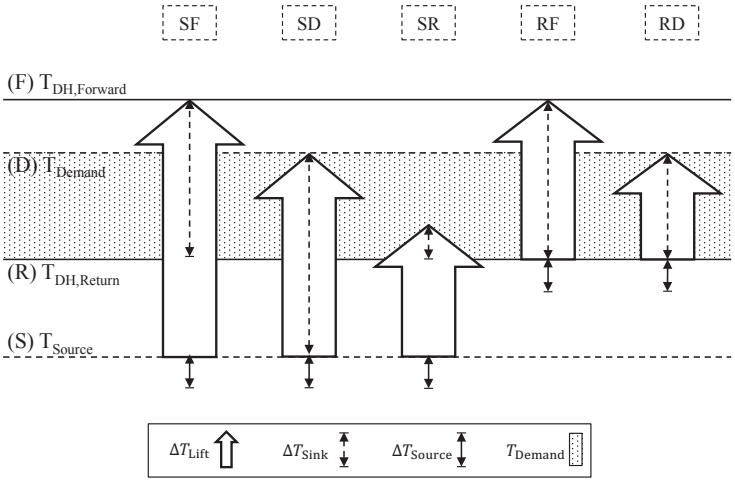

Figure 2.4: Five possible configurations for district heating heat pumps. Source: [P2]

individual configurations are thoroughly elaborated and presented in schematic diagrams. Each of the considered configurations can be found in the literature, or as existing units in DH networks at various locations.

The configurations SR and RD cannot be operated without other production technologies in the network. SF, SD and RF may operate independently. If SF and RF configurations are operated simultaneously with other production technologies it is possible to mix streams to achieve the desired temperature. In such a case, the sink temperature of the heat pump can be lowered, by increasing the temperature of the secondary forward stream. The changed temperature will typically reduce the electricity production of the CHP plant. For a very low forward temperature of the the SF heat pump configuration, the operation will tend to resemble the SR configuration.

Configurations RF and RD do not utilize an external heat source for the heat production. Assuming production of heat and electricity does not change significantly due to the source temperature offsets in other production equipment, the heat pump can be seen as a thermal short-circuit electric heater, as only the consumed electricity of the compressor is added to the DH network. Thus, the advantage of using these heat pump configurations rather than an electric boiler, will require significant operation advantages in other production technologies in the system.

An evaluation of pros and cons for the individual configurations was performed by combining two detailed energy system models. One represents the operation of an extraction CHP plant at various loads or with changes to production of

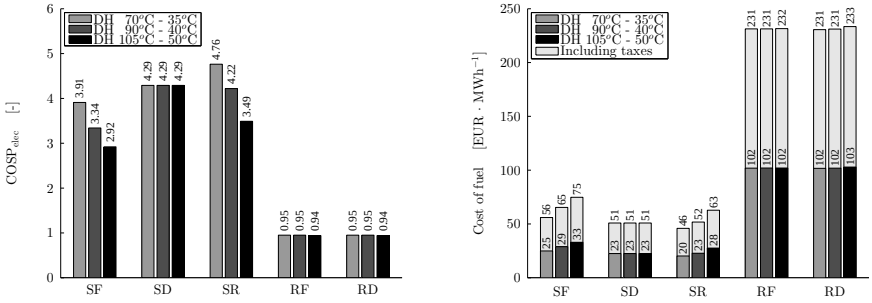

(a) Coefficient of system performance

(b) Cost of fuel including/excluding taxes

Figure 2.5: Comparison of five electric heat pump configurations in a district heating system fed by an extraction CHP plant. Source: [P2]

district heating. The second represents the operation of a heat pump in finite heat reservoirs according to section 2.1. The operational performance of the configurations was investigated based on four key performance factors. These include the coefficient of system performance (COSP) and the cost of fuel. The coefficient of system performance was defined on the basis of electricity consumption with fixed CHP load ($\mathrm{COSP_{elec}}$) and on the basis of fuel enthalpy rate (Primary Energy) with fixed electricity production ($\mathrm{COSP_{PE}}$). The five configurations were examined considering the shaft power delivered by either an electrical motor, or an internal combustion engine (ICE) operating on natural gas. In [P2] results are additionally presented for other combined heat and power technologies.

In Fig. 2.5 the performance of the configurations are compared for electrically driven heat pumps, considering 3 characteristic district heating network temperature levels. For lower DH temperatures (represented by DH 70°C - 35°C) the SR configuration was found to present the best performance when considering both cost of fuel and COSP. In high and medium temperature networks, the SD configuration was superior. The high COSP of the SD configuration may be explained by the high COP that can be achieved with a high sink temperature glide, by utilising the desuperheating and subcooling of the working fluid. As this configuration is not linked to the DH network, similar characteristics are found for all three DH types. RF and RD configurations showed COSP below 1, which translates to very high fuel costs.

In Fig. 2.6 the performance of electrically driven heat pumps are compared to heat pumps operated using ICE. In terms of COSP, the natural gas ICE driven configuration showed slightly increased performance for SF and SD, compared to the electricity driven configuration. For the remaining configurations, the COSP was similar or reduced. The change in system performance between the natural gas ICE and the electricity driven HP was within $\pm$ 8 % for all

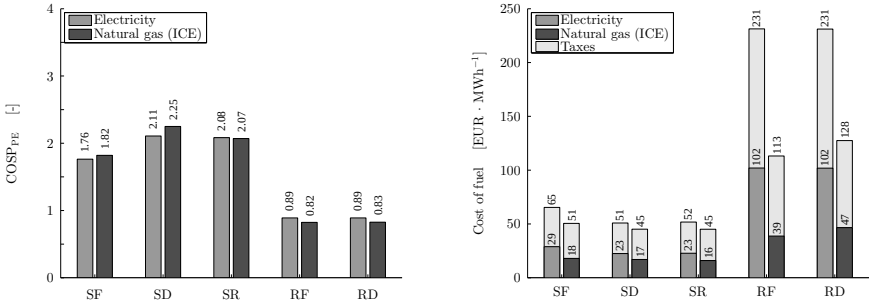

(a) Coefficient of system performance

(b) Cost of fuel

Figure 2.6: Comparison of the five configurations operated by electrical motor or internal combustion engine fed by natural gas. The network is supplied by an extraction CHP plant operating at 90°C - 40°C. (a) coefficient of system performance, (b) cost of fuel including/excluding taxes. Source: [P2]

configurations. The cost of fuel was lower for all of the considered natural gas ICE driven heat pumps, compared to the corresponding electricity driven ones. This is mainly due to the fuel cost, and not the taxation scheme.

The integration of an electrically driven heat pump in a district heating network increases the production possibilities of the combined technoloiges. To interpret these options, PQ-diagrams are typically used in CHP plants, where the curves with negative slope show the range of operation points at fixed boiler loads. The full lines of the PQ-diagrams of Fig. 2.7 correspond to a CHP plant (Avedøre unit 1) for a 90°C - 40°C network. In Fig. 2.7a and 2.7b the modified constraints are shown in the case of a 25 MWth heat capacity is added. The figures are for types SF and SR, respectively.

For SR configuration (as well as RF and RD), an significant increase in capacity (above 25 MWth) by integrating such configurations at Avedøre unit 1, would result in changes in performance due to constraits of the layout and capacity of the CHP plant. The changes occur due to the assumptions of fixed sink temperature variation and limited range of calculated changes to electricity efficiency. This is not the case for others (such as the SF configuration), where it is possible to increase capacity above the magnitude addressed in this analysis without reduction in performance.

The potential benefit from integrating thermally driven heat pumps such as the water-lithium bromide absorption HP is investigated in Kaniadakis (2014) as a SR configuration integrated in the Avedøre unit 1. The study show that the systems with electrically driven compression HPs generally have higher performance, but at some conditions the two systems show similar performance. In Martínez (2015) the study is continued by extending the exergy and economic analysis. The study show that the compression HP achieved the highest exergy

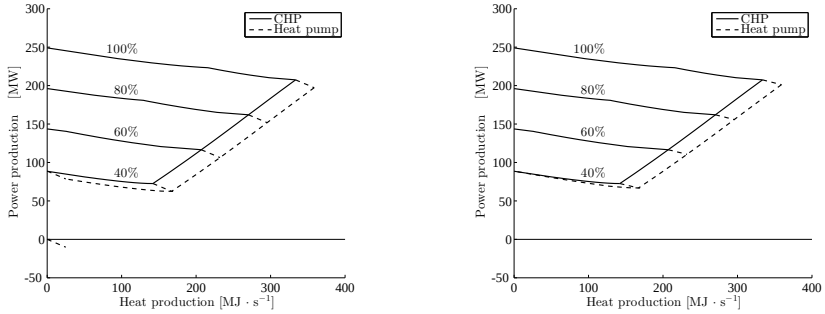

(a) SF configuration heat pump

(b) SR configuration heat pump

Figure 2.7: Comparison of the changed CHP plant operation with three applicable configurations operated by electrical motor. The network-configuration is fixed to 90°C - 40°C and the added capacity is fixed to 25 MW. (a) Modified PQ-diagram with SF configuration heat pump, (b) Modified PQ-diagram with SR configuration heat pump. Source: [P2]

efficiency, but that the absorption HP represents lower investment cost and a smaller pay back period.

2.5 Summary

Several renewable and non-renewable heat sources were proposed in various locations of a generic DH network. None of the proposed sources can be utilised without disadvantages such as fluctuations in capacity or temperature, intermittent availability or high investment cost. The location of the heat source may further influence the feasibility due to several considerations: Co-location with transmission or distribution facilities, availability of various fuels and possible storage options.

Depending on the chosen integration of the heat pump the unit will experience different performance characteristics. Such choices may also influence the other production technologies in the network. Five configurations were investigated in order to analyse the optimal performance in cooperation with typical combined heat and power technologies.

The analysis focused on key performance factors chosen to indicate the performance from a system perspective. In [P2] the differences between system performance and the performance of the heat pump unit are further investigated.

Two configurations (SD and SR) proposed the highest coefficient of system performance and lowest cost of fuel for the DH network temperatures evaluated. The highest coefficient of system performance was for SR configuration with

electric motor in a 70°C - 35°C DH network, where the $COSP_{elec}$ is reaching approximately five.
Using the return line of the DH network as the heat source for a HP, resulted in system performance close to or below what may be expected from an electric heater, depending on the technology mix for utility production.
Of the three configurations with high COSP, one (SD) must be located at the location of the demand, whereas SF and SR may be located "centrally" according to the availability of heat sources.

Chapter 3

Technical and economic working domains of industrial heat pumps

This chapter starts by a brief introduction to the concepts of working domains for determination of technical and economically feasible options for integration of HPs. Results are presented for a number of configurations including transcritical- and condensing vapour compression heat pumps (further addressed in [P3]), the compression-absorption hybrid heat pump ([P4]) and condensing vapour compression heat pumps operated in series ([P14]).

The aim is to provide detailed information of technically plausible and economically favourable technologies for a range of typically used configurations of sink and source streams in industry. This will assist in determination of optimal solutions for integration in DH networks according to Danish legislation.

3.1 Heat pump working domains

The use of working domains may be seen as a breakdown of recommendable HP solutions for a given industrial scale heat demand. The recommendation is based on thermoeconomic models used to determine the profitability and technical limitations of several specific thermodynamic cycles. For the technical constraints, the method for determination of limitations may be seen as similar to the one used for operation envelopes for compressors in HP and refrigeration industry (GEA Bock GmbH, 2012; Bitzer Kühlmaschinenbau GmbH, 2014).
The classification of HPs by use of technical and economic working domains was inspired by a paper by Brunin et al. (1997). The study includes many working fluids and presents technical working domains for temperature ranges reaching 200 °C. Economics are not considered as such, but two physical constraints are employed to represent economic feasibility. The constraints are COP and volumetric heating capacity (VHC). Maximum and minimum pressures are also considered as physical constraints. In the paper, temperature variations of the two secondary streams (sink and source) are fixed at 10 K. An example of a working domain utilising VHC, COP and min- & max pressures is presented in Fig. 3.1a.

A large fraction of the previously utilised working fluids are banned, or pending phaseout, throughout most of Europe (UN Ozone Secretariat, 2000; European Parliament, 2014), in particular when utilized in large industrial scale systems. This leaves fewer possibilities when designing systems to match certain thermal requirements. In addition, the design is constrained by currently available components from refrigeration and HP manufacturers.

In the case of integration of HPs within temperature reservoirs of limited heat capacity, such as in pinch analysis (Linnhoff and Hindmarsh, 1983) or DH networks (Ommen et al., 2014), the differences in temperature between inlet and outlet of both sink and source streams influence the performance and technical constraints of a HP solution. In this way, the best available technology may differ with a change in temperature variations for one of the heat exchange processes. Thus, the working domains were calculated for a range of representative configurations of sink and source streams. The examined temperature glides were: (sink/source): 10K/10K, 20K/10K, 20K/20K and 40K/10K. For heat production in DH networks, the HPs operation will resemble that of either 10K/10K or 40K/10K depending on the location and purpose of the unit.

In the following sections results corresponding to 40K/10K will be presented. Assuming DH forward and return temperatures of 80 °C and 40 °respectively, and a source temperature of 20 °C with a temperature variation of 10 K, the feasible technologies are found at sink temperature 80 °C and temperature lift of 60 K. With a 10 K increase in both forward and return temperature, the corresponding technologies are found for sink temperature 90 °C and temperature lift of 70 K.

An example of a working domain with both technical and economic constraints is presented in Fig. 3.1b. The purpose of the latter is to include influence of the HP performance and investment into the consideration. Two hatched areas represent sink and source temperature combinations where assumptions of the model are not fulfilled. One area is caused if $T_{\mathrm{source,out}}$ is below 0 °C, which restricts the use of pure water as heat transfer fluid. The second area corresponds to a case where $T_{\mathrm{sink,in}} < T_{\mathrm{source,in}}$. In such a case, heat should be exchanged directly (if possible) between the two streams before a HP is integrated in the process (Townsend and Linnhoff, 1983; Annex-21, 1995). The economic constraints are presented as green curves for net present value (NPV) and turquoise / dashed turquoise curves for pay back period (PBP). Red curves indicates high discharge temperatures, whereas blue curves show the pressure constraints for the considered systems.

Heat load and operating hours are key parameters for analysing economic feasibility. The impact of the two parameters were determined by a parametric variation, which is presented in Fig. 3.2a. The operating hours and HP capacity was fixed at 1000 (kW) and 3500 (h) respectively, which corresponds to a pay back period (PBP) of approximately 4 years.

Fig. 3.2b presents a variation of natural gas and electricity prices for the net present value criteria. Both natural gas and electricity prices were varied by ±

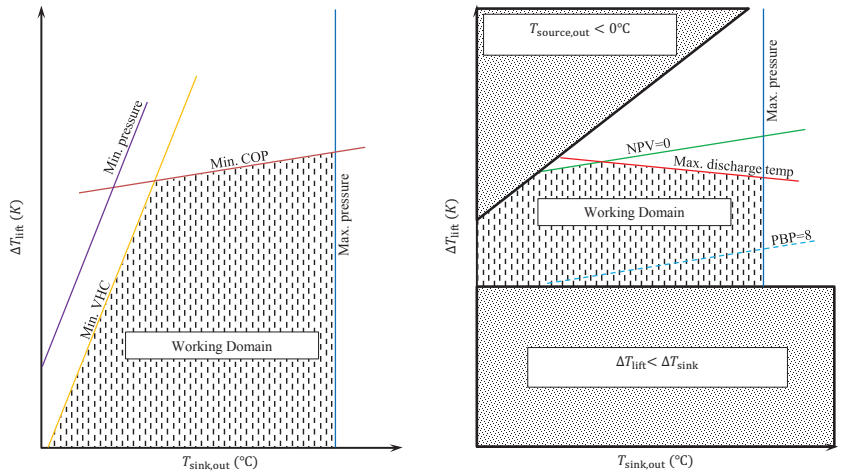

(a) Example of working domain with VHC and COP to represent economic feasibility (Brunin et al., 1997)

(b) Example of working domain with economic and technical constraints [P3].

Figure 3.1: Two typical examples of working domains with various technical and economic constraints

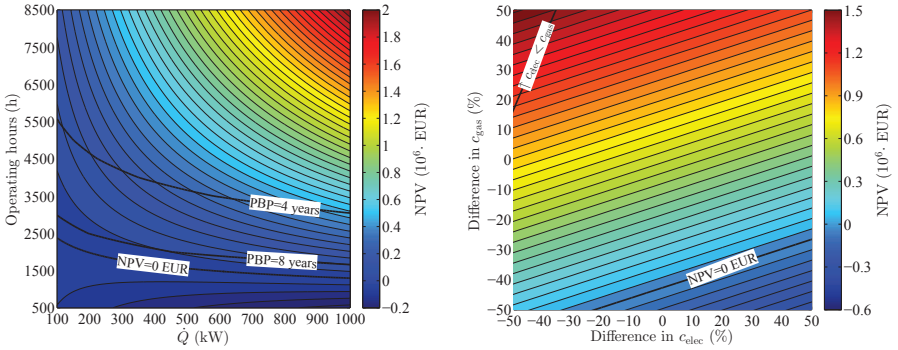

(a) NPV of HP system with variations in size and yearly operation hours

(b) NPV of HP system with variations in fuel cost

Figure 3.2: Influence of key economic assumptions on NPV
R717-HP heat pump operating at $T_{\text{sink,out}} = 60$°C, $T_{\text{lift}} = 20$°C, ΔT_{sink}=20 K, ΔT_{source}=10 K. Source: [P3]

50 % for the investigated HP solution. Based on the slope of constant NPV in Fig. 3.2b it was found that the system is more sensitive to the price of natural gas than of electricity, and that the gradients of fixed electricity or natural gas prices are close to constant. At high gas prices and low electricity prices an area is indicated, where the price of electricity is lower than natural gas. At low gas prices and high electricity prices, the HP NPV can become negative. In a comparison with similar plot of PBP (in [P3]), it was clear that the NPV is less sensitive to variations in fuel cost. Another benefit of the use of NPV as the economic criterion, is that the NPV evaluation returns a monotonic result.

3.2 Vapour compression heat pumps

Six single stage HP systems utilising natural working fluids were compared in terms of technical, thermodynamic and economic constraints. The considered natural working fluids were: R290, R600a, R744 and R717, where the latter utilises both low and high pressure components. One HFC working fluid (R134a) was included in the study for comparison of the feasibility of natural working fluids.

In Fig. 3.3 the various technical and economic constraints are presented for each of the considered HP systems. The working domains were typically limited by NPV and maximum allowable pressure in terms of temperature lift and temperature of sink respectively. The two R717 systems differ from this trend, as they were limited by the discharge temperature of the compressor. For R134a, the poor profitability for the HP resulted in the lack of a feasible working domain.

For all of the considered sink/source temperature variations, it was found that R717-LP configurations are the most profitable within the established technical boundaries for that type of system. For increasing sink temperatures, R717-HP units were most profitable of the technically feasible types. The technical and economical feasible temperature configurations of R717-HP extended beyond feasible areas of remaining types in terms of temperature lift. The R717-HP area was constrained by discharge temperatures and high pressure limit. For further increase in sink temperatures, R600a configurations were the only feasible option until the limitation on pressure is reached at approximately 115°C. The R600a and R290 configurations were limited by an economic constraint at ΔT_{lift} and 40 to 50 K for the 40K/10K glide.

Transcritical R744 was found to be the optimal configuration at high ΔT_{lift} if the sink temperature glide is large. A significant area exist, where the technology provides the only solutions which are technically and economically feasible. This is only the case for high temperature glides, as the technical constraints of R717-LP and R717-HP typically allow higher temperature lift than allowed by the economic constraint of R744.

Several steps to increase the working domain of individual HP systems may be

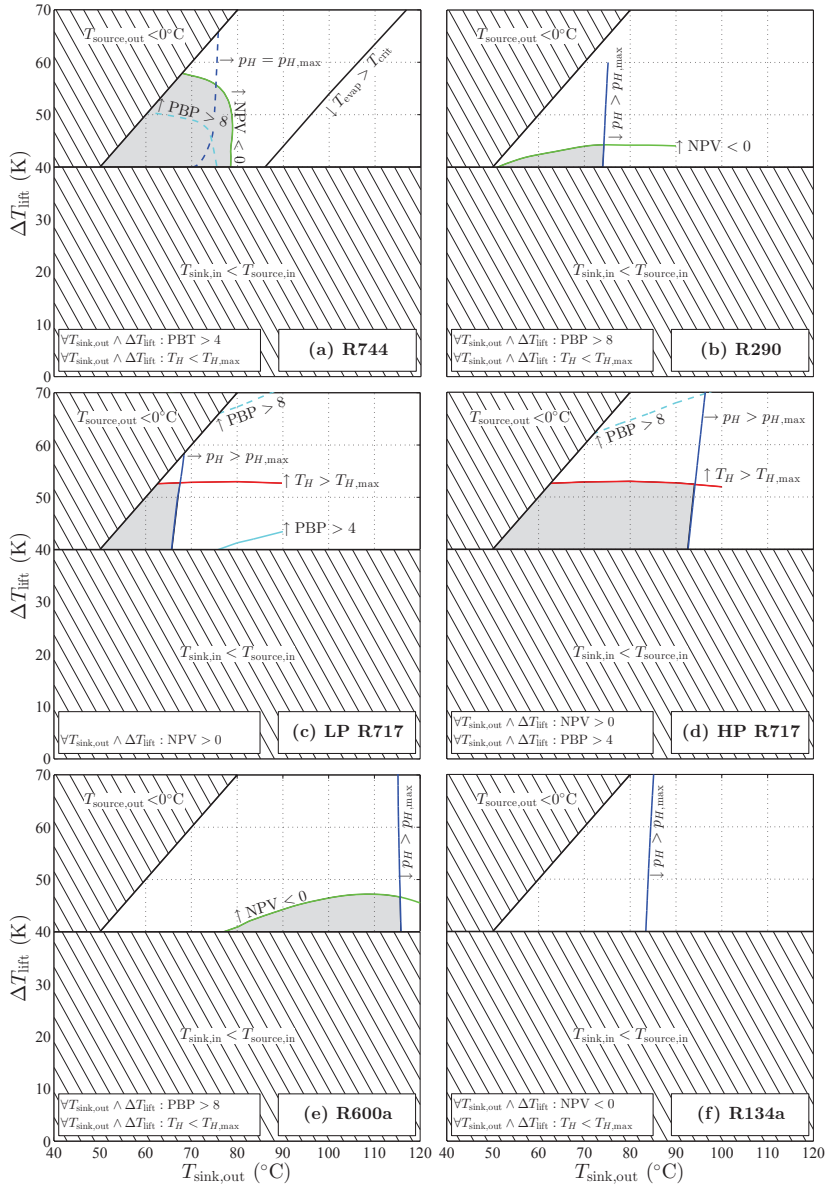

Figure 3.3: Working domains for the investigated HPs at ΔT_{sink}=40 K / ΔT_{source}=10 K. The various constraints are presented as contours. Areas complying with all technical and economic constraints are marked with gray color (working domains).

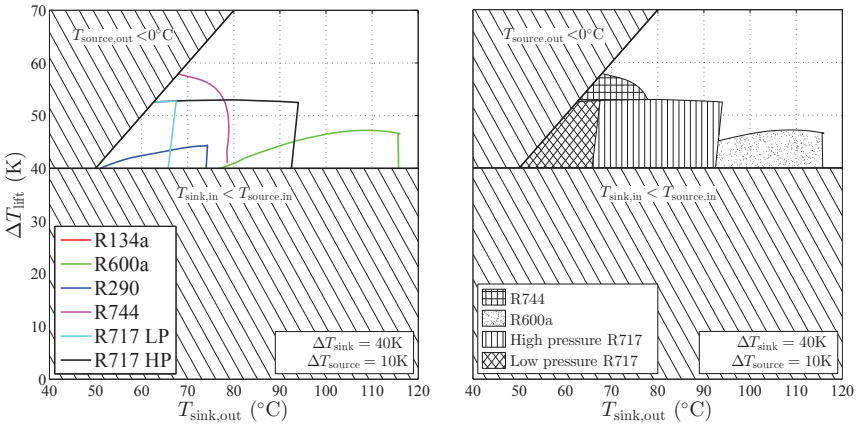

(a) Compilation of working domains

(b) Best available technology

Figure 3.4: Compilation of working domains and hatched areas with best available technology based on NPV for vapour compression HPs at ΔT_{sink}=40 K / ΔT_{source}=10 K. Source: [P3]

considered. Such options include:

- internal heat exchangers
- two stage HP cycle configurations
- two stage compression configurations
- HPs connected in series
- various working fluids in cascade configuration

The energetic or technical improvements of NPV for such systems are typically reduced by increased investment in terms of additional components for the thermodynamic cycle. At certain temperature configurations, where the best available technology may shift to a different system due to an expanded working domain (ie. from R600a to R717-HP) the gain in NPV may be significant. If a shift in best available technology is not possible, the maximal improvement due to cycle improvements (not including HPs in series) is typically below 10 % on COP (Granryd, 2005a). With additional investment according to the changed PI-diagram the gain in NPV will be lower than this figure.

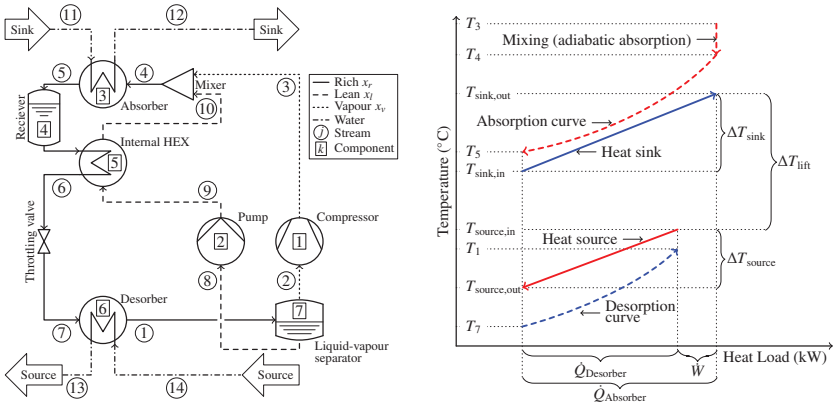

(a) Principle sketch of the HACHP

(b) HACHP process in temperature - heat load diagram

Figure 3.5: Principle sketch and temperature heat load diagram of HACHP. Source: [P4]

3.3 Ammonia-water hybrid absorption-compression heat pump

The hybrid absorption-compression heat pump (HACHP) is based on the Osenbrück cycle (Osenbrück, 1895). Compared to the vapour compression HP utilising R717, an ammonia-water HACHP may operate at lower pressure levels, and it is possible to match the temperature glide of the absorption/desorption process in order to minimise entropy generation caused by heat transfer over a finite temperature difference (Hultén and Berntsson, 1999, 2002; Jensen et al., 2014). These advantages result in high energetic performance, and technically feasible HP systems in the sink temperature range 70-120 °C using current day refrigeration equipment.

Due to the composition of the mixed working fluid, as well as the configuration of the solution circuit, the HACHP has two additional degrees of freedom for system design (Jensen et al., 2015). In previous comparisons between VCHP and HACHP (Brunin et al., 1997; Ommen et al., 2011) the design parameters are fixed at predefined ratios, which does not necessarily result in optimal criteria for comparison. In Ommen et al. (2011) an economic comparison of the HACHP with the VCHP shows that the technology is competitive. However, the study does not consider the degradation of heat transfer coefficients caused by the application of a zeotropic mixture working fluid (Radermacher and Hwang, 2005).

A process diagram of the HACHP is presented in Fig. 3.5a. The corresponding process is presented in a temperature heat load diagram in 3.5b.

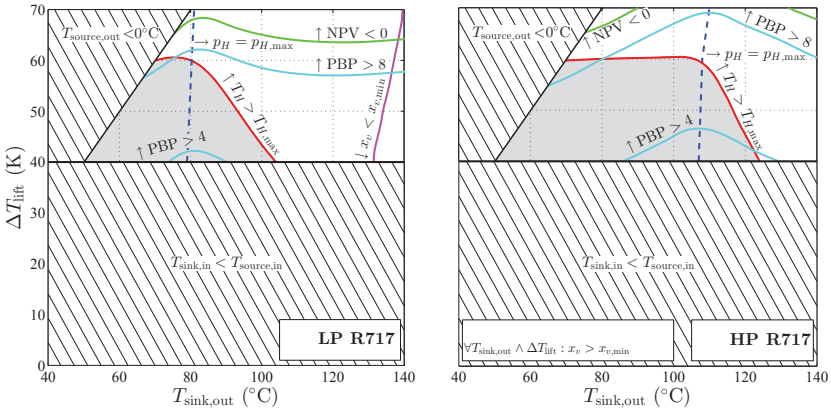

(a) R717-LP grade components

(b) R717-HP grade components

Figure 3.6: Working domains for HACHP at ΔT_{sink}=40 K / ΔT_{source}=10 K. Source: [P4]

In Fig. 3.6 the constraints for the HACHP are presented for two cases, corresponding to differences in the pressure limit of the utilised components. By changing working fluid composition and solution recirculation the absorber pressure may be reduced in exchange of deteriorated volumetric heat capacity and heat transfer characteristics, leading to increased investment, than what would be experienced at higher pressures. In this regard the influence of the pressure constraint was less decisive for the HACHP than what was experienced for the VCHP. But as shown by the difference between Fig. 3.6a and Fig. 3.6b the changed operation has a significant influence on discharge temperature of the compressor, which resulted in a substantial reduction of the working domain. Utilising R717-HP grade components, the HACHP achieved sink temperatures higher than 120 °C.

From comparing with the best available technology of VCHP in Fig. 3.4 it is clear, that the HACHP is capable to achieve higher temperature lifts (increase of approximately 10 K) than any of the competing VCHP. A direct comparison is presented in Fig. 3.7a, where the blue and yellow areas indicates whether the configuration utilising R717-LP or R717-HP grade components is preferable in terms of NPV. The relative difference in terms of present value (PV) is presented for all the comparisons. The differences are low when comparing PV of R717 VCHP to HACHP. Temperature configurations were found, where the difference is positive for the HACHP as well as areas with negative differences. For the remaining VCHP in the comparison, the PV of HACHP was significantly improved. In figure 3.7b the relative difference is presented in detail between the HACHP and the best competing VCHP. A red contour is presented where the relative difference to PV is zero. As seen in Fig. 3.7b

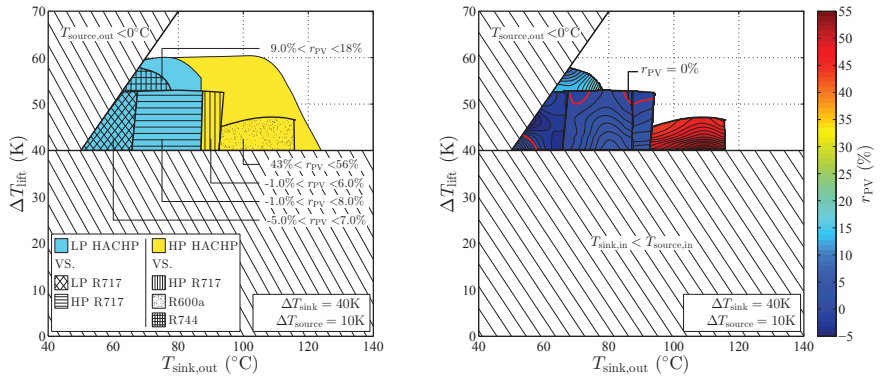

(a) Comparison of domain with best competing VCHP

(b) Relative difference in PV

Figure 3.7: Most profitable HACHP and comparison with the best available VCHP. Source: Fig. 3.7a is from [P4]

the improvements of PV from HACHP is largest at low temperature lifts, due to match of sink and source temperature glide, resulting in increase in COP. The performance increase may be explained by lower irreversibilities from heat exchange processes, in a thermodynamic cycle where irreversibility from heat exchange is a dominant factor.

As discussed in the paper [P4], the cost comparison between the two types was uncertain to an extend where small PV differences as the ones presented may be negligible (or substantial differences) if investment or electricity cost are altered for the two systems. From combining the results of papers [P3] and [P4] it was found that the investment of the HACHP is larger than for a similar R717 VCHP, but as the HACHP operates at a higher COP, the result was similar in terms of PV for the two systems. In Fig. 3.8 the calculated investment cost of both VCHP and HACHP are shown for ΔT_{sink}=10 K / ΔT_{source}=10 K. A small area was found where the investment of HACHP is lower than VCHP, but for many cases the HACHP investment may exceed VCHP by as high increases as 50 %.

It was expected that the case of 40K/10K would show the highest NPV improvement of the considered cases, as the HACHP would match the high temperature glides. But as high variations also involve a high temperature lift (due to $T_{sink,in} < T_{source,in}$), the improvement of NPV is actually higher at lower temperature glides, and highest for 20K/10K.

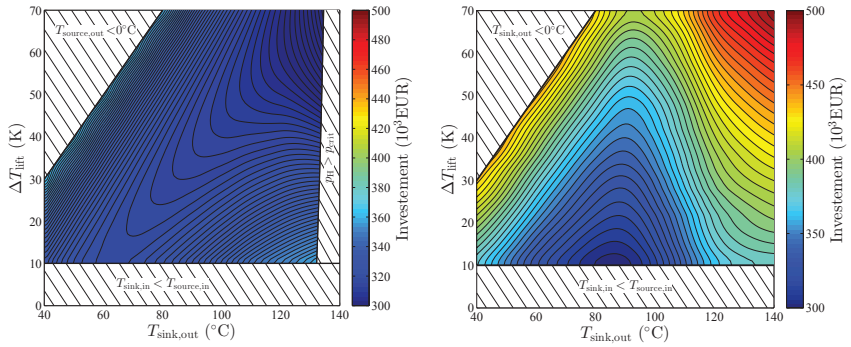

(a) VCHP (R717-HP) (b) HACHP (R717-HP)

Figure 3.8: Investment cost for VCHP and HACHP at ΔT_{sink}=10 K / ΔT_{source}=10 K. Source: Fig. 3.8b is from [P4]

3.4 Vapour compression heat pumps operated in series

In case of high temperature variation of either source or sink stream, serial connection of VCHP may provide an increase in HP COP (Prestmark and Schultz, 1984). This may be considered as another feasible measure for minimising entropy generation caused by heat transfer, in order to approach the efficiency limit as defined by Lorenz (1894).

Four serial connection schemes are presented in Fig. 3.9. Figure 3.9a presents the heat load/temperature diagram for two HPs in counter-current configuration considering both sink and source streams, as well as the refrigerant heat load and temperature profile for each of the HP systems. Figure 3.9b to 3.9d presents three alternative configurations for the sink and source streams. Counter- and Co-Current configurations are named according to Prestmark and Schultz (1984). The two remaining schemes are variations of the serial configuration, where either the evaporators or the condensers are split in parallel connection.

The four schemes for serial connection correspond to the same reference system when only one HP is installed. With a higher number of units, both economy and energetic efficiency is altered based on the changed temperature levels as presented in Fig. 3.9. The results in terms of COP and NPV are presented in Figure 3.10 for 20K/20K and 40K/10K. The results were calculated for an even split of the heat load for serial connected units which were two HPs of the type R717-HP.

The figures show, that serial connection of either two or three units results in an increase in COP and a decrease in NPV, when compared to the reference system

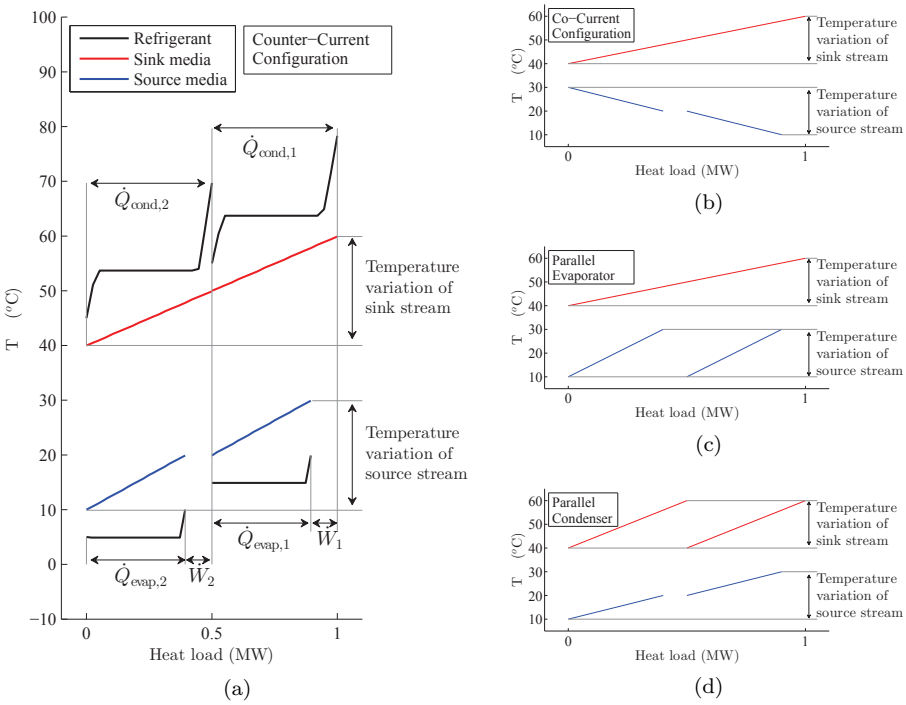

Figure 3.9: Temperature heat load diagrams for four serial connected HP schemes. (a) Two HPs in counter-current configuration. (b-d) Three alternative schemes for serial connection. Source: [P14]

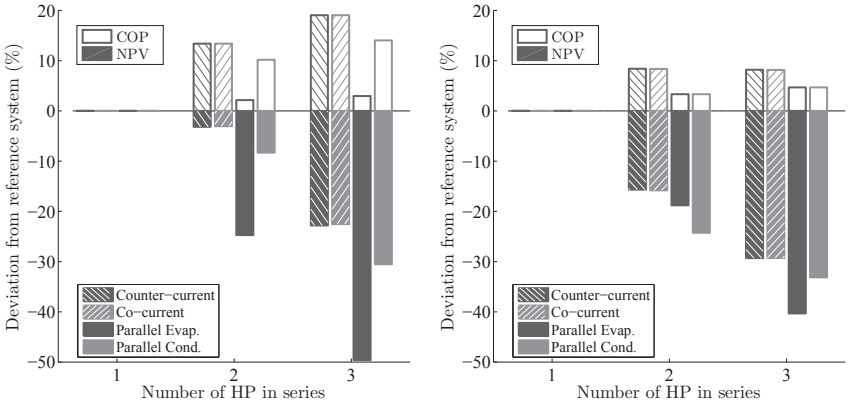

(a) ΔT_{sink}=20 K / ΔT_{source}=20 K (b) ΔT_{sink}=40 K / ΔT_{source}=10 K

Figure 3.10: Changes to COP and NPV for four serial connected HP schemes with even heat load for serial connected units. COP and NPV are calculated for R717-HP units in series. Source: [P14]

with only one HP. The decrease in NPV is the result of increased investment cost, which was not compensated by the decrease in operation cost. Serial connection of HP units presented a better NPV for the case 20K/20K compared to 40K/10K, as the increase in energetic performance was lower for the latter. Two configurations (Counter-current and Co-current) performed identically in both temperature cases, and were favourable both in terms of COP and NPV to the solutions with parallel connection of evaporator or condenser. Based on these findings, further investigation was calculated for two HPs in counter-current configuration, as this scheme resulted in lower maximum pressure ratio and consequently lower discharge temperatures compared to the co-current scheme.

The working domains were examined for two configurations of serial connected units (one for two R717-HP in series denoted "series # 1", and and one combining R717-HP and R600a denoted "series # 2"). Two main advantages were shown:

1 For large source temperature variations (the case of 20K/20K) it was possible to reduce the discharge temperature of "series # 1" significantly at minimal reduction in NPV. This lead to a significant increase in possible temperature lift, compared to one R717-HP unit.

2 It was possible to obtain a higher NPV for "series # 2" than the NPV of a single R600a unit, which at the same time was able to produce higher sink temperatures than a single R717-HP unit. This is possible due to the much higher NPV of R717-HP systems than R600a. It may be possible

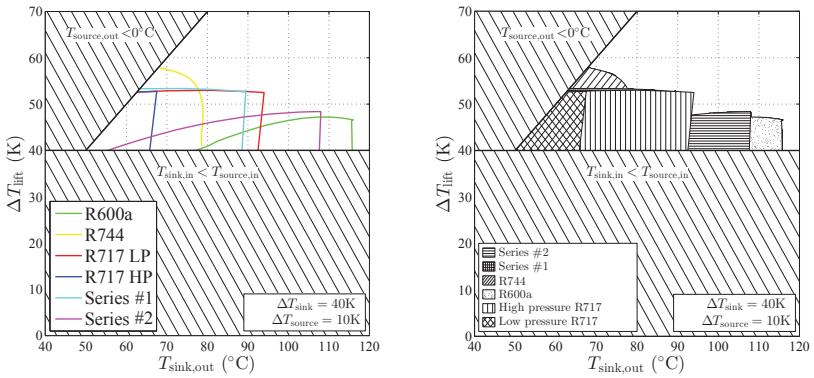

(a) Comparison of domain with VCHP

(b) Comparison with best competing VCHP

Figure 3.11: Serial connected VCHP working domains and best available technology plots at ΔT_{sink}=40 K / ΔT_{source}=10 K. Source: [P14]

to design other serial connected systems than the one considered here.

In Fig. 3.11 the serial connected HPs are added to the compilation of working domains and best available technology plots. In the case of 40K/10K the noticeable difference was only for "series # 2", which was found to be the most profitable technology between 90 °C and 105 °C. For "series # 1" a small increase in temperature lift compared to R717-HP was found, with a higher NPV than that of R744. The negative impact to NPV from increasing the amount of units (in serial connection) corresponds to the slope of an exponential function in the validated cost correlation. This indicates that the impact to investment may be smaller for larger systems. In the case where it is not possible to increase the size of the HPs (due to lack of component availability) the NPV should be compared to the case of two or more HPs in parallel. In this case the serial connected HPs may have a lower NPV than the alternative. Serially connected HPs may further prove increasingly beneficial at operation hours above the considered case of 3500 h/Year

3.5 Summary

By investigation of the four sink/source working domains it was found, that sink temperatures of up to 120 - 140 °C and temperature lifts 40 - 60 K can be achieved with positive NPV by a combination of VCHP and HACHP systems. For both VCHP and HACHP it was found, that the possible temperature lift increases with an increase in temperature variation of the sink (for a fixed source temperture variation).

For most of the vapour compression systems analysed in [P3], the maximal achievable temperature lift was limited by the economic profitability constraint. As indicated in Fig. 3.2 the NPV constraint is influenced by many parameters, but significant changes are found with variations in fuel cost. It may be difficult to access these parameters with high detail for the technical lifetime of an installation, as they depend on both technical achievements, energy policy, and security of supply. In the calculation examples presented, the operation and maintenance cost of the replaced burner was neglected. Including such sunk variable cost would further increase the profitability of the HP in real applications. Further, in the general case of new installations, the investment cost of the alternative boiler should be included in the NPV.

For the technologies utilising R717, both considering VCHP [P3] and the HACHP technology [P4], a technical constraint (the discharge temperature) limited the applicability in terms of temperature lift. The NPV constraint of these systems allowed much higher temperature lifts than any of the alternatives. Several methods may be utilized, in order to reduce the discharge temperature, or increase the application limits of the components.

For some applications, connecting HPs in series [P14] may ease technical constraints, but such setup typically resulted in small reductions of NPV compared to a single HP unit. For other applications (such as DH systems utilising 40K/10K), the technical constraints were not affected by the method. Combining characteristics of two HP types may result in improvements to NPV, compared to the profitability of e.g. R600a.

Considering the previously mentioned DH case, where a stream is heated to the sink temperature of 80 °C with source heat at 20 °C, only one technology (the HACHP) satisfy the considered constraints. With a higher temperature lift or sink temperature, neither of the technologies present working domains which cover such configurations. The main reason for lack of feasible domains is the requirement of a positive NPV.

Chapter 4

Centralised district heating heat pumps

As presented in Capter 3, the economic constraint of the working domain limited the feasible configurations for high temperature lifts. For integration in (urban) energy systems, where fluctuations in electricity cost are significant, a profitability evaluation of heat pump integration requires detailed energy system analysis to attain fuel cost and savings. In this case the energetic performance and investment cost of technically feasible units are important parameters for the analysis. The levelised cost of heat may be used to compare profitability in order to limit plausible technologies.

Eight heat pumps are compared based on the performance of exergoeconomic optimal systems for two typical district heating cases (SF and SR) according to the analysis in [P5]. The best available technology for various temperature configurations is found by considering technical constraints and operational economy of the units. The energetic performances of the best systems are presented, and (in [P5]) compared to the theoretical maximum for heat pumps in finite reservoirs.

4.1 Comparison of VCHP cycles for SF configuration at low forward temperatures

As mentioned in Chapter 3 the calculations for SR and SF integrations resemble that of working domains for (sink/source) 10K/10K and 40K/10K, respectively. An example of the calculation for configuration SF is presented, considering DH network at "new distribution" temperatures and fixed heat exchanger pinch point temperature difference (according to table 2.1. The comparison is presented in Table 4.1, where operating limits, electricity consumption, cycle efficiency and the cost of heat, as well as the three constituents (investments, fuel cost and taxes) of cost, are shown.
According to technical constraints, two of the HP systems can be disregarded due to a too high operating pressure (R407C and R717-LP). Out of the six

Table 4.1: Operating conditions for eight HP types for Configuration SF, "New distribution" DH network and heat source at $T_{\text{source},i} = 20$ °C

Type	High-pressure level (MPa)	Discharge temp. (°C)	Heat pump COP (–)	Lorenz efficiency (–)	Cost of heat C_{HP}(€/MWh)	Share of cost from invest. (%)	Share of cost from fuel cost (%)	Share of cost from taxes (%)
R134a	2.1	89	3.9	0.45	64	32	23	45
R1234ze	1.7	89	3.9	0.44	67	34	23	44
R290	2.6	87	3.9	0.44	64	31	24	46
R407C	3.0	95	4.3	0.49	56	25	25	49
R600a	1.2	77	3.9	0.44	71	37	21	41
R717-LP	3.1	176	3.9	0.45	54	20	27	53
R717-HP	3.1	176	3.9	0.45	56	23	26	51
R744	13.9	102	3.1	0.36	76	28	25	48

remaining, the R717-HP had the lowest cost of heat and was thus preferable for this operating condition. For the feasible configurations, it was found that the cost of heat was in the range of 56 €/MWh to 76 €/MWh, even though five of the HPs have the same COP of 3.9. For comparison with current systems, the cost for DH in Copenhagen in 2012 was 85 €/MWh (HOFOR, 2012). However it should be noted that none of the current areas in Copenhagen operates according to "New distribution" DH network temperatures. Further, the calculation was performed without considering distribution losses for the electricity network, which should be imposed on the electricity cost, depending on the electricity network at the location of the unit.
As presented in Table 4.1, the combined investment and electricity cost accounts for between 47 and 59 % of the total cost. For units with low investment cost, the share of total cost of heat from heat taxes may exceed 50 %.

4.2 Exergoeconomic optimal configurations

By careful investment allocation between the components of a heat pump, it is possible to optimize the economic performance criteria of the unit. The objective of the exergoeconomic evaluation is to examine the cost formation process of the product(s), to properly assess the contributions due to investments and the thermodynamic inefficiencies (irreversibilities). As a result, it is possible to focus the analysis on the components which have the highest impact. Exergoeconomic analysis is based on exergy analysis (Bejan et al., 1996).
By assuming that the compressor cost was a function of its volume flow (size of displacement volume) and unaffected by the isentropic efficiency, it was

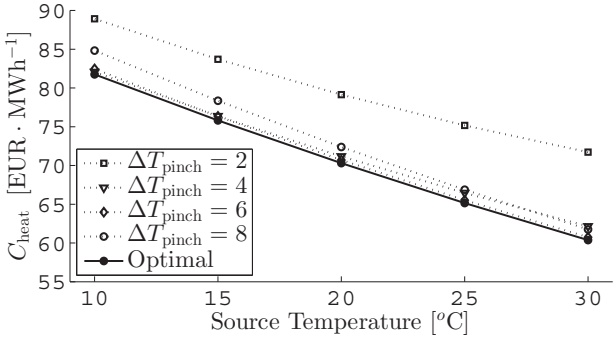

Figure 4.1: Optimal allocation of investment of R600a heat pump with variation of the source temperature. Sink temperatures according to configuration SF for district heating network with 70°C - 35°C.

found that the heat exchanger units were the primary area of interest of an economic optimisation. The heat exchangers provide the possibility to obtain increased performance of the cycle by increasing investment. An example of the impact of an exergoeconomic optimisation is presented in Fig. 4.1 for a heat pump with R600a as working fluid, considering a range of the considered source temperatures (10-30 °C) and sink temperatures according to a district heating network with 70°C - 35°C.

Four fixed heat exchanger pinch temperatures (ΔT_{pinch}) were compared to a case where both of the heat exchangers were optimised individually, in order to obtain the system with the lowest operation cost. The investment was not only changed for the heat exchanger, but all of the remaining components were affected correspondingly with significant magnitude, as the thermodynamic cycle was altered. Comparing a poor choice in pinch temperature difference (2 [K]) with the optimal pinch point (according to exergoeconomic optimisation) a reduction of 8-19 % in cost of heat was possible for the R600a heat pump.

By visual inspection of the curves for optimal and fixed pinch temperatures of Fig. 4.1 it may be seen that the level of the optimised heat exchanger temperature differences correspond to ΔT_{pinch} of approximately 4 - 6 K. The obtained magnitude matched well with the expected value for similar operating hours (Granryd, 2005a), but the obtained value differs with changed temperatures, configurations and working fluids. Exergo-economic optimal systems may present a fair comparison for systems where the predefined pinch temperature is not economically advantageous.

4.3 SF configuration

The SF configuration was investigated according to the sink and source temperature span considered in Sections 2.2 and 2.3. The exergo-economic optimum was determined for all combinations, and the type with lowest cost of heat was found by comparison. The individual systems are presented with a unique color in Fig. 4.2a in a (T_{source}, T_{sink}) plot, to indicate the temperature levels where the unit is favourable. Besides the indication of the best configuration, the COP of the best configuration (Fig. 4.2b), it's investment cost (Fig. 4.2c) and the levelised cost of heat (Fig. 4.2d) is presented.

At certain application limits, the favourable solution changes from one unit type to another. These changes are marked with black lines. For SF configurations five of eight units are favourable in a specific area.

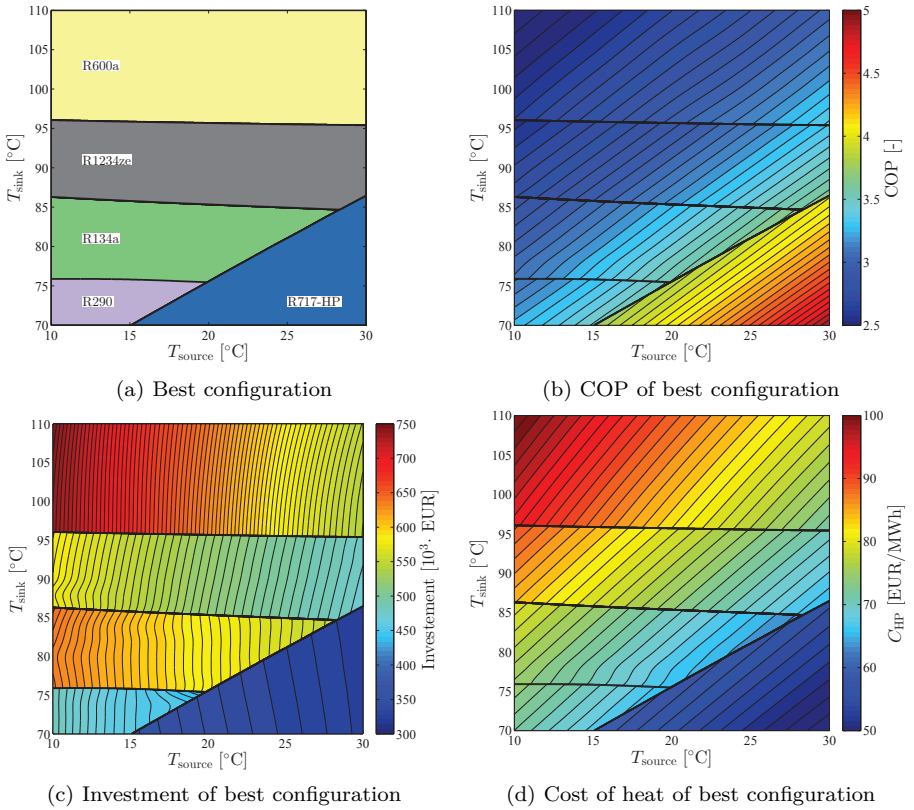

(a) Best configuration

(b) COP of best configuration

(c) Investment of best configuration

(d) Cost of heat of best configuration

Figure 4.2: COP, investment cost and cost of heat for best SF heat pump unit. The investigated temperature range correspond to sink and source temperatures for typical network configurations. Fig. 4.2a and 4.2b are from [P5]

For the SF configuration it was found, that R717-HP was the configuration with the best feasible economy, but due to component limitations, this was only in a limited area of the domain. The area of feasibility for the R717-HP system was limited by high discharge temperature, which is represented by a tilted constraint which allows highest sink temperatures at high source temperatures. The remaining technical constraints in Fig. 4.2 are due to pressure limitations. This constraint type is approximately horizontal, as the application limit may be considered unaffected by the source temperature. R290 was found to have a marginally lower cost than R134a (Fig. 4.2d), but the component limitations limits the applicability at approximately 75°C. The pressure limit of R134a was at approximately 85 °C and R1234ze was applicable below 95 °C. R600a was technically feasible in the full temperature span of sink and source, but with low levelised cost and thus not preferable at low sink outlet temperatures. R717-LP, R407C and transcritical R744 did not contribute with parts of the working domain either because of technical limitations or uncompetitive heat cost.
Considering the COP of the economically advantageous technologies (Fig. 4.2b) it may be seen that the COP is increasing for decreasing temperature lift, resulting in increased COP for approaching the lower right corner from the upper left corner. A shift in COP was experienced from changing from R1234ze, R134a and R290 to R717-HP. The shift is of a magnitude of 0.25-0.35 points of COP, which may be as high as 10 % increase. In terms of investment (Fig. 4.2c), the R717-HP was likewise favourable with investment cost of 3-400.000 €. R134a and R600a were found to have a significantly higher investment cost than the remaining configurations.
In case of HFC and HFO working fluid phaseout (already present for large quantities of working fluid in Denmark), the areas where R134a and R1234ze were determined as the best available technology, would change to an increased working domain for R600a, with an increase in cost of heat as a result. For the areas previously occupied by R1234ze the increase in cost was found to be in the order of 3 to 7 %. In the case of the R134a working domain, the increase was found to be between 8 and 12 %. This change is important as the working domains of R134a and R1234ze are representative for a high share of current DH networks. In terms of COP the differences were smaller, and in many cases in favour of R600a.

4.4 SR configuration

A similar analysis was performed for the SR configuration. The best available technology, COP, investment cost and cost of heat is presented in Fig. 4.3a, 4.3b, 4.3c and 4.3d respectively. For a large fraction of the working domain of the SR configuration, the R717-LP system proposed the lowest cost of heat. The R717-LP unit was constrained by two technical constraints. At

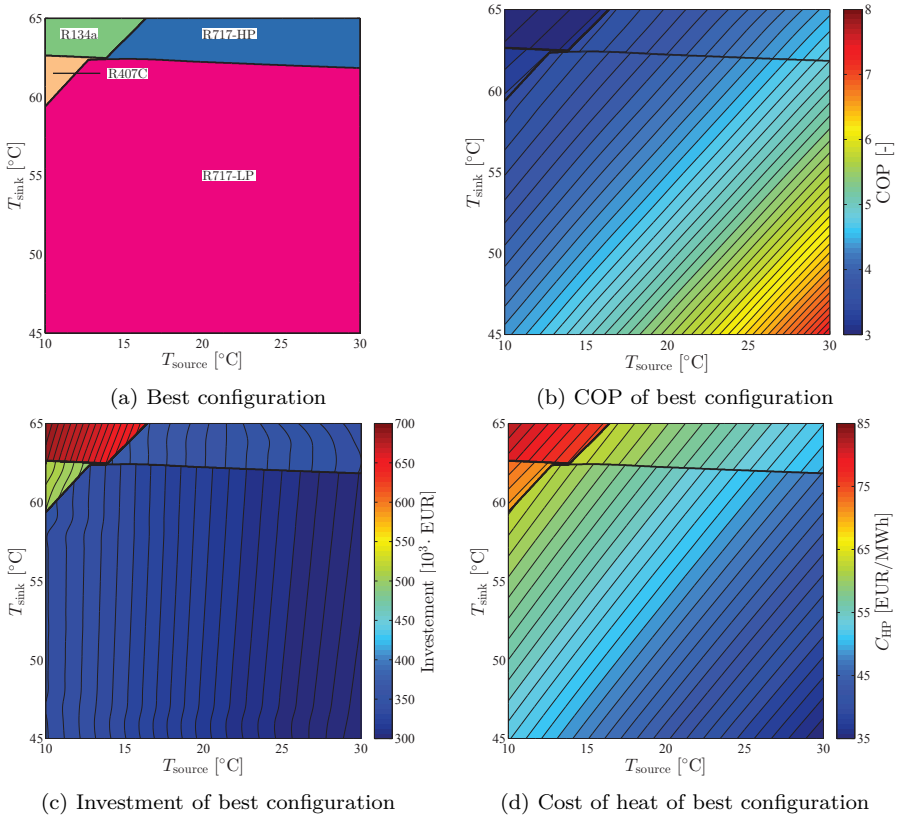

(a) Best configuration

(b) COP of best configuration

(c) Investment of best configuration

(d) Cost of heat of best configuration

Figure 4.3: COP, investment cost and cost of heat for best SR heat pump unit. The investigated temperature range correspond to sink and source temperatures for typical network configurations. Fig. 4.3a and 4.3b are from [P5]

low source temperatures the discharge temperature exceeded the set limitation. For higher source temperatures (approximately 13°C) the R717-LP system was constrained by the maximum high pressure limit corresponding to 62-63°C. Three systems (R407C, R134a and R717-HP) proposes the lowest cost of heat for the remaining sink temperature span.

According to Fig. 4.3c and 4.3d R407C and R134a units induce considerably higher investment cost and correspondingly higher cost of heat than the two units with R717 as the working fluid. The levelised cost is further deteriorated by lower COP for units utilising such HFC working fluids.

The COP of the best available SR systems were significantly higher than for SF configurations, due to the lower temperature lift of the HP. As a consequence the levelised cost of heat for SR was significantly lower, although investment

cost are similar.

4.5 Summary

Eight heat pump units were compared for their economic and energetic performances as SF and SR configurations in a district heating network. For a fixed case with set pinch temperatures it was found, that the cost of heat varies significantly between the considered feasible configurations, and is thus a superior selection criteria compared to the COP, which was similar for most of the considered HPs. For units with low investment cost, the share of total cost of heat from taxes exceeded 50 %.
For each of the examined temperature levels and working fluid configurations exergo-economic optimisation was performed to present a fair comparison to the heat pump units where the previously predefined pinch temperature was not economically advantageous.
Results show, that units utilising R717 as working fluid presents significantly lower levelised cost rates than the alternatives. The improved economic performance is a consequence of high COP and low investment cost. For both SR and SF integration in the district heating network, the configurations were limited by high discharge temperatures and high discharge pressures.
For the SF integration, five different units were preferable in individual areas of the working domain. In the case of SR, the R717-LP was advantageous in a large area of the working domain, but in the areas limited by technical constraints, three other configurations should be utilised, each in separate small working domains.
In case of HFC and HFO working fluid phaseout the recommendation for best available technology changed to an increased working domain for R600a, with an increase in cost of heat as a result. For the SF configuration the increase in cost was found to be in the order of 3 to 12 %. In terms of COP the differences were smaller, and in many cases in favour of R600a.
The investment cost for heat pump integration SR and SF were similar in magnitude and show similar trends for various working fluids for both configurations. The differences between low and high investment cost correspond approximately to a factor of 2-2.5.

Chapter 5

Energy system modelling

In order to analyse the benefits for HP integration schemes, considering HPs as a competing technology in market-based energy systems, the representation of other players in the economic optimisation is required. HP integration may change the load schedule of CHP plants or peak load boilers, compared to a system without this additional technology.

The influence of optimisation methods for energy system modelling is examined ([P1]) based on analysis of three comparable models utilising different optimisation schemes.

The key features of the derived mixed integer model are presented, and results are presented for three principal integration schemes in terms of consumer cost, carbon emission, operating hours and system efficiency for two different energy system scenarios.

To investigate the influences on system operation with integration of a specific HP configuration, an energy system model is required. The model should address the key interactions from both the various types of CHP-units, and different integration schemes of HPs. As interactions between the two technologies are investigated in both current and future energy system layouts, a generic model for various system layouts is desired.

5.1 Optimisation scheme

With high requirements for the level of technology detail, the impact of the choice of optimization algorithm in energy system dispatch models was investigated (in [P1]). The evaluation was based on a comparison of three different optimisation schemes for an energy system model.
A number of energy models have been developed during the last decade both with specific focus on the Danish system and for more general application (Connolly et al., 2010; Tuohy et al., 2009; Karlsson and Meibom, 2008; Ravn et al., 2005). Many of these models are continuously expanded and maintained. The majority of current models is using linear optimisation (Connolly et al., 2010).

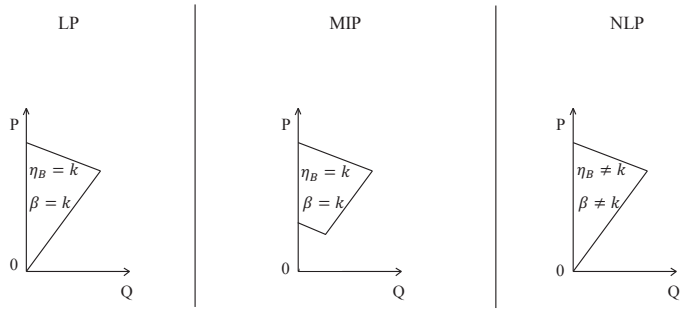

Figure 5.1: Three different representations of operation constraints, boiler efficiency and β-value for typical CHP models utilising three optimisation schemes. Source: [P1]

For many linear dispatch models, the level of detail of utility technologies is low, and the interdependence of the individual units is not representative for the constrained operation of the current Danish energy system. In such advanced optimisation models, the detail levels of individual technologies are not easily changeable, as they depend on the optimisation approach, which is a basic property of the model.

The analysis was carried out in General Algebraic Modelling System (GAMS) GAMS Development Corporation (1998) using two different solvers, three model types, different optimisation time frames and optimisation horizon. The production units in the system were represented by performance characteristics, which account for the network system parameters, such as e.g. temperatures in the district heating network.

A simplified visualisation of the impact of an optimisation scheme on the representation of an extraction CHP plant is presented in Fig. 5.1. The main differences occur for CHP units, as they due to their large sizes and the low quantity of units may experience a significant number of part load hours, compared to e.g. natural gas boilers which in comparison are aboundant, not significantly constrained in terms of load changes and of various sizes.

Four models where assessed: two utilising linear programming optimisation (LP) but with different optimisation time frame, one mixed integer programming optimisation (MIP) and one non-linear programming optimisation (NLP).

The optimisation type influenced the calculated operation and load characteristics of individual technologies to varying extend. The most affected technology was the HP units, as they may be used to circumvent technical constraints at the CHP-unit, at lower additional cost than other technologies in the system. Compared to LP, the results of MIP and NLP optimisation models showed

significant operation differences, as the technical constraints in the low load operating condition corresponds more closely to real performance. For these schemes, the HP units experienced a significantly higher amount of operating hours, and a changed load profile. The results in terms of HP operation was not similar for the two, but showed similar trends for various differences in a parametric analysis. As the NLP optimisation model was time-consuming, and the nature of the mathematical problem was non-convex, indicating that the solver does not guarantee the location of the global optimum, it was decided to continue with mixed integer programming optimisation.
At the time, it was found that no freely available and easily interchangeable models existed, and it was thus decided to continue development of a new model. Later it was found that the model was co-developed with an add-on to Balmorel based on a MIP optimisation scheme (Ravn, 2011), which allows some of the same properties as the developed model.

5.2 Mixed integer model

A detailed system model was developed for calculation of economic and environmental impact of integrating HPs in an energy system, where high shares of both CHP-plants and intermittent electricity production from renewable technologies (e.g. wind turbines) result in technically constrained optimum. The result was a validated heat and power system model, which features detailed representation of CHP technology as well as detailed representation of different HP technologies and integration possibilities.
The optimal production cost for the combined system can be achieved by minimisation of consumer cost for electricity and heat. This choice corresponds to the daily optimisation which is performed for both electricity and heat networks in the DK2 and Greater Copenhagen bidding area.
All cost rates associated with utility production (e.g. fuel, taxes and subsidies) were considered in the optimisation. In order to ensure the competitive conditions for import and export of electricity across taxation boarders, the taxes for electricity was put on consumption. This is opposite to taxation for heat, which is closely linked to the production.
In the model, all central power plant units were considered, as well as all units connected to the Greater Copenhagen DH network (such as waste incineration CHP-plants, smaller CHP units, boilers, electric heaters etc.). It was assumed, that electricity and heat production of small-scale decentralized CHP-plants and intermittent electricity production from wind turbines were operated independent of the electricity cost in the individual hour. Using this assumption, the production profile of such units was obtained from historical data.
The mathematical formulation of the heat and power system model is presented in Appendix A. The objective function in Eq. A.1 was subject to a number of economic and technical linear constraints. In the appendix, emphasis is placed

on the structure of the model, as well as constraints that differentiates the model in terms of detail of technology or specific Danish conditions.
The detailed representation of the CHP units includes various features which are briefly mentioned below:

- Four types of power plant units possible: Back-pressure, extraction, gas turbines/combined cycle or condensation.
- maximal hourly ramp rates and minimum technical production limits.
- Reduction in electricity production efficiency at part-load operation. May be set individually for each unit.
- Startup and shutdown costs corresponding to size and type of unit
- Extraction technology represented by two power loss factors from heat extraction (β^1, β^2) depending on production above or below the "no-loss" point Verbruggen (2007).
- Production at specific units may be prioritised, e.g. waste incineration.
- Availability (to market) may be set individually for all units. For validation these data were obtained from urgent market messages from Nord Pool Spot (2013b).
- Two different taxation schemes for heat production may be chosen for each unit.
- Steam bypass of turbine possible for backpressure CHP-units.
- Minimum available manual and frequency reserves may be set for the total system, and technical limitations of reserves are specified individually for each unit.
- Specific units may produce at higher capacity than their rating (overload) at reduced efficiency.

5.3 Current and future energy system scenarios

For each of the thermal CHP units in the current and planned utility system, specific information regarding capacity and efficiency, cost of fuels and maintenance, as well as capacities and consumption of the network were available online from various sources DONG Energy (2012); Vattenfall A/S (2012); Energinet.dk (2012b, 2011); Danish Energy Agency (2011); CTR, HOFOR and VEKS (2014a).

The individual specifications of CHP plants for the two scenarios are presented in [P14]. Most of the presented data correspond to operational parameters of the individual units, but the table also includes fuel cost for 2011 and 2025 using historical prices (corresponding to those used for validation in Appendix B) or prognoses Energinet.dk (2012b). It should be noted that both electric efficiency and energy utilisation were calculated for the plant in back-pressure operation mode.
The capacity and demand profile, as well as planned changes, of DH networks in 2012 and 2025 were based on information from CTR, HOFOR and VEKS (2014a). Such data are not presented due to non-disclosure agreement, but may be acquired from the homepage. Changes to the capacity of decentral CHP, on- and offshore windturbines, photovoltaics and spot-prices for electricity in 2025 were available from Energinet.dk (2012b).
As the process of converting old steam networks to water based networks is ongoing, the heat demand for these networks is increased according to the planned conversion, and the additional heat demand from integrating new areas. All in all the heat demand in 2025 is increased compared to today, due to expansion of the network, even though heat savings are included for a part of the building mass, and heat losses are reduced for the water based DH compared to steam networks.
In section 6.3 the two energy system scenarios are compared in terms of key parameters, including consumer cost and carbon emissions of heat and electricity.

5.4 Examples of various heat pump integration schemes

In section 2.2, various heat sources and integration schemes were considered depending on the location of the unit. Such heat sources and integration schemes should in principal be considered for each small addition of capacity for HPs in the DH network. In this way the best configuration incorporates the optimal choice in various factors such as concurrency, network constraints and temperature levels.
Examples of the possible benefits from integrating HPs in the two scenarios are presented (in table 5.1 and 5.2) in terms of three system parameters, and the amount of operational hours for the HP units. The considered HPs are three integration schemes from section 2.4, specifically SF, SR and SD configurations. For each type, 100 MW capacity is installed in the system at a beneficial location considering the type of location. Three locations are considered: transmission network (specifically at AMV where high transmission capacity is available), distribution network (location with high demand compared to installed capacity) and individual dwelling (even distribution of capacity in entire DH

Table 5.1: Integration of 100 MW HP capacity in current energy scenario

	Forward temp.	**(°C)**	**110**	**100**	**90**	**80**	**70**
SF transm.	Operating hours	(10^3 h)	1.1	**1.7**	2.1	3.0	4.5
	Consumer cost	(%)	-0.3	**-0.5**	-0.5	-0.8	-0.9
	CO2 emission heat	(%)	-1.1	**-1.8**	-2.3	-3.4	-5.7
	DK2 total efficiency	(%)	0.0	**-0.1**	-0.1	-0.1	-0.1
SF distr.	Operating hours	(10^3 h)	1.1	1.6	**2.1**	3.0	4.5
	Consumer cost	(%)	-0.4	-0.5	**-0.6**	-0.8	-0.8
	CO2 emission heat	(%)	-1.2	-1.8	**-2.3**	-3.4	-5.7
	DK2 total efficiency	(%)	0.0	-0.1	**-0.1**	-0.1	-0.1
	Return temp.	**(°C)**	**55**	**50**	**45**	**40**	**35**
SR transm.	Operating hours	(10^3 h)	3.3	**4.1**	4.7	4.9	5.2
	Consumer cost	(%)	-0.7	**-0.7**	-0.9	-1.0	-1.2
	CO2 emission heat	(%)	-3.3	**-4.5**	-4.8	-5.1	-5.2
	DK2 total efficiency	(%)	0.0	**-0.1**	0.0	0.1	0.1
	Demand temp.	**(°C)**	**35**	**45**	**55**	**55**	**55**
	Carnot eff.	**(-)**	**0.5**	**0.5**	**0.5**	**0.4**	**0.6**
SD air/w.	Consumer cost	(%)	1.0	1.7	**2.4**	3.4	1.8
	CO2 emission heat	(%)	-3.2	-2.6	**-1.9**	-1.0	-2.5
	DK2 total efficiency	(%)	-1.0	-1.1	**-1.2**	-1.3	-1.1

network). The sink temperature levels are not fixed, but calculated for representative forward or return temperatures. The results which are printed in **bold**, represent temperatures levels which are likely required as sink temperatures, in order to integrate HPs in the DH network at the considered location. The energetic performance of the individual HP configurations for SR and SF corresponds to that found for the economical optimal configurations in section 4.3 and 4.4. As heat source for the two central units, a fixed source temperature ($T_{\text{source}} = 20$ °C) was chosen. The temperature is not necessarily representative of an available source of approximately 50-70 MW capacity, but the considered areas for both transmission and distribution are co-located with heat sources such as waste water treatment and stack gasses from waste incineration. For the SR configuration, operation of the HP was constrained by corresponding co-production of heat at the central CHP plant or nearby waste incineration plant.

For the SD configurations, several heat sources are possible. However in practice each dwelling/apartment building in central Copenhagen is confined in terms of available area for installations, such as e.g. shallow geothermal. Air was utilised as the source, with temperatures corresponding to those at the considered location in 2011 (Danmarks Meteorologiske Institut, 2015). The performance of the units was calculated on basis of the Carnot limit, considering demand temperature of 35-55 °C and Carnot efficiency 0.4-0.6 (-). Examples

Table 5.2: Integration of 100 MW HP capacity in 2025 energy scenario

	Forward temp.	**(°C)**	**110**	**100**	**90**	**80**	**70**
SF Trans.	Operating hours	(10^3 h)	1.2	**1.3**	1.4	1.6	2.2
	Consumer cost	(%)	-0.3	**-0.4**	-0.5	-0.7	-1.3
	CO2 emission heat	(%)	-3.6	**-3.6**	-3.6	-3.6	-3.5
	DK2 total efficiency	(%)	0.2	**0.2**	0.3	0.3	0.4
SF Distr.	Operating hours	(10^3 h)	1.2	1.3	**1.4**	1.6	2.2
	Consumer cost	(%)	-0.3	-0.4	**-0.5**	-0.7	-1.3
	CO2 emission heat	(%)	-3.6	-3.6	**-3.6**	-3.6	-3.5
	DK2 total efficiency	(%)	0.2	0.2	**0.3**	0.3	0.4
	Return temp.	**(°C)**	**55**	**50**	**45**	**40**	**35**
SR Trans.	Operating hours	(10^3 h)	1.7	**2.0**	2.3	2.8	3.2
	Consumer cost	(%)	-0.8	**-1.1**	-1.3	-1.7	-2.0
	CO2 emission heat	(%)	-3.6	**-3.6**	-3.5	-3.5	-3.4
	DK2 total efficiency	(%)	0.0	**0.4**	0.5	0.5	0.6
	Demand temp.	**(°C)**	**35**	**45**	**55**	**55**	**55**
	Carnot eff.	**(-)**	**0.5**	**0.5**	**0.5**	**0.4**	**0.6**
SD air/w.	Consumer cost	(%)	0.2	0.9	**1.5**	2.4	0.9
	CO2 emission heat	(%)	-1.7	-1.2	**-0.7**	0.0	-1.1
	DK2 total efficiency	(%)	-0.6	-0.6	**-0.7**	-0.8	-0.7

of current "state of the art" recommended air/water heat pumps may be found at sparenergi.dk (2015), which shows that Carnot efficiency exceeding 0.45 is not likely possible today.

The results for current energy scenario show (in table 5.1), that regardless of forward or return temperatures in the DH network, SF or SR configurations result in reduction of both consumer cost (for both electricity and heat) and carbon emissions for heat. This is contrary to the total efficiency of the DK2 area, which for most cases is slightly decreased. Of the SF and SR configurations, only low return temperatures of SR allow a small increase in total efficiency of the bidding area DK2.

For comparing the location of transmission and distribution SF configurations, the four assessed parameters showed similar results for similar sink temperatures. The lack of difference for fixed temperatures, shows that the availability of storage (available in transmission network) does not influence production of heat. As performance is similar, it would seem that integration in distribution networks is beneficial, as the temperatures are always lower in these networks. The limit to integrating in distribution networks is when capacity exceeds the demand in many operating hours.

With lower sink temperatures (whether forward or return) the HP played an increasingly important role in terms of cost reductions and carbon emissions. Up to approx. 1 % reduction in consumer cost (combined for heat and power),

and more than 5 % reduction in carbon emissions from heat may be achieved. The SD air/water heat pump performed poorly in comparison with SF and SR. Regardless of the temperature of demand, or the performance in terms of Carnot efficiency, the cost for the total system was increased (up to 3.5 % increase in for electricity and power), the carbon emissions for heat were only slightly reduced (compared to SR and SF) and the total efficiency was reduced.
For the 2025 energy scenario, the main trends of the various configurations (in table 5.2) were similar to those observed for the current scenario. A significant difference was, that for most of the considered configurations, the total efficiency was increased by integration of HP capacity, and the consumer cost were further decreased. This was despite a significantly lower amount of operation hours for the heat pumps in 2025 compared to the current scenario (2011).
For the case of 2025, the use of SD heat pumps at the location of the dwellings affect the system efficiency less negatively, than for the results of 2011.

5.5 Summary

Three frequently used operation optimisation methods were examined, in order to investigate their impact on operation management of energy system technologies. By focussing on the physical representation of a CHP-plant, it was clear that a simple representation allows infeasible production.
Using MIP or NLP optimisation, the number of operation hours and the total production of heat from HPs was significantly increased, as the HPs were used to shave the load patterns of CHP units in significantly constrained energy systems. The results were further supported by a parametric investigation, which showed that the operational performances of the heat pumps were roughly similar in MIP and NLP optimisations compared to LP approaches. As the NLP was time consuming to solve, and did not guarantee the location of the global optimum, it was decided to continue development of a MIP optimisation energy system model.
The model was briefly introduced considering the detail level of features for representation of CHP units, and two energy scenarios were introduced for current and future technology mix in the DK2 area.
Three different HP configurations were integrated (100 MW capacity) in the network. The operational difference for the total energy system was considered based on three performance criteria. For current network, only few of the considered configuration and temperature combinations increases the total energy efficiency, but in the results for 2025, the integration of central HPs was typically a benefit for the system efficiency in all cases.
In terms of consumer cost, the integration of central HPs was typically an advantage. Similarly for carbon emissions of heat, which decreases for all (but one) considered heat pump integration schemes.

Chapter 6

Low temperature DH in current and future Danish energy scenarios

Operation of DH networks at low temperatures (LT) are proposed by several sources as a means to increase system performance. Especially three contributions are worth mentioning, the decreased DH heat losses, improvements in performance of CHP-plants, and improvements in performance for renewable technologies, either by direct utilisation (eg. solar thermal collectors) or by use of HP technology.

The topic is addressed from several perspectives in four of the attached papers. An essential difference between the considered studies is the origin of the produced DH and the entailed primary energy consumption.

Performance evaluation of LT DH as separate distribution networks supplied by high temperature transmission networks is examined in [P6]. Different consumer booster units are presented and analysed in [P8] and [P16]. The impact to system performance from lowering the DH temperature is analysed using the heat and power energy model. The analysis is performed for both current and future Danish energy scenarios in [P7].

The use of LT DH has been proposed for two quite different energy scenarios, both of which were analysed and assessed in following sections:

- The design of new or updated systems with better performance of utility units according to the production temperatures and low losses in DH network. A key aspect of lowering DH temperature is the increased performance for renewable technologies at lower forward temperatures.

- Expansion of existing DH networks, where troublesome capacity constraints may be addressed by lowering return temperature, by connecting LT DH networks at remote positions.

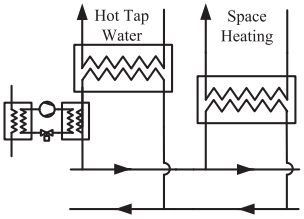

(a) Heat pump on primary side of the tap water heat exchanger.

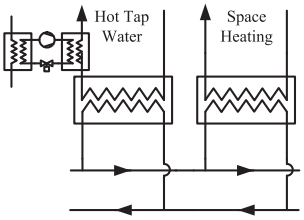

(b) Heat pump on secondary side of the tap water heat exchanger.

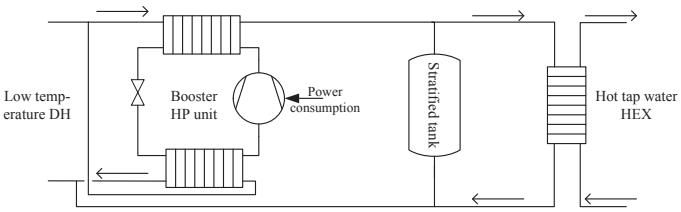

(c) specific layout of DH booster HP unit

Figure 6.1: Two DH booster HP integration schemes, and an example of a specific layout of booster HP unit. Source: [P7]

6.1 Performance evaluation of LT DH distribution networks

Traditional space heating in radiator systems requires temperatures of 50-70 °C, but modern low energy buildings equipped with efficient floor heating makes it possible to lower this temperature to about 30-40 °C. With lower demand temperatures, lower temperature may be possible in the distribution network. A direct effect of such temperature reduction in distribution networks is a reduction in heat losses.

However, for supply of hot tap water, two constraints are present, considering the Danish DH case. The requirements of the Danish building standard must be met (Danish Standards, 2009), where hot tap water is to be utilised at 45 °C. Additionally, a main concern is the issues related to the bacterium Legionella pneumophila. To avoid bacteria growth, either the hot tap water must exceed a predefined temperature limit, where the bacteria can no longer exist, or the tap water is not to be stored after being heated.

Two booster HP integration schemes were identified, corresponding to the schemes presented in Fig. 6.1a and 6.1b. The heat for hot tap water corresponds typically to 30-50 % of the combined heat consumption in a dwelling. In table 6.1 eight different configurations are presented for various distribu-

Table 6.1: Results of various DH distribution configurations. Source: [P6]

System	Distribution temperatures (°C)	Refrigerant	Heat pump COP (–)	Tank location	Preheating	Heat consumption (W)	Electricity consumption (W)	Energy Efficiency (%)	Exergetic Efficiency (%)	Cost (€/Y)
Conv. 1	80/40	–	–	Sec		1000	0	81	27	740
Conv. 2	65/55	–	–	Sec		970	0	84	27	710
Conv. 3	60/30	–	–	Sec		950	0	86	28	690
LT EL	45/25	–	1.0	Sec		790	150	89	16	970
LT HP 1	45/25	R134a	3.7	Sec		830	100	88	19	870
LT HP 2	45/25	R744	6.6	Sec		880	56	88	24	800
LT HP 3	45/25	R134a	3.5	Sec	×	890	41	89	24	760
LT HP 4	45/25	R134a	4.0	Prim	×	900	30	89	25	750

tion temperatures. Conventional 1 corresponds to distribution temperatures in a temperature range similar to that used in most networks today. Five LT configurations were considered of which four utilised a HP, and one employed direct electric heating, in order to boost the temperature of the DH stream to that required for hot tap water production. In the paper ([P6]) the details of the individual configurations are presented. The transmission system operates at 85/60 °C to cover all cases, and hot tap water was assumed to be approx. 44 % of the total DH usage in a low energy building.

For the conventional high temperature system (base case) it was found that the energy efficiency of the system was 81 % which illustrates the heat loss of the distribution network. The exergetic effciency was 29 % for the hot water supply and 24 % for space heating, and accordingly 27 % in total. The annual cost of the heat was 740 €.

Neither of the LT DH booster HP configurations showed exergetic efficiencies as high as the conventional solutions, but some showed significant increases in the energy efficiency. The most efficient LT DH booster configuration (heat pump on primary side of tap HEX) resulted in costs which are similar to the base case. As seen from the table, heat losses from the distribution network were reduced by approximately 8 percentage points, which account to 42 % reduction compared to base case.

Two other conventional systems, operating at lower temperatures of either forward and/or return, result in lower heat losses but similar high exergetic efficiency as the base case. The costs for these configurations (e.g. Conv. 3) were further reduced than the base case, and were thus the most competitive solutions.

6.2 Booster configurations

The specific design of the LT DH booster HP configurations are considered in detail in two contributions [P8] and [P16].
In [P8] three configurations (of which two corresponds to LT HP 3 and LT HP 4 of table 6.1) are examined in terms of performance at different temperature levels than 40/22 °C (forward/return temperatures at the consumer - corresponds to 45/25 °C at the distribution network). It was shown that the primary side configuration presented higher energy and exergetic performance at most temperature levels, compared to the booster HP unit at secondary side. The specific layout of the LT DH booster HP unit with storage tank on primary side is presented in Fig. 6.1c.
The economic implications related to investment and operating cost for the consumers are investigated in [P16]. Levelised yearly cost were calculated from a consumer perspective, and compared to various energy cost schemes. Six different configurations were considered, including the three above mentioned layouts, along with various layouts of electric heaters cooperated with LT DH systems. From the cost perspective, it was not obvious that booster HP configuration (Fig. 6.1c) was the most beneficial concept under current technology or energy prices scheme for the private consumers, or based on future socio-economic cost. Combined electric and DH water heater in the DH water tank was the competing technology, which proposes a compromise between low investment cost and increased operating cost. Small changes to electricity prices may however change the advantage towards the booster HP configurations.

6.3 Impact to system performance from lowering district heating temperatures

To assess the implications of lowering temperature levels in the DH network of Greater Copenhagen [P7], the variable performance characteristics of power plants as well as other types of utility units were calculated and analysed using thermodynamic models to represent the actual units. The changed performance parameters for various utility units are presented in Fig. 6.2a to 6.2d.
It is seen that the performance changes are of different magnitude for various technologies and miscellaneous performance parameters. For both extraction and backpressure CHP units, minor impact were experienced for the total efficiency of the unit, whereas it was considered significant for the combined cycle technology. Large variations were found for the COP of SF configuration HP units. If calculated as a ratio to the thermodynamic limit, the changes would be much lower. Further, the temperature difference between forward and return has an effect on the capacity of DH network pipelines and storage volumes. The temperature of forward and return lines follow that presented in Fig. 2.3.

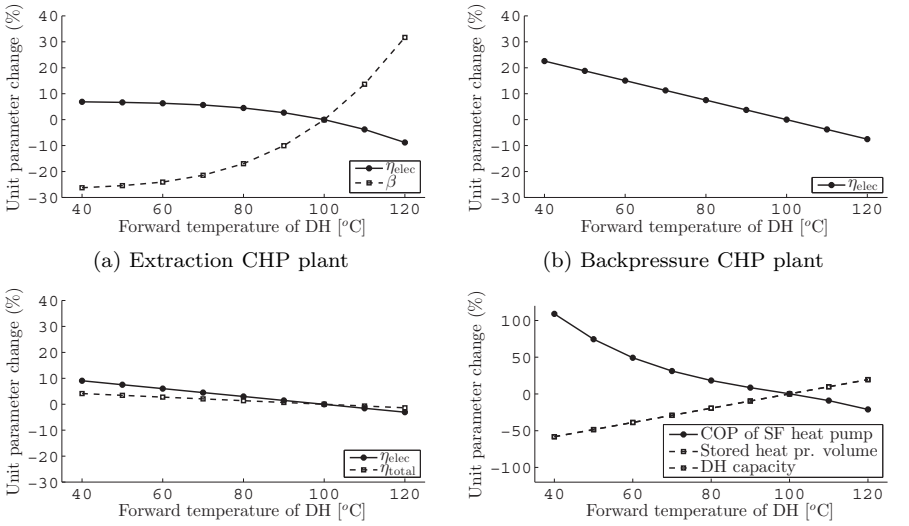

(a) Extraction CHP plant

(b) Backpressure CHP plant

(c) Combined cycle CHP plant

(d) Heat pump and changed temperature of DH

Figure 6.2: Changed performance parameters of three CHP types, HP and changed temperatures in DH network. Source: [P7]

The temperatures of the DH network forward and return streams correspond to the location of the utility unit (T_F and T_R) in Fig. 6.3. In the considered network, the heat is supplied from the utility plant to a transmission network, which transfers the heat to smaller distribution grids.

The heat losses for transmission and distribution were determined individually for 2011 as 2 % and 15 % respectively (Centralkomunernes Transmissionsselskab I/S, 2013; Dansk Fjernvarme, 2013). The transmission network is operated at 100-115 °C forward temperature, and 50-55 °C return temperatures. By assuming that the losses correspond to transmission network operation at 100 °C and 50 °C for forward and return temperatures, it was possible to find the heat transfer coefficient for each network, an thus the heat losses at changed temperature configurations.

For the case where the forward temperature at the location of the consumer T_C is lower than 55 °C (hot tap water requirement), it was assumed that booster HP units are installed in each dwelling, and operates according to the determined energetic performance which can be achieved for the temperature set (T_C and T_R) according to section 6.2.

In Fig. 6.4, a segment of the results of [P7] is presented. Fig. 6.4a show a comparison of the two energy scenarios based on the combined system cost (consumer cost) of both electricity and heat, as well as heat and electricity

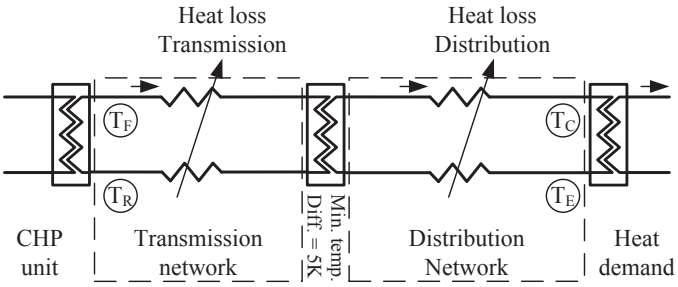

Figure 6.3: Schematic diagram of DH system with transmission and distribution networks. Source: [P7]

carbon emissions. The DH forward temperature is varied for both scenarios between 40 to 110 °C, with results presented as relative differences to the current scenario at 100 °C. Variations to the investigated parameters are presented with black for current scenario, and with gray lines for energy scenario of 2025 (future).

Although only separated by 14 years, the two energy system scenarios are quite different for the three parameters. The future scenario presented significantly increased system cost (typically approximately 14-15 % increase) but at the same time significantly reduced heat and electricity CO_2-emissions. The reductions in emissions were minimum 52 % for heat and 58 % for electricity.

The reference data (black) for cost and CO_2-emissions in Fig. 6.4a, are similar to those presented in Fig. 6.4b. It was found, that for the current technology mix, system costs were at a minimum for 60 °C. The minimum is caused by a improvement in utility technology at lower DH temperatures, which is reversed at low supply temperatures due to the increase in electricity demand from booster HP configurations, and the corresponding increase in taxes for electricity used for heating purposes. Considering carbon emissions for both heat and electricity, the minimum was observed at 50 °C and 60 °C respectively. In the paper [P7] both primary energy consumption and net. import of electricity is presented for all the considered cases. The general trend is, that primary energy consumption in DK2 is reduced for further reductions in temperature, whereas the electricity import is at its minimum at approximately 60 °C.

On the aspect of improving the performance for renewable technologies at lower forward temperatures, 200 MW HP (SF) capacity was introduced (in the paper). The consumer cost was reduced in most cases, and increasingly reduced for lower DH forward temperatures. It was shown that in some cases, the optimum for consumer cost and carbon emissions were moved towards lower temperatures, indicating that systems with LT DH benefit more from integrat-

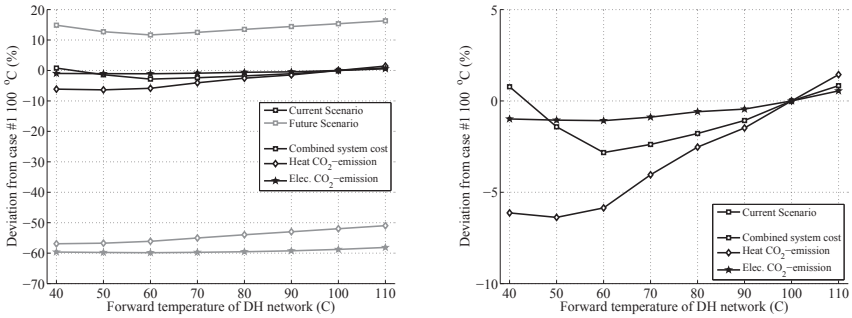

(a) Current and future energy scenario: System cost and CO_2 emissions

(b) Zoom of current energy scenario: System cost and CO_2 emissions

Figure 6.4: Comparison of system cost and CO_2 emissions for current and future energy system scenarios

ing renewable heat technologies than systems operating at conventional DH temperatures.

6.4 Summary

Low temperture DH networks and booster HP units have been proposed as a means to improve both current and future energy systems.

Eight configurations for supply of heat for tap water and space heating in a district heating system was examined with focus on energy, exergy and cost efficiency. The cost of heat from best to worst configurations was annually between 690 €and 970 €. The conventional systems presented better exergy utilisation than low temperature solutions, as the decrease in heat loss does not compensate the electricity demand to cover the energy consumption. This suggests that solutions where LT DH are feed by conventional transmission networks are poor in comparison with regular distribution networks. If possible the network temperature should be lowered to the limit where hot tap water may still be supplied (Conv. 3).

Three booster HP configurations were compared in terms of exergy efficiency, electricity consumption and DH heat flow, for a range of forward and return temperatures. One HP configuration presented improved performance compared to the alternatives at most temperature levels. An economic comparison showed, that at current energy prices, a similar configuration with an electric heater instead of HP was competitive due to the lower investment costs.

An analysis was performed with the assumption that lowered temperatures may result in lowered transmission network temperatures. The influence of DH network temperatures to the performance of utility production in Greater

Copenhagen is investigated for forward temperatures between 40 to 110 °C. Two energy scenarios were considered, one current, which was a validated for 2011, and a future scenario, as proposed by energy planners for 2025, where reductions in carbon emissions for heat is of major interest.
Compared to the current, the future scenario resulted in increased cost for consumers by approximately 15 %, but carbon reductions above 50 % for both electricity and heat. It was found, that for the current technology mix, system costs are at a minimum for 60 °C, which implies that booster HPs are needed, but only for a very limited temperature boost.
Integration of central HP became increasingly beneficial with reductions in DH temperatures. In a current scenario with central HPs installed, cost reductions of approximately 4-5 % may be achieved, which further reduces carbon emissions from DH by more than 15 %. For future scenarios, cost reductions were further increased, but reductions in carbon emissions were barely possible with the considered HP technology. For both cases the maximal reduction of consumer cost was found for 60 °C.
By integration of further sources of renewable heat, it is likely that optimum may shift to lower tempearutres for such systems. Further analysis is required to assess the possible capacity and availability of the renewable heat source.

Chapter 7

Concluding remarks

The presented study has focused on a number of areas related to integration of heat pumps in district heating networks, where a large part of the heat demand is supplied by various types of combined heat and power units.

Based on outlines from the subsidary subjects, the study has lead to a number of findings and recommendations, of which some may be the focus of further studies.

7.1 Summary of findings

7.1.1 HP in cooperation with CHP units

Several renewable and non-renewable heat sources were proposed in various locations of the network. None of the proposed sources can be utilised without disadvantages such as fluctuations in capacity or temperature, intermittent availability or high investment cost. The location of the heat source may further influence the feasibility due to several considerations: Co-location with transmission or distribution facilities, availability of various fuels and possible storage options.

Five configurations were investigated in order to analyse the optimal performance in cooperation with typical combined heat and power technologies. The analysis focussed on key performance factors chosen to indicate the performance from a system perspective. Two configurations (SD and SR) proposed the highest coefficient of system performance and lowest cost of fuel for the DH network temperatures evaluated. The highest coefficient of system performance was for SR configuration with electric motor in a 70°C - 35°C DH network, where the $COSP_{elec}$ is reaching approximately five. The results recommend further analysis of three configurations with high COSP, of which two are located centrally and one (SD) is located at the location of the demand (dwelling).

7.1.2 Competitive HP configurations

By investigation of four sink/source working domains, it was found that sink temperatures of up to 120 - 140 °C and temperature lifts 40 - 60 K can be achieved with positive NPV by a combination of VCHP and HACHP systems. For most of the vapour compression systems of the analysis, the maximal achievable temperature lift was limited by the economic profitability constraint. For the technologies utilising R717, both considering VCHP and the HACHP technology, a technical constraint (the discharge temperature) limited the applicability in terms of temperature lift. The NPV constraint of these systems allowed much higher temperature lifts than any of the alternatives.

The single stage VCHP and HACHP were compared to VCHP operated in series. The results showed that such systems may be used to expand working domains, in cases where key constraints may be bypassed, but with a reduction in NPV compared to a single heat pump unit.

The results of the working domain analysis showed, that the current requirements for SF configuration HPs are not covered by the working domains. Typical temperature lifts are of a magnitude where it is only possible to produce heat to 80 °C with positive NPV (the HACHP). The main reason for lack of feasible domains was the requirement of a positive NPV.

Eight heat pump units were compared for their economic and energetic performances as SF and SR configurations in a district heating network. For a fixed case with set pinch temperatures it was found, that the cost of heat varies significantly between the considered feasible configurations, and is thus a superior selection criteria compared to the COP, which was similar for most of the considered HPs. For units with low investment cost, the share of total cost of heat from taxes exceeded 50 %.

For each of the examined temperature levels and working fluid configurations exergo-economic optimisation was performed to present a fair comparison to the heat pump units where the previously predefined pinch temperature was not economically advantageous. Results showed, that units utilising R717 as working fluid presented significantly lower levelised cost rates than the alternatives. For the SF integration, five different units were preferable in individual areas of the working domain. In the case of SR, the R717-LP was advantageous in a large area of the working domain, but in the areas limited by technical constraints, three other configurations should be utilised, each in separate small working domains.

The investment cost for heat pump integration SR and SF were similar in magnitude and show similar trends for various working fluids for both configurations. The differences between low and high investment cost correspond approximately to a factor of 2-2.5.

In some of the considered cases taxes represented more than 50 % of the levelised cost of heat from both SF and SR heat pumps. High taxes may be seen as a restriction for large scale integration of HPs in the current energy system.

In case of HFC and HFO working fluid phaseout the recommendation for best available technology changed to an increased working domain for R600a. For the SF configuration the increase in cost was found to be in the order of 3 to 12 %. In terms of COP the differences were smaller, and in many cases in favour of R600a.

7.1.3 Energy system modelling

Three frequently used operation optimisation methods were examined, in order to investigate their impact on operation management of energy system technologies. By focussing on the physical representation of a CHP-plant, it was clear that a simple representation allows infeasible production. Using MIP or NLP optimisation, the number of operation hours and the total production of heat from HPs were significantly increased, as the HPs may be used to shave the load patterns of CHP units in significantly constrained energy systems.
A MIP energy system model was developed with focus on the detail level of features for representation of CHP units. Two energy scenarios were considered, one current, which is a validated model for 2011, and a future scenario, as proposed by energy planners for 2025, where reductions in carbon emissions for heat is of major interest.
Three different HP configurations were integrated (100 MW capacity) in the network. The operational difference for the total energy system was considered based on three performance criteria. For current network, only few of the considered configuration and temperature combinations increased the total energy efficiency, but in 2025 the integration of central HPs was typically found to be beneficial for the system efficiency in all cases.
In terms of consumer cost, the integration of central HPs was typically an advantage. Similarly for carbon emissions of heat, which decreases for all (but one) considered heat pump integration scheme. This was contrary to integration of individual HPs in dwellings, which tend to reduce system efficiency and increase consumer cost.
Compared to the current, the future scenario resulted in increased cost for consumers by approximately 15 %, but carbon reductions above 50 % for both electricity and heat. Further reduction in carbon may be achieved by reducing carbon footprint from waste.

7.1.4 Low temperature DH analysis

Low temperture DH networks and booster HP units have been proposed as a means to improve both current and future energy systems. The results suggest, that solutions where LT DH is feed by conventional transmission networks are poor in comparison with regular distrubution networks. If possible the network temperature should be lowered to the limit where hot tap water may still be supplied (Conv. 3).

If, on the contrary, the power plants and additional technologies for utility production are affected by significant changes to the transmission DH temperature, it is likely that LT DH systems with booster DH units are part of a future high effective energy system. An analysis was performed for forward temperatures between 40 to 110 °C. The impact to cost from reducing DH temperature were largest in cases where significant capacity of renewable sources for DH were installed. Increase in renewable capacity were possible for both cases.

7.2 Future work

The approach presented in the thesis and the papers is considered to be promising in terms of evaluation and comparison of individual integration possibilities. Various interdependencies are proposed, of which most of them may be further investigated using the developed tools and methods.

7.2.1 Short term

The below recommendations for future work may be considered short term perspective due to their short duration or ongoing/planed activity.

- With further integration of renewable electricity in the network, it may become increasingly important to assess the influence of control choices for intermittent technologies. Similar considerations may be required for decentral installations, which already today present some degree of operation flexibility due to increasing capacity of heat pumps and large heat storages.

- For the comparison of HP working domains a few additions should be made. Two of the key encountered constraints may possibly be met by considering two stage compression. Two stage compression may increase efficiency of selected cycles and reduce the discharge temperature of compression. The latter is considered a significant limitation for introduction of HPs in DH, as it eliminates the possibility to utilise R717 configurations, which is the most promising HP cycle in terms of levelised cost.

- The performance of the ammonia-water hybrid absorption-compression HP should be considered for the possible DH cases of chapter 4. Based on the results of working domain analysis, it is considered likely that the HACHP may benfit in terms of cost of heat and performance.

7.2.2 Medium and long perspectives

The following recommendations for future work require detailed analysis of the considered topics, and are at the time of writing not further planned.

- Methods to increase the allowable discharge temperatures of compressors for R717 working fluid should be considered. Alternatively it may be handled by discharge temperature reduction, but some of the presently utilised cycle configurations tend to reduce the thermodynamic performance of the unit and increase the investment. The economic analysis for working domains (chapter 3) and central DH HP configurations (chapter 4) show that the use of this technology in a broader temperature range may improve cost and efficiency of HP configurations in DH.

- The various models for optimisation of energy systems, including the one developed in this project, assume HPs to operate at fixed performance for part load operation. Typically it is also considered to be allowed to operate at very low loads or perform start-ups without delay. The operation limits and the performance at reduced load should be analysed and implemented in energy system modelling. It is likely that some configurations and/or working fluids present performance improvements compared to the economically optimal steady state configuation. This analysis should also include the technology of the HACHP, where solution differences may be used to improve performance.

- A mapping of available heat sources for HP technology in Greater Copenhagen area. By analysing all plausible configurations for DH HP integration, with appropriate taxes according to the heat source, it is likely that individual configurations reveal performance benefits, which are not considered today.

- Different HP taxation schemes may be utilised to achieve a fixed revenue but with various influences to the operational performance. It is possible that the current taxation scheme may be considered a limitation to achieve an efficient energy system. By examination of energy system efficiency for changed taxation schemes, the contribution to performance and taxation revenue may be illdisposed for the individual technologies. A key constraint to the optimisation can be net taxation revenue as current system, or calculation of optimal consumer economy.

- Investigation of the heat transfer properties and pressure drops for condensation of refrigerant in plate heat exchangers at elevated temperatures. An experimental set-up was produced during the project, which is currently in an initial testing phase. The possible experiments using the setup are expected to be a significant contribution.

Bibliography

Annex-21, 1995. Industrial Heat Pumps - Experiences, potential and Global Environmental Benefits. IEA Heat Pump Centre.

ARC, 2012. Environmental reports (in danish: Miljøredegørelse). URL: http://www.a-r-c.dk/media/123663/miljoredegorelse_2012-pdf-.pdf. [accessed 23.03.14].

Bach, B., 2014. Integration of Heat Pumps in Greater Copenhagen. Master's thesis. Technical University of Denmark.

Bejan, A., Tsatsaronis, G., Moran, M., 1996. Thermal Design & Optimization. 1'st edition ed., John Wiley & Sons, New York.

Berntsson, T., 2002. Heat sources - technology, economy and environment. International Journal of Refrigeration 25, 428–438.

Bitzer Kühlmaschinenbau GmbH, 2014. Semi-hermetic reciprocating compressors. URL: https://www.bitzer.de/documentation/kp-104-3.pdf. [accessed 03.03.15].

Blarke, M.B., 2012. Towards an intermittency-friendly energy system: Comparing electric boilers and heat pumps in distributed cogeneration. Applied Energy 91, 349–365.

Blarke, M.B., Lund, H., 2007. Large-scale heat pumps in sustainable energy systems: System and project perspectives. Thermal Science 11, 143–152.

Brunin, O., Feidt, M., Hivet, B., 1997. Comparison of the working domains of some compression heat pumps and a compression-absorption heat pump. International Journal of Refrigeration 20, 308.

Centralkomunernes Transmissionsselskab I/S, 2013. Technical key figures (in danish: Tekniske nøgletal). URL: http://www.ctr.dk/teknik.aspx. [accessed 02.02.15].

City Council of Copenhagen, 2013. CPH climate plan 2025 (in danish: KBH 2025 klimaplan - en grøn, smart og CO2-neutral by.). URL: http://cityclimateleadershipawards.com/copenhagen-cph-climate-plan-2025/. [accessed 25.03.14].

Connolly, D., Lund, H., Mathiesen, B.V., Leahy, M., 2010. A review of computer tools for analysing the integration of renewable energy into various energy systems. Applied Energy 87, 1059–1082.

CTR, HOFOR and VEKS, 2014a. Heat plan greater copenhagen 2 - options for CO2-neutral distict heating (in danish: Varmeplan hovedstaden 2 - handlemuligheder for en CO2-neutral fjernvarme). URL: http://www.varmeplanhovedstaden.dk/publikationer-og-moeder. [accessed 25.03.14].

CTR, HOFOR and VEKS, 2014b. Heat plan greater copenhagen 3 (in danish: Varmeplan hovedstaden 3). URL: http://www.varmeplanhovedstaden.dk/publikationer-og-moeder. [accessed 25.03.14].

Danish Energy Agency, 2011. Assumptions of socio- economic analysis in the energy sector [in danish: Forudsætninger for samfunds- økonomiske analyser påenergiområdet]. [accessed 10.10.13].

Danish Government, 2011. Government platform (in danish: Regeringsgrundlag). URL: http://www.stm.dk/publikationer/Et_Danmark_der_staar_sammen_11/Regeringsgrundlag_okt_2011.pdf. [accessed 25.03.14].

Danish Standards, 2009. Code of practise for domestic water supply installations (ds 439).

Danmarks Meteorologiske Institut, 2015. hourly temeprature data for roskilde and copenhagen in 2011. URL: http://www.dmi.dk/vejr/arkiver/maanedsaesonaar/. [accessed 13.01.15].

Dansk Fjernvarme, 2013. Benchmarking, statistics 2011/2012 (in danish: Benchmarking, statistik 2011/2012). URL: http://www.fjernvarmen.dk/Faneblade/HentMaterialerFANE4/~/media/Publikationer/Aarsstatistikker/BenchmarkingStatistik20112012.ashx. [accessed 26.09.13].

DONG Energy, 2012. Environmental reports 2011. URL: http://assets.dongenergy.com/DONGEnergyDocuments/com/Business%20Activities/Thermal%20Power/Environmental_Reports/2011/. [accessed 23.03.14].

DONG Energy, 2013. Thermal unit operation data - non-disclosure agreement. URL: http://www.dongenergy.com/en/business-activities/thermal-power. private communication.

DONG Energy, 2015. Annual report 2014 - Green, Independent and Cost-effective Energy. URL: http://assets.dongenergy.com/DONGEnergyDocuments/com/Investor/Annual_Report/2014/dong_energy_annual_report_en.pdf.

Energinet.dk, 2011. Download of market data - elspot price, capacity on transmission lines etc. URL: http://www.energinet.dk.

Energinet.dk, 2012a. Ancillary services to be delivered in denmark:tender conditions (in danish: Systemydelser til levering i danmark: Udbudsbetingelser). URL: http://www.energinet.dk.

Energinet.dk, 2012b. Energinet.dk Analytic prerequisites 2012-2035 [in danish: Energinet.dk's analyseforudsætninger 2012-2035]. Technical Report 1.

Energinet.dk, 2013. Introduction to system services (in danish: Introduktion til systemydelser, dok. 43532-13, sag 13/208). URL: http://www.energinet.dk.

Energinet.dk, 2014. Environmental statements 2004-2014 (in Danish: Miljødeklarationer 2004-2014). Technical Report 1. URL: http://www.energinet.dk/DA/KLIMA-OG-MILJOE/Miljoedeklarationer/Sider/Miljoedeklarering-af-1-kWh-el.aspx.

Energinet.dk, 2015. Guidelines for environmental statement of electricity (in Danish: Retningslinjer for miljødeklarationen for el). Technical Report 1. URL: http://www.energinet.dk/SiteCollectionDocuments/Danske%20dokumenter/Klimaogmiljo/Retningslinjer%20for%20milj%C3%B8deklarationen%20for%20el.pdf.

European Parliament, 2014. On fluorinated greenhouse gases and repealing regulation. The european parliament and the council of the european union.

Ferris, M.C., 2007. MATLAB and GAMS: Interfacing Optimization and Visualization Software. Technical Report 1.

GAMS Development Corporation, 1998. General algebraic modeling system. URL: http://www.gams.com/.

GEA Bock GmbH, 2012. Bock Open Type Compressors F. URL: http://www.bock.de/media/files/PDF/Kataloge/F-Catalog-_Gb.pdf. [accessed 03.03.15].

Granryd, E., 2005a. Refrigerating Engeneering - part I. Royal Institute of technology, KTH, Stockholm.

Granryd, E., 2005b. Refrigerating Engeneering - part II. Royal Institute of technology, KTH, Stockholm.

Gullev, L., 2006. The danish district heating history. Euroheat and Power (English Edition) 3, 24–29.

Hedegaard, K., Mathiesen, B.V., Lund, H., Heiselberg, P., 2012. Wind power integration using individual heat pumps - analysis of different heat storage options. Energy 47, 284–293.

Hendriksen, N.P., 2014. Utilization of waste heat from the industry. Master's thesis. Technical University of Denmark.

HOFOR, 2012. price of district heating 2012 (in danish: Prisen pÃ¥ fjernvarme 2012). URL: `http://www.hofor.dk/fjernvarme/prisen-pa-fjernvarme-2012-for-private/`. [accessed 25.03.15].

HOFOR A/S, 2012. Consumption of district heating in 2011. URL: `http://www.hofor.dk/`. [accessed 02.02.15].

HOFOR A/S, 2015. Environmental statement 2011 (in danish: Miljødeklaration 2011). URL: `http://www.hofor.dk/baeredygtige-byer/beregn-co2/miljodeklaration-2011/`. [accessed 25.03.14].

Hubeck-Graudal, H., 2015. Feasibility of using the copenhagen drinking water supply as a heat source in the district heating network. Master's thesis. Technical University of Denmark.

Hultén, M., Berntsson, T., 1999. The compression/absorption cycle - influence of some major parameters on cop and a comparison with the compression cycle. International Journal of Refrigeration 22, 91–106.

Hultén, M., Berntsson, T., 2002. The compression/absorption heat pump cycle - conceptual design improvements and comparisons with the compression cycle. International Journal of Refrigeration 25, 487–497.

IBM, 2009. IBM ILOG CPLEX. URL: `www.ibm.com`.

Jensen, J., Reinholdt, L., Markussen, W., Elmegaard, B., 2014. Investigation of ammonia/water hybrid absorption/compression heat pumps for heat supply temperatures above 100 °C.

Jensen, J.K., Ommen, T., Markussen, W.B., Reinholdt, L., Elmegaard, B., 2015. Technical and economic working domains of industrial heat pumps 2: Ammonia-water hybrid absorption-compression heat pumps. International Journal of Refrigeration .

Kaniadakis, G., 2014. Comparison of absorption and vapor compression heat pumps integrated in combined heat and power. Master's thesis. Technical University of Denmark.

KARA/NOVEREN I/S, 2012. Environmental reports (in danish: Grønne regnskaber). URL: `http://karanoveren.dk/karanoveren/organisation/groenne-regnskaber`. [accessed 23.03.14].

Karlsson, K., Meibom, P., 2008. Optimal investment paths for future renewable based energy systems-using the optimisation model balmorel. International Journal of Hydrogen Energy 33, 1777–1787.

Linnhoff, B., Hindmarsh, E., 1983. The pinch design method for heat exchanger networks. Chem. Eng. Sci. 38, 745–763.

Lorenz, V.H., 1894. Die ausnützung der brennstoffe in den kühlmaschinen. Zeitschrift für die gesammte Kälte-Industrie 1, 10–15.

Lowe, R., 2011. Combined heat and power considered as a virtual steam cycle heat pump. Energy Policy 39, 5528–5534.

Lund, H., Clark, W.W., 2002. Management of fluctuations in wind power and CHP comparing two possible Danish strategies. Energy 27, 471–483.

Lund, H., ller, B.M., Mathiesen, B.V., Dyrelund, A., 2010. The role of district heating in future renewable energy systems. Energy 35, 1381. URL: `http://www.sciencedirect.com/science/article/pii/S036054420900512X`.

Lund, H., Werner, S., Wiltshire, R., Svendsen, S., Thorsen, J.E., Hvelplund, F., Mathiesen, B.V., 2014. 4th generation district heating (4GDH). integrating smart thermal grids into future sustainable energy systems. Energy 68, 1–11.

Malinowska, W., Malinowski, L., 2003. Parametric study of exergetic efficiency of a small-scale cogeneration plant incorporating a heat pump. Applied Thermal Engineering 23, 459–472.

Mancarella, P., 2009. Cogeneration systems with electric heat pumps: Energy-shifting properties and equivalent plant modelling. Energy Conversion and Management 50, 1991–1999.

Martínez, M.V., 2015. Integration of Heat Pumps in Combined Heat and Power Plant. Bachelor thesis. Technical University of Denmark.

Meibom, P., Kiviluoma, J., Barth, R., Brand, H., Weber, C., Larsen, H., 2007. Value of electric heat boilers and heat pumps for wind power integration. Wind Energy 10, 321–337.

Münster, M., Morthorst, P.E., Larsen, H.V., k, L.B., Werling, J., Lindboe, H.H., Ravn, H., 2012. The role of district heating in the future danish energy system. Energy 48, 47.

Nord Pool Spot, 2013a. The power market. URL: `http://umm-archive.nordpoolspot.com/web/`. [accessed 02.02.15].

Nord Pool Spot, 2013b. Umm archive. URL: `http://www.nordpoolspot.com/How-does-it-work/`. [accessed 02.02.15].

Ommen, T., Markussen, C., Reinholdt, L., Elmegaard, B., 2011. Thermoeconomic comparison of industrial heat pumps, in: The 23rd IIR International Congress of Refrigeration - ICR 2011, pp. 1–8.

Ommen, T., Markussen, W.B., Elmegaard, B., 2014. Heat pumps in combined heat and power systems. Energy 76, 989–1000.

Ommen, T.S., Elmegaard, B., 2012. Exergetic evaluation of heat pump booster configurations in a low temperature district heating network, in: Desideri, U., Manfrida, G., Sciubba, E. (Eds.), The 25th International Conference on Efficiency, Cost, Optimization and Simulation of Energy Conversion Systems and Processes (Perugia, June 26th-June 29th, 2012), Firenze University Press.

Osenbrück, A., 1895. Verfahren zur Kälteerzeugung bei Absorptionsmaschinen. Deutsches Reichspatent [DRP 84084].

Prestmark, V., Schultz, J., 1984. Planning and design of a 15 MW geothermal heat pump installation in denmark, in: heat pumps for buildings, pp. 171–187.

Radermacher, R., Hwang, Y., 2005. Vapor Compression Heat Pumps with Refrigerant Mixtures. CRC Press.

Ravn, H., 2011. Addon unit commitment. URL: `http://www.balmorel.com/`. [accessed 25.03.14].

Ravn, H., Riisom, J., Schaumburg-Muller, C., 2005. A stochastic unit commitment model for a local chp plant, in: Power Tech, 2005 IEEE Russia, pp. 1–7.

Rinne, S., Syri, S., 2013. Heat pumps versus combined heat and power production as CO2 reduction measures in finland. Energy 57, 308–318.

SKAT, 2014. Examples for calculation of taxreduction for various heat production units (in danish: Eksempler på beregning af afgiftslempelse for forskellige varmeproduktionsanlæg). URL: `https://skat.dk/SKAT.aspx?oID=2061615`. [accessed 05.12.14].

Sørensen, T., 2014. Udnyttelse af industriel spildvarme. Bachelor thesis. Technical University of Denmark.

sparenergi.dk, 2015. Air to water heat pumps. URL: `http://sparenergi.dk/forbruger/vaerktoejer/varmepumpelisten`. [accessed 13.01.15].

Townsend, D., Linnhoff, B., 1983. Heat and power networks in process design. Part I: Criteria for placement of heat engines and heat pumps in process networks. AlChE J. 29, 742–748.

Tuohy, A., Meibom, P., Denny, E., O'Malley, M., 2009. Unit commitment for systems with significant wind penetration. IEEE Transactions on Power Systems 24, 592–601.

UN Ozone Secretariat, 2000. The Montreal Protocol on Substances that Deplete the Ozone Layer. United Nations Environment Programme.

Varmelast.dk, 2013. Heating plan (in danish: Varmeplaner). URL: `http://www.varmelast.dk/da/varmeplaner/varmeplaner`. [accessed 02.02.15].

Vattenfall A/S, 2012. Environmental reports 2011 (in danish: Grønne regnskaber 2011). URL: `http://corporate.vattenfall.dk/globalassets/danmark/om_os/gronne_regnskaber/amagervaerket-gront-regnskab-2013.pdf`. [accessed 23.03.14].

Verbruggen, A., 1982. A systemmodel of combined heat and power generation in district heating. Resources and Energy 4, 231–263.

Verbruggen, A., 2007. Combined heat and power (chp) essentials. International Journal of Energy Technology and Policy 5, 1–16.

Vestegnens Kraftvarmeselskab I/S, 2013. Current operationdata (in danish: Aktuelle driftdata). URL: `http://www.veks.dk/da/varmeproduktion/aktuelle-driftdata/driftdata`. [accessed 02.02.15].

Vestforbrænding, 2012. Measurement and results (in danish: Måling og resultater). URL: `http://www.vestfor.dk/web/10157/37@public`. [accessed 23.03.14].

Appendix A

Energy system model formulation

In the following appendix, the objective function and key technical and economical constraints are described for the developed energy system model. The described model is the result of adjustments according to the validation, and is used as a basis for obtaining the results of chapters 5 and 6.

A detailed system model was developed for calculation of economic and environmental impact of integrating heat pumps in an energy system with a high share of CHP plants and high shares of electricity from intermittent sources such as wind turbines. The objective of the research (as described in section 1.1) required adjustment of existing models (Connolly et al., 2010) or development of a tailored model. The result was a validated system model which features detailed representation of CHP technology as well as detailed representation of different heat pump technologies and integration possibilities.
The model was implemented in General Algebraic Modelling System (GAMS Development Corporation, 1998) using the mixed integer linear optimisation algorithm CPLEX (IBM, 2009). External data processing is handled by Matlab, using the interface gdxmrw (Ferris, 2007). The implementation of energy system layout (eg. CHP-units, heat pumps or transmission capacity) is generic and easy to change from one case to another.

Table A.1: Nomenclature for Appendix A

Variables	
$\dot{C}$	cost rate, €/h
c	cost factor, €/MWh or €
o	binary operation variable, -
P	power, MW
Q	quantity of heat in storage, MWh
r	ratio, -
UMM	availability input parameter, -
v	binary design input parameter, -
z	binary taxation input parameter, -

Greek symbols	
β	power loss factor by heat extraction, -
Δ	reduction, MJ/s
η	efficiency, -

Superscripts	
1	below the "no-loss" point
2	above the "no-loss" point
elec	electric
ex.	extraction
max	maximum
min	minimum
rel	relative to maximum

Subscripts	
f	other technologies
g	heat pumps
h	boilers
i	CHP plants
j	energy markets
k	thermal unit sites
l	transmission notes
m	transmission networks
n	distribution networks
o	heat pump sites in distribution networks
p	boiler sites in distribution networks

Abbreviations	
CHP	Combined Heat and Power
COP	Coefficient of Performance
HP(s)	Heat Pump(s)
HS	Heat storage
O&M	operation and maintenance
TL	transmission losses

A.1 Structure

The problem was considered over a period of time $\mathcal{T} = 1, \ldots, t$, which corresponds to the operation of the spot market. Relevant time periods are considered for a rolling horizon optimisation in [P1]. For each of the time periods, data for power plant load and the amount of stored heat at the termination of the period is passed on to the beginning of the subsequent period.
The heat and electricity demands of eastern Denmark were supplied as input to each of the time periods. In both cases the data series were obtained from transmission operators (i.e. without transmission- but including distribution losses) (Energinet.dk, 2011; Centralkomunernes Transmissionsselskab I/S, 2013; Vestegnens Kraftvarmeselskab I/S, 2013; HOFOR A/S, 2012). Besides the electricity demand, the electricity produced at decentral CHP-plants and by wind turbines in the region was supplied as an input (Energinet.dk, 2011). The deployment of historical data for seperate shares of the produced electricity, relies on the assumption that the production of electricity for such technologies is unaffected by the system operation. This limitation of the model, becomes increasingly critical with the introduction of heat pumps and large heat storages in decentral installations, as well as with increased flexibility for operation of wind turbines. Additionally, the cost of electricity in neighbouring areas, and the transmission capacity of import and export of the connections, was input to the model.
For the central thermal power plants, urgent market messages (UMM) are available from (Nord Pool Spot, 2013b). Such messages were included in the model, for the purpose of validation.

A.2 Objective function

The optimal production cost for the combined system can be achieved by minimisation of economic cost of the utility plant operation. When considering a system where capital cost can be considered as sunk cost, the objective function can be written as A.1.

$$\min \left[\sum_{t \in \mathcal{T}} \left(\sum_{i \in \mathcal{I}} (\dot{C}_{i,t}^{\mathrm{CHP}}) + \sum_{h \in \mathcal{H}} (\dot{C}_{h,t}^{\mathrm{boiler}}) + \sum_{g \in \mathcal{G}} (\dot{C}_{g,t}^{\mathrm{HP}}) + \sum_{f \in \mathcal{F}} (\dot{C}_{f,t}^{\mathrm{Other}}) + \sum_{j \in \mathcal{J}} (\dot{C}_{j,t}^{\mathrm{import}} - \dot{C}_{j,t}^{\mathrm{export}}) \right) \right] \quad \text{(A.1)}$$

Where $\dot{C}$ is the total cost rate of production at the individual plant. The cost rates include all cost associated with utility production (e.g. fuel, taxes and

subsidies) at the specific plant, and is further described in section A.3. The CHP units in the system are indexed by $\mathcal{I}$, boilers by $\mathcal{H}$, heat pumps by $\mathcal{G}$ and other heat and/or electricity production by $\mathcal{F}$. The neighbouring energy markets are indexed by $\mathcal{J}$.

A.3 Economic constraints

For most of the assessed technologies, the cost of utility production at an individual unit depends on the unit type, its efficiency, operation and maintenance cost and the type of fuel. Apart from direct fuel cost, the individual fuel types may further be affected by different taxation or subsidy schemes or by additional transportation and handling cost. The operation and maintenance cost included in the model correspond to the variable contribution.
Two different taxation schemes were used for electricity and heat production in the model. Taxes for electricity are placed on the consumption, where as taxes for heat are placed on the fuel. One reason for the difference, is that electricity is traded on Nord Pool Spot (2013a), where the competitive conditions for import and export across taxation boarders should not be misaligned. This implies that electricity cost is optimised without taxes and VAT. The heat production is optimised for low consumer cost, where fuel cost, O&M, taxes, CO_2 quota and electricity cost are included in the calculation (Varmelast.dk, 2013).
Several locations are used in the analysis. Traditional production areas for thermal units are indexed by $\mathcal{K}$. District heating transmission points (collection of streams) are indexed by $\mathcal{L}$. Transmission networks are indexed by $\mathcal{M}$ and the distribution networks by $\mathcal{N}$.
Due to the many possible locations for introduction of thermal units in a network, additional sets were created such as for heat pumps in distribution networks $\mathcal{O}$ and distribution network boilers $\mathcal{P}$.
In the following sections, the economic constraints are listed for individual unit types. Note that the description of power plants represents several types: extraction CHP, back pressure CHP and condensing power plants regardless of the specific technology configuration.

A.3.1 Power plants

The total cost rate of production at the individual plant was calculated based on various components. The method for calculation of the individual components was similar for most of the contributions. The total cost rate was calculated according to eq. A.2.

$$\begin{aligned}\dot{C}_{i,t}^{\mathrm{CHP}} =& \dot{C}_{i,t}^{\mathrm{fuel}} + \dot{C}_{i,t}^{\mathrm{CO_2}} + \dot{C}_{i,t}^{\mathrm{heattax}} \\ & - \dot{C}_{i,t}^{\mathrm{subsidy}} + \dot{C}_{i,t}^{\mathrm{VAT}} + \dot{C}_{i,t}^{\mathrm{startup/shutdown}} \qquad , i \in \mathcal{I}, t \in \mathcal{T}. \end{aligned} \tag{A.2}$$

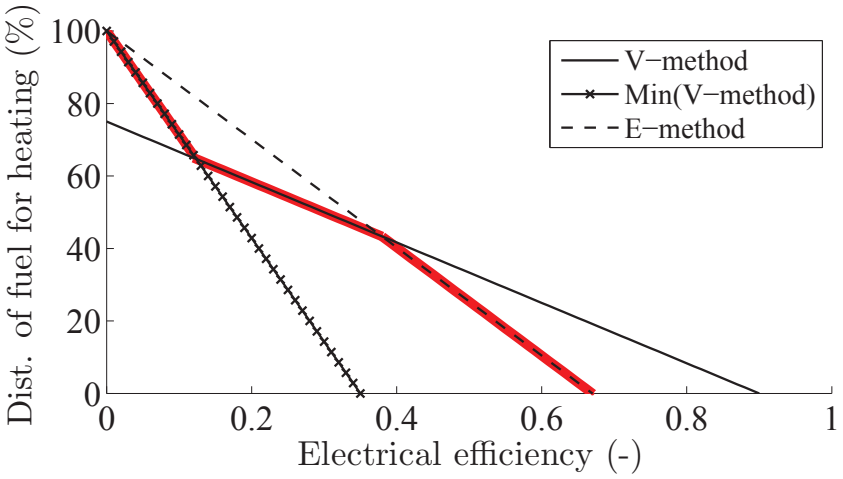

Figure A.1: Low distribution of fuel for heat production

The individual components of the total cost rate are dependent on the consumption of fuel and/or the production of electricity and heat. All of the individual contributions to the total cost rate for CHP units are required to be positive. In the case of fuel cost $\dot{C}_{i,t}^{\text{fuel}}$ the contributions are included in eq. A.3.

$$\dot{C}_{i,t}^{\text{fuel}} = c_i^{\text{fuel}} \cdot \dot{H}_{i,t} + c_i^{\text{O\&M}} \cdot P_{i,t} \qquad , i \in \mathcal{I}, t \in \mathcal{T}. \tag{A.3}$$

where $\dot{H}$ is the flow rate of enthalpy for combustion, and P is the produced electricity. The individual fuel cost factor c_i^{fuel} for the plants were calculated based on fuel type ([p7]) and transportation and handling cost (Danish Energy Agency, 2011). The cost factor for operation and maintenance c_i^{fuel} corresponds to the variable cost for utility production. A similar approach has been used to calculate the contribution from CO_2 quota $\dot{C}_{i,t}^{\text{CO}_2}$ and the contribution from subsidised fuels $\dot{C}_{i,t}^{\text{subsidy}}$.

Due to the above mentioned differences in taxation between electricity and heat, the operator of a CHP unit may choose (on a yearly basis) one of two calculation methods for distribution of fuel between the two utilities. The two distribution methods are named V and E. In neither case the fuel utilised for electricity production may exceed $P_{i,t}/0.35$. A visualisation of the two economic constraints is included as Fig. A.1. The full red highlighted line indicates the best choice of formula, if the purpose is to minimise fuel cost (and heat taxes) for the district heating consumers. The constraints are presented in eq. A.4 to

A.6.

$$\dot{C}_{i,t}^{\text{heattax}} \geq c_i^{\text{heattax}} \cdot \dot{Q}_{i,t}/1.2 \cdot (1 - z_i) \qquad ,i \in \mathcal{I}, t \in \mathcal{T}. \tag{A.4}$$

$$\dot{C}_{i,t}^{\text{heattax}} \geq c_i^{\text{heattax}} \cdot (\dot{H}_{i,t} - P_{i,t}/0.35) \cdot (1 - z_i) \qquad ,i \in \mathcal{I}, t \in \mathcal{T}. \tag{A.5}$$

$$\dot{C}_{i,t}^{\text{heattax}} \geq c_i^{\text{heattax}} \cdot (\dot{H}_{i,t} - P_{i,t}/0.67) \cdot z_i \qquad ,i \in \mathcal{I}, t \in \mathcal{T}. \tag{A.6}$$

where $\dot{Q}_{i,t}$ is the heat production of the CHP-plant, and c_i^{heattax} is the cost factor for taxes according to fuel and plant type. z_i is a binary input parameter used to classify if the plant is running according to V- or E-method.
The cost rate of VAT $\dot{C}_{i,t}^{\text{VAT}}$ collects the contributions of VAT for the heat production.
The cost rates for startup and shutdown were calculated as presented in eq. A.7.

$$\begin{aligned} \dot{C}_{i,t}^{\text{startup/shutdown}} =& c_i^{\text{startup}} \cdot o_{i,t}^{\text{startup}} + c_i^{\text{shutdown}} \cdot o_{i,t}^{\text{shutdown}} \\ & , o_{i,t}^{\text{startup}}, o_{i,t}^{\text{shutdown}} \in \{0,1\}, i \in \mathcal{I}, t \in \mathcal{T}. \end{aligned} \tag{A.7}$$

The cost c_i^{startup} and c_i^{shutdown} represents the variable cost of changing the operation between on and off. The binary variables $o_{i,t}^{\text{startup}}$ and $o_{i,t}^{\text{shutdown}}$ are controlled by the optimisation algorithm, and further described in section A.5.

A.3.2 Heat boilers

The employed method for calculation of the heat boilers was similar to the approach utilised for section A.3.1. The calculation of the total cost rate is presented in eq. A.8.

$$\dot{C}_{h,t}^{\text{boiler}} = \dot{C}_{h,t}^{\text{fuel}} + \dot{C}_{h,t}^{\text{CO}^2} + \dot{C}_{h,t}^{\text{heattax}} + \dot{C}_{h,t}^{\text{VAT}} \qquad ,h \in \mathcal{H}, t \in \mathcal{T}. \tag{A.8}$$

All of the individual contributions to the total cost rate for boilers are required to be positive. The fuel cost was calculated based on fuel consumption and the production-dependent element of the operation and maintenance cost, which corresponds to the produced heat.

$$\dot{C}_{h,t}^{\text{fuel}} = c_h^{\text{fuel}} \cdot \dot{H}_{h,t} + c_h^{\text{O\&M}} \cdot \dot{Q}_{h,t} \qquad ,h \in \mathcal{H}, t \in \mathcal{T}. \tag{A.9}$$

A similar approach was used to calculate the cost rates for the remaining elements of eq. A.8. In the case of heat boiler, the full consumption of fuel was used for calculation of heat taxes.

A.3.3 Electricity-driven heat pumps

In the case of electricity-driven heat pumps, the total cost rate does not include the cost of consumed electricity, as the electricity is covered by other elements

of the objective function eq. A.1 and by the energy balances in section A.4. The remaining elements are presented in Eq. A.10.

$$\dot{C}^{\mathrm{HP}}_{g,t} = \dot{C}^{\mathrm{O\&M}}_{g,t} + \dot{C}^{\mathrm{heattax}}_{g,t} + \dot{C}^{\mathrm{VAT}}_{g,t} \qquad , g \in \mathcal{G}, t \in \mathcal{T}. \tag{A.10}$$

All of the individual contributions to the total cost rate for HP units are required to be positive. The contribution from O&M corresponds to the variable expenses of operating a heat pump. For the case where the heat pump uses electricity supplied from the distribution grid, a network tariff is used, in order to take the distribution losses of such networks into account.

$$\dot{C}^{\mathrm{O\&M}}_{g,t} = c^{\mathrm{O\&M}}_{g} \cdot \dot{Q}_{g,t} + c^{\mathrm{networktariff}}_{g} \cdot P_{g,t} \qquad , g \in \mathcal{G}, t \in \mathcal{T}. \tag{A.11}$$

For electric heat pumps, the method for determination of heat taxes is chosen by the operator of the unit. Two methods are applicable depending on the COP of the unit. A graphical representation is presented in Fig. A.2 (SKAT, 2014). The cross between electric element law and the taxation for heat pump operating under DH conditions (2012) is approximately at COP = 2.3 (-). In the analysis, all heat pumps are operated according to the changed rules from 2012. In the case where electric elements are considered, the electric element taxation (2008) is applied.

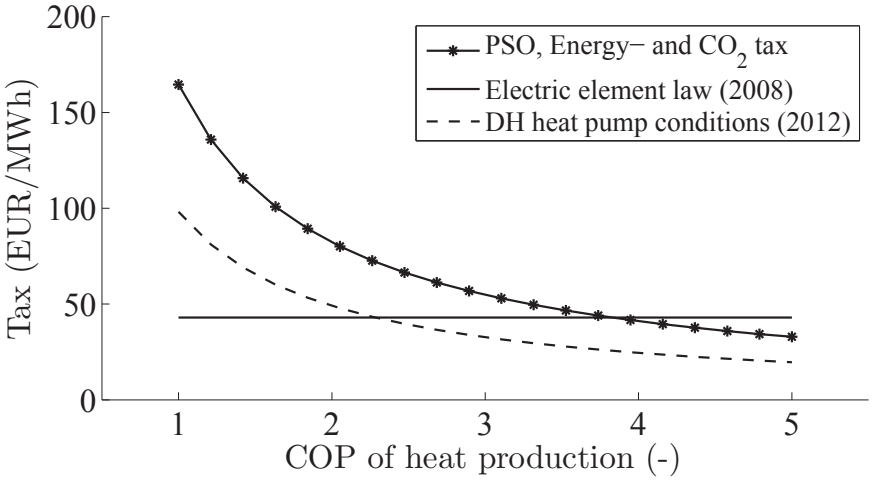

Figure A.2: Taxation schemes for electric heat pumps

A.3.4 ICE-driven heat pumps

In the case of heat pumps driven by use of ICE, the total cost rate is calculated according to A.12.

$$\dot{C}_{g,t}^{\mathrm{HP}} = \dot{C}_{g,t}^{\mathrm{fuel}} + \dot{C}_{g,t}^{\mathrm{CO_2}} + \dot{C}_{g,t}^{\mathrm{heattax}} + \dot{C}_{g,t}^{\mathrm{VAT}} \qquad , g \in \mathcal{G}, t \in \mathcal{T}. \tag{A.12}$$

In this case the cost rate of CO_2 and heattax were calculated based on the flow rate of enthalpy for combustion. All of the individual contributions to the total cost rate for ICE driven HP units are required to be positive. The calculation of fuel is presented in eq. A.13.

$$\dot{C}_{g,t}^{\mathrm{fuel}} = c_g^{\mathrm{fuel}} \cdot \dot{H}_{g,t} + c_g^{\mathrm{O\&M}} \cdot \dot{Q}_{g,t} \qquad , g \in \mathcal{G}, t \in \mathcal{T}. \tag{A.13}$$

The cost rate of fuel for an ICE operated heat pump, is thus calculated similarly to heat boilers in section A.3.2.

A.4 Electricity and heat balances

In modern energy systems, significant effort is put on balancing of the production and demand at correct location and time. The electricity transmission grid within the bidding area was modelled as one uniform network without bottlenecks for either of the utility units.
The electricity demand P_t^{consumer} including distribution losses was used for the analysis in the electricity balance eq. A.14.

$$P_t^{\mathrm{transmission}} - \sum_{g \in \mathcal{G}} P_{g,t} - \sum_{j \in \mathcal{J}} P_{j,t}^{\mathrm{export}} = P_t^{\mathrm{consumer}} \qquad , t \in \mathcal{T}. \tag{A.14}$$

where $P_t^{\mathrm{transmission}}$ is the flow of electricity from the transmission network.
The transmission is supplied by thermal units, wind turbines and import of electricity.

$$\sum_{i \in \mathcal{I}} P_{i,t} + P_t^{\mathrm{other}} + \sum_{j \in \mathcal{J}} P_{j,t}^{\mathrm{import}} = P_t^{\mathrm{transmission}} / (1 - \eta_{\mathrm{TL}}) \quad , t \in \mathcal{T}. \tag{A.15}$$

In this way all electricity flows into the network are subject to losses. The magnitude of transmission losses (η_{TL}) was determined based on historical data following a similar procedure. Both import and export of electricity are further constrained by the interconnection capacity of the two bidding areas. All of the variables in eq. A.14 and A.15 are required to be positive.
The heat balances used in the analysis followed a similar setup. The transmission network for heat is split into several areas, with detailed knowledge of the transmission capacity between each area. Opposite to the electricity demand, the heat demand is split into appropriate locations, according to the

detailed data from the transmission operators. The demand areas are denoted by $\mathcal{N}$ = {CTR, DSVM, DHCV, VEKS, VF1, SJ1, SJ2, NN}. The central CHP-plants are located at production locations $\mathcal{K}$ = {AMV1, AMV3, HCV, SVM, LYN, AMF, AVV, KARA, VF, ASV, NN}, which are not coherent with the demand areas. Other areas exist such as transmission points $\mathcal{L}$ and transmission areas $\mathcal{M}$ (location of heat storages), but individual data for these areas are not further addressed in this section. For all of the considered areas presented, energy balances ensure logic distribution and prevent accumulation in areas without storage options. Two examples of heat balances are presented for introduction of units in transmission and distribution networks in eq. A.16 and eq. A.17.

$$\sum_{i\in\mathcal{I}} \dot{Q}_{i,k,t} + \sum_{h\in\mathcal{H}} \dot{Q}_{h,k,t} + \sum_{g\in\mathcal{G}} \dot{Q}_{g,k,t} = \sum_{l\in\mathcal{L}} \dot{Q}_{l,k,t} \qquad , k \in \mathcal{K}, t \in \mathcal{T}. \tag{A.16}$$

where $\dot{Q}_{l,k,t}$ is the transferred heat from production area k to the transmission point l. An example of the capacity limitations of the transmission network is addressed in eq. A.18. In the heat distribution network, heat is transferred from a transmission area m to the distribution network n using the variable $\dot{Q}_{n,m,t}$.

$$\sum_{m\in\mathcal{M}} \dot{Q}_{n,m,t} + \sum_{o\in\mathcal{O}} \dot{Q}_{o,n,t} + \sum_{p\in\mathcal{P}} \dot{Q}_{p,n,t} = \dot{Q}_{n,t} \qquad , n \in \mathcal{N}, t \in \mathcal{T}. \tag{A.17}$$

where $\dot{Q}_{n,t}$ is the demand for heat in area n at time t. All of the variables in eq. A.16 and A.17 are required to be positive.
The limitations in transmission capacity, as well as in other connections of the DH network, is introduced as presented in eq. A.18.

$$\sum_{l\in\mathcal{L}} \dot{Q}_{l,k,t} \leq \dot{Q}^{\max}_{l,k} \qquad , k \in \mathcal{K}, t \in \mathcal{T}. \tag{A.18}$$

where $\dot{Q}^{\max}_{l,k}$ is the maximal allowed transmission capacity in (MJ/s)

A.4.1 Heat storages

Heat storages may be located at any position in the network, but according to the actual locations in the energy system case, the storages was only introduced in the transmission networks. Besides the integration in the network, five equations govern the operation of the storage. The overall heat balance for the unit is presented in eq. A.19.

$$Q_{m,t} + Q^{\text{in}}_{m,t} - Q^{\text{out}}_{m,t} - Q^{\text{heatloss}}_{m,t} = Q_{m,t+1} \qquad , m \in \mathcal{M}, t \in \mathcal{T}. \tag{A.19}$$

where $Q_{m,t}$ denotes the heat available in the storage at time t, and $Q_{m,t+1}$ in the subsequent time step. All five elements are required to be positive in the optimisation. The heat losses related to heat storage was calculated according to eq. A.20. Low heat losses for short time heat storage are expected due to mixing of stratified layers and temperature differences to the ambient.

$$Q_{m,t}^{out} \cdot (1 - \eta_{\mathrm{HS}}) = Q_{m,t}^{\mathrm{heatloss}} \qquad , m \in \mathcal{M}, t \in \mathcal{T}. \tag{A.20}$$

Three additional constraints were set to represent the physical dimensions and design of the heat storage. The constraints are presented in eq. A.21 to A.23. Eq. A.21 describes the installed capacity, where $Q_{m,t}^{\mathrm{max,size}}$ is the maximal allowed stored heat in (MWh). Eq. A.22 and A.23 limit the charge and discharge of the storage, where $Q_{m,t}^{\mathrm{max,rate}}$ is the maximal allowed rate per hour.

$$Q_{m,t} \leq Q_{m,t}^{\mathrm{max,size}} \qquad , m \in \mathcal{M}, t \in \mathcal{T}. \tag{A.21}$$

$$Q_{m,t}^{\mathrm{in}} \leq Q_{m,t}^{\mathrm{max,rate}} \qquad , m \in \mathcal{M}, t \in \mathcal{T}. \tag{A.22}$$

$$Q_{m,t}^{\mathrm{out}} \leq Q_{m,t}^{\mathrm{max,rate}} \qquad , m \in \mathcal{M}, t \in \mathcal{T}. \tag{A.23}$$

A.5 Technology constraints

The considered technologies are common utility units which are utilised in many large district heating networks. A large fraction of the utilized technology constraints are presented for each of the individual technologies.
In the following sections, the constraints are listed for the individual unit types.

A.5.1 Power plants

The technical constraints for the power plants were defined in order to represent several types. In this way it is possible to include extraction CHP, back pressure CHP and condensing power plants using few equations.
The maximum and minimum technical load in terms of fuel consumption for a power plant unit was described according to Eq A.24 and Eq. A.25. The operation of the unit is dependent on a binary operation variable $o_{i,t}$ and its availability $\mathrm{UMM}_{i,t}$ according to availability data (historical data for validation).
For the specific fuel load, the electricity production in full back pressure was calculated according to Eq. A.27. A reduction in electric efficiency was modelled assuming a constant contribution at full load. The trend of the derived model is presented in Fig. A.3. The high reduction scheme fits well with the results of the AVV1 model within the typical load range.

$$\dot{H}_{i,k}^{\max} \cdot o_{i,t} \cdot \mathrm{UMM}_{i,t} \geq \dot{H}_{i,k,t} \qquad , o_{i,t} \in \{0,1\}, i \in \mathcal{I}, k \in \mathcal{K}, t \in \mathcal{T}. \tag{A.24}$$

$$\dot{H}_{i,k}^{\min} \cdot o_{i,t} \leq \dot{H}_{i,k,t} \qquad , o_{i,t} \in \{0,1\}, i \in \mathcal{I}, k \in \mathcal{K}, t \in \mathcal{T}. \tag{A.25}$$

$$\eta_i^{\text{backp.}} = \eta_i^{\text{elec}} + \eta_i^{\text{reduc.}} \qquad , i \in \mathcal{I}. \tag{A.26}$$

$$P_{i,k,t}^{\text{backp.}} = \dot{H}_{i,k,t} \cdot \eta_i^{\text{backp.}} - \dot{H}_{i,k}^{\max} \cdot \eta_i^{\text{reduc.}} \cdot o_{i,t} \qquad , o_{i,t} \in \{0,1\}, i \in \mathcal{I}, k \in \mathcal{K}, t \in \mathcal{T}. \tag{A.27}$$

$$\dot{Q}_{i,k,t}^{\text{backp.}} = \dot{H}_{i,k,t} \cdot \eta_i^{\text{total}} - P_{i,k,t}^{\text{backp.}} \qquad , i \in \mathcal{I}, k \in \mathcal{K}, t \in \mathcal{T}. \tag{A.28}$$

$$\begin{aligned} P_{i,k,t} = {} & P_{i,k,t}^{\text{backp.}} + \beta_i^1 \cdot \Delta\dot{Q}_{i,k,t}^1 \cdot v_i^{\text{ex.}} + \beta_i^2 \cdot \Delta\dot{Q}_{i,k,t}^2 \cdot v_i^{\text{ex.}} \\ & - P_{i,k,t}^{\text{bypass}} \cdot v_i^{\text{bypass}} \end{aligned} \qquad , i \in \mathcal{I}, k \in \mathcal{K}, t \in \mathcal{T}. \tag{A.29}$$

$$\Delta\dot{Q}_{i,k,t}^1 - \dot{H}_{i,k}^{\max} \cdot o_{i,t}^{\text{no-loss}} \leq \dot{H}_{i,k}^{\max} \cdot r_i^{\text{no-loss}} \cdot (\eta_i^{\text{total}} - \eta_i^{\text{elec}}) \cdot v_i^{\text{ex.}} \qquad , o_{i,t}^{\text{no-loss}} \in \{0.1\}, i \in \mathcal{I}, k \in \mathcal{K}, t \in \mathcal{T}. \tag{A.30}$$

$$\Delta\dot{Q}_{i,k,t}^1 + \dot{H}_{i,k}^{\max} \cdot (1 - o_{i,t}^{\text{no-loss}}) \geq \dot{H}_{i,k}^{\max} \cdot r_i^{\text{no-loss}} \cdot (\eta_i^{\text{total}} - \eta_i^{\text{elec}}) \cdot v_i^{\text{ex.}} \qquad , o_{i,t}^{\text{no-loss}} \in \{0.1\}, i \in \mathcal{I}, k \in \mathcal{K}, t \in \mathcal{T}. \tag{A.31}$$

$$\Delta\dot{Q}_{i,k,t}^1 \leq \dot{H}_{i,k}^{\max} \cdot r_i^{\text{no-loss}} \cdot (\eta_i^{\text{total}} - \eta_i^{\text{elec}}) \cdot v_i^{\text{ex.}} \qquad , i \in \mathcal{I}, k \in \mathcal{K}, t \in \mathcal{T}. \tag{A.32}$$

$$\begin{aligned} \Delta\dot{Q}_{i,k,t}^2 \leq {} & \dot{H}_{i,k}^{\max} \cdot (1 - r_i^{\text{no-loss}}) \\ & \cdot (\eta_i^{\text{total}} - \eta_i^{\text{elec}}) \cdot o_{i,t}^{\text{no-loss}} \cdot v_i^{\text{ex.}} \end{aligned} \qquad , o_{i,t}^{\text{no-loss}} \in \{0.1\}, i \in \mathcal{I}, k \in \mathcal{K}, t \in \mathcal{T}. \tag{A.33}$$

$$\dot{Q}_{i,k,t}^{\text{backp.}} - \dot{Q}_{i,k,t}^1 = \Delta\dot{Q}_{i,k,t}^1 \cdot v_i^{\text{ex.}} \qquad , i \in \mathcal{I}, k \in \mathcal{K}, t \in \mathcal{T}. \tag{A.34}$$

$$\dot{Q}_{i,k,t}^1 - \dot{Q}_{i,k,t}^2 = \Delta\dot{Q}_{i,k,t}^2 \cdot v_i^{\text{ex.}} \qquad , i \in \mathcal{I}, k \in \mathcal{K}, t \in \mathcal{T}. \tag{A.35}$$

$$\dot{Q}_{i,k,t} = \dot{Q}_{i,k,t}^2 + \dot{Q}_{i,k,t}^{\text{bypass}} \cdot v_i^{\text{bypass}} \qquad , i \in \mathcal{I}, k \in \mathcal{K}, t \in \mathcal{T}. \tag{A.36}$$

$$\dot{Q}_{i,k,t}^{\text{bypass}} = P_{i,k,t}^{\text{bypass}} \cdot v_i^{\text{bypass}} \qquad , i \in \mathcal{I}, k \in \mathcal{K}, t \in \mathcal{T}. \tag{A.37}$$

$$0 \leq \dot{Q}_{i,k,t}, \dot{Q}_{i,k,t}^1, \dot{Q}_{i,k,t}^2, \dot{Q}_{i,k,t}^{\text{bypass}}, \dot{Q}_{i,k,t}^{\text{backp.}}, \Delta\dot{Q}_{i,k,t}^1, \Delta\dot{Q}_{i,k,t}^2$$

$$0 \leq P_{i,k,t}, P_{i,k,t}^{\text{bypass}}, P_{i,k,t}^{\text{backp.}}, \dot{H}_{i,k,t}$$

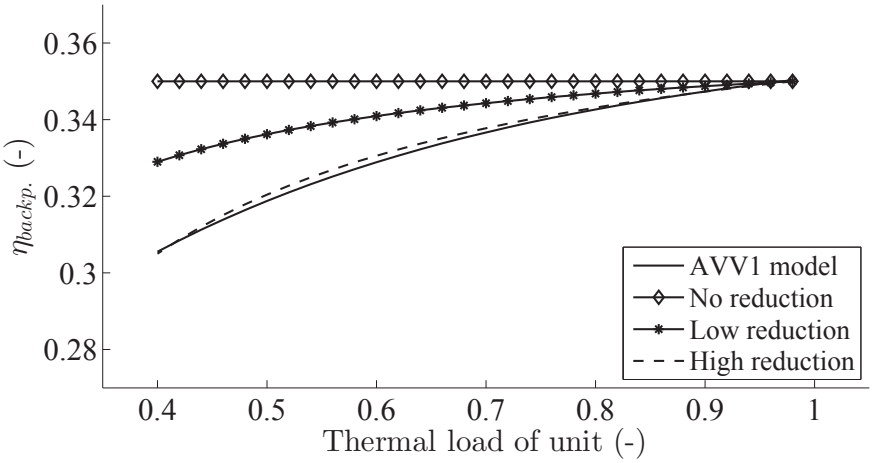

Figure A.3: Estimated reduction of electric efficiency at low unit loads

A constant boiler efficiency was assumed for the full range of applicable loads. The heat production in back pressure operation was evaluated as the residual of the total utilisation of fuel and the back pressure electricity production according to Eq. A.28, where the thermal efficiency η_i^{total} corresponds to the lower heating value of the utilised fuel.

The produced electricity of the unit was calculated according to Eq. A.29. A reduction in heat production of an extraction CHP plant ($\Delta\dot{Q}^1_{i,k,t} + \Delta\dot{Q}^2_{i,k,t}$) leads to increased power production according to power loss factors by heat extraction β^1,β^2 [-] (Verbruggen, 1982). β^1 corresponds to heat extraction below the "noloss" point, β^2 for heat extraction above this operational limit. The binary input parameter $v_i^{\text{ex.}}$ is used to distinguish between units with extraction points and units with only one production scheme (e.g. electricity only or back pressure units). Some of the investigated back pressure units allow the operator to bypass the turbine, in order to utilise the steam for boosting the heat production. The binary input parameter v_i^{bypass} is used to distinguish such units from the remaining. The reduction in electricity from bypassing the turbine is denoted $P^{\text{bypass}}_{i,k,t}$.

By use of eq A.30 and A.31 it was ensured that the change from one power loss factor to the other corresponds to the physical requirement of the extraction CHP plant. If the binary variable $o^{noloss}_{i,t}$ is 1, β^2 should be used, otherwise β^1. The no loss point was located as the ratio r_i^{noloss} between heat extracted above and below the no loss point. The binary variable $o^{noloss}_{i,t}$ was further used in Eq. A.32 and A.33 to determine the heat extraction.

The resulting heat from the extraction plant is determined by the Eq. A.34 to A.36. Eq. A.37 ensures that steam bypass corresponds to the bypassed amount

of electricity.
For the case where power plants are constrained by rapid ramping of the boiler load, the model includes constraints designed to describe this operation restriction. The constraints were modelled as a limiting difference in load $\dot{H}^{\text{rel}}_{i,k,t}$ of the boiler from one hour to the next. As in Eq. A.38 and A.39 the constraints for startup and shutdown were included in these constraints, and correpond to the additional cost described in A.7. The constraints of Eq. A.40 and A.41 ensure that startup and shutdown only occurs in case of changed production commitment.

$$\begin{aligned}\dot{H}^{\text{rel}}_{i,k,t+1} - \dot{H}^{\text{rel}}_{i,k,t} \leq & \dot{H}^{\text{rel,max}}_{i,k} \cdot (1 - o^{\text{startup}}_{i,t+1}) + \dot{H}^{\text{rel,startup}}_{i,k} \cdot o^{\text{startup}}_{i,t+1} \\ & , o^{\text{startup}}_{i,t} \in \{0,1\}, i \in \mathcal{I}, k \in \mathcal{K}, t \in \mathcal{T}. \end{aligned} \tag{A.38}$$

$$\begin{aligned}\dot{H}^{\text{rel}}_{i,k,t} - \dot{H}^{\text{rel}}_{i,k,t+1} \leq & \dot{H}^{\text{rel,max}}_{i,k} \cdot (1 - o^{\text{shutdown}}_{i,t+1}) + \dot{H}^{\text{rel,shutdown}}_{i,k} \cdot o^{\text{shutdown}}_{i,t+1} \\ & , o^{\text{shutdown}}_{i,t} \in \{0,1\}, i \in \mathcal{I}, k \in \mathcal{K}, t \in \mathcal{T}. \end{aligned} \tag{A.39}$$

$$\begin{aligned} o^{\text{startup}}_{i,t} \geq & o^{\text{CHP}}_{i,t} - o^{\text{CHP}}_{i,t-1} \\ & , o^{\text{CHP}}_{i,t}, o^{\text{startup}}_{i,t} \in \{0,1\}, i \in \mathcal{I}, t \in \mathcal{T}. \end{aligned} \tag{A.40}$$

$$\begin{aligned} o^{\text{shutdown}}_{i,t} \geq & o^{\text{CHP}}_{i,t} - o^{\text{CHP}}_{i,t+1} \\ & , o^{\text{CHP}}_{i,t}, o^{\text{shutdown}}_{i,t} \in \{0,1\}, i \in \mathcal{I}, t \in \mathcal{T}. \end{aligned} \tag{A.41}$$

A.5.2 Heat boilers

Two sets of heat boiler constraints were included in the model, one for each location type (central vs. decentral). In this section the constraints of the central installations are presented. The maximum technical load in terms of fuel consumption for a boiler unit was described according to Eq A.42.
The resulting heat production was described according to Eq. A.43, where the thermal efficiency η^{total}_{h} corresponds to the lower heating value of the utilised fuel.

$$\dot{H}^{\text{max}}_{h,k} \geq \dot{H}_{h,k,t} \qquad , h \in \mathcal{H}, k \in \mathcal{K}, t \in \mathcal{T}. \tag{A.42}$$

$$\dot{Q}_{h,k,t} = \dot{H}_{h,k,t} \cdot \eta^{\text{total}}_{h} \qquad , h \in \mathcal{H}, k \in \mathcal{K}, t \in \mathcal{T} \tag{A.43}$$

A.5.3 Heat pumps

Two sets of heat pump constraints were included in the model, one for each location type (central vs. decentral). In this section the constraints of the central installations are presented. The produced heat of the unit was calculated using a coefficient of performance, and the consumed electricity, as presented in Eq. A.44.
For certain types of installations, operation of the heat pump unit will depend on external factors, such as operation at a specific power plant or facility.

For other types, the unit capacity's and COP may vary according to ambient temperatures or heat source flow rates. In order to address such cases, the coefficient of performance $COP_{g,t}$ and the capacity constraint $\dot{Q}^{\max}_{g,k,t}$ of the heat pump units were split to hourly basis, and a binary operation variable $o^{\mathrm{HP}}_{g,t}$ was introduced. The capacity of such systems were calculated according to Eq. A.45.

$$\dot{Q}_{g,k,t} = COP_{g,t} \cdot P_{g,k,t} \quad , g \in \mathcal{G}, k \in \mathcal{K}, t \in \mathcal{T}. \tag{A.44}$$

$$\dot{Q}^{\max}_{g,k,t} \cdot o^{\mathrm{HP}}_{g,t} \geq COP_{g,t} \cdot P_{g,k,t} \quad , o^{\mathrm{HP}}_{g,t} \in \{0,1\}, g \in \mathcal{G}, k \in \mathcal{K}, t \in \mathcal{T} \tag{A.45}$$

A.6 System reserves and operational constraints

In order for the model to correspond to the operation of a specific energy system, additional constraints are needed to fully describe for cooperation of units and the different types of system reserves required. Many of the constraints are specified in publications from the systemoperator (Energinet.dk, 2013) (Energinet.dk, 2012a). For both manual and frequency reserve capacity the available reserve from a power plant unit was calculated according to Eq. A.46 and A.47. The individual reserve types were further constrained by minimum and maximum constributions from each unit.

$$\begin{aligned} P^{\mathrm{reserve}}_{i,t} \leq & \sum_{k \in \mathcal{K}} (\dot{H}_{i,k}) \cdot o_{i,t} \cdot \eta^{\mathrm{elec}}_{i} \cdot \dot{H}^{\mathrm{rel,reserve}}_{i} \\ & + \sum_{k \in \mathcal{K}} (\dot{H}_{i,k}) \cdot o_{i,t} \cdot (\eta^{\mathrm{total}}_{i} - \eta^{\mathrm{elec}}_{i}) \cdot \dot{H}^{\mathrm{rel,reserve}}_{i} \cdot (\beta^{1}_{i} + \beta^{2}_{i})/2 \\ & , o_{i,t} \in \{0,1\}, i \in \mathcal{I}, t \in \mathcal{T}. \end{aligned} \tag{A.46}$$

$$\begin{aligned} P^{\mathrm{reserve}}_{i,t} \leq & \sum_{k \in \mathcal{K}} (\dot{H}_{i,k}) \cdot o_{i,t} \cdot UMM_{i} \cdot \eta^{\mathrm{elec}}_{i} \cdot \dot{H}^{\mathrm{rel,reserve}}_{i} \\ & + \sum_{k \in \mathcal{K}} (\Delta\dot{Q}^{1}_{i,k,t}) \cdot \beta^{1}_{i} + \sum_{k \in \mathcal{K}} (\Delta\dot{Q}^{2}_{i,k,t}) \cdot \beta^{2}_{i} - \sum_{k \in \mathcal{K}} (P_{i,k,t}) \\ & , o_{i,t} \in \{0,1\}, i \in \mathcal{I}, t \in \mathcal{T}. \end{aligned} \tag{A.47}$$

Additional operational constraints exist, e.g. considerations for operating the steam network, as well as multifuel units with mutual steam turbines and/or gas turbines.

Ensuring short-circuit power, reactive reserves and voltage control was addressed by ensuring 3 large power plants ($P \geq 150$ MW) to be committed at all time.

Appendix B

Energy system model validation

This appendix contains data derived from the validation of the energy system model, which is described in Appendix A.

The system model has been validated against a number of data series from various sources. In one of the cases, data is protected by a non-disclosure agreement (NDA), which limit the detail-level of selected comparisons in this section.

By examination of the accuracy and detail of representative segments, it is shown that the model presents good agreement with the historical data. Thus the model is considered applicable to investigate the interaction between several production technologies in a system where both heat and electricity costs are optimized for each hour.

The model was validated with the previously mentioned data sets (in section A.1) on hourly basis for heat and electricity demand, decentral CHP production, wind-turbine production, transmission capacity and transmission cost for 2011.
A number of assumptions are used for performance of the individual plants, heat network capacities and fuel costs. Historical data are used where available. Both technology and cost data are presented in [P7]. The data representing various technologies and cost data are considered constant throughout the year, although the efficiency of many units will vary according to DH temperatures. The characteristic numbers used for V- and E-method (Section A.3.1) for heat taxes changed slightly in June 2011, but are assumed fixed (new rules) in the model throughout the year.

B.1 Optimisation Criteria

Optimisation of the presented mixed integer linear model is time-consuming due to the significant variations in external factors such as demand, auxiliary production, unit availability (UMM-data) and a high amount of competitive technologies. Optimisation of one period (36 hours) varies from 2.5 s to 6 s depending on the complexity, when the formulation of the model optimisation criteria is very strict (proven optimal solution). This results in calculation

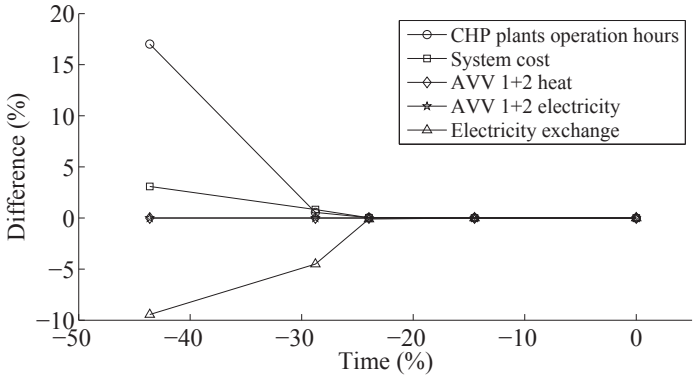

Figure B.1: Adjusting optimisation criteria for individual utility units versus calculation time

time of approximately 28 minutes for an optimisation of 365 days on a 3.2 GHz processor.

By adjusting the optimisation criteria for the energy system model, it is possible to reduce the calculation time, by allowing the current best integer solution within a relative criterion of the best possible integer solution. This results in solutions which are close to optimal, but where the individual operation of specific utility plants are not required to correspond exactly to the optimal choice. An example of the benefits and disadvantages of changing the optimisation criteria for a full yearly optimisation is presented in Fig. B.1. As presented in the figure, optimisation time may be cut significantly without real disadvantages until a limit (approximately 25 % time reduction). When the limit is reached, the optimised objective function increases slightly, whereas the optimised operation of individual units and of the electricity exchange varies significantly.

The results presented for both validation and results (sections B.2-B.5 and chapters 5-6, respectively) in this thesis corresponds to an optimisation criteria, which is below the limiting threshold.

B.2 Environmental reports

Based on data for environmental reports for 2011 from the companies (DONG Energy, 2012; Vattenfall A/S, 2012) and municipal cooperatives (ARC, 2012; Vestforbrænding, 2012; KARA/NOVEREN I/S, 2012) operating the considered thermal power plant, it is possible to compare the real production of the actual units, with the calculated production, for a given year (2011). The

two comparisons are presented in Fig. B.2a and B.2b for electricity and heat, respectively.
For most of the considered power plants, data is available for the entire power station, which may represent between 1 (eg. KARA) and 5 (Kyndby power station - KYB) units. For Avedøre power station, the data is available for unit 1 and unit 2 individually, where unit 2 represents a steam turbine with two boilers and two gas turbines in cooperation. The presented data series show close matches for both electricity and heat for the individual power plants.
In the case of KYB (peak load and backup unit), a very small separate district heating network exists, which was not included in the model. For the remaining power stations the difference between actual and modelled production is between 0-2 %, except for SVM where deviation of electricity production is approximately 3 % which in absolute value is only approximately 4 GWh. For ASV the considered heat demand of Kalundborg (Asnæs) and the corresponding data from the environmental report differs approximately 2 % or 16 GWh.
All together, the considered power plants produce a marginally higher amount of electricity and heat in the model compared to the operation data from 2011. This corresponds to approximately 31 GWh electricity and 29 GWh heat.

B.3 Environmental statements

From Energinet.dk (2014) and HOFOR A/S (2015) environmental statements for carbon emissions 2011 may be found representing Danish electricity production, and Copenhagen DH networks respectively. The two statements are calculated by two different methods, the 125 %- and the 200 %-method Energinet.dk (2015). The numbers are 359 g/kWh (125 % method) and 110 g/kWh (200 % method). Similar calculation was carried out based on the results of the energy model. In both cases the numbers are closely resembling the real values. The corresponding model results are 357 g/kWh (electricity: 125 % method) and 115 g/kWh (heat: 200 % method) respectively. The difference in both cases is below 5 %.
In the remaining parts of this report the 125 % method is utilised for both heat and electricity for reasons of unambiguity and relevance for comparison with existing litterature. Other frequently used methods are on basis of energy content (100 %) or on basis of exergy content. The carbon emission from model results of DH in Copenhagen using the 125 % method is 175 g/kWh.

B.4 Data from Energinet

As described in section A.4, import and export of electricity is handled by the model, based on capacity constraints of interconnections, the spot price

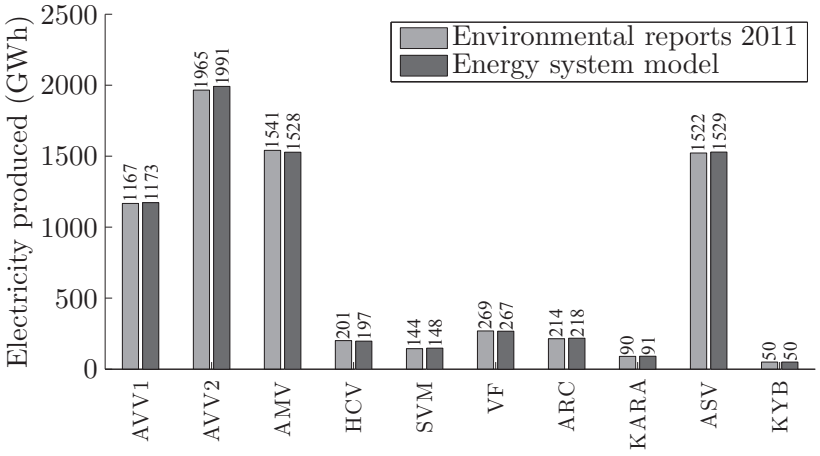

(a) Electricity

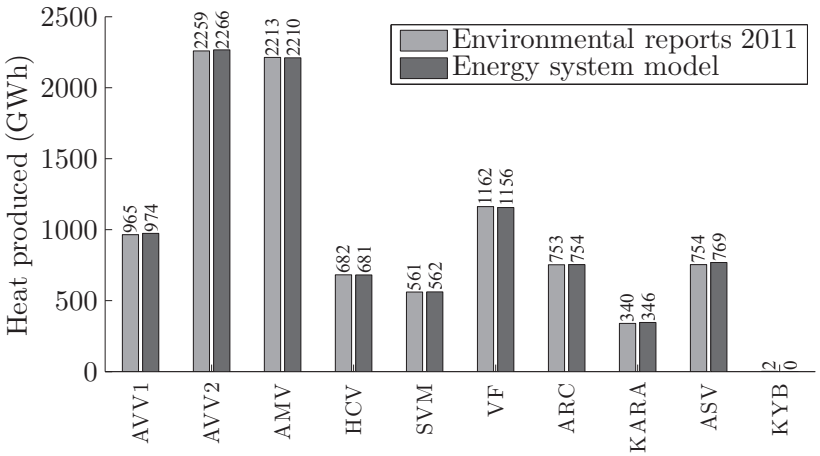

(b) Heat

Figure B.2: Comparison of produced electricity according to environmental reports 2011 and the model

of electricity at neighbouring markets and transmission losses. A comparison between the actual 2011 net imported electricity and the net exchange of the energy system model is presented in Fig. B.3 for two representative time frames.

It is found that the two data series show good coherence for a large part of the year. There are however some periods with less accurate coherence as e.g. during some hours in the summer (differences of approximately 150 MWh/h in Fig. B.3a).
A limitation of this approach is the lack of information about production and interconnection capacity constraints in neighbouring countries, which tend to result in an overestimation of the imported electricity, as the available transmission capacity becomes the only constraint. This however was found not to induce significant error in the exchanged electricity.

B.5 Data from DONG

By courtesy of DONG Energy (2013), production data (heat, steam and electricity) for both units in Avedøre power station (AVV1 & AVV2) and Asnæs power station (ASV2 & ASV5) was made available through a non-disclosure agreement. Selected data series was allowed to be shown for purpose of validation of the model. The presented data series are electricity production at representative time segments for two of the four units (Fig. B.4) , as well as summed production data for all hours of 2011 for AVV and ASV (Fig. B.5 and B.6 respectively).
For the comparison of electricity production at individual units, the figures show good agreement of the trends from day to day. For most of the considered time segments, the difference between the experienced and calculated electricity production at the unit is low (typically below 10 % relative difference). Some units are ramped up and down repeatedly (e.g. unit A and B), and some units experience a less fluctuating operation (e.g. unit C). For unit C (in Fig. B.4c) the deviation is experienced to be larger than this figure for some hours during the year. Despite larger deviations for this unit, the model is considered to represent the operation to a satisfactory degree.
It should be noted, that the procedure for optimisation of the unit operation, is not similar between the actual operation data and the model, as the model is deterministic in terms of both heat and electricity demand, where as the real operation corresponds to a system where the operator may optimise profit considering stochastic input parameters. The red line represents the available production capacity considering UMM data.
As presented in Fig. B.5 and B.6 the model represents the electricity and heat production of the four units well compared to the operation data from 2011, considering the differences in seasonal heat demand, electricity production and availability to the market. The unit with the largest relative inconsistency

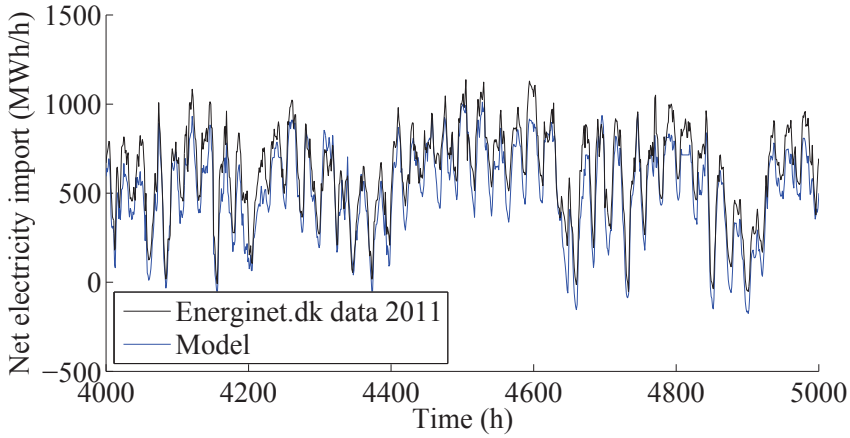

(a) spring/summer

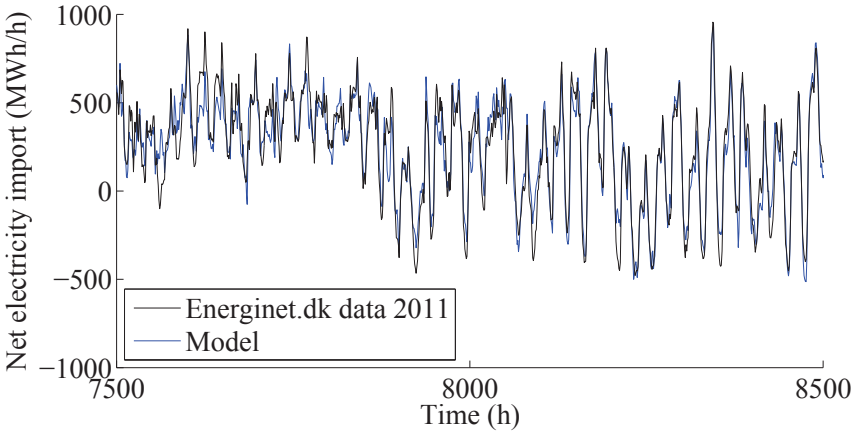

(b) fall/winter

Figure B.3: Comparison of net imported electricity from the neighbouring areas according to Energinet.dk (2011) and the model.

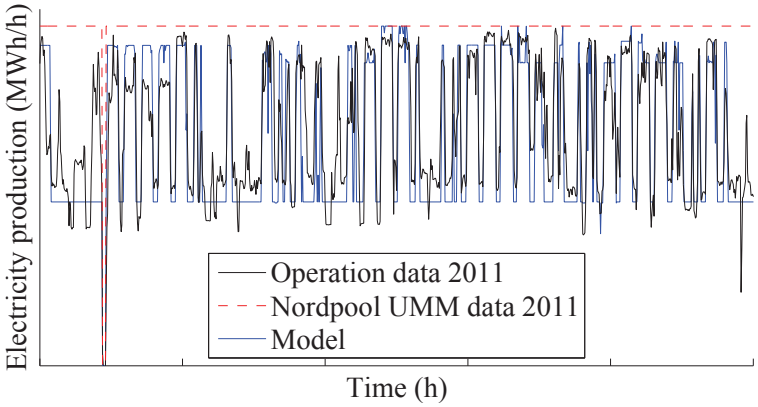

(a) Unit A - summer

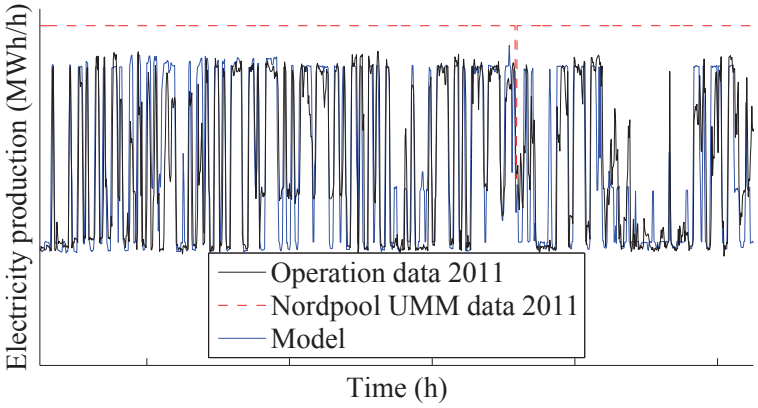

(b) Unit B - winter

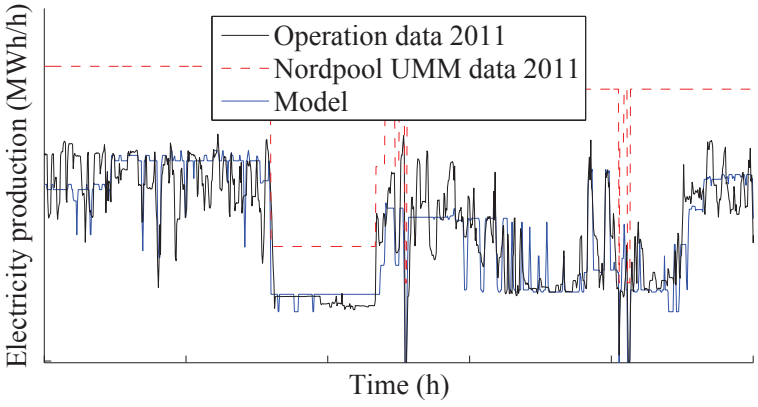

(c) Unit C - spring

Figure B.4: Comparison of produced electricity at three separate units according to operation data 2011 (DONG Energy, 2013) and the model

between model and operation data is electricity production at ASV2, with a summed difference of -3%, but which during spring/summer experiences hours with to high production. For AVV1, some difference is found between the modelled heat production during the spring and fall (represented by the difference in summed production during the summer) and the operation data. The difference may be a consequence of the lack of detail in heat demand for that specific unit, as a small steam network for industrial users is not considered in the model.

B.6 Summary

Based on the comparison of operation data as well as environmental reports, carbon emissions and imported electricity from neighbouring areas, the model is found to represent the heat and power system to a satisfactory degree of detail.
Some differences are found from comparison of operation data, but such discrepancy is likely to originate from differences between deterministic and stochastic optimisation schemes, as well as detailed knowledge of unit performance at various load and operation points.

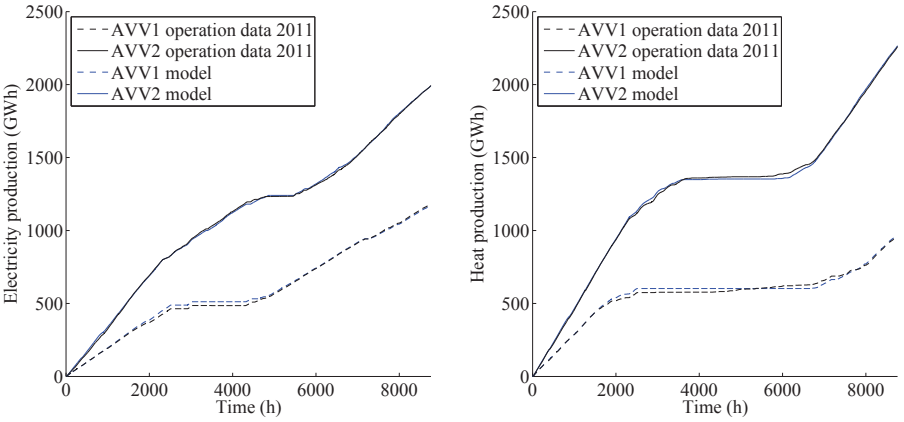

(a) Electricity (b) Heat

Figure B.5: Comparison of produced electricity and heat at the Avedøre plant according to operation data 2011 (DONG Energy, 2013) and the model

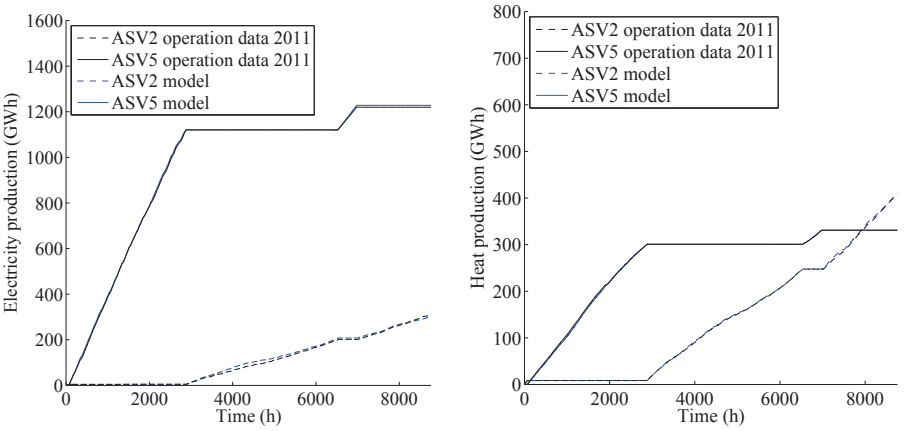

(a) Electricity (b) Heat

Figure B.6: Comparison of produced electricity and heat at the Asnæs plant according to operation data 2011 (DONG Energy, 2013) and the model

Appendix C

Paper 1 - Energy

Torben Ommen, Wiebke Brix Markussen and Brian Elmegaard

Comparison of linear, mixed integer and non-linear programming methods in energy system dispatch modelling

Energy, 74 (2014) 109-118

Energy 74 (2014) 109–118

Contents lists available at ScienceDirect

Energy

journal homepage: www.elsevier.com/locate/energy

Comparison of linear, mixed integer and non-linear programming methods in energy system dispatch modelling

Torben Ommen*, Wiebke Brix Markussen, Brian Elmegaard

Technical University of Denmark, Kgs, Lyngby, Denmark

ARTICLE INFO

Article history:
Received 17 September 2013
Received in revised form
5 March 2014
Accepted 8 April 2014
Available online 1 May 2014

Keywords:
CHP (combined heat and power)
Heat pumps
DH (district heating)
Dispatching
Optimisation methods

ABSTRACT

In the paper, three frequently used operation optimisation methods are examined with respect to their impact on operation management of the combined utility technologies for electric power and DH (district heating) of eastern Denmark. The investigation focusses on individual plant operation differences and differences between the solution found by each optimisation method. One of the investigated approaches utilises LP (linear programming) for optimisation, one uses LP with binary operation constraints, while the third approach uses NLP (non-linear programming). The LP model is used as a benchmark, as this type is frequently used, and has the lowest amount of constraints of the three. A comparison of the optimised operation of a number of units shows significant differences between the three methods. Compared to the reference, the use of binary integer variables, increases operation of selected units by 23%, while for a non-linear approach the increase can be higher than 39%. The results indicate a higher coherence between the two latter approaches, and that the MLP (mixed integer programming) optimisation is most appropriate from a viewpoint of accuracy and runtime.

1. Introduction

Increasing use of intermittent sources for power production may imply several severe effects in stability, economy and maintenance of central electricity production [1,2]. In areas with large shares of CHP (Combined Heat and Power) production, introduction of intermittent power production may further influence the operation management, as an increasing amount of operational constraints is included in the optimisation. Operation of some CHP-units may be required in order to satisfy heat demand, in time periods where utility production is not economically desirable for the plant operator. Methods to decouple the production constraints of the coproduced products, while maintaining the high energy efficiency, are investigated as they may prove highly valuable. DH (District heating) network heat pumps may pose this ability [3–7].

In a liberalised energy system the operation pattern of each plant is determined by optimisation of economics, such that the consumer prices are minimised in each time period. In the present work, different approaches to optimisation of operation are investigated and compared, in order to determine whether the choice of optimisation algorithm affects the results. The investigated energy system consists mainly of CHP-plants, boilers and heat pumps, constrained by high amounts of intermittent electricity production from wind turbines. In the strictly linear models, the outlines of thermal units such as CHP-plants appear to be simplified to an extent where the representation of the plant does not characterise the physical unit satisfactorily. Two alternative methods provide the possibility to increase the detail of the constraints.

When using a modelling approach to evaluate the interaction of several multi product technologies, early choices such as the applied modelling scheme may influence the final results significantly. In the case of heat pumps in a DH-network, the economic feasibility of the individual energy technologies will depend on several factors, e.g. the amount of annual operation hours, the average load, or an economic incentive in operation of the combined system. If the used modelling approach has significant influence on operation results, the economically optimal investment may not be derived, which will influence the cost of utility for society and the revenue for the investor.

A number of energy models has been developed during the last decade both with specific focus on the Danish system and for more general application [8–11]. Many of these models are continuously expanded and maintained. As noted by Connolly et al., many of the system models will require long training periods, depending on the level of complexity required. In the advanced models, the detail

* Corresponding author. Tel.: +45 45254037; fax: +45 45884325.
E-mail addresses: tsom@mek.dtu.dk (T. Ommen), wb@mek.dtu.dk (W. B. Markussen), be@mek.dtu.dk (B. Elmegaard).

http://dx.doi.org/10.1016/j.energy.2014.04.023
0360-5442/

level of individual technologies is not easily changeable, as the optimisation approach is a basic property of the model. The majority of the models is using linear optimisation [8].

The focus of this paper is to investigate and evaluate the impact of the choice of optimisation algorithm in energy system dispatch models. This choice will influence details of the calculated operation and load characteristics of individual technologies. As the derived operation characteristics are used in economic evaluations, faulty or incorrect estimations may impact the applicability or feasibility of a technology in the derived energy system.

The evaluation is based on a comparison of three different optimisation methods for an energy system model. The detail of the linear dispatch models used in the investigation represents the detail level of the technologies and demand characteristics in many of the considered references.

In the paper we describe the different detail levels of a dispatch models which represents the dynamic operation of heat and electricity markets. The production units in the system are represented by performance characteristics that account for the system parameters, such as temperatures in the DH-network and heat consumer units.

1.1. Energy system layout

As a specific case, the utility system for electricity and heat production of eastern Denmark has been used. The examined energy system has been chosen, as this is identified as a system, where heat pumps may contribute significantly in balancing both electricity and heat production with their individual demands.

The current utility production in this area distinguishes the system from other European utility areas, as electricity is only produced by wind turbines and CHP-plants. According to the statistics for the combined Danish energy system [12] (including the area of western Denmark) more than 99.7% of the produced electricity in 2011 originates from these two utility technologies.

Historical data are available online for the Danish electricity production and consumption in each region and for different production technologies from the TSO (Transmission System Operator) [13]. Hourly values for wind production, local production (decentralised CHP-plants) and gross consumption are used. The used data from this source is from January 2011.

The thermal electricity production in eastern Denmark origins from both small decentralised and large centralised CHP-plants. Out of 14 central power plant units, 10 are steam turbine-based CHP-plants, where a high part of the electricity is produced with simultaneous production of heat. Additionally, in 2011 there were 4 central CHP waste incineration steam power units in the energy system layout. In terms of installed capacity for electricity production the incineration plants represent a small fraction.

Most of the required heat production is handled by the abovementioned units, although additional DH incineration boilers are in use. For the majority of the central CHP-units and incineration plants, the produced heat is transmitted to one large DH-network that covers Copenhagen and the surroundings.

Two independent DH-networks have been included in the optimisation. The larger one (in reality consisting of three interconnected DH-networks) covers the major part of Copenhagen and suburbs, while the second network supplies heat to Kalundborg, a town in the western part of Zealand. The hourly demand of the networks has been collected from one of the network operators [14] for the entire year 2011. The data received is subdivided into five areas, ranging from central Copenhagen to one of the low intensity suburbs, and is thus considered representative for all the areas in the study. The hourly demand of the different DH-networks has been scaled by their individual yearly consumption. The derived central electricity demand and the total heat demand in the four DH-networks for January 2011 are presented in Fig. 1.

A graphical representation of the included technologies is shown in Fig. 2. The DH areas 1–3 are connected, and the capacity of the connections is not considered. Each plant in the figure represents one or more individual units. Only the large wind farms are included in the figure, but the total wind power capacity is included in the calculations. Transmission lines for import and export are not used in the analysis for this paper. The operation can thus be characterised as island operation.

1.2. Optimisation of utilities

In a liberalised electricity market, the installed utility technologies are cooperating in the effort to match electricity production and demand. The optimisation of electricity cost is handled by a common Nordic and Baltic market operator, while grid stability is handled by the TSO of the considered area. The optimisation is performed on a daily basis. Prices are calculated based on supply, demand and transmission capacity for the combined area, and the individual transmission systems. By accepting hourly- or block-bids from the power plant operators, the system operator decides the optimal allocation of power production between the producers.

For each individual DH-network, a similar system optimisation yields the cost of heat and the allocation of production. This optimisation is based on another set of production bids and demand characteristics. The combination of the two individual optimisations determines the production outlines for the individual utility producer for a given hour. The producer finally determines how he wishes to fulfil the production responsibility at the available units.

The production bids are based on various factors such as fuel prices, efficiencies and other variable cost. The bids can include both linear and non-linear constraints. The effect of some selected non-linearities is considered in this paper.

With fixed production bids from the producers, the production price is given and the system operators can optimise the utility cost using simple optimisation methods.

For the comparison of optimisation approaches, the optimisations performed in this paper is only the variable cost related to the consumption of the fuel. There are several reasons:

- The capital costs of already installed power plants can be considered sunk costs in the evaluated system.

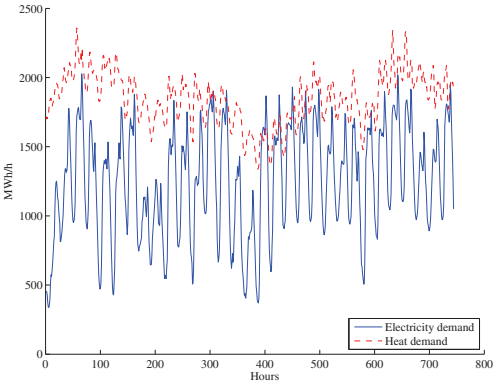

Fig. 1. Total electricity and heat demand for the considered units in January 2011.

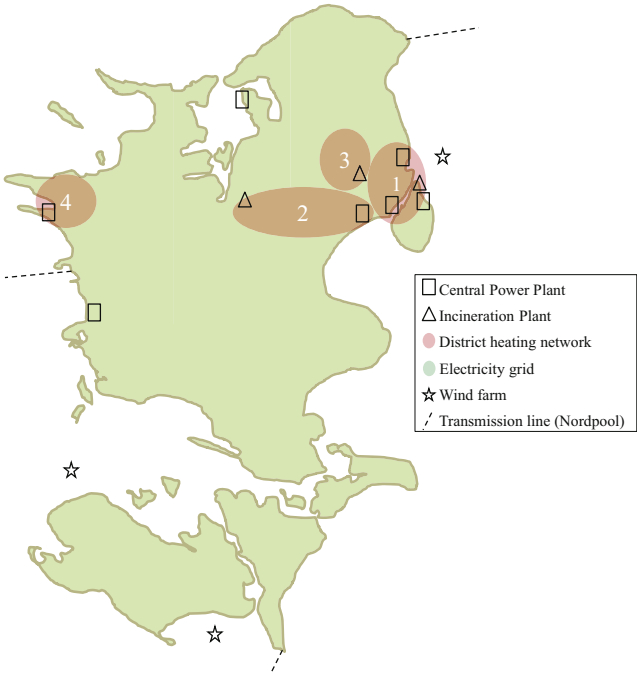

Fig. 2. The central CHP-plants and large incineration plants of eastern Denmark and the utility networks.

- Other variable costs related to operation and maintenance are not easy to quantify. Using a simple assumption would not differentiate the power plants in the assessment.
- Taxes on emissions and fuel will not be covered by the company operating the CHP-plant, but divided and paid by the end user of the utilities.
- For newly installed heat pumps in the DH-network, the capital cost would need to be covered. However, we assume that the capital costs and operation and maintenance costs are distributed equally to each unit energy produced.

2. Method

Several modelling schemes are compared in order to evaluate the gain or drawback of applying one scheme rather than the other. The numerical models are all implemented in GAMS (General Algebraic Modelling System) [15] using two different solvers for several model types, optimisation timeframe and optimisation horizon. External data processing is handled by Matlab, using the interface gdxmrw [16]. The implementation of energy system equipment in the model is generic and easy to change.

2.1. Modelling of the energy system

In the adaption of the thermal units layout into the numerical model, only the large central CHP-plants, the central power plants and the central incineration plants were included. It has been assumed, that the small-scale decentralised CHP-plants are operated with a strict policy to fulfil the heating demand of the decentralised DH-networks. With this assumption the operation of small-scale units can be handled using the previously discussed historical data from January 2011.

For the production units in the system, the optimal production cost for the combined system can be achieved by minimisation of economic cost of the plant dispatch [17]. When considering a system where capital cost can be considered as sunk cost, the objective function can be written as follows:

$$\min \sum_{i\in I} \sum_{t\in T} \left(C_{P,i,t}(P_{i,t}) + C_{\dot{Q},i,t}\left(\dot{Q}_{i,t}\right) \right) \tag{1}$$

The production units in the system are denoted by i [−], time is t [h] and the produced electricity and heat are denoted P [MW] and $\dot{Q}$ [MJ/s], respectively. The objective function in equation (1) is subject to a number of constraints, depending on the detail of the study, and the optimisation scheme. One important constraint requires the sum of produced products to satisfy the demand of both heat and power respectively for each hour. The cost of the products can be fixed or be calculated according to the efficiency of conversion of fuel in the units at time t (further discussed in Section 2.2).

For each of the 18 thermal power plant units in the utility system, information regarding capacity and consumption is available online, from either the plant owners, the Danish Energy Agency [18] or from the TSO [19]. From the information available it is possible to derive the plant characteristics listed in Table 1. Most of the data in the table is referring directly to the design parameters, but the table also includes prices of the used type of fuel for 2011 using IEA prices [20]. Waste has been assigned the cost of 2 [EUR/GJ].

Table 1
Thermal power plant unit characteristics.

Plant name	Area	Type	Capacity boiler [MW]	Elec. eff. in backp. [/]	Total efficiency [/]	Max. boiler ramp rate [/]	β [MW/MJs]	Fuel	Fuel price [EUR/GJ]
AMV1	1	Backp.	365	0.21	0.90	0.2	–	Biom.	6.5
AMV3	1	Extraction	600	0.36	0.91	0.2	0.11	Coal	3.5
HCV2	1	Backp.	180	0.18	0.90	0.2	–	NG	7.3
HCV7	1	Backp.	300	0.29	0.90	0.2	–	NG	7.3
HCV8	1	Backp.	125	0.20	0.90	0.2	–	NG	7.3
SVM1	1	Backp.	175	0.17	0.90	0.2	–	NG	7.3
SVM7	1	Backp.	485	0.17	0.90	0.2	–	NG	7.3
AMF1	1	Backp.	131	0.19	0.83	0.2	–	Waste	2.0
AVV1	2	Extraction	600	0.36	0.91	0.2	0.11	Coal	3.5
AVV2	2	Extraction	1150	0.43	0.93	0.2	0.14	Biom. & NG	6.9
KARA5	2	Backp.	65	0.18	0.81	0.2	–	Waste	2.0
VF5	3	Backp.	95	0.12	0.99	0.2	–	Waste	2.0
VF6	3	Backp.	110	0.18	0.99	0.2	–	Waste	2.0
ASV2	4	Extraction	430	0.34	0.90	0.2	0.12	Coal	3.5
STI1	–	Elec. only	900	0.30	0.30	0.2	–	Oil, heavy	8.5
KYB1	–	Elec. only	850	0.30	0.30	1	–	Oil, light	14.9
KYB2	–	Elec. only	850	0.30	0.30	1	–	Oil, light	14.9
KYB3	–	Elec. only	72	0.25	0.25	1	–	Oil, light	14.9
KYB4	–	Elec. only	504	0.25	0.25	1	–	Oil, light	14.9

It should be noted that both electric efficiency and total efficiency are calculated for the plant in back-pressure operation mode. In extraction power plants, the efficiency of the electricity production is variable according to the power loss factor by heat extraction β of the power plant [21]. A schematic representation of an extraction plant is presented in Fig. 3. The representation is similar to the one presented in Ref. [22].

For some of the energy technologies considered, it is required to include details about the ramp rate of the unit. Ramp rates are typically a concern in high pressure boilers, where material properties limit the boiler operational flexibility. The steam turbines of the power plant experience similar ramp constraints for cyclic loads and start-ups [23]. These constraints are included for all the plants in Table 1. The ramp rate denotes the maximal allowed change in boiler fuel input per operation hour. The ramp rate has been assumed for all CHP-plants. Four of the power plants (KYB1–KYB4) are emergency and peak load facilities. Thus the units must react quickly in case of imbalance between production and demand. The ramp rate has been set to 1 in this case.

Characteristics of the DH boilers are presented in Table 2. The heat incineration boilers are listed in the first part. Additionally, each DH area has a high amount of installed peak load boilers mainly operated on natural gas. These are included in the lower half of Table 2.

In three of the DH-networks, stratified storage tanks for hot DH-water are in use. The capacity and ramp rate of the storage have been included in Table 3. The ramp rate of a storage is defined as the maximum loading/unloading of stored heat to the network per hour. As the duration of the storage is short term (hours), no thermal losses are included.

One electric heater is installed in DH-network # 4 at the site of unit ASV2. Apart from the already installed units, four identical heat pumps, one for each DH-network, are included in the model for studying the options for optimal system operation with these installed. The inclusion of the four heat pumps is important as the purpose of the model is to investigate the relation between CHP-plants and heat pumps. The characteristics of the heat pumps are presented in Table 4. The Coefficient of Performance of the heat pumps is based on a mini-scale experiment [24], and within a plausible working domain as presented in Ref. [25]. The electricity consumed by heat pumps and the electric heater operation is priced in the optimisation using the hourly price of electricity. Heat loss in the DH-network is not considered as all consumption data are based on actual production from the plants, not end-user consumption.

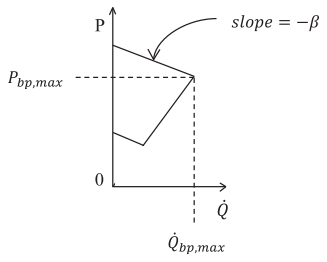

Fig. 3. Schematic representation of an extraction CHP-plant. Efficiency is calculated at full load back-pressure operation ($\dot{Q}_{bp,max}$, $P_{bp,max}$).

2.2. Unit formulation

For each individual optimisation model, the detailed formulations of units differ according to the requirements of the individual solver and model type. A generic formulation of the production constraints for an extraction CHP-plant is presented below for the linear case, as it constitutes the baseline for the comparison. The

Table 2
Boiler unit characteristics.

Plant name	Area	Type	Capacity boiler [MW]	Therm. efficiency [/]	Fuel	Fuel price [EUR/GJ]
LYN1	1	Heat only	14.0	0.95	Waste	2.0
AMF4	1	Heat only	43.6	0.85	Waste	2.0
KARA3	2	Heat only	40.6	0.69	Waste	2.0
VF1	3	Heat only	61.7	0.77	Waste	2.0
KBHb1	1	Heat only	2600	0.95	Nat. Gas	7.3
KBHb2	2	Heat only	1000	0.95	Nat. Gas	7.3
KBHb3	3	Heat only	200	0.95	Nat. Gas	7.3
ASVb1	4	Heat only	1000	0.95	Nat. Gas	7.3

Table 3
Storage units in DH (district heating) networks.

Unit name	Area	Type	Capacity [MW]	Therm. efficiency [/]	Ramp rate of storage [MWh/h]
STO1	1	Heat storage	750	1	300
STO2	2	Heat storage	2600	1	330
STO4	4	Heat storage	1200	1	300

equations correspond to the formulation used to derive the plant data in Table 1.

The relation between the products – electricity and heat – can be calculated based on equations (2) and (3) for back-pressure operation. Both heat and electricity depends directly on boiler load $\dot{Q}_b$ [MJ/s], and the heat production is calculated as the residual of electricity production.

$$P_{\mathrm{bp}} = \eta_{\mathrm{bp}} \cdot \dot{Q}_b \tag{2}$$

$$P_{\mathrm{bp}} + \dot{Q}_{\mathrm{bp}} = \eta_b \cdot \dot{Q}_b \tag{3}$$

where the electricity is denoted P_{bp} [MW], heat production is $\dot{Q}_{\mathrm{bp}}$ [MJ/s], boiler efficiency is η_b [−] and η_{bp} [−] is the electrical efficiency at back-pressure operation.

In the case of an extraction plant, the products can be found as formulated in equation (4).

$$P_{\mathrm{ex}} = P_{\mathrm{bp}} + \beta \cdot \left(\dot{Q}_{\mathrm{bp}} - \dot{Q}_{\mathrm{ex}}\right) \tag{4}$$

where the produced electricity and heat is denoted P_{ex} [MW] and $\dot{Q}_{\mathrm{ex}}$ [MJ/s] respectively, and β [−] is the power loss factor by heat extraction at a steam turbine. A graphical representation of the extraction CHP-plant in a linear optimisation model is presented in Fig. 4.

With this type of formulation, it is possible to include more than one unit type using in the same set of equations. In the case of a back-pressure CHP-plant, β can be fixed to 0. Similar, in the case of a separate electricity production plant, the electricity efficiency and total efficiency are equal, while β is fixed to 0.

It should be noted, that a lower operation limit is not allowed in a strictly linear optimisation. If a minimum load constraint is included in this approach, the CHP-plant will be forced to operate during all hours, regardless of the need for electricity or heat. Without the minimum constraint the plant will be allowed to shut-down when it is economically profitable. At the same time, this will allow the power plant to operate in very low load with the specified linear parameters. This may be allowed in linear dispatch models, as it may often be reasonable to assume that low load operation at one plant may be shifted to/from other plants in the network.

2.3. Causes of non-linearity

Representing non-linear relations as linear constraints in the optimisation model may have a significant impact on the results.

Table 4
Characteristics of heat pumps.

Plant name	Area	Type	Capacity Condenser [MW]	COP [/]	Fuel	Fuel price [EUR pr. GJ]
ASVe	4	Elec. Heat	98.0	0.95 [3]	Elec.	–
HP1	1	Elec. heat pump	100	3 [24]	Elec.	–
HP2	2	Elec. heat pump	100	3 [24]	Elec.	–
HP3	3	Elec. heat pump	100	3 [24]	Elec.	–
HP4	4	Elec. heat pump	100	3 [24]	Elec.	–

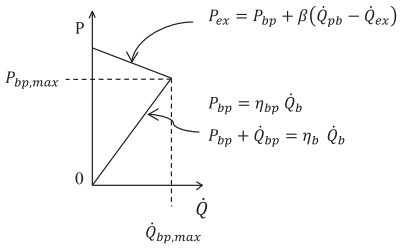

Fig. 4. Formulation of an extraction CHP-plant in a linear optimisation model. The formulation can also be used for a back-pressure CHP-plant and a 'power only' plant.

Considering the energy system in question, the vast majority of heat and electricity is produced in the CHP-plants, and consequently a linear representation for this plant type, may represent the largest error in the optimisation.

In the representation of both extraction and back-pressure CHP-plants (as well as separate power production plants) in a linear optimisation model, all parameters are assumed constant for the operating range of the plant. When considering the part-load performance of the equipment, it is clear that this assumption will lead to an error. Based on a literature review, two parameters have been identified as possible sources of error: the boiler efficiency [26] (applies to all power plants) and the design power to heat ratio [27,28] (only valid for extraction CHP-plants). Considering both parameters, the biggest deviations occur in "low" part-load operation, around 40% boiler load or below, close to the technical minimum limit of the boiler without auxiliary firing. For the remaining load range, variations in the two parameters are significantly lower.

2.4. The different optimisation model types

Three different numerical optimisation solvers are used to evaluate the effect of various assumptions. One of the investigated models utilises LP (linear programming) for optimisation, one uses LP with binary integer operation constraints (MIP), while the third model is solved using NLP (non-linear programming). The main characteristics of each individual model type are presented in Fig. 5 in the case of an extraction CHP-plant.

The LP model corresponds to the constraints and equations described in Section 2.2. With a LP model, the optimisation will return a global optimum.

A MIP (Mixed Integer Programming) model type, in this case with binary variables, allows the individual units to operate in on/off mode, as a minimum operation constraint is applied. In the used model type, the constraints are required to be linear. The cost of start-up and shut-down has been calculated based on the required fuel to comply with the ramp rate. The start-up and shut-down operation of a unit is consequently subject to a higher electricity and heat cost in the MIP model (compared to the LP), as the fuel price is included, without the corresponding production of utilities. The minimum constraint has been fixed at 35% of the boiler capacity in all units where a ramp rate is described in Section 2.1. Similarly to the LP model, the MIP model is guaranteed to return a global optimum.

Using a NLP solver a minimum constraint is not possible (similar reason as for the LP model). In the NLP model, the non-linear parameters η_b and β are varied according to the operation point of the individual unit. The part-load operation of all units follows similar

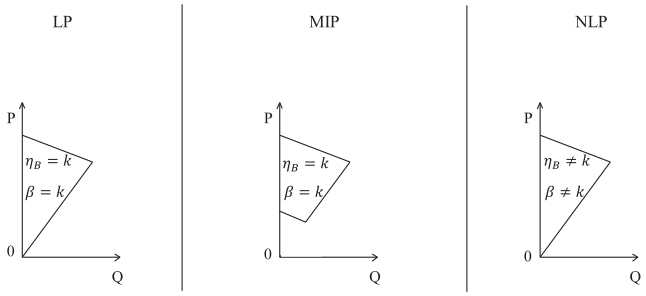

Fig. 5. Three different representations of operation constraints, boiler efficiency and β-value for the three optimisation models.

trend for boiler efficiency and β-value, but offset by the full load characteristics. As an example, a representation of the boiler efficiency is presented in Fig. 6. The full load (100%) boiler efficiency corresponds to a fixed value in all three cases. The remaining progress of the non-linear boiler efficiency corresponds to the variable function found in literature [26]. A similar approach is used for the non-linear representation of β. The NLP optimisation does not guarantee that the solution is a global optimum, unless the optimisation problem is convex. The type of problem investigated in this paper is not convex, indicating that a global optimisation is not guaranteed.

Two different optimisation software packages have been used in the study. Both packages can be used to solve several optimisation problem types. The CPLEX [29] package has been used for both the LP and MIP model, while the CONOPT3 [30] package has been used for the NLP optimisation.

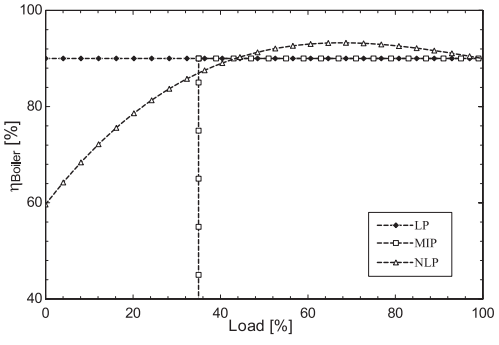

Fig. 6. Different representations of boiler efficiency in the three optimisation models.

3. Results

3.1. Optimisation timeframe and horizon

As some optimisation problems require a high amount of time consuming iterations, two different optimisation timeframes have been used in the evaluation. The full timeframe analysed in this paper is January 2011, which corresponds to 744 consecutive hours of operation optimisation for multiple utility units.

The reference approach is a direct optimisation of the complete time period in one iterative calculation. This approach can trigger a high amount of variables to optimise, depending on the amount of units in the system, and thus a long computation time. The second approach the rolling horizon procedure divides the investigated period into smaller time periods, typically to optimise individual calendar days. A graphical representation of the two different planning horizons is included in Fig. 7.

In order to obtain highly detailed results, the individual rolling optimisations must include knowledge of future demand, as knowledge of optimal storage and load must be included for each individual unit in each hour. The needed hours included in each optimisation is denoted by the term “Forecast”. The amount of hours is of particular interest, as the quality of the results relies on a lengthy forecast period, but at the same time the number of variables to optimise will increase correspondingly. The optimised period is defined as a 24 h plus a number of additional forecast hours. This period is the number of hours for which the optimisation algorithm estimates the electricity prices based on unit commitment. In practice this relates to the Nordic electricity market Nordpool in which all hourly electricity prices of the coming day are defined daily at noon by minimising the market price based on offers from all producers and consumer according to conventional price formation in a liberalised market [31].

Fig. 8 shows an evaluation of the difference in optimised cost when using the LP model with a perfect forecast and a rolling horizon approach. Each of the points represents an optimised solution

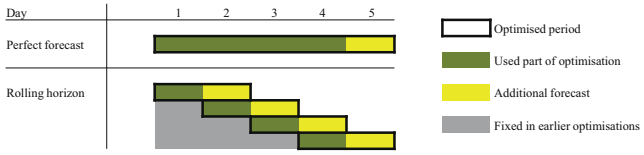

Fig. 7. Planning horizon for the optimisation problem.

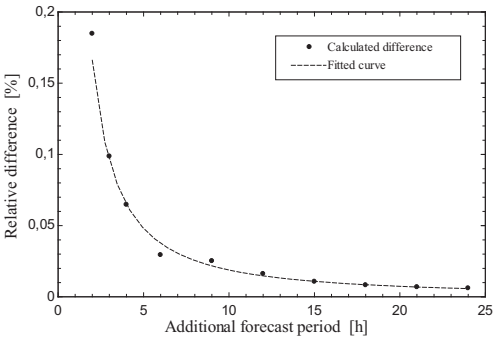

Fig. 8. Impact of the forecast period length to the optimised cost in the LP optimisation problem compared to an optimisation with perfect forecast.

for the full January 2011. The relative cost difference shown is the difference between the perfect forecast and the rolling horizon approach, with a variable forecast period. It is clear that the variation in terms of the optimised objective function is small, regardless of the length of forecast.

A larger relative difference is found when evaluating the effect of the changed forecast period on the amount of operating hours for the individual units. An example of the changed unit operation hours can be found in Fig. 9. The CHP-units with changed operation patterns are included (8 out of 16 units). Only smaller units experience a high difference in operation hours with a longer forecast period than 12 h, and consequently they do not contribute significantly to the cost calculation.

As a consequence of the above results and as this forecast length is typically used in daily optimisation of energy systems [19,31], a 12 h forecast period has been chosen for the remaining optimisations used in this study.

3.2. Computation time of the various approaches

Long computation times are required when optimising MIP and NLP problems using the perfect horizon approach. In both cases the amount of variables has a strong influence on the computation

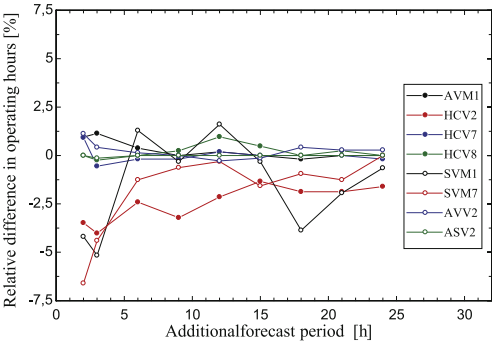

Fig. 9. Relative difference in operation hours for the CHP-plants that experience changed operation due to a changed forecast period. The units that are not included in the figure do not experience a change in the number of operation hours.

Table 5
Computation time for the four approaches.

Type	Planning horizon	Unit	Time
LP	Perfect Horizon	[s]	12
LP	Rolling horizon (12h)	[s]	23
MIP	Rolling horizon (12h)	[s]	56
NLP	Rolling horizon (12h)	[s]	50,400

time. For this reason, only the rolling horizon approach has been used for MIP and NLP. The computation time for the individual optimisation problems is listed in Table 5 using an Intel i5 laptop processor (2.67 GHz) with 64 bit windows 7.

In the case of LP optimisation, the combined computation time is prolonged for the rolling horizon approach. The increased processing time of the LP model is explained by pre- and post-processing of the individual optimisation problems, which becomes a significant factor when the amount of variables is low. For the MIP and NLP problems, the computation time for perfect horizon optimisation is significantly increased compared to the rolling horizon approach.

3.3. Comparison of the optimised unit operation

The main results of the different optimisation types are presented in Tables 6–8. Results from the rolling horizon LP, MIP and NLP optimisations are presented as relative to the perfect horizon LP solution. In Table 6 the operational hours for each unit are listed. Considering both the MIP and NLP optimisation solutions, significantly different numbers of operation hours are found for the CHP-plants of DH area 1. The main part of these plants operates with high fuel costs and low electric efficiency. In the LP approach the units are operated in the low part-load region. As this is not possible in both the MIP and the NLP approach, units must either be shut-down (MIP) or operate at a higher load or maintain the load at a lower efficiency (NLP).

The results indicate that an increased amount of operational constraints in the low part-load region of the CHP-plants lead to increased use of heat pumps in the proposed system. The highest increase in heat pump operation is experienced in the NLP model, where the variable efficiency of power plant boilers is included. The

Table 6
Comparison of operation hours for CHP and heat pump units from each model.

	Area	LP		MIP	NLP
		Perfect horizon [h]	Rolling horizon (12 h) [%]	Rolling horizon (12 h) [%]	Rolling horizon (12 h) [%]
AMV1	1	526	0.2	16.9	0.8
AMV3	1	744	0	0	0
HCV2	1	373	−2.1	−3.2	11.8
HCV7	1	541	0.2	5.4	2.2
HCV8	1	413	1.0	6.5	9.0
SVM1	1	310	1.6	−54.8	26.5
SVM7	1	318	−0.3	−46.5	22.3
AMF1	1	744	0	0	0
AVV1	2	744	0	0	0
AVV2	2	709	−0.3	2.5	−0.7
KARA5	2	744	0	0	0
VF5	3	744	0	0	0
VF6	3	744	0	0	0
ASV2	4	731	0.0	−1.4	0.5
HP1	1	222	−1.8	17.1	36.0
HP2	2	194	17.5	28.4	50.0
HP3	3	231	−6.1	10.4	35.1
HP4	4	20	15.0	180.0	30.0
ASVe	4	6	0.0	40.0	0

Table 7
Comparison of the average heat pump load.

	Area	LP		MIP	NLP
		Perfect horizon [MJ/s]	Rolling horizon (12 h) [%]	Rolling horizon (12 h) [%]	Rolling horizon (12 h) [%]
HP1	1	90.6	1.4	−1.0	−4.1
HP2	2	88.4	−0.6	3.7	−3.4
HP3	3	92.1	−1.3	−0.2	−8.6
HP4	4	78.0	2.0	−4.0	−6.3
ASVe	4	36.6	8.8	39.6	16.1

use of the heat pump capacity allows the optimisation to shift the production in the CHP-plant toward a higher efficiency, which results in an increase of approximately 100 operation hours compared to the MIP approach. The average load of the individual heat pumps is listed in Table 7. For all the investigated approaches the average heat pump load is close to constant. The average load of heat pumps in the NLP approach is generally slightly lower than for the remaining cases, which may be caused by the above described load shifting in CHP-plants.

Using the data from Tables 7 and 8, the full amount of heat produced by the heat pumps can be calculated. The production data is summed for each individual approach, and presented in Table 8. In this case, the increased heat production from heat pumps is 23% in the case of MIP and 32% using the NLP approach.

The combined cost of the produced utilities is presented in Table 9. MIP and NLP are constrained from efficient production in the low part-load regime. The start-up and shut-down costs in the MIP model correspond to consumption of fuel without utility production. The result is a higher cost for the MIP than in the NLP approach.

Fig. 10 presents the heat pump production with a variation of four key parameters when the optimisation is performed using the perfect horizon LP approach. In Table 10 a similar parametric investigation is presented for all four approaches. The results of the parametric variations for each algorithm are presented relative to the perfect horizon LP for the given parameter setting. The variation of the four chosen variables with ±10% show significant changes of the operation hours and heat production characteristics for all of the considered models. By investigation of the resulting heat production differences between the four programming methods, the MIP and NLP models show similar tendencies in all 9 considered cases compared to the LP optimisation methods, although with some deviation in the magnitude of the operational characteristics. NLP is assumed to be most accurate, but it is infeasible due to the huge solution times. The analysis shows that MIP is a reasonably accurate alternative.

4. Discussion

A comparison of the cost of produced utilities indicates a quite good overall representation of the energy system using only linear constraints. Although, when looking at the operation of a few of the considered CHP-plants and the heat pumps, operation hours and load may be subject to the changed optimisation approach. For both of the alternative approaches where the CHP-plant is subject to an increased amount of constraints, the heat pumps experience significantly increased operation.

Table 8
Heat production from heat pumps for each individual approach.

	LP		MIP	NLP
	Perfect horizon [GWh]	Rolling horizon (12 h) [%]	Rolling horizon (12 h) [%]	Rolling horizon (12 h) [%]
Produced heat	60.11	2.5	22.7	31.8

Table 9
Cost of produced utilities for each individual approach.

	LP		MIP	NLP
	Perfect horizon [Euro]	Rolling horizon (12 h) [%]	Rolling horizon (12 h) [%]	Rolling horizon (12 h) [%]
Cost	49.995.000	0.0	3.1	2.4

The principle of rolling horizon is used in daily energy planning optimisation. Considering the comparison in Section 3.1, optimisation using perfect horizon may consequently lead to imperfections in operation compared to practise. Additionally, the use of rolling planning will in most cases improve the calculation time.

Considering the non-linear operation dispatch model, the computation time, and the fact that optimal operation may not be reached, may result in applicability issues, depending on the application of the model. In the case where the model is used for optimisation of online equipment (such as operator production optimisation), the computation time and forecast period should be considered, such that the knowledge of intermittent production in the forecast period is not limited. For planning purposes, the computation time has a lower impact, although costly and troublesome for the researchers.

Only fuel cost was considered in the optimisation. If other variable costs were included, one possibility would be to include cost as a linear expression related to production. Using this approach would influence the relation between the optimised LP and MIP/NLP.

Many of the small-scale decentralised CHP-plants are now operated with heat storage, as this provides the possibility to shift production timeframe. The assumption of operation with a strict policy to meet the heating demand may thus be challenged. This impact may be assessed in future work.

The changed operation as a result of the MIP and NLP optimisation (compared to the LP) indicates, that increased detail of some

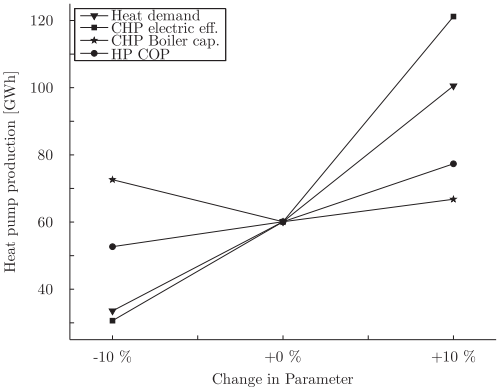

Fig. 10. Heat pump production with variation of four key parameters using the LP perfect horizon optimisation.

Table 10
Parametric variation of differences in heat pump heat production from individual programming methods. The perfect horizon LP optimisation is used as reference approach and presented as heat production in GWh. Remaining approaches are presented as changed production relative to LP perfect horizon.

	LP		MIP	NLP
	Perfect horizon [GWh]	Rolling horizon (12 h) [%]	Rolling horizon (12 h) [%]	Rolling horizon (12 h) [%]
Baseline	60.11	2.5	22.7	31.8
−10 % heat demand	33.55	4.3	48.7	29.7
+10 % heat demand	100.52	−0.9	−1.1	6.9
−10 % elec. eff. in CHP	30.64	5.9	33.2	48.4
+10 % elec. eff. in CHP	121.12	−0.1	3.1	−2.6
−10 % CHP boiler cap.	72.61	0.3	−0.1	−3.7
+10 % CHP boiler cap.	66.76	2.8	23.5	38.0
−10 % HP COP	51.67	2.0	24.5	37.8
+10 % HP COP	77.35	−0.4	9.7	12.5

of the technologies may impact the optimum system in several of the previously mentioned dispatch models. This is especially true for optimisations considering the combination of products from CHP-plants.

5. Conclusion

Three frequently used operation optimisation methods have been examined, in order to investigate their impact on operation management of energy system technologies. By focussing on the physical representation of a CHP-plant, it is clear that a simple representation allows infeasible production. In the present case the non-linearity occurs in the boiler efficiency of power plants and the β-value of an extraction plant.

The investigated optimisation types are LP, MIP and NLP. The LP model is used as a benchmark, as this type is frequently used, and has the lowest amount of constraints of the three. Comparisons of the derived operation of units show significant differences between the three methods. For the heat pumps, the linear optimisation yields the lowest amount of operation hours. Using MIP optimisation, the number of operation hours for heat pumps is increased by 23%, while for a NLP optimisation the increase is more than 39%. Considering the total production of heat from heat pumps, the two approaches differ by approx. 23% and 32% respectively. For the CHP-plants, significant operational changes occur in case of low efficiency electricity production with expensive fuels. The changes are especially visible in case of using the NLP optimisation, where the boiler efficiency is reduced in part load. The changed operation hours and production may lead to a different investment optimum. The results are further supported by a parametric investigation of 4 key parameters, which show that the operational performances of the heat pumps are roughly similar in MIP and NLP optimisations compared to LP approaches.

Acknowledgement

This work was supported by Copenhagen Cleantech Cluster (CCC), DONG Energy and Teknologisk Institut (DTI)

Nomenclature

β	power loss factor by heat extraction at a steam turbine
C	cost of produced product
P	electricity production, MW
$\dot{Q}$	heat production, MJ/s
η	efficiency

Subscripts

b	boiler
bp	back-pressure operation
ex	extraction operation
i	production unit
max	maximum
t	time

Abbreviations

CHP	Combined Heat and Power
COP	Coefficient Of Performance
DH	District Heating
LP	Linear Programming
MIP	Mixed Integer Programming
NLP	Non-Linear Programming

References

[1] Holttinen H. Estimating the impacts of wind power on power systems – summary of IEA wind collaboration. Environ Res Lett 2008;3(2).
[2] Kiviluoma J, Meibom P. Influence of wind power, plug-in electric vehicles, and heat storages on power system investments. Energy 2010;35(3):1244–55.
[3] Blarke MB. Towards an intermittency-friendly energy system: comparing electric boilers and heat pumps in distributed cogeneration. Appl Energy 2012;91(1):349–65.
[4] Oestergaard PA. Wind power integration in Aalborg municipality using compression heat pumps and geothermal absorption heat pumps. Energy 2013;49(1):502–8.
[5] Münster M, Morthorst PE, Larsen HV, Bregnbaek L, Werling J, Lindboe HH, et al. The role of district heating in the future Danish energy system. Energy 2012;48(1):47–55.
[6] Molyneaux A, Leyland G, Favrat D. Environomic multi-objective optimisation of a district heating network considering centralized and decentralized heat pumps. Energy 2010;35(2):751–8.
[7] Mancarella P. Cogeneration systems with electric heat pumps: energy-shifting properties and equivalent plant modelling. Energy Convers Manag 2009;50(8):1991–9.
[8] Connolly D, Lund H, Mathiesen BV, Leahy D. A review of computer tools for analysing the integration of renewable energy into various energy systems. Appl Energy 2010;87(4):1059–82.
[9] Ropenus S, Jacobsen HK, Schrüder ST. Network regulation and support schemes – how policy interactions affect the integration of distributed generation. Renew Energy 2011;36(7):1949–56.
[10] Tuohy A, Meibom P, Denny E, O'Malley M. Unit commitment for systems with significant wind penetration. IEEE Trans Power Syst 2009;24(2):592–601.
[11] Karlsson K, Meibom P. Optimal investment paths for future renewable based energy systems-using the optimisation model Balmorel. Int J Hydrogen Energy 2008;33(7):1777–87.
[12] Danish Energy Agency. Energy statistics 2011. Data, tables, statistics and maps. Tech. Rep.. Available at: http://www.ens.dk/sites/ens.dk/files/info/facts-figures/energy-statistics-indicators-energy-efficiency/annual-energy-statistics//Energy%20Statistics%202011.pdf; 2012 [accessed 13.09.13]
[13] Energinet.dk. Download of market data. Available at: http://www.energinet.dk/EN/El/Engrosmarked/Udtraek-af-markedsdata/Sider/default.aspx; 2011 [accessed 13.09.13].
[14] HOFOR A/S. Personal communication. Consumption of district heating in 2011; 2012.
[15] GAMS Development Corporation. General algebraic modeling system. Available at: http://www.gams.com/download/; 1998 [accessed 13.09.13], Licensed software.
[16] Ferris MC. MATLAB and GAMS: interfacing optimization and visualization software. Tech. Rep.. Available at: http://pages.cs.wisc.edu/ferris/matlabgams.pdf; 2005 [accessed 13.09.13]
[17] Schaumburg-Muller C, Clausen J, Ravn HV. Mathematical models and methods for analysis of distributed power generation on market conditions. PHD thesis. Kgs, Lyngby: DTU IMM; 2008.
[18] Danish Energy Agency. Technology data for energy plants. Tech. Rep. 1. Available at:, http://www.energinet.dk/SiteCollectionDocuments/Danske%20dokumenter/Forskning/Technology_data_for_energy_plants.pdf; 2010 [accessed 13.09.13].
[19] Energinet.dk. Energinet.dk analytic prerequisites 2012–2035 [Energinet.dk's analyseforudsaetninger 2012–2035] [in Danish]. Tech. Rep. 1. Available at:, http://www.energinet.dk/SiteCollectionDocuments/Danske%20dokumenter/El/Energinet.dk's%20analyseforuds%C3%A6tninger%202012-2035,%20juli%202012.pdf; 2012 [accessed 13.09.13].
[20] International Energy Agency. World energy outlook 2012; 2012. Tech. Rep. 1.
[21] Verbruggen A. Combined heat and power (CHP) essentials. Int J Energy Technol Pol 2007;5(1):1–16.

[22] Larsen HV, Palsson H, Ravn HF. Probabilistic production simulation including combined heat and power plants. Electr Power Syst Res 1998;48(1):45–56.
[23] Kosman G, Rusin A. The influence of the start-ups and cyclic loads of steam turbines conducted according to European standards on the component's life. Energy 2001;26(12):1083–99.
[24] Christensen KG, Patru LC, Poulsen CS, Rudmose C, Hansen EN, Hansen TM. Mini-scale heat pump using CO_2 for distributed cogeneration plants [Miniskala-varmepumpe med CO_2 som koelemiddel til decentrale kraftvarmevaerker] [in Danish]; 2007. Tech. Rep. 1373/03-0007.
[25] Brunin O, Feidt M, Hivet B. Comparison of the working domains of some compression heat pumps and a compression-absorption heat pump. Int J Refrigeration 1997;20(5):308.
[26] Effenberger H. Wirkungsgrad und Verluste. Dampferzeugung. Berlin: Springer; 2010. p. 611.
[27] Verbruggen A. A system model of combined heat and power generation in district heating. Resour Energy 1982;4(3):231–63.
[28] Johansen AO. Simulation and optimisation of thermal power stations by use of turabs. Tech. Rep. Elsam Engineering A/S; 2010. now: DONG Energy) 1
[29] IBM. IBM ILOG CPLEX 12.4.0.1; 2012. Licensed software.
[30] ARKI Consulting and Development. Conopt 3.15F; 2012. Licensed software.
[31] Nordpoolspot.com. The day-ahead market – Elspot. Available at: http://www.nordpoolspot.com/How-does-it-work/Day-ahead-market-Elspot-/; 2013 [accessed 13.09.13].

Appendix D

Paper 2 - Energy

Torben Ommen, Wiebke Brix Markussen and Brian Elmegaard

Heat pumps in combined heat and power systems

Energy, 76 (2014) 989-1000

Energy 76 (2014) 989–1000

Contents lists available at ScienceDirect

Energy

journal homepage: www.elsevier.com/locate/energy

Heat pumps in combined heat and power systems

Torben Ommen*, Wiebke Brix Markussen, Brian Elmegaard

Technical University of Denmark, Kgs. Lyngby, Denmark

ARTICLE INFO

Article history:
Received 24 January 2014
Received in revised form
14 August 2014
Accepted 6 September 2014
Available online 30 September 2014

Keywords:
Heat pumps
District heating
Combined heat and power

ABSTRACT

Heat pumps have previously been proposed as a way to integrate higher amounts of renewable energy in DH (district heating) networks by integrating, e.g., wind power. The paper identifies and compares five generic configurations of heat pumps in DH systems. The operational performance of the configurations is investigated at both local and system level considering different DH network temperatures, different fuels and different production technologies in the DH network. The results show that in terms of system performance and cost of fuel one or two configurations are superior for all of the considered cases. When considering a case where the heat pump is located at a CHP (combined heat and power) plant, a configuration that increases the DH return temperature proposes the lowest operation cost, as low as 12 EUR MWh^{-1} for a 90 °C – 40 °C DH network. Considering the volumetric heating capacity, a third configuration is superior in all cases. Finally, the three most promising heat pump configurations are integrated in a modified PQ-diagram of the CHP plant. Each show individual advantages, and for two, also disadvantages in order to achieve flexible operation.

1. Introduction

DH (district heating) systems are used as a means to increase overall energy efficiency and reduce consumption of fossil fuels in urban areas [1,2]. Such systems are implemented in many cities of northern Europe where CHP (combined heat and power) plants provide low carbon intensive heat from co-production with electricity. In order to further reduce the fossil fuel dependency of domestic heating, the use of renewable energy sources must be considered.

Heat pumps driven by electricity from renewable sources are proposed as a step to replace fossil-fuelled boilers [3–5]. The heat pump units can be installed in individual dwellings or as production units in DH networks. An advantage of implementing heat pumps in the DH networks is that they can be used to decouple the production constraints of the co-produced products at the CHP plants. This is especially important in systems with a high heat-to-power demand [6]. Using this ability, a higher amount of intermittent renewable power production can be integrated in energy systems with CHP plants, without further reducing the possibilities for efficient production in the thermal plants [7]. In this case, a reduction in carbon emissions can be achieved by utilising renewable energy sources for the heat pump compressor and evaporator.

For optimal utilization of the renewable energy and for economic reasons, the thermodynamic performance of the heat pump technology is of major interest. In liberalized energy markets, the installed utility technologies are optimized in an effort to reduce total production cost for each individual hour of production. Thus, a unit with low production cost and synergies with base load power production equipment will experience a higher amount of operating hours than that of a unit with higher heat price or a negative impact to the system operation. The fuel consumption of operating the heat pump and the derived effects in the system will thus have a major impact on the operation.

Only a few previous works discuss the optimal operation distribution between thermal power production, co-production of heat, and heat pumps: Blarke and Lund [8] discuss the impact of two different heat sources for a parallelly coupled HP at a small decentral CHP plant considering optimal operation of the units. In Malinowska and Malinowski [9] a study of exergetic efficiency is performed on a serially coupled HP and small-scale CHP plant. Lowe [10] assesses the heat production capabilities of a CHP by considering the combination of a conventional steam turbine cycle and an HP at varying condensing temperatures of the CHP plant. He finds that heat production of CHP plant is highly effective with a performance advantage in the order of a factor of 3 when compared to the coefficient of performance of heat pumps. In contrast, Dagilis [11] discusses the possibility of combining traditional power plants

* Corresponding author.
E-mail addresses: tsom@mek.dtu.dk (T. Ommen), wb@mek.dtu.dk (W.B. Markussen), be@mek.dtu.dk (B. Elmegaard).

http://dx.doi.org/10.1016/j.energy.2014.09.016
0360-5442/

and HP to obtain cost efficient CHP plants. None of these previous works discuss more than one configuration, or mentions the possibility of other plausible configurations.

In this paper, five basic configurations of heat pumps in district heating systems are identified. The operational performance of the configurations are investigated for different DH network temperatures, assuming that the network is supplied by a CHP plant and the heat pump is operated by electric motors. The analysis focusses on four key performance factors chosen to indicate the performance from a system perspective and differences between system performance and the performance of the heat pump. The target figures are the COP (coefficient of performance), COSP (coefficient of system performance), the VHC (volumetric heating capacity), and the cost of fuel. The five configurations are additionally examined considering the shaft power delivered by an ICE (internal combustion engine) operating on natural gas.

As another case, the DH network can be fed by surplus heat in stack gases or from various renewable sources. This case is also considered in the paper in order to make a fair comparison for the configurations where lower return temperatures may have a significant effect on the main production technology of the DH network.

1.1. Heat pumps in finite reservoirs

In industrial processes, and similarly in DH networks, the heat capacity of the reservoirs are finite and thus the difference in temperature between inlet and outlet of a stream, the temperature glide, may be of high importance for the efficiency of the new solutions. For heat pumps in such processes, it is important to consider the temperature glide of both sink and source in order to achieve optimal integration of the technology [12,13].

A schematic diagram of a single stage vapour compression heat pump is presented in Fig. 1. The nomenclature used matches that of several studies, e.g., Refs. [14,15]. The operating conditions of a heat pump can be evaluated based on four variables, considering the case where a fixed temperature difference is assumed for the two heat exchangers. The required variables are: the temperature of the sink process stream leaving the condenser T_{sink}, the temperature lift ΔT_{lift} and the process stream temperature glides from inlet to outlet in both heat exchangers (ΔT_{sink} and ΔT_{source}).

By using these four temperature variables and defining an expression for heat transfer in each of the heat exchangers, state points can be found for both heat exchangers using properties of sink, source and heat pump working fluid. We define the heat transfer of the condenser and evaporator by a pinch temperature difference, ΔT_{pinch}. An example of a the heat exchange processes for a pure refrigerant using finite temperatures of the reservoirs is presented in Fig. 2.

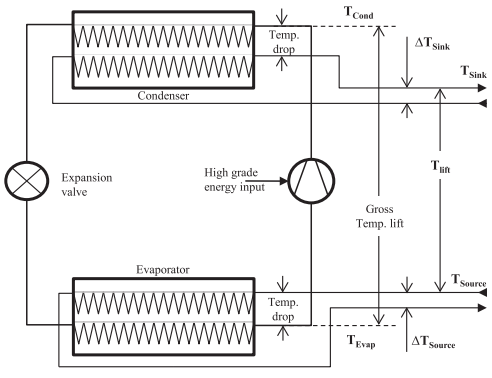

Fig. 1. Schematic diagram of a single stage heat pump system.

1.2. Heat pump configurations in a district heating network

District heating networks are not uniform in sizes or technology. The networks are built according to a large variety of specifications: temperature of demand, pressure levels, direct or indirect installations, with or without transmission lines etc. Thus, when considering the temperature levels of forward and return lines in DH networks, a span is needed rather than a fixed temperature. In a Danish context the forward temperature ($T_{\text{DH,Forward}}$) varies from 70 °C to 120 °C [16,17] mainly depending on size of the network and its commissioning year. The corresponding network return temperatures ($T_{\text{DH,Forward}}$) range from 35 °C to 55 °C. For the present study three different temperature levels of the network have been chosen as representative of the full range of temperatures. The temperature data is presented in Table 1.

Besides the temperature levels of the DH network, additionally two temperatures can be considered: the highest temperature of the available renewable heat source and the temperature of the demand of heat, which may be considered as the highest temperature of a finite heat capacity flow.

The temperature of the source is dictated by the type and location of the installation [18]. Smaller systems operate with source temperature according to the available media at the location of the heat demand. By using a DH network, larger installations can be located near heat sources of elevated temperatures (compared to ambient conditions), such as sewage water, industrial waste heat, power plants etc. Most of these heat sources tend to have a low yearly temperature variation and a finite heat capacity rate of the stream. In some cases the heat source can also be ocean or lakes

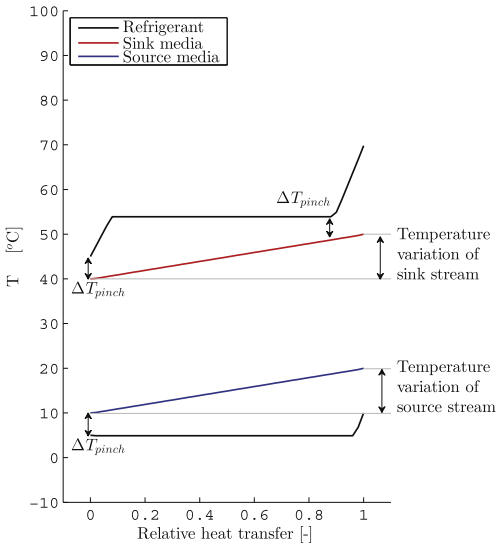

Fig. 2. Schematic diagram of condenser and evaporator in a single stage heat pump system. The transferred heat is normalised for each of the heat exchangers.

Table 1
Data of operating conditions of district heating networks.

Type	DH forward temperature	DH return temperature
1	105 °C	50 °C
2	90 °C	40 °C
3	70 °C	35 °C

where yearly variation in temperature would be expected. Table 2 presents typical values of available source heat in Danish conditions. The decentral heat source is assumed to utilise soil collectors at a sufficient depth in order to allow a temperature which is close to the average of ambient temperatures in the Danish design reference year [19].

Based on the four identified temperature levels of the district heating network, five possible heat pump configurations have been identified [8,18,20,21]. The configurations are presented in Fig. 3 where the white arrow indicates the temperature lift from T_{Source} to T_{Sink}, and the temperature glides (ΔT_{Sink} and ΔT_{Source}) are indicated by the dashed and full arrows, respectively. The span of demand temperatures is represented by the dotted area in the figure. If the DH network is mainly used to supply heat to dwellings and comfort heat for commercial businesses, the upper temperature of the heat demand can be assumed to be at 60 °C for Danish conditions [21].

The configurations are termed with the initial letter of both the source and the sink temperature level (e.g., the combination SF " (source-forward)" for Source and Forward, respectively):

SF (source-forward)

Heat pump with a temperature lift between $T_{DH,Forward}$ and T_{Source}. The sink process stream is heated from the temperature of the return line. The temperature glide of the source corresponds to the heat capacity of the finite heat capacity of the heat source.

The SF configuration can operate independently of other technologies in a DH network.

SD (source-demand)

Sink and source temperatures are T_{Demand} and T_{Source}, respectively. This configuration is similar to commercially available heat pump installations in dwellings. The sink process stream is heated from the temperature of the source. The temperature glide of the source corresponds to the heat capacity of the finite heat capacity of the heat source.

The SD (source-demand) configuration does not require a DH network in order to operate. The location of this heat pump type is de−central as the heat is delivered directly to the consumer.

SR (source-return)

The heat pump can be used to preheat the return line of a DH network before entering the CHP plant. Using this configuration, the temperature lift of the heat pump is the difference between $T_{DH,Return}$ and T_{Source}. Thus the temperature lift is significantly lower compared to configuration SF, which increases COP of the heat pump. This will reduce the electric efficiency of the CHP plant due to the increased condensing pressure [22]. ΔT_{Sink} is thus subject to optimisation in each individual DH system considering the generation technologies. The temperature glide of the source corresponds to the heat capacity of the finite heat capacity of the heat source.

The SR (source-return) configuration requires the use of other generation technologies in order to increase the temperature to that of the forward line.

Table 2
Heat pump source operating conditions.

Type	T_{source}	ΔT_{source}
Central	20 °C	10 K
Decentral	7.5 °C	5 K

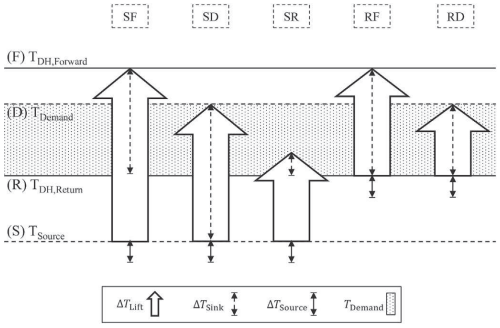

Fig. 3. Five possible configurations for district heating heat pumps.

RF (return-forward)

A heat pump configuration utilising the return line of the DH network as the heat source and forward line as sink. The source temperature glide is the lowered temperature of the return line of the DH network. The optimal temperature should be determined based on the coherence with other heat production units of the DH network.

The RF (return-forward) configuration requires the use of other generation technologies in order to increase the temperature to that of the forward line.

RD (return-demand)

Another configuration which utilises the return line as the heat source. The temperature lift is the difference between $T_{DH,Return}$ and T_{Demand}. This is similar to the sink glide, if it is assumed that the sink process stream is preheated by the DH return line. The source temperature glide is the lowered temperature of the return line of the DH network. The optimal temperature should be determined based on the coherence with other heat production units of the DH network.

The RD configuration requires the use of other generation technologies in order to increase the temperature to that of the forward line. The location of this heat pump type is de−central as the heat is delivered directly to the consumer. In this way, the heat pump can allow higher capacity in the DH network pipes, as the temperature difference between the forward and return is increased.

Schematic diagrams are shown in Fig. 4 for each of the five configurations. For the RF configuration two configurations are shown. Each of the diagrams are presented with two sets of dotted lines indicating two control volumes used for the analysis.

For configuration SF and configuration RF special cases are applicable. If operated concurrently with the CHP plant it is possible to mix streams, such that the sink temperature of the heat pump can be lowered, by increasing the temperature of the forward DH stream. The changed production of heat will reduce the electricity production of the CHP plant. These special cases are not further investigated in this paper. They will not influence the results significantly.

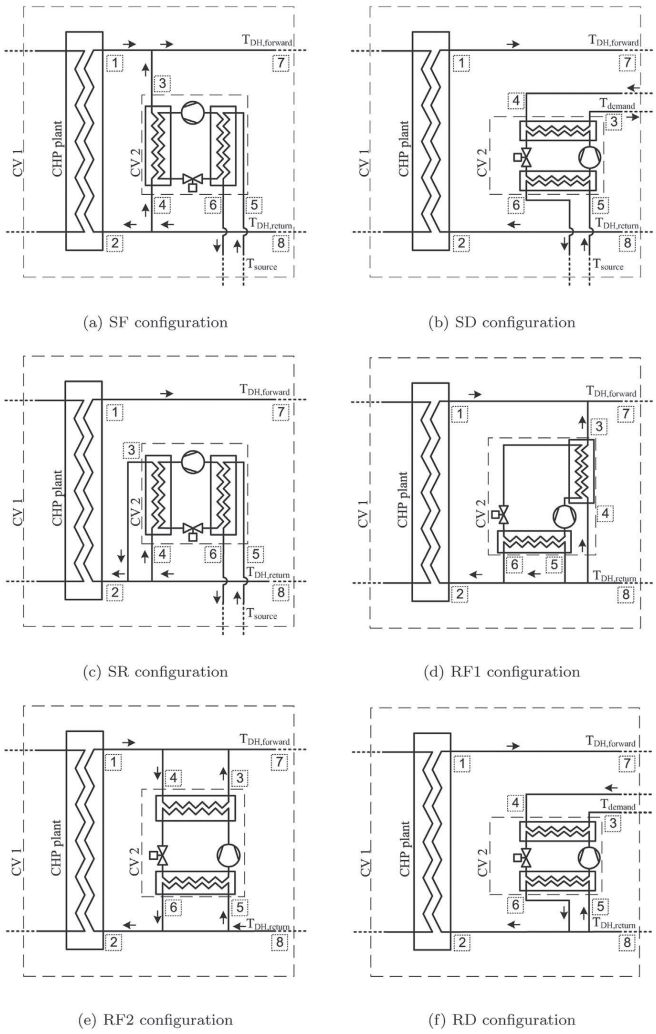

(a) SF configuration

(b) SD configuration

(c) SR configuration

(d) RF1 configuration

(e) RF2 configuration

(f) RD configuration

Fig. 4. Six schematic diagrams of the five identified configurations. Two similar schematic diagrams have been identified for the configuration RF. The dotted boxes indicate the two control volumes CV1 and CV2 considered when performing the system analysis and the heat pump analysis, respectively. Eight (similar) state points are identified for each configuration, these are further described in Section 3.2.

Configurations RF and RD do not utilize an external heat source for the heat production. Assuming production of heat and electricity does not change significantly due to the source temperature offsets in other production equipment, the heat pump can be seen as a thermal short-circuit electric heater, as only the consumed electricity of the compressor is added to the DH network. Thus, the advantage of using these heat pump configurations rather than an electric boiler will require significant operation advantages in other production technologies in the system.

2. Method

The different configurations are compared considering a single stage heat pump cycle. The comparison is done without considering possibilities for improved performance by, e.g., internal heat exchangers or several heat pumps connected in series. The refrigerant R134a has been used as working fluid for the heat pump cycle.

In the calculation of the heat pump cycle, some assumptions have been made. These include pressure drop in pipes and heat

exchangers, the extent of non-useful superheat and sub-cooling in gas and liquid lines, respectively, as well as compressor heat losses.

The calculations are performed for a heat pump system delivering 1 $MJ\,s^{-1}$ considering control volume 1 (system level) in Fig. 4. In this way the calculations include the changed heat production of the power plant. Only full load operation is considered.

A numerical model is implemented in EES (engineering equation solver) [23] for each of the heat pump configurations. The steady state models include between 440 and 480 algebraic variables and are solved in approximately 0.2 s.

2.1. Extraction CHP plant

In order to evaluate the effects of changing DH network temperatures, a separate model of an extraction CHP plant has been programmed in EES. The model follows the instructions of the proposal for simulator contest of ECOS 2003 [24,22], where specific information about the temperatures, isentropic efficiencies, temperature differences, auxiliary power consumption and pressure losses are defined.

Besides energy, entropy and mass balances, different expressions are used to establish the impulse balances in different parts of the system. For each section of the turbines, a turbine constant accounts for the swallowing capacity:

$$C_T = \frac{\dot{m}\cdot\sqrt{T_i}}{\sqrt{p_i^2 - p_o^2}} \tag{1}$$

For each of the valves, a flow characteristic has been fixed, in order to account for the pressure losses when the valve is operated between fully open and fully closed.

$$\dot{V} = \alpha_{\text{valve}}\cdot k\cdot\sqrt{\frac{\Delta p_{\text{valve}}}{\rho_i}}, \tag{2}$$

where α is the flow characteristic, k is the opening degree of the valve and Δp_{valve} is the pressure loss over the valve.

A schematic diagram of low pressure turbine section and the DH network heat exchanger in the modelled extraction CHP plant is presented in Fig. 5. The steam enters the low pressure part of the turbine train after expansion in the intermediate pressure turbine, Ip2, and may be used for power generation or district heating supply. The output of each product is controlled by adjusting the valves before the low pressure turbines and the district heating heat exchangers. With fully closed valves before the heat exchangers and fully open valves before low pressure turbines, the plant operates in condensing mode. It operates in full back pressure mode when the valves are in the opposite positions.

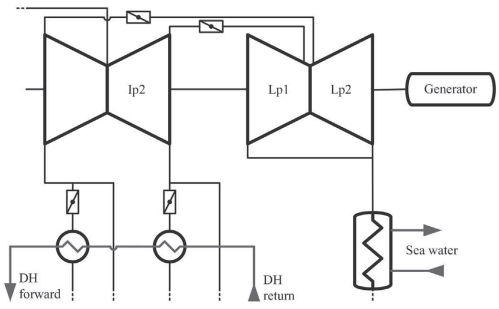

Fig. 5. Schematic diagram of the DH network heat exchanger in the modelled extraction CHP plant.

The model represents a plant with an electric efficiency of 42.0% and 34.9% at full boiler load and in condensing mode and full back pressure mode, respectively. In full back pressure mode the energy utilization is 91.5%.

2.2. Heat pump driven by electric motor or internal combustion engine

Each of the configurations presented in Fig. 4 proposes the possibility for the heat pump to be driven by an electrical motor or an internal combustion engine operated on either fossil or renewable fuels. In this paper, this option is represented by a natural gas driven ICE according to [25].

Both options imply mechanical losses in order to convert the energy content of the fuel to shaft power as defined in Table 4. In the case of the ICE, additional heat is available according to the total efficiency of the gas engine. The additional heat is assumed to be available at 90 °C.

2.3. DH networks fed by stack gases or renewables

As alternative heating sources for the DH network, surplus heat from stack gases or renewable energy technologies such as solar thermal systems are proposed and increasingly used. In such systems a significant increase in heat production can be achieved by lowering DH return temperatures.

A counterflow stack gas heat exchanger has been modelled in order to evaluate the performance of the configurations in a system where the DH network is not fed by CHP plants. The stack gas has been assumed to enter the heat exchanger at a temperature of 200 °C and with a minimum pinch point temperature difference in the heat exchanger of 20 K. The gas properties are assumed similar to those of air.

2.4. Energy efficiency, volumetric heating capacity and cost

The focus of the analysis is to evaluate the performance of the heat pump configurations from a system perspective. The analysis focusses on four performance factors, which are the coefficient of performance (COP), coefficient of system performance (COSP), the volumetric heating capacity (VHC) and the cost of fuel.

The coefficient of performance is calculated for the heat pump cycle using control volume 2 (CV2) as presented in Fig. 4.

$$\text{COP}_{\text{HP}} = \frac{\dot{Q}_{\text{cond}}}{\dot{W}_{\text{shaft}}} \tag{3}$$

On a system perspective, represented by control volume 1 (CV1) in Fig 4, the performance of the combined HP and CHP technologies can be calculated by two similar methods:

Table 3
Cost data for different fuel types from 2011, specific taxes apply for HP in DH depending on the operator of the unit.

Type	Unit	Consumer	Company
Electricity (excl. tax and network tarif)	EUR/MWh	49	49
Electricity (excl. tax)	EUR/MWh	96	96
Electricity (incl. tax)	EUR/MWh	219	219
Natural gas for ICE (excl. tax)	EUR/MWh	38	32
Natural gas for ICE (incl. tax)	EUR/MWh	102	92

Table 4
Data defining working point of heat pump and motor/engine performance.

Type of data	Value	Unit	Designation
Efficiency	0.8	/	Compressor isentropic efficiency
	0.8	/	Compressor volumetric efficiency
	0.95	/	Electric motor efficiency
	0.35	/	Gas engine shaft efficiency
	0.9	/	Gas engine total efficiency
Temperature	5	K	Evaporator superheat
	5	K	Minimum pinch point in condenser
	5	K	Minimum pinch point in evaporator
	3	K	Minimum pinch point in soil heat exchanger
Pressure	1.0	MPa	Pressure DH network

For the case where the CHP plant boiler is operated at constant load, and the heat pump is driven by electricity, a COSP can be calculated according to Eq. (4).

$$\mathrm{COSP}_{\mathrm{elec}} = \frac{\dot{Q}_{\mathrm{cond}} + \Delta\dot{Q}_{\mathrm{CHP}}}{\dot{W}_{\mathrm{elec}} - \Delta\dot{W}_{\mathrm{CHP}}} \tag{4}$$

where $\Delta\dot{Q}_{\mathrm{CHP}}$ represents the changed production on the CHP plant in terms of heat, and $\Delta\dot{W}_{\mathrm{CHP}}$ in terms of electricity, due to the changed production temperatures of DH.

For the case where the CHP plant is operated to produce the additional amount of electricity (i.e. fixed amount electricity sold to the market, rather than constant boiler load), the system performance can be calculated on basis of the required fuel for the CHP and HP units. The performance on basis of PE (primary energy) is according to Eq. (5). This calculation has the advantage, that the required fuel of an ICE driven HP can be compared directly to the primary energy needed for the electrically driven HP.

$$\mathrm{COSP}_{\mathrm{PE}} = \frac{\dot{Q}_{\mathrm{cond}} + \dot{Q}_{\mathrm{ICE}} + \Delta\dot{Q}_{\mathrm{CHP}}}{\dot{H}_{\mathrm{ICE}} - \Delta\dot{H}_{\mathrm{CHP}}} \tag{5}$$

where $\dot{Q}_{\mathrm{ICE}}$ is the available heat from the engine, and $\dot{H}$ is the flow rate of enthalpy of fuel for the two cycles. The two COSP factors are not comparable.

VHC represents a thermodynamic measure of the size of compressor required per heat production, given that a large part of the investment of a heat pump is the compressor. The VHC is calculated as the ratio between the displacement rate volume flow of suction gas and the useful heating capacity of the heat pump, using the system perspective according to CV1. A heat pump with limited investment is found if the configuration has a VHC above 2 [15].

$$\mathrm{VHC} = \frac{\dot{Q}_{\mathrm{cond}} + \Delta\dot{Q}_{\mathrm{CHP}} + \dot{Q}_{\mathrm{ICE}}}{\dot{V}_{\mathrm{HP}}} \tag{6}$$

COF (costs of fuel) are calculated according to Eq. (7). The individual components are multiplied by cost factors of the different energy types.

$$\mathrm{COF} = \left(\dot{W}_{\mathrm{elec}} + \Delta\dot{W}_{\mathrm{CHP}}\right)\cdot c_{f,\mathrm{elec}} + \dot{H}_{\mathrm{ICE}}\cdot c_{f,\mathrm{ng}} \tag{7}$$

The individual fuel cost factors for electricity ($c_{f,\mathrm{elec}}$) and natural gas ($c_{f,\mathrm{ng}}$) are calculated according to average yearly values. The prices of fuel and taxes are calculated according to [26–28] from industrial or consumer perspective, depending on the location of the heat pump. Cost data used for this study for different fuel types from 2011 is presented in Table 3. It should be noted that specific taxes apply for HP in DH, and only applies to specific DH production companies [28]. The taxes are not paid by the company, but added to the cost of heat, where the expences are subseqently covered by the DH consumer.

In all the cases studied in Section 3, the transmission cost of the fuel is included, given that the heat pump can be located in dwellings, centralised in the DH network or at the location of the power plant.

2.5. Additional assumptions required to define working condition

Additional parameters are needed to fully define the heat pump models. The relevant parameters are listed in Table 4. For the ICE unit shaft and total efficiency, the data are derived from investigation of manufacturer data sheets [29].

In the cases where DH return temperature is changed by the heat pump cycles, either increased or decreased, a fixed temperature glide of 10 K has been chosen. As an example, considering configuration SR where the return stream is preheated, a fixed sink temperature glide of 10 K has been assumed. Thus, the return stream is heated 10 K by the heat pump. A similar assumption is used for RF and RD configurations, although in this case for the evaporator. The heated or cooled stream is then mixed with the remaining DH stream, before evaluating the impact on the CHP plant. This temperature glide is, as previously mentioned, subject to optimisation in the individual DH Network, in order to further increase the COSP of the heat pump.

Heat losses are considered constant in the evaluation, as DH networks are operated in all configurations. The marginal changed temperatures of the network are assumed not to effect the overall losses. Similarly, it is assumed that the transmission losses of electricity are constant for decentral installations. This may not be applicable if a high amount of such installations are installed, especially when considering the losses in the distribution system. For systems utilising NG, the increased pressure losses of the distribution system are neglected. Such losses may be expected when increasing consumption significantly.

3. Results

The results are derived by investigating several heat pump configurations with different fuel types and energy system layouts.

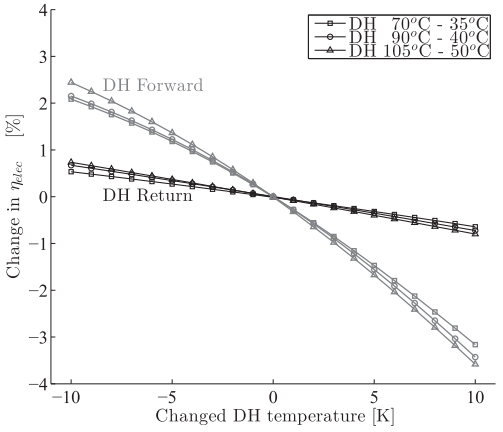

Fig. 6. Changes to electricity efficiency with variations in DH forward and return temperatures at CHP plants designed for different network types.

Table 5
Temperatures at state points 1 to 8 for electrical heat pumps - DH network type 2 - 1 MW added capacity.

State point	1	2	3	4	5	6	7	8
Description	CHP out	CHP in	Cond. out	Cond. in	Evap. in	Evap. out	DH forward	DH return
Unit	°C	°C	°C	°C	°C	°C	°C	°C
SF	90	40	90	40	20	10	90	40
SD	90	40	60	7.5	7.5	2.5	90	40
SR	90	40.1	50	40	20	10	90	40
RF1	90	39.3	90	40	40	30	90	40
RF2	89.4	39.6	99.4	89.4	40	30	90	40
RD	90	39.4	60	40	40	30	90	40

In the results, the interaction of both CHP plant and heat pumps are presented, and the synergies of combining the two technologies are presented as modified PQ-diagrams.

3.1. CHP operation at changed DH network temperatures

The impact of changing either forward or return stream temperature in a CHP plant is shown in Fig. 6 for the plant operating at 100% load with full heat production, i.e. back pressure operation. The results are presented as a relative change of the electric efficiency of the plant. The resulting efficiency is slightly increased with lower forward and return temperatures, as the temperatures of the CHP plant condenser approaches that of ambient. Due to the operation point, similar characteristics would be expected for a power plant without possibilities for extraction operation, i.e. an back pressure CHP plant.

The three network types show similar characteristics for variation of forward and return DH temperatures, although with slightly increased changed for higher temperature networks. Variation of forward and return temperatures are presented in grey and black colours respectively. It is found that a 10 K change in the return flow temperature has low impact on the power production, the electric efficiency changes less than 1%. A corresponding change in forward stream temperature results in a change of approximately 2.5%, if the temperature is reduced, and between 3 and 4% if the temperature of the forward stream is increased. 1% variation of the electric efficiency corresponds to approximately 0.35 percentage points.

Changes to the electricity production of the plants in back pressure operation will lead to a corresponding change in the heat production of the plant, due to energy balances of the plant.

3.2. Comparison of electrically driven heat pump configurations

The temperature levels for each of the identified configurations are presented in Table 5, according to the DH stream state points of Fig. 4. The states are calculated for the case where DH is produced by a CHP plant, a type 2 (90 °C − 40 °C) DH network and with the heat pumps operated by an electric motor. The temperatures in state points 7 and 8 are corresponding to the network type. The remaining temperatures are varied according to configuration and heat source type. For the four latter configurations, one or both temperatures of state point 1 and 2 are changed, leading to changed production of the CHP plant according to Fig. 6. Considering condenser and evaporator temperatures (state points 3-4 and 5-6 respectively) it is clear that the three latter configurations allow for a lower HP temperature lift, than the configurations utilizing an external heat source. Configurations SF, SD and RF1 utilise a high sink temperature glide.

Table 6 shows a comparison of the four key performance parameters from Section 2.4, along with the change in power generation of the CHP plant and the tax on the used fuel, considering Danish taxation scheme. The total fuel cost is the sum of fuel cost and tax cost for a Danish installation.

In terms of COP (considering CV2 in Fig. 4), the RD configuration allows the highest COP, followed by the RF1 configuration. This is in contrast to the performance when evaluated based on the system perspective (CV1), where the RD configuration - and both of the RF configurations - perform poorly, as the heat source originates from the CHP plant. From a system perspective (both $COSP_{elec}$ and $COSP_{PE}$), the SD and SR configurations are superior, despite the fact that the SR configuration has a negative impact on power generation of the CHP plant. The configurations are superior due to the high HP COP and the utilisation of renewable heat sources.

When considering the cost of fuel, configurations SD and SR are preferable, with SF as third best solution. The reason for the achievement of low cost of fuel, can be explained by the high COP and the utilisation of renewable heat sources. For VHC the SF configuration is the best, by a margin of approx. 8% compared to SR, which is second best.

As RF1 and RF2 configurations perform equally in terms of COSP, VHC and cost, only RF1 is presented in the following analysis (Sections 3.3 and 3.4).

3.3. Comparison of performance at different types of DH networks

In Fig. 7 the four key performance parameters are compared for the electrically driven heat pumps, when the district heating network temperatures are varied from type 1 to 3. It is seen that the results for changed DH temperatures show similar characteristics to the results of type 2 network presented in Table 6.

For lower DH temperatures (represented by DH 70 °C − 35 °C) the SR configuration has the best performance when considering both cost of fuel and COSP, and second best when considering VHC. In high and medium temperature networks, the SD configuration is

Table 6
Comparison of six configurations of electrical heat pumps - DH network type 2 − 1 MW added capacity.

	Unit	SF	SD	SR	RF1	RF2	RD
Heat pump COP	–	3.52	4.52	4.74	4.9	2.49	6.83
Changed power generation (Eq. (4))	MW	0	0	−0.02	+0.1	+0.39	+0.08
Coefficient of system performance (elec)	–	3.34	4.29	4.22	0.95	0.94	0.95
Coefficient of system performance (PE)	–	1.76	2.11	2.08	0.89	0.89	0.89
Volumetric heating capacity	MJ m^{-3}	2.7	2.2	2.5	0.9	0.9	0.6
Cost of fuel	EUR MWh^{-1}	29	23	23	102	103	102
Tax on fuel	EUR MWh^{-1}	37	28	29	129	131	129
Total fuel cost	EUR MWh^{-1}	65	51	52	231	234	231

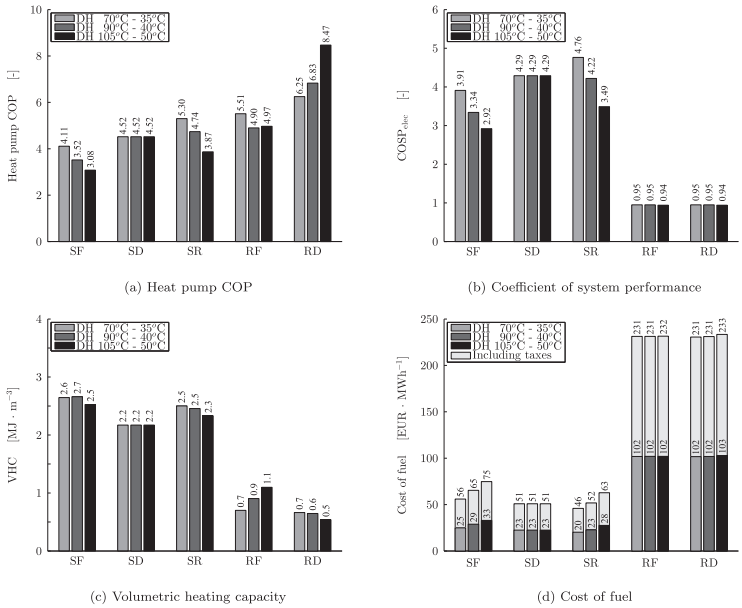

(a) Heat pump COP

(b) Coefficient of system performance

(c) Volumetric heating capacity

(d) Cost of fuel

Fig. 7. Five configurations compared considering a district heating system fed by extraction CHP plant. (a) heat pump COP, (b) coefficient of system performance, (c) volumetric heating capacity, (d) cost of fuel including/excluding taxes.

superior for COSP and cost of fuel. The high COSP of the SD configuration is explained by the high COP that can be achieved with a high sink temperature glide, by utilising the desuperheating and subcooling of the working fluid. As this configuration is not linked to the DH network, similar characteristics are found for all three DH types. RF and RD show high HP COP, but rank fourth or fifth in terms of COSP, VHC and cost. The main reason is the use of a DH network as heat source, from which the heat in reality is produced by the CHP plant itself.

In terms of VHC, the SF configuration is always the best configuration, but with inferior COSP and increased cost compared to SD and SR. By utilising the SR configuration an increase of between 20 and 25% in COSP can be achieved, when compared to the SF configuration in a similar DH network.

3.4. Comparison of electrical and ICE driven heat pumps

One focus of the research is the evaluation of appropriate fuels to produce the required shaft power. The performance of the configurations is evaluated by considering the heat pump driven by both an electric motor and a natural gas ICE, as introduced in Section 2.2. The comparison for each of the five configurations is presented in Fig. 8 for each of the four parameters of interest. The coefficient of system performance is presented according to Eq. (5) in Fig. 7b.

The changes to the heat pump COP are shown in Fig. 8a. The heat pump COP is changed as a consequence of the additional heat utilisation, according to the total efficiency of the engine. This allows all configurations to operate at a lower condensation pressure, as the available heat is used in serial connection at the highest possible temperature level. In terms of COSP, the natural gas ICE shows slightly increased performance for SF and SD, compared to the electricity driven configuration. For the remaining configurations the COSP is similar or reduced. The change in system performance between the natural gas ICE and the electricity driven HP is within ±8% for all configurations.

The cost of fuel is lower for all natural gas ICE driven heat pumps than the corresponding electricity driven ones, even though the configurations are subject to increased tax for utilising natural gas in combustion engines.

For the ICE driven HP, the VHC may be a misleading parameter, as this system requires investment in an ICE, which is not included in the factor, and thus only corresponds to the investment in the heat pump. In this way, the ICE driven heat pumps show higher VHC than the electrically driven as a consequence of the lower heat load required by the condenser in order to produce 1 MW added capacity, when the surplus heat from the ICE is utilised in the process.

3.5. Heat pumps in a DH network fed by stack gases

As introduced in Section 2.3, the comparison of the five configurations in DH (90 °C – 40 °C) networks fed by stack gases is presented in Fig. 9, where also the results of the initial investigation from Table 6 are presented for comparison. In Fig. 9 only $T_{DH,Return}$ and cost of fuel is presented, as the two remaining parameters resembles the already shown results.

Fig. 9a shows that in case of a system fed by stack gases – rather than a CHP plant - the performance of three previously uncompetitive configurations is significantly affected, as the HP allows better utilisation of the stack gas heat exchanger. Although the COSP of configurations RF1, RF2 and RD have increased significantly, their performances are still lower than the three remaining types. Of the configurations utilising the return stream as heat source, RF1 is superior in performance.

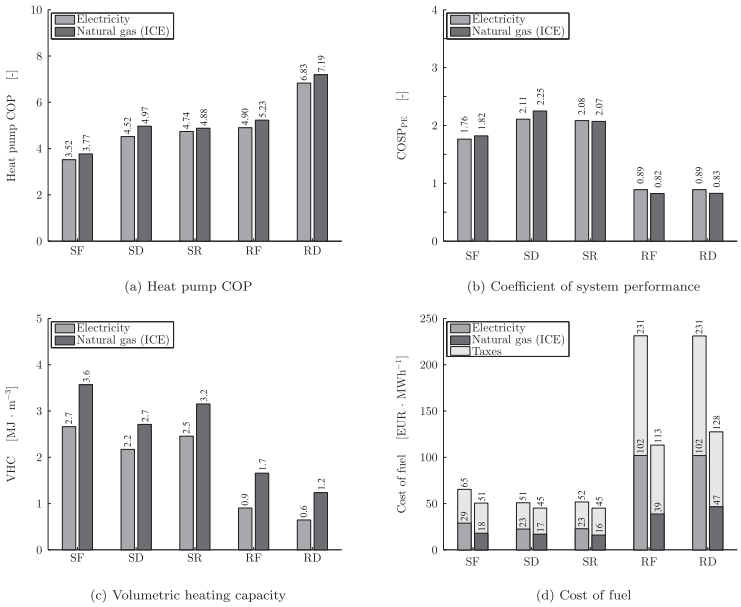

Fig. 8. Comparison of the five configurations operated by electrical motor or internal combustion engine fed by natural gas. The network-configuration is fixed to type 2 (Table 1) fed by an extraction CHP plant. (a) heat pump COP, (b) coefficient of system performance, (c) volumetric heating capacity, (d) cost of fuel including/excluding taxes.

An opposite effect is experienced using the SR configuration, where the system performance is reduced below the level of the SF configuration, as the utilisation of the stack gasses is significantly reduced due to the heat pump.

From considering the cost of fuel in Fig. 9b similar trends can be found. The cost of fuel for RF1 configuration is reduced by more than 60% when used in a system where the main production technology is a stack gas heat exchanger or a heat production technology with similar characteristics.

3.6. Three selected configurations integrated in the PQ-diagram of a CHP plant

The integration of an electrically driven heat pump in a DH network fed by a CHP plant increases the production possibilities of the power plant. To interpret these options, PQ-diagrams are typically used in CHP plants, where the curves with negative slope show the range of operation points at fixed boiler loads. Fig. 10a shows a traditional PQ-diagram of a CHP plant for a type 2 DH network. Fig. 10b – d are modified PQ-diagrams where a 25 MW added capacity is included for types SF, SD, and SR, respectively.

The SF configuration allows high flexibility, as the heat pump can be turned on when the power plant is in full back pressure operation. In this way, the use of the heat pump allows the combined plant to increase heat production, without increasing power production. At lower heat demand, the heat pump is turned off, as the trade off between heat and power at the CHP plant is better than in the heat pump. Additionally, the SF heat pump can be turned on without operating the CHP plant, indicated by the operation line below zero power production.

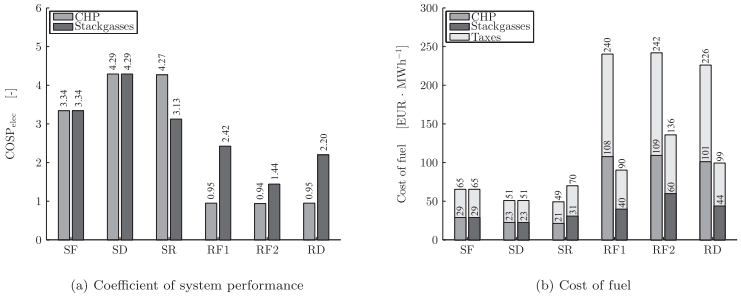

Fig. 9. Investigation of six electrically driven heat pump configurations when considering heat produced by two technolgies – extraction CHP plant and stack gases/boilers. (a) coefficient of system performance, (b) cost of fuel including/excluding taxes.

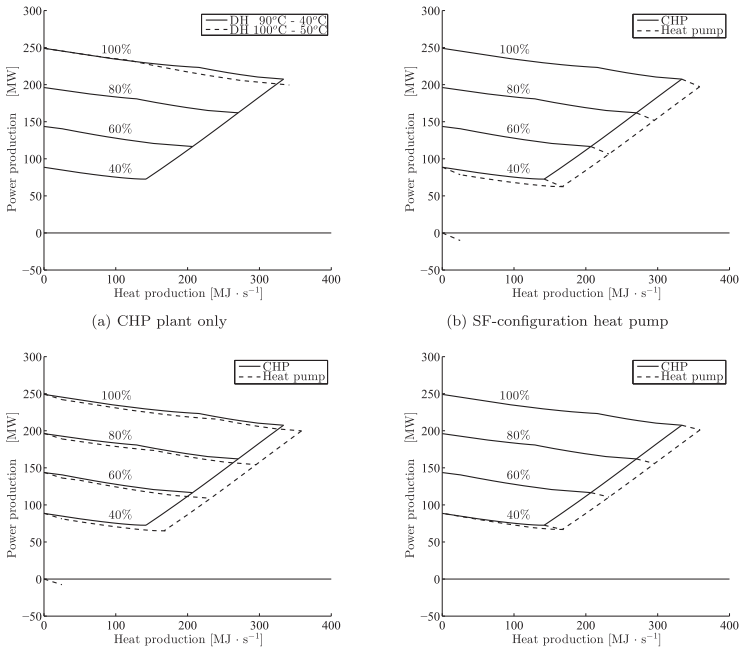

(a) CHP plant only

(b) SF-configuration heat pump

(c) SD-configuration heat pump

(d) SR-configuration heat pump

Fig. 10. Comparison of the changed CHP plant operation with three applicable configurations operated by electrical motor. The network-configuration is fixed to type 2 (Table 1) and the added capacity is fixed to 25 MW. (a) CHP plant PQ-diagram without HP, (b) Modified PQ-diagram with SF-configuration heat pump, (c) Modified PQ-diagram with SD-configuration heat pump, (d) Modified PQ-diagram with SR-configuration heat pump.

The SD configuration does not allow the same flexibility, as the heat pump unit is located near the consumer demand, without connection to the DH network. This implies that the heat pumps are operated according to the demand of the dwellings, and no heat production optimisation is possible. As for the SF configuration, it is possible to operate the heat pump when the power plant is shut down.

For the SR configuration to operate, the power plant is required to be in operation. Additionally, the operation is changed at low loads, as can be seen in Fig. 10d. On the other hand, the efficiency is higher than for configuration SF, and the heat pump can be operated when it is optimal from a system perspective.

4. Discussion

From interpretation of Fig. 6 it is clear that a changed forward temperature has a significant effect on power production compared to a corresponding change in return temperature. The previously considered special cases (introduced in Section 1.2) of configurations SF and RF may thus be disregarded in a system fed by a CHP plant, as this suggests a larger impact to power production and also higher condensation pressure in the heat pump compared to the SR configuration. If the primary production technology of heat is not sensitive to increased temperatures, as may be the case if a DH network is fed by co-production of electricity and heat from a ICE, these cases may be worth further investigation.

Fig. 6 also indicates that lowering temperatures in a DH network is mainly beneficial if it is possible to decrease the temperature of the forward stream. This is coherent with reduction of heat losses in the network, as the losses are highly influenced by the temperature differences between stream and soil.

In the case where the RF2 configuration is used to upgrade the temperature of a small part of a network heating demand, such that the temperature of the remaining network can be lowered, a COSP higher than 1 can be experienced, although it is questionable if an actual DH network exists where it would result in a better performance than SF, SD or SR configurations. Similarly, the RD configuration may improve COSP above 1 if the heat pump is only used for a fraction of the heat demand, e.g., the hot tap water heat demand in a dwelling is typically only a third or half of the combined heat demand.

The main results in Section 3.3 show, that in terms of COSP and cost of fuel the SD configuration is advantageous at high DH network temperatures. A number of arguments may question this outcome, as assumptions may be questionable for small de–central heat pumps. Mainly the isentropic and volumetric efficiencies (as well as shaft efficiency of ICE equipment) of a small system, may not reach the same levels as the ones used for large centralized units. Also the source temperature level, which is based on average values of the entire year, may not be possible to utilize in the shallow geothermal systems considered in this paper. If the depth is not sufficient to smoothen the variations, the heat pump will experience a reduced efficiency during months of high heat demand. On the other hand, trans-critical HPs are often used for this type of application, where the temperature glide of sink is high, as they allow increased HP COP compared to the sub-critical operation. In this way an increased COSP may be achieved.

Table 7
Cost of fuel without transmission costs for central installations at CHP plant – same conditions as results in.Table 6.

	Unit	SF	SD	SR	RF1	RF2	RD
Cost of fuel	EUR MWh^{-1}	15	23	12	53	53	102
Tax on fuel	EUR MWh^{-1}	33	28	26	118	118	129
Total fuel cost	EUR MWh^{-1}	48	51	38	170	171	231

As noted in Section 2.4, transmission costs are included in all configurations. If the heat pump is located at the CHP plant, as it is possible for the central installations, approximately half of the electricity cost can be disregarded. In this way the SR configuration provides a significantly lower production cost compared to the SD configuration. The changed cost of the configurations (Table 6) is presented in Table 7. Fluctuations in the electricity price may further influence the competitiveness of the SD configuration, as the centralised heat pumps may allow higher flexibility when electricity prices are low. Similar flexibility cannot be expected from the de–central installations, due to changed storage capacity and less knowledge of future electricity prices.

For the configurations utilizing an ICE to deliver the shaft power, the COSP will be lowered and cost will be increased (compared to Fig. 8) if the system is used for high temperature networks, as the additional heat is not at a sufficiently high temperature to lower the condensation temperature. This is only the case for DH network type 1 in Table 1.

The use of $COSP_{elec}$ or $COSP_{PE}$ may be important as it represents the changed performance of both technologies (when operated simultaneously), integrated in the characteristics of the heat pump. This may prove helpful in energy system modelling, where operational interdependencies are modelled, although typically without changed efficiency of either of the units.

5. Conclusions

Heat pumps have recently been proposed as a way to integrate higher amounts of renewable energy in the DH network. In this paper five configurations are investigated in order to analyse the optimal integration considering a network fed by two heat generation technologies, a CHP plant and stack gases.

The analysis focusses on four key performance factors chosen to indicate the performance from a system perspective and differences between system performance and the performance of the heat pump. The five configurations are examined considering the shaft power delivered by either an electric motor or an internal combustion engine operating on natural gas. Individually the results show similar tendencies for the two fuels, but the cost of fuel is lower when utilising natural gas, even though the system efficiency is significantly higher for electrical heat pumps.

Two configurations (SD and SR) propose the highest coefficient of system performance and lowest cost of fuel for the DH network temperatures evaluated. In terms of volumetric heating capacity the SF configuration is best. The highest coefficient of system performance was for SR configuration with electric motor in a low temperature DH network, where the COSP is almost 5.

If an electrical SR heat pump system is installed at the power plant, the cost of fuel can be as low as 12 EUR MWh^{-1} for 90 °C – 40 °C DH network, when neglecting taxes and transmission costs.

Acknowledgement

This work was supported by Copenhagen Cleantech Cluster (CCC), DONG Energy and Teknologisk Institut (DTI)

Nomenclature

c	cost, EUR/MWh
C	constant
$\dot{C}$	cost rate, EUR/h
$\dot{H}$	fuel enthalpy rate, KJ/s
k	opening degree, /
$\dot{m}$	mass flow, kg/s
p	pressure, Pa
$\dot{Q}$	heat production rate, KJ/s
T	temperature, °C
$\dot{V}$	volume flow, m^3/s
$\dot{W}$	work rate, KW

Greek symbols

α	flow characteristic, $\sqrt{K}$ $kg/bars$
η	efficiency, /

Subscripts

cond	condenser
elec	electricity
f	fuel
i	inlet
ng	natural gas
o	outlet
return	return stream in district heating network
sink	sink reservoir
source	source reservoir
t	turbine
valve	valve
forward	forward stream in district heating network

Abbreviations

CHP	combined heat and power
COP	coefficient of performance
COSP	coefficient of system performance
DH	district heating
HP	heat pump
ICE	internal combustion engine
PE	primary energy
VHC	volumetric heating capacity

References

[1] Münster M, Morthorst PE, Larsen HV, Bregnbæk L, Werling J, Lindboe HH, et al. The role of district heating in the future danish energy system. Energy 2012;48(1):47–55.
[2] Blarke MB. Towards an intermittency-friendly energy system: comparing electric boilers and heat pumps in distributed cogeneration. Appl Energy 2012;91(1):349–65.
[3] Lund H, Clark WW. Management of fluctuations in wind power and CHP comparing two possible danish strategies. Energy 2002;27(5):471–83.
[4] Rinne S, Syri S. Heat pumps versus combined heat and power production as CO_2 reduction measures in finland. Energy 2013;57:308–18.
[5] Hedegaard K, Mathiesen BV, Lund H, Heiselberg P. Wind power integration using individual heat pumps - analysis of different heat storage options. Energy 2012;47(1):284–93.
[6] Ommen T, Markussen WB, Elmegaard B. Comparison of linear, mixed integer and non-linear programming methods in energy system dispatch modelling. Energy 2014:1–10. http://dx.doi.org/10.1016/j.energy.2014.04.023 [Published 1, Sep 2014].
[7] Østergaard PA. Ancillary services and the integration of substantial quantities of wind power. Appl Energy 2006;83(5):451–63.
[8] Blarke MB, Lund H. Large-scale heat pumps in sustainable energy systems: system and project perspectives. Therm Sci 2007;11(3):143–52.
[9] Malinowska W, Malinowski L. Parametric study of exergetic efficiency of a small-scale cogeneration plant incorporating a heat pump. Appl Therm Eng 2003;23(4):459–72.
[10] Lowe R. Combined heat and power considered as a virtual steam cycle heat pump. Energy Policy 2011;39(9):5528–34.

[11] Dagilis V. Combined heat pump and power plant. part I: thermodynamic analysis. Mechanika 2013;19(1):19–24.
[12] Annex-21 Industrial heat pumps – experiences, potential and global environmental benefits. IEA Heat Pump Centre; 1995.
[13] Ommen T, Markussen CM, Reinholdt L, Elmegaard B. Thermoeconomic comparison of industrial heat pumps. In: Proceedings of the 23rd IIR International congress of refrigeration (ICR 2011); 2011.
[14] Eisa MAR, Best R, Holland FA. Working fluids for high temperature heat pumps. J Heat Recovery Syst 1986;6(4):305. URL: http://www.sciencedirect.com/science/article/B73H9-482GRG7-51/2/0d02c903939ec4893406524123a62e05.
[15] Brunin O, Feidt M, Hivet B. Comparison of the working domains of some compression heat pumps and a compression-absorption heat pump. Int J Refrig 1997;20(5):308. URL: http://www.sciencedirect.com/science/article/B6V4R-3SN6RKP-3/2/797a307487b127b05c41faab740a87c5.
[16] Centralkomunernes Transmissionsselskab I/S. Tekniske nøgletal [Technical key figures]. in danish. 2013. URL:, http://www.ctr.dk/teknik.aspx [accessed on 10.10.13].
[17] Fjernvarme Dansk. Benchmarking, statistik 2011/2012 [Benchmarking, statistics 2011/2012]. in danish. 2013. URL:, http://www.fjernvarmen.dk/Faneblade/HentMaterialerFANE4/~/media/Publikationer/Aarsstatistikker/BenchmarkingStatistik20112012.ashx [accessed on 10.10.13].
[18] Berntsson T. Heat sources – technology, economy and environment. Int J Refrig 2002;25(4):428–38.
[19] Wittchen K, Grunnet Wang P, Scharling M, Pagh Nielsen K, Kern-Hansen C. 2001 â€“ 2010 danish design reference year. DMI Technical Report. Danmarks Meteorologiske Institut; 2013.
[20] Granryd E. Refrigerating engineering – part II. Stockholm: Royal Institute of technology, KTH; 2005.
[21] Ommen TS, Elmegaard B. Exergetic evaluation of heat pump booster configurations in a low temperature district heating network. In: Proceedings of the 25th International conference on efficiency, cost, optimization, simulation, and environmental impact of energy systems (ECOS 2012). Firenze University Press; 2012.
[22] Elmegaard B, Houbak N. Simulaton of the Avedøreværket unit 1 cogeneration plant with DNA. In: Proceedings of the 16th International conference on efficiency, cost, optimization, simulation, and environmental impact of energy systems (ECOS 2003). Technical University of Denmark; 2003.
[23] F-Chart Software (LLC). Engineering equation solver EES. 1992. URL: http://www.fchart.com/ees/ [accessed on 10.10.13].
[24] Houbak N. Proposal for simulator contest. In: Proceedings of the 16th International conference on efficiency, cost, optimization, simulation, and environmental impact of energy systems (ECOS 2003). DTU, Technical University of Denmark; 2003.
[25] Danish Energy Agency. Technology data for energy plants – generation of electricity and district heating, energy storage and energy carrier generation and conversion. 2013. URL: http://www.ens.dk/node/2252 [accessed on 10.10.13].
[26] Energinetdk. Market price data. 2011. URL: http://www.energinet.dk [accessed on 10.10.13].
[27] Gaspoint Nordic A/S. Gaspoint nordic market data – history data 2012. 2012. URL: http://www.gaspointnordic.com/market-data [accessed on 10.10.13].
[28] SKAT. Afgiftslempelse for fjernvarme (el-patronordningen) [Taxreduction for district heating (electric boiler agreement)]. in danish. 2012. URL:, http://www.skat.dk/SKAT.aspx?oId=2061609&vId=208670 [accessed on 10.10.13].
[29] GE Energy. Gas engines, jernbacher type 2. 2012. URL: http://www.ge-energy.com/content/multimedia/_files/downloads/ETS_E_T2_12_screen.pdf [accessed on 10.10.13].

Appendix E

Paper 3 - International Journal of Refrigeration

Torben Ommen, Jonas Kjær Jensen, Wiebke Brix Markussen,
Lars Reinholdt and Brian Elmegaard

Technical and economic working domains of industrial heat pumps: Part 1 - single stage vapour compression heat pumps.

International Journal of Refrigeration, 2015; xx: 1–15.
doi:10.1016/j.ijrefrig.2015.02.012

ARTICLE IN PRESS

INTERNATIONAL JOURNAL OF REFRIGERATION XXX (2015) 1–15

Available online at www.sciencedirect.com

ScienceDirect

journal homepage: www.elsevier.com/locate/ijrefrig

Technical and economic working domains of industrial heat pumps: Part 1 – Single stage vapour compression heat pumps☆

Torben Ommen [a,*], *Jonas Kjær Jensen* [a], *Wiebke Brix Markussen* [a], *Lars Reinholdt* [b], *Brian Elmegaard* [a]

[a] *Technical University of Denmark, Kgs. Lyngby, DK-2800, Denmark*
[b] *Danish Technological Institute, Aarhus, DK-8000, Denmark*

ARTICLE INFO

Article history:
Available online xxx

Keywords:
Industrial heat pumps
Working domain
Economic evaluation
Natural working fluids
Pinch design method

ABSTRACT

A large amount of operational and economic constraints limit the applicability of heat pumps operated with natural working fluids. The limitations are highly dependent on the integration of heat source and sink streams. An evaluation of feasible operating conditions was carried out considering the constraints of available refrigeration equipment and a requirement of a positive net present value of the investment. Six heat pump systems were considered, corresponding to an upper limit of the sink temperature of 120 °C. For each set of heat sink and source temperatures the best available technology was determined. The results showed that four different heat pump systems propose the best available technology at different parts of the complete domain. Ammonia systems presented the best available technology at low sink outlet temperature. At high temperature difference between sink in- and outlet, the transcritical R744 expands the working domain for low sink outlet temperatures.

Domaines techniques et économiques de fonctionnement de pompes à chaleur industrielles : Partie 1- Pompes à chaleur à compression de vapeur mono-étagées

Mots-clés : Pompes à chaleur industrielles ; Domaine de fonctionnement ; Evaluation économique ; Fluides actifs naturels ; Méthode de conception de Pinch

☆ The original paper was presented on the 11th IIR Gustav Lorentzen Conference on Natural Refrigerants (GL2014), Aug.31 to Sept.2, 2014, Hangzhou, China.

* *Corresponding author*. Tel.: +45 4525 4037; fax: +45 4588 4325.
E-mail addresses: tsom@mek.dtu.dk (T. Ommen), jkjje@mek.dtu.dk (J.K. Jensen), wb@mek.dtu.dk (W.B. Markussen), lre@teknologisk.dk (L. Reinholdt), be@mek.dtu.dk (B. Elmegaard).

http://dx.doi.org/10.1016/j.ijrefrig.2015.02.012
0140-7007/

Please cite this article in press as: Ommen, T., et al., Technical and economic working domains of industrial heat pumps: Part 1 – Single stage vapour compression heat pumps, International Journal of Refrigeration (2015), http://dx.doi.org/10.1016/j.ijrefrig.2015.02.012

Nomenclature

Abbreviations

HP	high pressure
LP	low pressure
NDA	Non-disclosure agreement

Symbols

A	area (m^2)
AC	annual cost (€)
c	cost factor (€ kWh^{-1})
CRF	capital-recovery factor (–)
COP	coefficient of performance (–)
FC	annual cost of fuel consumption (€)
H	annual operating hours (h)
h	specific enthalpy (kJ kg^{-1})
i	rate of return (%)
$\dot{m}$	mass flow rate (kg s^{-1})
N	number of plates (–)
n	lifetime in years (years)
NPV	net present value (€)
OMC	operation and maintenance cost (€)
p	pressure (bar)
PBP	pay back period (year)
PV	present value (€)
PEC	purchased equipment cost (€)
TCI	total capital investment (€)
VHC	volumetric heating capacity (MJ m^{-3})
$\dot{Q}$	heat flow rate (kW)
s	specific entropy (kJ kg^{-1} K^{-1})
T	temperature (K)
U	heat transfer coefficient (kW m^{-2} K^{-1})
$\dot{W}$	work rate (kW)
υ	specific volume (m^3 kg^{-1})
$\dot{V}$	volume flow rate (m^3 s^{-1})
X	size or capacity of component

Greek symbols

α	cost function exponent (–)
Δ	difference
η	efficiency

Subscripts & Superscripts

b	boiler
eff	effective
el	electrical
H	high
HP	heat pump
j	denomination of technical project
L	inflation
max	maximum
NG	natural gas
W	equipment item with known cost
WF	working fluid
Y	equipment item with calculated cost

1. Introduction

Large vapour compression heat pumps (HP) may be used for process optimisation of industrial plants (Townsend and Linnhoff, 1983) or for utility supply in urban areas with heat networks (Ommen et al., 2014). For each individual process type (and temperature range) a wide span of design parameters and configuration options exists, which must be evaluated in order to calculate the best available heat pump technology for the assignment. The best available technology typically depends on the performance and investment of the heat pump systems at the specific layout of the sink/source process streams.

Besides the thermodynamic performance of the cycle and working fluid, it is important to consider the application limits of the individual components. Many systems have been built with sink temperatures between 50 °C and 90 °C for industrial applications, but the sink temperature span may likely be due to limitations of the heat pump technology or limited cost effectiveness, rather than a limited demand at higher temperatures (Annex-21, 1995).

Brunin et al. (1997) investigate the working domain of many working fluids in the temperature range up to 200 °C. A large fraction of the investigated working fluids are banned today (or will be shortly) throughout most of Europe (UN Ozone Secretariat, 2000; European Parliament, 2014) for large industrial scale systems. The study does not consider economics as such, but employs two physical constraints to represent economic feasibility. The constraints are coefficient of performance (COP) and volumetric heating capacity (VHC). The temperature variations of the two secondary streams (sink and source) are fixed at 10 K though out the investigation.

In the case of integration of heat pumps within temperature reservoirs of limited heat capacity, such as in pinch analysis (Linnhoff and Hindmarsh, 1983) or district heating networks (Ommen et al., 2014), the difference in temperature between inlet and outlet of a stream influences the performance of the investigated solution. Different temperature variations for sink or source, but for similar sink temperature and temperature lifts, may influence the choice of best available technology as well as the economic feasibility of such a modification.

The focus of this study was to reveal the possible working domains for several natural working fluids when considering variations in temperature lift and sink temperatures, and a range of different sink and source temperature variations. The investigation was limited to include only the single stage vapour compression heat pump cycle. Five heat pump systems utilising natural working fluids were compared in terms of technical, thermodynamic and economic constraints, in order to include the heat pump performance and investment into the consideration. The considered natural working fluids were: R290, R600a, R744 and R717, where the latter utilises both low and high pressure components. One HFC working fluid (R134a) was included in the study for comparison of the feasibility of natural working fluids. By comparing the net present value or pay back period of the heat pump integration, it was possible to determine which of the considered systems proposes the best available technology.

Please cite this article in press as: Ommen, T., et al., Technical and economic working domains of industrial heat pumps: Part 1 – Single stage vapour compression heat pumps, International Journal of Refrigeration (2015), http://dx.doi.org/10.1016/j.ijrefrig.2015.02.012

In part 2 of this paper (Jensen et al., 2015), the ammonia-water hybrid absorption-compression heat pump is studied and compared to the best available vapour compression HP technology determined in this paper.

2. Method

Examination of the working domain has been carried out for six single stage vapour compression HP systems. Various possibilities for improved performance by e.g. internal heat exchangers have been disregarded for the analysis. A model of each heat pump was implemented in Engineering Equation Solver (F-Chart, 1992).

The heat pumps were compared using both economic and technical constraints. The considered technical constraints may be caused by the behaviour of the working fluid or by limitations in the development of suitable components. This is further discussed in Section 2.3.

A few effects have been neglected as they are assumed of similar magnitude between the investigated heat pumps. Such effects include pressure drop in pipes, the extent of non-useful superheat and subcooling and compressor heat losses. Only full load steady state operation has been considered for the economic analysis.

2.1. *Vapour compression heat pump*

For industrial processes heat is often transferred by heat transfer fluids, which may be oil or water based. In this study it was assumed to be pure water, which was pressurized to avoid vaporisation of the secondary working fluid at elevated temperatures. Pinch point temperature difference was used to model heat exchange with both sink and source media (Nellis and Klein, 2009). A principle sketch of a vapour compression HP, and a temperature – heat load diagram for an azeotropic working fluid, are presented in Fig. 1. In the condenser, the working fluid was assumed sub-cooled until it reaches the pinch temperature difference at the sink entrance.

The performance of the HP was calculated using constant efficiencies for compressor and electrical motor, as well as fixed temperature differences in the heat exchangers. The used values are presented in Table 1.

For the case of R744, where heat rejection from the working fluid is at supercritical pressure, the heat pump performance is affected by the gas cooler pressure as presented in Nekså et al. (1998) and further discussed in Cecchinato et al. (2010). By changing the heat exchange process of the gas cooler, also the investment of the heat pump system is affected. For all the considered temperature configurations of transcritical heat pumps, the heat rejection pressure allowing the optimal net present value (further explained in section 2.4.1) was determined and used. This methodology is proposed in order to obtain a fair comparison with all configurations, where additional degrees of freedom allow optimisation of the system design.

2.2. *Estimation of plate heat exchanger area and pressure drop*

Heat exchange processes are important in any HP and a significant part of the physical system, with high influence to the investment and the derived heat cost. Detailed heat transfer correlations for both evaporators and condensers were implemented and used in moving boundary models of the heat exchangers.

Chevron type plate heat exchangers were considered, as they appear to be cost efficient and are typically used in such systems today. The correlations used for the analysis are presented in Table 2, while the plate dimensions are for a fixed type corresponding to pressure level and working fluid constraints (SWEP International AB, 2013). In this way an increment in heat exchange area will result in increased amount of plates.

For all of the considered heat pump systems, the calculated investment cost includes liquid receivers at an intermediate pressure for both subcritical and supercritical systems (Corberan, 2011; Kim et al., 2004). By using this option, it is possible to obtain the desired subcooling in the condenser, and operate the system freely at start-up and shut-down procedures.

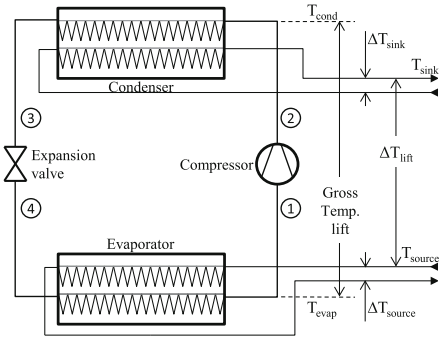

(a) Principle sketch of the vapour compression HP

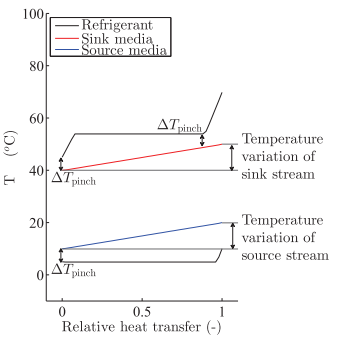

(b) Temperature - heat load diagram for condenser and evaporator. Temperature variation of both sink and source is 10 K

Fig. 1 – Principle sketch and temperature – heat load diagram of the vapour compression HP.

Please cite this article in press as: Ommen, T., et al., Technical and economic working domains of industrial heat pumps: Part 1 – Single stage vapour compression heat pumps, International Journal of Refrigeration (2015), http://dx.doi.org/10.1016/j.ijrefrig.2015.02.012

Table 1 – Operating point and performance of HP and natural gas boiler.

Type of data	Value	Unit	Designation
Efficiency	0.8	–	Compressor isentropic efficiency
	0.8	–	Compressor volumetric efficiency
	0.95	–	Compressor electric motor efficiency
	0.9	–	Natural gas burner efficiency
Temperature	5	K	Pinch point temperature difference in condensers, gascoolers and evaporators
	5	K	Compressor suction superheat

Table 2 – Applied heat transfer and pressure drop correlations for the evaporator, condenser and gascooler.

Component	Media	Zone	Heat transfer	Pressure drop
Condenser	H_2O		Martin (1996)	Martin (1996)
Condenser	Rxxx	Vapour only:	Martin (1996)	Martin (1996)
		Two-phase:	Yan et al. (1999)	Yan et al. (1999)
		Transcritical:	Martin (1996)	Martin (1996)
		Liquid only:	Martin (1996)	Martin (1996)
Evaporator	H_2O		Martin (1996)	Martin (1996)
Evaporator	Rxxx	Two-phase:	Yan and Lin (1999)	Yan and Lin (1999)
		Vapour only:	Martin (1996)	Martin (1996)

2.3. *Compressors and operating conditions*

In order to achieve the considered temperatures using vapour compression heat pumps, specially designed compressors are used. The pressure limit of the high pressure side may in many cases dictate the achievable sink temperatures, but also the suction pressure may pose limitations. Similarly for transcritical processes, where the pressure is not directly dependent on the sink temperature, the pressure limit has an effect on the heat pump performance.

The condensing temperature and pressure may in rare cases be lower than that of the sink stream leaving the condenser. This is possible in the case where a high fraction of heat dissipation is from superheated vapour.

Oil degradation may pose limitations due to high temperatures in the compressor. To reduce wear and excess degradation, the compressor discharge temperatures are limited to 180 °C (Nekså et al., 1998).

Compressors from large international manufactures were investigated, where both price and operation limits were available. Five different types were identified according to different working fluid properties, flammability and availability. The limiting operation data for these are presented in Table 3.

Compressor types 1–3 are similar, where type 1 is applicable for HFC working fluids, type 2 is prepared for flammable environments and type 3 is equipped for R717 specifically. Additionally two high pressure compressors are included, where type 4 is for R717 and type 5 is for transcritical R744 processes. The investigation was not constrained to individual compressor technologies, but due to data availability considering the compressor cost, the below results represent reciprocating piston compressors. For type 1–3 price data was aggregated from several manufacturers with similar operating limits and performance.

Table 3 – Available compressor technology with current operating limits.

Working fluid	Type –	Pressure limmit bar	Lubrication max. temp. °C	Capacity (1500 RPM) m^3/h
R134a	1	28	180	5–280
R290	2	28	180	5–280
R600a	2	28	180	5–280
R717-LP	3	28	180	5–180
R717-HP	4	50	180	90–200
R744	5	140	180	6–25

2.4. *Economic evaluation*

The economic evaluation of the heat pumps was based on the economic method presented by Bejan et al. (1996), where individual component costs are used to account for the overall collected system. The method requires detailed cost data for components presented in a process flow diagram.

In order to obtain coherent and comprehensive data for specific components, the aggregation of data required several assumptions. It was assumed that:

- Purchased Equipment Cost (PEC) for an open type compressor was solely dependent on the type (specified in Table 3) and the swept volume of the compressor.
- PEC for an electrical motor with a fixed efficiency was dependent on the shaft power.
- PEC for a heat exchanger was a function of the heat exchange area and pressure limit.
- PEC of an intermediate pressure receiver was a function of volume and pressure limit.
- The PECs of expansion valve and oil separator were neglected.
- Total Capital Investment (TCI) of a component was calculated as 4.16 higher than PEC of the component (Bejan et al., 1996). This was done to account for additional cost related to new investment at an existing facility. The costs include installation, piping, instrumentation, electrical equipment,

Please cite this article in press as: Ommen, T., et al., Technical and economic working domains of industrial heat pumps: Part 1 – Single stage vapour compression heat pumps, International Journal of Refrigeration (2015), http://dx.doi.org/10.1016/j.ijrefrig.2015.02.012

engineering and supervision, as well as startup and working capital etc.
- Electricity and natural gas prices correspond to the market cost for industrial consumers in the year 2012 according to Danish Energy Agency (2013a).
- The investment cost of already installed natural gas burners were neglected. This is the case if the heat pump replaces an existing installation.
- Source heat was assumed readily available as a process stream.
- Interest and inflation rate were fixed rates (7% and 2% respectively (Danish Energy Agency, 2011)).
- The technical lifetime of the plant was assumed to be 15 years (Fazelpour and Morosuk, 2014). This assumption may be seen as a conservative estimate, as higher technical lifetimes (20 years) are reported by other sources (Blarke, 2012; Danish Energy Agency, 2013b).
- Cost correlations are assumed to be valid for heat pump capacities between 100 kW and 2 MW. Restrictions are due to data availability for component correlations.

Purchased equipment cost (PEC) functions have been developed based on prices from intermediate Danish trade business and individual manufactures. The cost functions, Eq. (1), were constructed as proposed by Bejan et al. (1996) where the purchase cost of an equipment item PEC_Y at a size or capacity X_Y can be calculated based on knowledge of the cost PEC_W at a different size or capacity X_W by use of a scaling exponent α.

$$PEC_Y = PEC_W \left(\frac{X_Y}{X_W}\right)^{\alpha} \quad (1)$$

Data for the component cost correlations and references are listed in Table 4 for each of the investigated HP systems. In many cases, the data corresponds to several brands with similar characteristics in terms of economy and applicability. For some of the investigated components, the cost correlations are not presented due to non-disclosure agreements (NDA) with the manufacturers.

When comparing technical solutions the best available economically solution is preferred. Two different profitability criteria have been used for the analysis, the (simple) payback period (PBP) and the net present value (NPV). The method for determination of the two factors is explained in Sections 2.4.1 and 2.4.2.

2.4.1. *Net present value*

The profitability evaluation determines the net present value between two alternative systems, by considering the time value of cash flow streams during the lifetime of the investment. The present value of the proposed heat pump system was compared to the present value of the existing solution. The capital-recovery factor (CRF), Eq. (2) (Bejan et al., 1996), was used to calculate the levelized cost over the lifetime of the plant n:

$$CRF = \frac{i^{eff}(1+i^{eff})^n}{(1+i^{eff})^n - 1} \quad (2)$$

where i^{eff} is the effective interest rate over the life time of the system, calculated as seen in Eq. (3) (Bejan et al., 1996), where i is the interest rate, and i_L is the inflation rate.

$$i^{eff} = \frac{1+i}{1+i_L} - 1 \quad (3)$$

The annual fuel cost of the plant was calculated according to Eq. (4) for a heat pump or Eq. (5) for natural gas burner (Bejan et al., 1996).

$$FC_{HP} = \frac{\dot{Q}}{COP} \cdot c_{el} \cdot H \quad (4)$$

$$FC_{NG} = \frac{\dot{Q}}{\eta_{NG}} \cdot c_{NG} \cdot H \quad (5)$$

where $\dot{Q}$ is the desired heat rate of the demand. COP is the coefficient of performance of the heat pump, and the natural gas burner efficiency is denoted η_{ng}. c denotes the fuel price for either electricity or natural gas and H is the annual amount of operating hours.

The present value of the expenses associated with the project j was calculated as presented in Eq. (6) (Bejan et al., 1996).

Table 4 – Used cost correlations for component types divided by application limits.

Component	Type	PEC_W (€)	X_W	α(–)	Source
Compressor	R134a	10,631	178.4 ($m^3\ h^{-1}$)	0.79	trade business[a,b,c]
	R290, R600a	19,850	279.8 ($m^3\ h^{-1}$)	0.73	trade business[a,b]
	R717-LP	11,914	178.4 ($m^3\ h^{-1}$)	0.66	trade business[a,b]
	R717-HP	NDA	NDA	NDA	manufacturer[d]
	R744	12,109	25.6 ($m^3\ h^{-1}$)	0.42	trade business[a,b]
Electrical motor	R134a, R717-LP, R717-HP	10,710	250 (kW)	0.65	trade business[a]
	R290, R600a, R744	0	0	0	incl. in compressor[a,b]
Receiver	R134a, R290, R600a, R717-LP	1444	0.089 (m^3)	0.63	trade business[a]
	R717-HP	1934	0.089 (m^3)	0.66	trade business[a]
	R744	2744	0.050 (m^3)	1.12	trade business[a]
Plate heat exchanger	R134a, R290, R600a, R717-LP	15526	42 (m^2)	0.8	trade business[a,b,c]
	R717-HP	NDA	NDA	NDA	manufacturer[e]
	R744	NDA	NDA	NDA	manufacturer[e]

[a] H. Jessen Jörgensen A/S (2013).
[b] FK Teknik A/S (2013).
[c] Ahlsell Danmark ApS (2013).
[d] Johnson Controls, Inc. (2013).
[e] SWEP International AB (2013).

Please cite this article in press as: Ommen, T., et al., Technical and economic working domains of industrial heat pumps: Part 1 – Single stage vapour compression heat pumps, International Journal of Refrigeration (2015), http://dx.doi.org/10.1016/j.ijrefrig.2015.02.012

$$PV_j = TCI_j + \frac{FC_j}{CRF} + OMC_j \quad (6)$$

where TCI_j is the total capital investment of all required components for system j. OMC_j is the operation and maintenance cost (OMC) (not including fuel cost) for system j, which is assumed to be a fixed factor (20%) of TCI_j (Bejan et al., 1996). For natural gas burners the capital investments are considered as sunk cost ($TCI_{NG} = 0$) and thus the OMC costs are similarly neglected.

The NPV was calculated as presented in Eq. (7) for the case where a heat pump is proposed as an alternative for a natural gas burner in a facility.

$$NPV_{HP} = PV_{NG} - PV_{HP} \quad (7)$$

If the NPV is positive, the proposed heat pump is a cost effective alternative to the already installed burner.

2.4.2. Pay back period

The PBP determines the length of time required for the proposed installation to fully recover the TCI by reduction in FC and OMC compared to the existing solution. PBP is often used as a measure for feasibility of technical projects, but the factor does not include the time value of money or include cash flows that occur after the calculated period. The PBP was calculated as presented in Eq. (8) (Bejan et al., 1996).

$$PBP_{HP} = \frac{TCI_{HP}}{(FC_{NG} - FC_{HP}) + (OMC_{NG} - OMC_{HP}) \cdot CRF} \quad (8)$$

3. Results

Detailed results of the thermodynamic state points, heat transfer and costs are presented in appendix Appendix A for an R717-LP heat pump system operating at $T_{sink,out} = 60\ ^\circ C$, $T_{lift} = 20$ K, $\Delta T_{sink} = 20$ K, $\Delta T_{source} = 10$ K. For this analysis the heat pump operating hours and capacity was assumed to be 3500 h and 1000 kW respectively. Similar analysis was performed for the remaining systems.

For the analysis of the working domains, the operating hours and heat pump capacity have been kept constant. The operating point corresponds to that presented in appendix Appendix A. The impact of the two parameters were determined by a parametric variation, which is presented in Fig. 2a.

Contours of two different simple pay back periods (PBP) and the net present value of zero (meaning that both solutions are equally feasible for the technical lifetime of the heat pump system) are plotted. Similar variations of economic constraints, NPV = 0 as well as PBP = 4 years and PBP = 8 years have been included in each working domain, allowing the reader to decide the appropriate economic constraint.

It is worth noticing, that all solutions in Fig. 2a represent COP = 6.5 and VHC = 7.7 MJ/m^3 (according to calculation in Appendix Appendix A), which are within the recommended levels defined by Brunin et al. (1997). Although within the limits, a significant part of the solutions were found to be infeasible compared to the fuel cost of a natural gas boiler, which indicate that the use of semi-economical constraints may not include the required level of detail.

Based on the results of Fig. 2a the heat pump working domains were investigated for a case of 3500 operating hours yearly, and $\dot{Q}_{HP} = 1000$ kW. Fig. 2b presents a parametric variation of significant assumptions for calculation of the NPV at this operation point. The NPV is most sensitive to the assumptions of heat transfer coefficients and isentropic efficiency. The observed sensitivity is assumed not to limit the validity of the economic comparisons between the technologies, as offsets would result in similar changes for all the considered systems.

Fig. 3a–b presents a variation of natural gas and electricity prices for the two used economic criteria. Both natural gas and electricity prices were varied by ±50% for the investigated heat pump solution. Based on the slope of constant NPV in Fig. 3a it is found that the system is more sensitive of the price of natural gas than of electricity, and that the gradients of fixed electricity or natural gas prices are close to constant. At high gas prices and low electricity prices an area is indicated, where the price of electricity is lower than natural gas. At low gas prices and high electricity prices, the heat pump NPV can become negative.

For the PBP in Fig. 3b similar areas are indicated where the simple PBP becomes negative, or where the natural gas price exceeds the electricity price. Opposite to NPV, the gradients of fixed electricity or natural gas prices are far from constant throughout the investigated price span. By comparison of the two economic criteria, it is clear that the NPV is less sensitive to variations in fuel cost. Another benefit of the use of NPV as the economic criterion, is that the NPV evaluation returns a monotonic result.

The technical and economic limitations for heat pump operation were investigated for different sink and source temperature glides. The presented temperature glides are: (sink/source): 10 K/10 K, 20 K/10 K, 20 K/20 K and 40 K/10 K. In the study the working domains were established by considering the operational boundaries for each considered heat pump type for 10 K/10 K (Fig. 4) and 40 K/10 K (Fig. 5). The remaining temperature glides (20 K/10 K and 20 K/20 K) are presented in Appendix B as Fig. B.1 and Fig. B.2 respectively.

The hatched areas of the individual plots are areas where the considered technology is not appropriate. One area is caused if $T_{source,out}$ is below 0 °C, which requires another source media to be considered, and thus influences the heat transfer characteristics. This could be feasible if a brine was applied, but it would imply cooling the heat source below ambient temperatures, which may only be relevant if a cooling demand is satisfied. The second area corresponds to a case where $T_{sink,in} < T_{source,in}$. In such a heat transfer processes, heat should be exchanged directly between the two streams before a heat pump is integrated in the process (Townsend and Linnhoff, 1983; Annex-21, 1995).

The economic constraints are presented as green lines (NPV) and turquoise/dashed turquoise lines for PBP. Red lines indicates high discharge temperatures, whereas blue lines show the pressure constraints for the considered systems.

Each individual plot shows the constraints for the specific working fluid, showing both the components and the economic restrictions. By examination of Fig. 4 it can be seen, that combination of the four natural working fluids allows for a large working domain. The NPV constraints for R717-LP and R717-HP include a large fraction of the considered temperature span, but the technology is restricted by high compressor discharge temperatures, as well as the allowable high

Please cite this article in press as: Ommen, T., et al., Technical and economic working domains of industrial heat pumps: Part 1 – Single stage vapour compression heat pumps, International Journal of Refrigeration (2015), http://dx.doi.org/10.1016/j.ijrefrig.2015.02.012

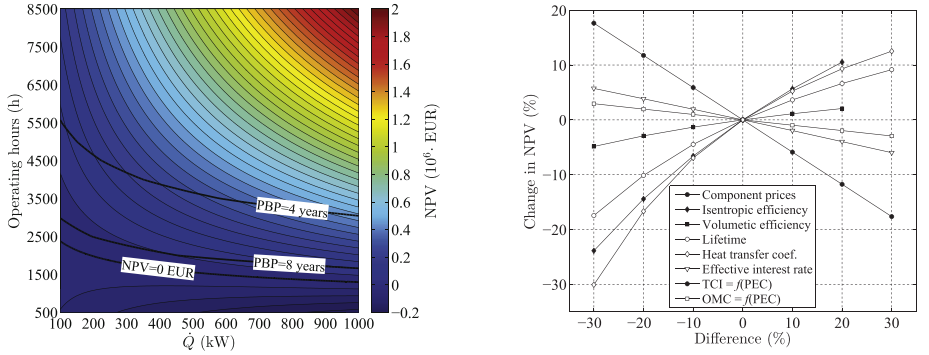

(a) NPV of HP system with variations in size and yearly operation hours

(b) Parametric variation of key economic assumptions

Fig. 2 – Influence of key economic assumptions on NPV R717-HP heat pump operating at $T_{sink,out} = 60$ °C, $T_{lift} = 20$ °C, $\Delta T_{sink} = 20$ K, $\Delta T_{source} = 10$ K.

pressure. For the four remaining heat pumps, the discharge temperatures are below the limit in all cases, but at the same time it may be seen that the NPV constraint is at a lower ΔT_{lift} compared to the two ammonia configurations.

Specifically for all R744 configurations (e.g. Fig. 4a) the critical pressure of the working fluid limits the working domain at high $T_{sink,out}$, as two-phase evaporation is not possible in some of the considered combinations. Furthermore, the dashed pressure constraint indicates where optimal pressure is above the maximum allowable for the compressor. Beyond this line the high pressure side is kept at the maximum allowable pressure, which results in decreased performance and changed slope of the economic constraints.

For 40 K/10 K (Fig. 5) similar plots are presented. At higher sink temperature glide, the high discharge temperature for R717 decreases the area of feasible solutions. At the same time, transcritical R744 is economically and technically feasible at even higher temperature lifts, than for the case 10 K/10 K. It can be seen that an area exist where R744 increases the allowable ΔT_{lift}, in the areas where R717 is constrained by discharge temperature. None of the considered heat pumps for sink/source glide of 40 K/10 K in Fig. 5a–f allow a PBT below 4 years.

From investigation of Figs. 4 and 5 it is found that the trends for NPV are similar for all subcritical systems, although at different magnitude for ΔT_{lift}. In order to further understand the mechanisms, an investigation of the thermodynamic performance and investment has been performed for one case (corresponding to R600a at 10 K/10 K sink/source glide in Fig. 4e). The trends for COP and investment are presented in Fig. 6a and b respectively. High COP is obtained for low temperature lifts resulting in low FC_{HP}. The investment TCI_{HP} is lowest at high sink outlet temperatures and medium (e.g. 30–50 K) temperature lift. At lower lift the investment required for the condenser is increased, while at low sink outlet temperature and high temperature lift the PEC of the

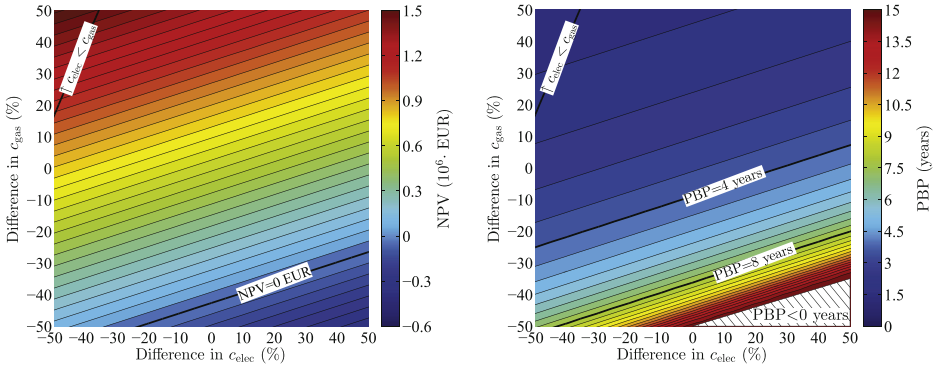

(a) NPV of HP system with variations in fuel cost

(b) PBP of HP system with variations in fuel cost

Fig. 3 – Impact of natural gas and electricity prices on NPV and PBP R717-HP heat pump operating at $T_{sink,out} = 60$ °C, $T_{lift} = 20$ °C, $\Delta T_{sink} = 20$ K, $\Delta T_{source} = 10$ K.

Please cite this article in press as: Ommen, T., et al., Technical and economic working domains of industrial heat pumps: Part 1 – Single stage vapour compression heat pumps, International Journal of Refrigeration (2015), http://dx.doi.org/10.1016/j.ijrefrig.2015.02.012

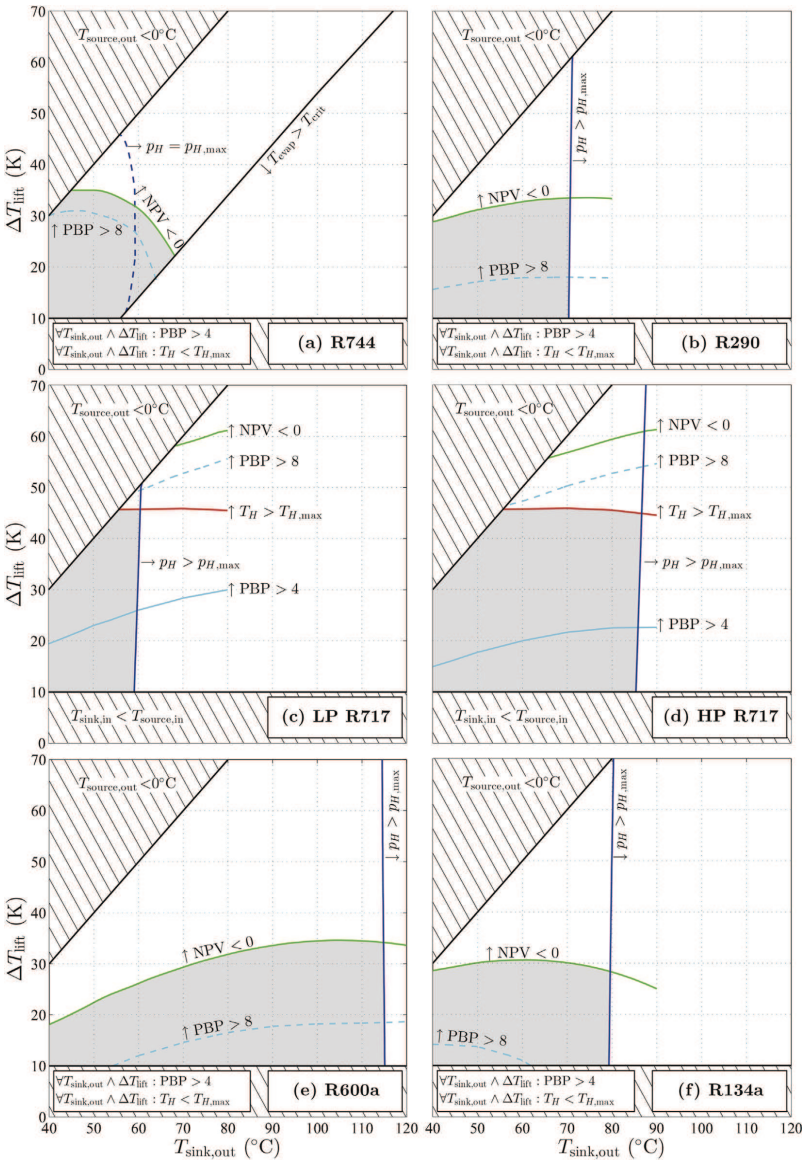

Fig. 4 – Working domains for six different heat pumps – ΔT_{sink} = 10 K/ΔT_{source} = 10 K.

compressor is significantly increased, as the suction volume of the heat pump is high.

High temperature glide in the source is typically used in the cases where the capacity of the source at low temperature glide does not fully match the heat demand. Optimal heat production may then be considered as a tradeoff between capacity and performance. By inspection of 20 K/20 K (Fig. B.2), it is clear that the working domains of the heat pumps are closely related to those of 20 K/10 K (Fig. B.1), although the economic constraints are moved towards a lower temperature lift. Because of the increased pressure ratio between evaporator and condenser, the R717 discharge temperature constraint is moved below a temperature lift of 40 K.

Please cite this article in press as: Ommen, T., et al., Technical and economic working domains of industrial heat pumps: Part 1 – Single stage vapour compression heat pumps, International Journal of Refrigeration (2015), http://dx.doi.org/10.1016/j.ijrefrig.2015.02.012

A full comparison of working domains for all heat pump systems is presented in Fig. 7 and Fig. 8 for all of the considered sink and source glides. Fig. 7a presents the combination of constraints for each individual working fluid for sink/source glide of 10 K/10 K and Fig. 7b highlights the economically best (NPV) solutions in the entire working domain. Similar plots are presented for the alternative glides. Fig. 7c–d correspond to 20 K/20 K glide. Fig. 8a–b and Fig. 8c–d are for 20 K/10 K and 40 K/10 K respectively.

For all of the sink/source glides, it is found that R717-LP configurations are optimal within the established technical and economical boundaries for the system. For increasing sink temperatures, R717-HP is cost optimal in the area constrained by discharge temperatures and high pressure limit. For further increase in sink temperatures, R600a configurations are the only feasible option until the limitations on pressure at approximately 115 °C. The R600a configurations are furthermore limited by an economic constraint at ΔT_{lift} between 30 and 40 K for most glides, and 40–50 K for the 40 K/10 K glide (Fig. 8d).

Transcritical R744 is the optimal configuration at high ΔT_{lift} if the sink temperature glide is large. For the glide 40 K/10 K a

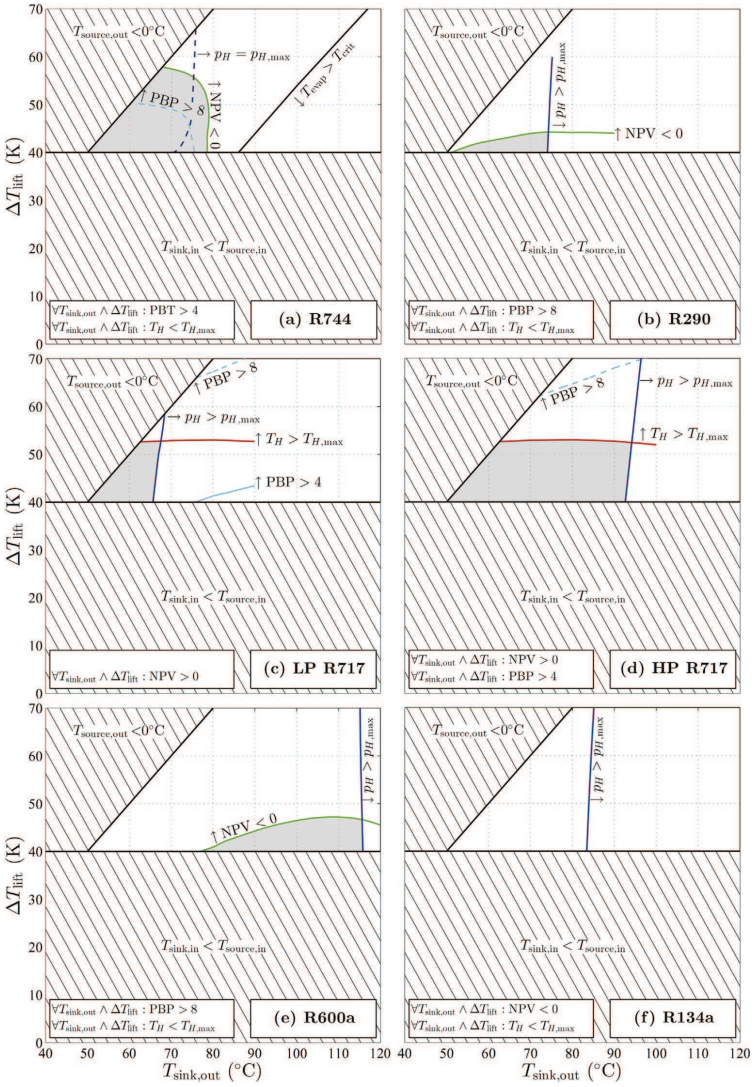

Fig. 5 – Working domains for six different heat pumps – $\Delta T_{sink} = 40$ K/$\Delta T_{source} = 10$ K.

Please cite this article in press as: Ommen, T., et al., Technical and economic working domains of industrial heat pumps: Part 1 – Single stage vapour compression heat pumps, International Journal of Refrigeration (2015), http://dx.doi.org/10.1016/j.ijrefrig.2015.02.012

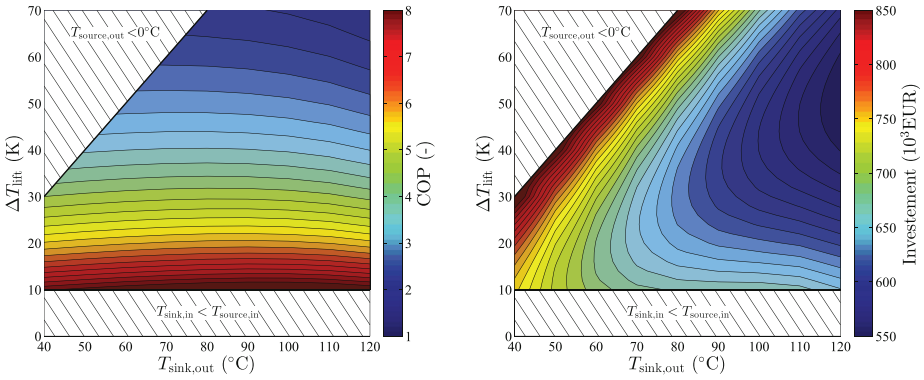

(a) COP (b) Investment

Fig. 6 – Trend of COP and investment for $T_{source,out}$ and ΔT_{lift} – R600a heat pump for 10 K/10 K sink/source glide.

significant area exsist, where the technology provides the only solutions which are technically and economically feasible. For the remaining cases with sink temperature glide at 20 K or below, the maximal ΔT_{lift} for R744 is below the constraints of R717-LP.

4. Discussion

The economic correlations used in the investigation are based directly on data from Danish suppliers or international manufacturers. List prices may be seen as a conservative estimate

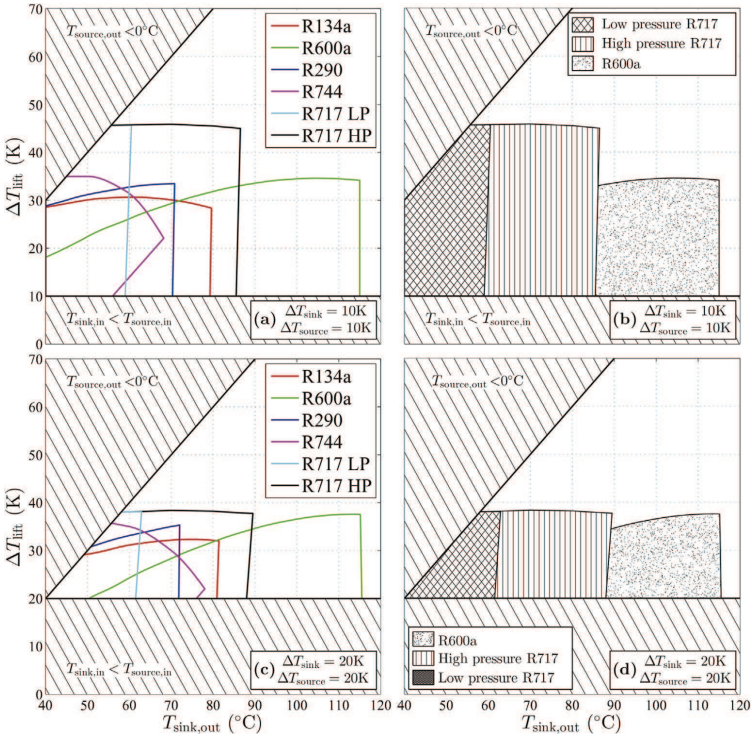

Fig. 7 – Compilation of working domains (a & c) and hatched areas with best available technology based on NPV (b & d) for selected heat pumps – (a & b) ΔT_{sink} = 10 K/ΔT_{source} = 10 K (c & d) ΔT_{sink} = 20 K/ΔT_{source} = 20 K.

Please cite this article in press as: Ommen, T., et al., Technical and economic working domains of industrial heat pumps: Part 1 – Single stage vapour compression heat pumps, International Journal of Refrigeration (2015), http://dx.doi.org/10.1016/j.ijrefrig.2015.02.012

on investment cost, as sealed price agreements may change the actual component investment cost. From Fig. 2b a 18% increased NPV is found for a 30% decrease in component cost. Such a change would significantly increase the feasible area for many of the considered heat pump types. It is expected that the cost reductions are similar for the investigated technologies, and as such the analysis would not change the relationship significantly between the types, but only between heat pumps and natural gas installations.

The results presented here stem from simulation results by verified models. Both economic correlations and heat transfer correlations are validated. Unfortunately, it is not possible to validate the investment cost of complete installations, due to lack of data availability in the open literature. However, the same approach has been applied for all investigations and thus it is assumed that if any fault occurs it will mainly effect the absolute values, and not the relation between the considered systems.

The heat transfer correlations used for condensation and evaporation are derived from experiments with R134a, but used in the evaluation for all working fluids, assuming that the individual transport properties of the fluids allow the required detail for calculating the correct heat transfer coefficient. An updated experimental investigation of the correlation at the correct temperature levels is being pursued at the time of writing. The used correlations have been compared to data from a few manufactures with promising results for several working fluids. Investigation of the parametric variations in Fig. 2b shows that the effect of changed heat transfer coefficient by ±30% is between −30% and 12% for the total heat transfer coefficient on NPV.

Several steps to increase the working domain of individual heat pump systems may be considered such as: two stage compression, liquid injection in suction line, internal heat exchangers, heat pumps connected in series or cascade solutions etc. The energetic or technical improvements of NPV are typically reduced by increased investment in terms of additional components for the thermodynamic cycle. Such improved working domains by energetic or technical improvements have not been considered in this study, but may be the focus of subsequent analysis. At certain temperature configurations, where the best available technology may shift to a different system due to an expanded working domain (ie. from R600a to R717-HP) the gain in NPV may be significant. If a shift in best available technology is not possible, the maximal improvement due to cycle improvements (not including heat pumps in series) is typically below 10% on COP (Granryd, 2005). With additional investment according to the changed PI-diagram the gain in NPV will be lower than this figure.

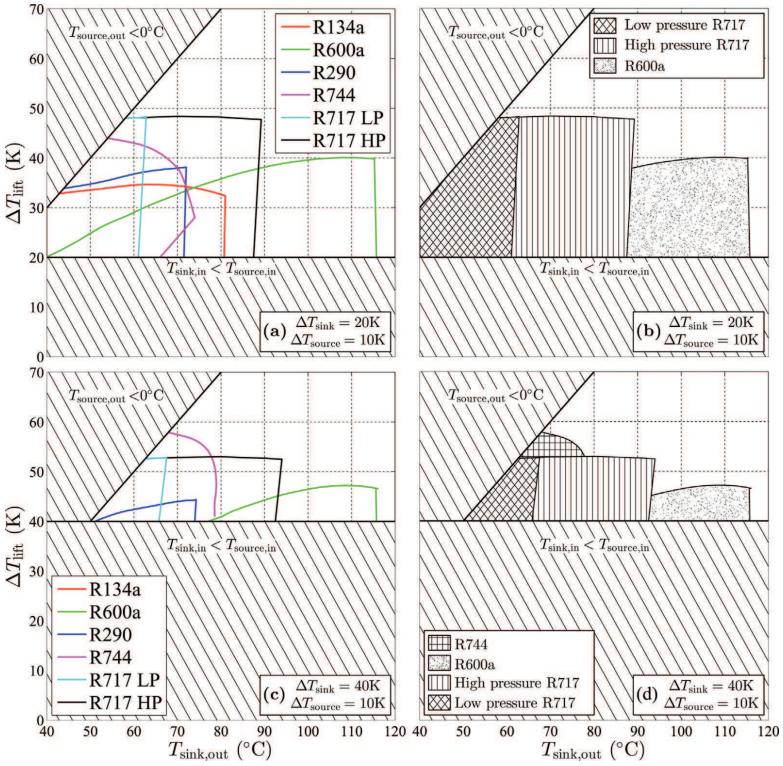

Fig. 8 – Compilation of working domains (a & c) and hatched areas with best available technology based on NPV (b & d) for selected heat pumps – (a & b) $\Delta T_{sink} = 20$ K/$\Delta T_{source} = 10$ K (c & d) $\Delta T_{sink} = 40$ K/$\Delta T_{source} = 10$ K.

Please cite this article in press as: Ommen, T., et al., Technical and economic working domains of industrial heat pumps: Part 1 – Single stage vapour compression heat pumps, International Journal of Refrigeration (2015), http://dx.doi.org/10.1016/j.ijrefrig.2015.02.012

5. Conclusion

From a variation of operation hours and heat production of a heat pump, it is found that the net present value or pay back period shows higher detail in the feasibility of investigated solutions than the use of semi-economic parameters such as COP and VHC.

All of the six considered heat pumps show working domains where net present value is positive, when compared to the fuel cost of a natural gas burner. Four of the heat pumps are advantageous when considering all of the presented constraints. These heat pumps are R717-LP, R717-HP, R600a and transcritical R744. In areas covered by the working domain of several configurations, the R717-LP and R717-HP allow the optimal NPV.

By investigation of the four sink/source working domains for vapour compression heat pumps it is found, that sink temperatures of up to 115 °C and temperature lifts up to 40 K can be achieved by four common heat pump systems. For both R717-LP and R717-HP heat pump systems, the discharge temperature is a significant limitation for expansion of the working domains, where as for the remaining technologies the economic constraints restrict feasible solutions.

Acknowledgements

This work was supported by DONG Energy, Copenhagen Cleantech Cluster (CCC), Danish Technological Institute and EUDP (Energy Technology Development and Demonstration) project number: 64011-0351.

Appendix A. Detailed results of the thermodynamic, heat transfer and economic model

Table A.1 – Thermodynamic state points.

j^{th} stream	Media	$\dot{m}_j$ (kgs^{-1})	T_j (°C)	p_j (bar)	h_j (kJkg^{-1})	s_j (kJkg^{-1} K^{-1})
(1)	R717-LP	0.79	30	10.03	1499	5.37
(2)	R717-LP	0.79	120.3	27.39	1684	5.47
(3)	R717-LP	0.79	45	27.39	415	1.72
(4)	R717-LP	0.79	25	10.03	415	1.74
Sink,out	Water	11.96	60	9.96	252	0.83
Sink,in	Water	11.96	40	10.00	168	0.57
Source,in	Water	20.43	40	10.00	168	0.57
Source,out	Water	20.43	30	9.96	126	0.43

Table A.2 – Heat and work load.

$\dot{Q}_{Evaporator}$	855	kW	COP	6.5	–
$\dot{Q}_{Condenser}$	1000	kW	$\dot{V}_1$	467	m^3 h^{-1}
$\dot{W}_{Comp.}$	146	kW	$V_{reciever}$	0.062	m^3
$\dot{W}_{Comp.,el}$	153	kW			

Table A.3 – Heat exchanger dimensions, heat transfer and pressure drop coefficients and working fluid charge estimation.

Evaporator:			Condenser:		
ΔP_{WF}	0.2	kPa	ΔP_{WF}	0.2	kPa
ΔP_{water}	3.8	kPa	ΔP_{water}	3.7	kPa
$U_{evaporation}$	1.483	kWm^{-2} K^{-1}	$U_{superheat}$	0.466	kWm^{-2} K^{-1}
$U_{superheat}$	0.380	kWm^{-2} K^{-1}	$U_{condensation}$	3.696	kWm^{-2} K^{-1}
			$U_{subcooling}$	1.494	kWm^{-2} K^{-1}
N	597	–	N	345	–
A	73.2	m^2	A	44.1	m^2

Table A.4 – PEC, TCI, total investment and operational cost.

Break down of TCI costs				Break down of FC, OMC, NPV and PBP		
Component	X_Y	PEC (€)	TCI (€)		PV (€)	AC (€)
Compressor	467 m^3 h^{-1}	22481	93521	TCI_{HP}	300228	–
Elec. motor	146 kW	7533	31337	TCI_{NG}	0	–
Evaporator	73.2 m^2	24919	103663	FC_{HP}	462937	44303
Condenser	44.1 m^2	16092	66942	FC_{NG}	1435810	137407
Receiver	0.062 m^3	1146	4767	OMC_{HP}	60052	5747
				OMC_{NG}	0	0
				PV_{HP}	823217	–
				PV_{NG}	1435810	–
Total HP investment (€)			300228	NPV (€)	612593	–
				PBP (year)	–	3.437

Please cite this article in press as: Ommen, T., et al., Technical and economic working domains of industrial heat pumps: Part 1 – Single stage vapour compression heat pumps, International Journal of Refrigeration (2015), http://dx.doi.org/10.1016/j.ijrefrig.2015.02.012

ARTICLE IN PRESS

INTERNATIONAL JOURNAL OF REFRIGERATION XXX (2015) 1–15

Appendix B. Technical and economical operating boundaries for 20/10 and 20/20

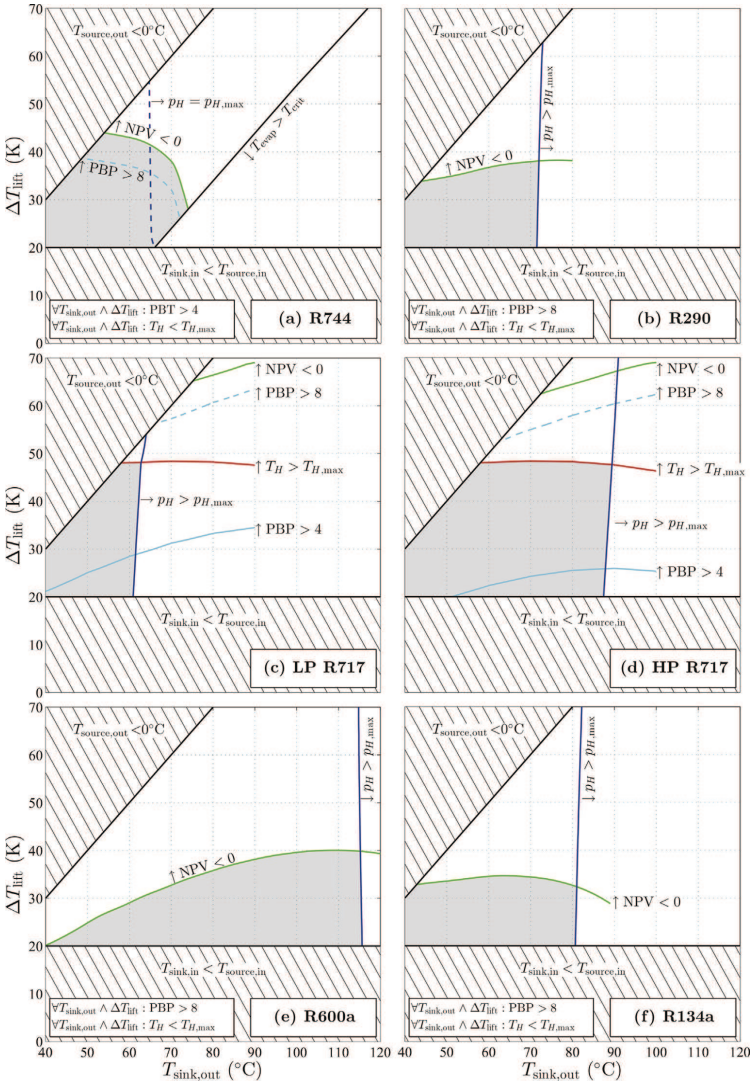

Fig. B.1 – Working domains for six different heat pumps – $\Delta T_{sink} = 20$ K/$\Delta T_{source} = 10$ K.

Please cite this article in press as: Ommen, T., et al., Technical and economic working domains of industrial heat pumps: Part 1 – Single stage vapour compression heat pumps, International Journal of Refrigeration (2015), http://dx.doi.org/10.1016/j.ijrefrig.2015.02.012

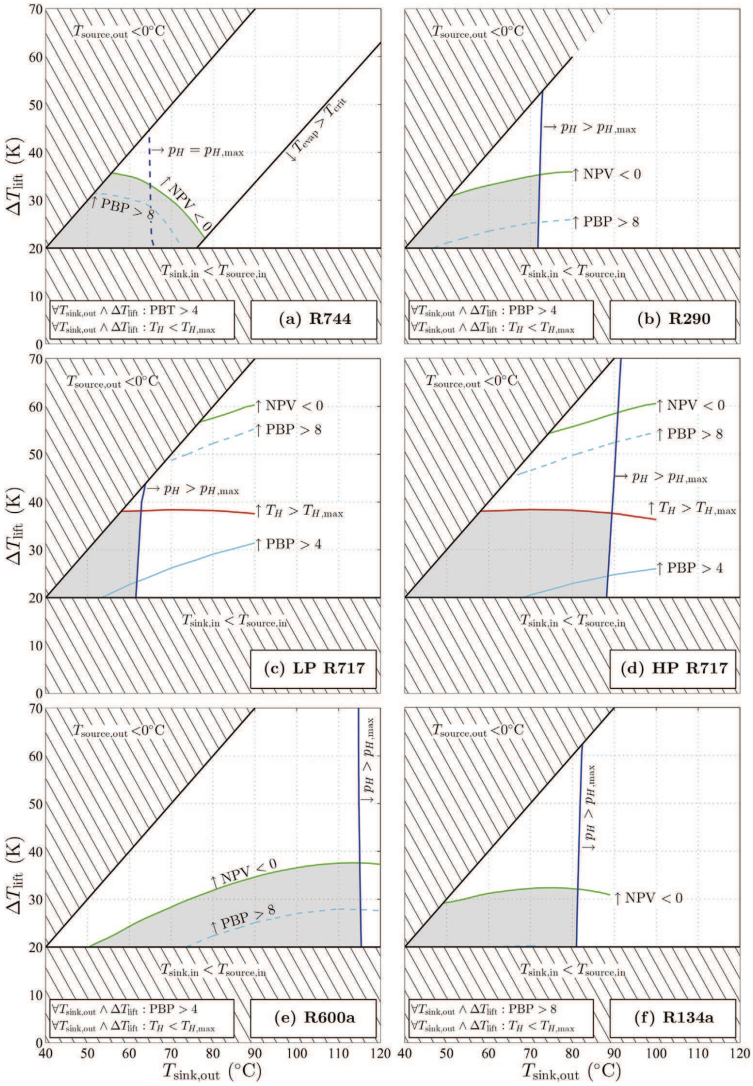

Fig. B.2 – Working domains for six different heat pumps – ΔT_{sink} = 20 K/ΔT_{source} = 20 K.

REFERENCES

Ahlsell Danmark ApS, 2013. Priskatalog 2013 (accessed 26.09.13.).

Annex-21, 1995. Industrial Heat Pumps – Experiences, Potential and Global Environmental Benefits. IEA Heat Pump Centre.

Bejan, A., Tsatsaronis, G., Moran, M., 1996. Thermal Design & Optimization, first ed. John Wiley & Sons, New York.

Blarke, M.B., 2012. Towards an intermittency-friendly energy system: comparing electric boilers and heat pumps in distributed cogeneration. Appl. Energy 91, 349–365.

Brunin, O., Feidt, M., Hivet, B., 1997. Comparison of the working domains of some compression heat pumps and a compression-absorption heat pump. Int. J. Refrigeration 20, 308.

Cecchinato, L., Corradi, M., Minetto, S., 2010. A critical approach to the determination of optimal heat rejection pressure in transcritical systems. Appl. Therm. Eng. 30.

Please cite this article in press as: Ommen, T., et al., Technical and economic working domains of industrial heat pumps: Part 1 – Single stage vapour compression heat pumps, International Journal of Refrigeration (2015), http://dx.doi.org/10.1016/j.ijrefrig.2015.02.012

Corberan, J.M., 2011. 2nd iir workshop on refrigerant charge reduction in refrigerating systems. Int. J. Refrigeration 34, 600.
Danish Energy Agency, 2011. Assumptions of Socio- Economic Analysis in the Energy Sector (Forudsætninger for samfunds-økonomiske analyser påenergiområdet). in danish: (accessed 10.10.13.).
Danish Energy Agency, 2013a. Data, Tables, Statistics and Maps, Energy in Denmark 2012 (accessed 30.06.14.).
Danish Energy Agency, 2013b. Technology Data for Energy Plants – Generation of Electricity and District Heating, Energy Storage and Energy Carrier Generation and Conversion (accessed 10.10.13.).
European Parliament, 2014. On Fluorinated Greenhouse Gases and Repealing Regulation (EC) No 842/2006. The European Parliament and the Council of the European Union.
F-Chart, S.L., 1992. Engineering Equation Solver (EES) (accessed 30.06.14.).
Fazelpour, F., Morosuk, T., 2014. Exergoeconomic analysis of carbon dioxide transcritical refrigeration machines. Int. J. Refrigeration 38, 128–139. Cited By 1.
FK Teknik A/S, 2013. Priskatalog 2013 (accessed 26.09.13.).
Granryd, E., 2005. Refrigerating Engeneering – Part I. Royal Institute of Technology, KTH, Stockholm.
H. Jessen Jörgensen A/S, 2013. Priskatalog 2013 (accessed 26.09.13.).
Jensen, J.K., Ommen, T., Markussen, W.B., Reinholdt, L., Elmegaard, B., 2015. Technical and economic working domains of industrial heat pumps: Part 2 - ammonia-water hybrid absorption-compression heat pumps. Int. J. Refrigeration. http://dx.doi.org/10.1016/j.ijrefrig.2015.02.011.
Johnson Controls, Inc, 2013. HPO R717 compressor cost – non-disclosure agreement. Priv. Commun..
Kim, M.H., Pettersen, J., Bullard, C.W., 2004. Fundamental process and system design issues in CO_2 vapor compression systems. Prog. Energy Combust. Sci. 30, 119–174.
Linnhoff, B., Hindmarsh, E., 1983. The pinch design method for heat exchanger networks. Chem. Eng. Sci. 38, 745–763. Cited By 594.
Martin, H., 1996. A theoretical approach to predict the performance of chevron-type plate heat exchangers. Chem. Eng. Process. Process Intensif. 35, 301–310.
Neksâ, P., Rekstad, H., Zakeri, G.R., Schiefloe, P.A., 1998. Co2-heat pump water heater: characteristics, system design and experimental results. Int. J. Refrigeration 21, 172.
Nellis, G., Klein, S., 2009. Heat Transfer. Cambridge University Press.
Ommen, T., Markussen, W., Elmegaard, B., 2014. Heat pumps in combined heat and power systems. Energy 76 (1), 989–1000.
SWEP International AB, 2013. SWEP – products & solutions (B400, B120T Fpressure, B17 product sheets) – non-disclosure agreement. Priv. Commun..
Townsend, D., Linnhoff, B., 1983. Heat and power networks in process design. Part I: criteria for placement of heat engines and heat pumps in process networks. AlChE J. 29, 742–748. Cited By 59.
UN Ozone Secretariat, 2000. The montreal protocol on substances that deplete the ozone layer. In: United Nations Environment Programme.
Yan, Y.Y., Lin, T.F., 1999. Evaporation heat transfer and pressure drop of refrigerant r-134a in a plate heat exchanger. J. Heat. Transf. 121, 118–127.
Yan, Y.Y., Lio, H.C., Lin, T.F., 1999. Condensation heat transfer and pressure drop of refrigerant r-134a in a plate heat exchanger. Int. J. Heat. Mass Transf. 42, 993–1006.

Please cite this article in press as: Ommen, T., et al., Technical and economic working domains of industrial heat pumps: Part 1 – Single stage vapour compression heat pumps, International Journal of Refrigeration (2015), http://dx.doi.org/10.1016/j.ijrefrig.2015.02.012

Appendix F

Paper 4 - International Journal of Refrigeration

Jonas Kjær Jensen, Torben Ommen, Wiebke Brix Markussen,
Lars Reinholdt and Brian Elmegaard

Technical and economic working domains of industrial heat pumps: Part 2 - ammonia-water hybrid absorption-compression heat pumps.

International Journal of Refrigeration, 2015; xx: 1–18.
doi:10.1016/j. ijrefrig.2015.02.011.

ARTICLE IN PRESS

INTERNATIONAL JOURNAL OF REFRIGERATION XXX (2015) 1–18

Available online at www.sciencedirect.com

ScienceDirect

journal homepage: www.elsevier.com/locate/ijrefrig

Technical and economic working domains of industrial heat pumps: Part 2 – Ammonia-water hybrid absorption-compression heat pumps☆

Jonas K. Jensen [a,*], *Torben Ommen* [a], *Wiebke B. Markussen* [a], *Lars Reinholdt* [b], *Brian Elmegaard* [a]

[a] *Technical University of Denmark, Department of Mechanical Engineering, Nils Koppels Alle, Building 403, DK-2800, Kgs. Lyngby, Denmark*

[b] *Danish Technological Institute, Kongsvang Allé 29 Aarhus, DK-8000, Denmark*

ARTICLE INFO

Article history:
Received 11 November 2014
Received in revised form
16 February 2015
Accepted 22 February 2015
Available online xxx

Keywords:
Industrial heat pumps
Working domain
Absorption-compression heat pump
Economic evaluation
Natural refrigerants

ABSTRACT

The ammonia-water hybrid absorption-compression heat pump (HACHP) has been proposed as a relevant technology for industrial heat supply, especially for high sink temperatures and high temperature glides in the sink and source. This is due to the reduced vapour pressure and the non-isothermal phase change of the zeotropic mixture, ammonia-water. To evaluate to which extent these advantages can be translated into feasible heat pump solutions, the working domain of the HACHP is investigated based on technical and economic constraints. The HACHP working domain is compared to that of the best available vapour compression heat pump with natural working fluids. This shows that the HACHP increases the temperature lifts and heat supply temperatures that are feasible to produce with a heat pump. The HACHP is shown to be capable of delivering heat supply temperatures as high as 150 °C and temperature lifts up to 60 K, all with economical benefits for the investor.

Domaines techniques et économiques de fonctionnement de pompes à chaleur industrielles : Partie 2 – Pompes à chaleur à ammoniac-eau hybrides à absorption-compression

Mots clés : Pompes à chaleur industrielles ; Domaine de fonctionnement ; Pompes à chaleur ; Evaluation économique ; Frigorigénes naturels

☆ The original paper was presented on the 11th IIR Gustav Lorentzen Conference on Natural Refrigerants (GL2014), Aug.31 to Sept.2, 2014, Hangzhou, China.

* *Corresponding author.*
E-mail addresses: jkjje@mek.dtu.dk (J.K. Jensen), tsom@mek.dtu.dk (T. Ommen), wb@mek.dtu.dk (W.B. Markussen), lre@teknologisk.dk (L. Reinholdt), be@mek.dtu.dk (B. Elmegaard).

http://dx.doi.org/10.1016/j.ijrefrig.2015.02.011
0140-7007/

Please cite this article in press as: Jensen, J.K., et al., Technical and economic working domains of industrial heat pumps: Part 2 – Ammonia-water hybrid absorption-compression heat pumps, International Journal of Refrigeration (2015), http://dx.doi.org/10.1016/j.ijrefrig.2015.02.011

Nomenclature

Abbreviations

CRF	Capital recovery factor
HACHP	Hybrid absorption-compression heat pump
HEX	Heat exchanger
LVS	Liquid-vapour separator
MRP	Manufacturer suggested retail price
NDA	Non-disclosure agreement
LP R717	Low pressure R717 components
HP R717	High pressure R717 components
TBP	Trade business price
VCHP	Vapour compression heat pump

Symbols

A_{HT}	Heat transfer area (m^2)
A_{IN}	Investment area (m^2)
c	Specific energy cost (€ kW^{-1})
c_p	Specific heat capacity (kJ kg^{-1} K^{-1})
b	Plate press depth (mm)
Bo	Boiling number (–)
COP	Coefficient of performance (–)
D_h	Hydraulic diameter (m)
f	Circulation ratio (–)
F	Two-phase enhancement factor (–)
FC	Annual cost of fuel consumption (€)
h	Specific enthalpy (kJ kg^{-1})
h_{fg}	Specific heat of vaporization (kJ kg^{-1})
G	Mass flux (kg s^{-1} m^{-2})
H	Yearly operating time (s)
i	Interest rate (–)
i^{eff}	Effective interest rate (–)
i_L	Inflation rate (–)
L	Plate length (m)
LT	Technical lifetime (years)
m	Mass (kg)
$\dot{m}$	Mass flow rate (kg s^{-1})
M	Number of channels (–)
N	Number of plates (–)
Nu	Nusselt number (–)
NPV	Net present value (€)
OMC	Operation and maintenance cost (€)
PBP	Payback period (years)
PEC	Purchased equipment cost (€)
TCI	Total capital investment (€)
p	Pressure (bar)
Δp	Pressure loss (bar)
Pr	Prandtl number (–)
PV	Present value (€)
q	Vapour mass fraction (–)
$\dot{Q}$	Heat rate (kW)
r	Relative difference (%)
Re	Reynolds number (–)
s	Specific entropy (kJ kg^{-1} K^{-1})
T	Temperature(°C)
ΔT	Temperature difference (K)
t	Plate wall thickness (–)
X	Size or capacity of component
x	Ammonia mass fraction (–)
X_{tt}	Lockhart–Martinelli parameter (–)
Z	Silver, Bell & Ghaly correlation factor
W	Plate width (m)
$\dot{W}$	Power (kW)
U	Overall heat transfer coefficient (kW m^{-2} K^{-1})
u_{SL}	Superficial liquid velocity (m s^{-1})
u_{SV}	Superficial vapour velocity (m s^{-1})
V	Volume (m^3)
v	Specific volume (m^3 kg^{-1})
$\dot{V}$	Volume flow rate (m^3 s^{-1})

Greek letters

α	Heat transfer coefficient (kW m^{-2} K^{-1})
β	Plate corrugation angle (°)
γ	Cost function exponent (–)
ε	Effectiveness (–)
η	Efficiency (–)
λ	Thermal conductivity (–)
Λ	Plate corrugation spacing (m)
μ	Viscosity (Pa s)
ϕ	Plate area enhancement factor (–)
φ	Plate corrugation inclination angle (°)
ξ	Pressure drop coefficient (–)

Subscripts

¯	Average
c	Critical
el	Electrical
dis	Displacement
HP	Heat pump (HACHP)
i	Index
is	Isentropic
j	Stream
k	Component
l	Liquid
lf	Liquid film
lo	Liquid only
LM	Logarithmic mean
max	Maximum
NG	Natural gas
pp	Pinch point
r	Rich
suc	Suction line
tp	Two phase
v	Vapour
vo	Vapour only
vol	Volumetric
w	Wall
W	Equipment with known cost
Y	equipment with calculated cost

Please cite this article in press as: Jensen, J.K., et al., Technical and economic working domains of industrial heat pumps: Part 2 – Ammonia-water hybrid absorption-compression heat pumps, International Journal of Refrigeration (2015), http://dx.doi.org/10.1016/j.ijrefrig.2015.02.011

1. Introduction

Industrial scale heat pumps may be applied to improve the energy efficiency of industrial processes (Townsend and Linnhoff, 1983) or for utility production in urban areas with district heating networks (Ommen et al., 2014b). The temperature range where heat pumps for such purposes are applicable is bound by several technical constraints. The technical constraints are governed by the thermodynamic behaviour of the working fluid and the limits of commercially available components, such as compressor discharge temperature and pressure. Further, for a heat pump to be a viable investment, the installation should be the more profitable alternative compared to a competitive technology such as a natural gas burner.

Many industrial scale heat pumps have been installed with a heat supply temperature in range 50–90 °C. The lack of installations above 90 °C is most likely due to the lack of cost efficient solutions in this temperature range, as seen in part 1 of this study (Ommen et al., 2014a) rather than a limited demand for high temperature heat pump solutions (Annex 21, 1995).

The hybrid absorption-compression heat pump (HACHP) or vapour compression heat pump with solution circuit is based on the Osenbrück cycle (Osenbrück, 1895). The advantage of the HACHP is the reduction of vapour pressure and the temperature glides of the absorption and desorption processes, (Altenkirch, 1950; Berntsson and Hultén, 1999, 2002).

The reduction of vapour pressure allows the design of high temperature heat pumps with standard pressure refrigeration components, (Brunin et al., 1997; Jensen et al., 2014). While the non-isothermal phase change allows the temperature profiles of the absorber and desorber to match those of the external circuits, thereby attaining a reduction of the entropy generation caused by heat transfer over a finite temperature difference. Consequently, the HACHP is one feasible measure of approaching the Lorenz cycle (Lorenz, 1894), thereby increasing the efficiency compared to a vapour compression heat pump (VCHP). These advantages make the HACHP a relevant technology, for industrial processes that require high temperatures and large temperature glides.

The HACHP has recently experienced gained interest, as commercial solutions have entered the market. The HACHP has been implemented for waste heat recovery and heat supply in industrial facilities such as dairies, abattoirs, district heating and sewage treatment plants (Hybrid Energy AS, 2015). These installations have a heat load ranging from 150 kW to 1200 kW and a heat supply temperature up to 85 °C (Hybrid Energy AS, 2015).

Brunin et al. (1997) evaluates the working domain of the HACHP based on one technical constraint: maximum pressure and two physical parameters applied as economic indicators: minimum coefficient of performance (COP) and minimum volumetric heat capacity (ratio between heat output and compressor displacement volume). The working domain by Brunin et al. (1997) is evaluated at a fixed 10 K temperature difference, between inlet and outlet, for both the heat sink and heat source. Under these constraints, Brunin et al. (1997) shows that the HACHP can attain allowable heat supply temperatures up to 140 °C with a maximum pressure of 20 bar.

In recent years the maximum pressure for standard refrigeration components have reached 28 bar and further high pressure components have entered the market for R717, allowing a maximum pressure of up to 50 bar, at the time of writing. It is thus relevant to investigate whether the increase in attainable pressures allows higher heat supply temperatures to be reached.

Further, Brunin et al. (1997) does not include the compressor discharge temperature as a constraint but, as discussed in Jensen et al. (2014) the compressor discharge temperature is a limiting factor for the development of a high temperature HACHP.

The use of COP and volumetric heat capacity as indicators for the economic viability of a heat pump investment may not always lead to a precise conclusion, as discussed in part 1 of this study (Ommen et al., 2014a). This is because components for different refrigerants may vary in cost due to e.g. different material requirements or different heat transfer coefficients and thus, the level of COP needed to attain a viable investment will differ based on the level of investment required for the specific refrigerant. Evaluating the working domain based on a complete economic evaluation of the heat pump installation, over the lifetime of the system may result in valuable information not provided by Brunin et al. (1997).

Further, the application of a complete economic analysis allows the different heat pump solutions to be compared based on an objective measure. Thus, evaluating the difference in the expected economic gain of the investment and thereby identifying the most relevant technologies.

Ommen et al. (2011) compared the economy of the HACHP to the VCHP and showed that the HACHP is a competitive technology. However, the study did not consider the degradation of heat transfer coefficients caused by the application of a zeotropic mixture working fluid. As discussed in Radermacher and Hwang (2005) the two-phase heat transfer coefficient is reduced due to mass diffusion resistance in the zone surrounding the liquid–vapour interface, which tends to be depleted of the volatile component. Consequently, the HACHP requires a larger heat transfer area compared to a pure R717 VCHP. Further, the reduced vapour pressure of the mixture increases the specific volume of the low pressure vapour and consequently entails the need for an increased compressor displacement volume. It is therefore relevant to evaluate, whether this increased investment in heat transfer area and compressor volume can be justified by the increased efficiency of the heat pump.

Due to the use of a mixed working fluid and the solution circuit configuration the design of the HACHP has two additional degrees of freedom. Both Brunin et al. (1997) and Ommen et al. (2011) use a fixed ammonia mass fraction and the concentration difference (difference between ammonia concentration in the rich mixture and the circulated lean

Please cite this article in press as: Jensen, J.K., et al., Technical and economic working domains of industrial heat pumps: Part 2 – Ammonia-water hybrid absorption-compression heat pumps, International Journal of Refrigeration (2015), http://dx.doi.org/10.1016/j.ijrefrig.2015.02.011

mixture) to satisfy these additional degrees of freedom. Jensen et al. (2014) applies the ammonia mass fraction and circulation ratio to determine the operation of the cycle and presents parameter variations of these. This shows that it is essential to determine the right combination of ammonia mass fraction and circulation ratio to attain a feasible high temperature HACHP, that complies with the constraints of commercially available components and further that the right combination is highly dependent on the operating conditions. As both Brunin et al. (1997) and Ommen et al. (2011) have restricted their HACHP analysis to a limited number of ammonia mass fractions and used a fixed value of concentration difference the HACHP is not necessarily analysed under the best possible design conditions, which may result in an unfair comparison.

Ommen et al. (2014a, b) shows that the heat sink and heat source temperature differences have a significant influence on both the economic and technical constraints of VCHPs. Ommen et al. (2014a, b) investigates four cases with different combinations of heat sink and heat source temperature differences. These are:

- $\Delta T_{sink} = 10$ K, $\Delta T_{source} = 10$ K
- $\Delta T_{sink} = 20$ K, $\Delta T_{source} = 20$ K
- $\Delta T_{sink} = 20$ K, $\Delta T_{source} = 10$ K
- $\Delta T_{sink} = 40$ K, $\Delta T_{source} = 10$ K

The same four cases will be applied in the present study of HACHP. In the following they will be referred to as sink/source configuration: 10 K/10 K, 20 K/20 K, 20 K/10 K and 40 K/10 K. The definition of ΔT_{sink} and ΔT_{source} is presented in detail in Sec. 2.1 and is presented graphically in Fig. 1b.

This study investigates the working domain of the HACHP for these four cases. For each case the operating conditions, defined by the heat supply temperature, $T_{sink,out}$, and the temperature lift, ΔT_{lift}, will be varied. The heat supply temperature from 40 to 140 °C and the temperature lift from 0 to 70 K. For each operating condition the ammonia mass fraction and circulation ratio are found by an optimisation of the net present value (NPV) under the technical constraints of the studied components. The working domains are presented graphically for all four cases, showing which operating conditions are possible to supply with a HACHP while respecting both the technical and economic constraints. Finally, the present value (PV) of the HACHP will be compared to the PV of the best available VCHP technology presented by Ommen et al. (2014a, b).

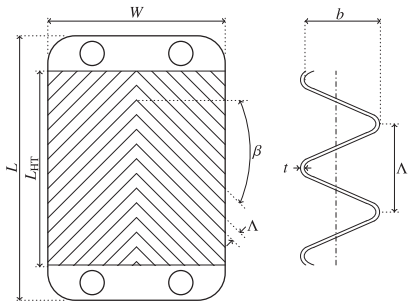

Fig. 2 – Plate dimension for chevron corrugation.

2. Methods

2.1. *The hybrid absorption-compression heat pump process*

The general layout of the HACHP is seen in Fig. 1a. In the desorber, heat is supplied from a heat source, stream 13–14, in order to desorb the ammonia from the mixture. The phase

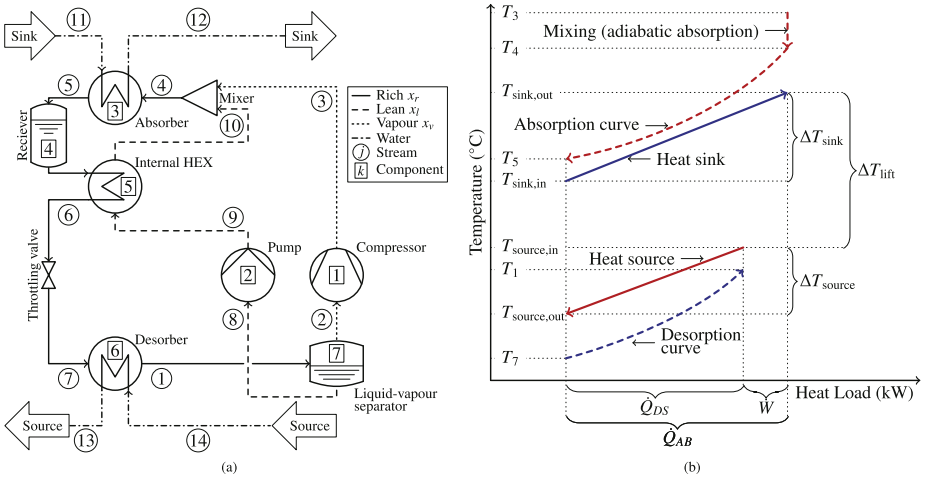

Fig. 1 – (a) Principle sketch of the HACHP, (b) HACHP process sketched in a temperature – heat load diagram.

Please cite this article in press as: Jensen, J.K., et al., Technical and economic working domains of industrial heat pumps: Part 2 – Ammonia-water hybrid absorption-compression heat pumps, International Journal of Refrigeration (2015), http://dx.doi.org/10.1016/j.ijrefrig.2015.02.011

change in the desorber is incomplete and thus stream 1 exiting the desorber is a liquid–vapour mixture. By separating the phases in a liquid–vapour separator (LVS), it can be ensured that only the vapour phase, stream 2, enters the compressor, while the liquid phase, stream 8, is supplied to the pump. The liquid stream will be lean in ammonia while the vapour stream consists mainly of ammonia. After the pump the lean mixture, stream 9, is heated in an internal Heat Exchanger (HEX) resulting in stream 10 which is mixed with stream 3, the vapour exiting the compressor. This causes an adiabatic absorption of the vapour phase into the lean liquid until equilibrium is reached, resulting in stream 4. In the absorber a diabatic absorption of the ammonia vapour into the liquid is undertaken, while releasing heat to the heat sink, stream 11–12. The exiting state, stream 5, is a saturated liquid mixture. As it is beneficial to sub-cool this stream, it is used as the heat source in the internal HEX. After this the sub-cooled liquid mixture, stream 6, is throttled to the low pressure resulting in a two-phase stream that enters the desorber, stream 7.

The process described above is sketched in a principle temperature – heat load diagram shown in Fig. 1b. Here the applied definitions of temperature lift, ΔT_{lift}, and heat sink and heat source temperature difference, ΔT_{sink} and ΔT_{source}, are illustrated. As seen ΔT_{lift} was defined as the temperature difference between the heat supply temperature, $T_{sink,out}$, and the temperature of the available heat source, $T_{source,in}$. ΔT_{sink} and ΔT_{source}, were defined as the temperature difference between the inlet and outlet of the sink and source, respectively.

From Fig. 1b it may be seen that the profiles of the equilibrium absorption and desorption processes are non-linear. This has been described in detail by Itard and Machielsen (1994). In Fig. 1b these are depicted as convex curves. Depending on ammonia mass fraction and circulation ratios these profiles could also exhibit a concave shape or have a convex and a concave part. This is further described in Zheng et al. (2013). When modelling the HACHP it is accordingly not sufficient to only ensure a positive temperature difference at the inlet and outlet of the absorber and desorber (Itard and Machielsen, 1994).

2.2. *Thermodynamic model of the hybrid absorption-compression heat pump*

The thermodynamic model of the HACHP was developed based on mass and energy balance equations and the second law of thermodynamics. Steady-state operation was assumed. Design variables were chosen on a component and system level. Component design variables were: isentropic and volumetric efficiency, η_{is} and η_{vol}, for compressor and pump, heat exchanger effectiveness, ε, for the internal HEX and the minimum temperature difference (in the following, referred to as the *pinch point* temperature difference), ΔT_{pp}, for the absorber and desorber. The applied values are stated in Table 1. On a system level the design variables were chosen as the ammonia mass fraction of the rich solution, x_r, (streams 4–7 and 1) and the circulation ratio, f, defined as the ratio between the mass flow rate of the rich and lean mixture, Eq. (1).

$$f = \frac{\dot{m}_l}{\dot{m}_r} \tag{1}$$

Table 1 – Fixed input variables applied in the thermodynamic model of the HACHP.

Input variable			Components to which they are applied	
η_{is}	0.80	–	Compressor	Pump
η_{vol}	0.80	–	Compressor	
η_{el}	0.95	–	Compressor	Pump
ΔT_{pp}	5.00	K	Absorber	Desorber
ε	0.90	–	Internal HEX	
$\dot{Q}$	1000	kW	Absorber	

Based on the high pressure, p_5 and low pressure, p_1, all other pressures in the system were determined. Pressure losses in piping and vessels were neglected. For the high pressure side:

$$p_6 = p_5 - \Delta p_{5-6} \tag{2}$$

$$p_4 = p_5 + \Delta p_{4-5} \tag{3}$$

$$p_3 = p_{10} = p_4 \tag{4}$$

$$p_9 = p_{10} - \Delta p_{9-10} \tag{5}$$

Likewise for the low pressure side:

$$p_7 = p_1 + \Delta p_{7-1} \tag{6}$$

$$p_2 = p_8 = p_1 \tag{7}$$

The values of Δp were determined from the HEX correlations described in detail in Sec. 2.3.

Based on the mass balance of the LVS it was found that the circulation ratio, f, directly relates to the vapour quality exiting the desorber, such that $q_1 = 1 - f$. Thereby the thermodynamic state of stream 1 was defined by x_r, q_1 and p_1.

Heat loss from the LVS was neglected and thermodynamic equilibrium between the two phases was assumed, hence: $T_1 = T_8 = T_2$. Stream 2 was assumed to be saturated vapour ($q_2 = 1$). The ammonia mass fraction and enthalpy of the lean liquid (stream 8) were found by energy, mass and element balances of the LVS.

The specific enthalpy of streams 3 and 9 were found using the isentropic efficiencies of the pump and the compressor. Heat loss from these components were neglected.

The heat transfer of the internal HEX was found by the Eq. (8), which was derived from an energy balance of the internal HEX and the definition of the heat exchanger effectiveness.

$$\dot{Q}_5 = \dot{m}_l(h_{10,max} - h_9)\varepsilon_5 \tag{8}$$

Here $h_{10,max}$ is the enthalpy of the lean solution evaluated at the temperature of stream 5, as the capacity rate of the rich solution is higher than the lean solution.

The enthalpy of stream 4 was calculated based on the energy and mass balances of the mixer. The throttling valve was assumed to be isenthalpic, $h_6 = h_7$.

The heat transfer rates and power consumption of the components were calculated by component energy balances, Eqs. (9)–(13).

$$(1)\ \text{Compressor}: \quad \dot{W}_1 = \dot{m}_v(h_3 - h_2) \tag{9}$$

Please cite this article in press as: Jensen, J.K., et al., Technical and economic working domains of industrial heat pumps: Part 2 – Ammonia-water hybrid absorption-compression heat pumps, International Journal of Refrigeration (2015), http://dx.doi.org/10.1016/j.ijrefrig.2015.02.011

(2) Pump : $\dot{W}_2 = \dot{m}_l(h_9 - h_8)$ (10)

(3) Absorber : $\dot{Q}_3 = \dot{m}_r(h_4 - h_5)$ (11)

(5) Internal HEX : $\dot{Q}_5 = \dot{m}_r(h_5 - h_6)$ (12)

(6) Desorber : $\dot{Q}_6 = \dot{m}_r(h_1 - h_7)$ (13)

The COP of the HACHP was defined as given in Eq. (14). The electrical efficiency of the electric motors driving the pump and compressor, η_{el}, was assumed to be the same for both the pump and compressor. The applied value of η_{el} is stated in Table 1.

$$COP = \frac{\dot{Q}_3}{\dot{W}_1 + \dot{W}_2} \cdot \eta_{el} \quad (14)$$

The displacement volume of the compressor, $\dot{V}_{dis}$, was found by Eq. (15), here $\dot{V}_{suc}$ is the suction line volume flow rate, calculated as seen in Eq. (16), and η_{vol} is the volumetric efficiency of the compressor.

$$\dot{V}_{dis} = \frac{\dot{V}_{suc}}{\eta_{vol}} \quad (15)$$

$$\dot{V}_{suc} = \dot{m}_2 \cdot v_2 \quad (16)$$

The thermodynamic model was implemented in the software Engineering Equation Solver (F-Chart, 1992). The thermodynamic properties of the ammonia-water mixture were calculated by the equations of state developed by Ibrahim and Klein (1993). Transport properties were calculated using correlations developed by El-Sayed (1988) and Conde (2004).

The model was implemented such that all equations are explicit for defined high and low pressure, p_5 and p_1. These pressures were solved iteratively to attain the desired values of the absorber and desorber ΔT_{pp}.

As enthalpy and temperature are not proportional during absorption and desorption, the absorber and desorber models were discretized equidistantly in heat load. From this the temperature difference for each step, ΔT_i, was evaluated based on the equilibrium temperature of the ammonia-water mixture. The pinch point temperature difference was then determined as seen in Eq. (17).

$$\Delta T_{pp} = \min(\Delta T_i) \quad i \in \{1; I\} \quad (17)$$

$I = 50$ steps was applied to both the absorber and desorber to determine the pinch point temperature differences.

2.3. *Dimensioning heat exchangers*

All three heat exchangers were assumed to be of a plate type with a chevron corrugation, as depicted in Fig. 2. The use of plate heat exchangers for industrial processes have increased significantly over the last decades (Abu-Khader, 2012) and is therefore assumed to be the preferred option.

The plate size correspond to either the "V120T" or the "V10T" (SWEP international AB, 2014a, 2014b), for which a complete list of the applied dimensions are given in Table 2. The small plate size (V10T) was applied when the pressure loss using the large plate (V120T) exceeds $\Delta p = 0.5$ bar. This tends to happen when there is a large difference in the mass flow rate between the exchanging fluids. This occurred in the absorber and desorber when ΔT_{sink} and ΔT_{source} were small and in the internal HEX when the circulation ratio, f, was large.

Table 2 – Plate dimensions for V120 T and V10 T, variable designation on the plate is seen in Fig. 2

	V120 T	V10 T	
L	525	289	(mm)
L_{HT}	456	243	(mm)
W	243	119	(mm)
β	30	30	(°)
Λ	8.0	8.0	(mm)
b	1.8	1.8	(mm)
t	0.5	0.5	(mm)
λ	16.0	16.0	($Wm^{-1}K^{-1}$)

As the plate size was given, the objective of the HEX dimensioning was to determine the number of plates, N, needed to attain a heat transfer area, A_{HT}, capable of transferring the required heat load, $\dot{Q}$. These parameters relate as seen in Eq. (18).

$$A_{HT} = N \cdot L_{HT} \cdot W \cdot \phi = \frac{U \cdot \Delta T_{LM}}{\dot{Q}} \quad (18)$$

Here U is the overall heat transfer coefficient of the HEX and ΔT_{LM} is the logarithmic mean temperature difference. Further, L_{HT} is the length of the heat transfer section of the plate, W is the plate width and ϕ is the plate area enhancement factor calculated as suggested by Martin (1996) (see Appendix A) to account for the complex geometry of the channels. The area for which the cost has been correlated, A_{IN}, is the full area of the purchased plates and is thus determined as seen in, Eq. (19).

$$A_{IN} = N \cdot L \cdot W \cdot \phi \quad (19)$$

The overall heat transfer coefficient was calculated as the inverse of the sum of the convective resistance of both streams and the conductive resistance through the plate, see Eq. (20).

$$U = \left(\frac{1}{\bar{\alpha}_1} + \frac{t}{\lambda} + \frac{1}{\bar{\alpha}_2}\right)^{-1} \quad (20)$$

Here, $\bar{\alpha}$ is the average heat transfer coefficient of the individual streams, t is the plate thickness and λ is the thermal conductivity of the plate. Detailed heat transfer coefficient correlations were applied to both the absorber, desorber and internal HEX to determine $\bar{\alpha}$. The applied correlations are listed in Table 3 and the equations are stated in Appendix A.

The HEX pressure losses, Δp, were calculated as seen in Eq. (21).

$$\Delta p = \frac{2 \cdot \bar{\xi} \cdot G^2 \cdot v \cdot L_{HT}}{D_h} \quad (21)$$

Here G is the mass flux and D_h is the hydraulic channel diameter, set to $D_h = 2b\phi$ as suggested by Martin (1996). Further, $\bar{\xi}$ is the average friction factor, which was determined

Please cite this article in press as: Jensen, J.K., et al., Technical and economic working domains of industrial heat pumps: Part 2 – Ammonia-water hybrid absorption-compression heat pumps, International Journal of Refrigeration (2015), http://dx.doi.org/10.1016/j.ijrefrig.2015.02.011

Table 3 – Applied heat transfer and pressure drop correlations for the absorber, desorber and internal heat exchanger.

Absorber				
Water	α:	Martin (1996)	ξ:	Martin (1996)
NH_3–H_2O	α_{vo}:	Martin (1996)		
	α_{lf}:	Yan et al. (1999)		
	α_{tp}:	Silver (1947), Bell and Ghaly (1972)	ξ_{tp}:	Yan et al. (1999)
Internal HEX				
NH_3–H_2O	α:	Martin (1996)	ξ:	Martin (1996)
Desorber				
Water	α:	Martin (1996)	ξ:	Martin (1996)
NH_3–H_2O	α_{lo}:	Martin (1996)	ξ_{lo}:	Martin (1996)
	α_{tp}:	Táboas et al. (2012)	ξ_{tp}:	Táboas et al. (2012)

based on the correlations listed in Table 3 the equations are equally presented in Appendix A.

For the sink and source streams of the absorber and desorber and both streams in the internal HEX $\overline{\alpha}$ and $\overline{\xi}$ were evaluated at the mean temperature and pressure. This is a reasonable approach as the transport properties of the liquids only show a weak dependence on the pressure and temperature.

For the ammonia-water streams of the absorber and desorber this approach was not applicable as the ammonia mass fraction of the liquid and vapour phase changes through the HEX, which can lead to significant variations in the transport properties of the two phases. Further, α and ξ are strongly dependent on the vapour quality, q which also varies greatly during absorption and desorption. To account for these variations $\overline{\alpha}$ and $\overline{\xi}$ were determined based on a one-dimensional discretization in heat load and averaged as seen in Eqs. (22) and (23).

$$\overline{\alpha}_{tp} = \left(\sum_{i=1}^{I} \alpha_{tp,i}\right) \cdot I^{-1} \tag{22}$$

$$\overline{\xi}_{tp} = \left(\sum_{i=1}^{I} \xi_{tp,i}\right) \cdot I^{-1} \tag{23}$$

Here $\alpha_{tp,i}$ and $\xi_{tp,i}$ are the two-phase heat transfer coefficient and friction factor for the i^{th} cell, calculated based on the cell averages of: vapour quality, temperature, pressure and liquid and vapour ammonia mass fraction.

Further, for the absorber and desorber the logarithmic mean temperature difference could not be directly applied as enthalpy and temperature are not proportional during absorption and desorption (Itard and Machielsen, 1994; Zheng et al., 2013). To account for this an average logarithmic mean temperature difference was defined as seen in Eq (24).

$$\Delta\overline{T}_{LM} = \dot{Q}\left(\sum_{i=1}^{I} \frac{\dot{Q}}{I} \cdot \frac{1}{\Delta T_{LM,i}}\right)^{-1} \tag{24}$$

Here $\Delta T_{LM,i}$ is the logarithmic mean temperature difference of the i^{th} cell calculated by the same discretization as applied in the heat transfer correlation ($I = 50$).

2.4. Refrigerant charge estimation and dimensioning of high pressure receiver

Based on the calculated size of the three heat exchangers the working fluid charge, m, was estimated by evaluating the volume occupied by the working fluid and the mean specific volume, $\overline{v}$, of the HEX, see Eq. (25)

$$m_k = M_k \cdot W_k \cdot b_k \cdot \frac{1}{\overline{v}_k} \tag{25}$$

Here M is the number op channels occupied by the working fluid. The total m_{tot} was defined as the sum of the working fluid charge in the absorber, desorber and internal HEX.

The high pressure receiver was dimensioned such that it can contain the entire charge at the high pressure (state of stream 5). The receiver was over-sized by 25% as suggested by Stoecker (1998). The receiver volume, V_4, was calculated as stated in Eq. (26).

$$V_4 = (m_3 + m_5 + m_6) \cdot v_5 \cdot 1.25 \tag{26}$$

The application of an oversized high pressure receiver ensures a saturated state at the outlet from the absorber (stream 5, Fig. 1a) (Corberan, 2011).

2.5. Compressors and technological constraints

The maximum heat supply temperature achievable by a heat pump is restricted by the maximum pressure of the applied compressor technology. Further, the maximum achievable temperature lift is restricted by the compressor discharge temperature and in some cases differential pressure. This is to ensure the thermal stability of the lubricating oil and to reduce wear by thermal stress. As discussed in Ommen et al. (2014a, b), the compressor discharge temperature is of special concern for ammonia heat pumps.

In the present study two compressor technologies were investigated: low pressure ammonia (Ommen et al. (2014a, b): Type 3) and high pressure ammonia (Ommen et al. (2014a, b): Type 4). The low pressure ammonia compressor (LP R717) has a maximum pressure of 28 bar. The discharge temperature is limited to 180 °C. The high pressure ammonia compressor (HP R717) has a maximum pressure of 50 bar and can equally tolerate discharge temperatures up to 180 °C.

Generally the water content in the compressed vapour stream is negligible but as shown by Jensen et al. (2014): for low ammonia mass fractions the water content can be substantial for some operating conditions. These solutions should be avoided and therefore solutions with $x_v < 0.95$ were deemed infeasible.

2.6. Economic evaluation

The basis of the economic analysis was the replacement of an existing gas burner with a HACHP of the same heat load. Thus, it was necessary to evaluate the total capital investment (TCI) of the HACHP. To determine TCI_{HP}, first the purchased equipment cost (PEC) of all major components was found. PEC

Please cite this article in press as: Jensen, J.K., et al., Technical and economic working domains of industrial heat pumps: Part 2 – Ammonia-water hybrid absorption-compression heat pumps, International Journal of Refrigeration (2015), http://dx.doi.org/10.1016/j.ijrefrig.2015.02.011

functions were developed for all major components based on Danish intermediate trade business prices (TRB) and individual manufacturers suggested retail prices (MRP). The cost functions were constructed as proposed by Bejan et al. (1996), see Eq. (27).

$$PEC_Y = PEC_W \left(\frac{X_Y}{X_W}\right)^{\gamma} \quad (27)$$

Here PEC_Y is the PEC of the component at capacity X_Y, while PEC_W is the PEC at a chosen base capacity, X_W. The correlated capacities for the different components were as follows:

- PEC for a compressor was a function of the compressor displacement volume and the pressure limit.
- PEC for an electrical motor with a fixed efficiency was dependent only on the shaft power.
- PEC for a heat exchanger was a function of the HEX area and the pressure limit.
- PEC for a pump was a function of the shaft power.
- PEC for an LVS was a function of the compressor suction line volume flow rate. The size was chosen to attain a vapour velocity of 0.4 m s^{-1} in the separator. This corresponds to an entrained liquid droplet size with a maximum diameter of 0.25 mm (Stoecker, 1998).
- PEC for a high pressure receiver was a function of the volume and pressure limit.

The values of PEC_W, X_W and γ attained are stated in Table 5 together with the source from which the cost information was supplied. Cost information for some components were supplied under a non-disclosure agreement (NDA) and thus the coefficients of the developed cost functions are not published.

Once the PEC costs of all components were determined the total capital investment (TCI) of the HACHP installation was found. As suggested by Bejan et al. (1996), it was assumed that the TCI was a factor of 4.16 higher than the PEC of the component, Eq. (28).

$$TCI_{HP} = \sum_{k=1}^{K} PEC_k \cdot 4.16 \quad (28)$$

The factor of 4.16 was applied to account for additional costs related to new investment at an existing facility. It was thus applied to account for additional direct costs such as: piping, instrumentation and control, electrical equipment, civil and structural work and service facilities as well as indirect costs such as: engineering and supervision costs and construction and contractor profit costs (Bejan et al., 1996).

Annual costs for the fuel consumption of both the existing gas burner and the proposed HACHP was determined as seen in Eqs. (29) and (30) (Bejan et al., 1996), respectively.

$$FC_{NG} = \frac{\dot{Q}}{\eta_{NG}} \cdot c_{NG} \cdot H \quad (29)$$

$$FC_{HP} = \frac{\dot{Q}}{COP} \cdot c_w \cdot H \quad (30)$$

Here c_{NG} and c_w are the natural gas and electricity prices, H is the operating time per year and η_{NG} is the assumed gas burner efficiency. The applied values of H and η_{NG} are stated in Table 4, while c_{NG} and c_w corresponding to an industrial consumer in the Danish fiscal environment for year the 2012, prices from Danish Energy Agency (2013) were applied.

Table 4 – Fixed parameters applied in the economic analysis.

Interest rate	i	7%
Inflation rate	i_L	2%
Technical lifetime	LT	15 years
Operating time	H	3500 h pr. year
Gas burner efficiency	η_{NG}	0.9 -
Gas burner investment cost	TCI_{NG}	0 €
Gas burner maintenance cost	OMC_{NG}	0 €

To account for the time value of money the capital recovery factor (CRF), see Eq. (31) (Bejan et al., 1996), was applied to discount future expenditure to a PV.

$$CRF = \frac{i^{eff}(1+i^{eff})^{LT}}{(1+i^{eff})^{LT}-1} \quad (31)$$

As seen in Eq. (31), CRF depends on the effective interest rate over the life time of the system, i^{eff}, and the technical life time LT. The effective interest rate was calculated from the interest rate, i, and inflation rate, i_L, as seen in Eq. (32) (Bejan et al., 1996). The assumed value of LT,i and i_L are stated in Table 4.

$$i^{eff} = \frac{1+i}{1+i_L} - 1 \quad (32)$$

The PV of the two alternatives: keeping the natural gas burner or replacing it with a HACHP was found using Eq. (33).

$$PV_i = TCI_i + \frac{FC_i}{CRF} + OMC_i \quad (33)$$

Table 5 – Used cost correlations coefficients for the component types divided by application limits.

Equipment	PEC_W	X_W	γ	Source
Compressor:	(€)	($m^3\ h^{-1}$)		
LP R717	11,914	178.4	0.66	TBP[a,b]
HP R717	NDA	NDA	NDA	MRP[d]
Electrical motor:	(€)	(kW)		
LP/HP R717	10,710	250.0	0.65	TBP[a]
Receiver:	(€)	(m^3)		
LP R717	1444	0.089	0.63	TBP[a]
HP R717	1934	0.089	0.66	TBP[a]
Plate HEX:	(€)	(m^2)		
LP R717	15,526	42.0	0.80	TBP[a,b,c]
HP R717	NDA	NDA	NDA	MRP[e]
Pump:	(€)	(kW)		
LP/HP R717	NDA	NDA	NDA	MRP[f]
LVS:	(€)	($m^3\ h^{-1}$)		
LP/HP R717	12,702	525	0.39	TBP[a]

[a] H. Jessen Jürgensen A/S (2013).
[b] FK Teknik A/S (2013).
[c] Ahlsell Danmark ApS (2013).
[d] Johnson Controls (2013).
[e] SWEP International AB (2014b).
[f] Grundfos DK A/S (2014).

Please cite this article in press as: Jensen, J.K., et al., Technical and economic working domains of industrial heat pumps: Part 2 – Ammonia-water hybrid absorption-compression heat pumps, International Journal of Refrigeration (2015), http://dx.doi.org/10.1016/j.ijrefrig.2015.02.011

For the natural gas burner the capital investment was assumed as sunk costs ($TCI_{NG} = 0$ €) and further the operation and maintenance cost (OMC) were neglected ($OMC_{NG} = 0$ €). Thus, PV_{NG} is equivalent to the discounted FC over the technical life time of the project. For the HACHP the OMC were assumed to attain a PV equivalent to 20% of the TCI as suggested by Bejan et al. (1996).

The criteria for the economic viability of the HACHP installation was a positive NPV when replacing a natural gas boiler as the source of heat supply. The NPV was defined as the difference in PV of the two alternatives as seen in Eq. (34).

$$NPV = PV_{NG} - PV_{HP} \tag{34}$$

Thus, if the NPV is positive the HACHP investment will be profitable while if the NPV is negative keeping the natural gas burner would be the more profitable solution.

Further, a simple pay back period (PBP) was determined as stated in Eq. (35). The PBP is calculated as the ratio of the TCI_{HP} and the yearly savings in running costs.

$$PBP = \frac{TCI_{HP}}{(FC_{NG} - FC_{HP}) + (OMC_{NG} - OMC_{HP}) \cdot CRF} \tag{35}$$

PBP is not a precise measure of the economic viability of an investment as it does not account for the time value of money and thus should be used with caution (Bejan et al., 1996). However, PBP is often used as a selection criterion in industry typically with a maximum allowable value (Bejan et al., 1996). The maximum PBP is not easily defined as this depends highly on the industry and the type of investment. For the present study PBPs of 4 and 8 years will be reported, however the overall criteria for the economic viability will be NPV > 0 €, regardless of the actually allowed PBP. NPV = 0 € indicates that the PBP equals the technical lifetime of the system, which was assumed to be 15 years.

3. Results

Detailed results from one run of the thermodynamic, heat transfer and economic model are provided in Appendix B. The results are provided for $x_r = 0.65$ and $f = 0.65$, an operating condition of $T_{sink,out} = 80$ °C and $\Delta T_{lift} = 30$ K and a sink/source configuration of 20 K/20 K.

3.1. The influence of x_r and f on the HACHP working domain

Fig. 3 shows the HACHP working domain for two fixed combinations of x_r and f. Fig. 3a has a high ammonia mass fraction of $x_r = 0.9$ while 3b has a low ammonia mass fraction of $x_r = 0.5$. The circulation ratio, f, was chosen to give high values of COP and thus as suggested by Jensen et al. (2014) the circulation ratio is reduced with an increase in ammonia mass fraction. Fig. 3a has a circulation ratio of $f = 0.35$ while 3b has a circulation ratio of $f = 0.85$.

The working domains in Fig. 3 are presented with the heat supply temperature, $T_{sink,out}$, as the abscissa and the temperature lift, ΔT_{lift}, as the ordinate. Further, a fixed sink/source configuration of 10 K/10 K is applied and thus ΔT_{sink} and ΔT_{source} are both fixed at a value of 10 K. Thus, for a given $T_{sink,out}$: $T_{sink,in}$ is determined from ΔT_{sink}. Likewise, from a given ΔT_{lift} and $T_{sink,out}$: $T_{source,in}$ is determined and finally $T_{source,out}$ is found from ΔT_{source}.

The hatched areas in Fig. 3 define operating conditions for which heat pump implementation is not applicable. The upper left corner indicates operating points that are infeasible as these require $T_{source,out} < 0$ °C, which implies a phase change for the chosen heat transfer fluid (water). This could be feasible if a brine was applied. However, it should be noted that this also implies cooling the heat source well below ambient temperature, which might not be reasonable unless a cooling demand is met.

The bottom rectangle indicates operating points at which $T_{sink,in} < T_{source,in}$. These operating points are neglected as for these conditions, direct heat transfer between the sink and source is possible for some range of the heat transfer process. Therefore, this should be applied first, as suggested by the principles of pinch analysis (Kemp, 2011; Townsend and Linnhoff, 1983).

The resulting working domains are indicated in Fig. 3 by the grey areas. These areas represent values of $T_{sink,out}$ and ΔT_{lift} where the HACHP simultaneously complies with all technical and economic constraints.

Further, all constraints are presented in Fig. 3. The dark blue line (in web version) indicates the $T_{sink,out}$ and ΔT_{lift} at which the high pressure is equal to the maximum allowable pressure, $p_{H,max}$, for Fig. 3a and b 28 bar, corresponding to LP R717 components. Solutions to the left of the blue line (in web version) thus have high pressures within the limit of the applied technology, while solutions to the right of the blue line (in web version) have pressures above the allowable limit and are thus infeasible. As seen, the high pressure constraint only shows a weak dependence on ΔT_{lift}. Further, it is seen that the $T_{sink,out}$ at which $p_{H,max}$ is reached differs significantly for the two values of x_r presented. As seen in Fig. 3a with $x_r = 0.9$: heat supply temperature of only 70 °C can be reached while, as seen in Fig. 3b with $x_r = 0.5$: a heat supply temperature up to 115 °C can be attained.

The red line (in web version) indicates the $T_{sink,out}$ and ΔT_{lift} at which the compressor discharge temperature is equal to the maximum allowable temperature, $T_{H,max}$. As seen $T_{H,max}$ depends mainly of ΔT_{lift}. Hence, solutions with $T_{sink,out}$ and ΔT_{lift} below the red line (in web version) have compressor discharge temperatures below $T_{H,max}$ while solutions with $T_{sink,out}$ and ΔT_{lift} above the red line (in web version) exceed the limitations of $T_{H,max}$ and are thus infeasible. As seen the higher the $T_{sink,out}$ the lower the ΔT_{lift} is possible. When comparing the compressor discharge temperature constraint in Fig. 3a and b it is clear that the choice of ammonia mass fraction has an impact on attainable temperature lifts. As seen a reduction of the ammonia mass fraction entails a reduction of the attainable temperature lift.

The green line (in web version) indicates the $T_{sink,out}$ and ΔT_{lift} at which the NPV of the investment is zero and thus where the installation of a HACHP is equivalent to keeping the existing natural gas burner. Solutions with $T_{sink,out}$ and ΔT_{lift} below the green line (in web version) have positive NPV and are thus economically feasible while solutions above the green line (in web version) have a negative NPV and are thus not economically viable.

Please cite this article in press as: Jensen, J.K., et al., Technical and economic working domains of industrial heat pumps: Part 2 – Ammonia-water hybrid absorption-compression heat pumps, International Journal of Refrigeration (2015), http://dx.doi.org/10.1016/j.ijrefrig.2015.02.011

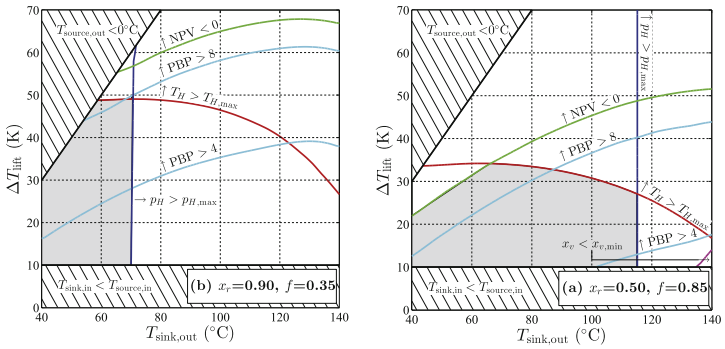

Fig. 3 – Working domain for a HACHP with fixed ammonia mass fraction and circulation ratio. (a) $x_r = 0.90$ and $f = 0.35$, (b) $x_r = 0.50$ and $f = 0.85$. Both for a sink/source configuration of 10 K/10 K. The technical and economic constraints correspond to the LP R717 components.

As seen, NPV is dependent on both $T_{sink,out}$ and ΔT_{lift}, because an increase in ΔT_{lift} decreases the COP and consequently increases the annual fuel costs. Further, increasing ΔT_{lift} for a given $T_{sink,out}$ reduces the temperature level of the heat source, which results in a reduction of the low pressure and consequently an increased suction line volume flow and the need for a larger compressor investment. Likewise, increasing $T_{sink,out}$ for a given ΔT_{lift} increases the temperature of the heat source subsequently resulting in a reduced compressor investment.

When comparing the NPV constraint in Fig. 3a and b it is clear that the choice of ammonia mass fraction also influences NPV. As seen a reduction of the ammonia mass fraction reduces the number of economically viable solutions. This is due to the an increase in TCI_{HP} caused by the sum of three phenomena:

- The reduction of vapour pressure results in an increased suction line volume flow rate, and thus a large compressor investment.
- The reduction of the two-phase heat transfer coefficient, results in a larger absorber and desorber investment.
- The increase in circulation ratio increases the heat transfer in the internal HEX and thus the internal HEX investment

The light blue lines (in web version) indicate the $T_{sink,out}$ and ΔT_{lift} at which the PBP is 4 and 8 years, respectively. As seen the PBP follows the same trend as the NPV.

Finally, the magenta line, seen only in the bottom right corner of Fig. 3b, indicates the $T_{sink,out}$ and ΔT_{lift} at which the ammonia mass fraction of the vapour stream supplied to the compressor is equal to the minimum allowable value. Solutions below this line are thus infeasible as these have too low a vapour ammonia mass fraction.

When comparing the two working domains presented in Fig. 3a and b it is clear that the choices of ammonia mass fraction and circulation ratio influence the amount of feasible HACHP solutions. As seen, when the ammonia mass fraction is high temperature lifts up to 49 K can be attained, while the HACHP under these conditions is only capable of reaching a heat supply temperature of 70 °C. Conversely, the low ammonia mass fraction solution is capable of reaching heat supply temperatures up to 115 °C but can only attain temperature lifts up to 35 K.

Consequently, defining the HACHP working domain based on fixed values of ammonia mass fraction and circulation ratio may not fairly represent the strengths and limitations of the HACHP technology as a whole.

3.2. *Optimization of x_r and f to determine complete HACHP working domain*

In order to assess the complete working domain of the HACHP technology, a selection criterion was defined to choose the economically optimal design at each operating condition (defined by $T_{sink,out}$ and ΔT_{lift}). Values of x_r and f have been set individually for each computed operating condition for all four cases, to maximize the NPV of the installation. The technical constraints of the high pressure, p_H, compressor discharge temperature, T_H, and vapour ammonia mass fraction, x_v, have been imposed on the optimization of NPV.

Fig. 4a and b shows the optimum value of x_r and f, respectively, for a sink/source configuration of 10 K/10 K and with the application of the HP R717 components. The corresponding COP is presented in Fig. 4c, and TCI in Fig. 4d. As seen the optimum value of x_r is 0.9 up to a heat supply temperature of approximately, $T_{sink,out} = 100$ °C. At this point the high pressure with $x_r = 0.9$ attains a value 50 bar, corresponding to the limits of the HP R717 compressor. When increasing the supply temperature beyond this point the ammonia mass fraction must consequently be reduced to comply with the high pressure constraint. All optimal solutions beyond this point have the maximum allowable pressure and thus the maximum allowable ammonia mass fraction. This is in alignment with what was shown in Fig. 3 and is also in alignment with the conclusions of studies such as Berntsson and Hultén (1999, 2002).

Please cite this article in press as: Jensen, J.K., et al., Technical and economic working domains of industrial heat pumps: Part 2 – Ammonia-water hybrid absorption-compression heat pumps, International Journal of Refrigeration (2015), http://dx.doi.org/10.1016/j.ijrefrig.2015.02.011

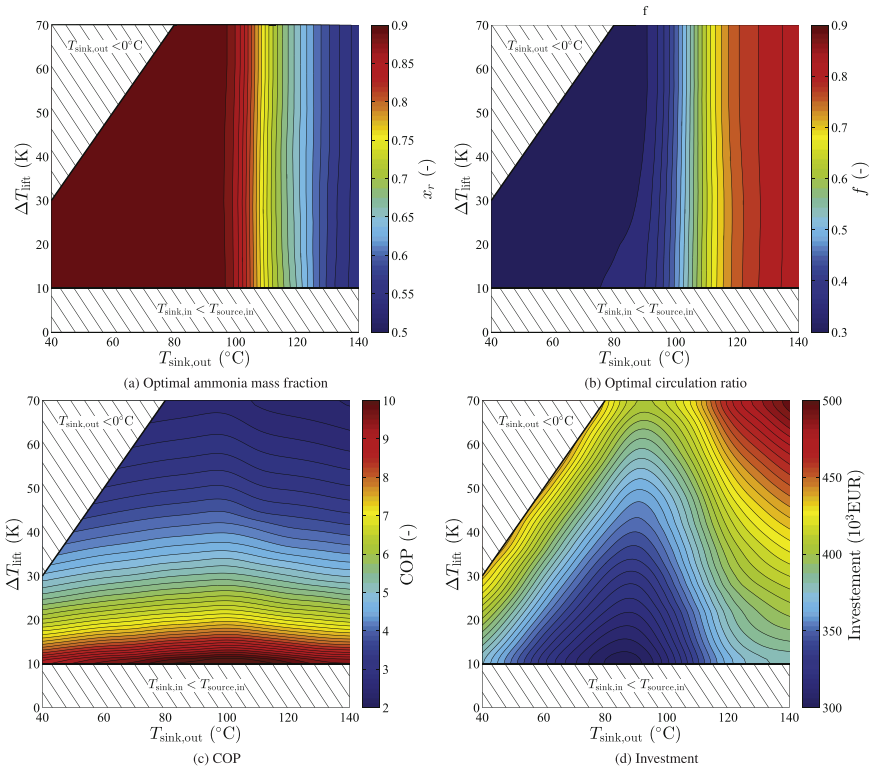

Fig. 4 – Optimal choice of x_r and f and the corresponding COP and TCI for a sink/source configuration of 10 K/10 K.

From Fig. 4b it is be seen that optimal choice of f remains close to constant as long as $x_r = 0.9$, while it starts to increase when the ammonia mass fraction is reduced.

As seen from Fig. 4c the COP increases slightly up to the point at which the ammonia mass fraction is reduced. Moving beyond this point COP decreases slightly. However, it is seen that the COP is more sensitive to the value of ΔT_{lift} than to $T_{sink,out}$.

Fig. 4d shows that the TCI decreases up to the point at which the ammonia mass fraction is reduced. The reduction of TCI combined with the increased COP results in an improved NPV up to the point at which $p_{H,max}$ is reached. Moving beyond this point, TCI increases while COP decreases, thus reducing NPV. However, it may be seen that the increase of the investment flattens out for $T_{sink,out} > 120$ °C. This occurs as the higher temperatures increase the specific volume in the suction line thus countering the increase due to the reduction of x_r. Further, going below an x_r of approximately 0.5 will cause the two-phase heat transfer coefficient to increase again as pure water is approached.

3.3. *HACHP working domain*

Figs. 5 and 6 show the derived working domains of the HACHP under the four investigated sink/source configuration cases and under the application of both the LP R717 and HP R717 components.

Fig. 5 shows the working domain for the sink/source configurations of 10 K/10 K (5b) and 20 K/20 K (5c & 5d). Fig. 5a and c correspond to the use of the LP R717 components while the HP R717 components have been applied in Fig. 5b and d.

Fig. 6 shows the working domain for the sink/source configuration of 20 K/10 K (6a & 6b) and 40 K/10 K (6c & 6d). Equally, Fig. 6a and c are for LP R717 components, while Fig. 6b and d are with the HP R717 components.

As in Fig. 3 the grey areas in Figs. 5 and 6 indicate the operating conditions that comply with all technical and economic constraints. Further, all constraints are presented as in Fig. 3. However, it should be noted that the dashed blue line (in web version) presented in Figs. 5 and 6 indicate the point at which the optimal solution attains the maximum allowable pressure. Thus, all solutions to the left of the dashed blue line

Please cite this article in press as: Jensen, J.K., et al., Technical and economic working domains of industrial heat pumps: Part 2 – Ammonia-water hybrid absorption-compression heat pumps, International Journal of Refrigeration (2015), http://dx.doi.org/10.1016/j.ijrefrig.2015.02.011

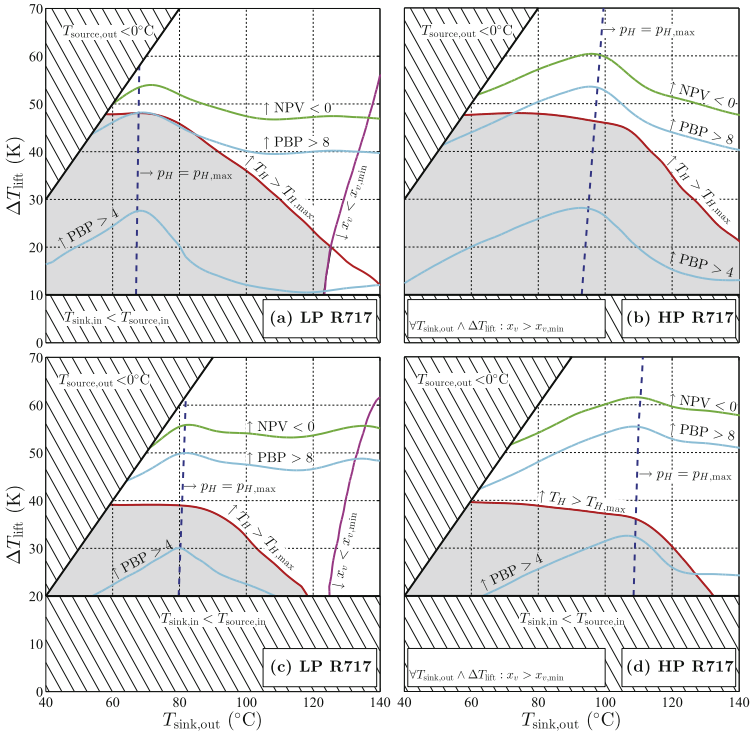

Fig. 5 – Feasible working domains indicated by grey background for HACHP using LP R717 and HP R717 compressors at $\Delta T_{sink} = 10$ K, $\Delta T_{source} = 10$ K (a) and (b) and $\Delta T_{sink} = 20$ K, $\Delta T_{source} = 20$ K (c) and (d). Hatched areas define technically infeasible domains. Curves indicate technical operating limits of components and economic limits.

(in web version) have pressures below $p_{H,max}$ while all solutions to the right of the dashed blue line (in web version) have $p_H = p_{H,max}$. The solutions to the right of dashed blue line (in web version) are thus feasible solutions but they operate on the pressure boundary to attain the best economy.

As may be seen from Fig. 5a, the HACHP using the LP R717 components at a sink/source configuration of 10 K/10 K can deliver a maximum heat supply temperature of $T_{sink,out} = 125$ °C and a maximum temperature lift of $\Delta T_{lift} = 48$ K. It can be seen that the maximum heat supply temperature is limited by the vapour ammonia mass fraction, x_v, while the maximum temperature lift is limited by the compressor discharge temperature. Further, it may be seen that all technically feasible solutions attain a positive NPV and almost all attain a simple PBP lower than 8 years. To attain a PBP below 4 years a maximum temperature lift of 28 K can be attained at a heat supply temperature of 65 °C.

Applying the HP R717 compressors to the 10 K/10 K sink/source configuration, the maximum heat supply temperature is increased to above $T_{sink,out} = 140$ °C, see Fig. 5b. Further, it can be seen that the maximum lift of 48 K can be retained at higher heat supply temperatures when applying the high pressure compressor. It can be seen that the maximum heat supply temperature and maximum temperature lift are both bound by the compressor discharge temperature. Again all technically feasible solutions attain a positive NPV.

For the sink/source configuration of 20 K/20 K, Fig. 5c and d, the maximum temperature lift is 42 K while the maximum heat supply temperature is 119 °C for LP R717 and 130 °C for HP R717. For 20 K/10 K, Fig. 6a and b, this is reduced to a maximum temperature lift of 54 K and a maximum heat supply temperature of 125 °C for LP R717 and 135 °C for HP R717. For sink/source configuration 40 K/10 K, Fig. 6c and d, the maximum temperature lift is 60 K while the maximum heat supply temperature is 100 °C and 125 °C for LP and HP R717 respectively.

It can be seen that mainly the working domain for the LP R717 compressor at a sink/source configuration of 10 K/10 K is bound by the x_v constraint. For 20 K/10 K a minor area is also limited by x_v. All other working domains are limited entirely by the compressor discharge temperature. Further, all technically feasible solutions have a positive NPV and almost all

Please cite this article in press as: Jensen, J.K., et al., Technical and economic working domains of industrial heat pumps: Part 2 – Ammonia-water hybrid absorption-compression heat pumps, International Journal of Refrigeration (2015), http://dx.doi.org/10.1016/j.ijrefrig.2015.02.011

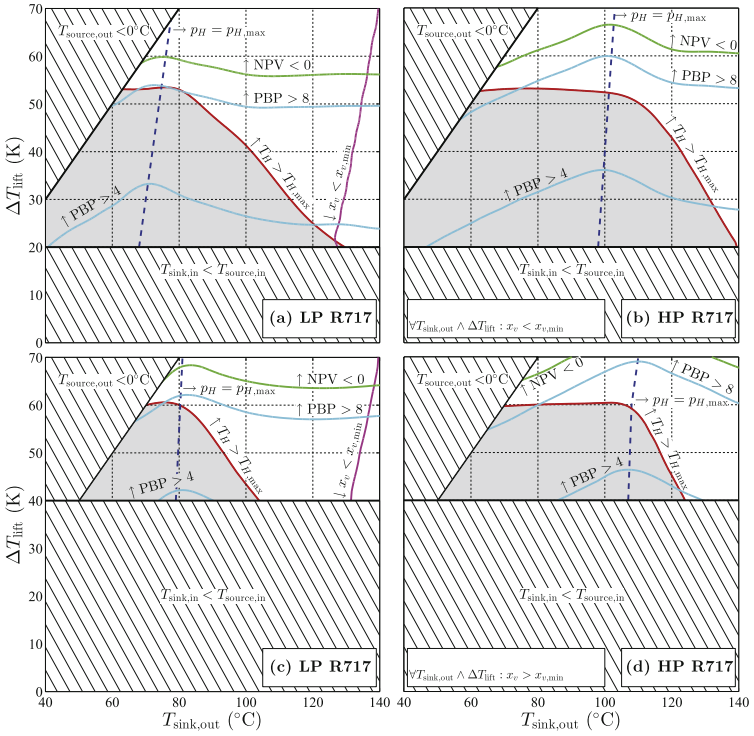

Fig. 6 – Working domains for HACHP using LP R717 and HP R717 compressors at $\Delta T_{\text{sink}} = 20$ K, $\Delta T_{\text{source}} = 10$ K (a) and (b) and $\Delta T_{\text{sink}} = 40$ K, $\Delta T_{\text{source}} = 10$ K (c) and (d).

have a PBP below 8 years. In general, when increasing the sink glide the maximum heat supply temperature is reduced while the maximum lift is increased.

3.4. *Best available HACHP and comparison with the VCHP*

From Figs. 5 and 6 it can be seen that the working domains of the LP and HP R717 components overlap in the low temperature range. It is therefore relevant to evaluate when it is more profitable to chose a high pressure solution over the low pressure solution. Fig. 7 shows which component technology yields the highest possible NPV for all four evaluated sink/source configurations. As seen, this results in two regions: a low temperature region (blue) in which the LP R717 components should be used and a high temperature region (yellow) in which the HP R717 components should be used. The supply temperature at which the high pressure option becomes favourable is approximately $T_{\text{sink,out}} = 75$ °C for 10 K/10 K, $T_{\text{sink,out}} = 85$ °C for 20 K/20 K, $T_{\text{sink,out}} = 78$ °C for 20 K/10 K and $T_{\text{sink,out}} = 90$ °C for 40 K/10 K. If this is compared to the dashed blue lines in Figs. 5 and 6 it may be seen that the switch from LP to HP R717 happens approximately 5–8 °C above the point where the LP R717 reaches $p_{H,\max}$. This is due the retention of the high ammonia mass fraction for the HP R717 meaning that the compressor volume will be smaller and the heat transfer coefficient will be higher. Hence, the HP R717 investment becomes smaller than the LP R717 investment although the investment in the HP R717 components are higher per unit of displacement volume and heat transfer area (Fig. 8).

Further, Fig. 7 shows the working domain of the best available VCHP, as concluded from Ommen et al. (2014a, b). As seen, the HACHP competes mainly with low and high pressure R717 and R600a but also with R744 for 40 K/10 K. Comparing the working domain of the HACHP to the working domain of the best possible VCHP solution it is clear that the HACHP expands the range of operating conditions for which heat pump application is technically feasible and economically viable. The HACHP allows both higher temperature lifts and higher heat supply temperatures, especially when ΔT_{sink} is large.

Fig. 7 also shows the difference in cost between the HACHP and the VCHP. This is represented by the relative difference in present value: $r_{\text{PV}} = ((\text{PV}_{\text{VCHP}} - \text{PV}_{\text{HACHP}})/\text{PV}_{\text{VCHP}}) \cdot 100\%$. As

Please cite this article in press as: Jensen, J.K., et al., Technical and economic working domains of industrial heat pumps: Part 2 – Ammonia-water hybrid absorption-compression heat pumps, International Journal of Refrigeration (2015), http://dx.doi.org/10.1016/j.ijrefrig.2015.02.011

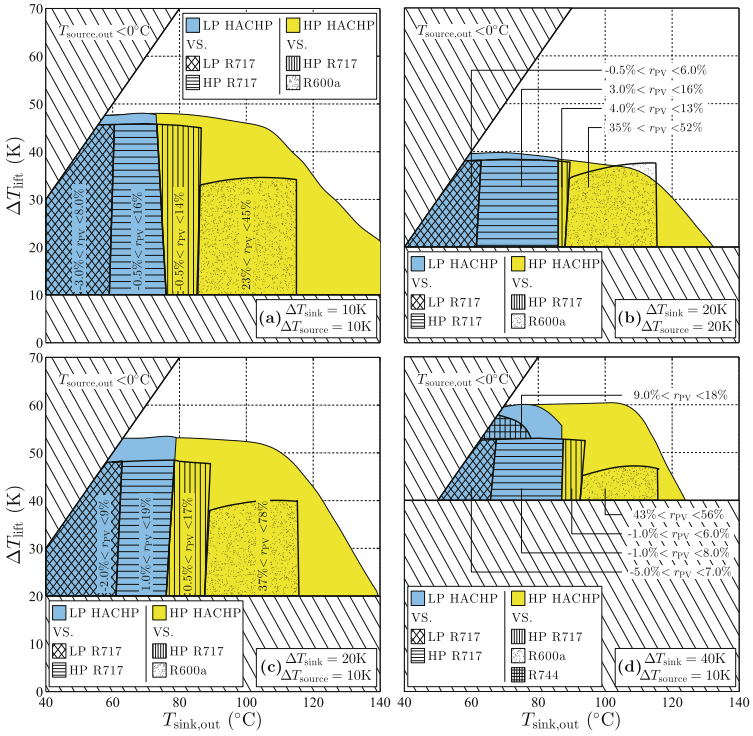

Fig. 7 – Most profitable HACHP and comparison with the best available VCHP. The blue area indicates the region in which the NPV of the LP R717 is higher than the NPV of the HP R717 solution. The hatched areas indicate which VCHP is the best competing technology. (For interpretation of the references to colour in this figure legend, the reader is referred to the web version of this article.)

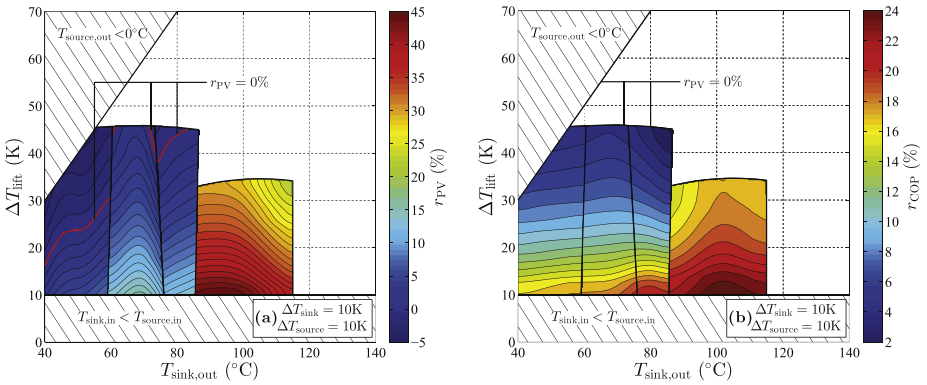

Fig. 8 – Contours of relative difference in PV, r_{PV}, (a) and the relative difference in COP, r_{COP}, between the best available HACHP and VCHP. Both for a sink/source configuration of 10 K/10 K.

Please cite this article in press as: Jensen, J.K., et al., Technical and economic working domains of industrial heat pumps: Part 2 – Ammonia-water hybrid absorption-compression heat pumps, International Journal of Refrigeration (2015), http://dx.doi.org/10.1016/j.ijrefrig.2015.02.011

seen, r_{PV} is between −5.0% and +9% for the range in which low pressure HACHP competes with low pressure R717. For low pressure HACHP against high pressure R717, r_{PV} is between −1.0% and +19% while high pressure HACHP versus high pressure R717 results in r_{PV} is between −1.0% and +17%.

For the range where the HACHP competes with R600a the r_{PV} is between 23% and 78%. This is due to the large investment and poor COP associated with R600a. Hence, for heat supply temperatures above $T_{sink,out} = 90$ °C where R717 can no longer be applied, the HACHP seem to be the more profitable solution.

Also for the range where LP HACHP competes with the transcritical R744 heat pump, the HACHP seem to be the preferred option with r_{PV} between 9 and 18%.

Fig. ?? shows the trend of r_{PV} for the sink/source configuration of 10 K/10 K. As seen, the economic advantage of the HACHP is larger at low temperature lifts. Further, it may be seen that the advantage increases with increasing heat supply temperature. Fig. ?? shows the relative difference in COP between the HACHP and VCHP: $r_{COP} = ((COP_{HACHP} - COP_{VCHP})/COP_{VCHP})\cdot 100\%$. As seen, the HACHP offers significantly increased COP at low lifts. However, when the temperature lift is increased the COP of the HACHP and the VCHP approach one another. This as the advantage of the HACHP is the reduction of irreversibilities related to the heat exchange processes. However, as the temperature lift is increased the irreversibilities related to the compression is more dominant and thus the efficiency of the two systems become similar. This results in the trend of r_{PV} seen in Fig. ?? As seen, for low temperature range (LP R717 versus LP HACHP), where compressor investment is high, this results in an area where the HACHP is not economically favourable compared to the VCHP. This is indicated by the red line in Fig. 8a

As seen from Fig. 7 the HACHP offers the best economic improvement for the sink/source configuration of 20 K/10 K. One could expect the improvement to be even higher for 40 K/10 K due to the large sink temperature difference, but this is not the case as a high sink temperature difference also entails a high temperature lift and thus the HACHP and VCHP are only compared at lifts where the COP is similar.

4. Discussion

Comparing R717 VCHP to the HACHP, the r_{PV} for most operating points is between 5 and 10%. However, the PEC cost of commercial components may vary with up to 40% from the indicated price. This might be an advantage for large manufactures where large quantities are purchased and PEC thereby can be reduced. This could cause the R717 VCHP to attain equal or higher NPV as VCHPs are a more mature technology with more competition between the suppliers. As shown in Ommen et al. (2014a, b) one of the highest uncertainty on the NPV is related to the electricity price. An increased electricity cost would be an advantage for the HACHP over the VCHP due to the higher COP, while a reduction of the electricity price would be an advantage for the VCHP as the NPV would be more influenced by investment.

Further, the performance of VCHP could be further optimized by the application of exergoeconomic optimization (Bejan et al., 1996) to the temperature difference in the evaporator and condenser. This would allow the best trade-off between investment and running cost to be determined for each refrigerant and at each operating point. This, however could also be applied to HACHP. If exergoeconomic optimization was applied the technologies would be compared at the best possible design, which might change the conclusion from this study.

Further, the HACHP is just one method for vapour compression systems to approach the Lorenz cycle. Conventional vapour compression heat pumps set in series are an alternative measure of this. This could prove to be a more cost efficient solution and should be investigated.

It should be noted that the application of the high pressure compressor to the HACHP did not increase the range of feasible heat supply temperatures compared to those concluded from Brunin et al. (1997). This is mainly due to the applied constraint on the compressor discharge temperature, which was neglected in Brunin et al. (1997). The use of a cooled screw compressor or an oil free compressor could relax the constraints on the compressor discharge temperature and allow heat supply temperatures above 150 °C. Alternatively, the application of a gas cooler prior to the mixing of vapour and lean solution can reduce the compressor discharge temperature as shown in Jensen et al. (2014). Further, a two-stage compression could be a measure of reducing the compressor discharge temperature and thus extending the working domain of the HACHP.

5. Conclusion

The feasible working domain of a HACHP has been evaluated based on a detailed economic analysis and a comprehensive investigation of the design variables: ammonia mass fraction and circulation ratio. The results show that the HACHP is capable of delivering both higher heat supply temperatures and higher temperature lifts than conventional VCHP.

Heat supply temperatures up to 150 °C and temperature lifts up to 60 K can be attained with commercially available components and with an economic benefit compared to gas combustion. It is found that the dominating constraint for the HACHP is the compressor discharge temperature. Further, it is found that reducing the sink/source temperature difference increases the maximum attainable heat supply temperature while reducing the maximum attainable lift.

When comparing the PV of the HACHP with the VCHP at the operating points where both are applicable: the cost of the HACHP is lower for almost all operating conditions with a heat supply temperature above 80 °C. For the range where the HACHP competes with R717 the difference in PV can be insignificant and both technologies should be considered. For the high temperature range where the only applicable VCHP technology is R600a the difference in PV is large and the HACHP should be applied.

Acknowledgements

This research project is financially funded by EUDP (Energy Technology Development and Demonstration), project title:

Please cite this article in press as: Jensen, J.K., et al., Technical and economic working domains of industrial heat pumps: Part 2 – Ammonia-water hybrid absorption-compression heat pumps, International Journal of Refrigeration (2015), http://dx.doi.org/10.1016/j.ijrefrig.2015.02.011

"Development of ultra-high temperature hybrid heat pump for process application", project number: 64011-0351 and by the Copenhagen Cleantech Cluster (CCC), DONG Energy and the Danish Technological Institute.

Appendix A. Heat transfer and pressure drop correlations

Table A. 1 – Heat transfer and pressure drop correlations.

General equations

$$G = \frac{\dot{m}}{M \cdot W \cdot b} \quad (A.1)$$

$$Re = G \cdot D_h / \mu \quad (A.2)$$

$$Re_{lo} = G \cdot D_h / \mu_{lo} \quad (A.3)$$

$$Bo = \frac{\dot{Q}}{G \cdot h_{lg} \cdot A_{HT}} \quad (A.4)$$

Martin (1996)

$$\varphi = \beta - 90^{\circ} \quad (A.5)$$

$$\phi = \frac{1}{6}\left(1 + \sqrt{1 + \frac{b_{\pi}}{\Lambda^2}} + 4\sqrt{1 + \frac{b_{\pi}}{2\Lambda^2}}\right) \quad (A.6)$$

If $\frac{Re}{\phi} < 2000$:

$$\xi_0 = 64\phi / Re \quad (A.7)$$

$$\xi_{1.0} = \frac{597\delta}{Re} + 3.85 \quad (A.8)$$

If $Re/\phi \geq 2000$:

$$\xi_0 = \left(1.8 \log_{10}\frac{Re}{\phi} - 1.5\right)^{-2} \quad (A.9)$$

$$\xi_{1.0} = \frac{39}{(Re/\phi)^{0.289}} \quad (A.10)$$

$$\frac{1}{\xi} = \frac{\cos\varphi}{\sqrt{0.18\ \tan\varphi + 0.36\ \sin\varphi + \xi_0/\cos\varphi}} + \frac{1 - \cos\varphi}{\sqrt{3.8\xi_{1.0}}} \quad (A.11)$$

$$Nu = \phi \cdot 0.122 \cdot Pr^{1/3} \frac{\mu}{\mu_w}^{1/6} \left(\xi \cdot \left(\frac{Re}{\phi}\right)^2 \sin(2\varphi)\right)^{0.374} \quad (A.12)$$

$$\alpha = Nu \cdot \lambda / D_h \quad (A.13)$$

$$\Delta p = \frac{2 \cdot \xi \cdot G^2 \cdot v \cdot L_{HT}}{D_h} \quad (A.14)$$

Yan et al. (1999)

$$G_{eq} = G\left(1 - q + q\left(\frac{v_{go}}{v_{lo}}\right)^{1/2}\right) \quad (A.15)$$

$$Re_{eq} = G_{eq} \cdot D_h / \mu_{lo} \quad (A.16)$$

$$\alpha = \frac{\lambda}{D_h} \cdot 4.188 \cdot Re_{eq}^{0.4} \cdot Pr_{lo}^{1/3} \quad (A.17)$$

$$\xi \cdot Re_{lo}^{0.4} \cdot Bo^{-0.5} \cdot \left(\frac{p}{p_c}\right)^{-0.8} = 94.75 \cdot Re_{eq}^{-0.0467} \quad (A.18)$$

Bell and Ghaly (1972)

$$\alpha = (1/\alpha_{lf} + Z/\alpha_{vo})^{-1} \quad (A.19)$$

$$Z = q \cdot c_{p,v} \cdot \frac{dT}{dh} \quad (A.20)$$

Táboas et al. (2012)

$$X_{tt} = \left(\frac{\mu_{lo}}{\mu_{vo}}\right)^{0.1} \left(\frac{1-q}{q}\right)^{0.9} \left(\frac{v_{lo}}{v_{vo}}\right)^{0.5} \quad (A.21)$$

$$F = (1 + 3/X_{tt} + 1/X_{tt}^2)^{0.2} \quad (A.22)$$

$$u_{SL} = G \cdot (1 - q) \cdot v_{lo} \quad (A.23)$$

$$u_{SV} = G \cdot q \cdot v_{vo} \quad (A.24)$$

If: $u_{SV} < 111.88 \cdot u_{SL} + 11.848\ ms^{-1}$:

$$\alpha = 5 \cdot Bo^{0.15} \alpha_{lo} \quad (A.25)$$

If: $u_{SV} > 111.88 \cdot u_{SL} + 11.848\ ms^{-1}$:

$$\alpha = F \cdot \alpha_{lo} \quad (A.26)$$

$$\xi_{lo} = 4.779 \cdot Re_{lo}^{-0.118} \quad (A.27)$$

$$\Delta p = \frac{2 \cdot \xi_{lo} \cdot F \cdot G^2 \cdot v_{lo} \cdot L_{HT}}{D_h} \quad (A.28)$$

Appendix B. Detailed results of the thermodynamic, heat transfer and economic models

Table B. 1 – Thermodynamic state points for a HACHP with $x_r = 0.65$ and $f = 0.65$, $T_{sink,out} = 80\ ^{\circ}C$, $\Delta T_{lift} = 30\ K$ and $\Delta T_{sink} = \Delta T_{source} = 20\ K$.

j^{th} stream	Media	$\dot{m}_j$(kg s^{-1})	x_j(–)	T_j (°C)	p_j (Bar)	h_j (kJ kg^{-1})	s_j (kJ kg^{-1} K^{-1})	v (10^{-3} m^3 kg^{-1})
(1)	NH_3–H_2O	1.929	0.650	45.00	4.957	459.1	2.07	106
(2)	NH_3–H_2O	0.6750	0.993	45.00	4.957	1382	4.95	300
(3)	NH_3–H_2O	0.6750	0.993	169.9	17.60	1653	5.08	118
(4)	NH_3–H_2O	1.929	0.650	91.01	17.60	609.2	2.31	31.8
(5)	NH_3–H_2O	1.929	0.650	65.62	17.59	90.98	0.832	1.39
(6)	NH_3–H_2O	1.929	0.650	54.25	17.39	37.01	0.670	1.36
(7)	NH_3–H_2O	1.929	0.650	24.85	4.964	37.01	0.697	30.0
(8)	NH_3–H_2O	1.254	0.465	44.91	4.957	−37.86	0.512	1.21
(9)	NH_3–H_2O	1.254	0.465	45.12	17.51	−35.96	0.513	1.21
(10)	NH_3–H_2O	1.254	0.465	63.58	17.60	47.07	0.766	1.24
(11)	Water	11.94		60.00	2.000	251.3	0.831	
(12)	Water	11.94		80.00	1.875	335.0	1.08	
(13)	Water	9.738		50.00	2.000	209.5	0.704	
(14)	Water	9.738		30.00	1.929	125.8	0.436	

Please cite this article in press as: Jensen, J.K., et al., Technical and economic working domains of industrial heat pumps: Part 2 – Ammonia-water hybrid absorption-compression heat pumps, International Journal of Refrigeration (2015), http://dx.doi.org/10.1016/j.ijrefrig.2015.02.011

ARTICLE IN PRESS

INTERNATIONAL JOURNAL OF REFRIGERATION XXX (2015) 1–18

Table B. 2 – Heat and work load COP and volume flow rates and receiver model.

$\dot{W}_{Comp.}$	183.1	kW	$\dot{Q}_{Absorber}$	1000	kW	COP	5.122	–
$\dot{W}_{Comp.,el}$	192.7	kW	$\dot{Q}_{Desorber}$	814.5	kW	$\dot{V}_2$	0.2024	$m^3\ s^{-1}$
$\dot{W}_{Pump}$	2.39	kW	$\dot{Q}_{iHEX}$	104.1	kW	$\dot{V}_{dis}$	0.2530	$m^3\ s^{-1}$
$\dot{W}_{Pump,el}$	2.514	kW				V_4	0.1106	m^3

Table B. 3 – HEX dimensions, heat transfer and pressure drop coefficients and refrigerant charge estimation.

Absorber:			Desorber:			Internal HEX:		
Plate type	SWEP V120T		Plate type	SWEP V120T		Plate type	SWEP V120T	
$\overline{\alpha}_{tp}$	7.30	$kWm^{-2}\ K^{-1}$	$\overline{\alpha}_{tp}$	5.847	$kW\ m^{-2}\ K^{-1}$	$\overline{\alpha}_r$	10.36	$kW\ m^{-2}\ K^{-1}$
$\overline{\alpha}_{sink}$	8.484	$kWm^{-2}\ K^{-1}$	$\overline{\alpha}_{source}$	5.58	$kW\ m^{-2}\ K^{-1}$	$\overline{\alpha}_l$	6.587	$kW\ m^{-2}\ K^{-1}$
$\overline{\xi}_{tp}$	0.03352	–	$\overline{\xi}_{tp}$	5.036	$-(\xi_{lo}\cdot F)$	$\overline{\xi}_r$	1.941	–
$\overline{\xi}_{sink}$	2.037	–	$\overline{\xi}_{source}$	2.241	–	$\overline{\xi}_l$	2.174	–
Δp_{3-4}	0.0008421	bar	Δp_{7-1}	0.007692	bar	Δp_{5-6}	0.204	bar
Δp_{11-12}	0.1255	bar	Δp_{14-13}	0.07065	bar	Δp_{9-10}	0.08604	bar
U	3.495	$kWm^{-2}\ K^{-1}$	U	2.621	$kW\ m^{-2}\ K^{-1}$	U	3.577	$kW\ m^{-2}\ K^{-1}$
$\Delta\overline{T}_{LM}$	6.551	K	$\Delta\overline{T}_{LM}$	6.286	K	ΔT_{LM}	4.725	K
N	353	–	N	400	–	N	52	–
A_{HT}	43.67	m^2	A	49.43	m^2	A_{HT}	6.163	m^2
A_{IN}	45.03	m^2	A_{IN}	51.03	m^2	A_{IN}	6.634	m^2
m	25.08	kg	m	28.59	kg	m	8.997	kg

Table B. 4 – PEC, TCI, total HACHP investment and operational cost.

Break down of HACHP TCI costs						Break down of HACHP FC, OMC, NPV and PBP		
k^{th}	component	X_Y		PEC_Y (€)	TCI_k (€)		PV (€)	Annual costs (€)
(1)	Compressor	910.8	$m^3\ h^{-1}$	34,944	145,365	TCI_{HP}	415,864.8	–
	Compressor motor	183.1	kW	8747.7	36,390.4	TCI_{NG}	0	–
(2)	Pump	2.514	kW	2243.7	9333.94	FC_{HP}	590,247.6	56,489.6
(3)	Absorber	45.03	m^2	16,356	68,038.9	FC_{NG}	1,435,741	137,407
(4)	Receiver	0.1116	m^3	1656.6	6891.57	OMC_{HP}	83,172.76	7960.04
(5)	Internal HEX	6.163	m^2	3533.8	14,700.8	OMC_{NG}	0	0
(6)	Desorber	51.03	m^2	18076	75,194.4	PV_{HP}	1,089,284	–
(7)	LVS	728.7	$m^3\ h^{-1}$	14,411	59,948.7	PV_{NG}	1,435,741	–
						Annual net cash flow		72,957.4
Total HACHP investment					415,864	NPV	346,456.5	–
						PBP	–	5.70

REFERENCES

Abu-Khader, M.M., 2012. Plate heat exchangers: recent advances. Renew. Sust. Energ. Rev. 16 (4), 1883–1891. ISSN: 1364–0321. http://dx.doi.org/10.1016/j.rser.2012.01.009.

Ahlsell Danmark ApS, 2013. Priskatalog 2013 (accessed 26.09.13.). URL. https://webshop.ahlsell.com/vivp/index.jsp.

Altenkirch, E., 1950. Kompressionskältemachine mit lösungskreislauf. Kältetechnik 2 (10,11,12), 251–259,310–315,279–284.

Annex–21, 1995. Industrial Heat Pumps – Experiences, Potential and Global Environmental Benefits. IEA Heat Pump Centre.

Bejan, A., Tsatsaronis, G., Moran, M.J., 1996. Thermal Design and Optimization. Wiley-Interscience Publication, Wiley, ISBN 9780471584674.

Bell, K.J., Ghaly, M.A., 1972. An approximate generalized design method for multicomponent/partial condensers. In: 13th National Heat Transfer Conference, Denver, Colorado, USA. AIChE-ASME.

Berntsson, T., Hultén, M., 1999. The compression/absorption cycle – influence of some major parameters on COP and a comparison with the compression cycle compression – absorption. Int. J. Refrigeration 22, 91–106.

Berntsson, T., Hultén, M., 2002. The compression/absorption heat pump cycle - conceptual design improvements and comparisons with the compression cycle. Int. J. Refrigeration 25, 487–497.

Brunin, O., Feidt, M., Hivet, B., 1997. Comparison of the working domains of some compression heat pumps and a compression-absorption heat pump. Int. J. Refrigeration 20 (5), 308–318. ISSN: 0140–7007.

Conde, M., 2004. Thermophysical Properties of NH3 + H2O Solutions for the Industrial Design of Absorption Refrigeration Equiptment. Technical report. M. Conde Engineering.

Corberan, J.M., 2011. 2nd IIR workshop on refrigerant charge reduction in refrigerating systems. Int. J. Refrigeration 34 (2), 600, 3.

Danish Energy Agency, 2013. Data, Tables, Statistics and Maps, Energy in Denmark 2012 (accessed 30.06.14.).

El-Sayed, Y.M., 1988. On exergy and surface requirements for heat transfer processes involving binary mixtures. In: Proceedings of ASME Winter Annual Meeting, Chicago, pp. 19–24. ASME-AES Vol. 6, HTD – Vol. 97.

Please cite this article in press as: Jensen, J.K., et al., Technical and economic working domains of industrial heat pumps: Part 2 – Ammonia-water hybrid absorption-compression heat pumps, International Journal of Refrigeration (2015), http://dx.doi.org/10.1016/j.ijrefrig.2015.02.011

F-Chart, S.L., 1992. Engineering Equation Solver (EES). http://www.fchart.com/ees (accessed 30.06.14.).
FK Teknik A/S., 2013. Priskatalog 2013 (accessed 26.09.13.). URL. http://www.fkteknik.dk/kataloger.html.
Grundfos DK A/S, 2014. Indicative Retail Prices.
H. Jessen Jürgensen A/S, 2013. Price catalog 2013 (accessed 26.09.13). http://www.hjj.dk/indhold_prisliste.html.
Hybrid Energy AS. 2015, (accessed 28.01.15.) URL http://www.hybridenergy.no/en/clients/.
Ibrahim, O.M., Klein, S.A., 1993. Thermodynamic properties of ammonia-water mixtures. In: ASHRAE Trans.: Symposia, p. 21, 2 1495–1502.
Itard, L.C.M., Machielsen, C.H.M., 1994. Considerations when modelling compression/resorption heat pumps. Int. J. Refrigeration 17 (7), 453–460.
Jensen, J.K., Reinholdt, L., Markussen, W.B., Elmegaard, B., 2014. Investigation of ammonia/water hybrid absorption/compression heat pumps for heat supply temperatures above 100 °C. In: International Sorption Heat Pump Conference, March 31-April 2. University of Maryland, Washington D.C.
Johnson Controls, 2013. HPO R717 Compressor Cost. Personal Communication with Sørensen, K.
Kemp, I.C., 2011. Pinch analysis and process integration: a user guide on process integration for the efficient use of energy. Elsevier Science, ISBN 9780080468266.
Lorenz, H., 1894. Beiträge zur Beurteilung von Kühlmaschinen. Z VDI 38, 62–68, 98–103, 124–130.
Martin, H., 1996. A theoretical approach to predict the performance of chevron-type plate heat exchangers. Chem. Eng. Process.: Process Intensif. 35 (4), 301–310. ISSN: 0255–2701.
Ommen, T., Markussen, C.M., Reinholdt, L., Elmegaard, B., 2011. Thermoeconomic comparison of industrial heat pumps. In: ICR 2011, August 21-26-Prague, Czech Republic.
Ommen, T., Jensen, J.K., Markussen, W.B., Reinholdt, L., Elmegaard, B., 2014a. Technical and economic working domains of industrial heat pumps 1: vapour compression heat pumps. Int. J. Refrigeration. http://dx.doi.org/10.1016/j.ijrefrig.2015.02.012.
Ommen, T., Markussen, W.B., Elmegaard, B., 2014b. Heat pumps in combined heat and power systems. Energy 79, 989–1000. http://dx.doi.org/10.1016/j.energy.2014.09.016. Nov.
Osenbrück, A., 1895. Verfahren zur Kälteerzeugung bei Absorptionsmaschinen. Deutsches Reichspatent, [DRP 84084].
Radermacher, R., Hwang, Y., 2005. Vapor Compression Heat Pumps with Refrigerant Mixtures. Mechanical Engineering. Taylor & Francis, ISBN 9781420037579.
Silver, L., 1947. Gas cooling with aqueous condensation: a new procedure for calculating heat transfer coefficients. Industial Chem. 380–386 (June).
Stoecker, W., 1998. Industrial Refrigeration Handbook. McGraw-Hill Education, ISBN 9780070616233.
SWEP international AB, 2014a. Technical Information v120t anf v10t [accessed 01.06.14]. URL. http://www.swep.net/en.
SWEP International AB., 2014b, private communication SWEP – products & solutions (B400, B120T F-pressure, B17 product sheets) – non-disclosure agreement URL http://www.swep.net/en/products_solutions/productfinder/Pages/B120T.aspx.
Táboas, F., Vallès, M., Bourouis, M., Coronas, A., 2012. Assessment of boiling heat transfer and pressure drop correlations of ammonia/water mixture in a plate heat exchanger. Int. J. Refrigeration. ISSN: 01407007 35 (3), 633–644. May.
Townsend, D., Linnhoff, B., 1983. Heat and power networks in process design. Part I: criteria for placement of heat engines and heat pumps in process networks. AIChE J. 35 (3), 742–748, 29.
Yan, Y.Y., Lio, H.C., Lin, T.F., 1999. Condensation heat transfer and pressure drop of refrigerant r-134a in a plate heat exchanger. Int. J. Heat. Mass Tran. 42 (6), 993–1006.
Zheng, N., Song, W., Zhao, L., 2013. Theoretical and experimental investigations on the changing regularity of the extreme point of the temperature difference between zeotropic mixtures and heat transfer fluid. Energy. ISSN: 03605442 55, 541–552. June.

Please cite this article in press as: Jensen, J.K., et al., Technical and economic working domains of industrial heat pumps: Part 2 – Ammonia-water hybrid absorption-compression heat pumps, International Journal of Refrigeration (2015), http://dx.doi.org/10.1016/j.ijrefrig.2015.02.011

Appendix G

Paper 5 - To be submitted

Torben Ommen, Vittorio Verda, Jonas Kjær Jensen, Wiebke Brix Markussen and Brian Elmegaard

Exergoeconomic comparison of heat pumps in district heating systems

[to be submitted]

Exergoeconomic comparison of heat pumps in district heating systems

Torben Ommen[a,*], Vittorio Verda[b], Jonas Kjær Jensen[a], Wiebke Brix Markussen[a], Brian Elmegaard[a]

[a] *Technical University of Denmark, Department of Mechanical Engineering, Kgs. Lyngby, Denmark*
[b] *Politecnico di Torino, Department of Energetics, Torino, Italy*

Abstract

Compression heat pumps (HPs) are frequently considered as part of future production capacity for urban district heating demands. The feasibility of HPs in such systems depends on the cost of the heat production, which is closely related to the efficiency of the plant. Two HP configurations are studied in detail, as they may supply heat at a central location in the network, while operating at high system efficiency. Central solutions are key in order to obtain the favourable effects from economy of scale. Eight systems are examined in terms of applicability, and the systems are optimised for each operating condition using exergoeconomic theory. The HPs are compared based on cost of heat. The results show that including the practical applicability of components causes a significantly increased cost at high temperature lifts, compared to the most competitive thermodynamic cycle. At high and medium temperature lifts cycle efficiencies of 45 - 50 % of the theoretical maximum (Lorenz cycle limit) can be achieved, whereas for low temperature lifts, efficiencies as low as 36 % may be expected.

Keywords: Heat pumps, District heating, Exergoeconomic optimisation

1. Introduction

Heat pumps (HPs) have been proposed as a way to replace fossil fuels with high amounts of renewable energy in district heating (DH) networks in Northern Europe [1–6]. This may be achieved by utilisation of renewable electricity, e.g. from wind turbines, and heat from ambient or geothermal sources. For the considered networks in Copenhagen [7], the main fraction of heat is typically supplied by combined heat and power plants. If the operational flexibility in such systems is limited by many production constraints, the production efficiency of the central thermal plants may be reduced [8]. By carefully integrating the HPs, the added technology can be used to decouple the production constraints of the cogenerated products [9].
HP units may be installed in individual dwellings or at several locations in the district heating networks, e.g., the forward or return stream, transmission or distribution grids. Each location results in differences in performance in terms of energy efficiency, operational constraints and economic feasibility.

In studies of the complete energy system, assumptions about the performance for HPs (such as the COP or the capacity of the units) are critical, as incorrect estimates impact the system and the potential benefit of the technology. The result may be non-optimal implementation proposals or system configurations. Of the above mentioned studies, some use a fixed value of the COP independent of load and temperatures (often a value of 3 [/]) and unlimited capacity, without further consideration of the temperature or availability of source heat. The available heat sources are crucial for the operation of a HP and will impact the performance.

Considering the case where both the electricity and heat services are traded in a liberalised energy market, the installed utility technologies are operated in an effort to reduce the utility cost for the consumers. Thus, a unit with low production cost will undergo a higher number of operating hours than a unit with higher production cost. For a given electricity price, the main factor for the heat pro-

*Corresponding author, Tel.: +45 4525 4037, Fax.: +45 4588 4325.
Email addresses: tsom@mek.dtu.dk (Torben Ommen), vittorio.verda@polito.it (Vittorio Verda), jkjje@mek.dtu.dk (Jonas Kjær Jensen), wb@mek.dtu.dk (Wiebke Brix Markussen), be@mek.dtu.dk (Brian Elmegaard)

Nomenclature

$\hat{a}$	amplitude of corrugation, m
b	constant /
Bo	Boiling number, /
C	cost, €/MWh
$\dot{C}$	cost rate, €/h
c	constant
d	diameter, m
G	mass flux, kg/m^{2}s
h	heat transfer coefficient, W/m^{2}K
i	enthalpy, J/kg
k	thermal conductivity, W/mK
L	channel length, m
Nu	Nusselt number, /
p	pressure, Pa
Pr	Prandtl number, /
$\dot{Q}$	heat production, MJ/s
q''	imposed heat flux, W/m^2
Re	Reynolds number, /
T	temperature, °C
$\bar{T}$	Log mean temperature, °C
u	velocity, m/s
X	vapour quality, /
$\dot{Z}$	non-exergy-related cost rate,

Greek symbols

Δ	variation or glide
η	efficiency, /
μ	viscosity, Pa s
ξ	friction factor
ρ	density, kg/m^3
φ	corrugation inclination angle, /

Subscripts

discharge	at discharge of compressor
eq	equivalent to all liquid
F	fuel
fg	evaporation
h	hydraulic
high	high pressure side
HP	heat pump
i	inlet
inv	investment
k	component
l	liquid, saturated
Lorenz	thermodynamic limit according to Lorenz
o	outlet
p	plate
P	product
return	return stream in district heating network
sink	sink reservoir
source	source reservoir
supply	supply stream in district heating network
tax	taxes and VAT
v	vapour, saturated
w	wall temperature

Abbreviations

CHP	Combined Heat and Power
COP	Coefficient Of Performance
DH	District Heating
HP(s)	Heat Pump(s)
PEC	Purchased Equipment Cost
VHC	Volumetric Heating Capacity

duction cost of a HP is the electricity consumption and plant investment. The relationship between the variable and fixed costs can be altered by changing equipment sizes and efficiencies. By using exergoeconomic optimisation, optimal heat production prices can be found by applying the correct allocation of investment cost in relation to the operation hours of the plant [10].

In this paper, a comparison of exergoeconomic optimal systems is performed for two types of centralised district heating HPs. This determines the best available technology for the given application and the corresponding HP efficiency. Eight different single-stage HP systems are considered, of which 5 are based on natural working fluids [11]. Of the 3 remaining working fluids, two are HFC-refrigerants and one is part of the novel HFO generation. Many of the considered working fluids are in practice restricted by pressure and temperature limits for the individual components according to current application envelopes. By comparing investment, performance and working regime of the individual HP systems, this analysis examines the cost, applicability and efficiency of the best available technology in a given DH system.

1.1. Heat pumps using finite reservoirs

In DH networks, the temperature reservoirs are of limited heat capacity, which influences the performance of HPs significantly. Thus the temperature difference between the inlet and the outlet of a stream may be of high importance for the efficiency of the investigated solutions.

A schematic diagram of a single-stage vapour compression HP is presented in Fig. 1. The nomen-

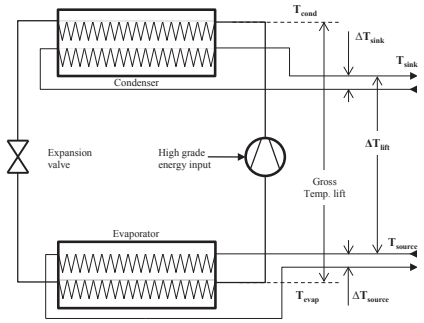

Figure 1: Schematic diagram of a single-stage HP system

clature matches that of several studies such as Eisa et al. [12] and Brunin et al. [13]. With fixed parameters for the compressor efficiency and a fixed minimum temperature difference in heat exchangers, the performance of a HP can be determined based on only four variables representing the integration of the sink and source streams. The variables typically used are the temperature of the sink process stream leaving the condenser T_{sink}, the temperature of the source process stream entering the evaporator T_{source} and the process stream temperature glides from the inlet to outlet in both heat exchangers (ΔT_{sink} and ΔT_{source}).
For finite reservoirs with significant temperature glide, the Carnot COP is not representative for the thermodynamic limit [14]. In this case, a corresponding calculation based on the logarithmic mean temperature of the finite heat reservoirs can be used. The logarithmic mean temperatures of sink and source are defined as in Equations 1 and 2:

$$\bar{T}_{\text{sink}} = \frac{T_{\text{sink,o}} - T_{\text{sink,i}}}{\ln(T_{\text{sink,o}}) - \ln(T_{\text{sink,i}})} \tag{1}$$

$$\bar{T}_{\text{source}} = \frac{T_{\text{source,o}} - T_{\text{source,i}}}{\ln(T_{\text{source,o}}) - \ln(T_{\text{source,i}})} \tag{2}$$

The log mean temperature lift can be calculated as the difference between $\bar{T}_{\text{sink}}$ and $\bar{T}_{\text{source}}$. The thermodynamic limit of COP can be calculated according to Lorenz:

$$\text{COP}_{\text{Lorenz}} = \frac{\bar{T}_{\text{sink}}}{\bar{T}_{\text{sink}} - \bar{T}_{\text{source}}} \tag{3}$$

The Lorenz efficiency determines the actual COP of an application compared to the theoretical limit:

$$\eta_{\text{Lorenz}} = \frac{\text{COP}_{\text{HP}}}{\text{COP}_{\text{Lorenz}}} \tag{4}$$

1.2. Current district heating networks

As DH networks are not uniform in sizes or technology, several HP configurations are needed. Different network specifications include the temperature of demand, pressure levels, direct or indirect installations, with or without transmission lines, etc. When considering the temperature levels of supply and return lines in DH networks, a span is needed rather than a fixed temperature. In a Danish context the supply temperature ($T_{\text{DH,supply}}$) varies from 70 °C to 120 °C [7, 15] mainly depending on the size of the network and its commissioning year. The corresponding network return temperatures ($T_{\text{DH,return}}$) range from 35 °C to 55 °C. In Table 1, three commonly used temperature sets are presented.
The temperature of the source is dictated by the type and location of the installation [16]. Smaller systems operate with source temperatures according to the available media/type at the location of the heat demand. By using a DH network, larger installations can be located near heat sources of higher and more constant temperatures compared to, e.g., the temperature of ambient air. Examples of these are sea or sewage water, geothermal or aquifer bore holes, power plant stack gasses, etc. Most of these heat sources tend to have a low yearly temperature variation and a finite heat capacity of the stream.

1.3. Heat pump configurations in a district heating network

Based on the identified finite temperature levels, five generic HP configurations are identified and compared in [9]. In this paper, two of these configurations are studied in detail, as they provide the possibility to supply heat to the DH network from a

Table 1: Three common temperature sets for DH networks

Network type	DH forward temperature	DH return temperature
Transmission	110°C	55°C
Old distribution	90°C	45°C
New distribution	70°C	35°C

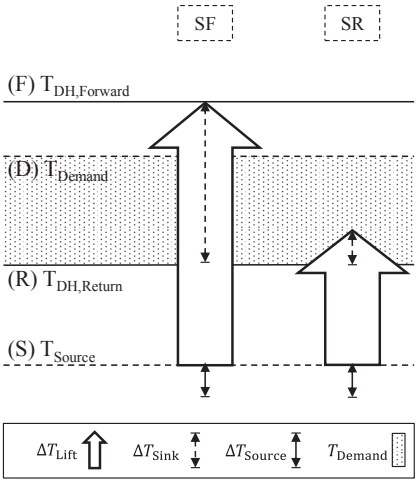

Figure 2: HP configurations for supplying district heating from a central location

central location. The configurations are presented in Fig. 2 where the white arrow indicates the temperature lift from T_{sink} to T_{source}, and the temperature glides (ΔT_{sink} and ΔT_{source}) are indicated by the dashed and solid arrows, respectively.
The details of the two HP configurations are described below:

Source-Forward (SF) HP with a temperature lift from T_{source} to $T_{\text{DH,forward}}$. The sink process stream is heated from the temperature of the return line. The temperature glide of the source corresponds to the heat capacity of the finite heat capacity of the heat source.

The SF configuration can operate independently of other technologies in a DH network.

Source-Return (SR) HP with a temperature lift from T_{source} to $T_{\text{DH,return}}$. The HP can be used to preheat the return water of a DH network before entering the CHP plant. The temperature lift is significantly lower compared to configuration SF, which results in an increased COP of the HP. This will, on the other hand, reduce the electric efficiency of the CHP plant [17]. ΔT_{sink} is thus subject to optimisation in each individual DH system when considering the applied generation technology. The temperature glide of the source corresponds to the finite heat capacity of the heat source.

The SR configuration requires the use of other generation technologies in order to increase the temperature to that of the forward line.

According to the heat demand of a DH network, the installed capacity of such installations is typically large, in the range of 100 kW - 100 MW, due to the favourable effects from economy of scale.

2. Method

The single-stage vapour compression HP cycle was considered for the analysis in this paper. The work rate for the compressor was supplied by an electric motor. The comparison was carried out without considering possibilities for improved performance by, e.g., internal heat exchangers or two-stage compression.
Looking at a specific HP technology, several constraints must be considered, whereof some are determined by the working fluid, and some by component construction and materials. Some effects were disregarded in the comparison, as these do not result in significant differences between the different HP systems. These effects include the pressure drop in pipes, the extent of non-useful superheat and subcooling, and compressor heat losses. Only full load steady state operation was considered.
A model for each HP was implemented in Engineering Equation Solver (EES) [18]. The developed models include exergy analysis and exergoeconomic analysis [10]. For each of the considered temperature sets of DH networks and source temperature, the models were optimised in order to obtain the minimum heat cost. The method for calculation and optimisation of exergoeconomics is further described in section 2.5.

2.1. Heat exchangers

As one of the significant processes of a physical HP system, optimal heat transfer is key in terms of optimisation. In order to include fully the various effects of the different cycles, the thermophysical properties of the working fluids must be included. This can be achieved by integrating detailed heat transfer correlations for both the evaporator and condenser.

For both heat exchangers a combination of single and two-phase heat transfer is present in the refrigerant channel. For components with different zones of heat transfer processes, moving boundary models are often used in order to assign the correct heat transfer coefficient and pressure loss for each process [19]. Thus, the heat exchangers are divided in heat transfer zones such as condensation, desuperheating and subcooling.
The application of chevron type plate heat exchangers has increased significantly within the last two decades [20, 21], and has now reached a point where plate heat exchangers are highly competitive for HP systems. In order to ensure competitive prices, all heat transfer coefficients, pressure losses and resulting heat transfer areas have been calculated for this type of heat exchangers. The heat transfer coefficient and pressure losses in plate heat exchangers have been the focus of many studies. Claesson [19] compares different correlations to experimental data from a manufacturer. Many findings are summarized in Palm and Claesson [22].

- The single-phase correlation for heat transfer coefficients and pressure losses proposed by Martin [23] is used to evaluate single-phase heat transfer coefficients. See Appendix A.1 for further details.
- The heat transfer coefficients of the evaporation and condensation processes are evaluated using Yan and Lin [24] and Yan et al. [25], respectively. See Appendix A.2 for further details.

For the resulting heat transfer coefficient, heat transfer area and pressure losses, the correlations correspond well with several on-line calculation tools made available by some of the major manufacturers [26, 27]. For sizes and further specification of the plate heat exchangers, the reader is referred to SWEP International AB [28]. The considered types are B400 for up to 2.8 MPa, B120T (F-pressure specification) for up to 5 MPa, and B17 for transcritical processes below 14 MPa.
For the calculation of the HP thermodynamic cycle and heat transfer coefficients, it was assumed that the working fluid was subcooled until the minimum temperature difference was reached between the working fluid outlet and sink stream inlet. Exiting the evaporator, the working fluid was assumed superheated, until the temperature of the fluid was 5 K above the evaporation temperature.

2.2. Compressors and operating conditions

For a high temperature HP, the pressure limit of the high pressure side will in many cases dictate the achievable sink temperatures. In some cases also the suction pressure or pressure ratio of the compressor poses limitations.
For trans-critical processes, where the pressure limit cannot be directly converted into a temperature limit, the maximum pressure for cost optimisation has an effect on the working regime, performance and economic profitability of the unit.
Oil and valve degradation due to high temperatures at the compressor discharge may also pose limitations [29]. High temperatures may also influence the performance and lifetime of selected refrigerants.
Prices and operational limits of compressors from large international manufacturers are available from data sheets (see Table 4 for references). Compressors for five different working fluid types (WF-type) were identified according to different refrigerant properties, flammability and availability. The data are presented in Table 2. Operating limits correspond to reciprocating piston compressors, as data for other types are not available.
Compressors for WF-type 1, 2 and 3 have similar pressure constraints but are designed for different fluids. WF-type 1 is for HFC refrigerants, WF-type 2 is for flammable gases and WF-type 3 is for R717 specifically. Additionally two high pressure component types are included. WF-type 4 is for R717 up to 5.2 MPa, and WF-type 5 is for transcritical R744 processes up to 14 MPa.
The performance parameters for all compressors are addressed in section 2.4.

2.3. Temperature ranges of DH networks and heat source

The HPs were examined within the temperature range discussed in section 1.2 and Table 1. The return and forward temperatures were interpolated linearly for the range of $T_{\mathrm{DH,forward}}$ = 70-110 °C and $T_{\mathrm{DH,return}}$ = 35-55 °C as presented in Fig 3.
The heat sources for central HPs were assumed to be in the temperature range of $T_{\mathrm{source}} = 10 - 30\,^{\circ}\mathrm{C}$. All source temperature glides were assumed constant at 10 K for both SF and SR configurations presented in Fig. 2.
The forward and return temperatures of the DH network determine the temperature glide of configuration SF. Considering configuration SR, where

Table 2: Current operating limits of available piston compressor types

WF-type #	Refrigerant	Pressure limit MPa (°C)	Lubrication max. temp. °C	Capacity (1500 RPM) m^3/h
1	R134a	2.8 (83)	180	5-280
1	R1234ze	2.8 (96)	180	5-280
1	R407C	2.8 (65)	180	5-280
2	R290	2.8 (74)	180	5-280
2	R600a	2.8 (119)	180	5-280
3	R717-LP	2.8 (63)	180	5-180
4	R717-HP	5.2 (91)	180	90-200
5	R744	14.0 (N/A)	180	6-25

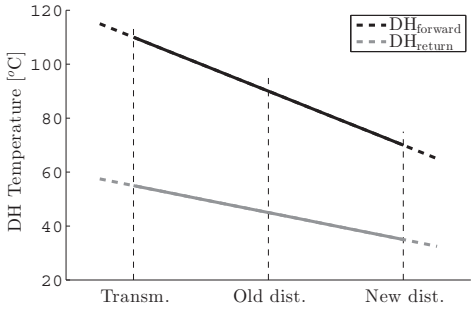

Figure 3: Temperature spans applied to the modelled DH networks

the return stream is preheated, a fixed sink temperature glide of 10 K was assumed. Thus for a transmission network (as specified in Table 1), the return stream is heated from 55 °C to 65 °C by the HP unit before being returned to the CHP plant.

2.4. Heat pump capacity and compressor efficiencies

The additional parameters needed to define fully the HP models are listed in Table 3.
The performances of the compressors are calculated using a fixed value for the isentropic and volumetric efficiencies. The impact of the estimated parameters is investigated in section 3.5.

2.5. Exergoeconomics

By detailed investment allocation between the components of a HP, optimal performance in terms of production cost can be obtained. The objective of the exergoeconomic evaluation is to examine the cost formation process of the product(s), to assess properly the contributions due to investments and the thermodynamic inefficiencies (irreversibilities). As a result, it is possible to focus the analysis on the components which have the highest impact.
Exergoeconomic analysis is based on exergy analysis. An exergy cost balance is written, for each HP cycle, by calculating the exergetic resources, products, destructions and losses for each individual component. In the cost balance, the exergy cost of a product includes the cost associated with owning and operating the considered component, including the cost associated with the exergetic fuel(s) for the component. The cost balance for component k is given by:

$$\sum \dot{C}_{o,k} = \sum \dot{C}_{i,k} + \dot{Z}_k \tag{5}$$

where o are outlet streams and i are inlet streams. $\dot{Z}_k$ represents the appropriate cost rate due to capital investment and maintenance expenses.
In this way, the price of the fuel for one component is dictated by the investment and running cost of the other components in the cycle. Changing investment or performance of one component changes the price of the final product. Nomenclature and development of the exergoeconomic evaluation are based on Bejan et al. [10] and Tsatsaronis [30].
The optimal configuration in terms of minimum heat cost during the lifetime of a HP system can be found by minimising the objective function:

$$\text{Min}\,(\dot{C}_{P,\text{HP}} = \dot{C}_{F,\text{HP}} + \sum \dot{Z}_k) \tag{6}$$

where the variables on the right-hand side of the equation are functions of the decision variables. In this analysis, the decision variables are minimum temperature differences in heat exchangers.
As the allocation of investment between components is the subject of consideration, the model re-

Table 3: HP capacity and compressor efficiencies

	Value	Unit	Designation
Efficiency	0.8	/	Compressor isentropic efficiency
	0.8	/	Compressor volumetric efficiency
	0.95	/	Compressor electric motor efficiency
Capacity	1000	kW	HP capacity

quires detailed cost data for all components. Thus, detailed cost correlations for components are developed to reflect variations in the values of decision parameters, such as size or efficiency. As mentioned in section 2.2, coherent and comprehensive data for specific components are not easily uncovered. In order to aggregate from the data at hand, it is assumed that:

- The Purchased Equipment Cost (PEC) for an open type compressor is a function of the type (specified in Table 2 - differentiated by eg. pressure level and explosive atmosphere) and the swept volume of the compressor.
- The PEC for an electrical motor with a fixed efficiency is dependent on the shaft power.
- The PEC for a heat exchanger is a function of the heat exchange area and pressure limit.
- The PEC of a receiver is a function of the volume and the pressure limit.
- The PECs of the expansion valve and oil separator are neglected.
- The capital investment of a component is 4.16 higher than the PEC of the component. This accounts for additional costs related to new investment [10] at an existing facility.
- The electricity cost corresponds to the market price for industrial consumers in the year 2012 according to [31]. As connection to the electricity grid is not known in advance, only transmission losses are included in the cost. If the HP is connected to low voltage networks, a significant increase (up to +20 %) in electricity cost should be expected. Taxes on heat from HP systems are calculated for 2012 [32]. The full cost of electricity utilised for the analysis is 171 €/MWh.
- Source heat is readily available as a process stream.
- Interest and inflation rate are constant at 7% and 2%, respectively.
- The cost correlations fit equipment for capacities between 100 kW and 2 MW.

The PEC functions have been developed based on prices from intermediate Danish trade business and individual manufactures. The cost functions, Eq. 7, were constructed as proposed by [10]. The purchase cost of an equipment item PEC_Y at a size or capacity X_Y can be calculated based on knowledge of the cost PEC_W at a different size or capacity X_W by use of a scaling exponent α.

$$\mathrm{PEC}_Y = \mathrm{PEC}_W \left(\frac{X_Y}{X_W} \right)^{\alpha} \tag{7}$$

Data for the component cost correlations and references are listed in Table 4 for each of the investigated WF-types. In many cases, the data corresponds to more than one brand with similar characteristics in terms of economy and applicability. For some of the investigated components, the cost correlations are not presented due to non-disclosure agreements (NDA) with the manufacturers. The presented cost correlations correspond to the ones used in Ommen et al. [33] and Jensen et al. [34].

The plant has a specified amount of annual operation hours, 3500 h/year, with a technical lifetime of 15 years. The amount of annual operating hours are found for the SF configuration in an energy system analysis for Greater Copenhagen using various specific heat sources at limited capacity Bach [39], CTR, HOFOR and VEKS [40].

For the case of R744, where heat rejection from the working fluid is at super-critical pressure, the performance of the HP is affected by the gas cooler pressure as presented in [29] and further discussed in [41]. By changing the heat exchange process of the gas cooler, also the investment of the HP system is affected. For all the considered temperature configurations of tran-scritical HPs, the gas cooler pressure resulting in the minimum cost of heat is determined and used. In this way it is possible to utilize the additional degree of freedom in the system design to obtain a lower cost of heat.

Table 4: Used cost correlations for component types divided by application limits

Component	WF-type	PEC_W (€)	X_W	$\alpha(-)$	Source
Compressor	1	10631	178.4 (m^3 h^{-1})	0.79	trade business [35–37]
	2	19850	279.8 (m^3 h^{-1})	0.73	trade business [35, 36]
	3	11914	178.4 (m^3 h^{-1})	0.66	trade business [35, 36]
	4	NDA	NDA	NDA	manufacturer [38]
	5	12109	25.6 (m^3 h^{-1})	0.42	trade business [35, 36]
Electrical motor	1,3,4	10710	250 (kW)	0.65	trade business [35]
	2,5	0	0	0	incl. in compressor [35, 36]
Receiver	1,2,3	1444	0.089 (m^3)	0.63	trade business [35]
	4	1934	0.089 (m^3)	0.66	trade business [35]
	5	2744	0.050 (m^3)	1.12	trade business [35]
Plate heat exchanger	1,2,3	15526	42 (m^2)	0.8	trade business [35–37]
	4	NDA	NDA	NDA	manufacturer [28]
	5	NDA	NDA	NDA	manufacturer [28]

3. Results

The eight HP configurations are compared based on the production cost of heat and cycle efficiency for the integrated configurations SF and SR, respectively. As an example of the comparison, a calculation of configuration SF is presented, considering DH network at new distribution temperatures and fixed heat exchanger pinch point temperature difference. The comparison is presented in Table 5, where operating limits, electricity consumption, cycle efficiency, Volumetric Heating Capacity (VHC) and the cost of heat (C_{heat}), as well as the three constituents (investments, fuel cost and taxes) of cost, are shown. VHC expresses the ratio between the heat transfer rate of the condenser and the compressor swept flow. For low ratios of VHC (e.g. below 2) the system should be disregarded due to the high investment cost for compressors according to the volume flow rate [13].

According to the limitations defined in Table 2, two of the HP systems are disregarded due to a too high operating pressure (R407C and R717-LP). Out of the six remaining, the R717-HP has the lowest cost of heat and is thus preferable for this operating condition. The cycle efficiency for this configuration is among the highest presented. From the table it is clear that the economically preferable solutions operate at high cycle efficiency and high VHC. For the feasible configuration, it is found that the cost of heat is in the range of 56 €/MWh to 76 €/MWh, even though five of the HPs have the same COP of 3.9. For comparision with current systems, the cost for DH in Copenhagen in 2012 was 85 €/MWh [42]. However it should be noted that none of the current areas in Copenhagen operates according to "New distribution" DH network temperatures. Additionally, as the comparison is for distribution network, distribution losses should be imposed on the electricity cost, depending on the electricity network at the location of the unit.

As presented in Table 5, the sum of investment and electricity cost accounts for between 47 and 59 % of the full cost of heat from the considered HPs. For units with low investment cost, the cost according to heat taxes may exceed 50 %.

3.1. Optimal allocation of investment

Considering the component cost functions of the HP cycle as specified in section 2.5, the heat exchanger units are the primary area of interest for an economic optimisation, as this component type provides the possibility to obtain increased performance of the cycle by increasing investment. An example of the impact of an exergoeconomic optimisation is presented in Fig. 4 for the R600a HP, considering a range of the considered source temperatures (10-30 °C) and sink temperatures according to "New distribution" DH network temperatures (in Fig. 3 or Table 1).

Four cases with predefined condenser and evaporator pinch temperature differences (ΔT_{pinch}) are compared to a case where the heat exchangers are optimised individually in order to obtain the lowest operation cost of the HP in consideration. In

Table 5: Operating conditions for eight HP types for Configuration SF, "New distribution" DH network, $T_{\text{source},i} = 20$ °C, fixed minimum pinch point in heat exchangers $\Delta T_{\text{pinch}} = 5$ K

	P_{high} [MPa]	$T_{\text{discharge}}$ [°C]	COP [/]	η_{Lorenz} [/]	VHC [MJ m^{-3}]	C_{heat} [€ MWh^{-1}]	$C_{\text{heat,inv}}$ [€ MWh^{-1}]	$C_{\text{heat},F}$ [€ MWh^{-1}]	$C_{\text{heat,tax}}$ [€ MWh^{-1}]
R134a	2.1	89	3.9	0.45	2.6	64 (100 %)	20 (32 %)	15 (23 %)	29 (45 %)
R1234ze	1.7	89	3.9	0.44	2.0	67 (100 %)	22 (34 %)	15 (23 %)	29 (44 %)
R290	2.6	87	3.9	0.44	3.5	64 (100 %)	20 (31 %)	15 (24 %)	30 (46 %)
R407C	3.0	95	4.3	0.49	4.3	56 (100 %)	14 (25 %)	14 (25 %)	28 (49 %)
R600a	1.2	77	3.9	0.44	1.4	71 (100 %)	26 (37 %)	15 (21 %)	29 (41 %)
R717-LP	3.1	176	3.9	0.45	4.6	54 (100 %)	11 (20 %)	15 (27 %)	28 (53 %)
R717-HP	3.1	176	3.9	0.45	4.6	56 (100 %)	13 (23 %)	15 (26 %)	29 (51 %)
R744	13.9	102	3.1	0.36	19.1	76 (100 %)	21 (28 %)	19 (25 %)	36 (48 %)

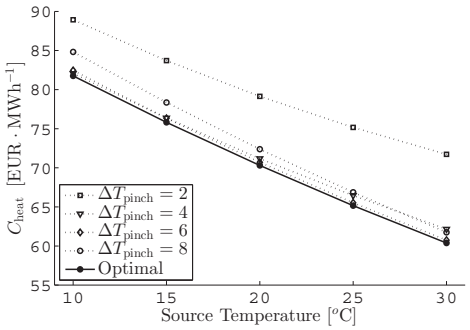

Figure 4: Cost of heat for R600a HP with variable source temperature. Sink temperatures according to configuration SF for "New distribution" DH network temperatures.

addition to the optimisation of investment in heat exchangers, also the remaining components of the cycle are affected, as the sizes (and volume flow rate) of components are changed. Comparing a poor choice in pinch temperature difference (2 [K]) with the optimal pinch point according to exergoeconomic optimisation, a reduction of 8-19 % in the heat cost is possible.

From the fixed pinch temperature differences of Fig. 4, it is clear that the levels of the optimised heat exchanger temperature differences are in approximately $\Delta T_{\text{pinch}} = 4-6$ K. The obtained magnitude of cost optimal temperature differences in evaporators and condensers matches well with values from literature Granryd [43] for similar operating hours. Based on observations from the derived results for changed temperatures, configurations and working fluids, it is found that the optimum changes as much as from 2 K to 11 K, considering both evaporator and condenser.

3.2. Performance of SF and SR configurations at fixed source temperature (20 °C)

The exergoeconomic optimum has been calculated for each of the eight systems for the range of temperatures presented in Fig. 3 considering both SF and SR configurations. The results correspond to a source temperature of $T_{\text{source}} = 20$ °C.

The resulting levelized cost per exergy unit (including operation and investment cost for the lifetime of the plant), levelized cost of heat and Lorenz efficiencies are presented in Fig. 5a, Fig. 5b and Fig. 5c, respectively. The technical constraints presented in Table 2 are examined for each of the configurations. Feasible solutions are indicated by filled markers in the curves. Solutions that are allowed thermodynamically, but are practically infeasible due to technical constraints, are indicated by open markers. For a few of the considered configurations, results for part of the temperature span are not presented, due to other limitations, such as e.g. condenser pressure above the critical pressure of the working fluid. This is the case for, e.g., R407C and R290 in small parts of the sink temperature span. R744 is limited by a constraint on the upper pressure level in the gas cooler.

By investigation of the two DH HP configurations in Fig. 5, it appears that the levelized cost per exergy unit decreases with higher sink temperatures. This trend is, however, opposite to the trend of the cost of heat, which increases with the sink temperature. Both the cost per exergy unit and heat cost curves are not continuous between the two configurations SR and SF, but the trends of the curves are similar, corresponding to the characteristics of the working fluid. The main thermodynamic difference between

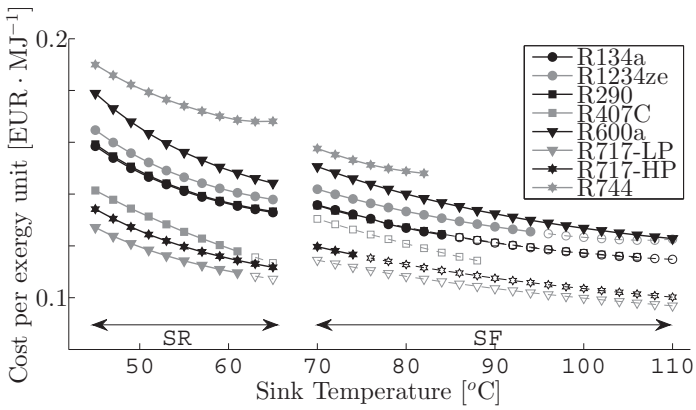

(a) Cost per exergy unit for cost optimal HP system

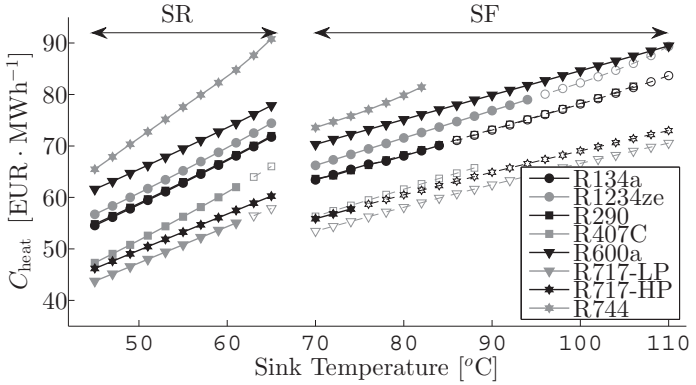

(b) Levelized heat cost of HP system for $\dot{Q}_{\text{heat}} = 1\text{MW}$

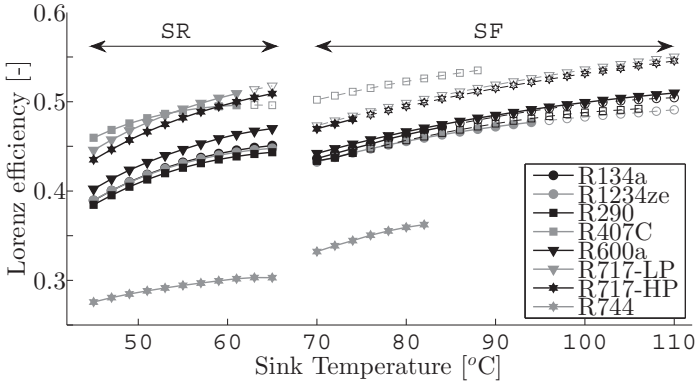

(c) Lorenz efficiency for cost optimal HP system

Figure 5: Cost per exergy unit, levelized heat cost and Lorenz efficiency for optimised SF and SR configurations with a fixed heat source temperature (20 °C). Open markers indicate that the calculated solution exceeds limits given in Table 2

the two configurations is a larger sink temperature glide for the SF configuration.
Considering only the technically feasible solutions, it is found that the lowest cost per exergy unit is from a HP integrated as a SR configuration with sink temperature at approximately 60 °C. For the production cost of heat, the lowest cost is found for SR at the lowest possible sink temperature. In the case of a DH network operated at low temperatures (e.g. "new distribution"), the cost of exergy for installing the SF unit (sink temperature 70 °C) is approximately 5 % lower than installing the corresponding SR unit (sink temperature 45 °C). For the same configurations and sink temperature, the cost of heat for SF is 25 % increased compared to the SR configuration. Considering high DH network temperatures (e.g. "Transmission") the SR configuration proposes the lowest cost considering both cost per exergy unit and production cost of heat.
At high sink temperatures, only a few of the HP systems are applicable. This is mainly a consequence of the pressures on the high pressure side. The refrigerants R717 and R407C are highly competitive throughout the investigated temperature span when comparing cost of heat, but both working fluids experience limitations in applicability of components for a significant part. The limited applicability of the R717-HP system is due to high discharge temperatures as presented in Table 5, whereas the limitations for the R717-LP is mainly due to the pressure constraint. At the high sink temperatures, only the R600a HP system is applicable, but at about 30 % increased costs compared to the configuration with lowest cost (R717-LP).
For both the SR and the SF configurations transcritical R744 HP systems are not competitive. It is clear from Fig. 5b that the cost of heat is significantly higher than for other systems. This is due to several factors such as higher component cost due to increased pressure limitations and problematic sink temperature glide for both configurations. Transcritical R744 systems typically benefit from a sink outlet temperature below the critical temperature of the working fluid [44], which is not the case in any of the investigated configurations. This explains why R744 approaches the heat cost of the remaining systems at very low sink temperatures, as the sink outlet temperature approaches that of the two-phase fluid at critical pressure of R744.
The difference in heat production costs from the most to the least cost effective (not including R744) is at a constant level of 16.5 to 20 [€/MWh^{-1}] throughout the investigated sink temperature span. This results in a relative span of between 27 - 41 % increased cost for the least cost effective systems.
The efficiencies of the optimised HP systems range from 0.27 to 0.55 [/]. Examination of the Lorenz efficiency reveals similar tendencies for the HP systems. The HP systems experience slightly increasing cycle efficiency with increasing sink temperature. As for the cost of heat, the Lorenz efficiency is not continuous when changing from the SR to the SF configuration.
For the case of source temperatures at 20 °C, four working fluids are recommended for SF configurations, whereas for the SR only two different types should be utilised. In terms of increasing temperatures, the recommendation for SF is R717-HP, R134a, R1234ze, R600a. For SR the R717-LP should be utilised until infeasible due to a technical constraint (high pressure), after which the R717-HP is the solution with lowest cost of heat.

3.3. Performance of SF and SR configurations at a range of source temperatures

Similar results are obtained for other values of source temperatures. The result of each of the individual source temperature sets resembles the results of Fig. 5b and Fig. 5c, but with variation in the temperature lift of the HP. The results of the heat cost and efficiency change, as well as the constraints related to component limitations result in changed temperature limits.
The obtained results are presented in (T_{source}, T_{sink}) plots for the HP heat production cost and the corresponding COP. The production costs are evaluated for all combinations of sink and source temperatures (as in section 3.2), and the type with lowest cost of heat is selected among the feasible systems. At certain points, the cheapest solution changes from one system to another. These changes are presented by a black line. For SF configurations the most cost effective HP system is presented in Fig. 6a with the corresponding HP COP in Fig. 6b, whereas the SR configuration is presented in Fig. 6c and 6d, respectively.
For the SF configuration, it is found that the R717-HP is the configuration with the best economy, but due to component limitations, this is only in a limited area of the domain. The area of feasibility for the R717-HP system is limited by high discharge temperature, which is represented by a tilted constraint allowing the highest sink temperatures at

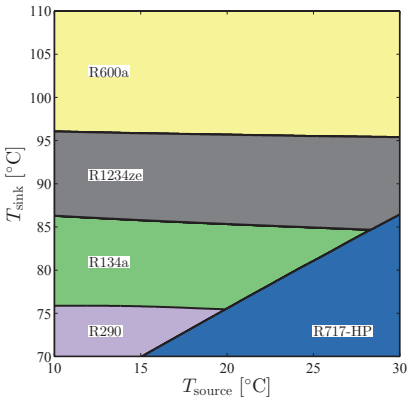

(a) Cost effective HP systems for SF configuration

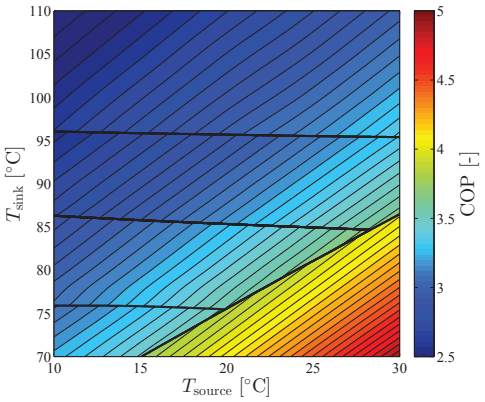

(b) COP of optimal SF configuration

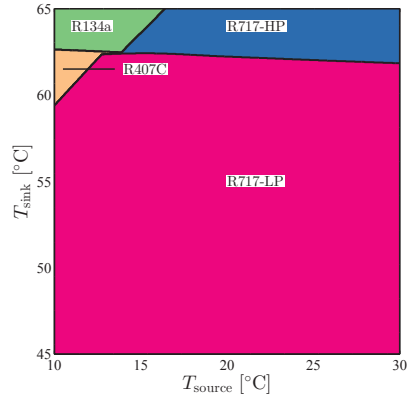

(c) Cost effective HP systems SR configuration

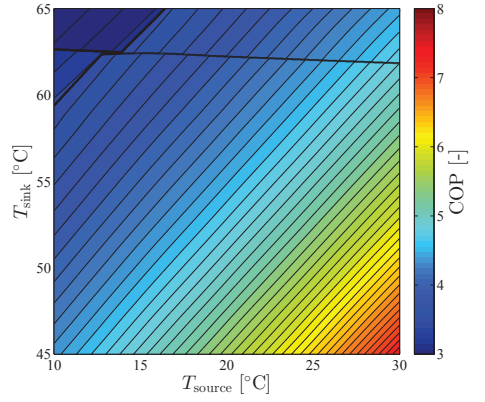

(d) COP of optimal SR configuration

Figure 6: Most cost-effective HP systems and corresponding COP for the two DH configurations SF and SR. The presented working domain corresponds to a range of sink and source temperatures according to typical network configurations.

high source temperatures. The second constraint is due to pressure limitations. This constraint is close to horizontal, as the application limit is almost without influence from the source temperature. R290 has a marginally lower cost than R134a, but the component limitations limit the applicability at approximately 75 °C. The pressure limit of R134a is at approximately 85 °C and R1234ze is applicable below 95 °C. R600a is a feasible solution in the full temperature span of sink and source. R744, R717-LP and R407C are not optimal in any part of the working domain either because of component limitations or uncompetitive heat cost.

The COP of the economically competitive technologies is presented for each of the HP systems in the chosen working domain of Fig. 6b. The COP is increasing for decreasing temperature lift, resulting in an increased COP when approaching the lower right corner from the upper left corner.

For a large fraction of the working domain of the SR configuration, the R717-LP system proposes the lowest cost of heat and the highest cycle efficiency. The system is constrained by two component limitations. At low source temperatures, the discharge temperature exceeds the set limitation. For higher source temperatures than approximately 13 °C, the R717-LP system is constrained by the maximum high pressure limit corresponding to 62-63 °C. Three systems (R407C, R134a and R717-HP) propose the lowest cost of heat for the remaining sink temperature span. The COP of the corresponding systems are significantly higher for SR systems than for the SF ones due to the lower temperature lift of the HP.

3.4. Lorenz efficiency of optimised district heating heat pumps

Fig. 7 presents the cycle efficiency of the two configurations. The data set is identical to the results presented in Fig. 6b and Fig. 6d, but the data are compared based on sink temperatures and the logarithmic mean temperature lift $\bar{T}_{\text{lift}}$. The investigated sink and source temperature span results in a parallelogram, where the upper left corner and lower right corner correspond to source temperatures below or above the considered temperature span.

Investigation of the two figures (especially for the SR configuration in Fig. 7b) indicates that for a limited sink temperature range, the Lorenz efficiency of a DH HP system can be estimated as constant for a specific $\bar{T}_{\text{lift}}$. The sink temperature may change the Lorenz efficiency significantly in the case where technical constraints limit the applicability of a system. An example with a significant offset is the horizontal constraint (discharge temperature) for R717-LP in Fig. 7a.

All of the investigated Lorenz efficiencies are between 0.36 and 0.52. A significant increase in efficiency is found for high logarithmic mean temperature lifts.

3.5. Parametric investigation

Several assumptions and technical parameters have been used in the analysis. In order to evaluate the possible deviations of incorrectly estimated parameters, a parametric investigation is carried out, considering both the price of heat and the Lorenz efficiency. The results are presented in Fig. 8 for operating temperatures of the HP (Figs. 8a-8b) and for input parameters and economic assumptions (Figs. 8c-8d), respectively. The parametric study is made for two HP systems (R717-LP and R600a) at a source temperature of 20 °C for the SF configuration in network type 3 (Table 1). Results for R717-LP and R600a are in gray and black, respectively. Generally the effects of changed assumptions are identical for the two invested HP systems, which indicate that the cost and cycle efficiency may be affected by the assumed parameters, but with similar trend and magnitude for the investigated HP systems. In this way, we conclude that the presented results for the optimal HP systems will not be affected by different parameter values.

The steepest gradients in Fig. 8a are for the source outlet temperature and sink outlet temperature. The two temperatures directly affect the evaporation and condensation pressures and thus the power consumption of the HP. This is contrary to the Lorenz efficiency (in Fig. 8b) where the two temperatures have a smaller impact, compared with the two inlet temperatures.

Considering the economic assumptions in Fig. 8c, electricity cost and isentropic efficiency have a large impact on heat cost (approximately 20-22 % changed production price for 30 % change in the parameter). The corresponding changes for the remaining parameters, such as component cost and heat transfer coefficient, are below ± 10 % for a 30 % change compared to the assumption.

For the corresponding impact of assumptions on the Lorenz efficiency, only one parameter has a significant influence. A 30 % decrease of isentropic efficiency results in up to 20 % reduction in the Lorenz

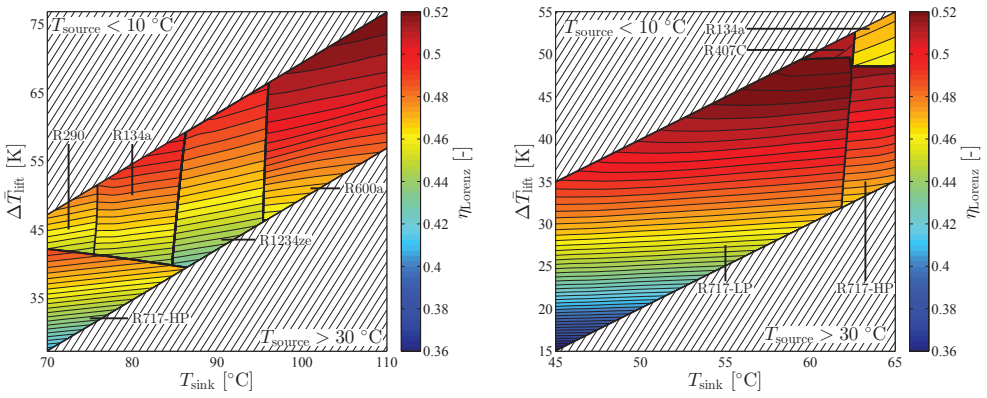

(a) SF configurations

(b) SR configurations

Figure 7: Lorenz efficiency of the two DH configurations SF and SR depending on (T_{sink} and $\bar{T}_{\text{lift}}$).

efficiency. A corresponding change for all of the remaining parameters yields at maximum ± 3 % on Lorenz efficiency.

4. Discussion

The use of (exergo-)economic optimisation may result in large reductions in the heat cost for a utility plant, if compared to a rule of thumb minimum temperature differences for heat exchangers. The relative reduction of heat cost by exergoeconomic optimisation (up to 19 % in Fig. 4) is similar in magnitude to the largest impact of the parametric investigation (up to 22 % for a 30 % reduction in electricity cost). An energy-based optimisation would result in low minimum temperature differences for heat exchangers, which is not in line with the results of the economic optimum. For the calculations performed for the assessment, variable cost represents approximately two-thirds of the combined cost of heat, indicating that investment costs are important in order to establish a competitive system.

The cost of heat is not directly comparable when considering the configurations SF and SR, as the configuration SR will require other production technologies in order to accommodate the supply temperature of the DH network. Using exergoeconomic analysis, it is found that the cost per exergy unit should be considered when making a decision whether to install the (cost of heat) optimal SR or SF configuration.

Depending on the technology, preheating of the stream may affect the efficiency of production, and may thus increase heat production prices of other producers such as combined heat and power plants. Electric heaters or fossil fuel boilers would in most cases not be affected, and preheating would typically present the lowest cost of heat. The change in cost per exergy unit of the CHP-plant (or other main heating technology in the DH network) can assist in addressing whether or not the installation of SR systems should be recommended.

Other types of compressors have been identified for high volumetric capacities, and such technologies may reduce investment cost for the system. The absence of detailed cost data has omitted such technologies from the comparison. The pressure or temperature levels, as well as the isentropic and volumetric efficiencies, have to be updated appropriately, and may in such case alter the working domain. A 10 % reduction in isentropic efficiency (leading to 5-6 % reduction in the cost of heat) corresponds to approximately 20 % reduction in component cost (5-7 % in the cost of heat), of which the compressor is only one of the considered components.

The results presented in the paper are derived from simulations of verified models. Heat transfer correlations are validated with experimental results and verified by manufacturer data. Equipment cost correlations stem from manufacturer data or trade businesses. The same approach has been applied for all investigations, and thus any incorrect data

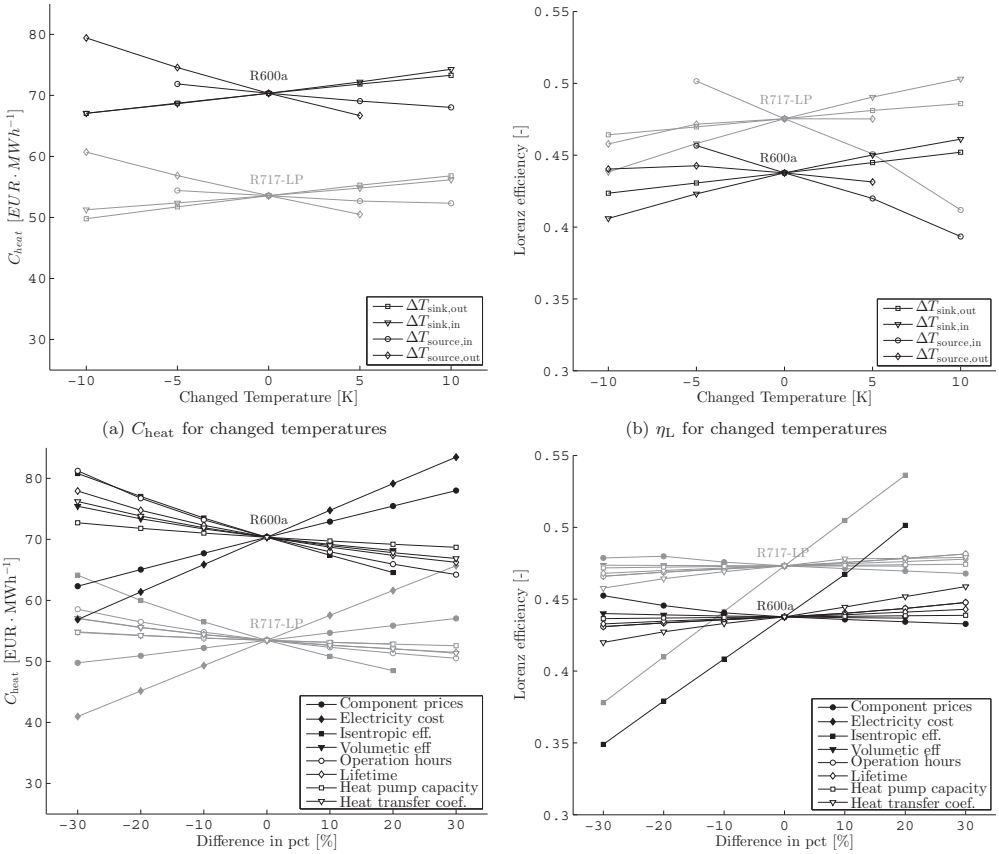

(a) C_{heat} for changed temperatures

(b) η_{L} for changed temperatures

(c) C_{heat} for changed parameters

(d) η_{L} for changed parameters

Figure 8: Parametric study of individual parameters and cost functions for both the optimised cost of heat and Lorenz efficiency.

will mainly affect the absolute values and not the interrelations of the technologies.
The results of this paper may address researchers involved in energy system studies where HPs and their performance are of high importance. The preferred technologies and corresponding Lorenz efficiency may be obtained from the paper using only a few temperature levels corresponding to pinch point analysis and the HP configuration.

5. Conclusion

The technology constraints and economic relationships regarding two HP configurations for DH networks are studied in order to establish the cost of heat for the best available technology and corresponding cycle efficiency. The two identified configurations may supply heat from a central location, which may lead to favourable effects from economy of scale and the use of high temperature heat sources.
Eight systems are examined from based on applicability, and the systems are optimised for each operating condition using exergoeconomic theory. The HPs are compared based on cost of heat, but the analysis indicates that the cost per exergy unit should be considered in order to ensure capable decisions regarding investment in either the SR or SF configuration.
When considering the applicability of components, a high number of infeasible operating conditions are found. The result is up to 27-32 % increased cost at high sink temperatures for the best practically feasible system (R600a), compared to the most competitive thermodynamic cycle. At low sink temperatures, the R717-LP provides the lowest cost of heat for the SR configuration, and the R717-HP for the SF configuration.
At high and medium temperature lifts, cycle efficiencies of 45 - 50 % of the theoretical maximum (Lorenz) can be achieved, whereas for low temperature lifts, efficiencies as low as 36 % can be expected.

Acknowledgement

This work was supported by Copenhagen Cleantech Cluster (CCC), DONG Energy, and Danish Technological Institute (DTI).

References

[1] Lund, H., Clark, W.W.. Management of fluctuations in wind power and CHP comparing two possible Danish strategies. Energy 2002;27(5):471–483.
[2] Rinne, S., Syri, S.. Heat pumps versus combined heat and power production as CO2 reduction measures in Finland. Energy 2013;57:308–318.
[3] Hedegaard, K., Mathiesen, B.V., Lund, H., Heiselberg, P.. Wind power integration using individual heat pumps - analysis of different heat storage options. Energy 2012;47(1):284–293.
[4] Münster, M., Morthorst, P.E., Larsen, H.V., Bregnbaek, L., Werling, J., Lindboe, H.H., et al. The role of district heating in the future Danish energy system. Energy 2012;48(1):47–55.
[5] Blarke, M.B.. Towards an intermittency-friendly energy system: Comparing electric boilers and heat pumps in distributed cogeneration. Applied Energy 2012;91(1):349–365.
[6] Ommen, T., Markussen, W.B., Elmegaard, B.. Comparison of linear, mixed integer and non-linear programming methods in energy system dispatch modelling. Energy 2014;74(1):109–118.
[7] Centralkomunernes Transmissionsselskab I/S, . Technical key figures (in Danish: Tekniske nøgletal). 2013. [accessed 26.09.13].
[8] Østergaard, P.A.. Ancillary services and the integration of substantial quantities of wind power. Applied Energy 2006;83(5):451–463.
[9] Ommen, T., Markussen, W., Elmegaard, B.. Heat pumps in combined heat and power systems. Energy; 2014; 76(1):989–1000.
[10] Bejan, A., Tsatsaronis, G., Moran, M.. Thermal Design & Optimization. 1st edition ed.; New York: John Wiley & Sons; 1996.
[11] Lorentzen, G.. The use of natural refrigerants: a complete solution to the CFC/HCFC predicament. International Journal of Refrigeration 1995;18:190–197(8).
[12] Eisa, M.A.R., Best, R., Holland, F.A.. Working fluids for high temperature heat pumps. Journal of Heat Recovery Systems 1986;6(4):305.
[13] Brunin, O., Feidt, M., Hivet, B.. Comparison of the working domains of some compression heat pumps and a compression-absorption heat pump. International Journal of Refrigeration 1997;20(5):308.
[14] Lorenz, H.. Die ausnützung der brennstoffe in den kühlmaschinen. Zeitschrift für die gesammte Kälte-Industrie 1894;1:10–15.
[15] Dansk Fjernvarme, . Benchmarking, statistics 2011/2012 (in Danish: Benchmarking, statistik 2011/2012). 2013. [accessed 26.09.13].
[16] Berntsson, T.. Heat sources - technology, economy and environment. International Journal of Refrigeration 2002;25(4):428–438.
[17] Elmegaard, B., Houbak, N.. Simulaton of the Avedøreværket Unit 1 Cogeneration Plant with DNA. Proceedings of The 16th International Conference on Efficiency, Cost, Optimization, Simulation, and Environmental Impact of Energy Systems (ECOS 2003),; Technical University of Denmark; 2003,.
[18] F-Chart Software (LLC.), . Engineering equation solver (EES). 1992.
[19] Claesson, J.. Thermal and hydraulic performance of compact brazed plate heat exchangers operating as

evaporators in domestic heat pumps. Ph.D. thesis; KTH, Energy Technology; 2005.

[20] Thonon, B., Vidil, R., Marvillet, C.. Recent research and developments in plate heat exchangers. Journal of Enhanced Heat Transfer 1995;2(1-2):149–155.

[21] Qiao, H., Aute, V., Lee, H., Saleh, K., Radermacher, R.. A new model for plate heat exchangers with generalized flow configurations and phase change. International Journal of Refrigeration 2013;36(2):622–632.

[22] Palm, B., Claesson, J.. Plate heat exchangers: Calculation methods for single and two-phase flow. Heat Transfer Engineering 2006;27(4):88–98.

[23] Martin, H.. A theoretical approach to predict the performance of chevron-type plate heat exchangers. Chemical Engineering and Processing: Process Intensification 1996;35(4):301–310.

[24] Yan, Y.Y., Lin, T.F.. Evaporation heat transfer and pressure drop of refrigerant R-134a in a plate heat exchanger. Journal of Heat Transfer 1999;121(1):118–127.

[25] Yan, Y.Y., Lio, H.C., Lin, T.F.. Condensation heat transfer and pressure drop of refrigerant R-134a in a plate heat exchanger. International Journal of Heat and Mass Transfer 1999;42(6):993–1006.

[26] SWEP International AB, . SSP G7, V 7.0.3.19. 2013. [accessed 26.09.13].

[27] GEA Heat Exchangers, Inc. PHE Division, . FlatPlate-SELECT - ONLINE. 2013. [accessed 26.09.13].

[28] SWEP International AB, . SWEP - products & solutions (B400, B120T (F-pressure), B17 product sheets) - non-disclosure agreement. 2013. Private communication.

[29] Nekså, P., Rekstad, H., Zakeri, G.R., Schiefloe, P.A.. CO_2-heat pump water heater: characteristics, system design and experimental results. International Journal of Refrigeration 1998;21(3):172.

[30] Tsatsaronis, G.. Definitions and nomenclature in exergy analysis and exergoeconomics. Energy 2007;32(4):249–253.

[31] DONG Energy, . Development of electricity cost (in danish: Prisudvikling). 2012. URL: `http://www.dongenergy.dk/erhverv/El/omprisen/basiselkvartal/Pages/Prisudvikling.aspx`; [accessed 23.06.13].

[32] SKAT. Examples for calculation of taxreduction for various heat production units (in danish: Eksempler på beregning af afgiftslempelse for forskellige varmeproduktionsanlæg). 2014. URL: `https://skat.dk/SKAT.aspx?oID=2061615`; [accessed 05.12.14].

[33] Ommen, T., Jensen, J., Markussen, W., Reinholdt, L., Elmegaard, B.. Technical and economic working domains of industrial heat pumps: Part 1 - single stage vapour compression heat pumps. International Journal of Refrigeration 2015;doi:10.1016/j.ijrefrig.2015.02.012.

[34] Jensen, J., Ommen, T., Markussen, W., Reinholdt, L., Elmegaard, B.. Technical and economic working domains of industrial heat pumps: Part 2 - ammonia-water hybrid absorption-compression heat pumps. International Journal of Refrigeration 2015;doi:10.1016/j.ijrefrig.2015.02.011.

[35] H. Jessen Jörgensen A/S, . Priskatalog 2013. 2013. [accessed 26.09.13].

[36] FK Teknik A/S, . Priskatalog 2013. 2013. [accessed 26.09.13].

[37] Ahlsell Danmark ApS, . Priskatalog 2013. 2013. [accessed 26.09.13].

[38] Johnson Controls, Inc., . HPO R717 compressor cost - non-disclosure agreement; 2013. Private communication.

[39] Bach, B.. Integration of heat pumps in greater Copenhagen. Master's thesis; Technical University of Denmark; 2014.

[40] CTR, HOFOR and VEKS, . Heat plan greater copenhagen 3 (in danish: Varmeplan hovedstaden 3). 2014. URL: `http://www.varmeplanhovedstaden.dk/publikationer-og-moeder`; [accessed 25.03.14].

[41] Cecchinato, L., Corradi, M., Minetto, S.. A critical approach to the determination of optimal heat rejection pressure in transcritical systems. Applied Thermal Engineering 2010;30(13).

[42] HOFOR. Price for district heating 2012 (in Danish: Prisen på fjernvarme 2012). 2012. URL: `http://www.hofor.dk/fjernvarme/prisen-pa-fjernvarme-2012-for-private/`; [accessed 25.03.15].

[43] Granryd, E.. Refrigerating Engeneering - part I. Royal Institute of Technology, KTH, Stockholm; 2005.

[44] Kim, M.H., Pettersen, J., Bullard, C.W.. Fundamental process and system design issues in CO2 vapor compression systems. Progress in Energy and Combustion Science 2004;30(2):119–174.

[45] Thonon, B., Bontemps, A.. Condensation of pure and mixture of hydrocarbons in a compact heat exchanger: Experiments and modelling. Heat Transfer Engineering 2002;23(6):3–17.

[46] Longo, G.A.. Heat transfer and pressure drop during hfc refrigerant saturated vapour condensation inside a brazed plate heat exchanger. International Journal of Heat and Mass Transfer 2010;53(5-6):1079–1087.

Appendix A. Heat transfer correlations

Appendix A.1. Single-phase heat transfer coefficients

Martin [23] derives theoretical equations for the friction factor and heat transfer coefficients, which are compared to experimental observations. The correlation shows high coherence with manufacturer data for the full range of application.
The friction factor is defined as:

$$\xi = \frac{2 \cdot \Delta p \cdot d_h}{\rho \cdot u^2 \cdot L_p} \tag{A.1}$$

where Δp is the pressure drop, L_p is the length of the plate, and

$$d_h = \frac{4\hat{a}}{\Phi} \tag{A.2}$$

is the hydraulic diameter, dependent on the amplitude of the plate corrugation $\hat{a}$ and the area enlargement factor Φ of the plate.
The friction factor can be calculated from the corrugation inclination angle φ and the friction factor for straight longitudinal flow $\xi_0(\mathrm{Re})$ and wavy longitudinal flow $\xi_1(\mathrm{Re})$:

$$\frac{1}{\sqrt{\xi}} = \frac{\cos\varphi}{b \cdot \tan\varphi + c\sin\varphi + \xi_0(\mathrm{Re})/\cos\varphi + \frac{1-\cos\varphi}{\sqrt{\xi_1(\mathrm{Re})}}} \tag{A.3}$$

where the constants b and c are fixed friction parameters. The Nusselt number can then be calculated using viscosity μ and the corrugation inclination angle φ:

$$\mathrm{Nu} = 0.122\mathrm{Pr}^{1/3} \cdot (\mu/\mu_w)^{1/6} \cdot [\xi \cdot \mathrm{Re}^2 \sin(2\varphi)]^{0.374} \tag{A.4}$$

Appendix A.2. Two-phase heat transfer coefficients

Several studies have examined the effect of two-phase flow in a chevron-type plate heat exchanger in order to correlate heat transfer coefficients and pressure losses [24, 45, 46]. The heat transfer coefficients of the evaporation and condensation process are evaluated using Yan and Lin [24] and Yan et al. [25], respectively. The studies report local heat transfer coefficients as a function of vapour quality. This is done by calculating an equivalent all liquid mass flux G_{eq} defined as:

$$G_{\mathrm{eq}} = G(1 - X_m + X_m(\frac{\rho_l}{\rho_v})^{1/2}) \tag{A.5}$$

where X_m is the average vapour quality, and ρ_l and ρ_v are densities of saturated liquid and vapour. Using this definition the equivalent Reynolds number can be calculated as:

$$\mathrm{Re}_{\mathrm{eq}} = \frac{G_{\mathrm{eq}} \cdot d_h}{\mu_l} \tag{A.6}$$

and correspondingly the equivalent Boiling number:

$$\mathrm{Bo}_{\mathrm{eq}} = \frac{q''_w}{G_{\mathrm{eq}} \cdot i_{fg}} \tag{A.7}$$

where i_{fg} is the enthalpy of vaporization, and q''_w is the imposed wall heat flux.
Using these definitions, the heat transfer coefficients for evaporation and condensation are calculated from as Eq. A.8 and Eq. A.9, respectively.

$$(\frac{h \cdot d_h}{k_l})\mathrm{Pr}_l^{-1/3}\mathrm{Re}^{0.5}\mathrm{Bo}_{\mathrm{eq}}^{0.3} = 1.926\mathrm{Re}_{\mathrm{eq}} \tag{A.8}$$

$$(\frac{h \cdot d_h}{k_l}) = 4.118\mathrm{Re}_{\mathrm{eq}}^{0.4}\mathrm{Pr}_l^{1/3} \tag{A.9}$$

For further reading and the corresponding friction factors required in order to calculate pressure losses, the reader is referred to the cited literature. The two-phase heat transfer correlations and pressure drop correlations generally show good agreement with manufacturer data.

Appendix H

Paper 6 - Energy & Buildings

Brian Elmegaard, Torben Ommen, Michael Markussen, Johnny Iversen

Integration of space heating and hot water supply in low temperature district heating

Energy & Buildings, [accepted for publication], doi:10.1016/j.enbuild.2015.09.003.

Integration of Space Heating and Hot Water Supply in Low Temperature District Heating

Brian Elmegaard[a,*], Torben Schmidt Ommen[a], Michael Markussen[b], Johnny Iversen[c]

[a] *DTU Technical University of Denmark, Department of Mechanical Engineering, 2800 Kgs. Lyngby, Denmark*
[b] *DONG Energy, 2830 Virum, Denmark*
[c] *Grontmij, 2600 Glostrup, Denmark*

Abstract

District heating may supply many consumers efficiently, but the heat loss from the pipes to the ground is a challenge. The heat loss may be lowered by decreasing the network temperatures for which reason low temperature networks are proposed for future district heating. The heating demand of the consumers involves both domestic hot water and space heating. Space heating may be provided at low temperature in low energy buildings. Domestic hot water, however, needs sufficient temperatures to avoid growth of legionella. If the network temperature is below the demand temperature, supplementary heating is required by the consumer. We study conventional district heating at different temperatures and compare the energy and exergetic efficiency and annual heating cost to solutions that utilize electricity for supplementary heating of domestic hot water in low temperature district heating. This includes direct electric heating and three heat pump solutions applying R134a and R744. The results show that conventional solutions at lowest possible temperature have the highest exergetic efficiency of 28% and lowest annual cost of € 690 for a 159 m^2 house. The best low temperature system is an R134a heat pump with hot water storage on the district heating side, which reaches 25% exergetic efficiency.

Keywords: Low temperature district heating, space heating, domestic hot water, heat pumps, exergy

1. Introduction

District heating provides a means for efficient heating in urban environments. In particular, the integration with combined heat and power (CHP) plants and heat storage makes it possible to produce power and heat with significant flexibility and at high efficiency. The Danish energy system is an example of a system for which extensive expansion of CHP has contributed to make it possible to not increase the energy consumption of society over the last decades [1].

Figure 1 illustrates a generic district heating system which involves combined heat and power production as the main heat supplier. It supplies district heating to a stratified storage tanks, which is connected to the transmission network in order to fulfil the consumer demand. The transmission network operates at high temperatures and has a high annual utilization of capacity, which results in relatively low heat loss. The heat is transferred to the distribution system via substations. The distribution system works with lower temperatures, but due to smaller pipe

*Corresponding author
Email addresses: be@mek.dtu.dk (Brian Elmegaard), tsom@mek.dtu.dk (Torben Schmidt Ommen), mimom@dongenergy.dk (Michael Markussen), johnny.iversen@grontmij.dk (Johnny Iversen)

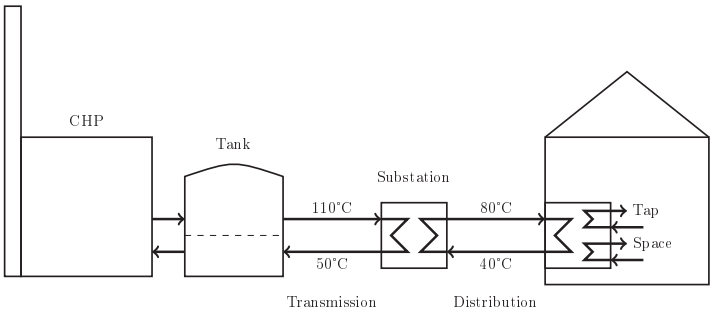

Figure 1. Illustration of district heating system

dimensions and lower capacity, the heat loss is relatively high. Heat is eventually supplied to the consumers by service pipes.

The configuration and performance of the heat supply of a district heating system is governed by a number of criteria. These include:

Energy source The energy input to the district heating system may be fossil fuels, renewable fuels or alternative renewable energy sources. These may be heat sources, e.g., solar or geothermal, or electric power from wind, hydro, or photovoltaics.

For larger systems more heat producers may be connected to the system, such that the heat is based on a mixture of sources.

Conversion Efficiency The conversion efficiency of the energy input to heat supply involves efficiency of the plants, which may be combined heat and power, CHP, or separate heat production.

Heat pumps will most likely play a larger role in the future. For these the Coefficient of Performance, COP, will have an impact on the efficiency of the heat supply.

Heat loss from the network is another important factor. This factor is closely related to the temperature of the forward and return lines of the system.

System Configuration The system may include a number of subsystems which are connected by pipes with a given capacity.

For larger systems with longer distances and with different supply systems on the consumer side, the network will be constituted of a transmission system and distribution systems for each consumer subsystem.

District heating has the potential of being an efficient and cost-effective heat production. A drawback of district heating is, however, the heat loss from transmission and distribution pipes. This is, however, the only energy loss that occurs in the system, and avoiding any heat loss would result in a 100% efficient supply based on first law approach.

But heat loss is not the only source of thermodynamic irreversibilities in district heating. Heat transfer at finite temperature differences and pressure loss in fluid flow results in exergy destruction.

On average the heat loss amounts to about 20 % of the energy consumption for Danish district heating systems [1]. For further developing district heating solutions low temperature transmission

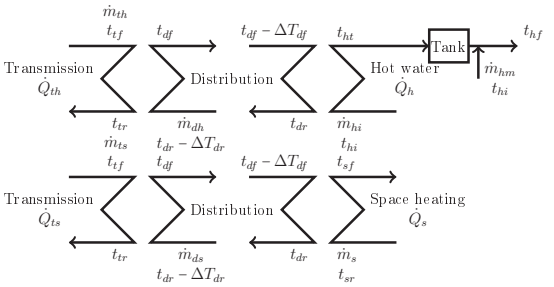

Figure 2. Conventional system

and distribution systems are currently investigated by different researchers as this will increase the efficiency of the total system.

Song [2] develops an exergy-based methodology for investigating the total performance of heating systems based on CHP and heat pumps. It is shown that exergetic efficiency of conventional heating is less than 10 % and that up to 50 % efficiency may be reached by improved systems including waste heat recovery.

Olsen et al. [3] discuss the potential of using low temperature district heating for low energy buildings and the demand for minimum heat loss. In [4] a heating system for space heating with low temperature district heating is investigated. [5] also discusses the potential benefits of low temperature district heating, specifically reduced heat loss, integration of additional heat sources and increased efficiency. Brand [6] describes solutions for low temperature systems for buildings of various standards.

By integrating heat pumps in the district heating system, low temperature sources, e.g., waste heat, may be integrated. The heat pumps may also provide means for lowering the temperatures in the network by boosting the temperatures by the consumers. Lorentzen [7, 8] suggests R744 (CO_2) as an anternative natural refrigerant for low temperature district heating. Several heat pump configurations are investigated by [9].

Low temperature district heating has been investigated based on energy and exergy criteria by e.g., [10]. In [11] the costs of low temperature district heating in terms of both energy and exergy are studied. A detailed study of exergy losses in a complete district heating network is studied in [12]. Pirouti [13] presents a comprehensive study of both high and low temperature district heating.

1.1. District Heating Configurations

District heating may be connected to the consumer system in different ways as illustrated below. The heat demand of the urban environment is assumed to consist of space heating and domestic hot water. The difference between the systems is in the domestic hot water supply, as the space heating system is the same in all cases for a low energy building with floor heating. In the analysis and illustrations, the configurations for both domestic hot water and space heating are considered.

Conventional configuration. A conventional district heating system is illustrated in figure 2. It connects the heating plant(s) and the consumers by a transmission network from the plants to substations and distribution networks from the substations to the consumers. The consumers need heat both for space heating and hot water consumption. The figure illustrates the two supply

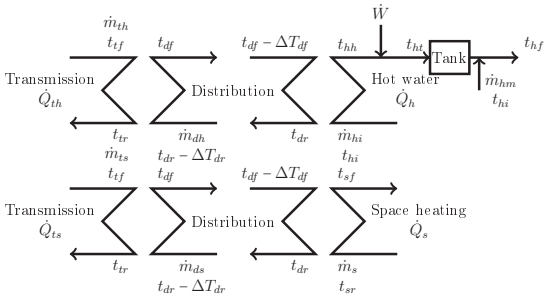

Figure 3. Low temperature system with electric heating of hot water

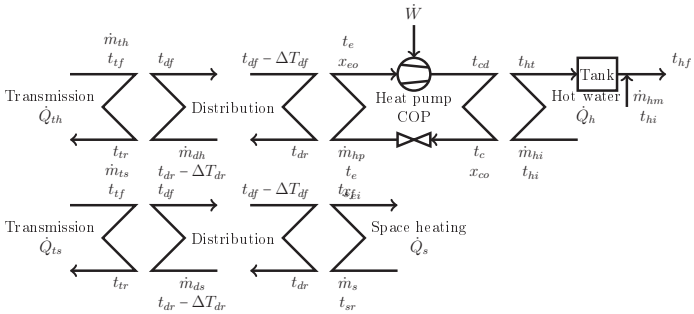

Figure 4. Low temperature system with heat pump and secondary side tank

systems individually, but this is obviously not how the installation would be in practice, as the house is only connected to one supply system from the district heating.

Low temperature configuration with electric heating. Space heating in radiator systems requires temperatures of 50-70 °C, but modern low energy buildings equipped with floor heating makes it possible to lower this temperature to about 30-40 °C. Thus, lower temperature may be possible in the distribution network and accordingly lower heat loss would be acquired. However, if domestic hot water is stored in a tank, it must be heated to 50-60 °C to avoid health risks caused by legionalla bacteria growth. This means that even if the space heating demand can be covered by lower temperature networks, the hot water temperature cannot be avoided. An example of an installation is ilustrated in figure 3. The required hot water temperature is obtained by supplementary electric heating between the district heating and the hot water tank. However, direct electric heating is thermodynamically inefficient. For this reason heat pumps for boosting the hot water temperature are considered. Three heat pump configurations are considered depending on the location of the hot water tank.

Low temperature configuration with heat pump and secondary side tank. The tank may be installed on the consumer side, the secondary side, as illustrated in figure 4. In this configuration the district heating supplies the heat pump evaporator. The heat pump directly heats the domestic hot water, which is stored in a hot water tank. As the fresh water enters at a temperature which is significantly lower than the condenser temperature a significant exergy loss occurs. This makes it relevant to investigate the performance of a transcritical R744 heat pump, which utilizes the temperature glide

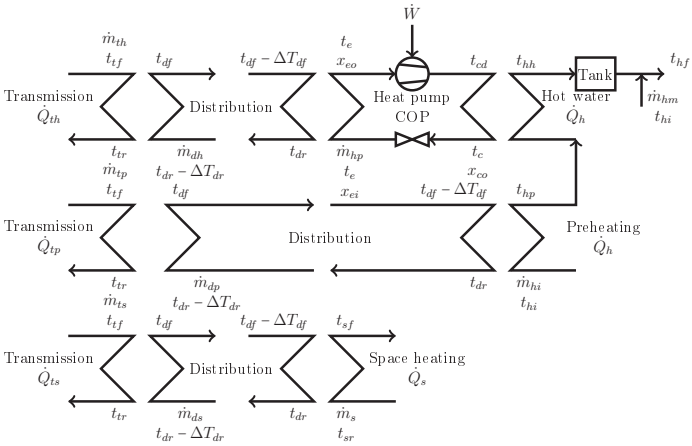

Figure 5. Low temperature system with heat pump, secondary side tank and preheating of domestic hot water

of the working fluid in the gas cooler.

Low temperature configuration with heat pump, secondary side and and preheating. Another way to decrease the irreversibility of the heat transfer is illustrated in figure 5. In this configuration, the fresh water is preheated by district heating before entering the condenser of the heat pump. This configuration would in practice require two storage tanks in order to limit the load on the district heating supply at high demands for hot water.

Low temperature configuration with heat pump and primary side tank. The secondary side hot water tank implies a risk of legionella bacteria growth of the water due to the storage at increased temperature. For this reason, it is required to reach a sufficiently high temperature to eliminate the health risk. This situation may be avoided by a configuration with hot water storage on the district heating side, the primary side, instead. By storing hot water on this side, the fresh water entering the system may be heated by the water in the tank, and no need for storage of the consumer water is involved. This configuration is illustrated in figure 6. As a lower temperature is required in the storage, the heat pump will have a higher efficiency. The district heating supply is both used as the heat source for the heat pump evaporator in the upper part of the configuration, and as the heat sink for the condenser in the middle part of the system and connected to the heat pump by nodes A and B. The temperature in the tank, t_{hh}, is in this case lower than required in the previous configurations and no mixing is made to reach the actual consumer temperature.

1.2. Scope of work

The present paper compares the described concepts for space heating and domestic hot water in conventional district heating and low temperature district heating networks based on annual time-averaged calculations. The development and installation of a heat pump for this purpose is explained in detail in [14], [15] and [16].

Case study for low energy building. The basis of the work is a new settlement of 116 buildings. We study a house of 159 m^2 with 4 inhabitants. It has an annual consumption of 4010 kWh for space heating and 3200 kWh for hot water [14]. The space heating demand occurs about 4000

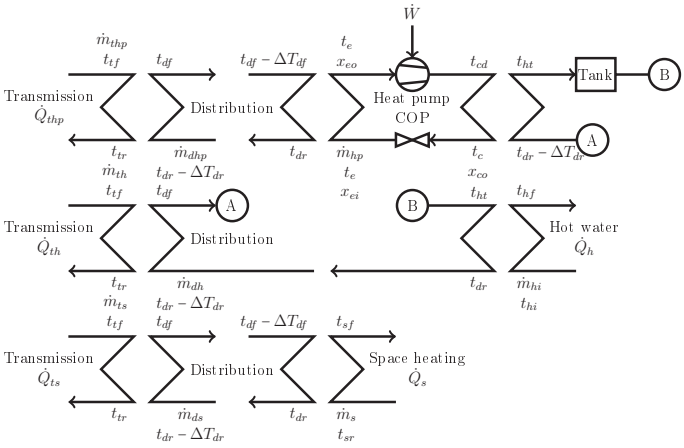

Figure 6. Low temperature system with heat pump and primary side tank

Figure 7. Micro Booster Heat Pump for Hot Water Production

hours annually, whereas hot water is used daily for e.g., showers, dish washing and hand washing. This results in that annual averages of 365 W hot water and 458 W space heating are consumed. Space heating is provided at 30/22°C and hot water at 50/10°C in the house. Hot water is supplied from a tank which may be located on the primary (district heating distribution) side or on the secondary (consumption) side in the system. In the cases where the hot water storage is located on the secondary side a temperature of 60 °C is required in the tank.

Heat loss calculations are based on data and are given as a coefficient per unit pipe length of 65 W/km K in total for both the forward and return sides of the twin pipe. The length of forward and return pipes in the network is 3.6 km. The ground temperature is assumed to be 10 °C. Heat loss is only considered in the distribution network.

The objective of the work is to understand the performance of low-temperature district heating systems compared to conventional systems. The low temperature systems are characterized by the need of supplementary electric heating, e.g., heat pumps, for providing hot water. The work considers the integration of low temperature distribution systems in combination with, possibly existing, transmission systems. This means that the transmission system temperatures are maintained, because it is difficult to change the operation temperatures of such a system. The benefit of low temperature systems is that significantly lower heat loss is obtained while it on the other hands introduces demands for electricity for heat pump operation. The system is assumed to mostly utilize large extraction steam cycle CHP plants as described in e.g., [17] as these are flexible and efficient. If a new system was considered it would be possible to dimension it for low temperature operation. This would mean that the CHP plant would be able to operate at a higher electric efficiency. The effect is however minor as explained in [18].

2. Methods

Based on a screening of the possible configurations, the following cases are studied:

- Conventional system 80/40°C
- Conventional system 65/55°C
- Conventional system 60/30°C
- Low temperature system with electric heating 45/25°C
- Low temperature system with heat pump and secondary side tank 45/25°C
- Low temperature system with heat pump and secondary side tank and preheating 45/25°C
- Low temperature system with heat pump and primary side tank 45/25°C

The heat pump systems are calculated for both a conventional R134a heat pump cycle and a transcritical CO_2 cycle.

The transmission system operates at 85/60°C to cover all cases.

The consumer cost of the energy supply is calculated by estimated electricity and district heating prices of 0.30 €/kWh (2.26 DKK/kWh) [19] and 0.10 €/kWh (0.77 DKK/kWh) [20], respectively, in a conventional system. The benefits resulting of decreased heat loss is assigned to the consumer prices in low temperature scenarios.

2.1. Modeling

The different configurations have been implemented as models in DNA [21]. The models consist of component models which include heat exchangers, distribution pipes and the components of the heat pumps, i.e., evaporator, condenser, compressor and valves. The fundamental laws of thermodynamics are respected in all component models.

The following parameters are used throughout the calculations:

Minimum temperature difference in heat exchangers in cycle	2.5	K
Minimum temperature difference in heat exchangers in network	5	K
Minimum temperature difference in tank coil	5	K
Isentropic efficiency of heat pump compressor	50	%
Heat transfer coefficient from network (distribution and service lines) to ground	1.9	W/K
Ground temperature	10	°C
Pressure loss	0	Pa

for the heat pump compressor heat loss, as well as condenser subcooling and evaporator superheating are neglected.

Heat loss from the network is calculated individually for the forward and return pipes based on the heat transfer coefficient and the temperature difference between water and ground.

2.2. Evaluation of Performance

The results of the calculations are the required heat supply from the transmission system, the electricity demand, the total heat loss and annual cost of heat. The analysis is based on annual averages of heat demands for both space heating and hot water consumption.

The results are quantified in terms of energy, exergy and consumer costs. For energy a unit energy from district heat and electricity are equal, which makes it difficult to define a meaningful efficiency. Contrary, exergy not only measures the energy content, but also takes the "quality" of the energy into account. In thermodynamics exergy is defined as the maximum work that may be extracted from a given amount of energy. This theoretical measure may, however, be described in several ways that show the value of exergy as a measure of quantity and quality of energy. Exergy may namely also be stated to be the part of an amount of energy that can be converted into any other energy form by a thermodynamically reversible process. For, e.g., electric, mechanical, kinetic and potential energy this fraction is unity, whereas for heat and substances at finite temperature the fraction is smaller.

The exergy analysis in this study is based on the approach described in [22].

Exergy will due to irreversible energy conversion be destroyed and is closely related to entropy that is generated, due to the Guoy-Stodola theorem. It states that exergy destruction and entropy generation are proportional:

$$\dot{E}_{\mathtt{dest}} = T_0 \dot{S}_{\mathtt{gen}} \tag{1}$$

The two quantities are related by the reference temperature. This shows that exergy resembles a state variable when the reference conditions p_0, T_0 are decided. In the present case they are set to 1 bar and 10°C, respectively.

Primary energy sources as fuel, solar, and wind can all be found to be exergy within 5% accuracy. This shows that exergy destruction is also a quantification of the primary energy supply to a system.

Primary energy utilization in the system may thus be evaluated by the exergetic efficiency:

$$\eta_x = \frac{\dot{E}_{\mathrm{prod}}}{\dot{E}_{\mathrm{cons}}} \tag{2}$$

In the present case the exergy consumption is electricity and district heat, the exergetic product is the space heating and domestic hot water.

$$\eta_x = \frac{\dot{E}_{\mathrm{dhw}} + \dot{E}_{\mathrm{sh}}}{\dot{E}_{\mathrm{dh}} + \dot{E}_{\mathrm{el}}} \tag{3}$$

As changes in kinetic and potential energy are neglected and chemical reactions do not occur, only the physical exergy of the flows is calculated. It is given as:

$$\dot{E} = \dot{m}(h - h_0 - T_0(s - s_0)), \text{ where } h_0 \text{ and } s_0 \text{ are found at } (p_0, T_0) \tag{4}$$

In the present case the exergy input to the heat supply system is defined by the transmission network. We thus neglect the exergy destruction in the CHP plant. This means that it is assumed that the heat in the transmission system is assumed to have been produced by a reversible heat engine driving a reversible heat pump that produces the heat in the system at 85 °C/60°C. Similarly, the consumed electricity is assumed to be produced by a reversible heat engine. This is naturally not the case, so in order to quantify the primary energy utilization the calculated exergetic efficiencies should be multiplied by the exergetic efficiency of the CHP production to the transmission system. In the Danish energy system, this efficiency is about 45%, presently.

The exergy content of the energy supply to the consumers is 1 kWh exergy/kWh electricity and 0.18 kWh exergy per unit district heat from the transmission grid.

The exergy cost per unit of electricity supply is equal to the electricity price of 0.30 €/kWh. For heat the cost per unit exergy is 0.57 €/kWh based on 0.10 €/kWh energy.

This shows that even though exergy is a common measure of any energy supply, the price of an exergy unit is not the same in practice. In this case heat almost has the double cost compared to electricity based on the exergy content.

For the economic evaluation the cost of district heating per unit energy is kept constant at the production side. This means that the consumer receives the benefit of lower loss, as the cost is lowered proportionally with the heat loss when the network temperature is lowered.

3. Results

3.1. Conventional District Heating

The base case is a conventional high temperature system where all heat is provided by the district heating without supplementary electricity. Figure 8 illustrates the flows and temperatures in this configuration. The energy flows in this configuration are presented in table 1. It is seen that the energy efficiency of the system is 81% which illustrates the heat loss of the distribution network. The exergetic efficiency is 29 % for the hot water supply and 24 % for space heating, and accordingly 27 % in total. The annual cost of the heat is € 740 (5500 DKK).

For a lower temperature conventional system utilizing temperatures of 65 °C and 35 °C for forward and return, respectively, the results are presented in table 2. The heat loss is lower in this configuration and higher efficiencies are obtained, even if the differences are small.

A configuration with even lower temperatures in the distribution network is presented in table 3. Naturally higher efficiency and lower cost is found is this case. However, the case is not fully applicable, as the requirement of 60 °C cannot be respected in the tank. The case is only acceptable if lower temperature can be allowed, without compromising the health concerns.

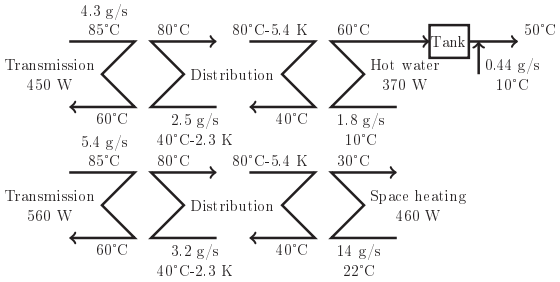

Figure 8. Conventional system at 80/40°C

Table 1. Conventional system 80/40 °C

	Energy [W]	Exergy [W]	Price [€/y]
Hot water			
Hot water supply	370	23	330
Heat loss	81	13	
District heat consumption	450	81	330
Efficiency [%]	*82*	*29*	
Space heating			
Heat supply	460	25	410
Heat loss	110	17	
District heat consumption	570	100	410
Efficiency [%]	*81*	*24*	
Total			
Heat supply	820	48	740
Heat loss	190	30	
Heat consumption	1000	180	740
Power consumption	0	0	
Efficiency [%]	*81*	*27*	

Table 2. Conventional system 65/35 °C

	Energy [W]	Exergy [W]	Price [€/y]
Hot water			
Hot water supply	370	23	320
Heat loss	66	8.8	
District heat consumption	430	78	320
Efficiency [%]	*84*	*30*	
Space heating			
Heat supply	460	25	400
Heat loss	85	11	
District heat consumption	540	98	400
Efficiency [%]	*84*	*25*	
Total			
Heat supply	820	48	710
Heat loss	150	20	
Heat consumption	970	180	710
Power consumption	0	0	
Efficiency [%]	*84*	*27*	

Table 3. Conventional system 60/30 °C

	Energy [W]	Exergy [W]	Price [€/y]
Hot water			
Hot water supply	370	23	310
Heat loss	58	7	
District heat consumption	420	76	310
Efficiency [%]	*86*	*31*	
Space heating			
Heat supply	460	25	390
Heat loss	74	9.2	
District heat consumption	530	96	390
Efficiency [%]	*86*	*26*	
Total			
Heat supply	820	48	690
Heat loss	130	16	
Heat consumption	950	170	690
Power consumption	0	0	
Efficiency [%]	*86*	*28*	

Table 4. Low temperature system 45/25 °C with electric heating

	Energy [W]	Exergy [W]	Price [€/y]
Hot water			
Hot water supply	370	23	590
Heat loss	41	3.7	
District heat consumption	260	47	190
Electricity consumption	150	150	390
Efficiency [%]	*89*	*12*	
Space heating			
Heat supply	460	25	390
Heat loss	74	9.2	
District heat consumption	530	96	390
Efficiency [%]	*89*	*26*	
Total			
Heat supply	820	48	970
Heat loss	180	13	
Heat consumption	790	140	590
Power consumption	150	150	390
Efficiency [%]	*89*	*16*	

3.2. Low Temperature District Heating 45/25°C with Electric Heating

For the simplest low temperature configuration using electric heating the results are presented in table 4. It is found that a significant share of electricity is required to reach the target domestic hot water temperature, i.e., 150 W out of the 370 W demand. This results in low exergetic efficiency of the hot water heating, and an efficiency of only 16 % of the total system. The annual cost is € 970 (7300 DKK).

3.3. Low Temperature District Heating with Heat Pump

The three different heat pump configurations reach higher efficiency than the simple low temperature system with electric heating.

Secondary side tank. With the hot water tank on the consumer side an exergetic efficiency of 20 % is obtained with R134a as shown in table 5. The heat pump has a COP of 4.2 and consumes 86 W power.

For the system with R744, table 6, instead higher efficiency results are obtained. The exergetic efficiency is 24 %. This heat pump reaches a COP of 6.6 and consumes only 56 W power.

The preheat configuration with R134a is competitive with R744 and reaches an efficiency of 24 % as well, as presented in table 7. The heat pump COP is still 3.5 but it is utilitzed for higher temperature heating and thus only consumes 41 W.

The annual cost of heat for the three configurations are € 820 (DKK 6100), € 800 (DKK 5900) and € 760 (DKK 5700), respectively. The lowest electricity consumption is thus most attractive.

The configuration has a minimum temperature difference of 2.5 K between the fluids in the gas cooler.

Primary Side Tank. The best configuration for the low temperature system is the configuration with hot water storage on the district heating side. The calculations are presented in table 8.

Table 5. Low temperature system at 45/25°C with R134a and secondary side tank

	Energy [W]	Exergy [W]	Price [€/y]
Hot water			
Hot water supply	370	23	450
Heat loss	41	3.7	
District heat consumption	280	58	210
Electricity consumption	86	86	230
Efficiency [%]	*90*	*16*	
Space heating			
Heat supply	460	25	390
Heat loss	74	9.2	
District heat consumption	530	96	390
Efficiency [%]	*89*	*26*	
Total			
Heat supply	820	48	820
Heat loss	120	13	
Heat consumption	810	150	590
Power consumption	86	86	230
Efficiency [%]	*92*	*20*	

Table 6. Low temperature system at 45/25°C with R744 and secondary side tank

	Energy [W]	Exergy [W]	Price [€/y]
Hot water			
Hot water supply	370	23	400
Heat loss	41	3.8	
District heat consumption	350	63	260
Electricity consumption	56	56	150
Efficiency [%]	*90*	*20*	
Space heating			
Heat supply	460	25	390
Heat loss	74	9.2	
District heat consumption	530	96	390
Efficiency [%]	*89*	*26*	
Total			
Heat supply	820	48	800
Heat loss	120	13	
Heat consumption	880	140	650
Power consumption	56	56	150
Efficiency [%]	*88*	*24*	

Table 7. Low temperature system at 45/25°C with R134a and secondary side tank and preheating of domestic hot water

	Energy [W]	Exergy [W]	Price [€/y]
Hot water			
Hot water supply	370	23	370
Evaporator side			
Heat loss	17	1.5	
District heat consumption	120	22	90
Preheating			
Heat loss	25	2.3	
District heat consumption	240	44	180
Heat Pump			
Electricity consumption	38	38	100
Efficiency [%]	*90*	*22*	
Space heating			
Heat supply	460	25	390
Heat loss	74	9.2	
District heat consumption	530	96	390
Efficiency [%]	*89*	*26*	
Total			
Heat supply	820	48	750
Heat loss	120	13	
Heat consumption	890	160	650
Power consumption	38	38	100
Efficiency [%]	*89*	*24*	

Table 8. Low temperature system at 45/25°C with R134a and primary side tank

	Energy [W]	Exergy [W]	Price [€/y]
Hot water			
Hot water supply	370	23	350
Evaporator side			
Heat loss	12	1.0	
District heat consumption	130	24	97
Condenser side			
Heat loss	28	2.4	
District heat consumption	240	44	180
Heat pump			
Electricity consumption	29	29	76
Efficiency [%]	*90*	*24*	
Space heating			
Heat supply	460	25	390
Heat loss	74	9	
District heat consumption	530	96	390
Efficiency [%]	*89*	*26*	
Total			
Heat supply	820	48	740
Heat loss	110	12	
Heat consumption	930	170	660
Power consumption	29	29	76
Efficiency [%]	*87*	*25*	

The heat pump has a COP of 9.6 and consumes only 29 W to produce domestic hot water. The exergetic efficiency of the system is 25 % and is thus almost competitive with the conventional system. The annual cost of heat is € 740 (DKK 5600).

3.4. Overall Results

In summary the results of the above calculations are given in table 9.

The results show that the exergetic efficiency of the conventional system configurations is higher than in the low temperature cases. This is caused by the low exergy content of heat at the relatively low temperatures in the system. However, the difference in efficiency is low if compared to the best low temperature solutions which are R134a heat pump with primary side tank and with secondary side tank and preheating. The former is considered to be the best solution and it will reach exergetic efficiency of the same values as the conventional system if the minimum temperature differences in the heat pump evaporator and condenser are lowered to 2.5 K.

It should also be noted that the best solution with a 60/30°C distribution network actually involves a temperature crossover, which means that it is not a realisable solution without allowing a little lower temperature in the storage tank.

The three latter heat pump solutions are close in performance. The R744 system may be competitive even though the efficiency is lower than for the R134a solutions. R744 has several advantages such as being a natural refrigerant with very low global warming potential (GWP), a low safety classification and a low price. Other refrigerants that do not operate in a transcritical cycle may have similar performance as R134a and may thus also be competitive.

Table 9. Summary of results

System	Distribution temperatures [°C]	Refrigerant	Heat pump COP [–]	Tank location	Preheating	Heat consumption [W]	Electricity consumption [W]	Energy Efficiency [%]	Exergetic Efficiency [%]	Cost [€/y]	CO_2 emissions [Mg/y]
Conv. 1	80/40	–	–	Sec		1000	0	81	27	740	1.0
Conv. 2	65/55	–	–	Sec		970	0	84	27	710	1.0
Conv. 3	60/30	–	–	Sec		950	0	86	28	690	1.0
LT EL	45/25	–	1.0	Sec		790	150	89	16	970	1.4
LT HP 1	45/25	R134a	4.2	Sec		830	100	92	20	820	1.3
LT HP 2	45/25	R744	6.6	Sec		880	56	88	24	800	1.1
LT HP 3	45/25	R134a	3.5	Sec	×	890	41	89	24	750	1.1
LT HP 4	45/25	R134a	9.6	Prim	×	930	29	89	25	740	1.1

Regarding climate impact of the heat supply for the building, the conventional systems all have a CO_2 emission of close to 1000 kg per year based on the average emission for power and district heating in the Danish energy statistics [1]. The emissions of the best heat pump solutions are close to this value, while the solutions with low efficiency may reach up to 40% higher emissions.

3.5. Sensitivity Analysis

The most relevant heat pump-based solution is the LT HP 3, with a conventional hot water tank. This has been analyzed in further detail to investigate sensitivity of the results with respect to the assumed values. None of the investigated parameters have a very significant impact on the annual cost or the exergetic efficiency.

Low electricity prices is a quite important factor. If the price was 33% lower it would benefit the heat pump solutions, and the annual cost would be 730 €.

Out of the technical parameters, the estimated value of isentropic efficiency of the compressor is conservative, but not unrealistic, as it is based on the component used in the demonstration unit. If it reaches 80% the annual cost would be reduced to 740 € and the exergetic efficiency 25%.

A similar result would be found if the supply temperature of the hot water was reduced to 45 °C and all the condenser temperautre was reduced accordingly.

If the heat loss in the network was reduced 50% the cost would be 750 €.

Heat pump parameters as evaporator temperature, condenser temperature, and evaporator superheat all have little significance for the annual result and exergetic efficiency.

4. Discussion

The results show that the low losses of the low temperature systems are not sufficient to make these competitive regarding cost or exergy utilization, when compared to conventional systems, even at high temperatures. This is to some extent caused by the high share of domestic hot water in the low energy building.

The exergy flows illustrate the differences due to the lower temperatures through the system. The exergetic efficiency of a modern combined heat and power plant is on the order of 45%, which means that the overall exergetic efficiency of the district heating system is as low as 10%. This shows that there is a significant room for improvement, if the whole chain of energy conversion from fuel to low temperature consumption by the consumer is considered. This involves several heat transfer processes which result in exergy destruction or loss. If low temperature was introduced in the transmission system as well as in the distribution system, lower exergy destruction would be introduced. However, the exergy difference is likely not sufficient to compensate the difference in efficiency fully.

Another consequence of lowering the temperatures in the transmission systems would be that higher electric efficiency could be obtained from the power plant. A similar improvement would be found in smaller systems with distribution network only.

Improved performance of low temperature district heating may be obtained by integrating it with cheap heat sources which are not possible to use at the temperatures in conventional systems. This idea has been suggested by e.g., [23]. [24] integrates industrial waste heat in district heating by use of absorption heat pumps. Other cheap, low temperature heat sources may also benefit the low temperature system, e.g., waste heat, flue gas condensation from biomass-based power and solar heating.

The risk of legionella has in this study been assumed to be avoided by reaching a temperature of 60 °C in domestic hot water tanks. The actual temperature requirement varies in different studies. However, the results are considered to be similar if lower temperatures is required, even if the systems with storage on the consumer side will be improved. Other means of legionella treatment are being developed. They may make it possible to avoid the high temperature of the hot water, but they will require cost for investment and operation.

The prices used in calculations are based on average numbers in Danish conditions. In other countries or in future situations, other values may occur such that electric may be favoured compared to district heating. On the other hand, future systems with improved building standards will require less space heating, and thus the domestic hot water will have an increased share of the demand. From an efficiency viewpoint it would be better to consider heating at different temperatures, such as floor heating and domestic hot water, as two different products, which might be produced in separate systems.

The calculations are based on yearly average consumption rates. This is an important assumption, but it is assumed that taking the seasonal variations into account would not change the overall picture significantly. However, in practical heating installations, the high temperature needed for legionella treatment may only be obtained e.g. weekly. This solution is beneficial for the heat pump solutions as the COP, and thus the power consumption, is directly linked to the water temperature.

The calculations are based on large district heating networks for cities including both transmission and distribution networks with heat production from primarily extraction steam cycle CHP units, but also back-pressure mode cycles. Such systems account for the largest share of the district heating in Denmark. These will have an increase in efficiency if lower temperatures are used in the district heating system, in particular the forward lines. This benefit is not taken into account, but it will not impact the results significantly, as only minor efficiency improvement will be obtained [18]. The transmission system will usually be difficult to change. For other CHP plant types and for smaller networks with single CHP units, other options for improvement may be utilized by lower temperatures in the district heating system. Such systems may benefit more from low temperature solutions and heat pump integration.

Table 9 presents the COP of the heat pump cycle of each of the systems. These are not the *System COP* of the domestic hot water heat pump system, which might be introduced as well. For the system with primary side tank this would be as high as 12, as 370 W heat are supplied by consumption of 30 W electricity. However, the value should be taken with a grain of salt, as COP is always dependent on the exact system configuration. For instance, the electric heating system apparently has a System COP of 2.5 which is not intuitive.

5. Conclusion

Eight configurations for supply of heat for tap water and space heating in a district heating system have been studied to determine the demands for heat and electricity supply. It is found that the systems all have a primary energy utilization, i.e., exergetic efficiency, of 16-28%, and thus that significant potential for improvement theoretically exists. The exergy utilization in the presented systems does not include the CHP production, so the primary energy utilization is only about half of the presented values. The cost of heat is annually between € 690 and € 970. The cost is not proportional to the exergetic efficiency, but the trends are similar.

Conventional systems with higher temperatures in the network have a better utilization than low temperature solutions, as the decrease in heat loss does not compensate the electricity demand to cover the energy consumption. However, district heating will probably in general be converted to lower temperature and thus a heat pump solution is required.

In the complete district heating system, the largest sources of exergy destruction are due to the fuel conversion at the CHP plant and the heat transfer in substations and by consumers. The exergy loss due to heat loss is only a minor contributor to the overall irreversibility.

The results show that a solution with R134a, or other subcritical systems, with heat storage on the primary side, will have the lowest primary energy consumption. A transcritical R744 solution or an R134a solution with preheating both with heat storage on the primary side may also be considered as they have similar performance.

6. Acknowledgments

The work has been funded by Danish Energy Agency, Energy Technology Development and Demonstration Program, Project EUDP 11-I, J. nr. 64011-0076, Heat Pumps for Domestic Hot Water Preparation in Connection with Low Temperature District Heating.

Nomenclature

COP Heat pump Coefficient of Performance [–]

$\dot{E}$ Exergy flow [W]

$\dot{E}_{\mathtt{dest}}$ Exergy destruction rate [W]

$\dot{E}_{\mathrm{cons}}$ Exergy consumption flow [W]

$\dot{E}_{\mathrm{dhw}}$ Exergy flow of domestic hot water [W]

$\dot{E}_{\mathrm{dh}}$ Exergy flow of district heat supply [W]

$\dot{E}_{\mathrm{el}}$ Exergy flow of electricity [W]

$\dot{E}_{\text{prod}}$ Exergy product flow [W]

$\dot{E}_{\text{sh}}$ Exergy flow of space heating [W]

η_x Exergetic efficiency [–]

h Specific enthalpy [kJ/kg]

h_0 Dead state specific enthalpy [kJ/kg]

$\dot{m}$ Mass flow [kg/s]

$\dot{m}_{dhp}$ Mass flow for heat pump heating in distribution [kg/s]

$\dot{m}_{dh}$ Mass flow for hot water in distribution [g/s]

$\dot{m}_{dp}$ Mass flow for preheating in distribution [g/s]

$\dot{m}_{ds}$ Mass flow for space heating in distribution [g/s]

$\dot{m}_{hi}$ Mass flow of fresh water to hot water tank [g/s]

$\dot{m}_{hm}$ Mass flow of fresh water for mixing to supply temperature [g/s]

$\dot{m}_{hp}$ Heat pump refrigerant mass flow [kg/s]

$\dot{m}_s$ Mass flow for space heating in house [g/s]

$\dot{m}_{thp}$ Mass flow for heat pump heating in transmission [kg/s]

$\dot{m}_{th}$ Mass flow for hot water in transmission [g/s]

$\dot{m}_{tp}$ Mass flow for preheating in transmission [g/s]

$\dot{m}_{ts}$ Mass flow for space heating in transmission [g/s]

p_0 Dead state pressure [bar]

$\dot{Q}_h$ Hot water demand [W]

$\dot{Q}_h$ Space heat preheating demand [W]

$\dot{Q}_s$ Space heating demand [W]

$\dot{Q}_{thp}$ Heat pump heating transmission demand [W]

$\dot{Q}_{th}$ Hot water transmission demand [W]

$\dot{Q}_{tp}$ Space heat preheating transmission demand [W]

$\dot{Q}_{ts}$ Space heating transmission demand [W]

$\dot{S}_{\text{gen}}$ Entropy generation rate [W/K]

s Specific entropy [kJ/kg K]

s_0 Dead state specific entropy [kJ/kg K]

ΔT_{df} Distribution forward temperature difference [K]

ΔT_{dr} Distribution return temperature difference [K]

T_0 Dead state temperature [K]

t_c Heat pump condenser temperature [°C]

t_e Heat pump evaporator temperature [°C]

t_{cd} Heat pump compressor discharge temperature [°C]

t_{df} Distribution forward temperature [°C]

t_{dr} Distribution return temperature [°C]

t_{hf} Hot water forward temperature [°C]

t_{hh} Hot water temperature after district heating [°C]

t_{hi} Fresh water temperature [°C]

t_{hp} Temperature after preheating [°C]

t_{ht} Hot water tank temperature [°C]

t_{sf} Space heating forward temperature [°C]

t_{sr} Space heating return temperature [°C]

t_{tf} Transmission forward temperature [°C]

t_{tr} Transmission return temperature [°C]

$\dot{W}$ Electric power [W]

x_{co} Heat pump condenser outlet vapor quality [–]

x_{ei} Heat pump evaporator inlet vapor quality [–]

x_{eo} Heat pump evaporator outlet vapor quality [–]

References

[1] Anonymous, Energy statistics 2012, Tech. Rep. ISBN 978-87-93071-40-7 www, Danish Energy Agency, Copenhagen, Denmark (Feb. 2014).

[2] Z.-P. Song, Total energy system analysis of heating, Energy 25 (9) (2000) 807 – 822. doi:http://dx.doi.org/10.1016/S0360-5442(00)00021-9.

[3] P.K.Olsen, H. Lambertsen, R. Hummelshøj, B. Bøhm, C. Christiansen, S. Svendsen, C. Larsen, J. Worm, A new low-temperature district heating system for low-energy buildings, in: The 11th International Symposium on District Heating and Cooling,, Reykjavik, Iceland, 2008.

[4] M. Brand, P. Lauenburg, J. Wollestrand, V. Zboril, Optimal space heating system for low-energy single-family house supplied by low-temperature district heating, in: Passivhus Norden 2012, Trondheim, Norway, 2012.

[5] O. Gudmundsson, The effects of lowering the network temperatures in existing networks, in: DHC13, the 13th international symposium on district heating and cooling, September 3rd to September 4th, 2012, pp. 116–121.

[6] M. Brand, S. Svendsen, Renewable-based low-temperature district heating for existing buildings in various stages of refurbishment, Energy 62 (2013) 311–319.

[7] G. Lorentzen, Revival of carbon dioxide as a refrigerant, International Journal of Refrigeration 17 (5) (1994) 292–301.

[8] G. Lorentzen, The use of natural refrigerants: a complete solution to the cfc/hcfc predicament, International Journal of Refrigeration 18 (3) (1995) 190–97.

[9] T. Ommen, B. Elmegaard, Exergetic evaluation of heat pump booster configurations in a low temperature district heating network, in: Proceedings of ECOS 2012 - The 25th International Conference on Efficiency, Cost, Optimization, Simulation and Environmental Impact of Energy Systems, Pergugia, Italy, 2012.

[10] H. Li, S. Svendsen, Energetic and exergetic analysis of low and medium temperature district heating network integration, in: 2nd International Exergy, Life Cycle Assessment, and Sustainability Workshop & Symposium (ELCAS2), Nisyros, Greece, 2011.

[11] V. Vittorio, A. Kona, Thermoeconomic approach for the analysis of low temperature district heating systems, in: Proceedings of ECOS 2012 - The 25th International Conference on Efficiency, Cost, Optimization, Simulation and Environmental Impact of Energy Systems, Pergugia, Italy, 2012.

[12] A. Ljubenko, A. Poredos, T. Morosuk, G. Tsatsaronis, Performance analysis of a district heating system, Energies 6 (2013) 1298–1313, doi:10.3390/en6031298.

[13] M. Pirouti, Modelling and Analysis of a District Heating Network, 2013.

[14] M. Markussen, B. Elmegaard, T. S. Ommen, M. Brand, J. E. Thorsen, Heat pumps for domestic hot water preparation in connection with low temperature district heating, Tech. Rep. EUDP 11-I, J. nr. 64011-0076, Grontmij (Oct. 2013).

[15] E. Zvingilaite, T. Ommen, B. Elmegaard, M. L. Franck, Low temperature district heating consumer unit with micro heat pump for domestic hot water preparation, in: DHC13, the 13th International Symposium on District Heating and Cooling, Copenhagen, Denmark, 2012.

[16] O. Gudmundsson, J. E. Thorsen, J. Iversen, Ultra low temperature district heating substation, Euroheat and Power (English Edition) 11 (1) (2014) 43–45.

[17] B. Elmegaard, N. Houbak, Simulation of the Avedøreværket Unit 1 Cogeneration Plant with DNA, in: 16th International Conference on Efficiency, Costs, Optimization, Simulation and Environmental Impact of Energy Systems.

[18] T. Ommen, W. B. Markussen, B. Elmegaard, Heat pumps in combined heat and power systems, Energy 76 (0) (2014) 989 – 1000. doi:http://dx.doi.org/10.1016/j.energy.2014.09.016. URL http://www.sciencedirect.com/science/article/pii/S036054421401072X

[19] Anonymous, Energy statistics 2012, Tech. rep., Danish Energy Agency (2013).

[20] J. Tang, Notat: Fjernvarmeprisen i danmark 2013, Tech. rep., Danish District Heating Association (2013).

[21] B. Elmegaard, N. Houbak, DNA – A General Energy System Simulation Tool, in: J. Amundsen (Ed.), Proceedings of SIMS 2005 - 46th Conference on Simulation and Modeling, Trondheim, Norway, 2005.

[22] A. Bejan, G. Tsatsaronis, M. Moran, Thermal Design and Optimization, John Wiley & Sons, 1996.

[23] R. Wiltshire, Low temperature district energy systems, in: 16th Building Services, Mechanical and Building Industry Days, Debrecen, hungary, 2011.

[24] H. Fang, J. Xia, K. Zhu, Y. Su, Y. Jiang, Industrial waste heat utilization for low temperature district heating, Energy Policy 62 (2013) 236–246.

Appendix I

Paper 7 - Energy

Torben Ommen, Wiebke Brix Markussen and Brian Elmegaard

Lowering district heating temperatures - Impact to system performance in current and future Danish energy scenarios

Energy, [Submitted]

Lowering district heating temperatures - Impact to system performance in current and future Danish energy scenarios

Torben Ommen[a,*], Wiebke Brix Markussen[a], Brian Elmegaard[a]

[a] *Technical University of Denmark, Kgs. Lyngby, Denmark*

Abstract

Combined heat and power (CHP) production in connection with district heating (DH) systems has previously demonstrated a significant reduction in primary energy consumption. With extended installation of intermittent sustainable sources, such as eg. wind turbines rather than thermal units, the changed distribution of generation technologies may suggest a reconsideration of optimum for DH network temperatures, in order to achieve low cost and minimize carbon emissions. A mixed integer linear optimisation model was used to investigate the changed operation based on changed network characteristics. Utility plants and demand curves corresponded to the current and future scenarios for the DH system of Greater Copenhagen. Performance curves from typical CHP-plant technologies were used to represent the changed operation of power and heat production for changed DH temperatures. The results show that primary fuel consumption is reduced approximately 5-7 % at DH design temperatures of 60 - 70 ˚C. Further reduction in DH temperatures resulted in opposing tendencies, as hot tap water requires electricity to reach the required temperatures. The results are network-specific, as they represent the given network and production units, but similar trends can be expected for other large networks.

Keywords: Heat pumps, District heating, Combined heat and power, Optimisation.

1 Introduction

Combined heat and power (CHP) production in connection with district heating (DH) systems has resulted in significant reduction in primary energy consumption in Denmark [1]. With power production investments moving from thermal units to intermittent renewable sources, such as eg. wind turbines or solar photovoltaics technology [2], the excess heat co-generated with power is decreased. The changed distribution between thermal and intermittent technologies for electricity suggest changes to the corresponding technologies for supplying heat to the DH network. As investment in new utility technologies is required, it is suggested also to consider the influence of DH network temperatures for a complete system optimization. The choice of temperatures does not only affect network heat losses, but also impacts network capacities, and changes the possible benefit of different technologies. Thus it is likely that two different choices in network temperatures will result in two significantly different optimal technology distributions, and vice versa.

In Denmark, the investment in future utility production units is constrained to renewable technologies due to political zero carbon emission ambitions (eg. Danish Government [3]). Such ambitions are also represented in the local communities. The city council of Copenhagen agreed in 2013 on a climate plan attempting to make Copenhagen the first CO_2 neutral capital in 2025 [4]. Carbon neutral heating and power production is naturally key focuses to achieve such goals. As the DH network supplies 98% of the heat demand in the Copenhagen municipality, these utility production units are of main concern. The climate plan proposes to convert central CHP units to biomass and integrating central, large-scale heat pumps (HPs) in the DH networks as two feasible measures.

*Corresponding author

Email addresses: tsom@mek.dtu.dk (Torben Ommen), wb@mek.dtu.dk (Wiebke Brix Markussen), be@mek.dtu.dk (Brian Elmegaard)

Nomenclature

$\dot{C}$	cost rate, €/h
C	constant
k	opening degree, -
$\dot{m}$	massflow, kg/s
p	pressure, Pa
T	temperature, °C
Greek symbols	
α	flow characteristic
β	power loss factor for heat extraction
Δ	variation or glide
ρ	density, kg/m^3
Subscripts	
C	consumer
cond	condensation
E	exiting consumer
evap	evaporation
elec	electric
F	forward
f, g, h, i, j	index
in	inlet
out	outlet
R	return
sink	sink reservoir
source	source reservoir
T	turbine
t	hours
total	total utilisation
Abbreviations	
CC	Combined Cycle
CHP	Combined Heat and Power
COP	Coefficient Of Performance
DH	District Heating
Gen	Generator
HP(s)	Heat Pump(s)

A series of previously published reports named "Heat Plan Greater Copenhagen" (in Danish "Varmeplan Hovedstaden"), of which the newest at the time of writing is number 3, concludes that a limited share (300 MW installed capacity) of central heat pumps, may provide small reductions in heat cost after 2030-35 [5]. According to their calculations, the use of sustainable biomass is the major driver for cost and carbon reductions in the future system. With one highly dominant fuel type, the system may, however, experience a significant reduction in security of supply.
Four explanations are conceivable for the expected poor penetration of heat pumps in the future technology composition for DH:

1 The extraction CHP plant technology provides highly efficient conversion of electricity to heat (typically approx. ratio: 7-11:1 [6]) according to the power loss factors by heat extraction [7]. This is a performance advantage in the order of a factor of 3 compared to the HP technology [8].

2 Low coefficient of performance (COP) from integrating HPs to supply heat in the transmission network at 90 °C or above [9]. With low COP the HP utilises large quantities of electricity, which in addition to the cost of electricity also carries significant network losses and taxes. Heat can be co-supplied at lower temperatures to increase COP (e.g. to the return stream of the network) but such integration schemes increase the operational constraints of the system, and the HPs can in this case not be utilised as a stand alone technology.

3 Taxation for HPs reaches above 50 % of the levelized cost for heat [10] considering the Danish taxation scheme [11].

4 Insufficient heat sources with high temperature, which are located within or close to the DH network perimeter [5, 12]. In case the heat sources are not co-located with the large DH-streams, the investments for HPs are increased significantly.

Item 2 and 3 are addressed by lowering DH temperatures, in this way increasing the COP of the HP unit. As taxation is based on the consumption of electricity for heat production, increasing COP will lower the quantity of the heat cost that originate from taxes.
When the temperature in the DH network is changed, all of the existing types of utility technologies will experience performance changes. In order to fully evaluate the improved performance of the HPs at changed DH temperatures, the performance estimates for existing technologies should also correspond to the changed temperatures.
In this paper, the effects of changing DH temperatures are evaluated in terms of the total cost

for heat and electricity for the consumers, carbon emissions and primary fuel consumption. Performance curves from typical CHP-plant technologies are used to represent the changed operation of power and heat production.
As large changes are expected for the current network within a limited time-frame, two cases are considered in order to evaluate the implications of changing DH temperatures for the current and future network and utility units. The current energy scenario is assessed by utilising a validated layout for 2011 where steam-based DH networks are utilised in central areas of the network [13]. The future scenario (2025) corresponds closely to that considered in "Heat Plan Greater Copenhagen 2" [14]. Neither of the two scenarios utilises central HPs in DH networks. In the paper two corresponding scenarios are included considering a significant integration (200 MW capacity) of HPs.
To assess the changes to the network capacity corresponding to the current and future design, a DH network model is included, where the changed capacity at changed temperature levels is considered. This allows an analysis of the possibilities for changing network temperatures without further investment in the large transmission and distribution lines of Greater Copenhagen.
The developed model thus represents an existing system as a case, but it is intended to be an illustration of current and future energy systems in cities with high penetration of CHP-based district heating and thus high-efficient heat supply. The study shows the possibilities for optimal integration of intermittent renewables when accounting for the performance of different technologies under different operating temperature conditions.

2 Method

Thermodynamic models of representative technologies were used in order to analyse the change in performance of the individual units with changes in temperature of the DH network. The models were programmed in Engineering Equation Solver [15]. These models are further described in section 2.1, 2.2 and 2.3.
A detailed mixed integer linear optimisation model was used to investigate the new operation based on the changed parameters. The model was programmed in Matlab and GAMS using the CPLEX solver [16, 17, 18]. The model was designed and used for the case study of the production technologies and network characteristics of Greater Copenhagen [13], but the implementation of energy system equipment in the model is generic and easy to change to other systems. The heat and power system model is further described in section 2.5 and appendix A.

2.1 Temperature of current and future DH networks, network capacities and DH heat losses

Generally, the temperatures for a district heating network are kept as low as possible in order to reduce heat losses and increase efficiency of electricity co-production. The lower limit for traditional DH forward temperatures is reached when the required temperature of certain constituents of the demand (often approximately 55 °C due to hot tap water) is no longer met.
In a Danish context the forward temperature ($T_{\mathrm{DH,forward}}$) varies from 70 °C to 120 °C [19, 20]. The corresponding network return temperatures ($T_{\mathrm{DH,return}}$) range from 35 °C to 55 °C. The design temperatures of the current DH network and utility units are 100 °C, with temperature variations of 95-110 °C to account for network capacity constraints in cold periods and energy savings in the summer.
In Lund et al. [21] further reduction in temperatures is proposed, with a lower limit of DH design temperatures reaching as low as 40 °C, which is the limit allowed by modern space heating technology (4GDH). In this case electric heaters or booster HP units are required for production of hot tap water [22, 23, 24]. The performance of booster HP units is further addressed in section 2.4. In table 1 both current and future proposals for temperature in DH networks are presented.

Table 1: Current and future temperature sets for DH networks

Network type	Media	DH forward temperature	DH return temperature
Transmission	H_2O	110°C	55°C
Old distribution	H_2O	90°C	45°C
New distribution	H_2O	70°C	35°C
4GDH (low limit)	H_2O	40°C	20°C

Based on the considered temperature sets, the return and forward temperatures were interpolated linearly for the range of $T_{\mathrm{DH,forward}}$ = 40-110 °C and $T_{\mathrm{DH,return}}$ = 20-55 °C as shown in Fig 1.

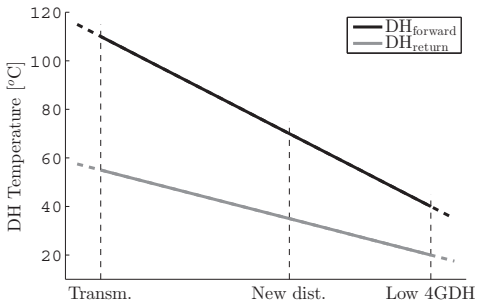

Figure 1: Temperature spans applied of the modelled DH networks.

The temperature levels do not only influence the production technologies, but also the volume flow of DH fluid is significantly changed for a constant amount of transferred heat. As the pressure losses become significant for increasing flow rates in the network [25, 26, 27], the various transmission lines were constrained to a maximal volume flow. The maximal flow rates for the two scenarios were based on a data from a corresponding network model for 2012 and 2025 [5, 12]. Only transmission lines and capacity constraints for large distribution lines were included in the model. The capacity of the individual transmission lines was varied according to the changed temperatures in the model.
Similar constraints were found for sensible heat storages, where the energy content of a volume of stored water changes with changed DH temperature.
The relative variation of the two technologies is presented in Fig. 4d, where 100 ˚C forward design temperature is used as the base. As seen from the figure, the relative differences of stored heat per volume and capacity of DH network are coinciding.
The temperatures of the DH network forward and return streams were defined to be at the location of the utility unit (T_f and T_r) in Fig. 2. In the considered network, the heat is supplied from the utility plant to a transmission network, which transfers the heat to smaller distribution grids.
The heat losses for transmission and distribution were determined individually for 2011 as 2 % and 15 % respectively [19, 20]. By assuming that the losses correspond to transmission network operation at 100 ˚C and 50 ˚C for forward and return temperatures, the combined heat transfer characteristics of each individual heat network to the ground was found [28, 29]. Using this assumption, it was possible to estimate the heat losses, as well as the consumer temperature T_C for variations in DH temperatures corresponding to Fig. 1. The temperature of the soil was estimated as the average of yearly temperature variation for the area (8.8 ˚C).

2.2 Performance of CHP units at changed DH temperatures

In order to evaluate the effects of changing DH network temperatures, three separate models of CHP plants was programmed in EES. The developed models are:

- Extraction: Extraction type steam turbine (Rankine) cycle.
- Back-pressure: Back-pressure steam turbine (Rankine) cycle.
- Combined cycle: Gas turbine (open Brayton) and steam turbine (Rankine) cycle.

Schematic diagrams of the three considered CHP technologies are presented in Fig. 3. The layout of the three units was modelled to represent specific units in the current utility production.
Besides energy, entropy and mass balances, different, representative expressions were used to establish the impulse balances in different parts of the systems.
For each section of the modelled turbines, a turbine constant accounts for the swallowing capacity of a specific unit:

$$C_T = \frac{\dot{m} \cdot \sqrt{T_{\text{in}}}}{\sqrt{p_{\text{in}}^2 - p_{\text{out}}^2}} \tag{1}$$

where the massflow of working fluid $\dot{m}$, the temperature of entering fluid T_{in} and pressures at inlet p_{in} and outlet p_{out} are used. Once installed, the swallowing capacity should be considered constant throughout the lifetime of the unit. The constant is required to calculate the off-design operation of such units.

2.2.1 Extraction CHP

In the current energy scenario based on todays Eastern Danish energy system, the Nordpool DK2

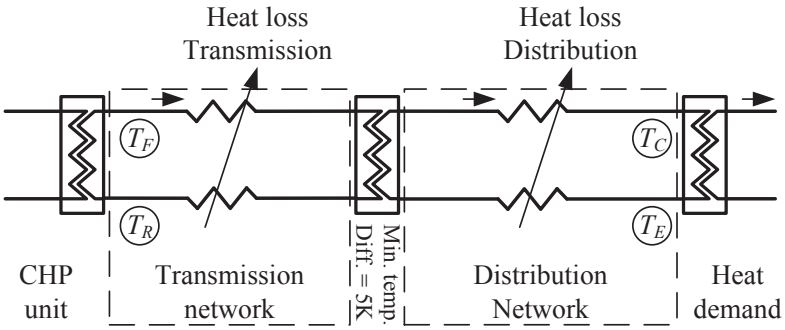

Figure 2: Schematic diagram of DH system with transmission and distribution networks.

area [30], four central extraction CHP units are operated (five in case the reserve unit at Asnæsværket (ASV5) is included), of which three are located within the DH network. The same units are expected to be operating in 2025, although two of the units (which are identical) require overhaul and conversion to biomass fuel.

The model for extraction type steam turbine (Rankine) cycles represent one of these units (AVV1 or AMV3). The model follows the instructions of the proposal for simulator contest of ECOS 2003 [31, 6], where specific information about the temperatures, isentropic efficiencies, temperature differences, auxiliary power consumption and pressure losses are defined. The model used for this analysis corresponded closely to the one used in Ommen et al. [9]. The steam enters the intermediate and low pressure part of the turbine train after expansion in the preceding turbine, IP1, and may be used for power generation or to supply district heating. The output of each product is controlled by adjusting the valves before the low pressure turbines and the district heating heat exchangers.

For each of the valves, a flow characteristic was fixed, in order to account for the pressure losses when the valve is operated between fully open and fully closed. The constant is required to calculate the off-design operation of such units.

$$\dot{V} = \alpha_{\text{valve}} \cdot k \cdot \sqrt{\frac{\Delta p_{\text{valve}}}{\rho_{\text{in}}}}, \tag{2}$$

where α is the flow characteristic, k is the opening degree of the valve and Δp_{valve} is the pressure loss over the valve.

Considering DH temperatures of 100 °C and 50 °C for forward and return temperatures, the model represents a plant with an electric efficiency of 42.0 % at full boiler load and in condensing mode and 34.9 % at full back-pressure mode, respectively. In full back-pressure mode the total energy utilization is 91.5 %.

2.2.2 Back-pressure CHP

Back-Pressure CHP units are extensively used in Copenhagen today and in future scenarios (see section 2.6). The units are typically fuelled by biomass, or used for waste incineration. A few of the units allow the steam to bypass the turbine, in order to be utilised directly for heat production.

The back-pressure CHP unit was modelled to represent the Amagerværket unit 1 (AMV1), which is a biomass-fuelled unit located centrally in Copenhagen. The component details corresponded to those used for the extraction plant. In the current energy scenario, only a high pressure turbine is installed, as the unit supplies steam to a central network. When the steam network has been phased out (expected before 2025) a low-pressure turbine will be added to the unit.

Considering DH temperatures of 100 °C and 50 °C for forward and return temperatures, the model represents a plant with an electric efficiency of 29.5 % and total energy utilization of 92 %.

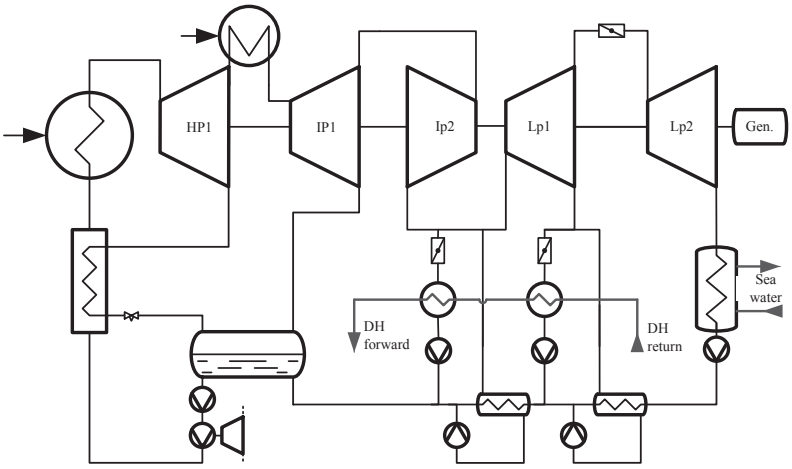

(a) Extraction CHP plant

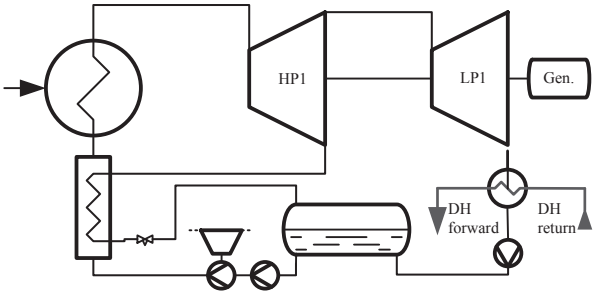

(b) Back-pressure CHP plant

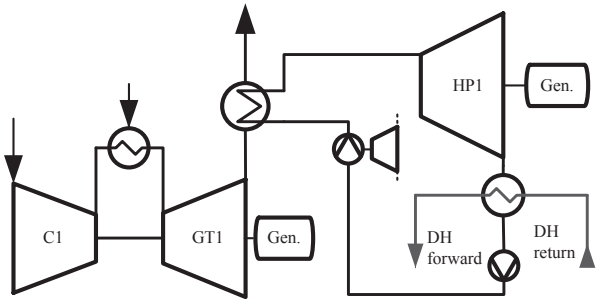

(c) Combined cycle CHP plant

Figure 3: Schematic diagram of the three considered combined heat and power plants.

2.2.3 Combined cycle CHP

The combined cycle CHP plant corresponds to the two combined cycle units at Avedøreværket unit 2. For the Rankine cycle, the component details correspond to those used for the extraction plant. Combined cycle units represent a small fraction of the current electricity and heat production, and are expected to play an even smaller role in the system of 2025. Out of the four current units, two will be retired as they are used for the steam network, and the two at AVV2 will be utilised exclusively as electricity reserve measures.

For DH forward and return temperatures of 100 °C and 50 °C respectively, the model represents a plant with an electric efficiency of 51 % and total energy utilization of 85 %.

2.2.4 Performance improvement of CHP technologies from reduction in temperatures of DH network

The individual models of CHP units were varied according to the district heating temperature levels presented in Fig. 1. In this way, the potential improvements for the individual plants were determined. By assuming, that the models are representative for the individual CHP-plant types, the influence from DH temperatures are found for all considered units in the current and future energy scenarios. The changed performance parameters are presented in Fig. 4a, 4b and 4c for extraction, back-pressure and combined cycle CHP, respectively.

For extraction CHP units, the temperature variations contributed to significant modifications to the electricity efficiency and to the power loss factor by heat extraction β. For back-pressure units the electricity efficiency was significantly changed. For both extraction and back-pressure CHP units, minor impact was experienced for the total energy utilization of the unit.

For the combined cycle technology, the electric efficiency has changed with variation of DH temperature. Opposed to the above-mentioned technologies, the alteration of DH temperature affects the total efficiency significantly, although less than the corresponding change in electrical efficiency.

2.3 Heat pumps in DH

In Ommen et al. [9] five possible heat pump configurations in DH networks are analysed. The operational performance of the configurations are investigated based on four key performance factors, which are the coefficient of performance, the coefficient of system performance, the volumetric heating capacity and the cost of fuel.

The SF configuration was utilised for the present analysis. In this configuration the sink DH stream is heated from the temperature of the return line to that of the forward stream. The main advantage of the SF configuration is that this configuration allows operation independently of other technologies. A schematic diagram of a single stage vapour compression heat pump is presented in Fig. 5.

The performance of the HP was evaluated based on four variables and fixed temperature differences for both evaporator and condenser. The utilised variables were: the temperature of the sink process stream leaving the condenser T_{sink}, the temperature of the source T_{source} and the process stream temperature variation from inlet to outlet in both heat exchangers (ΔT_{sink} and ΔT_{source}). Both the sink temperature, and the variation of the sink was determined for a SF configuration HP as the forward temperature of DH, or the difference between DH forward and return in Fig. 1, respectively.

The temperature of the source is dictated by the type and location of the installation [32]. By using a DH network, large installations can be located near heat sources of elevated temperatures (compared to ambient conditions), such as sewage water, industrial waste heat, power plant stack gasses etc. Most of these heat sources tend to have a low yearly temperature variation and a finite heat capacity rate of the stream. In some cases the heat source can also be ocean or lakes where yearly variation in temperature would be expected. The performance of the considered heat pump was calculated using constant efficiencies for compressor and electrical motor, as well as fixed temperature differences in the heat exchangers. The used values for heat source and performance of equipment are presented in Table 2.

For DH forward and return temperatures of 100 °C and 50 °C respectively, the HP model represents a unit with a COP of 2.97 (-) including electric motor efficiency (3.12 (-), if only the thermodynamic cycle is considered).

2.4 DH booster heat pump

For supply of hot tap water, two constraints are to be respected, considering the Danish DH case. The requirements of the Danish building standard must be met [33], where hot tap water is utilised

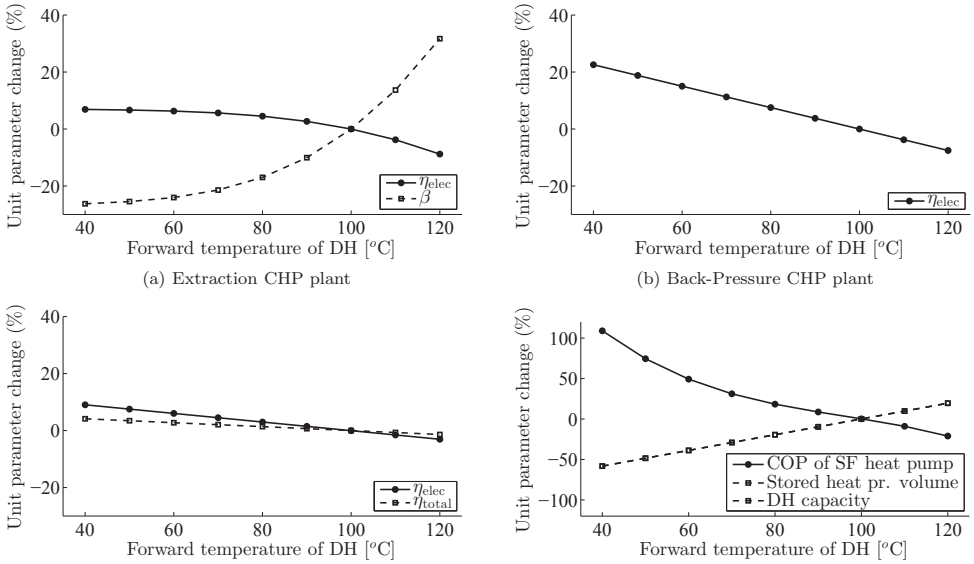

(a) Extraction CHP plant

(b) Back-Pressure CHP plant

(c) Combined cycle CHP plant

(d) Heat pump and changed temperature of DH

Figure 4: Changed performance parameters of three CHP types, HP and changed temperatures in DH network when design conditions (100 °C forward temperature) are altered to off-design operation.

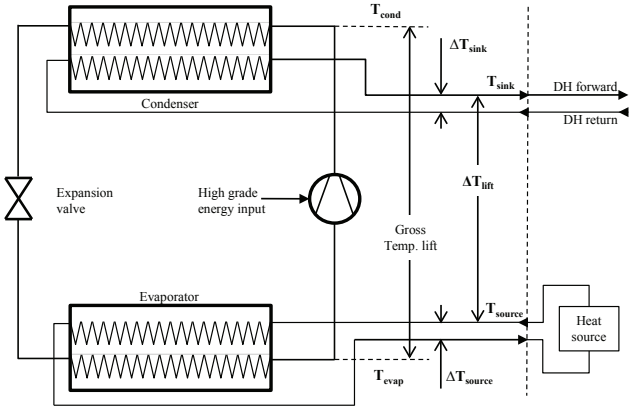

Figure 5: Schematic diagram of a single stage heat pump system for DH (configuration SF)

Table 2: Operational parameters for SF configuration HP

	Value	Unit	Designation
Type	R134a	-	Working fluid
Efficiency	0.8	-	Compressor isentropic efficiency
	0.95	-	Electric motor efficiency
Temperature	20	°C	Temperature of heat source
	10	K	Temperature variation of heat source
	5	K	Evaporator superheat
	5	K	Minimum pinch point in heat exchangers

at two temperature levels 45 °C and 40 °C, respectively. Additionally, a main concern is the issues related to the Legionella bacterium. To avoid bacteria growth, the hot tap water must either exceed a predefined temperature limit, where the bacteria can no longer exist when stored, or the tap water is not to be stored after being heated.

Two HP booster integration schemes were identified, corresponding to the schemes presented in Fig. 6a and 6b. In Ommen and Elmegaard [23] various specific configurations are investigated and compared based on their exergy efficiency. It is found that a heat pump on the primary side of the hot tap water heat exchanger, is superior in terms of COP and exergy efficency at almost all temperature configurations of low temperature DH. The considered configuration is presented in Fig. 6c.

In case the temperature of the DH network at the location of the consumer (in Fig. 2) is lower than 55 °C, it is assumed that the hot tap water constitutes a fixed share of DH heat demand. The share was determined by assessing the heat demand of the individual area (without heat losses) during the periods of the year where space heating is not needed. The remaining part of the supplied heat is utilised for space heating, and it was assumed that this fraction did not require boosting of the temperature.

For district heating consumer forward temperature of 40 °C and return temperature of 22 °C, the model represents a unit with a COP of 5.6 (-) and a power consumption of 0.066 kWh per kWh of hot tap water. For a forward temperature approaching 55 °C, the heat load is reduced and the COP of the unit increases. Thus at 55 °C the electricity consumption for boosting tap water temperatures becomes zero.

2.5 Heat and power system model

A detailed system model was developed for calculation of the economic and environmental impact of integrating heat pumps in an energy system with a high share of CHP-plants and intermittent electricity production from renewable technologies, e.g. wind turbines. The result was a validated heat and power system model, which features detailed representation of CHP technology as well as detailed representation of different heat pump technologies and integration possibilities [13].
The optimal production cost for the combined system can be achieved by minimisation of consumer cost for electricity and heat in daily auctions on hourly basis [34]. The optimal daily market clearances are then added for the duration of the year. When considering a system where capital cost can be considered as sunk cost, the objective function can be written as 3.

$$\min \left[\sum_{t \in \mathcal{T}} \left(\sum_{i \in \mathcal{I}} \dot{C}_{i,t}^{\mathrm{CHP}} + \sum_{h \in \mathcal{H}} \dot{C}_{h,t}^{\mathrm{boiler}} + \sum_{g \in \mathcal{G}} \dot{C}_{g,t}^{\mathrm{HP}} + \sum_{f \in \mathcal{F}} \dot{C}_{f,t}^{\mathrm{Other}} + \sum_{j \in \mathcal{J}} \dot{C}_{j,t}^{\mathrm{import}} - \dot{C}_{j,t}^{\mathrm{export}} \right) \right] \quad (3)$$

Where $\dot{C}$ is the total cost rate of production at the individual plant. The CHP units in the system are indexed by $\mathcal{I}$, boilers by $\mathcal{H}$, heat pumps by $\mathcal{G}$ and other heat and/or electricity production by $\mathcal{F}$. The neighbouring energy markets are indexed by $\mathcal{J}$.
It was assumed, that electricity and heat production of small-scale decentralized CHP-plants and intermittent electricity production from wind turbines are independent of the electricity cost in the individual hour. Using this assumption, the production profile of such units can be obtained from historical data.

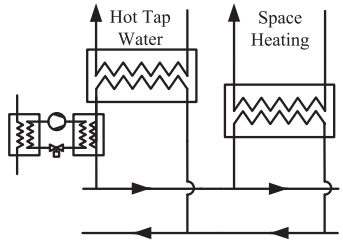

(a) Heat pump on primary side of the tap water heat exchanger

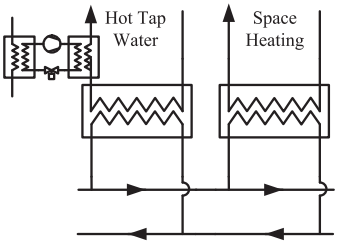

(b) Heat pump on secondary side of the tap water heat exchanger

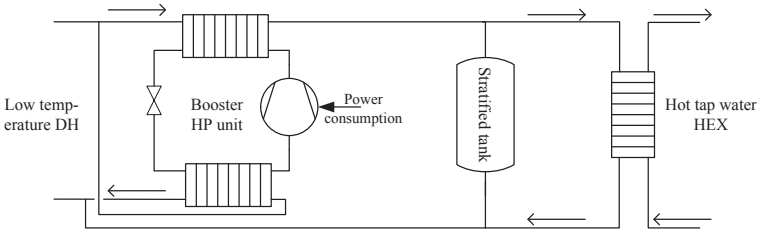

(c) Specific layout of DH booster HP unit

Figure 6: Two DH booster HP integration schemes.

The objective function shown in Eq. 3 was subject to a number of economic and technical constraints, of which the most important ones are presented and explained in appendix A. The economic constraints related to taxation are autonomous for each country, and are thus not presented in detail here. We refer to [13] for further information. The cost rates include all costs associated with utility production (e.g. fuel, taxes and subsidies) at the specific plant. In order to ensure the competitive conditions for import and export of electricity across taxation borders, the taxes for electricity are placed on the consumption. This is opposite to taxation for fuel, which is closely linked to the production.
The detailed representation of the CHP units includes various features which are briefly mentioned below:

- Four types of power plant units possible: Back-pressure, extraction, gas turbines/combined cycle or condensation.
- Limitation for hourly ramp rates and minimum technical production limits.
- Reduction in electricity production efficiency at part-load operation, which is specified individually for each unit.
- Startup and shutdown costs corresponding to size and type of unit
- Extraction technology represented by two power loss factors by heat extraction (β^1, β^2) depending on production above or below the "no-loss" point [7].
- Production at specific units can be prioritised, e.g. waste incineration.
- Availability (to market) is set individually for all units. For validation these data were obtained from urgent market messages from Nord Pool Spot [35].
- Different Danish taxation schemes for heat production are preprogrammed for each unit.
- Steam bypass of turbine possible for back-pressure CHP-units.
- Minimum available manual and frequency reserves are included for the total system, and technical limitations of reserves may be specified individually for each unit.

- Specific units may produce at higher capacity than their rating (overload) at reduced efficiency.

2.6 Current and future energy scenarios for Copenhagen

For each of the thermal CHP units in the current and planned utility system, specific information regarding capacity and efficiency, cost of fuels and maintenance, as well as capacities and consumption of the network were available online from various sources [36, 37, 38, 39, 40, 14].

In this way it was possible to derive the plant characteristics for current (Table 3a) and future (2025) energy scenario (Table 3b). Most of the data in the table is referring directly to the operational parameters of the individual units, but the table also includes fuel cost for 2011 and 2025 using historical prices or prognoses [38]. It should be noted that both electric efficiency and energy utilization were calculated for the plant in back-pressure operation mode.

The capacity and demand profiles, as well as planned changes, of DH networks in 2012 and 2025 were based on information from CTR, HOFOR and VEKS [14]. Changes to the demand, capacity of decentral CHP, on- and offshore wind turbines, photovoltaics and spot-prices for electricity in 2025 were available from Energinet.dk [38].

As the process of converting old steam networks to water-based networks is ongoing, the heat demand for water-based networks increases its demand faster than that which can be related to the heat demand from new areas. In the current scenario a number of units produces heat for the steam network, and is thus not effected by changes to the network temperature for water based DH systems. The units are AMV1, HCV4-8 and SMV7.

The scenarios were named as four different cases, Case #1-4. The details of the cases are presented in table 4. The difference between case #1 and #2 as well as case #3 and #4 is the use of temperature dependency for capacity constraints in the DH network, as well as temperature dependency for storage systems. The objective of including case #2 and #4 was to show the effects of the temperature dependency in the specific case that no further investments were made to the transmission network or to the storage facilities. This can be seen as a conservative estimate.

The objective of case #1 and #3 was to analyse the effects of lowering temperature, with similar capacity constraints as proposed for the traditional temperature levels. This assumption reflects that some critical network and storage capacity constraints in the transmission network can be low cost changes, compared to the magnitude of investments for the remaining system. Such investments would further imply additional work to DH pumps, due to increased volume flow, which is not included for the analysis. This may thus be seen as a high estimate.

Table 4: Four different cases for analysis of impact to system performance from lowering DH temperatures

	Energy scenario	Capacity dependent on temperature of DH
Case #1	2011	no
Case #2	2011	yes
Case #3	2025	no
Case #4	2025	yes

The four energy system cases were further expanded by introduction of a significant capacity of central SF configuration heat pumps (as presented in section 2.3). For each of the four cases the system was analysed without introduction of HP capacity, as well as a case with 200 MW capacity installed in the transmission network of the DH system (denoted "W/HP" for cases with HP installed). The installed capacity was divided equally at two locations, namely the location of Amagerværket (AMV) and Avedøreværket (AVV).

Carbon emissions for heat and electricity production in CHP plants were calculated based on the 125 % method for heat, assuming that heat is produced at 125 % efficiency, whereas the remaining part correspond to electricity production [41]. Other methods are also utilised for splitting contributions, such as 200 %, energy basis or quality (exergy) of content. Carbon emissions from combustion of fuel correspond to the Danish Energy Agency [40]

3 Results

The various energy system scenarios were compared based on six different parameters. The parameters were: Combined system cost, CO_2-emissions from heat and electricity individually, primary energy consumption, net imported electricity and the production ratio between electricity and heat in the extraction CHP units. The calculated results represent the entire bidding area, ex-

Table 3: Thermal power plant unit characteristics for central power plants and waste inceneration plants in DK2 bidding area.

(a) Current (2011) energy scenario

	Fuel type	Cost fuel (€/GJ)	Type	Priority	Turb. byp.	η_{elec} (-)	η_{total} (-)	β^1 (-)	β^2 (-)	Ramp rate (-)	Min. load (-)	Man. reserve (-)	Freq. reserve (-)	η_{elec} reduction (%)	Boiler capacity (MW)
AMV1	bio/straw	9.4	Backp.		X	0.20	0.92			0.25	0.50		0.05	0.08	350
AMV3	coal	3.3	Extr.			0.35	0.89	0.14	0.10	0.25	0.50		0.05	0.08	595 (+75)
HCV4	nat. gas	5.9	Backp.		X	0.11	0.82			0.25	0.45	0.03	0.05	0.08	157
HCV7	nat. gas	5.9	Backp.		X	0.26	0.89			0.25	0.45	0.03	0.05	0.08	285
HCV8	nat. gas	5.9	CC			0.20	0.89			1.00	0.55	0.05	0.10	0.16	127
SVM7	nat. gas	5.9	CC			0.23	0.92			1.00	0.50	0.05	0.10	0.16	275
AMF1	waste	4.0	Backp.	X	X	0.21	0.83			0.25	0.70			0.08	132
AVV1	coal	3.3	Extr.			0.35	0.89	0.14	0.10	0.25	0.50	0.03	0.05	0.08	595 (+75)
$AVV2_{B1}$	bio	9.9	Extr.			0.36	0.92	0.18	0.12	0.25	0.45	0.03	0.05	0.08	805
$AVV2_{B2}$	straw	8.0	Extr.			0.34	0.91	0.16	0.12	0.25	0.45			0.08	100
$AVV2_{cc1}$	nat. gas	5.9	CC			0.51	0.85	0.11	0.11	1.00	0.55	0.05	0.10	0.16	135
$AVV2_{cc2}$	nat. gas	5.9	CC			0.51	0.85	0.11	0.11	1.00	0.55	0.05	0.10	0.16	135
KARA5	waste	4.0	Backp.	X	X	0.17	0.80			0.25	0.70			0.08	65
VF5	waste	4.0	Backp.	X		0.13	0.82			0.25	0.70			0.08	90
VF6	waste	4.0	Backp.	X		0.19	0.82			0.25	0.70			0.08	105
ASV2	coal	3.3	Extr.			0.31	0.88	0.18	0.15	0.25	0.20	0.03	0.05	0.08	368
ASV5	coal	3.3	Extr.			0.26	0.88	0.18	0.15	0.25	0.40	0.03	0.05	0.08	1750
KYB1	oil	11.9	Elec. only			0.33	0.33			0.60	0.48	0.03	0.05	0.08	790
KYB2	oil	11.9	Elec. only			0.33	0.33			0.60	0.48	0.03	0.05	0.08	790

(b) Future (2025) energy scenario

	Fuel type	Cost fuel (€/GJ)	Type	Priority	Turb. byp.	η_{elec} (-)	η_{total} (-)	β^1 (-)	β^2 (-)	Ramp rate (-)	Min. load (-)	Man. reserve (-)	Freq. reserve (-)	η_{elec} reduction (%)	Boiler capacity (MW)
AMV1	bio/straw	8.9	Backp.		X	0.30	0.92			0.25	0.50		0.05	0.08	350
AMV3	bio	9.9	Extr.			0.34	0.89	0.14	0.10	0.25	0.50		0.05	0.08	640
AMF1	waste	4.0	Backp.	X	X	0.21	0.99			0.25	0.70			0.08	203
FLIS1	bio	9.9	Backp.		X	0.20	0.99			0.25	0.45			0.08	150
AVV1	bio	9.9	Extr.			0.34	0.89	0.14	0.10	0.25	0.50	0.03	0.05	0.08	640
AVV2	bio	9.9	Extr.			0.36	0.92	0.18	0.12	0.25	0.45	0.03	0.05	0.08	960
AVV3	straw	5.7	Extr.			0.34	0.91	0.16	0.12	0.25	0.45			0.08	125
KARA5	waste	4.0	Backp.	X	X	0.17	0.80			0.25	0.70			0.08	65
KARA6	waste	4.0	Backp.	X	X	0.22	0.99			0.25	0.70			0.08	82
VF5	waste	4.0	Backp.	X		0.12	0.99			0.25	0.70			0.08	90
VF6	waste	4.0	Backp.	X		0.18	0.99			0.25	0.70			0.08	105
VF7	waste	4.0	Backp.	X		0.27	0.99			0.25	0.70			0.08	102
KKV7	bio	9.9	Backp.		X	0.18	0.90			0.25	0.45			0.08	45
KKV8	bio	9.9	Backp.		X	0.25	0.90			0.25	0.45			0.08	55
ASV2	coal	3.2	Extr.	X		0.31	0.88	0.18	0.15	0.25	0.20	0.03	0.05	0.08	368
KYB1	oil	16.0	Elec. only			0.33	0.33			0.60	0.48	0.03	0.05	0.08	790
KYB2	oil	16.0	Elec. only			0.33	0.33			0.60	0.48	0.03	0.05	0.08	790

cept for carbon emissions of heat, where the results represent the emissions in the Greater Copenhagen DH area.

The results of the analysis were calculated as relative differences, compared to the energy scenario base case - either state of the art (2011) or compared to the future scenario (2025) as presented in [14]. This implies, that the results of a specific calculation (e.g. Case #1 at 60 ˚C) correspond to the relevant scenario (2011) at DH network design temperature of 100 ˚C. Each of the six calculated system parameters are presented in table 5 for both current and future energy scenario.

Although only separated by 14 years, the two energy system scenarios are quite different in terms of cost and carbon emissions. The main reason for the reductions in primary energy use and net import of electricity in 2025 was the significant increase in intermittent electricity production.

The reason for the discrepancy between the calculated emissions and the previously mentioned zero carbon emission goal, was the difference in imposition for carbon expenditure for waste as a fuel. In *Heat plan Greater Copenhagen* a significant effort is placed for recycling the carbon constituents from waste [14], whereas the performed calculations in this paper assume similar carbon composition as that of today.

The influence to CO_2-emission for exported electricity corresponds to the overall emissions from electricity, which thus influences not only the specific bidding area, but also to a limited extent the emissions of neighbouring transmission networks.

3.1 Current energy scenario

The results for case #1 and #2 are presented in Fig. 7 relative to the 2011 scenario. For case #1, system cost and CO_2-emissions are presented in Fig. 7a, whereas primary energy use, net imported electricity and extraction CHP production ratio are presented in Fig. 7b. For case #2, similar parameters are presented in Fig. 7c and 7d respectively. The results of DH temperature variations for the base case (without HPs) is presented in black color, whereas results representing configurations with the additional installed heat pump capacity, are presented in gray.

By reducing DH temperatures for Case #1 (Fig. 7a), the consumer cost were reduced up to approximately 2.8 %, and emissions by approximately 1 % and 6.4 % for electricity and heat respectively. The performance improvements were consequences of the increased electricity production efficiency at CHP plants, as well as reduction in heat losses from the network.

Both system cost and carbon emissions from electricity reached a minimum at 60 ˚C, whereas the minimum emissions for heat were found for forward temperatures of 50 ˚C. The minimum can be explained by the utilisation of additional electricity to increase the temperature of the hot tap water, when the consumer temperature decreases below the set value of 55 ˚C.

The electricity and heat demands are similar for all results corresponding to a specific energy scenario, and thus also the interdependency for the specific CO2 emissions for the overall emissions.

By integration of the considered central HP capacity the cost was further reduced. For the reference temperature level (100 ˚C) a reduction in system cost of 1.2 % was possible, with a corresponding reduction in emissions for heat of 3.6 %. CO_2 emissions for electricity was reduced slightly. The trend for system cost for a system with HPs resembles that of the base case, but with an offset in favour of the HP case of approximately 2 percentage-points. The combination of reduction in DH temperatures and integration of central HP capacity in the network resulted in large reductions of CO_2 emissions for heat. The maximal reduction was 19 %, which was found for DH forward temperature of 40 ˚C. For forward temperatures below 80 ˚C the CO_2 emissions for electricity was increased compared to the system without HP capacity (up to 2 % increase).

It was found that both primary fuel usage and import of electricity decreased when decreasing DH temperatures for case #1 (Fig. 7b). For the case with HP integration, the primary energy usage decreased further, whereas the net import of electricity increased significantly. Such results suggest that the constrained production of CHP units was reduced by integrating HPs. This presumption was further supported by increased electricity production ratio of extraction CHP plants in the case with HPs compared to case #1, and correspond to the increased CO_2 emissions for electricity, as less heat was produced from thermal units, which shifts carbon emissions from the consumed fuel towards electricity. The increased production ratio of extraction CHP plants in case #1 (without HP) may be explained by the increase in back-pressure efficiency from reduction in DH temperatures.

Table 5: Results of energy scenarios base case (100 ˚C) for six system parameters

Parameter	Unit	2011 scenario	2025 scenario
Total system cost	10^8 €	5.16	5.95
Heat CO_2-emission	kg/MWh	0.13	0.05
Electricity CO_2-emission	kg/MWh	0.36	0.15
Primary energy use	10^7 GJ	8.42	7.38
Net. Imported Electricity	10^6 MWh	2.09	1.10
Extr. CHP prod. ratio	%	0.00	-2.20

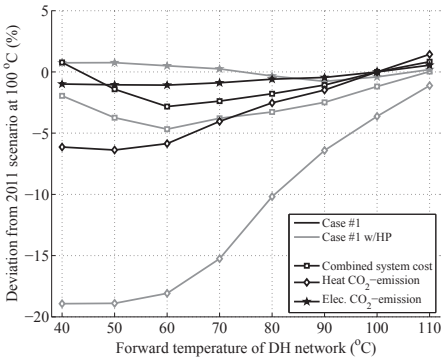

(a) Case #1: System cost and CO_2 emissions

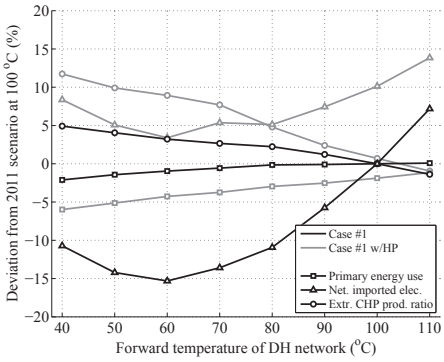

(b) Case #1: Primary energy use, net import of electricity and extraction CHP prod. ratio

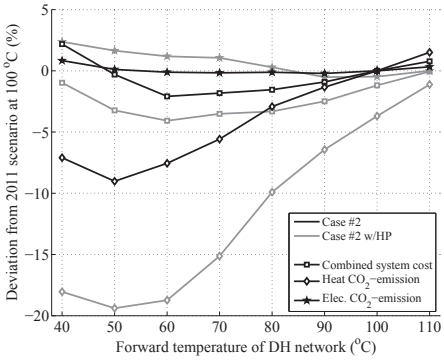

(c) Case #2: System cost and CO_2 emissions

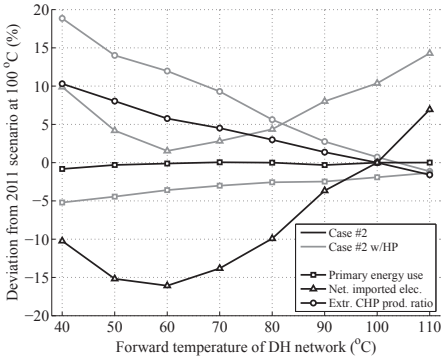

(d) Case #2: Primary energy use, net import of electricity and extraction CHP prod. ratio

Figure 7: Impact to key parameters for lowering DH network temperature for Case #1 and #2 and with integration of 200 MW central HP capacity

For case #2 (capacity and storage constraints according to change in DH temperature levels) the obtained results resemble those presented above. Comparing Fig. 7a and 7b with 7c and 7d respectively, it was found that trends are similar at high DH temperatures, whereas the performance improvements at low DH forward temperatures were reduced. The impact was increasingly significant at forward temperatures below 60 °C. The potential benefits at the temperature levels of maximal reductions from case #1 were reduced, but even with capacity constraints in place, the benefit was significant. As an example, the combined system cost reduction was changed from 2.8 % to 2.1 % for the system without HP integration, and reductions in carbon emissions for the system with HPs integrated are even slightly increased. A significant difference was found for the production ratio of extraction CHP plants, which at low forward temperatures increased approximately 5 % for the system without HP, and 6 % for the system with integration of HPs. The difference was particularly large for DH temperatures of 40-60 °C. This could suggest that the production ratio was changed due to limited network capacity at periods with high heat consumption.

3.2 Comparison of the two energy scenarios

The two reference scenarios (2011 and 2025) are compared in Fig. 8. The results of both scenarios were calculated on the basis of the 2011 scenario (in table 5). Variations from the investigated parameters are presented in black colour for case #1, and by gray curves for case #3.

The case #1 data for cost and CO_2-emissions in Fig. 8a, as well as primary fuel usage and import in Fig. 8b, are similar data as those presented in Fig. 7a and 7b, respectively. Compared to case #1, case #3 presented significantly increased system cost (typically around 14-15 % increase) but at the same time significantly reduced heat and electricity CO_2 emissions. The reductions in emissions were minimum 52 % for heat and 58 % for electricity.

From Fig. 8b it is found, that case #3 implied a significantly lower net import of electricity (between 40 and 50 %), and lower consumption of primary energy (approximately a reduction of 14 %). The reduction was due to a large increases of intermittent electricity in the future scenario. This was obtained without significantly affecting the production ratio of the extraction plants compared to todays operation.

The impact of changing DH temperatures on the performance of the two cases was shown to be equal in magnitude and experience similar trends at various temperature levels.

3.3 2025 energy scenario

Results for future scenario cases #3 and #4 are presented in Fig. 9. The reference data (black) of Fig. 9a and 9b, corresponds to the gray curves presented in Fig. 8a and 8b, respectively.

The maximal reduction in system cost, by decreasing the DH temperatures, was 3.2 % for case #3, and a reduction of 6 % when the considered additional HP capacity was integrated. For both cases this was marginally higher savings, than those presented for case #1. For case #3 with HP, the savings at forward temperatures of 50 °C was similar to that of 60 °C. The gain from integrating HP technology in low temperature DH in terms of cost was larger in 2025 low temperature scenarios, compared to 2011. For the case of 50 °C, the gain of central HP units were at a magnitude, where the technology compensates for the additional electricity consumption at the consumer booster HP.

The gain in terms of CO_2 emissions of lowering DH temperatures for case #3 were small, considering systems with or without central HP integration. The maximal reduction was for heat, which was 5.8 and 7.2 % respectively, but as the base scenario was already significantly reduced, the actual reductions were low. From Fig. 9b it was found that net imported electricity was significantly reduced, with a minimum at -24 to -28 % for 60 - 70 °C depending on whether or not HP capacity was included.

As for the similarities between case #1 and #2, corresponding characteristics were found for the differences between case #3 and #4. The effects of DH temperature capacity constraints were large at DH temperature levels below 60 °C. A difference for the future scenario was that a reduction in carbon emissions was not achieved for case #4 at DH temperatures between 70 and 110 °C.

3.4 Parametric analysis

A detailed parametric analysis is presented for four significant input parameters, and analysed for three of the six presented parameters, as well as HP operation hours for the two units. The parametric analysis was performed for the 2025 energy scenario, case #4 w/HP, and is presented in Fig. 10 with variations of ± 20 % of the individual input

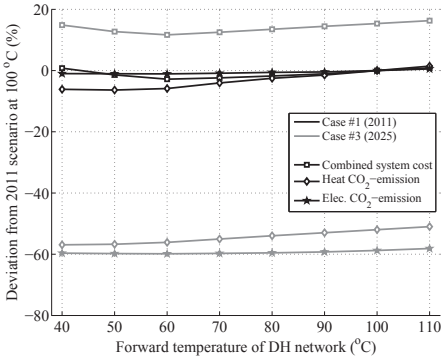

(a) Case #1 and #3: System cost and CO_2 emissions

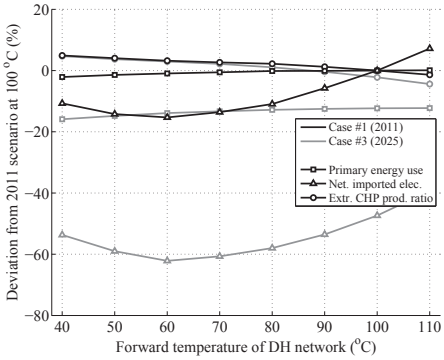

(b) Case #1 and #3: Primary energy use, net import of electricity and extraction CHP prod. ratio

Figure 8: Comparison of key parameters for current and future energy system scenarios

parameters. The results were calculated as relative to DH network temperatures of 100 °C for 2025 scenario.
The four considered input parameters are presented below:

- Mean spot price for bidding area. Capacity of interconnections remain as specified by Energinet.dk [38].
- Biomass fuel cost.
- Production of electricity from residual technologies. This parameter is for both intermittent sources as well as decentral CHP units.
- The COP of the considered HP.

In Fig. 10a the influence of the four input parameters is presented for the combined system cost. It was found that the spot price, biomass fuel cost and the changes in production of residual electricity technologies affected the results with similar magnitude: approximately 5 to 7 % changed cost for a 20 % change in input parameter. Changes to HP COP influenced the cost of the system to a minor degree.
For carbon emissions from electricity, the chosen input parameter of biomass fuel cost was highly sensitive. A reduction of 14 % on carbon emissions for 20 % reduction in fuel cost was experienced, according to Fig. 10b. The influence was not as significant if the fuel cost was increased. Minimal changes were found for changes to CO_2 emissions from heat (Fig. 10c), where the fuel cost of biomass again was the most sensitive.
In Fig. 10d heat pump operation hours were presented. It was shown, that one unit (the one located at Avedøreværket) experienced significantly less operation hours than the sibling (located at Amagerværket). This was included to show that for case #4 w/HP, at 70 °C, the DH network capacity constraints were a significant limitation to the considered technologies, especially for the marginal cost unit of the network capacity.

4 Discussion

In the analysis, the influence of varying DH temperatures for several different utility technologies was examined. This was done in order to establish the potential for reductions in cost and primary fuel consumption. In such large systems with many cooperating units, minor misrepresentation for individual technologies can have affected the production distribution, but not significantly influenced the total consumer cost, carbon emissions or total primary fuel use. The litterature study revealed no similar studies or analysis, and comparison with relevant literature was thus not possible.
The energy system model which was utilised for the analysis has been validated against historical data of 2011. The scenario of the current energy system was based directly on the validated calculation. The future energy scenario was based on

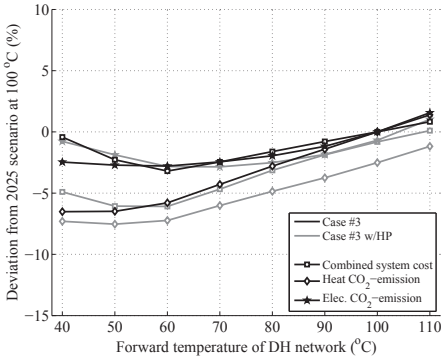

(a) Case #3: System cost and CO_2 emissions

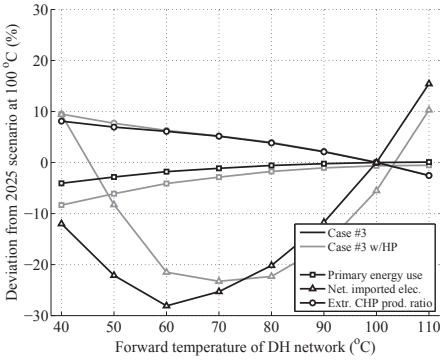

(b) Case #3: Primary energy use, net import of electricity and extraction CHP prod. ratio

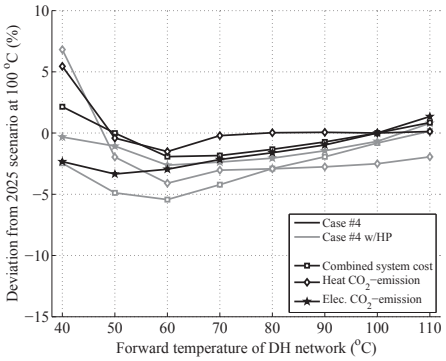

(c) Case #4: System cost and CO_2 emissions

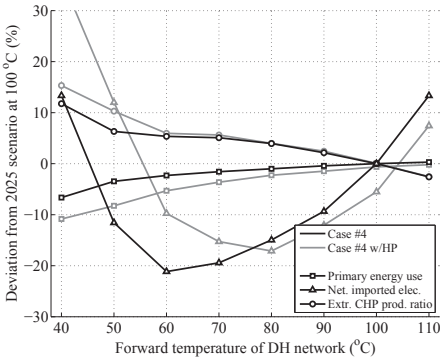

(d) Case #4: Primary energy use, net import of electricity and extraction CHP prod. ratio

Figure 9: Impact to key parameters for lowering DH network temperature for Case #3 and #4 and with integration of 200 MW central HP capacity

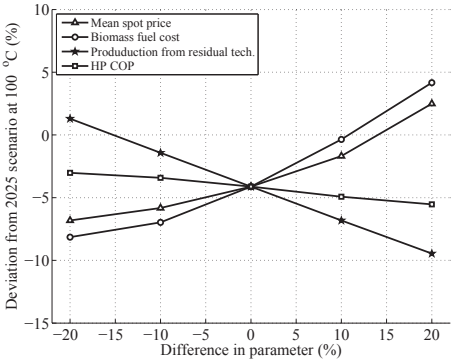

(a) Case #4 w/HP: Combined system cost

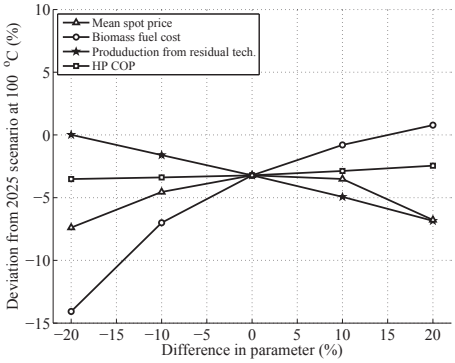

(b) Case #4 w/HP: CO_2-emissions of electricty

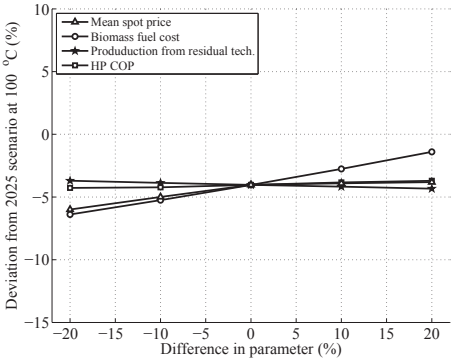

(c) Case #4 w/HP: CO_2-emissions of heat

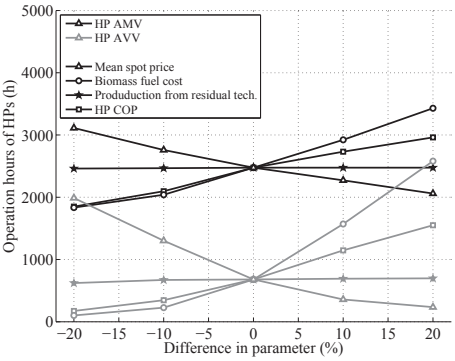

(d) Case #4 w/HP: Operation hours for the two HP units

Figure 10: Parametric analysis of the results from case #4 w/HP at forward temperatures of 70 °C

a prognosis of demand and planned energy system changes such as design data for new units [38, 14].

The impact of lowering temperatures for utility technologies in the network were calculated based on a series of thermodynamic models. Due to lack of data, only the model for the extraction CHP plant was validated (against Elmegaard and Houbak [6]), but the remaining models was verified for operation within the considered temperature span for DH. The model for the DH booster HP configuration was previously published and the technology is currently close to commercially available [42].

Several of the findings (e.g. Fig. 7 and 9) suggested choosing temperatures at 60 °C, as this technically is the optimal temperature for achieving low operation cost. In the analysis, the investment cost related to changes in the system were not included, which likely would change recommendation towards higher temperatures. Additionally, at 60 °C forward temperatures, the consumer temperature was below 55 °C, which thus required DH booster HP units in all dwellings. As the reduction in terms of cost and emissions were low from utilising temperatures above this investment limit, forward temperatures of e.g. 70 °C would likely result in increased relevance for the consumer.

The presented results may be seen as case specific, as they represent the specific generation technologies, demand curves and capacity constraints of the Greater Copenhagen network. But, as shown in the analysis, the two energy scenario cases result in quite similar trends for development in terms of cost, carbon emissions and primary fuel consumption. Thus, it is expected that similar trends would be representative for other large networks.

The transmission network was included in the calculation, due to the impact of such constraints to cost reductions or energy efficiency in the current system. By changing the DH network temperatures further capacity constraints may occur, e.g. in the distribution network. Such information was not available, and would require significant changes to the utilised models. On the other hand, the constraints of network capacities in distribution networks could be assessed individually, as transmission network flow profiles can be supplied as an input, based on the presented study.

5 Conclusion

The influence of DH network temperatures to the performance of utility production in Greater Copenhagen was investigated for forward temperatures between 40 to 110 °C. Two energy scenarios were considered, one current, which was validated model for 2011, and a future scenario, as proposed by energy planners for 2025, where reductions in carbon emissions for heat were of major interest. As neither of the two scenarios utilise central HPs for DH production, two additional scenarios were created to investigate if changed DH temperatures influenced the performance of this technology.

Compared to the current, the future scenario resulted in increased cost for consumers by approximately 15 %, but also carbon reductions above 50 % on both electricity and heat. The two scenarios showed similar trends for cost and emissions for reduced DH temperatures. Reduction in consumer cost were possible, with increasing magnitude with reductions in DH temperatures, until the point where electricity was needed to boost the temperatures of hot tap water in the individual dwellings.

Integration of central HPs became increasingly beneficial with reductions in DH temperatures. In a current scenario with central HPs installed, cost reductions of approximately 4-5 % were achieved, which further reduces carbon emissions from DH by more than 15 %. For future scenarios, cost reductions were further increased, but further reduction in carbon emissions for 2025 were barely possible with the considered HP technology. For both cases the maximal reduction of consumer cost was found for 60 °C forward temperature.

Based on the results, the authors recommend the use of 65-70 °C as the optimal forward temperature for DH networks, since lower temperatures require high investment, among others DH booster HP units in each dwelling. The difference between 60 and 70 °C forward temperatures corresponds to a difference of approximately 1.5-2 % on consumer costs for the future scenario.

The results were network specific, as they represent the specific generation technologies and demand curves and network capacities, but similar trends were found for the two different scenarios, and similar effects may thus also be expected for other large DH networks.

Acknowledgement

This work was supported by Copenhagen Cleantech Cluster (CCC), DONG Energy and Danish Technological Institute (DTI)

References

[1] Blarke, M.B.. Towards an intermittency-friendly energy system: Comparing electric boilers and heat pumps in distributed cogeneration. Applied Energy 2012;91(1):349–365.

[2] DONG Energy, . Annual report 2014 - Green, Independent and Cost-effective Energy. 2015. URL: http://assets.dongenergy.com/DONGEnergyDocuments/com/Investor/Annual_Report/2014/dong_energy_annual_report_en.pdf.

[3] Danish Government, . Government platform (in danish: Regeringsgrundlag). 2011. URL: http://www.stm.dk/publikationer/Et_Danmark_der_staar_sammen_11/Regeringsgrundlag_okt_2011.pdf; [accessed 25.03.14].

[4] City Council of Copenhagen, . CPH climate plan 2025 (in danish: KBH 2025 klimaplan - en grøn, smart og CO2-neutral by.). 2013. URL: http://cityclimateleadershipawards.com/copenhagen-cph-climate-plan-2025/; [accessed 25.03.14].

[5] CTR, HOFOR and VEKS, . Heat plan Greater Copenhagen 3 (in danish: Varmeplan Hovedstaden 3). 2014. URL: http://www.varmeplanhovedstaden.dk/publikationer-og-moeder; [accessed 25.03.14].

[6] Elmegaard, B., Houbak, N.. Simulaton of the Avedøreværket Unit 1 Cogeneration Plant with DNA. Proceedings of The 16th International Conference on Efficiency, Cost, Optimization, Simulation, and Environmental Impact of Energy Systems (ECOS 2003),; Technical University of Denmark; 2003,.

[7] Verbruggen, A.. Combined heat and power (CHP) essentials. International Journal of Energy Technology and Policy 2007;5(1):1–16.

[8] Lowe, R.. Combined heat and power considered as a virtual steam cycle heat pump. Energy Policy 2011;39(9):5528–5534.

[9] Ommen, T., Markussen, W.B., Elmegaard, B.. Heat pumps in combined heat and power systems. Energy 2014;76(0):989–1000.

[10] Ommen, T., Verda, V., Jensen, J.K., Markussen, W.B., Elmegaard, B.. Exergoeconomic optimisation of heat pumps in district heating systems. Energy 2015;xx(0):1–18. [submitted].

[11] SKAT, . Examples for calculation of taxreduction for various heat production units (in danish: Eksempler p beregning af afgiftslempelse for forskellige varmeproduktionsanlæg). 2014. URL: https://skat.dk/SKAT.aspx?oID=2061615; [accessed 05.12.14].

[12] Bach, B.. Integration of heat pumps in greater copenhagen. Master's thesis; Technical University of Denmark; 2014.

[13] Ommen, T.. Heat pumps in CHP systems - high-efficiency energy system utilising combined heat and power and heat pumps. Ph.D. thesis; Technical University of Denmark; 2015.

[14] CTR, HOFOR and VEKS, . Heat plan Greater Copenhagen 2 - options for CO2-neutral distict heating (in danish: Varmeplan Hovedstaden 2 - handlemuligheder for en CO2-neutral fjernvarme). 2014. URL: http://www.varmeplanhovedstaden.dk/publikationer-og-moeder; [accessed 25.03.14].

[15] F-Chart Software, . Engineering equation solver. 1992.

[16] Ferris, M.C.. Matlab and gams: Interfacing optimization and visualization software. Tech. Rep. 1; 2007.

[17] GAMS Development Corporation, . General algebraic modeling system. 1998. URL: http://www.gams.com/.

[18] IBM, . IBM ILOG CPLEX. 2009. URL: www.ibm.com.

[19] Centralkomunernes Transmissionsselskab I/S, . Technical key figures (in danish: Tekniske nøgletal). 2013. URL: http://www.ctr.dk/teknik.aspx; [accessed 02.02.15].

[20] Dansk Fjernvarme, . Benchmarking, statistics 2011/2012 (in danish: Benchmarking, statistik 2011/2012). 2013. URL: http://www.fjernvarmen.dk/Faneblade/HentMaterialerFANE4/~/media/Publikationer/Aarsstatistikker/BenchmarkingStatistik20112012.ashx; [accessed 26.09.13].

[21] Lund, H., Werner, S., Wiltshire, R., Svendsen, S., Thorsen, J.E., Hvelplund, F., et al. 4th generation district heating (4GDH). integrating smart thermal grids into future sustainable energy systems. Energy 2014;68:1–11.

[22] Zvingilaite, E., Ommen, T., Elmegaard, B., Franck, M.. Low Temperature District Heating Consumer Unit with Micro Heat Pump for Domestic Hot Water Preparation. District Energy Development Center; 2012, p. 136–143.

[23] Ommen, T.S., Elmegaard, B.. Exergetic evaluation of heat pump booster configurations in a low temperature district heating network. In: Desideri, U., Manfrida, G., Sciubba, E., editors. The 25th International Conference on Efficiency, Cost, Optimization and Simulation of Energy Conversion Systems and Processes (Perugia, June 26th-June 29th, 2012). Firenze University Press; 2012,.

[24] Elmegaard, B., Ommen, T.S., Markussen, M., Iversen, J.. Integration of space heating and hot water supply in low temperature district heating. Energy and Buildings 2015;:–doi:http://dx.doi.org/10.1016/j.enbuild.2015.09.003.

[25] Pirouti, M., Bagdanavicius, A., Ekanayake, J., Wu, J., Jenkins, N.. Energy consumption and economic analyses of a district heating network. Energy 2013;57:149–159. doi:10.1016/j.energy.2013.01.065.

[26] Dalla Rosa, A., Christensen, J.. Low-energy district heating in energy-efficient building areas. Energy 2011;36(12):6890–6899. doi:10.1016/j.energy.2011.10.001.

[27] Lin, F., Yi, J., Weixing, Y., Xuzhong, Q.. Influence of supply and return water temperatures on the energy consumption of a district cooling system. Applied Thermal Engineering 2001;21(4):511–521. doi:10.1016/S1359-4311(00)00046-6.

[28] Kvisgaard, B., Hadvig, S.. Varmetab fra fjernvarmeledninger : Heat loss from pipelines in district heating systems. Teknisk forlag; 1980. ISBN 8757106355, 9788757106350.

[29] Bøhm, B.. Simple methods for determination of heat losses from district heating pipes under normal con-

ditions [in danish: Enkle metoder til bestemmelse af varmetab fra fjernvarmeledninger under normal drift]. Danmarks Tekniske Højskole, Lyngby (Denmark) and Sønderborg Fjernvarmeselskab A.m.b.A., Sønderborg (Denmark).; 1990. ISBN 8788038181, 9788788038187.

[30] Nord Pool Spot, . The power market. 2013. URL: http://umm-archive.nordpoolspot.com/web/; [accessed 02.02.15].

[31] Houbak, N.. Proposal for simulator contest. Proceedings of the 16th International ECOS conference. Volume 1, 2, and 3; DTU, Technical University of Denmark; 2003,.

[32] Berntsson, T.. Heat sources - technology, economy and environment. International Journal of Refrigeration 2002;25(4):428–438.

[33] Danish Standards, . Code of practise for domestic water supply installations (DS 439). 2009.

[34] Ommen, T., Markussen, W.B., Elmegaard, B.. Comparison of linear, mixed integer and non-linear programming methods in energy system dispatch modelling. Energy 2014;74:109–118.

[35] Nord Pool Spot, . UMM archive. 2013. URL: http://www.nordpoolspot.com/How-does-it-work/; [accessed 02.02.15].

[36] DONG Energy, . Environmental reports 2011. 2012. URL: http://assets.dongenergy.com/DONGEnergyDocuments/com/Business%20Activities/Thermal%20Power/Environmental_Reports/2011/; [accessed 23.03.14].

[37] Vattenfall A/S, . Environmental reports 2011 (in danish: Grønne regnskaber 2011). 2012. URL: http://corporate.vattenfall.dk/globalassets/danmark/om_os/gronne_regnskaber/amagervaerket-gront-regnskab-2013.pdf; [accessed 23.03.14].

[38] Energinet.dk, . Energinet.dk analytic prerequisites 2012-2035 [in danish: Energinet.dk's analyseforudsætninger 2012-2035]. Tech. Rep. 1; 2012.

[39] Energinet.dk, . Download of market data - elspot price, capacity on transmission lines etc. 2011. URL: http://www.energinet.dk.

[40] Danish Energy Agency, . Assumptions of socio-economic analysis in the energy sector [in danish: Forudsætninger for samfunds- økonomiske analyser påenergiområdet]. 2011. [accessed 10.10.13].

[41] Energinet.dk, . Guidelines for the environmental declaration of electricity [in danish: Retningslinjer for miljødeklarationen for el]. Tech. Rep. 1; 2015.

[42] EUDP - Energiteknologisk udvikling & demonstration, . Heat pumps for hot tap water in low temperature district heating networks. (in danish: Varmepumper til brugsvand i forbindelse med lavtemperaturfjernvarme). 2015. URL: http://www.energiteknologi.dk/da/project/varmepumper-til-brugsvand-i-forbindelse-med-lavtemperaturfjernvarme; [accessed 25.03.15].

[43] Verbruggen, A.. A systemmodel of combined heat and power generation in district heating. Resources and Energy 1982;4(3):231–263.

[44] Energinet.dk, . Introduction to system services (in danish: Introduktion til systemydelser, dok. 43532-13, sag 13/208). 2013. URL: http://www.energinet.dk.

[45] Energinet.dk, . Ancillary services to be delivered in denmark:tender conditions (in danish: Systemydelser til levering i danmark: Udbudsbetingelser). 2012. URL: http://www.energinet.dk.

[46] Amager Ressourcecenter, . Environmental reports (in danish: Miljøredegørelse). 2012. URL: http://www.a-r-c.dk/media/123663/miljoredegorelse_2012-pdf-.pdf; [accessed 23.03.14].

[47] Vestforbrænding, . Measurement and results (in danish: Måling og resultater). 2012. URL: http://www.vestfor.dk/web/10157/37@public; [accessed 23.03.14].

[48] KARA/NOVEREN I/S, . Environmental reports (in danish: Grønne regnskaber). 2012. URL: http://karanoveren.dk/karanoveren/organisation/groenne-regnskaber; [accessed 23.03.14].

Nomenclature

$\dot{C}$	cost rate, €/h
c	cost factor, €/MWh or €
$\dot{H}$	flow rate of enthalpy, MWh/h
o	binary operation variable, -
P	power, MW
Q	quantity of heat in storage, MWh
$\dot{Q}$	heat production, MJ/s
r	ratio, -
UMM	availability input parameter, -
v	binary design input parameter, -

Greek symbols

β	power loss factor by heat extraction, -
Δ	reduction, MJ/s
η	efficiency, -

Superscripts

1	below the "no-loss" point
2	above the "no-loss" point
elec	electric
ex.	extraction
max	maximum
min	minimum
rel	relative to maximum

Subscripts

f	other technologies
g	heat pumps
h	boilers
i	CHP plants
j	energy markets
k	thermal unit sites
l	transmission notes
m	transmission networks
n	distribution networks
t	hours

Abbreviations

CHP	Combined Heat and Power
COP	Coefficient of Performance
HP(s)	Heat Pump(s)
HS	Heat storage
O&M	operation and maintenance
TL	transmission losses

Appendices

A Energy system model formulation **22**
A.1 Structure . . . 23
A.2 Economic constraints . . . 23
A.3 Electricity and heat balances . . . 24
A.4 Technology constraints . . . 26
A.5 System reserves and operational constraints . . . 29

B Energy system model validation **29**
B.1 Environmental reports . . . 30

A Energy system model formulation

In this appendix, the key technical and economical constraints of the detailed system model are presented. As the economic constraints related to taxation are autonomous for each country, the reader is referred to [13] for further information on this specific topic for Danish conditions.

The model was implemented in General Algebraic Modelling System [17] using the mixed integer linear optimisation algorithm CPLEX [18]. External data processing is handled by Matlab, using the interface gdxmrw [16]. The implementation of energy system layout (eg. CHP-units, heat pumps or transmission capacity) is generic and easy to change from one case to another.

A.1 Structure

The problem was considered over a period of time $\mathcal{T} = 1, \ldots, t$, which corresponds to the operation of the spot market. For each time periods, data for power plant load and the amount of stored heat at the termination of the period is passed on to the beginning of the subsequent period.
The heat and electricity demands, as well as the electricity produced at decentral CHP plants and by wind turbines in the region, were supplied as input to each of the time periods.
For the case where capital cost are considered as sunk cost, the objective function for minimisation of each time period was calculated as presented in Eq. 3 and further explained in section 2.5.
Several locations are used in the analysis. Traditional production areas for thermal units are indexed by $\mathcal{K}$. District heating transmission points (collection of streams) are indexed by $\mathcal{L}$. Transmission networks are indexed by $\mathcal{M}$ and the distribution networks by $\mathcal{N}$.

A.2 Economic constraints

For most of the assessed technologies, the cost of utility production at an individual unit depends on the unit type, its efficiency, operation and maintenance cost and the type of fuel. Apart from direct fuel cost, the individual fuel types may further be affected by different taxation or subsidy schemes or by additional transportation and handling cost. The operation and maintenance cost included in the model correspond to the variable contribution.
In the following sections, the economic constraints are listed for individual unit types. Note that the description of power plants represents several types: extraction CHP, back pressure CHP and condensing power plants.

A.2.1 Power plants

The total cost rate of production at the individual plant was calculated based on various components. The method for calculation of the individual components was similar for most of the contributions. The total cost rate was calculated according to eq. A.1.

$$\dot{C}_{i,t}^{\text{CHP}} = \dot{C}_{i,t}^{\text{fuel}} + \dot{C}_{i,t}^{\text{taxes}} - \dot{C}_{i,t}^{\text{subsidy}} + \dot{C}_{i,t}^{\text{VAT}} + \dot{C}_{i,t}^{\text{startup/shutdown}} \qquad , i \in \mathcal{I}, t \in \mathcal{T}. \tag{A.1}$$

The individual components of the total cost rate are dependent on the consumption of fuel and/or the production of electricity and heat. All of the individual contributions to the total cost rate for CHP units are required to be positive. In the case of fuel cost $\dot{C}_{i,t}^{\text{fuel}}$ the contributions are included in eq. A.2.

$$\dot{C}_{i,t}^{\text{fuel}} = c_i^{\text{fuel}} \cdot \dot{H}_{i,t} + c_i^{\text{O\&M}} \cdot P_{i,t} \qquad , i \in \mathcal{I}, t \in \mathcal{T}. \tag{A.2}$$

where $\dot{H}$ is the flow rate of enthalpy for combustion, and P is the produced electricity. The individual fuel cost factor c_i^{fuel} for the plants were calculated based on fuel type and transportation and handling cost [40]. The cost factor for operation and maintenance c_i^{fuel} corresponds to the variable cost for utility production. A similar approach has been used to calculate the contribution from subsidised fuels $\dot{C}_{i,t}^{\text{subsidy}}$.
The cost rates for startup and shutdown were calculated as presented in eq. A.3.

$$\begin{aligned} \dot{C}_{i,t}^{\text{startup/shutdown}} = & c_i^{\text{startup}} \cdot o_{i,t}^{\text{startup}} + c_i^{\text{shutdown}} \cdot o_{i,t}^{\text{shutdown}} \\ & , o_{i,t}^{\text{startup}}, o_{i,t}^{\text{shutdown}} \in \{0,1\}, i \in \mathcal{I}, t \in \mathcal{T}. \end{aligned} \tag{A.3}$$

The cost c_i^{startup} and c_i^{shutdown} represent the variable cost of changing the operation between on and off. The binary variables $o_{i,t}^{\text{startup}}$ and $o_{i,t}^{\text{shutdown}}$ are controlled by the optimisation algorithm, and further described in section A.4.

A.2.2 Heat boilers

The employed method for calculation of the heat boilers was similar to the approach utilised for section A.2.1. The calculation of the total cost rate is presented in eq. A.4.

$$\dot{C}_{h,t}^{\text{boiler}} = \dot{C}_{h,t}^{\text{fuel}} + \dot{C}_{h,t}^{\text{taxes}} + \dot{C}_{h,t}^{\text{VAT}} \qquad , h \in \mathcal{H}, t \in \mathcal{T}. \tag{A.4}$$

All of the individual contributions to the total cost rate for boilers are required to be positive. The fuel cost was calculated based on fuel consumption and the production-dependent element of the operation and maintenance cost, which corresponds to the produced heat.

$$\dot{C}_{h,t}^{\text{fuel}} = c_h^{\text{fuel}} \cdot \dot{H}_{h,t} + c_h^{\text{O\&M}} \cdot \dot{Q}_{h,t} \qquad , h \in \mathcal{H}, t \in \mathcal{T}. \tag{A.5}$$

A similar approach was used to calculate the cost rates for the remaining elements of eq. A.4.

A.2.3 Electricity-driven heat pumps

In the case of electricity-driven heat pumps, the total cost rate does not include the cost of consumed electricity, as the electricity is covered by other elements of the objective function eq. 3 and by the energy balances in section A.3. The remaining elements are presented in Eq. A.6.

$$\dot{C}_{g,t}^{\text{HP}} = \dot{C}_{g,t}^{\text{O\&M}} + \dot{C}_{g,t}^{\text{taxes}} + \dot{C}_{g,t}^{\text{VAT}} \qquad , g \in \mathcal{G}, t \in \mathcal{T}. \tag{A.6}$$

All of the individual contributions to the total cost rate for HP units are required to be positive. The contribution from O&M corresponds to the variable expenses of operating a heat pump. For the case where the heat pump uses electricity supplied from the distribution grid, a network tariff is used, in order to take the distribution losses of such networks into account.

$$\dot{C}_{g,t}^{\text{O\&M}} = c_g^{\text{O\&M}} \cdot \dot{Q}_{g,t} + c_g^{\text{networktariff}} \cdot P_{g,t} \qquad , g \in \mathcal{G}, t \in \mathcal{T}. \tag{A.7}$$

A.3 Electricity and heat balances

In modern energy systems, significant effort is put on balancing of the production and demand at correct location and time. The electricity transmission grid within the bidding area was modelled as one uniform network without bottlenecks for either of the utility units or consumers.
The electricity demand P_t^{consumer} including distribution losses was used for the analysis in the electricity balance eq. A.8.

$$P_t^{\text{transmission}} - \sum_{g \in \mathcal{G}} P_{g,t} - \sum_{j \in \mathcal{J}} P_{j,t}^{\text{export}} = P_t^{\text{consumer}} \qquad , t \in \mathcal{T}. \tag{A.8}$$

where $P_t^{\text{transmission}}$ is the flow of electricity from the transmission network, $P_{g,t}$ is the consumed electricity from a specific heat pump, and $P_{j,t}^{\text{export}}$ is the export of electricity to a specific area.
The transmission is supplied by thermal units, other units such as wind turbines and decentral CHP units, and import of electricity.

$$\sum_{i \in \mathcal{I}} P_{i,t} + \sum_{f \in \mathcal{F}} P_{f,t}^{\text{other}} + \sum_{j \in \mathcal{J}} P_{j,t}^{\text{import}} = P_t^{\text{transmission}} / (1 - \eta_{\text{TL}}) \qquad , t \in \mathcal{T}. \tag{A.9}$$

In this way all electricity flows into the network are subject to losses. The magnitude of transmission losses (η_{TL}) was determined based on historical data following a similar procedure. Both import and export of

electricity are further constrained by the interconnection capacity of the two bidding areas. All of the variables in eq. A.8 and A.9 are required to be positive.
The heat balances used in the analysis followed a similar setup. The transmission network for heat is split into several areas, with detailed knowledge of the transmission capacity between each area. Opposite to the electricity demand, the heat demand is split into appropriate locations, according to the detailed data from the transmission operators. For all of the considered areas, energy balances ensure logic distribution and prevent accumulation in areas without storage options.
Two examples of heat balances are presented for introduction of units in transmission and distribution networks in eq. A.10 and eq. A.11.

$$\sum_{i\in\mathcal{I}} \dot{Q}_{i,k,t} + \sum_{h\in\mathcal{H}} \dot{Q}_{h,k,t} + \sum_{g\in\mathcal{G}} \dot{Q}_{g,k,t} = \sum_{l\in\mathcal{L}} \dot{Q}_{l,k,t} \qquad , k \in \mathcal{K}, t \in \mathcal{T}. \tag{A.10}$$

where $\dot{Q}_{l,k,t}$ is the transferred heat from production area k to the transmission point l. An example of the capacity limitations of the transmission network is addressed in eq. A.12. In the heat distribution network, heat is transferred from a transmission area m to the distribution network n using the variable $\dot{Q}_{n,m,t}$.

$$\sum_{m\in\mathcal{M}} \dot{Q}_{n,m,t} + \sum_{o\in\mathcal{O}} \dot{Q}_{o,n,t} + \sum_{p\in\mathcal{P}} \dot{Q}_{p,n,t} = \dot{Q}_{n,t} \qquad , n \in \mathcal{N}, t \in \mathcal{T}. \tag{A.11}$$

where $\dot{Q}_{n,t}$ is the demand for heat in area n at time t. All of the variables in eq. A.10 and A.11 are required to be positive.
The limitations in transmission capacity, as well as in other connections of the DH network, is introduced as presented in eq. A.12.

$$\sum_{l\in\mathcal{L}} \dot{Q}_{l,k,t} \leq \dot{Q}^{\max}_{l,k} \qquad , k \in \mathcal{K}, t \in \mathcal{T}. \tag{A.12}$$

where $\dot{Q}^{\max}_{l,k}$ is the maximal allowed transmission capacity in (MJ/s)

A.3.1 Heat storages
Heat storages may be located at any position in the network, but according to the actual locations in the energy system case, the storages was only introduced in the transmission networks. Besides the integration in the network, five equations govern the operation of the storage. The overall heat balance for the unit is presented in eq. A.13.

$$Q_{m,t} + Q^{\mathrm{in}}_{m,t} - Q^{\mathrm{out}}_{m,t} - Q^{\mathrm{heatloss}}_{m,t} = Q_{m,t+1} \qquad , m \in \mathcal{M}, t \in \mathcal{T}. \tag{A.13}$$

where $Q_{m,t}$ denotes the heat available in the storage at time t, and $Q_{m,t+1}$ in the subsequent time step. All five elements are required to be positive in the optimisation. The heat losses related to heat storage was calculated according to eq. A.14. Low heat losses for short time heat storage are expected due to mixing of stratified layers and temperature differences to the ambient.

$$Q^{out}_{m,t} \cdot (1 - \eta_{\mathrm{HS}}) = Q^{\mathrm{heatloss}}_{m,t} \qquad , m \in \mathcal{M}, t \in \mathcal{T}. \tag{A.14}$$

Three additional constraints were set to represent the physical dimensions and design of the heat storage. The constraints are presented in eq. A.15 to A.17. Eq. A.15 describes the installed capacity, where $Q^{\mathrm{max,size}}_{m,t}$ is the maximal allowed stored heat in (MWh). Eq. A.16 and A.17 limit the charge and discharge of the storage, where $Q^{\mathrm{max,rate}}_{m,t}$ is the maximal allowed rate per hour.

$$Q_{m,t} \leq Q_{m,t}^{\max,\text{size}} \quad , m \in \mathcal{M}, t \in \mathcal{T}. \tag{A.15}$$

$$Q_{m,t}^{\text{in}} \leq Q_{m,t}^{\max,\text{rate}} \quad , m \in \mathcal{M}, t \in \mathcal{T}. \tag{A.16}$$

$$Q_{m,t}^{\text{out}} \leq Q_{m,t}^{\max,\text{rate}} \quad , m \in \mathcal{M}, t \in \mathcal{T}. \tag{A.17}$$

A.4 Technology constraints

The considered technologies are common utility units which are utilised in many large district heating networks. A large fraction of the utilized technology constraints are presented for each of the individual technologies.
In the following sections, the constraints are listed for the individual unit types.

A.4.1 Power plants

The technical constraints for the power plants were defined in order to represent several types. In this way it is possible to include extraction CHP, back pressure CHP and condensing power plants using few equations. The maximum and minimum technical load in terms of fuel consumption for a power plant unit was described according to Eq A.18 and Eq. A.19. The operation of the unit is dependent on a binary operation variable $o_{i,t}$ and its availability $\text{UMM}_{i,t}$ according to availability data (historical data for validation).
For the specific fuel load, the electricity production in full back pressure was calculated according to Eq. A.21. A reduction in electric efficiency was modelled assuming a constant contribution at full load. The trend of the derived model is presented in Fig. A.1. The high reduction scheme fits well with the results of the AVV1 model within the typical load range.
A constant boiler efficiency was assumed for the full range of applicable loads. The heat production in back pressure operation was evaluated as the residual of the total utilisation of fuel and the back pressure electricity production according to Eq. A.22, where the thermal efficiency η_i^{total} corresponds to the lower heating value of the utilised fuel.
The produced electricity of the unit was calculated according to Eq. A.23. A reduction in heat production of an extraction CHP plant ($\Delta\dot{Q}_{i,k,t}^{1} + \Delta\dot{Q}_{i,k,t}^{2}$) leads to increased power production according to power loss factors by heat extraction β^1,β^2 [-] [43]. β^1 corresponds to heat extraction below the "no-loss" point, β^2 for heat extraction above this operational limit. The binary input parameter $v_i^{\text{ex.}}$ is used to distinguish between units with extraction points and units with only one production scheme (e.g. electricity only or back pressure units). Some of the investigated back pressure units allow the operator to bypass the turbine, in order to utilise the steam for boosting the heat production. The binary input parameter v_i^{bypass} is used to distinguish such units from the remaining. The reduction in electricity from bypassing the turbine is denoted $P_{i,k,t}^{\text{bypass}}$.
By use of eq A.24 and A.25 it was ensured that the change from one power loss factor to the other corresponds to the physical requirement of the extraction CHP plant. If the binary variable $o_{i,t}^{\text{no-loss}}$ is 1, β^2 should be used, otherwise β^1. The no-loss point was located as the ratio $r_i^{\text{no-loss}}$ between heat extracted above and below the no loss point. The binary variable $o_{i,t}^{\text{no-loss}}$ was further used in Eq. A.26 and A.27 to determine the heat extraction.
The resulting heat from the extraction plant is determined by the Eq. A.28 to A.30. Eq. A.31 ensures that steam bypass corresponds to the bypassed amount of electricity.
For the case where power plants are constrained by rapid ramping of the boiler load, the model includes constraints designed to describe this operation restriction. The constraints were modelled as a limiting difference in load $\dot{H}_{i,k,t}^{\text{rel}}$ of the boiler from one hour to the next. As in Eq. A.32 and A.33 the constraints for startup and shutdown were included in these constraints, and correspond to the additional cost described in A.3. The constraints of Eq. A.34 and A.35 ensure that startup and shutdown only occurs in case of changed production commitment.

Technical and operational power plant constraints:

$$\dot{H}^{\max}_{i,k} \cdot o_{i,t} \cdot \mathrm{UMM}_{i,t} \geq \dot{H}_{i,k,t} \qquad , o_{i,t} \in \{0,1\}, i \in \mathcal{I}, k \in \mathcal{K}, t \in \mathcal{T}. \tag{A.18}$$

$$\dot{H}^{\min}_{i,k} \cdot o_{i,t} \leq \dot{H}_{i,k,t} \qquad , o_{i,t} \in \{0,1\}, i \in \mathcal{I}, k \in \mathcal{K}, t \in \mathcal{T}. \tag{A.19}$$

$$\eta^{\mathrm{backp.}}_{i} = \eta^{\mathrm{elec}}_{i} + \eta^{\mathrm{reduc.}}_{i} \qquad , i \in \mathcal{I}. \tag{A.20}$$

$$P^{\mathrm{backp.}}_{i,k,t} = \dot{H}_{i,k,t} \cdot \eta^{\mathrm{backp.}}_{i} - \dot{H}^{\max}_{i,k} \cdot \eta^{\mathrm{reduc.}}_{i} \cdot o_{i,t} \qquad , o_{i,t} \in \{0,1\}, i \in \mathcal{I}, k \in \mathcal{K}, t \in \mathcal{T}. \tag{A.21}$$

$$\dot{Q}^{\mathrm{backp.}}_{i,k,t} = \dot{H}_{i,k,t} \cdot \eta^{\mathrm{total}}_{i} - P^{\mathrm{backp.}}_{i,k,t} \qquad , i \in \mathcal{I}, k \in \mathcal{K}, t \in \mathcal{T}. \tag{A.22}$$

$$\begin{aligned} P_{i,k,t} = {} & P^{\mathrm{backp.}}_{i,k,t} + \beta^{1}_{i} \cdot \Delta\dot{Q}^{1}_{i,k,t} \cdot v^{\mathrm{ex.}}_{i} + \beta^{2}_{i} \cdot \Delta\dot{Q}^{2}_{i,k,t} \cdot v^{\mathrm{ex.}}_{i} \\ & - P^{\mathrm{bypass}}_{i,k,t} \cdot v^{\mathrm{bypass}}_{i} \end{aligned} \qquad , i \in \mathcal{I}, k \in \mathcal{K}, t \in \mathcal{T}. \tag{A.23}$$

$$\Delta\dot{Q}^{1}_{i,k,t} - \dot{H}^{\max}_{i,k} \cdot o^{\mathrm{no-loss}}_{i,t} \leq \dot{H}^{\max}_{i,k} \cdot r^{\mathrm{no-loss}}_{i} \cdot (\eta^{\mathrm{total}}_{i} - \eta^{\mathrm{elec}}_{i}) \cdot v^{\mathrm{ex.}}_{i} \qquad , o^{\mathrm{no-loss}}_{i,t} \in \{0.1\}, i \in \mathcal{I}, k \in \mathcal{K}, t \in \mathcal{T}. \tag{A.24}$$

$$\Delta\dot{Q}^{1}_{i,k,t} + \dot{H}^{\max}_{i,k} \cdot (1 - o^{\mathrm{no-loss}}_{i,t}) \geq \dot{H}^{\max}_{i,k} \cdot r^{\mathrm{no-loss}}_{i} \cdot (\eta^{\mathrm{total}}_{i} - \eta^{\mathrm{elec}}_{i}) \cdot v^{\mathrm{ex.}}_{i} \qquad , o^{\mathrm{no-loss}}_{i,t} \in \{0.1\}, i \in \mathcal{I}, k \in \mathcal{K}, t \in \mathcal{T}. \tag{A.25}$$

$$\Delta\dot{Q}^{1}_{i,k,t} \leq \dot{H}^{\max}_{i,k} \cdot r^{\mathrm{no-loss}}_{i} \cdot (\eta^{\mathrm{total}}_{i} - \eta^{\mathrm{elec}}_{i}) \cdot v^{\mathrm{ex.}}_{i} \qquad , i \in \mathcal{I}, k \in \mathcal{K}, t \in \mathcal{T}. \tag{A.26}$$

$$\begin{aligned} \Delta\dot{Q}^{2}_{i,k,t} \leq {} & \dot{H}^{\max}_{i,k} \cdot (1 - r^{\mathrm{no-loss}}_{i}) \\ & \cdot (\eta^{\mathrm{total}}_{i} - \eta^{\mathrm{elec}}_{i}) \cdot o^{\mathrm{no-loss}}_{i,t} \cdot v^{\mathrm{ex.}}_{i} \end{aligned} \qquad , o^{\mathrm{no-loss}}_{i,t} \in \{0.1\}, i \in \mathcal{I}, k \in \mathcal{K}, t \in \mathcal{T}. \tag{A.27}$$

$$\dot{Q}^{\mathrm{backp.}}_{i,k,t} - \dot{Q}^{1}_{i,k,t} = \Delta\dot{Q}^{1}_{i,k,t} \cdot v^{\mathrm{ex.}}_{i} \qquad , i \in \mathcal{I}, k \in \mathcal{K}, t \in \mathcal{T}. \tag{A.28}$$

$$\dot{Q}^{1}_{i,k,t} - \dot{Q}^{2}_{i,k,t} = \Delta\dot{Q}^{2}_{i,k,t} \cdot v^{\mathrm{ex.}}_{i} \qquad , i \in \mathcal{I}, k \in \mathcal{K}, t \in \mathcal{T}. \tag{A.29}$$

$$\dot{Q}_{i,k,t} = \dot{Q}^{2}_{i,k,t} + \dot{Q}^{\mathrm{bypass}}_{i,k,t} \cdot v^{\mathrm{bypass}}_{i} \qquad , i \in \mathcal{I}, k \in \mathcal{K}, t \in \mathcal{T}. \tag{A.30}$$

$$\dot{Q}^{\mathrm{bypass}}_{i,k,t} = P^{\mathrm{bypass}}_{i,k,t} \cdot v^{\mathrm{bypass}}_{i} \qquad , i \in \mathcal{I}, k \in \mathcal{K}, t \in \mathcal{T}. \tag{A.31}$$

$$\begin{aligned} 0 \leq {} & \dot{Q}_{i,k,t}, \dot{Q}^{1}_{i,k,t}, \dot{Q}^{2}_{i,k,t}, \dot{Q}^{\mathrm{bypass}}_{i,k,t}, \dot{Q}^{\mathrm{backp.}}_{i,k,t}, \Delta\dot{Q}^{1}_{i,k,t}, \Delta\dot{Q}^{2}_{i,k,t} \\ 0 \leq {} & P_{i,k,t}, P^{\mathrm{bypass}}_{i,k,t}, P^{\mathrm{backp.}}_{i,k,t}, \dot{H}_{i,k,t} \end{aligned}$$

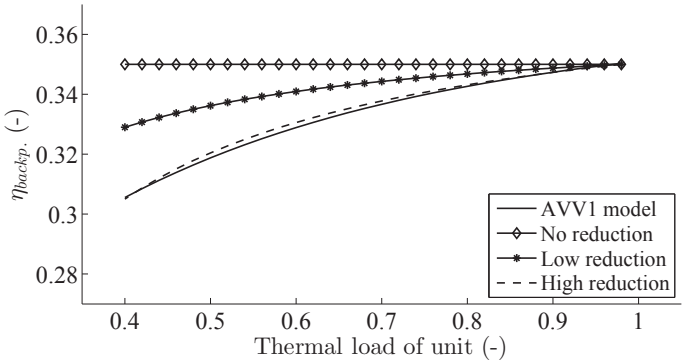

Figure A.1: Estimated reduction of electric efficiency at low unit loads

$$\dot{H}^{\text{rel}}_{i,k,t+1} - \dot{H}^{\text{rel}}_{i,k,t} \leq \dot{H}^{\text{rel,max}}_{i,k} \cdot (1 - o^{\text{startup}}_{i,t+1}) + \dot{H}^{\text{rel,startup}}_{i,k} \cdot o^{\text{startup}}_{i,t+1}$$
$$, o^{\text{startup}}_{i,t} \in \{0,1\}, i \in \mathcal{I}, k \in \mathcal{K}, t \in \mathcal{T}. \tag{A.32}$$

$$\dot{H}^{\text{rel}}_{i,k,t} - \dot{H}^{\text{rel}}_{i,k,t+1} \leq \dot{H}^{\text{rel,max}}_{i,k} \cdot (1 - o^{\text{shutdown}}_{i,t+1}) + \dot{H}^{\text{rel,shutdown}}_{i,k} \cdot o^{\text{shutdown}}_{i,t+1}$$
$$, o^{\text{shutdown}}_{i,t} \in \{0,1\}, i \in \mathcal{I}, k \in \mathcal{K}, t \in \mathcal{T}. \tag{A.33}$$

$$o^{\text{startup}}_{i,t} \geq o^{\text{CHP}}_{i,t} - o^{\text{CHP}}_{i,t-1}$$
$$, o^{\text{CHP}}_{i,t}, o^{\text{startup}}_{i,t} \in \{0,1\}, i \in \mathcal{I}, t \in \mathcal{T}. \tag{A.34}$$

$$o^{\text{shutdown}}_{i,t} \geq o^{\text{CHP}}_{i,t} - o^{\text{CHP}}_{i,t+1}$$
$$, o^{\text{CHP}}_{i,t}, o^{\text{shutdown}}_{i,t} \in \{0,1\}, i \in \mathcal{I}, t \in \mathcal{T}. \tag{A.35}$$

A.4.2 Heat boilers

Two sets of heat boiler constraints were included in the model, one for each location type (central vs. decentral). In this section the constraints of the central installations are presented. The maximum technical load in terms of fuel consumption for a boiler unit was described according to Eq A.36.

The resulting heat production was described according to Eq. A.37, where the thermal efficiency η^{total}_{h} corresponds to the lower heating value of the utilised fuel.

$$\dot{H}^{\text{max}}_{h,k} \geq \dot{H}_{h,k,t} \qquad , h \in \mathcal{H}, k \in \mathcal{K}, t \in \mathcal{T}. \tag{A.36}$$

$$\dot{Q}_{h,k,t} = \dot{H}_{h,k,t} \cdot \eta^{\text{total}}_{h} \qquad , h \in \mathcal{H}, k \in \mathcal{K}, t \in \mathcal{T} \tag{A.37}$$

A.4.3 Heat pumps

Two sets of heat pump constraints were included in the model, one for each location type (central vs. decentral). In this section the constraints of the central installations are presented. The produced heat of the unit was calculated using a coefficient of performance, and the consumed electricity, as presented in Eq. A.38.

For certain types of installations, operation of the heat pump unit will depend on external factors, such as operation at a specific power plant or facility. For other types, the unit capacity and COP may vary according to ambient temperatures or heat source flow rates. In order to address such cases, the coefficient of performance $COP_{g,t}$ and the capacity constraint $\dot{Q}^{\text{max}}_{g,k,t}$ of the heat pump units were split at hourly basis,

and a binary operation variable $o_{g,t}^{\mathrm{HP}}$ was introduced. The capacity of such systems were calculated according to Eq. A.39.

$$\dot{Q}_{g,k,t} = COP_{g,t} \cdot P_{g,k,t} \quad , g \in \mathcal{G}, k \in \mathcal{K}, t \in \mathcal{T}. \tag{A.38}$$

$$\dot{Q}_{g,k,t}^{\max} \cdot o_{g,t}^{\mathrm{HP}} \geq COP_{g,t} \cdot P_{g,k,t} \quad , o_{g,t}^{\mathrm{HP}} \in \{0,1\}, g \in \mathcal{G}, k \in \mathcal{K}, t \in \mathcal{T} \tag{A.39}$$

A.5 System reserves and operational constraints

In order for the model to correspond to the operation of a specific energy system, additional constraints are needed to fully describe for cooperation of units and the different types of system reserves required. Many of the constraints are specified in publications from the system operator [44] [45]. For both manual and frequency reserve capacity the available reserve from a power plant unit was calculated according to Eq. A.40 and A.41 for the individual units. The individual reserve types were further constrained by minimum and maximum contributions from each unit.

$$\begin{aligned} P_{i,t}^{\mathrm{reserve}} \leq & \sum_{k \in \mathcal{K}} (\dot{H}_{i,k}) \cdot o_{i,t} \cdot \eta_i^{\mathrm{elec}} \cdot \dot{H}_i^{\mathrm{rel,reserve}} \\ & + \sum_{k \in \mathcal{K}} (\dot{H}_{i,k}) \cdot o_{i,t} \cdot (\eta_i^{\mathrm{total}} - \eta_i^{\mathrm{elec}}) \cdot \dot{H}_i^{\mathrm{rel,reserve}} \cdot (\beta_i^1 + \beta_i^2)/2 \\ & , o_{i,t} \in \{0,1\}, i \in \mathcal{I}, t \in \mathcal{T}. \end{aligned} \tag{A.40}$$

$$\begin{aligned} P_{i,t}^{\mathrm{reserve}} \leq & \sum_{k \in \mathcal{K}} (\dot{H}_{i,k}) \cdot o_{i,t} \cdot UMM_i \cdot \eta_i^{\mathrm{elec}} \cdot \dot{H}_i^{\mathrm{rel,reserve}} \\ & + \sum_{k \in \mathcal{K}} (\Delta \dot{Q}_{i,k,t}^1) \cdot \beta_i^1 + \sum_{k \in \mathcal{K}} (\Delta \dot{Q}_{i,k,t}^2) \cdot \beta_i^2 - \sum_{k \in \mathcal{K}} (P_{i,k,t}) \\ & , o_{i,t} \in \{0,1\}, i \in \mathcal{I}, t \in \mathcal{T}. \end{aligned} \tag{A.41}$$

The sum of the individual reserves were required to exceed a predefined value for both types of reserves.
Additional operational constraints exist, e.g. considerations for operating the steam network, as well as multifuel units with mutual steam turbines and/or gas turbines.
Ensuring short-circuit power, reactive reserves and voltage control was addressed by ensuring 3 large power plants ($P \geq 150$ MW) to be committed at all time.

B Energy system model validation

The system model has been validated against a number of data series from various sources and with different time resolutions. The comparison with one of the data sources is presented in this appendix. Further results of the validation may be found in [13].
A number of assumptions are used for performance of the individual plants, heat network capacities and fuel costs. Historical data are used where available. Both technology and cost data are presented in Table 8a. Such data are considered constant throughout the year, although the efficiency of many units will vary according to DH temperatures.
By examination of the accuracy and detail of representative segments, it is shown that the model presents good agreement with the historical data. Thus the model is considered applicable to investigate the interaction between several production technologies in a system where both heat and electricity costs are optimized for each hour.

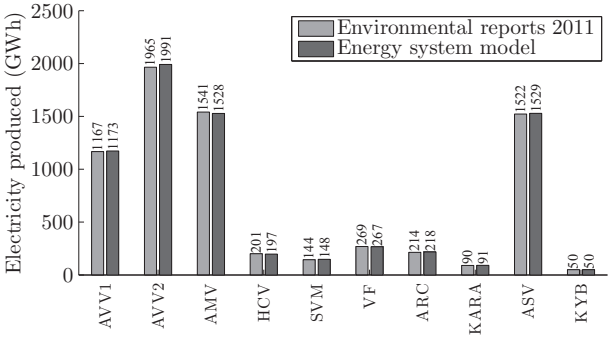

(a) Electricity

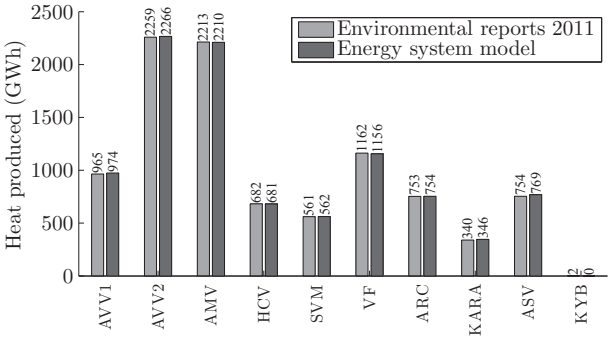

(b) Heat

Figure B.2: Comparison of produced electricity according to environmental reports 2011 and the model. Results correspond to entire power stations, except for AVV1 and AVV2 units.

B.1 Environmental reports

Based on data for environmental reports for 2011 from the companies [36, 37] and municipal cooperatives [46, 47, 48] operating the considered thermal power plant, it is possible to compare the real production of the actual units, with the calculated production, for a given year (2011). The two comparisons are presented in Fig. B.2a and B.2b for electricity and heat, respectively.

For most of the considered power plants, data is available for the entire power station, which may represent between 1 (eg. KARA) and 5 (Kyndby power station - KYB) units. For Avedøre power station, the data is available for unit 1 and unit 2 individually, where unit 2 represents a steam turbine with two boilers and two gas turbines in cooperation. The presented data series show close matches for both electricity and heat for the individual power plants.

In the case of KYB (peak load and backup unit), a very small separate district heating network exists, which was not included in the model. For the remaining power stations the difference between actual and modelled production is between 0-2 %, except for SVM where deviation of electricity production is approximately 3 % which in absolute value is only approximately 4 GWh. For ASV the considered heat demand of Kalundborg (Asnæs) and the corresponding data from the environmental report differs approximately 2 % or 16 GWh. All together, the considered power plants produce a marginally higher amount of electricity and heat in the model compared to the operation data from 2011. This corresponds to approximately 31 GWh electricity

and 29 GWh heat.

Appendix J

Paper 8 - ECOS 2012

Torben Ommen and Brian Elmegaard

Exergetic evaluation of heat pump booster configurations in a low temperature district heating network

ECOS 2012 The 25th international conference on efficiency, cost, optimization, simulation and environmental impact of energy systems, 2012, Perugia, Italy.

PROCEEDINGS OF ECOS 2012 – THE 25TH INTERNATIONAL CONFERENCE ON
EFFICIENCY, COST, OPTIMIZATION, SIMULATION AND ENVIRONMENTAL IMPACT OF ENERGY SYSTEMS
JUNE 26-29, 2012, PERUGIA, ITALY

Exergetic evaluation of heat pump booster configurations in a low temperature district heating network

Torben Ommen [a], Brian Elmegaard [b]

[a] *Technical University of Denmark, Kgs. Lyngby, Denmark, tsom@mek.dtu.dk* ***CA***
[b] *Technical University of Denmark, Kgs. Lyngby, Denmark, be@mek.dtu.dk*

Abstract:

In order to minimise losses in a district heating network, one approach is to lower the temperature difference between working media and soil. Considering only direct heat exchange, the minimum forward temperature level is determined by the demand side, as energy services are required at a certain temperature. As domestic hot water is required at a temperature range where legionella is no longer a threat, forward temperatures in a traditional low temperature district heating network cannot be lowered beyond approximately 55 °C. One solution is to boost the temperature of the forward tap water stream with a heat pump, as the remaining heat demands are often not required at temperature levels as high as the tap water. The scope of this work is to evaluate the power consumption and second law efficiency of booster heat pumps for tap water production in a low temperature district heating network. The heat pump and storage arrangement is evaluated based on a tapping sequence from the Danish standards (DS439). Based an initial investigation of possible designs, three configurations have been chosen for the evaluation. Of the three heat pumps, two are implemented on the primary side to boost the network stream, and one is intended to increase the temperature of the tap water directly. Results show that one of the three configurations are superior to the two remaining, when considering temperature levels of forward stream between 35 °C and 47 °C. The overall results remain the same regardless of heat exchanger sizes and the isentropic efficiency of the compressor used in the heat pump. The superior configuration shows exergetic efficiencies higher than 0.5 when forward temperatures is around 45 °C.

Keywords:

Domestic hot water, Exergy analysis, Heat pumps, Low temperature district heating.

1. Introduction

Using district heating in urban areas is a measure to increase overall energy efficiency and reduce consumption of fossil fuels. These systems are implemented in many northern cities and even rural areas where incineration plants provide surplus waste heat. As the market value of heat is increasing (due to numerous reasons - mainly due to increase in fuel prices), so is the interest in lowering the losses affiliated with transportation of heat. One simple measure is to reduce the temperature of the network, as this reduces the driving potential of the heat loss in the distribution system.

Novel parts of existing Danish district heating networks tend to be built with a forward temperature of around 60-55 °C [1] as this is the lowest temperature for which direct conversion into domestic hot water is possible. Domestic hot water (hot tap water) and space heating are the common heat demands in residential areas, of which the domestic hot water constitute approximately one third of the combined consumption [2]. Lowering the forward temperatures of the district heating network could potentially be beneficial, if only a small amount of electricity is required to increase the temperature of the tap water, while the temperature is high enough to provide space heating without using additional means. In this way heat losses of the combined district heating stream can be minimized while using only a small amount of electricity to boost the temperature of a minor part. Many of the new networks are coupled to the existing district heating networks. In case of the build of a completely new network and production unit (combined heat and power plant or district

heating boiler) several effects may be experienced from changing the temperatures levels of both forward and return in the network [3]. Changed production or efficiencies of these production units are not considered in this paper, as the entire production facility and district heating network must be changed for these effects to become realized.

Several heat pump solutions have been considered in the on-going research affiliated with this paper. Below the most promising candidates are evaluated based on electricity consumption, district heating network considerations and exergetic efficiency.

2. Concept considerations for low temperature DH systems.

2.1. Main obstacles

In trying to reach a lower supply temperature in the district heating system - beyond 55 ^{o}C, new steps must be taken to utilise the heat, as several constraints appear in this temperature range. In residential areas, the load for the district heating system consists mainly of two parts; space heating and hot tap water.

For space heating, the temperature difference between indoor heaters and the room temperature is minimised when using the lowered temperature in the system. Assuming a constant heat demand, the low temperature difference requires larger surfaces for heat transfer. In these situations floor heating is often utilised. Still quite some temperature difference is needed, as building materials are often inferior to slim iron constructions in terms of heat transfer. A minimum of 15 K higher floor heating inlet temperatures, compared to the required room temperature is considered a requirement in this evaluation [4]. In addition to this heat transfer consideration, the flow rates and pressure losses in both the district heating network and the house installations must be considered before choosing the appropriate temperature levels.

Considering the tap water requirements, the main issues are related to the bacterium “Legionella”. To prevent problems with bacteria two simple measures can be taken. Either the hot tap water must exceed a predefined temperature limit where the bacteria can no longer exist when stored, or the tap water is not to be stored after being heated. Either way, some constraints are encountered.

Additionally the Danish building standard must be met, where hot tap water is assumed at two temperature levels – 45 ^{o}C and 40 ^{o}C, respectively, differentiated by their use in kitchens or bathrooms. Even with small pinch temperature differences in the heat exchanger network, it is unlikely that forward temperatures in district heating can be reduced below 50 ^{o}C without considering heat pumps or other efforts to increase the temperature of tap water. In order to evaluate an overall conversion efficiency of systems with very low forward temperature (below 50 ^{o}C), small heat pump installations for individual houses are considered.

2.2. Different implementation schemes

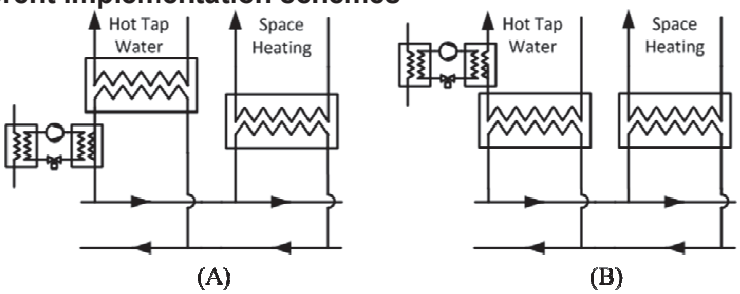

Fig. 1. Two different implementation schemes: (A) Heat pump on primary side of the tap water heat exchanger. (B) Heat pump on secondary side of the tap water heat exchanger.

In individual house installations for low temperature networks, heat pumps can be implemented in two different operating schemes, either to boost the temperature level of the district heating water prior to heat exchange with the tap water (named “primary”), or to boost the tap water temperature after the district heat network heat exchanger (“secondary”).

Within these two schemes, many individual concepts are plausible. Several different conceptual ideas have been tested and evaluated, based on “back of the envelope” calculations. The three most promising concepts are presented in this paper. This focus is to evaluate the most promising candidates in terms of energy efficiency. The evaluated systems consist principally of the tap water heat exchanger, heat pump and the storage system. The evaluation is considering both first and second laws of thermodynamic.

The results presented are intended for further analysis, as the impact of reducing supply temperature will influence the entire district heating system, among others; space heating requirements, pressure losses, cost of implementation and dimensioning of the piping system. Tap-water corresponds to between one half and one third of the combined heat consumption in the house.

2.3. Assumptions

The calculations are based on the assumptions presented in Table 1. Assumptions are made based on estimates of state of the art technology for a small decentralized heat pump producing hot tap water by use of low temperature district heating network.

Table 1 - Assumptions for low temperature district heating network heat pump

Variable	Assumption
Pinch temperature in Tap-water HEX (Q_{MAX}=32 kW)	8 [K]
Initially assumed forward temperature of DH network	40 [°C]
Initially assumed return temperature of DH network	22 [°C]
Refrigerant	R134a
Isentropic efficiency of compressor	0.5 [/]
HEX pinch temperature difference in both Condenser and Evaporator	2.5 [K]
Hot tap water	45 [°C]
Tap water in	10 [°C]
Minimum temperature if water stored on secondary side	58 [°C]

In the conducted calculations heat exchange between district heating water and tap water is assumed to have a constant pinch temperature of 8 K, as high flow rates occur in the tap water system. The assumed pinch temperature corresponds to the highest flow of tap water, but is assumed constant across the entire range of tap water flows. In practice the temperature difference would decrease at lower flow.

As the temperature difference between the forward and return stream of the district heating network is reduced (by a factor of minimum 2) [2] while assuming no change in the demand profile, significantly higher flow rates are required in the district heating network. Furthermore the high flow rates in the system will require high heat exchanger area and intermittent operation of the heat pump. To reduce these issues, storage of hot water is introduced in each scenario. The storage is regarded as a means to lower heat exchanger sizes and service life of components and will as such require an economic optimisation, which is not part of this paper.

In order to dimension the different heat pumps and storage tank sizes, the heat demand profile from DS439 is used [5]. As the recovery time for the system (storage empty -> storage full) is not expected to exceed 3 hours, only the time interval between 6.00 AM and 7.05 AM (morning showers and cooking) is considered in these calculations, as the time until next tap is almost 2 hours according to the standard. Only for the tapping sequence from 6.00 AM to 7.05 AM the full capacity of the heat storage will be needed. The preceding hours are assumed without any tapping,

thus the storage can be full before the tapping sequence. In the calculations presented below, the interaction between heat pump and storage tank is dimensioned to allow a "refilling" (leaving a heated volume of water corresponding to the desired) in two hours.

Regarding heat storage and heat pump on either primary or secondary side, some assumptions are introduced:

- With heat pump and storage on primary side of the network, only the tapping temperature dictates the temperature of the storage in the calculations.
- Employing the Heat pump on the secondary side of the system, the tap water is stored at high temperatures. Concern must be regarded towards legionella, so the heat pump system must be able to prevent and even remove the bacteria. Taking into account some of the heat losses that may emerge in a real system, the heat pump must deliver the tap water at minimum 58 °C.

The profile presented in figure 2 corresponds to the tapping and refilling profile considered. The concept considered in the figure corresponds to configuration A, but identical profiles are experienced in the two remaining configurations. The tapping sequence is assumed to correspond to a tapping temperature of 45 °C during the entire profile (this is a small offset from standard – where some are 40 °C).

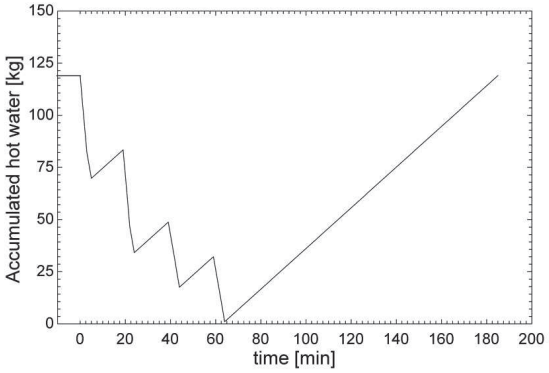

Fig. 2. Tapping and refilling sequence considered.

It is assumed that the heat pump is in operation from the initial tapping sequence and until the heated water volume is restored. The heat pump is working continuously during the tapping procedure in order to reduce the required amount of stored hot water. The tapping and refilling sequence is presented in Fig. 2. Thus proper dimensioning of the heat pump capacity can reduce the required volume of storage. Heat loss from the hot storage of water is neglected, as an almost equivalent amount of stored hot water is required in all the configurations at equally comparable temperature levels.

3. Method

Numerical models have been implemented in Engineering Equation Solver (EES) [6], corresponding to each individual heat pump implementation scheme. Operation assumptions are listed either in Table 1 or in the section considering each individual heat pump solution. The calculation of the state of all streams is primarily based on energy and mass balances. Pressure losses in heat exchange and pipes are neglected throughout the paper.

Heat exchange is modelled according to Nellis and Klein [7] using pinch temperatures in heat exchangers both with and without phase change. The used formulation of pinch point results in

lowered condensation pressure as the pinch point is not assumed at either end of the considered heat exchanger, but at the location of minimum temperature difference.

Calculation of the exergetic efficiency is based on the formulation of physical exergy presented in Bejan et al [8]. There are no changes in chemical composition of the working media or district heating media, leaving only changes in the physical exergy of each separate stream:

$$\dot{E}_i^{PH} = \dot{m}_i((h_i - h_0) - T_0(s_i - s_0)), \qquad (1)$$

Massflow $\dot{m}_i$, enthalpy h_i and entropy s_i is based on the above mentioned EES calculations for each concept. The dead state is based on $t_0 = 10\,^{o}\text{C}$ and $p_0 = 1\,\text{bar}$, from where h_0 and s_0 can be calculated for the working media. The dead state is related to the cold tap water at ambient pressure.

Exergetic efficiency is modelled according to the formulation in Bejan et al. [8]. As exergetic efficiency is calculated as a relative term, the location of the dead state does not matter for the final results presented [9].

4. Individual concepts and initial calculations

4.1. A (primary side)

The heat pump is modelled according to the simplified PI-diagram presented in Figure 3. The forward stream supplies DH water for both the evaporator and the condenser. The two streams are mixed in the return flow, combining the residue heat from the evaporator and tap water HEX. During tapping, heated water is removed from the hot layer in the stratified tank, heat is transferred in the tap water heat exchanger and returned to the cold bottom layer in the tank. This is done to avoid high mass flows of district heating water in the heat pump condenser and in the district heating network. During recharging heated water is filled in the tank, displacing the bottom cold layer, which is returned to the District heating network.

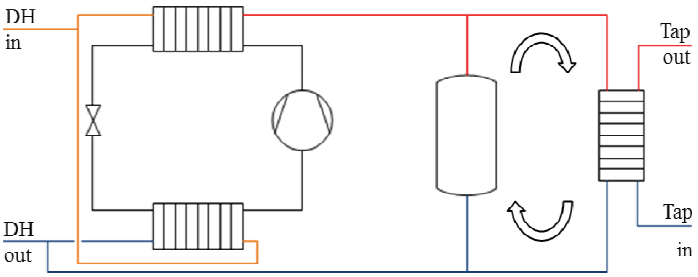

Fig. 3. Simplified diagram of A, with arrows to indicate the short circuit during tapping

Table 2. Initial calculations of variant A based on information from table 1.

Variant	$\dot{V}_{DH}$ [m^3/h]	Condenser [kW]	P [kW]	Heat pump COP [/]	Water Volume [m^3]	Exergetic eff. [/]
A	0.107	0.89	0.157	5.62	0.118	0.44

The results shown in Table 2 indicate that condenser capacity of approximately 0.9 kW is required in order to boost the temperature of the district heating water. The temperature levels in both the condenser and the evaporator allow the heat pump to operate with a COP of approx. 5.6. The combination of the tapping profile and the temperature of the boosted storage dictate the required amount of water in the storage.

4.2. B (primary side)

Source heat for the heat pump system can also be supplied from other sources than the forward district heating line. Heat can be extracted from space heating return flow, or even from the system return line. High temperatures in the heat supply for the evaporator is of cause an advantage in order to minimize the temperature lift between condenser and evaporator. The advantage of this system is a reduction in the district heating network forward flow compared to the variant A. This is achieved by increasing the temperature difference between DH forward and return beside the assumptions in Table 1.

To allow evaluation of introducing additional "waste" heat before the evaporator, two different calculations is performed in this variant.

- 'B1 is only using the return stream from either the tap water heat exchanger or the storage tank.
- 'B2' is an additional amount of return flow (most likely from the space heating circuit) with temperature 22 °C and mass flow corresponding to the assumption that the district heating requirement of a house can be divided into 2/3 space heating and 1/3 tap water [2]. The additional flow is subject to some uncertainties, as it is not always likely that the space heating flow is available when the tap water is required. On the other hand, utilising the space heating return flow would enable a lower return temperature than the one otherwise considered, which is dictated by the space heating heat transfer.

Figure 4 presents the simple flow diagram. The concept is quite similar to A, except for the addition of surplus waste heat prior to the evaporator.

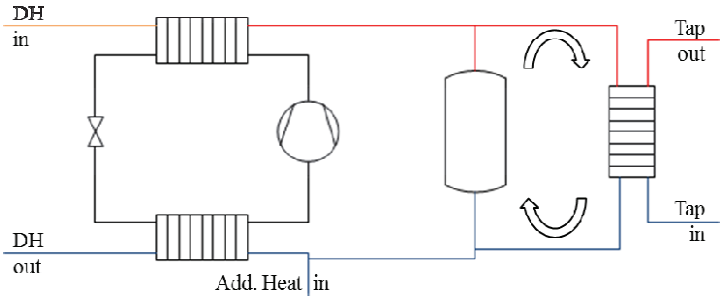

Fig. 4. Simple diagram of variant B (primary), with arrows to indicate the "short circuit" during tapping

Table 3. Initial calculations of variant B based on information from table 1.

Variant	$\dot{V}_{DH}$ [m³/h]	Condenser [kW]	P [kW]	Heat pump COP [/]	Water Volume [m³]	Exergetic eff. [/]
'B1'	0.059	0.89	0.252	3.52	0.118	0.38
'B2'	0.059	0.89	0.207	4.27	0.118	0.42

Table 3 shows the initial calculations of both variant B1 and B2. The condenser load is in both cases equal to the one presented in table 2, as the hot DH water stream for the condenser is identical to the one in variant A. Due to the changed temperature levels of the evaporator in both B1 and B2 the heat pump COP is changed, which calls for a higher electricity consumption. Considering available surplus heat (according to 'B2'), the system efficiency improves, as this reduces the temperature lift between heat pump sink and source. As the system changes only influence the evaporator, the new system provides similar effects with a variation in forward temperature. In

cases with no additional heat requirements in the house, the heat pump unit will operate on only the return stream from the tap water heat exchanger.

As the two systems have similarities in operation, only the 'B1' system is considered for further analysis, as this system composes the simple solution, where both streams from Figure 1 are not available in the same location due to practical constraints.

4.3. C (secondary side)

The last variant proposes the most efficient solution for boosting the tap water with the heat pump (secondary side implementation). The configuration of this system allows preheating to be utilized in an efficient way, where the high flow rates of the tap water does not influence the temperature lift. The forward stream of the district heating network is supplied both to the evaporator of the heat pump and the heat exchanger for preheating of tap water. In modelling the system the preheater was considered both as a tap water heat exchanger (pinch temperature in tap-water HEX = 8 K) or as a separate type (pinch temperature in HEX = 2.5 K = Condenser pinch temperature). As only a limited constant stream of tap water is heated, the heat exchanger (named 'preheater') was assumed to resemble the condenser based on the load profile. The pinch temperature defines the thermal load of the heat pump, and as such the losses in this heat exchanger must be minimised for efficient water heating.

The simple diagram of B2 is presented below in Figure 5. The arrow represents the continuous heating of tap water, which is independent of the tapping stream. The high flow from the Tapping procedure will only affect the amount of hot water in the stratified tank.

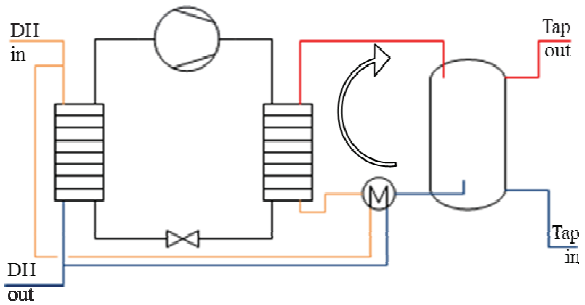

Fig. 5. Simple diagram of C, the arrow represents the continuous heating of tap water through the heat pump.

Table 4. Initial calculations of variant C based on information from table 1.

Variant	$\dot{V}_{DH}$ [m^3/h]	Condenser [kW]	P [kW]	Heat pump COP [/]	Water Volume [L]	Exergetic eff. [/]
C	0.105	1.02	0.193	5.26	0.086	0.40

Table 4 reveals a slightly increased heat pump condenser load is in variant C compared to the primary configurations. The increased load is due to the heat exchanger losses introduced in the secondary solution, where the district heating water is directly used (without temperature loss) in variant A and B. The configuration has a slightly lower requirement of DH flow than configuration A, and a lower storage volume than the both A and B.

As the heated water in the tank is hotter than the desired tapping temperature, cold tap water is mixed with the hot tap water during tapping, as is common practise when using district heating water today.

4.4. Evaluation

Based on table 2 to 4, a simple evaluation of electricity consumption and exergetic efficiency is possible. However, a variation of some of the parameters from table 1 may reveal changes in performance of the different booster configurations.

Heat exchanger sizes is a major interest, as the assumptions in Table 1 may not prove the economic optimum in later calculations. Other economic evaluations may include improvement in isentropic efficiency of the heat pump compressor, which may become possible through the use of different compression technologies and/or development of a compressor specifically designed for the temperature levels of the booster heat pump.

Heat exchange pinch temperature difference: In the evaluation of different heat exchangers, an increase in pressure losses from a decrease in pinch temperature difference is neglected. Such pressure losses would only affect the heat pump performance, as the pressure difference between forward and return DH stream is controlled at the district heating central, and as such not included in this paper.

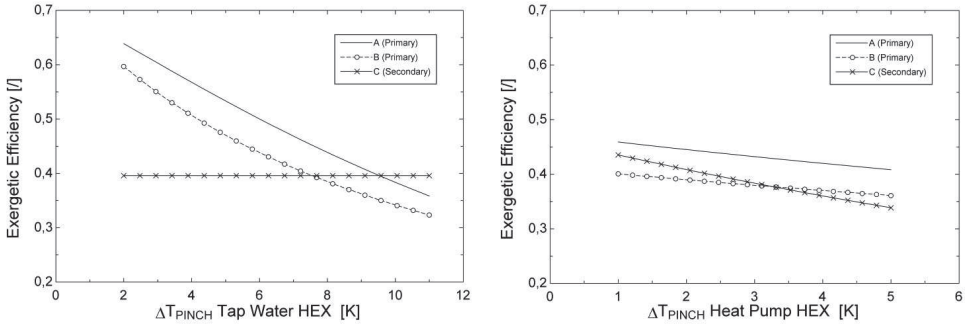

Fig. 6. (A) The impact of tap water HEX pinch temperature on the 3 proposed configurations. (B) Impact of pinch temperature difference in evaporator and condenser on the 3 proposed configurations.

From Figure 6 (A) it is clear that the tap water HEX performance will influence the efficiency of Variant A and B, indicating that with poor heat exchange in these system, optimal performance will shift from variant A to variant C (as described in section 4.3, the heat exchanger in configuration C is not regarded as a tap water heat exchanger due to the constant flow rate of the HEX) . The steeper gradient of variant C in Figure 6 (B) is due to a higher number of HEX controlled by this pinch temperature difference (same explanation as in Fig. 6 (A))

Isentropic efficiency of heat pump compressor: The evaluation presented in Figure 7 cover a broader band of isentropic efficiency than what is reasonable to expect. A compressor for high temperature heat pumps in the condenser capacity range expected and at a reasonable cost is unlikely to have a higher efficiency than 0.65 [/] [9].

The evaluation presents the COP (coefficient of performance) for the heat pump pack and exergetic efficiency for the combined system with variable isentropic efficiency of the compressor. It is noticeable from Figure 7 (B), that an increase of isentropic efficiency above 0.65 [/] changes the relation between variant B and C. Configuration A has the highest performance of the three in both fig. 7 (A) and (B).

The difference between the first and the second law evaluation of performance is the influence of the condenser load on the electricity consumption. The increased load for the heat pump in configuration C is mainly due to the pinch temperature differences discussed above.

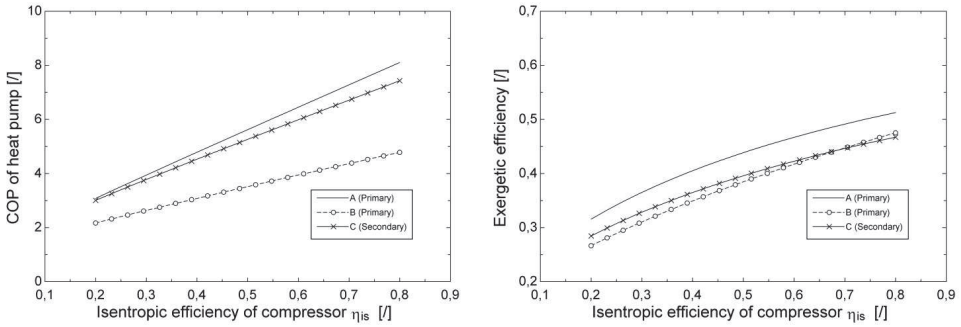

(A) (B)

Fig.7. (A) COP of heat pump with variable isentropic efficiency for each of the 3 proposed configurations. (B) Exergetic efficiency of individual configurations with variable isentropic efficiency.

5. Results

5.1. Variation of forward temperature of the DH network

The forward temperature of the DH has a high impact on the system performance, as the temperature is directly linked to the heat pump capacity and temperature lift in all the different configurations. Figure 8 shows the variation of the described configurations in terms of both volume flow of district heating water and electricity consumption, with variation in forward temperatures of the district heating network. Electricity consumption is presented as a function of the product – this is to represent how much power (and the remaining heat load) is required in order for the system to produce one [kWh] of hot tap water at 45 ^{o}C according to the assumptions explained above and the Danish building standard.

Heat is calculated on the basis of enthalpy difference between forward and return temperatures (in the case of Figure 8 the return temperature can be found in Table 1). The full heat content between forward and the lowered return temperature can be found by subtracting the curve of variant B from Figure 8 (B) from the product (energy balance calculation where the product is 1).

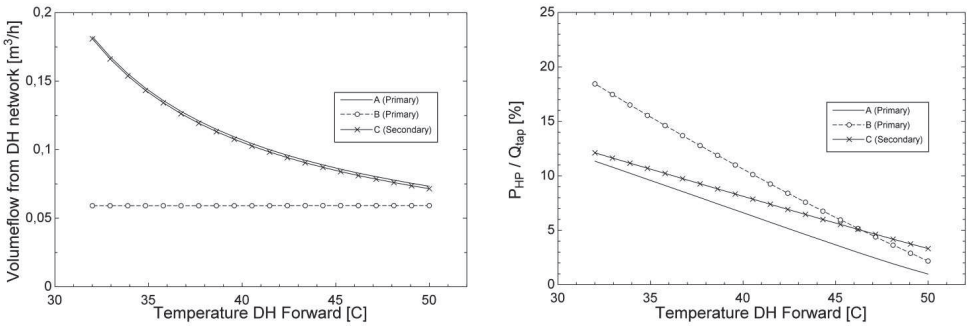

(A) (B)

Fig. 8. (A) Required volume flow of hot DH stream with variable forward DH temperature. (B) Relation between electricity consumption and product with variable forward DH temperature.

When the DH forward temperature approaches the temperature required for tap water heating (53 ^{o}C for primary side when considering a pinch temperature of 8 K, 58 ^{o}C for secondary side

according to the assumptions of Table 1), the consumption of electricity is reduced significantly; while almost the full energy flow is required from the district heating network. This is due to the significantly reduced thermal load in each of the heat pump configurations. As discussed above, configuration C has a slightly higher condenser load as in variant A, thus increasing the electricity consumption for the heat pump correspondingly at all temperature levels.

5.2. Variation of return temperature of the DH network

Changes in return temperatures are highly important, as not only the electricity consumption of the heat pump booster configuration is affected, but also the temperature difference between the forward and return of the district heating network. Thus the optimal heat pump must perform with high efficiency in a range of high temperature differences between forward and return temperatures.

Assuming tap water at 10 ^{o}C, and a finite heat exchanger (8 K), 18 ^{o}C is the lowest reachable temperature for the return water in the district heat system by direct heat exchange. Lower temperatures can only be achieved by using the heat pump evaporator to cool the stream further, which in this study only is considered in variant B.

With an increase in return temperature of the district heating network, power consumption is reduced as the evaporation temperature of the heat pump refrigerant can be increased. An evaluation of the heat pump characteristics with a change in return temperature is considered in Figure 9 (constant forward temperature corresponding to Table 1). From the curvature of variant A and C in Figure 9 (B) it is clear that an optimum exists if the district heating water from Figure 9 (A) has a change in value.

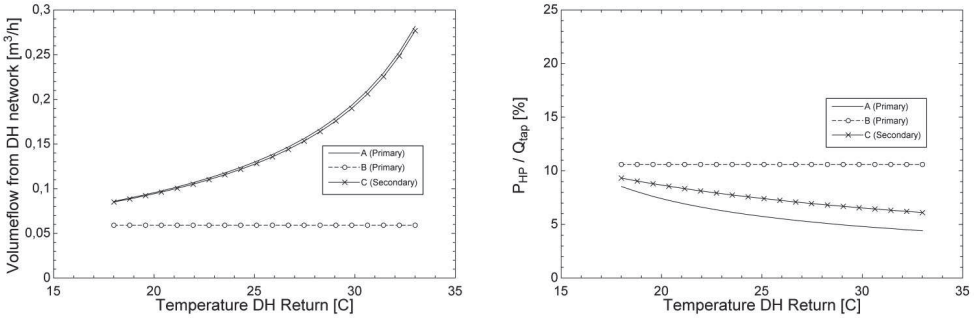

(A) (B)

Fig. 9. (A) Required volume flow of hot DH stream with variable forward DH temperature. (B) Relation between electricity consumption and product with variable return DH temperature

The differences between configurations A and C are quite hard to spot in Figure 9. In principle it does not make sense to display variant B, as the return temperature of the DH network is not controlled. The visible changes in Figure 9 (A) correspond to the previously addressed wish to show the differences in flow of DH water required to fulfil the tapping process.

5.3. Comparison of results using exergy

Exergy is used as another way to evaluate the performance of the different concepts. In this evaluation the different temperature levels of the district heating network is evaluated. Exergy is furthermore a good evaluation parameter when more than one fuel stream combine into only one product, as optimum between the different fuel streams is easily spotted.

The lower electricity consumption of configuration A is rewarded in the calculation of exergetic efficiency throughout the entire range of forward and return temperatures considered in the paper. Considering the initial calculations, and the sensitivity study of heat exchanger performance and

isentropic efficiency, the distribution between the performances of the individual configurations is distinct.

Figure 10 shows the exergetic efficiency of the three different variants, considering both the forward and the return temperatures. From Figure 10 (B) it seems that the second law efficiency is not improved with a return temperature above 25 ^{o}C in either of the cases, because the trade-off between reductions in electricity consumption is no longer compensating the increased exergy content of the heat consumption. The influence of pressure losses on exergy destruction is not considered in the systems and would lower efficiency further at the higher temperature due to higher flow rates. Increasing the forward temperature seems to be beneficial to the point where heat pump is no longer needed in the system. This is further discussed in section 6.

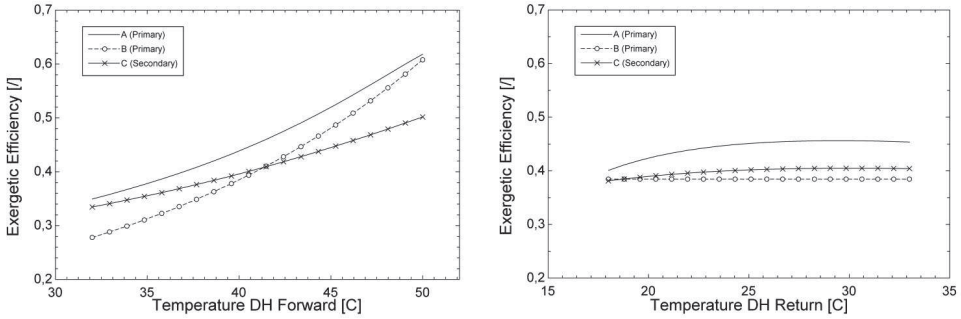

(A) (B)

Fig. 10. (A) Exergetic efficiency of individual configurations with variable DH forward temperature. (B) Exergetic efficiency of individual configurations with variable DH return temperature.

Variant B performs well with a low temperature return stream, or very high forward temperatures. Allowing this configuration additional heat from the space heating as proposed in section 4.2 might improve the performance of the configuration considerably, but in the temperature regime proposed in the above calculations, the configuration is not advantageous in any part of the temperature span considered.

5.4. Constant temperature difference between forward and return

As it is not easy to find the optimal forward temperature from the above calculations, an additional calculation has been performed with a constant temperature difference (18 K) between forward and return of the district heating network. This is to rule out the coinciding effects of very high temperature lifts in the heat pump in one end and high thermal heat pump load in the other end of the studied temperature range.

In figure 11, most of the range is clearly covered by the configuration A. Only at very high temperature levels configuration B is advantageous. The secondary system C is inferior in the entire range.

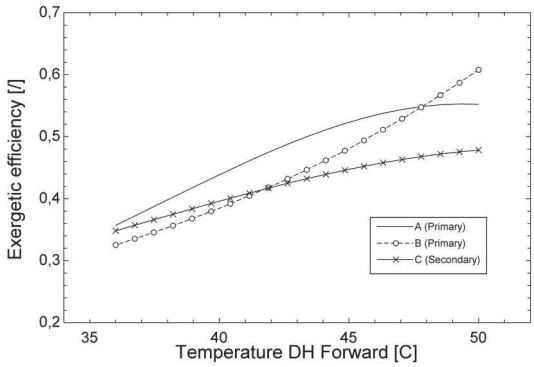

Fig. 11. Exergetic efficiency of the individual configurations with constant temperature difference between forward and return line of the district heating network.

6. Discussion

Several system configurations have been considered in the initial work of the project based on forward and return temperatures corresponding to table 1. Of the investigated systems, the three configurations presented in this paper have provided the best performance. It is not unlikely that other energy efficient solutions can exist. The three variants have been chosen based on the criteria considered in the overall project, not only to satisfy energy efficiency, but also to comply with e.g., state of the art technology and DH network considerations.

Considering both Fig. 8 and Fig. 10 (A), the optimal operation temperature of the district heating forward is not easily determined. The method used in fig. 11 show, that with a reasonable temperature difference throughout the range (18 K), the thermal load is the important factor to observe, as the COP is (almost) constant. Determination of optimal forward temperature of a low temperature district heating network will therefore not depend on the heat pump booster unit, but rather on external factors such as heat loses in the distribution network, sustainable sources and optimum production criteria for the combined heat and power plant.

This effect is also shown in In Fig. 10 (B), as the exergetic efficiency levels out without consideration to the improvement in COP from increasing the evaporator temperature.

From the same figure it is clear, that with a constant forward temperature (40 ^{o}C), the return temperature has an optimum (25 ^{o}C – 30 ^{o}C), which presumably would not be beneficial for the remaining network.

Consulting Figure 10 (A) it is clear that the exergetic efficiency decreases with consumption of electricity in the heat pump configurations. When approaching the temperatures where direct heat exchange is possible, the exergetic efficiency increases, as heat losses are not considered in the network.

If the heat pump booster unit is used in a system where it is coupled with a traditional district heating network, changes in the heat and power prices can be neglected. The reason for this is that the new system does not significantly change the operating conditions of the combined heat and power plant or the capacity of the transmission line in the district heating network. In this case only the heat losses in the novel DH system, and the increased end user capacity of the DH system from using lower temperatures can be compared with the additional electricity consumption.

7. Conclusion

Three heat pump schemes were singled out for evaluation in a low temperature district heating network in order to increase tap water temperature to meet the Danish standard. Out of the three

heat pumps, two are used to boost the network temperature prior to heat exchange with the tap water, while the third is used to boost the temperature of the heated tap water. Variant A was found to be the most efficient configuration in the temperature range considered. In the expected temperature range the heat pump has an exergetic efficiency between 0.4 [/] and 0.6 [/]. Variant B proved that power consumption might not become significantly increased, if the heat pump is used to actively lover the temperature of the return flow as source heat. This would allow for lower flow rates to meet the tap water requirements.

Acknowledgments

This work was supported by the Danish Energy Technology Development and Demonstration Programme (EUDP).

Nomenclature

$\dot{E}$ Time rate of exergy, kW

h Enthalpy, kJ/kg

$\dot{m}$ Mass flow rate, kg/s

p Pressure, kPa

P Electricity, kW

Q Heat, kW

s Entropy, kJ/(kg*K)

t Temperature, C

$\dot{V}$ Volume flow rate, m^3/h

subscripts

0 Dead state

i Index (component)

DH District heating network

References

[1] Thorsen J E, Christiansen C H, Brand M, Olesen P K, Larsen C T. Experiences on Low-Temperature District Heating in Lystrup – Denmark. Procedings of International Conference on District Energy 2011, Slovenia.

[2] Bøhm B, Danig P O. Monitoring the energy consumption in a district heated apartment building in Copenhagen, with specific interest in the thermodynamic performance. Energy and Buildings 2004; 36; 229 – 236

[3] Elmegaard B, Houbak N. Simulation of the Avedøreværket Unit 1 Cogeneration Plant with DNA. Proceedings of The 16th International Conference on Efficiency, Cost, Optimization, Simulation, and Environmental Impact of Energy Systems 2003; 1659-1666

[4] Asada H, Boelman EC. Exergy analysis of a low temperature radiant heating system. Building Services Engineering Research & Technology 2004; 25 (3); 197-209

[5] Danish Standards. Code of Practise for domestic water supply installations (DS 439). 2009; Fourth edition.

[6] Engineering Equation Solver (EES). 2011 F-Chart Software, LLC. http://www.fchart.com/ees/ [accessed 20.01.2012]

[7] Nellis G., Klein S A. Heat Transfer. Cambridge university press, NY. 2008. ISBN 978-0-521-88107-4.

[8] Bejan A, Tsatsaronis G, Moran M. Thermal Design and Optimization. Wiley, NY. 1996 ISBN 978-0-471-58467-4

[9] Rosen M A, Dincer I. Effect of varying dead state properties on energy and exergy analyses of thermal systems. Int J Therm Sci 2004; 43: 121–133

Appendix K

Paper 14 - ICR 2015

Torben Ommen, Jonas Kjær Jensen, Wiebke Brix Markussen
and Brian Elmegaard

Enhanced technical and economic working domains of industrial heat pumps operated in series

ICR 2015, [accepted for publication]

ENHANCED TECHNICAL AND ECONOMIC WORKING DOMAINS OF INDUSTRIAL HEAT PUMPS OPERATED IN SERIES

Torben OMMEN(*), Jonas Kjær JENSEN(*), Wiebke Brix MARKUSSEN(*), Brian ELMEGAARD(*)
(*) Technical University of Denmark, Department of Mechanical Engineering, Nils Koppels Allé, Kgs. Lyngby, DK-2800, Denmark
tsom@mek.dtu.dk

ABSTRACT

By operating heat pumps (HPs) in series, it is possible to obtain closer match between working fluid and sink- and source streams, resulting in higher coefficient of performance (COP). For industrial HPs, it was found that serial connection of either two or three units results in an increase in COP and a decrease in net present value (NPV), due to the effects of economy of scale. However, connecting HPs in series may reduce the discharge temperature, which is of particular interest when assessing R717 HPs. Another possibility from serial connection is to mix different types of HP units, in order obtain specific characteristics. The technical and economical working domains were calculated for two serial connections. Both configurations result in an increased working domain for the investigated dual unit serial connections.

1. INTRODUCTION

Economically viable applications for large heat pumps (HPs) include industrial process optimisation and utility production in district heating networks (Ommen, et al, 2015). For many of such applications, the temperature variation of either source or sink stream may be of a magnitude, where serial connection of HPs may provide an increase in HP coefficient of performance (COP) (Prestmark and Schultz, 1984). On the other hand the economy of scale may suggest that the investment of a single unit is lower than two smaller units, when considering similar heat load. The most profitable solution may further vary with HP parameters such as sink temperature, temperature lift and temperature variation of sink and source streams.

The working domains of several single stage vapour compression HPs (VCHP) were investigated in Ommen, et al (2015). The results were compared to similar results for the hybrid absorption-compression HP (HACHP) in Jensen, et al, (2015). The best available technology typically depends on the performance and investment of the HP systems at the specific layout of the sink/source process streams. Besides the thermodynamic performance of the cycle and working fluid, it is important to consider the application limits of the individual components.

This paper will investigate if the working domains of VCHP may be expanded by connecting the units in series. Four different schemes for serial connection are investigated. Finally the most profitable solution is determined for different sink temperatures, temperature lifts and temperature variations.

2. METHOD

The enlargement of working domains due to serial operation of units was investigated for two single stage vapour compression HP systems. The individual unit configurations correspond to the previously investigated solutions of single stage vapour compression systems, where improved performance measures such as internal heat exchangers or two stage compression schemes were disregarded. A model of each HP system was implemented in Engineering Equation Solver (F-Chart Software (LLC.), 1992).

The two HP systems (R717HP and R600a) were chosen in order to enhance the working domain of VCHP at high sink outlet temperatures (Ommen, et al, 2015). Of the previously examined VCHP, the two considered systems each contribute with individual benefits and drawbacks. The profitability of R717 systems are typically higher than other natural refrigerants, but the thermodynamic cycle results in very high discharge temperatures which limit the practical applications. The thermodynamic characteristics of R600a results in high COP as well as low pressures and low discharge temperatures, but the economic constraint is decreased

by high investment costs which is explained by a low volumetric heating capacity (large volume flow of refrigerant at compressor suction line for a given heat capacity in the condenser).

The HPs were compared using both economic and technical constraints. The considered technical constraints may be caused by either the thermodynamic cycle or by limitations in the development of suitable components. The economic constraints correspond to a combination of capital investment, fuel cost and operation and maintenance. Both topics are further addressed in the following sections.

A few causes of inefficiencies were neglected, as they are assumed of similar magnitude between the investigated HPs. Examples include pressure drop in pipes, the extent of non-useful superheat and subcooling and compressor heat losses. Only full load steady state operation was considered for the economic analysis.

2.1. Vapour compression heat pump

For many industrial processes heat is transferred by heat transfer fluids, such as oil or water. In this study it was assumed to be pure water, which was pressurized to avoid vaporisation of the secondary working fluid at elevated temperatures. Pinch point temperature differences were used to model heat exchange with both sink and source media. A principle sketch of a vapour compression HP, and a temperature - heat load diagram for an azeotropic working fluid, are presented in Figure 1. In the condenser, the working fluid was assumed sub-cooled until it reaches the pinch temperature difference at the sink entrance. Depending on the slope of temperature variation of the source steam, one of two (or both) locations may be possible for the pinch point of the evaporator. The correct location of the pinch point is handled by the model.

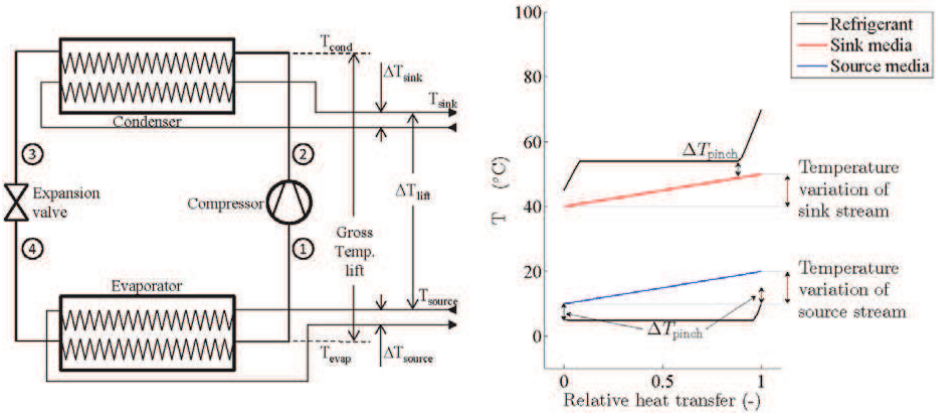

Figure 1: Principle sketch and temperature - heat load diagram of the vapour compression HP

The performance of the HP was calculated using constant efficiencies for compressor and electrical motor, as well as fixed temperature differences in the heat exchangers. The used values are presented in Table 1. The data used for the analysis corresponds to the values used in the two previous studies (Ommen, et al, 2015,Jensen, et al, 2015), where a parametric analysis is performed for key parameters.

Table 1: Fixed input variables for heat pumps

Input variable	Value	Unit
Compressor isentropic efficiency	0.8	-
Compressor volumetric efficiency	0.8	-
Compressor electric motor efficiency	0.95	-
Pinch point temperature difference heat exchangers	5	K
Compressor suction superheat	5	K

Four serial connection schemes are presented in Figure 2. Figure 2a presents the heat load/temperature diagram for two HPs in counter-current configuration considering both sink and source streams, as well as

the refrigerant heat load and temperature profile for each of the HP systems. Figure 2b presents three alternative configurations for the sink and source streams. Counter- and Co-Current configurations are named according to Prestmark and Schultz (1984). The two remaining schemes are variations of the counter-current configuration, where either the evaporators or the condensers are split in parallel connection. The four schemes are further investigated in section 3.

In the case of HP systems operated in series, the optimal configuration depends on the split of heat load between the units. In order to conduct a fair comparison with between various configurations the additional degrees of freedom should be optimised for the system design (Ommen, et al, 2015). The impact of heat load distribution for the individual units is further investigated in section 3.

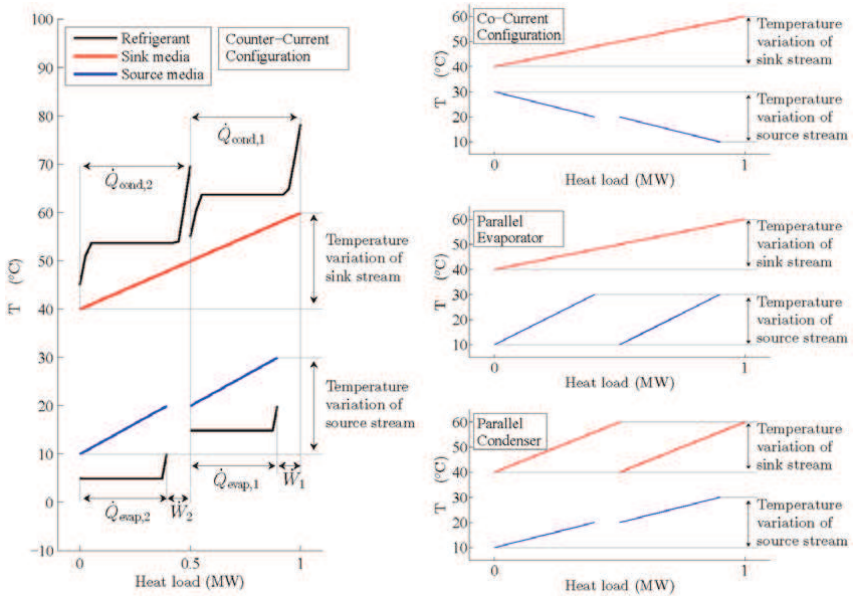

Figure 2: Temperature heat load diagrams of four serially connected HP schemes. (a) Two HPs in counter-current configuration with even split in heat load. (b) Three alternative serial connection schemes.

2.2. Estimation of plate heat exchanger area and pressure drop

Heat exchange processes are important in any HP and a significant part of the physical system, with high influence to the investment and the derived heat cost. Detailed heat transfer correlations for both evaporators and condensers were implemented and used in moving boundary models of the heat exchangers.

In accordance with the applied method of Ommen, et al. (2015), the heat exchange process and required heat exchanger size was calculated for chevron type plate heat exchangers. The correlations used for the analysis are presented in Table 2. The plate dimensions are for a fixed type corresponding to pressure level and working fluid constraints. In this way an increment in heat exchange area will result in increased amount of plates.

Table 2: Applied heat transfer and pressure drop correlations for the evaporator and condenser

Component	Media	Zone	Heat Transfer	Pressure drop
Condenser	H_2O		(Martin, 1996)	(Martin, 1996)
	Refrigerant	vapour only	(Martin, 1996)	(Martin, 1996)
		two phase	(Yan, et al, 1999)	(Yan, et al, 1999)
		liquid only	(Martin, 1996)	(Martin, 1996)
Evaporator	H_2O		(Martin, 1996)	(Martin, 1996)
	Refrigerant	two-phase	(Yan and Lin, 1999)	(Yan and Lin, 1999)
		vapour only	(Martin, 1996)	(Martin, 1996)

2.3. Compressors and operating conditions

In HP applications for industrial processes and district heating, specially designed compressors are used. For most vapour compression HPs, the pressure limit of the high pressure dictates the achievable sink temperatures. For selected fluids (e.g. R717), the condensing temperature (and corresponding pressure) can be lower than that of the sink stream leaving the condenser. This is possible in the case where a high fraction of heat dissipation is from superheated vapour.

The compressor types were identified according to different working fluid properties, flammability and availability. The considered operating limits for the two HP systems are presented in Table 3 (Ommen, et al, 2015).

Table 3: Current operating limits

Working fluid	Pressure limit Bar	Lubrication max. temp ^{o}C
R600a	28	180
R717-HP	50	180

2.4. Economic evaluation

The economic evaluation of the HPs was based on the economic method presented by Bejan et al. (1996), where individual component costs are used to account for the overall collected system. The method requires detailed cost data for components presented in a process flow diagram.
In order to obtain coherent and comprehensive data for specific components, the aggregation of data required several assumptions. It was assumed that:

- Purchased Equipment Cost (PEC) for an open type compressor was solely dependent on the type and the swept volume of the compressor.
- PEC for an electrical motor with a fixed efficiency was dependent on the shaft power.
- PEC for a heat exchanger was a function of the heat exchange area and pressure limit.
- PEC of an intermediate pressure receiver was a function of volume and pressure limit.
- The PECs of expansion valve and oil separator were neglected.
- Total Capital Investment (TCI) of a component was calculated as 4.16 higher than PEC of the component (Bejan, et al, 1996). This was done to account for additional cost related to new investment at an existing facility. The costs include installation, piping, instrumentation, electrical equipment, engineering and supervision, as well as start-up and working capital etc.
- Electricity and natural gas prices correspond to the market cost for industrial consumers in the year 2012 according to Danish Energy Agency (2013).
- The investment costs of already installed natural gas burners were neglected. This is the case if the HP replaces an existing installation.
- Source heat was assumed readily available as a process stream.

Table 4: Parameters applied in the economic analysis

Parameter	Value	Unit
Heat pump load	1000	kW
Interest rate	7	%
Inflation rate	2	%
Natural gas burner efficiency	0.9	-
Technical lifetime	15	Years
Operating time	3500	Hours pr. year
Gas burner investment cost	0	€
Gas burner maintenance cost	0	€

Purchased equipment cost functions were developed based on prices from intermediate Danish trade businesses and individual manufactures. The cost functions were constructed as proposed by Bejan et al. (1996) where the purchase cost of an equipment item PEC_Y at a size or capacity X_Y can be calculated based on knowledge of the cost PEC_W at a different size or capacity X_W by use of a scaling exponent α. Data for the component cost correlations and references are listed in Ommen et al. (2015) for the investigated HP systems. Cost correlations were estimated to be valid for HP capacities between 100 kW and 2 MW.

When comparing technical solutions the economically best available solution is preferred. Two different profitability criteria were used for the analysis, the (simple) payback period (PBP) and the net present value (NPV) utilising discounted cash flows. The methods for determination of the two factors are explained in Ommen, et al. (2015).

3. RESULTS

In Ommen et al. (2015) it is shown that temperature variation of both heat sink and heat source streams have significant influence on both the economic and technical constraints of VCHPs. In the present study two of the proposed cases with high temperature variations were examined. The two cases are denominated: ΔT_{sink}/ ΔT_{source} = 20K/20K and 40K/10K. Temperature variations are presented graphically in Figure 2.

The four schemes for serial connection were compared to the same reference system, containing only one HP. With a higher number of units, both economy and energetic efficiency is altered based on the changed temperature levels as presented in Figure 2a. The results in terms of COP and NPV are presented in Figure 3 for the two temperature variation cases, i.e. the changes of the sink and source streams in the condenser or evaporator, respectively. All systems were calculated for 1000 kW, and with even heat load distribution for serial connected units. For both ΔT_{sink}/ ΔT_{source} variations it was found that serial connection of either two or three units result in an increase in the COP and a decrease in NPV, when compared to the reference system with only one HP. The decrease in the NPV is the result of a significant increase in investment cost, which is not fully compensated by the decrease in operation cost. Accordingly, it was found that HP units in serial connection perform best for the case 20K/20K compared to 40K/10K, as the increase in energetic performance is lower for the latter. This may be the case as the change to evaporation temperature is larger with a large variation in source temperature. Additionally, the two configurations 'Counter-current' and 'Co-current' perform similar in both temperature cases, and are favourable both in terms of COP and NPV to the solutions with parallel connection of evaporator or condenser. Based on the results presented in Figure 3, further investigation of economic and technical working domains were limited to include two HPs in counter-current configuration, as this scheme results in lower maximum pressure ratio and consequently lower discharge temperatures compared to the co-current scheme.

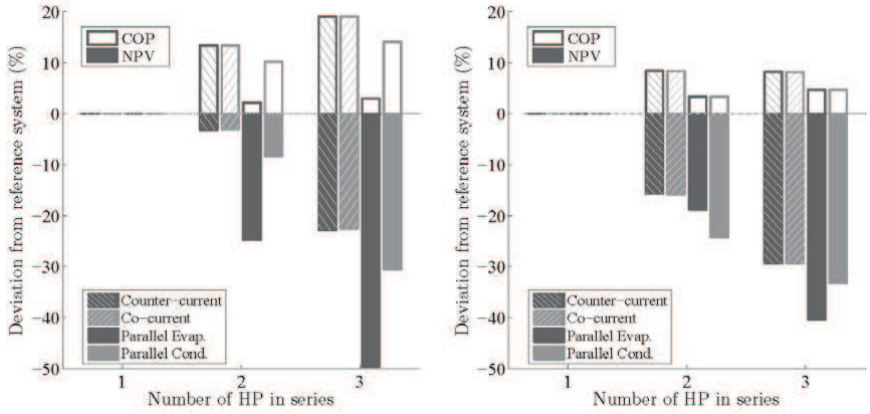

Figure 3: Changes to COP and NPV for four serial connected HP schemes with even heat load for serial connected units. In the considered case, all units were of the same type (R717-HP).
(a) ΔT_{sink}/ ΔT_{source} = 20K/20K. (b) ΔT_{sink}/ ΔT_{source} = 40K/10K

For the serially connected HPs, the split of heat load between the units is an additional degree of freedom which should be considered. The impact of variation of the load distribution is presented as contours in Figure 4a and Figure 4b for the COP and NPV, respectively. The load distribution for HP_1 is defined as the heat load of HP_1 compared to the combined load (sum of load for HP_1 and HP_2 - 1 MW for the presented results). In Figure 4b curves for technical constraints are presented for the unit with the highest discharge temperature (180°C), as well as the condenser pressure for the unit with the highest high side pressure. Based

on the slope of constant COP and NPV contours, the heat load distribution has a higher impact to the COP than to the NPV. For both performance criteria it is clear that the temperature lift has a high influence. As NPV is not sensitive to the heat load distribution, other influences to the technical constraints may prove significant. It is seen that an even heat load split allows higher temperature lift of the total installation, compared to the case where one of the units has a significantly higher share of heat load than the other. At a fixed temperature lift the highest condenser pressure may vary by approximately 2 bar. The gain from even heat load split to the case with the lowest condenser pressure is a reduction of approximately 1 bar. As the discharge temperature is found to be a major factor to limitations of working domains in Ommen et al. (2015) the heat load fraction of the configuration utilised for calculation of the working domains was kept at 0.5 (-).

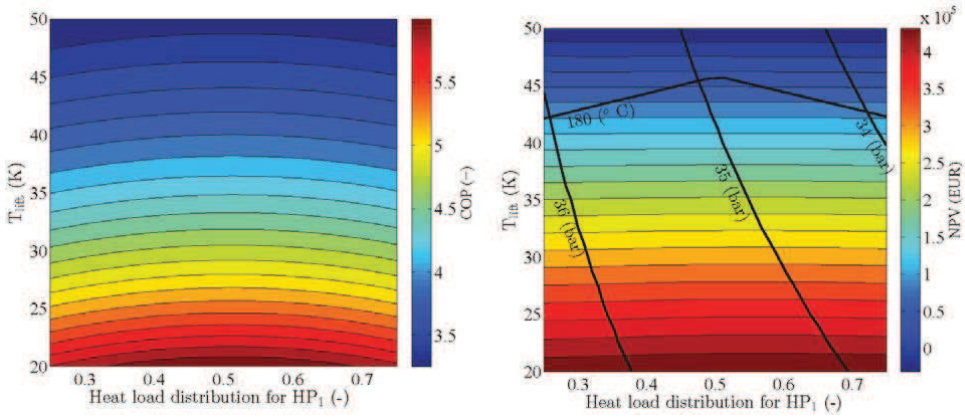

Figure 4: COP and NPV variations with variation of the heat load fraction and temperature lift. Results are calculated for T_{sink} = 70 (°C) and ΔT_{sink}/ ΔT_{source} = 20K/20K.

The enhanced working domains for VCHP are presented in Figure 5. Each individual plot shows the constraints for the serially connected HP units, showing both the technical and the economic restrictions. The economic constraints are presented as green curves (NPV) and turquoise curves for PBP = 8 years. Red curves indicate high discharge temperatures, whereas blue curves show the pressure constraints. Series #1 corresponds to two R717-HP HPs, Series #2 corresponds to R600a for unit 1 and R717-HP for unit 2. For the two plots presenting Series #1 (Figure **5**a and Figure **5**b) it was found that the working domain is constrained by two technical constraints (maximum allowable pressure and discharge temperature). For both cases the pressure constraint limits the working domain at sink temperatures below 90 °C, whereas the temperature lift is constrained at approximately 45 K for the 20K/20K case, and 53 K for the 40K/10K case, respectively. For Series #2, the economic NPV constraint is limiting the working domain in terms of high temperature lift. The pressure constraint (limitation in terms of high sink temperatures) of Figure **5**c and d corresponds to the technical constraint of R717-HP components of the HP_2 unit, which result in sink temperatures of approximately 96 °C for the 20K/20K case and 107 °C for the 40K/10K case. The difference in achievable sink temperatures is due to the sink temperature glide for the two cases.
In Figure **6** the working domains of Series #1 and #2 are compared to the best available working domains of the previous study. Figure 6 (a & b) compares the limiting constraints, and in (c & d) the areas are hatched with the most profitable vapour compression technology based on NPV. For both ΔT_{sink} / ΔT_{source} variations, the serially connected HPs expand the working domain in areas, which are not possible to operate by other configurations. In parts of the areas where the previous recommendation was installation of an R600a unit, Series #2 replaces the area due to higher profitability.

4. DISCUSSION

For an in depth discussion of the assumptions for working conditions, economic parameters and the applied correlations for heat exchangers and component costs, the reader is referred to Ommen et al. (2015) and Jensen et al. (2015). A possible improvement would be the use of polytropic efficiency for the comparison

of VCHP operated in series with a single VCHP. The differences in terms of NPV and discharge temperatures are expected to be low.

It is important to note, that the negative impact to NPV from increasing the amount of units (in serial connection) corresponds to economy of scale. In the HP model this effect corresponds to the slope of the validated cost correlation. In the case where it is not possible to utilise larger components (due to lack of availability) the NPV should be compared to the case of two or more HPs in parallel. In this case the serial connected HPs may have a lower NPV than the alternative.

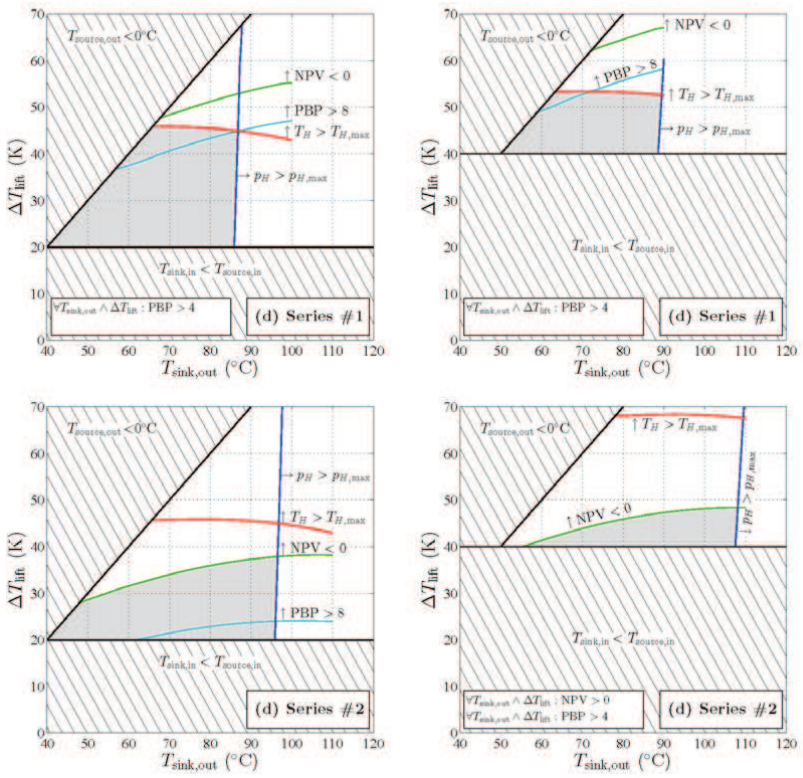

Figure 5: Feasible working domains indicated by grey background for serial connected vapour compression HPs. The considered temperature glides are (ΔT_{sink}/ ΔT_{source}) 20K/20K (a & c) and 40K/10K (b & d). Series #1 correspond to two R717-HP HPs, Series #2 correspond to R600a for unit 1 and R717-HP for unit 2.

5. CONCLUSION

Four schemes for serial connection of industrial HPs were investigated in the paper. It is found that serial connection of either two or three units results in an increase in COP and a decrease in NPV, when compared to the reference system with only one HP. On the other hand, the serial connection reduces the discharge temperature, which is of particular interest when assessing R717 HPs. Another possibility is to mix different types of HP units, in order obtain specific characteristics. Both improvements result in enlarged working domains for both investigated dual unit serial connections.

ACKNOWLEDGEMENTS

This work was supported by DONG Energy, Copenhagen Cleantech Cluster (CCC), Danish Technological Institute and EUDP (Energy Technology Development and Demonstration) project number: 64011-0351.

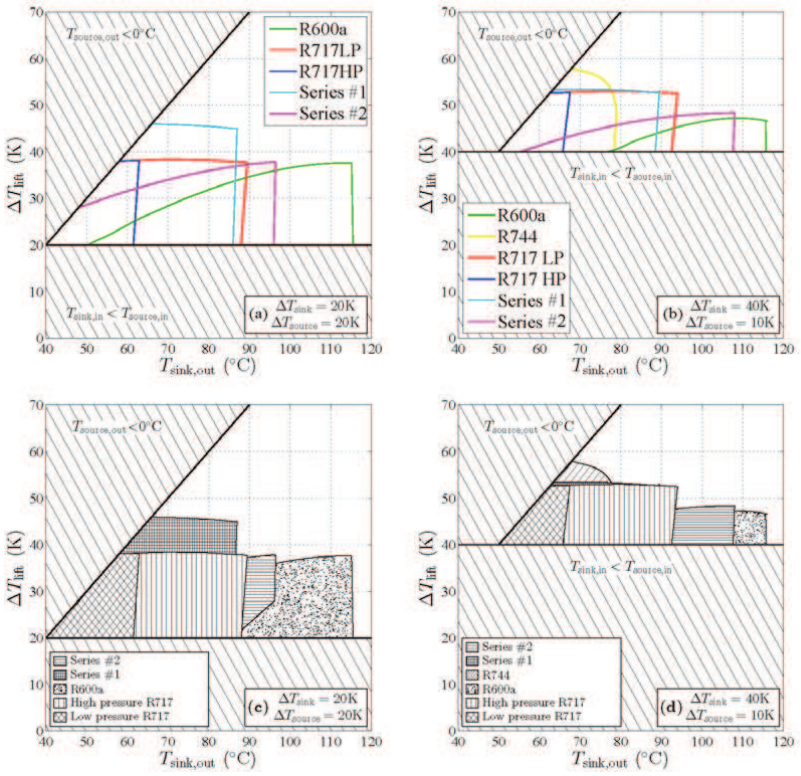

Figure 6: Compilation of working domains (a & b) and hatched areas with most profitable vapour compression technology based on NPV (c & d). The considered temperature glides are (ΔT_{sink}/ ΔT_{source}) 20K/20K (a & c) and 40K/10K (b & d).

REFERENCES

Danish Energy Agency, Data, tables, statistics and maps, ENERGY IN DENMARK 2012, http://www.ens.dk/ [accessed 23.03.14].

A Bejan, G Tsatsaronis, M Moran, Thermal Design & Optimization. 1'st edition ed., John Wiley & Sons, New York, 1996.

F-Chart Software (LLC.), Engineering Equation Solver, EES. V9.710 (6/28/12) (1992) http://www.fchart.com/ees/. [accessed 23.03.14].

JK Jensen, T Ommen, WB Markussen, L Reinholdt, B Elmegaard, Technical and economic working domains of industrial heat pumps: Part 2 - ammonia-water hybrid absorption-compression heat pumps, Int.J.Refrigeration. (2015).

H Martin, A theoretical approach to predict the performance of chevron-type plate heat exchangers, Chemical Engineering and Processing: Process Intensification. 35 (1996) 301-310.

T Ommen, JK Jensen, WB Markussen, L Reinholdt, B Elmegaard, Technical and economic working domains of industrial heat pumps: Part 1 - single stage vapour compression heat pumps, Int.J.Refrig. (2015).

V Prestmark, J Schultz, Planning and design of a 15 M geothermal heat pump installation in Denmark, Heat pumps for buildings. (1984) 171-187.

Y- Yan, T- Lin, Evaporation heat transfer and pressure drop of refrigerant R-134a in a plate heat exchanger, Journal of Heat Transfer. 121 (1999) 118-127.

Y- Yan, H- Lio, T- Lin, Condensation heat transfer and pressure drop of refrigerant R-134a in a plate heat exchanger, Int.J.Heat Mass Transfer. 42 (1999) 993-1006.

Appendix L

Paper 15 - ICR 2015

Jonas Kjær Jensen, Martin Ryhl Kærn, Torben Ommen, Wiebke Brix Markussen, Lars Reinholdt and Brian Elmegaard

Effect of liquid/vapour maldistribution on the performance of plate heat exchanger evaporators

ICR 2015, [accepted for publication]

EFFECT OF LIQUID/VAPOUR MALDISTRIBUTION ON THE PERFORMANCE OF PLATE HEAT EXCHANGER EVAPORATORS

Jonas K. JENSEN(*), Martin R. KÆRN(*), Torben OMMEN(*), Wiebke B. MARKUSSEN(*), Lars REINHOLDT(**), Brian ELMEGAARD(*)

(*) Department of Mechanical Engineering, Technical University of Denmark, Nils Koppels Allé Building 403, Kgs. Lyngby, DK-2800, Denmark
jkjje@mek.dtu.dk

(**) Danish Technological Institute, Kongsvang Allé 29, Aarhus, DK-8000, Denmark

ABSTRACT

Plate heat exchangers are often applied as evaporators in industrial refrigeration and heat pump systems. In the design and modelling of such heat exchangers the flow and liquid/vapour distribution is often assumed to be ideal. However, maldistribution may occur and will cause each channel to behave differently due to the variation of the mass flux and vapour quality. To evaluate the effect of maldistribution on the performance of plate heat exchangers, a numerical model is developed in which the mass, momentum and energy balances are applied individually to each channel, including suitable correlations for heat transfer and pressure drop. The flow distribution on both the refrigerant and secondary side is determined based on equal pressure drop while the liquid/vapour distribution is imposed to the model. Results show that maldistribution may cause up to a 25 % reduction of the overall heat transfer coefficient, compared to a lumped model with uniform distribution.

1. INTRODUCTION

Plate heat exchangers (PHE) are often applied as evaporators for industrial scale refrigeration or heat pump systems. The performance of such heat exchangers is thus important for the design and evaluation of these systems. Often, when dimensioning such heat exchangers, a lumped model with uniform flow and vapour quality distribution is applied. Thus, the effect of the end-plates is neglected. Maldistribution may occur and pose an impact on the heat transfer performance (Mueller and Chiou, 1988).

Kandlikar and Shah (1989) provides correction factors for the logarithmic mean temperature difference, for several types of PHE configurations, to account for the end-plate effects. However, these are applicable only for liquid/liquid heat transfer without flow maldistribution. Bassiouny and Martin (1983) investigated the flow distribution in PHE and found that flow maldistribution can be avoided if the area ratio between the inlet port and outlet port is chosen correctly. However, again for liquid/liquid heat transfer only.

The effect of maldistribution in evaporators was investigated for mini-channel heat exchangers in Brix et al. (2009) and Brix et al. (2010) and for fin and tube evaporators in Kærn et al. (2011). These studies were focused on quantifying the effect of a non-uniform airflow distribution and found that the refrigerant distribution was affected by the airflow distribution and that the distribution has an effect on the evaporator performance.

Lin et al. (2014) experimentally investigated the in-channel distribution of refrigerant and its effect on the heat transfer characteristics of PHE. Vist and Pettersen (2004) experimentally investigated the quality distribution in compact heat exchanger manifolds and showed that the liquid/vapour maldistribution can be severe and cause a significant reduction of the thermal performance of the heat exchanger.

In the present study, a numerical model of a PHE capable of solving heat transfer, pressure loss and mass flow distribution will be presented. In this model the vapour quality distribution (the vapour quality at the inlet of the refrigerant channels) is imposed. Thus the effect of the vapour quality distribution and the induced mass flow maldistribution can be quantified.

2. METHOD

2.1. Plate heat exchanger correlations, maldistribution parameter and operating conditions

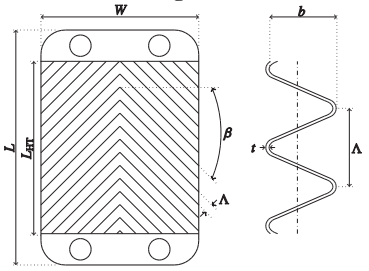

Figure 1. Schematic diagram of a chevron corrugated plate.

Table 1. Plate dimensions of plate 1 & 2

	Plate 1	Plate 2
W	115 mm	243 mm
L	522 mm	525 mm
L_{HT}	476 mm	456 mm
β	35 °	35 °
Λ	8 mm	8 mm
t	0.5 mm	0.5 mm
b	2.3 mm	2.3 mm
λ	16 W/m-K	16 W/m-K
D_h	$2(b-t)\,\phi^{-1}$	

The numerical model was developed in MatLAB (2013) using the thermophysical property database CoolProp (Bell et al., 2014). Correlations proposed by Han et al. (2003) were applied for calculating heat transfer and pressure drop in the two-phase region, while Martin (1996) was applied for the single-phase regions of both the refrigerant and the secondary sides.

The refrigerant was R134a and the secondary side was assumed to be water. Two plate dimensions were investigated: Plate 1 and Plate 2. The dimensions of these two plates are stated in Table 1. As seen Plate 1 has a smaller length to width ratio than Plate 2. The PHE had 20 refrigerant channels.

In order to best isolate the effect of the vapour quality distribution, fixed operating conditions were applied. The applied operating conditions for the secondary side consisted of a fixed inlet and outlet temperature: $T_{\mathrm{sec,in}}$=40 °C and $T_{\mathrm{sec,out}}$=30 °C. For the refrigerant, a fixed superheat temperature difference: ΔT_{SH}=5 K and a constant inlet specific enthalpy were applied. The inlet specific enthalpy was evaluated at saturated liquid conditions at 60 °C.

The vapour quality distribution was imposed by the parameter Δx, which is the difference between the inlet vapour quality of the first and last refrigerant channel. The vapour quality distribution profile was assumed to be linear and thus the inlet quality, $x_{\mathrm{in},n}$, of the remaining channels was found as shown in Eq. (1). Here N is the total number of refrigerant channels and n is the index of the refrigerant channels. The value of $x_{\mathrm{in},1}$ is solved iteratively to ensure mass conservation. This will be described in detail in section 2.2.

$$x_{\mathrm{in},n} = x_{\mathrm{in},1} - (1-n)\frac{\Delta x}{N-1} \qquad \text{for } n \in \{1,\mathrm{N}\} \tag{1}$$

2.2. Solving heat transfer and pressure loss

The heat transfer and pressure loss was solved for given boundary conditions (refrigerant and secondary side inlet conditions) using a successive substitution approach. The control volume and grid structure are illustrated in Figure 2. As seen the PHE is constructed such that both the first and the last channels are secondary channels and thus: M=N+1, where N and M are the number of refrigerant and secondary channels, respectively. Further, the total number of plates, I, can be determined as I=2N+2 in which two of the plates are end plates and therefore do not transfer heat: $\dot{Q}_{1,j} = \dot{Q}_{I,j} = 0$. Thus the number heat transfer plates are I=2N. A total of J=100 lengthwise discretizations were applied.

The structure of the successive substitution procedure is seen in Figure 3 (A). As seen first initial guess values were supplied for: $\dot{Q}_{i,j}, T_{w,\mathrm{sec},i,j}, T_{w,\mathrm{ref},i,j}, \Delta p_{ref,i,j}$ and $\Delta p_{\mathrm{sec},i,j}$. From $\Delta p_{ref,i,j}$ and $\Delta p_{\mathrm{sec},i,j}$ the pressure of the remaining cells was found as seen in Eq. (2)-(3). From $\dot{Q}_{i,j}$ the enthalpy of all cells was found from the energy balances: Eq. (4)-(5)

$$p_{\mathrm{ref},n,j+1} = p_{\mathrm{ref},n,j} + \Delta p_{\mathrm{ref},n,j} \quad \text{for } n \in \{1, N\} \quad \text{and } j \in \{1, \mathrm{J}\} \quad (2)$$

$$p_{\mathrm{sec},m,j+1} = p_{\mathrm{sec},m,j} - \Delta p_{\mathrm{sec},m,j} \quad \text{for } m \in \{1, M\} \quad \text{and } j \in \{1, \mathrm{J}\} \quad (3)$$

$$h_{ref,n,j+1} = h_{ref,n,j} + \frac{\dot{Q}_{2\cdot n,j} + \dot{Q}_{2\cdot n+1,j}}{\dot{m}_{\mathrm{ref},n}} \quad \text{for } n \in \{1, N\} \quad \text{and } j \in \{1, \mathrm{J}\} \quad (4)$$

$$h_{sec,m,j+1} = h_{sec,m,j} - \frac{\dot{Q}_{2\cdot m-1,j} + \dot{Q}_{2\cdot m,j}}{\dot{m}_{\mathrm{sec},m}} \quad \text{for } m \in \{1, M\} \quad \text{and } j \in \{1, \mathrm{J}\} \quad (5)$$

From the pressure and enthalpy, the temperatures at the inlet and outlet of all cells were determined and subsequently the log mean temperature difference, $\Delta T_{\mathrm{LM},i,j}$ between each control volume was found as seen in Eq. (6). Here $p(i)$= {1, 1, 2, 2, 3, 3, … M, M} and $q(i)$= {-, 1, 1, 2, 2, 3, 3, ... N, N,-} for $i \in \{1, \mathrm{I}\}$ which ensures that the correct channel is chosen for each plate.

$$\Delta T_{LM,i,j} = \frac{\left(T_{\mathrm{sec},p(i),j} - T_{ref,q(i),j}\right) - \left(T_{\mathrm{sec},p(i),j+1} - T_{ref,q(i),j+1}\right)}{ln\left(\frac{T_{\mathrm{sec},p(i),j} - T_{ref,q(i),j}}{T_{\mathrm{sec},p(i),j+1} - T_{ref,q(i),j+1}}\right)} \quad \text{for } i \in \{2, \mathrm{I}-1\} \quad \text{and } j \in \{1, \mathrm{J}\} \quad (6)$$

The heat transfer coefficient and friction factor were determined from the applied correlations. Transport properties were evaluated at the cells mean temperature and pressure. From the heat transfer coefficients of the cell walls the overall heat transfer coefficient between each control volume was determined from Eq. (7).

$$U_{i,j} = \left(\frac{1}{\alpha_{\mathrm{sec},i,j}} + \frac{t}{\lambda} + \frac{1}{\alpha_{\mathrm{ref},i,j}}\right)^{-1} \quad \text{for } i \in \{2, \mathrm{I}-1\} \quad \text{and } j \in \{1, \mathrm{J}\} \quad (7)$$

Subsequently $\dot{Q}_{i,j}, T_{w,\mathrm{sec},i,j}, T_{w,\mathrm{ref},i,j}, \Delta p_{ref,n,j}$ and $\Delta p_{\mathrm{sec},m,j}$ was updated based on the calculated temperature difference, heat transfer coefficient and friction factor. This was done as seen in Eq. (8)-(12). For the cell pressure loss an average of the friction factors of the cell's two opposing plates were applied as: $\bar{\xi}_{\mathrm{ref},n,j} = 0.5 \cdot \left(\xi_{\mathrm{ref},2\cdot n,j} + \xi_{\mathrm{ref},2\cdot n+1,j}\right)$ and $\bar{\xi}_{\mathrm{sec},n,j} = 0.5 \cdot \left(\xi_{\mathrm{sec},2\cdot m,j} + \xi_{\mathrm{sec},2\cdot m+1,j}\right)$.

$$\dot{Q}_{i,j} = q''_{i,j} A_{i,j} = U_{i,j} \cdot A_{i,j} \cdot \Delta T_{LM,i,j} \quad \text{for } i \in \{2, \mathrm{I}-1\} \quad \text{and } j \in \{1, \mathrm{J}\} \quad (8)$$

$$T_{w,\mathrm{sec},i,j} = 0.5 \cdot \left(T_{\mathrm{sec},m,j} + T_{\mathrm{sec},m,j+1}\right) - q''_{i,j} \frac{1}{\alpha_{\mathrm{sec},i,j}} \quad \text{for } i \in \{1, \mathrm{I}\} \quad \text{and } j \in \{1, \mathrm{J}\} \quad (9)$$

$$T_{w,\mathrm{ref},i,j} = T_{w,\mathrm{sec},i,j} - q''_{i,j} \frac{t}{\lambda} \quad \text{for } i \in \{2, \mathrm{I}-1\} \quad \text{and } j \in \{1, \mathrm{J}\} \quad (10)$$

$$\Delta p_{\mathrm{ref},n,j} = \frac{2 \cdot G^2_{\mathrm{ref},n} \cdot \bar{\xi}_{\mathrm{ref},n,j} \cdot \frac{L_{HT}}{J}}{\rho_{\mathrm{ref},n,j} \cdot D_h}, \quad \text{for } n \in \{1, N\} \quad \text{and } j \in \{1, \mathrm{J}\} \quad (11)$$

$$\Delta p_{\mathrm{sec},m,j} = \frac{2 \cdot G^2_{\mathrm{sec},m} \cdot \bar{\xi}_{\mathrm{sec},n,j} \cdot \frac{L_{HT}}{J}}{\rho_{\mathrm{sec},m,j} \cdot D_h} \quad \text{for } m \in \{1, M\} \quad \text{and } j \in \{1, \mathrm{J}\} \quad (12)$$

To determine if a solution was reached, the relative difference between the guess values and the updated values of: $\dot{Q}_{i,j}, T_{w,\mathrm{sec},i,j}, T_{w,\mathrm{ref},i,j}, \Delta p_{ref,i,j}$ and $\Delta p_{\mathrm{sec},i,j}$ was calculated. If the maximum relative difference was below the desired tolerance the procedure was terminated. If it was greater than the desired tolerance: the updated values were supplied as guess values for the next iteration.

2.3. Solving flow distribution and operating conditions

To solve the flow distribution and the operating conditions a Newton-Raphson solver was applied. The structure of the procedure is seen in Figure 3 (B). The flow distribution was solved for both refrigerant and secondary side such that equal pressure loss over each channel was attained. The objective was to find a mass flow rate for each channel such that this criterion was satisfied. The pressure loss in each channel was found using the successive substitution approach described above. The flow distribution was calculated to satisfy Eq. (13) – (14). The first *N*-1 and *M*-1 equations ensure that equal pressure loss is attained, while equations *N* and *M* ensure mass conservation.

$$\sum_{j=1}^{J} \Delta p_{\mathrm{ref},n,j} = \frac{1}{N} \sum_{n=1}^{N} \sum_{j=1}^{J} \Delta p_{\mathrm{ref},n,j} \qquad \text{for } n \in \{1, N-1\} \qquad \dot{m}_{\mathrm{ref,tot}} = \sum_{n=1}^{N} \dot{m}_{\mathrm{ref},n} \tag{13}$$

$$\sum_{j=1}^{J} \Delta p_{\mathrm{sec},m,j} = \frac{1}{M} \sum_{m=1}^{M} \sum_{j=1}^{J} \Delta p_{\mathrm{sec},m,j} \qquad \text{for } m \in \{1, M-1\} \qquad \dot{m}_{\mathrm{sec,tot}} = \sum_{m=1}^{M} \dot{m}_{\mathrm{sec},m} \tag{14}$$

To solve the fixed operating conditions described in Section 2.1 equations Eq. (15)-(17) were applied. Here Eq. (15) was used to determine the needed refrigerant mass flow rate, $\dot{m}_{\mathrm{ref,tot}}$, in order to ensure that the desired superheat was attained at the outlet of the PHE. The superheat was defined using enthalpies thus avoiding the zero singularity at ΔT_{SH}=0 K (two-phase refrigerant outlet). $h_{\Delta T_{SH}}$ was evaluated at the outlet pressure and a temperature ΔT_{SH} above the corresponding saturation temperature. Eq. (16) was applied to determine the evaporation temperature needed to ensure the desired secondary outlet temperature. $h_{T_{\mathrm{sec},o}}$ was evaluated at the desired secondary outlet temperature and the calculated pressure. Finally, Eq. (17) was applied to determine the inlet vapour quality of the first channel to ensure conservation of the inflowing vapour.

$$h_{\Delta T_{SH}} = \frac{1}{\dot{m}_{\mathrm{ref,tot}}} \sum_{n=1}^{N} \dot{m}_{\mathrm{ref},n} \cdot \mathrm{h}_{\mathrm{ref},n} \tag{15}$$

$$h_{T_{\mathrm{sec},o}} = \frac{1}{\dot{m}_{\mathrm{sec,tot}}} \sum_{m=1}^{M} \dot{m}_{\mathrm{sec},n} \cdot \mathrm{h}_{\mathrm{sec},n} \tag{16}$$

$$\mathrm{x}_{\mathrm{ref,in}} \cdot \dot{m}_{\mathrm{ref,tot}} = \sum_{n=1}^{N} \dot{m}_{\mathrm{ref},n}\, x_{\mathrm{ref,in},n} \tag{17}$$

The flow distribution and operating conditions were solved to a relative tolerance one order of magnitude higher than that applied in the successive substitution procedure, which had a tolerance of 10^{-5}.

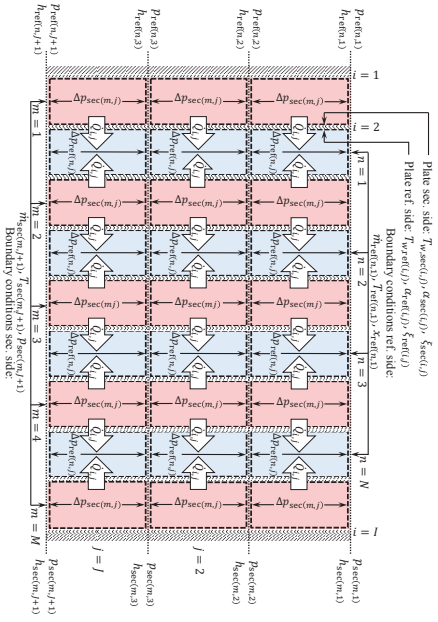

Figure 3. Control volume and grid structure diagram

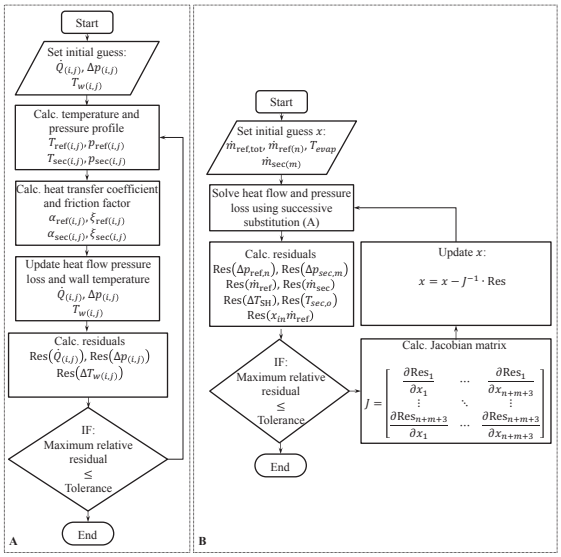

Figure 2. Procedure for solving the numerical model. A: solves the heat transfer and pressure drop. B: solves flow distribution and operating conditions.

3. RESULTS

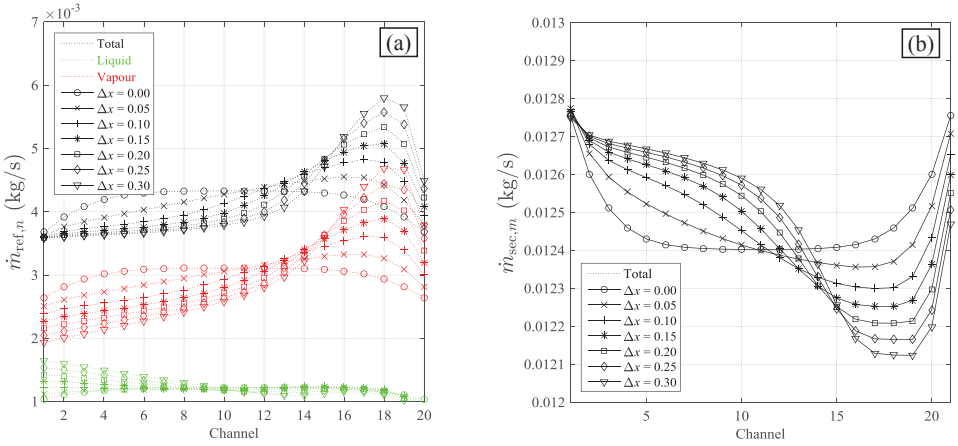

Figure 4. Refrigerant (a) and secondary (b) mass distribution profile for plate type 1 with a mean heat flux of 5000 W/m^2 and a variation of the vapour quality distribution.

In order to quantify the effect of a non-uniform distribution of vapour quality a series of simulations have been conducted. The simulations have been carried out for the two plate sizes listed in Table 1 under four different mean heat fluxes: 2500 W m^{-2}, 5000 W m^{-2}, 7500 W m^{-2}, 10,000 W m^{-2}, yielding a total of eight cases. For these eight cases the quality distribution was varied from a uniform distribution (Δx=0) to high maldistribution (Δx=0.4). All simulations were performed with N=20 refrigerant channels and the operating conditions described in Section 2.1.

An example of the mass distribution variation is shown in Figure 4 for a mean heat flux of 5000 W m^{-2} and plate size 1. As seen, even with a uniform distribution of the vapour quality (Δx=0) maldistribution of the mass flow rates will occur for both the refrigerant and the secondary side. This maldistribution is caused by the effects of the end plates and affects the mass flow rate of the first and last five channels for the presented case.

When increasing Δx, it is seen that the variation of the mass flow rates is increased such that more refrigerant mass flow is supplied to the channels with low vapour quality. Conversely, less secondary mass flow is supplied to the adjacent secondary channels. Overall it is seen from Figure 4 that the variation of the mass flow rate is more profound on the refrigerant side than on the secondary side.

Figure 5 shows the temperature and heat flux profile for two cases: uniform vapour quality distribution (Δx=0) and with vapour quality maldistribution of Δx=0.3. Figure 5 (a) & (b) shows the temperature of the refrigerant and secondary channels as well as the wall temperature on both sides. As seen from Figure 5 (a), a uniform temperature profile occurs in the centre of the heat exchangers when the vapour quality distribution is ideal. However, the first and last 5 channels will differ from this due to the effect of the end plates, which results in a low temperature difference at the refrigerant outlet side, consequently reducing the heat flux in this area, see Figure 5 (c).

Imposing a vapour quality maldistribution of Δx=0.3 results in a non-uniform temperature profile as seen in Figure 5 (b). As seen the high vapour quality of the 10 first channels result in a large region in which the refrigerant is superheated. This region will subsequently suffer from both low temperature differences and poor heat transfer coefficients. These unfavourable conditions are enhanced by the additionally low mass flux caused by the high pressure loss associated with the superheated vapour. Consequently, the heat flux in this region will be low as is evident from Figure 5 (d).

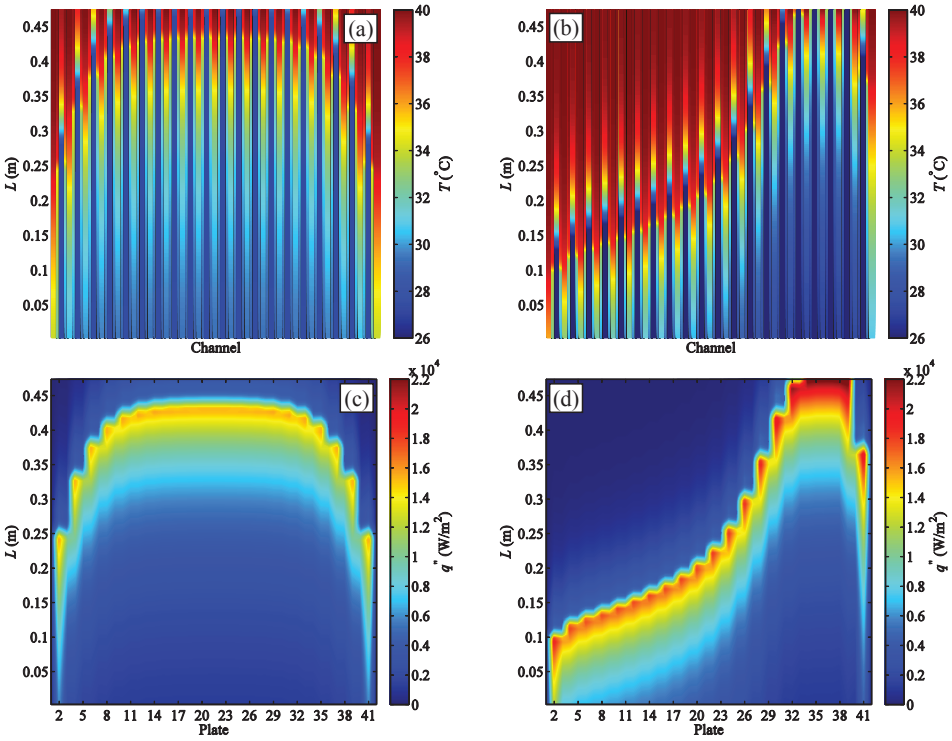

Figure 5 Temperature (a) & (b) and heat flux (c) & (d) profile for plate type 1 with a mean heat flux of 5000 W m^{-2}. Even vapour quality distribution (Δx=0) is presented in (a) & (c). Vapour quality maldistribution (Δx=0.30) is presented in (b) & (d).

Figure 6 summarizes the results of the eight simulated cases. Here the needed evaporation temperature, T_{evap}, the overall heat transfer coefficient reduction factor, F, and the relative standard deviation, RSD, for both the refrigerant and secondary mass flow distribution, is presented. These four parameters are all shown as functions of the imposed vapour quality distribution parameter Δx.

As seen from Figure 6 (a) the evaporation temperature only shows a weak dependence on the plate size while exhibiting a large dependence on both the mean heat flux and Δx. Further, it may be seen that the larger the heat flux, the more sensitive the evaporation temperature will be on the vapour quality distribution. Figure 6 (b) shows the reduction factor, F, of the overall heat transfer coefficient compared to a lumped model in which uniform vapour quality distribution is assumed and the effect of the end plates are neglected. As seen, even with Δx=0 there is a reduction of the overall heat transfer coefficients due to the end plates. This reduction depends on both the plate size and mean heat flux. As seen, when the heat flux is increased the heat transfer coefficient is more affected by the end plates. This is however caused by the increased mass flux associated with the increased heat flux as the plate geometry is fixed. Further, it may be seen that Plate 1 is more influenced by the end plates than Plate 2. This is attributed to the small length to width ratio for Plate 1: ≈ ¼ compared to the larger ratio of ≈ ½ for Plate 2. Thus the mass flux for will be higher for Plate 1 than for Plate 2. It is seen that the two plate sizes are equally influenced by Δx.

Figure 6 (c) & (d) show the relative standard deviation (RSD) of the mass distribution and is thus a measure of the variability of the mass flow profiles. Hence, if RSD=0 % the mass flow rates do not deviate from the mean and a uniform distribution is attained. As seen this is never the case. From Figure 6 (c) it is clear that the maldistribution induced by the end plates increases with increasing heat flux and that the maldistribution is influenced by the plate size. The refrigerant maldistribution increases with the mean heat flux while it is

seen that the secondary side maldistribution decreases. Furthermore, the refrigerant maldistribution is more influences by the plate size than the secondary side.

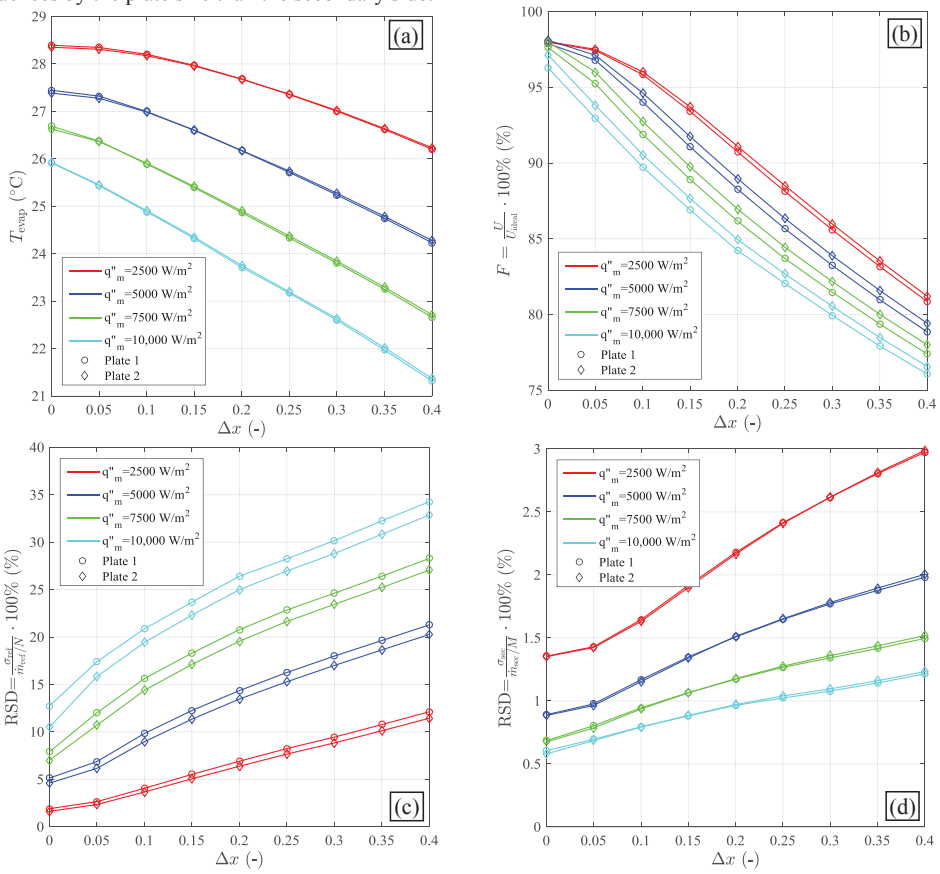

Figure 6. Evaporation temperature (a), the overall heat transfer coefficient reduction factor (b) and the relative standard deviation, RSD, for both the refrigerant (c) and secondary (d) mass flow distribution.

4. DISCUSSION

The results presented stem solely from numerical simulations using validated heat transfer and pressure loss correlations. However, it is unclear from the sources of the correlations to which extent they include some effect of maldistribution. Therefore, the absolute values of the local overall heat transfer coefficients attained by the described model may be inaccurate. However, the relative reduction of heat transfer coefficient and the RSD should be justified, as the same correlations are applied.

5. CONCLUSIONS

A numerical model of a plate evaporator was developed such that a vapour quality distribution profile could be imposed, thus allowing the influence of the distribution to be quantified. Eight cases were simulated: four mean heat fluxes and two plate sizes. This showed that vapour quality maldistribution can reduce the *U*-value up to 25% when the vapour quality distribution difference is 0.4. Further it was found that even with a uniform vapour quality distribution; flow maldistribution will occur and may cause a reduction of the *U*-value from 2-4%. This is caused by the end plates and the effect is increased with increasing mean heat flux. Further the plate with the smallest length to width ratio showed a stronger tendency for maldistribution.

6. REFERENCES

Bassiouny, M.K., Martin, H., 1983. Flow distribution and pressure drop in plate heat exchangers - I. Chem. Eng. Sci. 39, 693–700.

Bell, I.H., Wronski, J., Quoilin, S., Lemort, V., 2014. Pure and Pseudo-pure Fluid Thermophysical Property Evaluation and the Open-Source Thermophysical Property Library CoolProp. Ind. Eng. Chem. Res. 53, 2498–2508.

Brix, W., Kærn, M.R., Elmegaard, B., 2009. Modelling refrigerant distribution in microchannel evaporators. Int. J. Refrig. 32, 1736–1743.

Brix, W., Kærn, M.R., Elmegaard, B., 2010. Modelling distribution of evaporating CO2 in parallel minichannels. Int. J. Refrig. 33, 1086–1094.

Han, D.H., Lee, K.J., Kim, Y.H., 2003. Experiments on the characteristics of evaporation of R410A in brazed plate heat exchangers with different geometric configurations. Appl. Therm. Eng. 23, 1209–1225.

Kandlikar, S.G., Shah, R.K., 1989. Multipass plate heat exchangers - effectiveness-NTU results and guidelines for selecting pass arrangements. J. Heat Transfer 111, 300–313.

Kærn, M.R., Brix, W., Elmegaard, B., Larsen, L.F.S., 2011. Performance of residential air-conditioning systems with flow maldistribution in fin-and-tube evaporators. Int. J. Refrig. 34, 696–706.

Lin, Y.-H., Li, G.-C., Yang, C.-Y., 2014. An experimental observation of the effect of flow direction for evaporation heat transfer in plate heat exchanger. Appl. Therm. Eng. 1–8.

Martin, H., 1996. A theoretical approach to predict the performance of chevron-type plate heat exchangers. Chem. Eng. Process. 35, 301–310.

MatLAB, version: 2013b, publisher: Mathworks, 2013.

Mueller, A.C., Chiou, J.P., 1988. Review of various types of flow maldistribution in heat exchangers. Heat Transf. Eng. 9, 36–50.

Vist, S., Pettersen, J., 2004. Two-phase flow distribution in compact heat exchanger manifolds. Exp. Therm. Fluid Sci. 28, 209–215.

7. NOMENCLATURE

Symbols

A	Area	m^2
b	Plate press depth	m
D_h	Hydraulic diameter	m
F	Heat transfer reduction factor	%
G	Mass flux	kg s^{-1} m^{-2}
h	Specific enthalpy	kJ kg^{-1}
I	Number of plates	-
J	Number of discretization	-
L	Plate length	m
M	Number of secondary channels	-
$\dot{m}$	Mass flow rate	kg s^{-1}
N	Number of refrigerant channels	-
p	Pressure	Pa
$\dot{Q}$	Heat load	kW
q''	Heat flux	kW m^{-2}
RSD	Relative standard deviation	%
T	Temperature	°C
t	Plate thickness	m
U	Overall heat transfer coefficient	kW m^{-2} K^{-1}
W	Plate width	m
x	Vapour quality	-

Greek

α	Heat transfer coefficient	kW m^{-2} K^{-1}
β	Plate corrugation angle	°
Δ	Difference	-
λ	Thermal conductivity	kW m^{-1} K^{-1}
Λ	Plate corrugation spacing	m
μ	Viscosity	Pa s
ξ	Fanning friction factor	-
ρ	Density	kg m^{-3}
σ	Standard deviation	-
ϕ	Plate enhancement factor	-

Subscripts & indices

HT	Plate heat transfer section
i	Plate index
j	Discretization index
m	Secondary channel index
n	Refrigerant channel index
sec	Secondary
ref	Refrigerant
w	Wall

Appendix M

Paper 16 - DHC13 2012

Erika Zvingilaite, Torben Ommen, Brian Elmegaard and Martin Franck

Low temperature district heating consumer unit with micro heat pump for domestic hot water preparation.

DHC13 2012, 13th International Symposium on District Heating and Cooling 2012. District Energy Development Center.

DHC13, the 13th International Symposium on District Heating and Cooling
September 3rd to September 4th, 2012, Copenhagen, Denmark

LOW TEMPERATURE DISTRICT HEATING CONSUMER UNIT WITH MICRO HEAT PUMP FOR DOMESTIC HOT WATER PREPARATION

E.Zvingilaite[1], T.Ommen[2], B. Elmegaard[2] and M.L.Franck[1]

[1] District Energy Application Centre, Danfoss A/S, DK-Nordborg
[2] Department of Mechanical Engineering, Technical University of Denmark

Keywords: Low temperature District Heating, DH consumer unit, Domestic hot water, Micro booster heat pump

ABSTRACT

In this paper we present and analyse the feasibility of a district heating (DH) consumer unit with micro heat pump for domestic hot water (DHW) preparation in a low temperature (40 °C) DH network.

We propose a micro booster heat pump of high efficiency (COP equal to 5,3) in a consumer DH unit in order to boost the temperature of the district heating water for heating the DHW. The paper presents the main designs of the suggested system and different alternative micro booster heat pump concepts. Energy efficiency and thermodynamic performance of these concepts are calculated and compared. The results show that the proposed system has the highest efficiency. Furthermore, we compare thermodynamic and economic performance of the suggested heat pump-based concept with different solutions, using electric water heater. The micro booster heat pump system has the highest annualised investment (390 EUR/year) and the lowest operation (320 EUR/year) expenditures. Electric heater-based concepts consume 5-14 times more electricity, which leads to relatively high annual operation costs (530-970 EUR/year); while investment costs are lower (326-76 EUR/year). The suggested DHW heat pump-based system is cost-efficient for private consumers already today. Furthermore, application of the micro booster heat pump in low energy houses complies with the energy consumption requirements, set by the recent Danish Building Regulations. The use of electrical heater variants would exceed this limit.

INTRODUCTION

District heat in Denmark is mainly produced in heat boilers or combined heat and power plants [1]. The average yearly district heating supply and return temperatures in distribution networks are 80 °C and 40 °C respectively [2]. Clearly, lower DH temperatures are desired in order to reduce energy losses in the district heating networks. Reducing district heating supply temperature becomes possible with increasing focus on energy efficiency improvements in energy supply systems and in the buildings. In Denmark energy performance requirements for new buildings set progressively lower limits on energy consumption for space heating and hot water preparation. At the same time renovations of the existing buildings are required to include certain minimum energy saving measures, such as insulation of roofs and walls and replacement of windows with more efficient ones etc. Consequently, with decreasing heat demand, low temperature heating becomes feasible in the increasing share of the building stock.

According to the proposal by the Danish Government [3] for future energy, heat and power supply and transport systems should solely rely on renewable energy (RE) resources by 2050. An important milestone is in 2035 where the entire heat and power supply should be 100 % renewable. Clearly, energy efficiency plays an important role in achieving these targets – reducing energy resource consumption and additional capacity investments. In the district heating sector biomass will play an important role in the 100 % renewable energy system. However, both national and global biomass resources are scarce. Therefore, other energy resources and technologies will have to be used in addition to biomass plants. For district heating production alternative sources are solar, geothermal, ambient and waste heat resources. The utilisation efficiency of energy resources depends on the required district heating water temperature and increases with decreasing DH temperatures

In this context the benefits of low temperature district heating (LTDH) are multiple. First, heat losses from the district heating network can be reduced. For example, by reducing DH supply temperature from 80 to 40-45 °C, heat losses in a DH system can be lowered by approximately 37 % or even more [4]. Second, low temperature DH in local networks opens for possibilities to connect new users to existing DH systems without necessarily requiring additional capacity investments[1]. Moreover, LTDH enables efficient use of low temperature renewable energy resources, such as solar, geothermal, industrial waste heat.

[1] Depends on a specific DH system and generation technology

DHC13, the 13th International Symposium on District Heating and Cooling
September 3rd to September 4th, 2012, Copenhagen, Denmark

The viability of a LTDH consumer substation with DH supply at just above 50 °C has been proven and demonstrated in Denmark [7]. Here it is possible to prepare domestic hot water of 45 °C without any additional energy source. Further lowering DH supply temperature could for example enable use of the DH return water (40 °C) in the traditional networks (and connect more consumers without significant increase in capacity). However, while district heating supply at 40-45 °C is in principle sufficient for space heating, it cannot be used for domestic hot water preparation.

In this paper possibilities for preparation of domestic hot water, when DH supply temperature is as low as 40 °C are discussed. We analyse different heat pump and electric heater concepts for utilising additional energy source – electricity for heating DHW. The concepts are compared on the basis of thermodynamic and economic calculations, described in the article. We recommend using a small heat pump for boosting DH water to 53 °C. As it was mentioned earlier, such temperature is sufficient for DHW preparation.

ENERGY CONSUMPTION FOR SPACE HEATING AND DOMESTIC HOT WATER

We assume that low temperature district heating is supplied to a low energy detached single family house. The house is built according to the requirements of the recent Danish Building Regulations (BR10) for low energy buildings of class 2015. The total yearly energy demand for space heating, domestic hot water preparation, operation of ventilators and pumps should not exceed the maximum annual energy demand set by the BR10 – the energy frame (E_{frame}, kWh/m^2), calculated by the following equation (1):

$$E_{frame} = 30 + \frac{1000}{A} \quad (1)$$

Here A is gross heated floor area (m^2).

Different weight coefficients are applied for consumed district heat and electricity – 0,8 and 2,5 respectively – when comparing the calculated energy consumption of a designed building with the energy frame.

Table 1 Energy consumption in the low energy house

Space heating demand, kWh/year	2570
DHW demand (250l/m2 per year at 55 °C (BR10)), kWh/year	2083
Electricity in pumps and ventilators, kWh/year	525
Total energy consumption, kWh/year	5178
Total allowed energy consumption by energy frame, kWh/year	5771

The analysed single family house has a heated area of 159 m^2, thus the energy frame is 36,3 kWh/m^2. The calculated energy demand is presented in Table 1. The energy consumption for domestic hot water heating accounts for a considerable share (40 %) of the total energy demand in the low energy house according to Table 1.

The single family house is heated by under floor heating. Consequently, with low energy demand and under floor heating systems the house is well suited for low temperature (40°C) district heating supply.

Different hot water consumption rates are assumed by various literature sources. For comparison of energy consumption in the building when different domestic hot water preparation alternatives are applied with the energy frame, hot water consumption calculated according to BR10 (Table 1), is used. For energy and economic cost calculations a more conservative and higher DHW [4] demand of 3200 kWh/year has been assumed (800 kWh per person per year and 4 occupants), which is 54 % higher than according to BR10.

DOMESTIC HOT WATER SYSTEM AND LOW TEMPERATURE DISTRICT HEATING

When considering domestic hot water preparation systems, three main aspects/requirements need to be taken into account:

- The required temperature of DHW is 40 - 45 °C, depending on the tapping place (kitchen or bathroom);
- The risk of bacterium 'Legionella' (especially if storing the hot tap water), which can be avoided either by increasing temperature of the DHW to around 55 °C or by avoiding storing it;
- The Danish water standard DS 439, which includes hot water tapping profile, has to be met when dimensioning DHW system, meaning that the peak load of 32,3 kW has to be satisfied and the hot water storage tank has to be large enough to cover the most critical DHW tapping profile during morning hours.

Previously a low temperature DH network and consumer substations have been developed and demonstrated, when district heating supply temperature was lowered to around 50 °C [7]. The Danish full-scale demonstration project of the low-temperature DH supply to low-energy buildings has proven that the concept works – both space heating and hot water demand can be satisfied.

In this article we take a step further and reduce DH supply temperature to 40 °C. Clearly this temperature is too low for heating the tap water up to 45 °C, thus additional energy is needed for domestic hot water preparation. This energy could come from electricity – in a heat pump or electric heater. For evaluation of energy systems with multiple fuels and products, the

thermodynamic quantity *Exergy* is commonly used [5]. The exergy level of a stream expresses the availability to do technical work, as temperature, pressure and chemical composition of the stream reaches equilibrium with the ambient. Electricity has a very high availability to do work, normally considered to be 100 %. If the ambient is represented by the cold tap water, the exergy of district heating water at 40 °C is very low (10 %) compared to electricity. Exergy expresses the minimum demand of primary energy supply theoretically needed to fulfil the DHW demand and should thus be minimized. The total energy demand for DHW supply may thus be quantified by the total exergy consumption of electricity and DH. From this viewpoint it will be advantageous to substitute one unit of electricity by up to ten units of DH. The further lowering of the district heating supply temperature is from a thermodynamic point of view more beneficial if the share of electricity in total energy, consumed for DHW, is small. Compared to an electric heater, where one unit (kW) of electricity input results in one unit (kW) of heat output, heat pumps can reduce this consumption by several units. To optimise the DHW production we have designed a small heat pump-based unit for hot tap water preparation in the low temperature DH system – a *microbooster heat pump unit*. Clearly, such DHW unit has to fulfil also the 2 latter requirements regarding legionella and sufficient capacity. This has been also taking into account when designing different DHW system concepts.

CONSUMER DHW UNIT WITH MICROBOOSTER HEAT PUMP

The additional energy, needed for DHW can be added either on the secondary side, directly to the tap water, or to the district heating water on the primary side, which is then used to heat the tap water. Different system configurations regarding hot source for the heat pump (DH supply or return water), pre-heating of tap or return water, configuration of the heat pump and storage tank type are possible for the two options. We have selected the three most promising concepts for further analysis (see Figure 1).

In variant **A** the district heating water entering the hot water system is divided into two flows. The temperature of the first flow is boosted from 40 °C to 53 °C as it flows through the condenser of the heat pump. The second DH flow runs through the evaporator and is the heat source for the heat pump (and is cooled down to around 25 °C). The heated DH water is stored in a stratified accumulator tank and instantaneously heats tap water in a micro plate heat exchanger [10], when the tapping starts. Here the district heating storage tank is used in order to lower DH flow, heat pump capacity and investment cost.

Variant **B** resembles **A** - the only difference is that return water from hot water heat exchanger (and possibly space heating) is used as hot source in the heat pump. This variant has a reduced DH flow when compared to **A**.

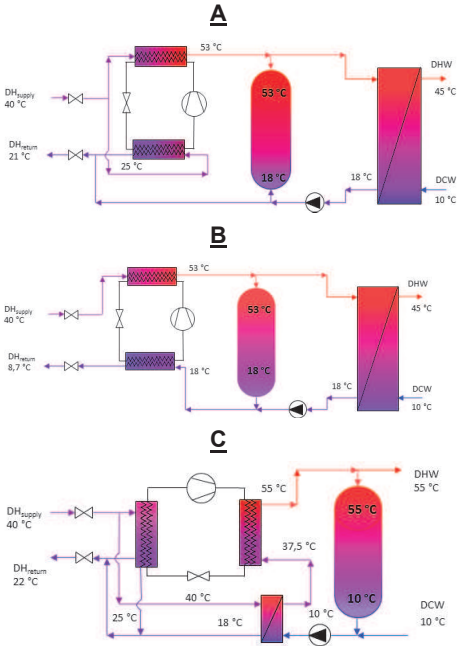

Figure 1 Analysed microbooster heat pump DHW concepts

In Variant **C** cold tap water is heated to 55 °C in the heat pump. DHW is stored at higher temperature than DH water in order to avoid formation of 'legionella' bacterium. In order to reduce required heat pump capacity, the cold water is preheated in a heat exchanger by using district heating water. The heat source of the heat pump is, as in variant **A**, district heating supply water.

For each micro booster heat pump variant, a numerical model has been implemented in Engineering Equation Solver (EES) using the assumptions presented in Table 2. More details on the numerical models and some results has been published previously [6]. In this paper some assumptions have been changed for the heat pump, to better represent the actual working conditions in the considered system. The heat pump is switched on from the start of the tapping sequence until the re-filling of the stratified tank is completed. Steady state operation can be assumed for the heat pump, as fluctuations from the hot water tapping profile are managed in the stratified tank. The storage volume of all the considered solutions has been calculated individually to allow similar operation patterns and operation time for all the heat pumps.

Table 2 Assumptions used in modelling DHW systems with micro booster heat pump

Variable	Assumption
Refrigerant	R600a
Isentropic efficiency of compressor, /	0.5
HEX pinch temperature difference in both Condenser and Evaporator, K	2.5
Pinch temperature in Tap-water HEX (Q_{MAX}=32 kW), K	8
Temperature of DH return from the evaporator (variants A & C) , °C	25

The main results of the calculations are summarised in Table 3. The flow of DH water, electricity consumption and exergetic efficiency are averaged values, which is possible due to steady state operation in the heat pump units.

Table 3 The results of three micro booster heat pump-based DHW system calculations

	Microbooster Heat Pump variants		
	A	B	C
DH flow, l/h	85	50	75
Power, W	142	214	155
Coefficient of performance (COP)	5,3	3,5	5,0
Exergetic efficiency	0,43	0,41	0,42
Storage size required, l	128	128	100

From the table it can be seen that variant A has the lowest required power capacity and the highest district heat flow. When DH flow is reduced and the return water is used in the evaporator in variant B, more power is needed to boost the DH water temperature. The reason is low temperature of the return water (around 18 °C), entering the evaporator. As a consequence the heat pump in variant B has low COP. In variant C more energy has to be used to heat the DHW. Here domestic hot water is heated to 55 °C, i.e. 2 °C higher than in the case of primary DH water. Furthermore, even though the cold tap water is pre-heated to 37,5 °C before entering the heat pump it is still lower than the temperature of the DH water entering the heat pump in variants A and B.

The differences in district heating water flow in the three analysed hot water systems will not have any effect on the size of service pipes, since they are already oversized due to low energy consumption of the house and the fact that the smallest DH pipe size available on the market has been assumed.

The relation between the required heat (DH flow) from the district heating network and the additional electricity needed is of primary interest, as both are needed to produce hot water with the micro booster heat pump unit. Heat and electricity are in many cases produced as main products in the Combined Heat and Power (CHP) plant, and in this way the interaction becomes important. As exergetic efficiency is a measure of both the inputs and products (the product is in this case the constant amount of domestic hot water) the objective is to minimize the amount of heat and power required as the energy source for the heat pump. As the DH supply water has lower exergy content than electricity [5], the heat pump configuration with the lower power consumption and the higher heat consumption has the highest exergetic efficiency. With the highest exergetic efficiency the lowest amount of exergy (or available work) is used to complete the process, and thereby the highest fuel efficiency is reached. It is observed that due to the differences in heat pump configuration the significant differences in COP are not reflected equally significant in the exergetic efficiency. Thus, it is of importance to take both measures into account to do a consistent evaluation.

In variants A and B district heating and not domestic hot water is stored in the tank (Figure 1), which eliminates the risk of legionella formation in the DHW. The content of hot water after the heat exchanger on its secondary side, in DHW pipes, is possible to be kept under 3 litres. This is the maximum permissible hot water amount in the DHW system in order to avoid legionella if no additional treatment is applied, according to the German guidelines (DVGW, W551) for hot water systems [7]. In variant C the possibility of bacteria formation increases, as DHW is stored in the tank. In order to reduce the risk additional energy is needed to occasionally increase the temperature in the tank to 60 °C.

When comparing the required storage tank size (Table 3) variant C has an advantage of smaller hot water storage requirement. Usually smaller storage tanks are desired due to practical reasons, such as available space for the consumer DH station at the households. A smaller tank could also lead to lower heat losses. On the other hand DHW is stored at higher temperature (variant C) than the heated DH water in variants A and B, which would lead to higher heat losses. Heat losses are neglected in the calculations, as they are assumed of similar magnitude when considering the total installation.

When comparing A and B concepts, it seems that heat pump in variant A will have more stable operation conditions, as district heating supply water flows through both, condenser and evaporator. Whereas in case of variant B, temperature of the return water, flowing through evaporator, can vary, depending on e.g. cold tap water temperature.

Based on the lowest electricity consumption as well as other advantages and disadvantages variant A has been chosen for further development.

DHC13, the 13th International Symposium on District Heating and Cooling
September 3rd to September 4th, 2012, Copenhagen, Denmark

CONSUMER DHW UNIT WITH ELECTRIC HEATER AND COMPARISON WITH MICRO BOOSTER HEAT PUMP

Even though the micro booster heat pump is expected to use significantly less additional electricity than electric water heaters, the latter solution can be expected to have lower investment costs and more simple design (Figure 2). In order to compare the costs and benefits of micro-booster heat pump and electric water heater DHW concepts for low temperature district heating, three electric heating alternatives have been calculated. The chosen micro-booster variant A is then compared with the 3 electric heater alternatives.

In the first electric heating alternative (D) the heat pump is replaced by an instantaneous electric heater, which boosts DH temperature from 40 °C to 53 °C. The design is more simple when compared to the variant A and only one DH flow is used for hot water preparation. In the alternative E district heating water flows through a coil, which is mounted in a hot water tank. Cold tap water in the tank is pre-heated to 35 °C by the coil and further heated up to the required 55 °C by an electrical heater, also installed in the tank. Finally, in the alternative F only electricity is used to heat domestic hot water in the tank with the installed electric heater.

The microbooster heat pump and the electric heating alternatives are compared, based on energy (e.g. increased electricity) consumption, exergetic efficiency, CO_2 emissions, as well as annualised investment and operation costs. Thermodynamic analysis has been performed using the same tool and assumptions as described in the previous section. The yearly costs have been calculated for assumed hot water consumption of 3200 kWh.

Cost calculations are performed for private consumers, assuming low temperature district heating supply to the single family houses. Additionally, socioeconomic costs of hot water preparation are compared based on the projected future energy costs in order to include the expected development of the Danish energy system into the analysis [9]. Investment costs of different alternatives include only costs, related to hot water installations of a consumer substation in a low energy single family house with low temperature district heating supply. The heating part of the substation is assumed to be the same for the analysed house, regardless of the hot water installation. All hot water units are assumed to have 15 years economic lifetime. A 6 % discount rate has been used for the private consumer and 3 % in the socioeconomic calculations.

District heating and electricity prices for private consumers are based on the latest data by the Danish Energy Regulatory Authority [8] (see Table 4). District heating prices for households include only variable heat costs, since the house is connected to a DH network and the fixed yearly fees have to be paid anyway. District heating prices in Denmark vary depending on the DH company and span between 3 and 21 ¢/kWh. For the calculations average and minimum DH price has been used. Electricity prices are based on the price level for consumers with yearly consumption of 4000 kWh and include energy and CO_2 taxes. Private investment costs and energy prices also include VAT, which in Denmark reaches 25 %. Socioeconomic district heating and electricity costs (Table 4) as well as CO_2 emission rates (kg/GJ) of district heat and electricity are based on the estimations by the Danish Energy Agency [9].

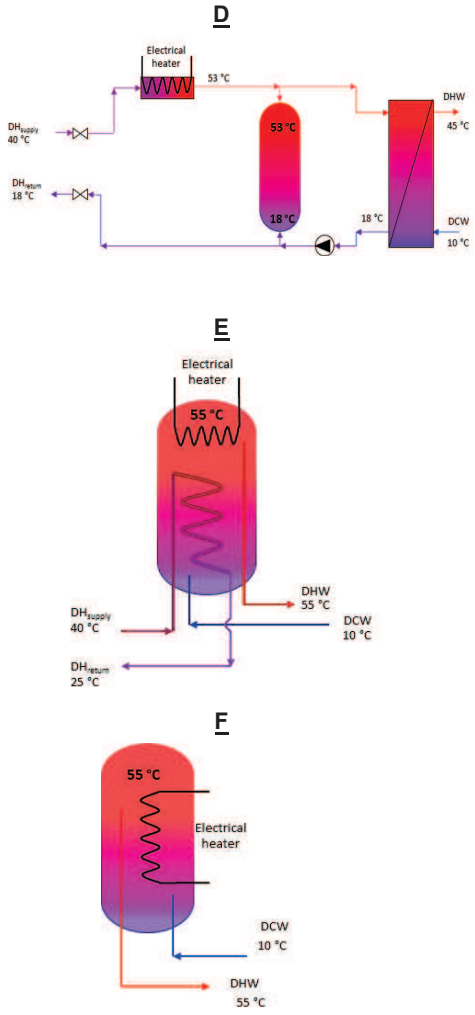

Figure 2 Analysed electric heater DHW concepts

DHC13, the 13th International Symposium on District Heating and Cooling
September 3rd to September 4th, 2012, Copenhagen, Denmark

CO_2 emissions are based on district heating and electricity production in 2011, while socioeconomic energy prices reflect DH and electricity costs in 2030.

Table 4 District heating and electricity prices

¢/kWh	Average	Min
DH price, private	8,4	3,0
DH price, socioeconomic, 2030	3,5	
EL price, private	30,3	
EL price, socioeconomic, 2030	11,2	

The main calculation results regarding DH and electricity capacities needed and system efficiencies are summarised in Table 5.

Table 5 The results of micro booster heat pump- and electric heater- based DHW system calculations

	Microbooster heat pump and electric heater variants			
	A	D	E	F
DH flow, l/h	85	50	65	0
Power, W	142	749	896	2017
Coefficient of performance (COP)	5,3	1,0	1,0	1,0
Exergetic efficiency	0,43	0,14	0,12	0,06
Storage size required, l	128	128	100	100

The highest exergetic efficiency of the system is achieved in variant A, where the heat pump is used for boosting the DH water temperature. At the same time the highest share of the total energy for hot water heating comes from district heating in this alternative (93 %), see Figure 3. Other variants (D, E and F) have considerably higher electricity consumption, which is not desired. When electricity consumption increases, exergetic efficiency decreases. Thus, the advantage of micro booster heat pump – only moderate increase in electricity consumption – is clearly illustrated here. If a large share of electricity is produced in wind power plants and other non-dispatchable renewable energy technologies, higher electricity consumption can be acceptable, also due to the possibility for providing balancing services for the electricity grid (since the boosted DH or domestic hot water is stored in the tank making electricity consumption flexible). However, increased power consumption might require reinforcements of electricity distribution networks if considerable share of consumers would choose e.g. variant F.

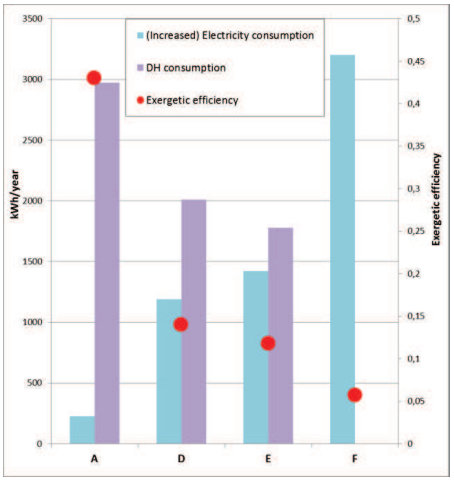

Figure 3 Energy consumption in DHW system and exergetic efficiency

From Figure 4 it can be seen that, based on the fuel mix in production of district heat and electricity today, the microbooster heat pump alternative causes the lowest yearly CO_2 emissions. Clearly, the emissions from DH production can be significantly lower if low temperature and renewable energy sources, such as solar, geothermal energy or biomass, are used. For electricity it also depends on whether fossil fuel-based production will be repalced by renewable energy ressources (e.g. wind or biomass).

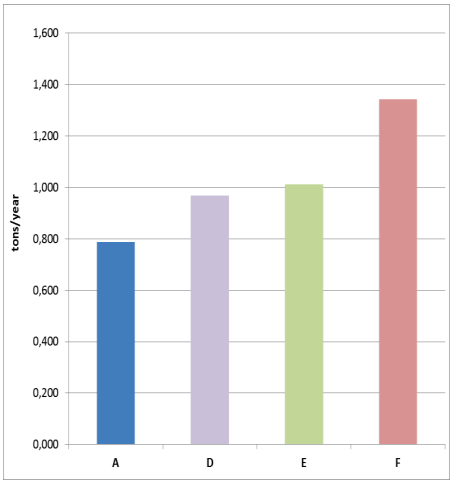

Figure 4 CO_2 emissions, caused by different hot water heating alternatives

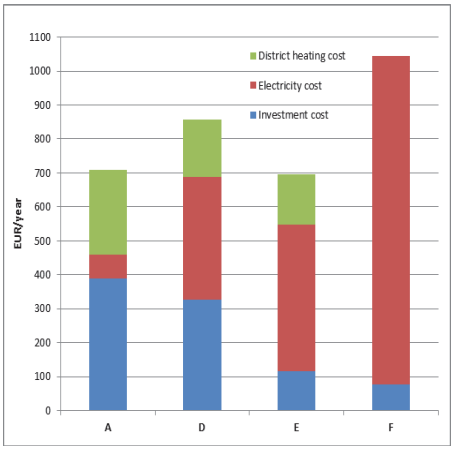

Figure 5 Yearly costs for private consumers, average DH price and 6 % interest rate

Figure 5 and Figure 6 include yearly costs of different hot water heating alternatives for private consumers with average and lowest variable district heating prices respectively.

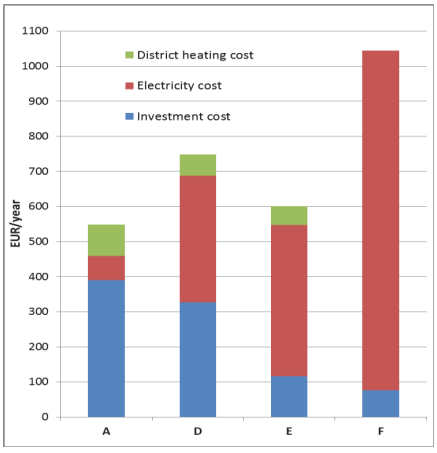

Figure 6 Yearly costs for private consumers, minimum DH price and 6 % interest rate

Investment costs account for the largest share (55 %) of the yearly expenditures when the micro booster heat pump alternative is chosen. At the same time yearly operation costs are high when electric water heaters are installed – between 62 % and 93 % of the total yearly costs. From the figures it can be seen that the least cost alternatives are A and E. With average DH price (Figure 5) variant E has the lowest yearly cost, which is only marginally lower than for variant A. Low DH price (Figure 6) leads to reduced operation costs for all hot water installations (except for variant F) – but most significantly when the micro booster heat pump is used. Hence, variant A is the least cost alternative in this case.

If hot water consumption is lower (e.g. 1240 kWh/year) than the one, used in the calculations (3200 kWh/year), operation costs decrease and the electric heating alternatives become more cost efficient than heat pump-based system. While the investment in a micro booster heat pump is more beneficial with high DHW consumption.

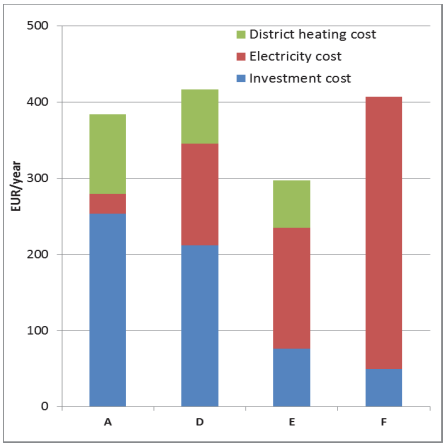

Figure 7 Yearly socioeconomic costs (2030 prices), 3 % interest rate

In general, the conclusion can be made that it is critical to reduce investment costs of the micro booster heat pump. Clearly, use of heat pump in the low temperature DH consumer substation can already today be cost-efficient for private consumers with hot water consumption of around 3200 kWh/year. When looking at the results of the socioeconomic calculations with 2030 energy prices (Figure 7) it is obvious that the cost of the micro booster unit has to be reduced by approximately one third for this concept to be more cost efficient than variant E from the socioeconomic point of view. The micro booster heat pump hot water unit is at the prototype stage today, thus a certain cost reduction might be expected.

Figure 8 compares the total energy consumption in the low energy single family house with different hot water installations. Here hot water demand is calculated according to the guidelines in the recent Danish Building Regulations (Table 1) and is lower than the demand, used for cost calculations.

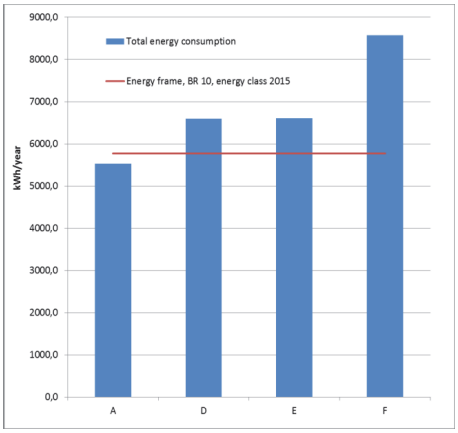

Figure 8 Comparison of total energy consumption in a building with energy frame, according to BR 10

Only variant A complies with the energy frame for buildings of low energy class 2015. The reason is high electricity consumption of electric heating alternatives, which is in this calculation weighted by a factor 3 when compared to the district heating consumption. Thus, energy policy of today encourages district heating consumption and promotes electricity savings in building installations. Consequently, a micro booster heat pump-based hot water installation is the most suitable concept, with low temperature (~40 °C) district heating supply according to the Danish Building Regulations.

CONCLUSION

Different concepts for domestic hot water preparation when district heating supply temperature is reduced to 40 °C have been presented and compared in the article. The reduction of DH temperature implies the use of an additional energy source (electricity) for DHW preparation. Two main concepts of utilising the additional energy have been compared – based on heat pump and electric heater technologies.

Based on the performed calculations several main conclusions can be drawn. From the cost perspective it is not obvious that heat pump use in DHW system (variant A) is the most beneficial concept under current technology and energy prices for the private consumers or based on future socioeconomic costs. Combined electric and DH water heater in the DHW tank (variant E) is the competing technology. On the other hand, heat pump alternative reduces electricity consumption by more than 6 times, which is an important advantage in the light of the expected more rapid increase in electricity prices, when compared to the prices of the district heat. The benefits of reduced electricity consumption are reflected in the calculated exergetic efficiencies of the two alternatives (0,43 and 0,12 for variant A and E respectively), which reflect consumption of primary energy. According to the recent Danish Building Regulations the DHW system with the micro heat pump is the best alternative, due to the lowest electricity consumption.

FUTURE WORK

As a part of the Danish Energy Technology Development and Demonstration project (EUDP 11-I, J. nr. 64011-0076) the first prototype of the DHW system with micro booster heat pump has been built according to the design of the variant A. The laboratory tests have shown that it is possible to achieve high heat pump COP and prepare the domestic hot water at the required temperature. Five consumer DH stations with the micro booster heat pump will be installed in single family houses, supplied with 40 °C district heating, for demonstration of the technology during the heating season 2012/2013.

REFERENCES

[1] Danish Energy Agency, “Basic facts on Heat Supply in Denmark”, http://www.ens.dk, accessed on 10 July 2012

[2] Rambøll, “Varmeplan Danmark”, Virum, Denmark (2008), pp. 22.

[3] Danish Ministry of Climate, Energy and Buildings, “Vores energi”, The Danish Government, Copenhagen (2011), pp.5.

[4] Grontmij, “Heat pumps for domestic hot water preparation in connection with low temperature district heating”, draft report (2012).

[5] A. Bejan, G. Tsatsaronis M. Moran, “Thermal Design and Optimization” Wiley, NY. 1996 pp. 113-163

[6] T. Ommen and B. Elmegaard, ”Exergetic evaluation of heat pump booster configurations in a low temperature district heating network”, in Proc. ECOS2012, vol. 1, pp 148(1-14)

[7] C. H. Christiansen, A. Dalla Rosa, M. Brand, P. K. Olsen, J. E. Thorsen, “Results and experiences from a 2-year study with measurements on a new low-temperature district heating system for low-energy buildings”, final draft (2012)

[8] Danish Energy Regulatory Authority, homepage, http://www.energitilsynet.dk/, accessed on 5 July 2012

[9] Danish Energy Agency, Forudsætninger for samfundsøkonomiske analyser på energiområdet, Copenhagen (2011), pp. 18, 23.

[10] Hämäläinen, T. et.al. Dimple Pattern – A challenger in plate heat exchanger Technology, SDDE 2010, 21-23 March, Portoroz, Slovenia

Appendix N

Paper 17 - Coolenergy 2013

Torben Ommen, Wiebke B. Markussen and Brian Elmegaard

Heat pumps in district heating networks

Coolenergy 2013, Dansk Køledag f.m.b.a.

Heat pumps in district heating networks

Torben Ommen [a], Wiebke Brix Markussen [b] and Brian Elmegaard [c]
[a] *Technical University of Denmark, Kgs Lyngby, Denmark, tsom@mek.dtu.dk, CA*
[b] *Technical University of Denmark, Kgs Lyngby, Denmark, wb@mek.dtu.dk*
[c] *Technical University of Denmark, Kgs Lyngby, Denmark, be@mek.dtu.dk*

Abstract:
In the current Danish energy system, the majority of electricity and heat is produced in combined heat and power plants. With increasing shares of intermittent renewable power production, it becomes a challenging task to match power and heat production, as heat demand and production capacity constraints limit the power plants. Efficient heat pumps can be used to decouple the constraints of electricity and heat production, while maintaining the high energy efficiency needed to match the politically agreed carbon emission goals. The requirements in terms of COP, location, capacity and economy are calculated using an energy system model which includes power plants, heat pumps and district heating consumption profiles. The model is developed with focus on accurate representation of the performance of the units in different locations and operating modes. The model can assist in investment decisions and strategic planning in the energy sector. The paper presents a case study of optimal implementation of heat pumps in the present energy system of the Copenhagen area. By introduction of the correct capacity of heat pumps, a 1,6 % reduction in fuel consumption for electricity and heat production can be obtained at present conditions in a month with high heating demand.

Keywords:

Combined heat and power, Heat pumps, District heating, Energy systems analysis, Optimisation.

1. Introduction

In areas with large shares of Combined Heat and Power (CHP) production, a significant introduction of intermittent power production may influence the operation management of both heat and electricity production. CHP plants may be needed to operate in hours where the electricity price is not favourable, as demand for heat production exceeds supply. Methods to decouple the production constraints of both utility products, while maintaining high energy efficiency, are investigated as they may prove highly valuable. Integration of heat pumps in in district heating may pose this ability [i].
In the liberalized, Nordic electricity market, the operation pattern of each plant is determined by optimization of economics. In order to evaluate the feasibility of installation of heat pumps, the numerical models used in the optimization should include the complete characteristics of the operation of both CHP plants and heat pumps utility optimisation of utilities. Today, the Danish energy system consists mainly of CHP plants, peak production boilers and wind turbines. In the coming years an increased number of wind turbines will be installed, and the intermittent power production may assign further constraints to the remaining utility units.
A number of energy system models have been developed during the last decade both in Denmark and worldwide [ii], and many of these models are continuously expanded and maintained. Some of the system models will require a training period up to several months, "depending on the level of complexity required". The majority of the models are using linear optimisation [ii].
In the linear programming (LP) models, the outlines of thermal units such as CHP-plants appear to be simplified to an extent where the representation of the plant does not characterise the physical unit satisfactory at the full operating range. Two alternative methods, i.e., Non-linear programming (NLP) and Mixed Integer Linear Programming (MIP) are increasingly used, as they both provide a possibility to increase the detail of the constraints.

The influence of using the three different optimisation approaches has been investigated in a recent paper [iii]. This study shows that the operation of heat pumps is highly affected by the representation of CHP-plants in the model. Both alternative approaches estimate increased supply of heat from heat pump operation, but the results differ to some extent. The increase is respectively 23 % (MIP optimisation) and 39% (NLP optimisation) in a month where heating demand is high. The difference for a full year is lower, however, and from an overall system perspective the two optimisations show similar results. We thus conclude that the difference in the optimised operation by using the two methods is reasonable, and that the MIP optimisation is most appropriate from a viewpoint of accuracy and runtime.
The MIP optimisation model has been used in this paper, to reveal trends regarding optimal location, COP and capacity of heat pumps in the current Eastern Denmark system.

2. Method

The numerical model is implemented in General Algebraic Modelling System (GAMS) [iv] using the CPLEX solver. The model utilises the rolling horizon optimisation principle. The model is built to represent the dynamic operation of heat and electricity markets using based on the physical principles, such as the thermodynamic laws. External data processing is handled by Matlab, using the interface gdxmrw [v]. The model approach used for implementation of the plants in the energy system is generic and easily customisable .
The energy system of eastern Denmark has been used as a case. The current operation of the utility production in this area distinguishes the system from other European utility areas, as electricity is produced by wind turbines and by CHP-plants. According to the statistics for the combined Danish energy system [vi] (including the area of western Denmark) more than 99.7% of the produced electricity in 2011 originates from the two utility technologies.
Historical data are available online for electricity production and consumption in each region [vii]. Hourly values for wind production, local production (small scale CHP-plants) and gross consumption are used. The used data from this source is from 2011.

The electricity production system in eastern Denmark is composed mainly of small scale and central CHP-plants, along with a high number of wind turbines. Additionally there are 4 central CHP waste incineration units in the energy system layout, but in terms of installed capacity for electricity production they represent a small fraction. For the majority of the central CHP-units and incineration plants, the produced heat is transmitted to only one large district heating network (network #1). One central CHP-plant is connected to a separate network (network #2). The hourly demand of the networks has been collected from one of the network operators (HOFOR) for the entire year 2011. The data received is subdivided into five areas, ranging from central Copenhagen to one of the low intensity suburbs, and is thus considered representative for all the areas in the study. The derived “central” electricity demand and the total heat demand in the DH-networks for 2011 are presented in Fig.1.

Transmission lines for import/export with neighbouring regions are not studied in the analysis. Thus, the operation can be characterised as an island operation.

For each of the 18 thermal power plant units in the utility system, information regarding capacity and consumption is available online, from either the plant owners [viii] or from the TSO [ix]. From the information, it is possible to derive the plant characteristics listed in table 1. Most of the data in the table is referring directly to the design parameters, but the table also includes prices of the used type of fuel for 2011 using IEA prices [x]. Waste has been estimated to have a cost of 2 [EUR pr. GJ].

It should be noted that both electric efficiency and maximal thermal efficiency is calculated for the plant in back pressure operation mode. In extraction power plants, the efficiency of the electricity production is variable according to the c_v value of the power plant. A schematic representation of an extraction plant is presented in Fig. 2.

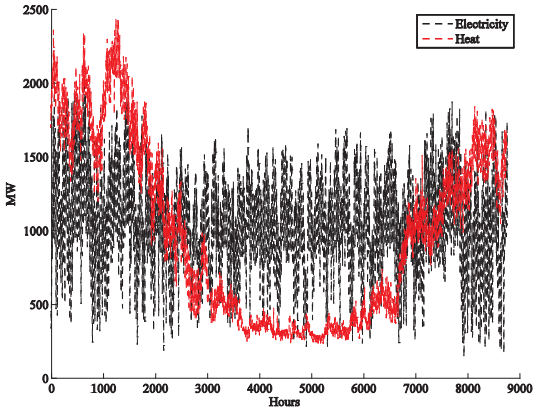

Fig. 1. Total electricity and heat demand for the system (2011).

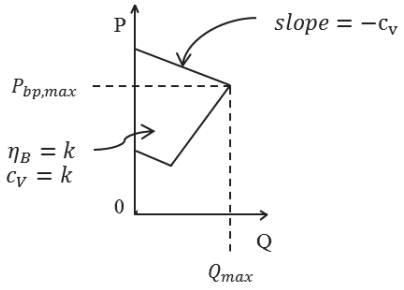

Fig. 2. Schematic representation of an extraction CHP-plant with linear constraints. Efficiency is calculated at full load back pressure operation (Q_{max} , $P_{bp,max}$).

For some of the energy technologies considered, it is required to include detail about the unit's ramp rate. Ramp rates are typically a concern in high pressure boilers, where material properties limit the boiler operational usability. These constraints are included for all the plants in table 1. The ramp rate denotes the maximal allowed change in boiler fuel input per operation hour. The ramp rate has been assumed for all CHP-plants. Four of the power plants (KYB1, KYB2, KYB3 and KYB4) are emergency and peak load facilities. Thus the units must react quickly in case of imbalance between production and demand. The ramp rate has been set to 1 in this case.

In both DH-networks, stratified storage tanks for hot DH-water are in use. The capacity and ramp rate of the storage are included in table 2. As the duration of the storage is short term (hours), thermal losses are neglected.

Table 1. Thermal power plant unit characteristics

Plant name	DH Area	Type	Capacity Boiler [MW]	Elec. eff. in backp. [/]	Max. Therm. eff. [/]	Max. boiler Ramp rate [/]	C_V value [MW/MJs]	Fuel	Fuel price [EUR pr. GJ]
AMV1	1	Backp.	365	0.21	0.90	0.2	-	Biom.	6.5
AMV3	1	Extraction	600	0.36	0.91	0.2	0.11	Coal	3.5
HCV2	1	Backp.	180	0.18	0.90	0.2	-	Nat. Gas	7.3
HCV7	1	Backp.	300	0.29	0.90	0.2	-	Nat. Gas	7.3
HCV8	1	Backp.	125	0.20	0.90	0.2	-	Nat. Gas	7.3
SVM1	1	Backp.	175	0.17	0.90	0.2	-	Nat. Gas	7.3
SVM7	1	Backp.	485	0.17	0.90	0.2	-	Nat. Gas	7.3
AMF1	1	Backp.	131	0.19	0.83	0.2	-	Waste	2.0
AVV1	1	Extraction	600	0.36	0.91	0.2	0.11	Coal	3.5
AVV2	1	Extraction	1150	0.43	0.93	0.2	0.14	Biom. & Nat. Gas	6.9
KARA5	1	Backp.	65	0.18	0.81	0.2	-	Waste	2.0
VF5	1	Backp.	95	0.12	0.99	0.2	-	Waste	2.0
VF6	1	Backp.	110	0.18	0.99	0.2	-	Waste	2.0
ASV2	2	Extraction	430	0.34	0.90	0.2	0.12	Coal	3.5
STI1	-	Elec. only	900	0.30	0.30	0.2	-	Oil, heavy	8.5
KYB1	-	Elec. only	850	0.30	0.30	1	-	Oil, light	14.9
KYB2	-	Elec. only	850	0.30	0.30	1	-	Oil, light	14.9
KYB3	-	Elec. only	72	0.25	0.25	1	-	Oil, light	14.9
KYB4	-	Elec. only	504	0.25	0.25	1	-	Oil, light	14.9

Table 2. Storage units in district heating networks

Unit name	DH Area	Type	Capacity [MW]	Assumed Therm. eff. [/]	Ramp rate of storage [MWh/h]
STO1	1	Heat storage	750	1	300
STO2	1	Heat storage	2600	1	330
STO4	2	Heat storage	1200	1	300

One electric heater is installed in DH-network #2 at the site of unit ASV2. The Coefficient of Performance (COP) of the electric heater is estimated to be 95%. Its characteristics are presented in table 3.
Also presented in table 3 are the basic properties of a typical heat pump unit. The COP of the considered heat pumps is estimated to 3, based on already installed units in other DH networks [xi]. Several types of heat pumps for this temperature range are investigated in [xii]. The COP is highly influenced by the availability of the heat source and the sink temperature. The appropriate area and condenser capacity are not fixed, but are determined by the optimisation.

Table 3. Characteristics of electric boiler and heat pump unit.

Plant name	DH Area	Type	Capacity Condenser [MW]	COP [/]	Fuel	Fuel price [EUR pr. GJ]
ASVe	2	Elec. Heat	98.0	0.95	Elec.	-
Heat Pump	??	Elec. Heat	??	3	Elec.	-

3. Results

In order to utilise the already installed CHP units optimally, the correct capacity of DH-network heat pumps is of main concern. The two networks far from identical, so each network must be considered. Results of a study of heat pump capacity for DH area #1 are presented in Fig 3 A and for DH area #2 in Fig. 3 B.

The figures illustrate the relative, equivalent full load operation as a function of heat pumps capacity for the optimum system operation. The evaluation covers the period of January 2011. We find that the installation of heat pumps result in up to 2% lower fuel consumption. More heat pump capacity will result in higher total heat production, even though the capacity ratio decreases. The heat pumps will also substitute operation of the less efficient electric heater.

A significant improvement in fuel savings with a fixed capacity of heat pumps is found for area #1, compared to the area #2. Several factors contribute to the results, of which two are mentioned here:

- Area #1 is subject to a significantly higher district heating demand, than in area #2.
- Operation optimisation of multiple CHP units (in contrast to one unit) allows higher flexibility for variables such as ramp rate and minimum/maximum load.

Considering the results in figures 3 A and 3 B, the capacity is fixed for the remaining of this study to 300 [MW] in area #1 and 100 [MW] in area #2.

The operation of the considered heat pump capacity for the full year of 2011 is presented in Fig. 4. The capacity installed in DH-area #1 has an operational time of 1389 hours a year, with an average load of approximately 228 [MW]. The heat pump capacity considered for DH-area #2, is only operated 247 hours with an average load of 71,5 [MW]. The electric heater is used as little as 22 hours during the full year with an average load of 48 [MW].

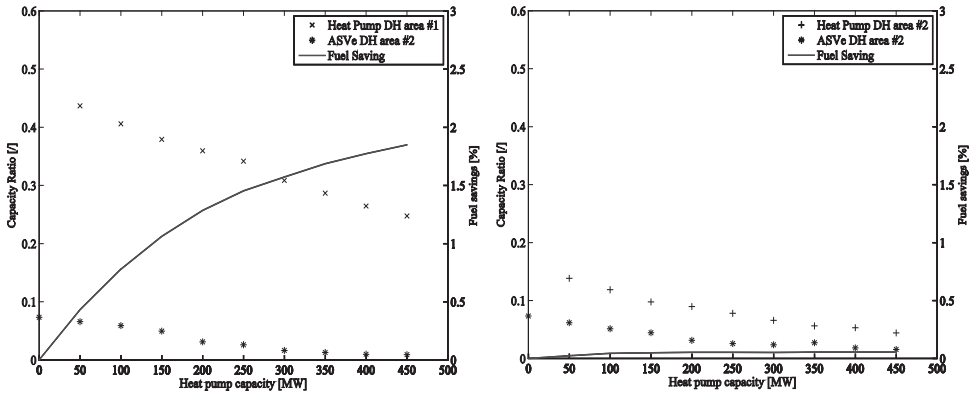

(A) (B)

Fig. 3. Capacity ratio and fuel savings of heat pump integrations as a parametric study of the capacity to be installed in DH-area #1 (Fig 3 A) and DH-area #2 (Fig 3 B) for January 2011. In both figures, the capacity ratio of the electric heater, for the 'ASVe'-unit, is included as the operation pattern of this unit will be significantly changed.

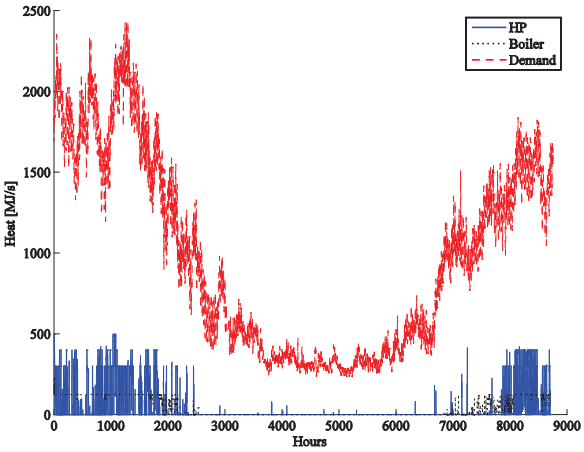

Fig. 4. Operation of heat pumps based on demand and production data from 2011.

On a monthly scale, the operation hours of each individual heat pump is presented in table 4. The heat pumps are mainly operated in four months during winter. A small part of the operation is during spring and fall, and during summer period, the operation is negligible.

Table 4 Operational hours of separate months in 2011.

	Jan	feb	mar	Apr	may	jun	jul	Aug	sep	oct	Nov	Dec
HP DH - Area #1	240	418	226	33	1	3	0	0	2	18	54	394
HP DH - Area #2	40	73	32	1	1	4	3	2	0	0	2	89
ASVe – Area #2	0	19	0	0	0	0	0	0	0	0	1	2

The load/duration curves of both heat and electricity production for the four central extraction CHP plants are presented in Fig 5. The extraction plants present an important control possibility in a highly constrained energy system. Comparing the operation hours of electricity production (Fig. 5 A) with the operation hours of heat production (Fig. 5 B) it is clear, that the extraction plants are still mainly operated for electricity production. This suggests, that heat pump introduction mainly is advantageous due to the high fluctuations of electricity production, as heat pumps may assist in levelling the demand.

Both AVV2 and ASV2 run in full load back pressure operation approximately 280 hours a year. This suggests, that the operation pattern of heat pumps is not related to constraints from installed utility capacity, but rather to:

- High fluctuations in boiler load for the CHP-units.
- Mismatch between heat and electricity demand concurrency.
- Mismatch between heat and electricity demand and CHP-plant production.
- Introduction of heat pumps shift power plant production from units with high fuel cost, to units with lower cost.

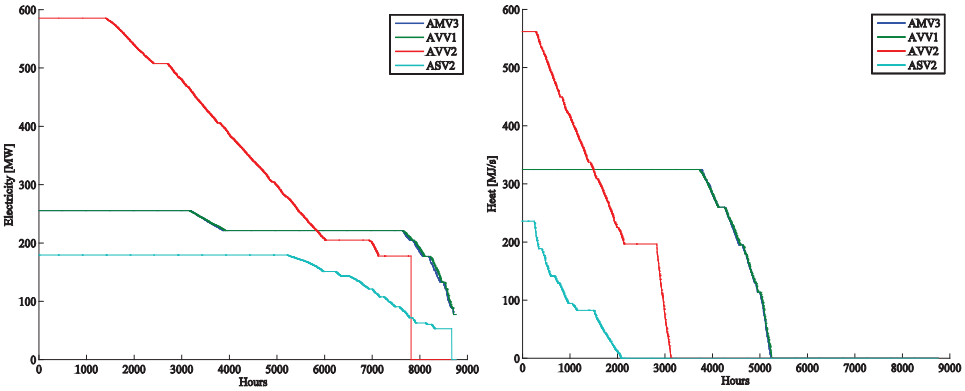

(A) (B)

Fig. 5. Load duration curve for the operation of the central extraction CHP-plants in terms of electricity (Fig. 5 A) and heat (Fig. 5 B) for 2011.

As the input parameters may affect some of the above stated considerations, a parametric study has been conducted, based on the data from January 2011. This type of evaluation may highlight the influence of assumptions, or possible allow a more in depth understanding of the mechanisms represented by the model. The evaluation is presented in Fig 6. Only key input parameters are considered.

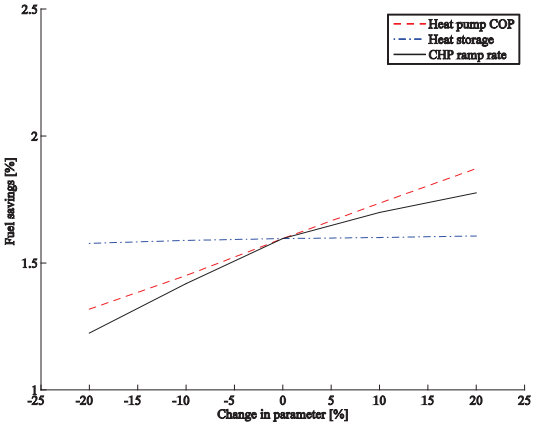

Fig. 6. Parametric study of selected input parameters in the numerical model. The study is based on data from January 2011.

The evaluation express how a slight change in the selected parameter will affect the result of the objective function, expressed as the fuel savings compared to the reference case, where no heat pumps are introduced.
Based on the evaluation it is clear, that the size of heat storage has a very low impact on the derived fuel savings from introduction of heat pumps. On the other hand, the magnitude of some of the key assumptions - heat pump COP and power plant ramp rate - influences the derived results significantly. In the case of a too high estimate of the parameters, the power plant ramp rate has the main influence on the results. If the estimated parameters are too low, the changed COP is the main influence in the system.

4. Discussion

Large scale heat pumps for high temperature applications are not easily available from manufacturers, and require in depth knowledge about the heat source and system integration. As the COP of the heat pump has a high impact on the results, further investigation is necessary, to establish the correct range of the COP.
Similarly, the ramp rate for each individual unit must be investigated, in order to establish the correct fuel savings in Eastern Denmark. Furthermore the level of detail can be increased for a few of the power plant units.

5. Conclusion

Efficient heat pumps can be used to decouple the constraints of electricity and heat production, and at the same time address the high energy efficiency needed to match the politically agreed carbon emission goals.
A newly developed energy system model can address the requirements in terms of COP, location, capacity and economy. At present, the model includes power plants, heat pumps and district heating consumption profiles. The model is developed with focus on accurate representation of the performance of the units in different locations and operating modes.
As a case study, the Copenhagen area is used. By introduction of the correct capacity of heat pumps, a 1,6 % reduction in fuel consumption for both heat and electricity production can be obtained in East Denmark in a month with high heating demand.

Acknowledgement

This work was supported by Copenhagen Cleantech Cluster (CCC), DONG Energy and Teknologisk Institut (DTI)

References

[i] Blarke, M.B. Towards an intermittency-friendly energy system: Comparing electric boilers and heat pumps in distributed cogeneration (2012) Applied Energy, 91 (1), pp. 349-365. Cited 8 times.
[ii] D. Connolly, H. Lund, B.V. Mathiesen, M. Leahy, A review of computer tools for analysing the integration of renewable energy into various energy systems, Applied Energy (2009)
[iii] T. Ommen, W. B. Markussen, B. Elmegaard. Comparison of operation optimization methods in energy system modelling, ECOS 2013.
[iv] General Algebraic Modeling System (GAMS), http://www.gams.com/

[v] Michael C. Ferris, MATLAB and GAMS: Interfacing Optimization and Visualization Software, May 26, 2005, http://pages.cs.wisc.edu/~ferris/matlabgams.pdf
[vi] Energistyrelsen, Energy statistics 2011, http://www.ens.dk/
[vii] Energinet.dk, www.energinet.dk
[viii] Dong Energy and Vattenfall, power plant details available online.
[ix] Energinet.dk, Energinet.dk's analyseforudsætninger 2012-2035
[x] IEA's World Energy Outlook, november 2011.
[xi] Kent Krøyer, Nu køre r Danmarks første kæmpe -varmepumpe på billig mølle strøm, Ingeniøren, 2009.
[xii] T. Ommen, C. M. Markussen, L. Reinholdt, B. Elmegaard, Thermoeconomic comparison of industrial heat pumps. ICR 2011.

DTU Mechanical Engineering
Section of Thermal Energy
Technical University of Denmark

Nils Koppels Allé, Bld. 403
DK- 2800 Kgs. Lyngby
Denmark
Phone (+45) 4525 4131
Fax (+45) 4588 4325
www.mek.dtu.dk
ISBN: 978-87-7475-426-2

DCAMM
Danish Center for Applied Mathematics and Mechanics

Nils Koppels Allé, Bld. 404
DK-2800 Kgs. Lyngby
Denmark
Phone (+45) 4525 4250
Fax (+45) 4593 1475
www.dcamm.dk
ISSN: 0903-1685